NIRS-R-53
ISBN 4-938987-32-5

プルトニウム内部被ばく研究報告書

平成１８年３月

放射線医学総合研究所

目次

1. 緒言

放射線医学総合研究所におけるプルトニウム研究の発端は、1960年代にまで遡るが、プルトニウム内部被ばく研究を目的とした内部被ばく研究部の発足は1982(昭和56)年、内部被ばく実験棟の竣工は1985(昭和59)年になる。**表1**には、その後の内部被ばく実験棟におけるプルトニウム研究の経緯について、年代ごとに研究課題をまとめて示した。

実際にプルトニウムを使用した吸入曝露実験は1989（平成元）年より開始した。途中経過と成果については、『特別研究「公衆被曝のリスク評価に関する生物学的調査研究」最終報告書 88(S63)ー92(H4) NIRS-R-24』と『特別研究「放射線被ばくのデトリメントとその修飾に関する生物学的調査研究」最終報告書 93(H5)ー97(H9) NIRS-R-37』にまとめられて既に刊行されており、また保健物理学会誌(*保健物理*, **33**, 1998)にも総説が出されている。

本報告書では生物研究を中心に、プルトニウムの代謝・体内挙動に関する研究成果と、上記特別研究が終了した97年以降のプルトニウム生物影響研究の最終結果が、取りまとめられて報告されている。また、生物影響研究に関する詳しいデータおよび標本は、アーカイブとしてまとめられており、『Pathological Archives of Life-span Animal Studies on Carcinogenesis Following Internal Exposures to Plutonium Compounds, NIRS-M-186』として刊行されているほか、放医研のインターネットホームページ(http://www.nirs.go.jp:8080/anzendb/PuDB/ PuDB.html) にも公開されているので参照していただきたい。

さらに、内部被ばく実験棟における研究成果のまとめとして、巻末に89年以降のプルトニウム研究に関わる著書目録（原著論文、総説・プロシーディング)、および報告書目録（年報、業務報告書）を掲載した。

プルトニウム研究は、実験動物施設の建設とその管理、吸入曝露技術・装置の開発、内部被ばく線量評価、代謝・体内挙動解析、及び生物影響のリスク評価といった一連の技術開発・実験研究が有機的に統合され、はじめて遂行することが可能となったプロジェクト研究の一つであった。本報告書を刊行するにあたり、研究に関与した全ての研究者および技術者にこの場を借りて感謝を申し上げる。

表１　プルトニウム内部被ばく研究の経緯

1）1985-1990 年（施設・設備・技術開発から予備的試験研究）

①内部被ばく実験棟竣工・廃棄物処理施設の完成（1985-1988 年）

②吸入実験装置・体外計測装置・動物飼育装置等大型機器・設備の開発・設置

③線源（^{239}Pu：酸化物）の入手と硝酸塩への化学変換

④特別研究（生物効果特研中課題）：非 RI 次いで RI を用いて以下の小課題を実施

・放射性核種の代謝に関する比較動物学的研究

・体外計測法の開発と線量評価に関する研究

・吸入毒性と生物効果に関する研究

・放射性エアロゾルの挙動に関する研究

・キレート剤等による放射性核種除去法に関する研究

2）1990-1998 年（本格的実験研究開始から生涯飼育動物実験研究）

特別研究（公衆被曝・デトリメント特研中課題）により、プルトニウムを用いて、以下の小課題を実施

①吸入プルトニウム・エアロゾルの呼吸気道内挙動・代謝に関する研究

②体外計測法による吸入プルトニウムの線量算定と評価に関する研究

③プルトニウムの内部被ばくによる生物効果（発がん）に関する研究

④プルトニウムの体外除去とリスク低減化に関する研究

3）1998-2000 年（生涯発がん実験研究等の継続）

安全解析研究により、以下の小課題を継続・実施

①アルファ放射体の体内線量評価法開発とバイオドシメトリに関する研究

②プルトニウム曝露動物の生涯発がんとその機構に関する研究

③キレート剤によるプルトニウム内部被ばくリスク低減化に関する研究

4）2000 年-2006 年（発がん研究の継続と集約）

独法化後の組織改変により、基盤研究課題「プルトニウム化合物内部被ばく発がんに関する研究」として以下の小課題を実施

①酸化プルトニウム吸入曝露ラットにおける肺がんの線量効果

②クエン酸プルトニウム注射投与マウスにおける発がんの特異性

2. プルトニウムの代謝・体内挙動

2.1 プルトニウムの体内動態研究

2.1.1 酸化プルトニウム吸入曝露後のラット体内におけるプルトニウムの残留、移行、排泄に関する研究

酸化プルトニウムは粒子状のプルトニウムとして吸入されて気道内に沈着する。特に肺深部、すなわち肺胞へ沈着したプルトニウムの生体への影響が重大である。肺胞（以下、肺）に沈着した後の動態はプルトニウムの化学形、粒子径、肺への初期沈着量等、種々の要因により変化する。酸化プルトニウムは一般には不溶性であるが、酸化プルトニウムを生成する際の焼結温度により溶解性が異なってくる。したがって、その後の動態にも違いが生じると考えられる。この点を明らかにするため、焼結温度の異なる酸化プルトニウムのラットへの吸入実験を行い、焼結温度の違いによるプルトニウムの体内動態を比較した。

【目的】水酸化プルトニウムを高温（1,150℃）と低温（400℃）でそれぞれ焼結させて生成した２種類の酸化プルトニウムをラットに吸入曝露し、曝露後のプルトニウムの肺への沈着、肺から他の臓器への移行、体外への排泄が焼結温度の異なるプルトニウムでどのように違うかを明らかにする。

【方法】肺、肝や腎、糞尿中に存在するプルトニウムの放射能を液体シンチレーションカウンターで計測した。肺、肝、腎等の臓器は濃硝酸で溶解し、500℃で 24 時間灰化処理した後、フッ化水素酸を含む７M 硝酸に溶解して測定用試料とした。糞は蒸留水に十分懸濁させた後、一定量を坩堝にとり臓器と同様にして測定用試料とした。尿はろ過したロ液を測定用試料とする。測定用試料の全量または一部を計測用バイアルに取りシンチレーターを加えて計測した。

【結果および考察】高温及び低温焼結酸化プルトニウムを吸入させて１ヵ月後と１年後の肺と肝に存在するプルトニウムの割合、糞尿中への排泄率を**表２**に示した。

表２．焼結温度による酸化プルトニウムの代謝の違い

		臓器分布		排泄	
焼結温度(℃)	吸入後の時間	肺	肝	糞	尿
1150	1ヶ月	79#	0.04	20	3.2
	12ヶ月	17	0.12	52	31
400	1ヶ月	58	0.08	32**	3.8
	12ヶ月	8.9	0.17	68**	23*

#：初期沈着量に対する割合、(significance level * $p<0.05$、** $p<0.005$)

1ヶ月後、高温及び低温焼結酸化プルトニウムを吸入させたラットの肺残留率はそれぞれ初期沈着量の79及び58%で、低温焼結の方が肺から他臓器への移行が速いという結果を得た。1年後の肺残留率も、高温及び低温焼結酸化プルトニウムでそれぞれ17および9%となり、低温焼結の方が高温焼結の約半分まで減少した。肝のプルトニウムは吸入1ヶ月及び1年後で0.04～0.17%となり、量としては少ないが、低温焼結の方が高い傾向を示した。一方、体外へのプルトニウムの排泄率は肺からの移行が速い低温焼結酸化プルトニウム吸入ラットの方が高く、吸入後1ヶ月間に糞及び尿へ35%が排泄された。これは高温焼結酸化プルトニウム吸入ラットの約1.5倍に相当する。

【結果のまとめ】

1）肺への残留率は高温で焼結させた酸化プルトニウムを吸入したラットの方が高い。

2）糞へ排泄されたプルトニウムは1ヵ月後と1年後と、ともに低温で焼結させた酸化プルトニウムを吸入したラットの方が多い。

3）肝へ移行し、1年後も肝に残留するプルトニウムは低温で焼結させた酸化プルトニウムを吸入したラットの方が多い。

4）骨に移行し、1年後も骨に残留するプルトニウムは高温で焼結させた酸化プルトニウムを吸入したラットの方が多い。

【発表原著論文】 98)，99)

2.1.2 水酸化プルトニウム気管内投与ラットのプルトニウム体内動態に対するガドリニウムの影響に関する研究

使用済み燃料を再処理してプルトニウムを取り出す際、中性子吸収剤として硝酸ガドリニウムが使用されている。再処理工程に携わる作業者はプルトニウムとガドリニウムを同時に体内へ摂取する可能性があり、その際にはプルトニウムのみを吸入摂取した場合と吸入後の動態が異なることが考えられる。この点を明らかにするため、プルトニウムと硝酸ガドリニウムの混合溶液の気道内投与実験を行い、ガドリニウムの共存によるプルトニウムの体内動態を比較した。

【目的】ガドリニウムの共存によってプルトニウムの体内動態が変化するか否かを確認し、変化するならばどのように変化するのかを明らかにする。

【方法】硝酸プルトニウムの硝酸溶液に２種類の濃度の硝酸ガドリニウムを加え、中和することによりガドリニウムを含むコロイド状の水酸化プルトニウムを生成させた。ガドリニウム濃度の高い高ガドリニウム含有水酸化プルトニウム（以下、Ｐｕ－Ｇｄ－H）とガドリニウム濃度の低い低ガドリニウム含有水酸化プルトニウム（以下、Ｐｕ－Ｇｄ－Ｌ）をラットに麻酔下で気管内投与し、投与後４日目と４週後まで１週間ごとに肺、肝、腎、脾、大腿骨、糞尿を採取し、それぞれに含まれるプルトニウムの放射能を計測した。

【結果および考察】Ｐｕ－Ｇｄ－HおよびＰｕ－Ｇｄ－Ｌを投与して４週間後の肺への残留率、糞および尿中への総排泄率を**図１**に示した。高濃度のガドリニウムが共存すると、４週間後のプルトニウムの肺への残留率はガドリニウムが存在しない場合に比べて1.7倍も高い。肺に炎症があると粒子状物質の肺からの移行が遅くなることが知られている。ガドリニウムは濃度が高いと炎症を起こすことが知られており、水酸化プルトニウムは粒子状物質である。したがって、ガドリニウム濃度が高いＰｕ－Ｇｄ－Hを投与したラットでは肺に炎症が起きたためにプルトニウムの肺からの移行が妨げられ、４週間後においても依然として肺残留率が高かったと考えられる。

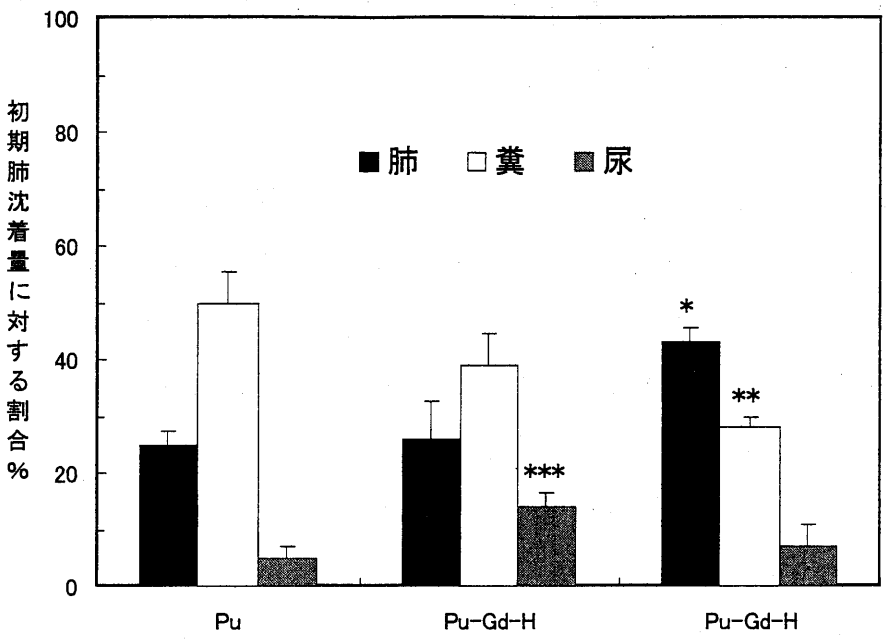

図1. 水酸化プルトニウム（Pu）およびPu-Gd-L、Pu-Gd-Hをラットに気管内投与4週間後の肺への残留率と糞尿中への総排泄率

(significance level *p<0.05, **p<0.01, ***p<0.005)

【結果のまとめ】

1）高濃度のガドリニウムが存在するとプルトニウムの肺からの移行は抑えられる。

2）低濃度のガドリニウムの存在により尿中への排泄が増加する。

【発表原著論文】 63), 113)

2.2 胎児におけるプルトニウムの代謝・影響研究

女性が妊娠中にプルトニウムを摂取した場合、胎児に移行したプルトニウムが、胎児或いは出生後の子供の健康に影響を与える可能性が示唆され、線量評価のための精密な代謝データや胚、胎児組織の放射線感受性に関する知見等、胎児におけるプルトニウムのリスク評価に必要なデータを提供することが求められてきた。その要求に応えるために、本研究では妊娠動物（マウス、ラット）に投与したプルトニウムの胚、胎児への移行率、胚、胎児に与える線量及びその生物影響を明らかにした。

2.2.1 妊娠動物に投与したプルトニウムの胚、胎児への移行に関する研究

【目的】胎児は驚くべき速度で成長、分化し、それに伴いプルトニウムの分布や濃度も刻々と変化するので、胎児組織に与えられる正確な線量を評価するには精密な代謝データが要求される。そのため、妊娠日齢毎に胎児胎盤組織へのプルトニウムの移行率を求め、その平均線量を算出する研究を実施した。また、未解明であったプルトニウムの胎児胎盤への移行に係わる機序の解明を目的とした研究を実施した。

【方法】妊娠日齢が1日ずつ異なる妊娠10.5日（妊娠中期）から16.5日（妊娠後期）のマウスにクエン酸プルトニウムを投与し、24時間後に胎児、羊水および胎児血液、卵黄嚢および羊膜、胎盤を含む脱落膜を採取し、各組織の放射能を液体シンチレーションカウンターで測定した。プルトニウムの胎児移行に係わる機序の解明を目的とした研究では、クエン酸プルトニウムをラットに投与し、またラットの胚を培養（全胚培養）した培地にクエン酸プルトニウム或いはプルトニウムの水酸化コロイドを投与し、それぞれの胎児と卵黄嚢に存在するプルトニウムの比率を比較した。

【結果および考察】

(1) 妊娠日齢毎の胎児胎盤組織へのプルトニウムの移行

図2に示すように、投与量に対する胎盤、胎児各組織へのプルトニウム移行率は妊娠日齢が進むとともに増加した。特に胎児への移行率の増加が顕著であり、妊娠後期における胎児の急激な成長により移行率も増加したと考えられた。

試験したすべての妊娠日齢を通じて胎盤、胎児組織に沈着したプルトニウムのほとんど（89%以上）は卵黄嚢と脱落膜にあり、胎児への移行率が増加する妊娠16.5日

でも、胎児に沈着する割合は胎盤、胎児組織全沈着量の数%であった。卵黄嚢と脱落膜がプルトニウムの胎児移行の強力なバリアとなっており、胎児がプルトニウムの主要な標的器官ではないことが証明された。

胎盤、胎児各組織へのプルトニウムの移行を濃度（組織 1g 当たり沈着したプルトニウムの投与量に対する%）で表すと、すべての妊娠日齢を通じて卵黄嚢が極めて高い値を示し、妊娠中期に卵黄嚢に存在する胎児造血幹細胞が被ばくする可能性が示唆された。

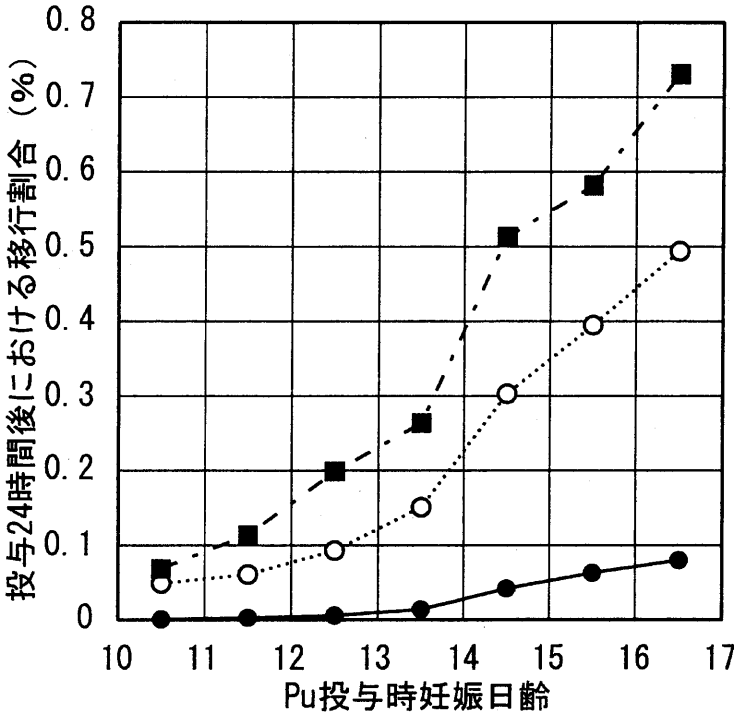

図２．妊娠日齢毎の胎児胎盤組織へのプルトニウムの移行；

○：脱落膜、■：卵黄嚢、●：胎児

(2) プルトニウムの胎児胎盤への移行に係わる機序

図３に示すように、胚に対する卵黄嚢のプルトニウム濃度比は、全胚培養系ではプルトニウム投与後の時間経過およびプルトニウムの形態（クエン酸、水酸化コロイド）に係わらずほぼ一定であるのに対し、クエン酸プルトニウムを母体に投与した場合は投与後の時間とともに増加した。本結果は、クエン酸プルトニウムを動物に投与した

場合、投与後の時間経過とともに、プルトニウムの化学形がクエン酸プルトニウムからおそらく水酸化コロイド或いはタンパク質複合体のような高分子形に変化したためと考えられ、クエン酸プルトニウムを動物に投与して１日後の胚に対する卵黄嚢のプルトニウム濃度比が極めて高いこと、全胚培養系にプルトニウムの水酸化コロイドを投与した場合も卵黄嚢の濃度が非常に高い実験結果を鑑みると、母体血液から卵黄嚢へのプルトニウムの移行の主要な機序は、高分子形に変化したプルトニウムがピノサイトーシス（貪飲）によって卵黄嚢にとりこまれることによると推察された。

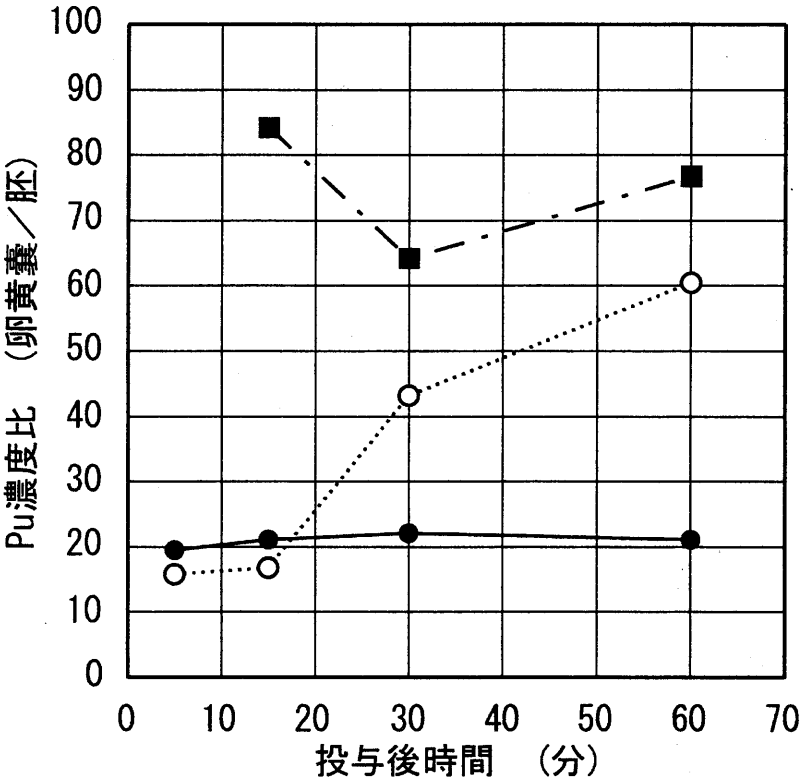

図３．母体にクエン酸プルトニウムを投与後、または全胚培養系にクエン酸プルトニウムあるいは水酸化コロイドプルトニウムを投与後の、胚に対する卵黄嚢のプルトニウム濃度比；

○：クエン酸プルトニウム母体投与、●：クエン酸プルトニウム全胚培養投与、

■：水酸化プルトニウムコロイド全胚培養投与

【発表原著論文】 28)，41)

2.2.2 妊娠動物に投与したプルトニウムの胎児造血組織に及ぼす影響に関する研究

【目的】胚、胎児組織は成体と比べて放射線高感受性であることが実証されており、さらに英国セラフィールドの核燃料再処理工場の近郊で小児白血病の多発を示唆する疫学調査研究がセンセーショナルに報道されたのを機に、プルトニウムやアメリシウムなど超ウラン元素の妊娠動物への投与が、胎児肝臓或いは出生児の骨髄に明らかな造血障害を引き起こすことを実証した研究が相次いで報告された。本研究は、妊娠マウスにプルトニウムを投与し、胎児肝臓の造血障害と胚、胎児に付与されるアルファ線の線量とを関連付けることを目的に実施した。

【方法】C3H 雄マウスと交配した C3H 雌マウス及び DBA2 雄マウスと交配した B6 雌マウスにクエン酸プルトニウムを妊娠 4 日目に投与し、妊娠 17 日目に胎児肝臓を採取し、胎児肝臓中に存在する造血幹細胞数を CFU-S アッセイ（致死量放射線照射された同系マウスに測定対象の細胞試料を静注し、12 日後に脾臓に形成されるコロニー数から試料中の造血幹細胞数を算定する方法）により測定した。また、妊娠 6, 8, 10 日の胚、胎児、胎盤組織におけるプルトニウムの分布をオートラジオグラフィーにより、妊娠 13, 17 日目の胎児、胎盤組織におけるプルトニウム量を液体シンチレーションカウンターで測定した。

【結果及び考察】

表 3 に見られるように、BDF1 マウスの胎児肝臓中の造血幹細胞数は 30kBq/kg 体重以上のプルトニウムの投与で有意に減少した。本結果は BDF1 マウスを使用した他の研究者の報告と同じであった。一方、C3H マウスでは多量のプルトニウム（BDF1 マウスで影響が見られる量の 30 倍）を投与しても、胎児肝臓中の造血幹細胞数に影響が見られなかった。このプルトニウムの生物影響に見られるマウス系統差が、プルトニウムの胚、胎児組織への移行や分布の相違によるものなのか、組織のオートラジオグラフィーや胎児、胎盤組織のプルトニウムの定量化によって検証したが、マウス系統間でプルトニウムの移行率や分布に差は認められず、胎児造血幹細胞の発生、分化に及ぼす放射線の影響がマウスの系統間で異なることが示唆された。

表３．妊娠４日目に投与されたプルトニウムが妊娠17日目の胎児肝臓中の造血幹細胞数に及ぼす影響[a]

投与量[b] (kBq/kg)	投与経路	マウス系統	
		C3H	BDF1
0	-	1877±291 (8)	2389±109 (8)
30	腹腔内	1801±204 (4)	1636±276[c] (4)
300	静脈内	2035±568 (3)	1192±492[c] (3)
300	腹腔内	1951±342 (7)	1255±210[c] (7)
900	腹腔内	1947±287 (3)	1304± 79[c] (3)

[a] 胎児肝臓当たりのCFU-S数の平均値と標準偏差。括弧内は母親の数。

[b] クエン酸プルトニウムは妊娠４日目に投与（kBq/kg体重）。

[c] コントロールとプルトニウム投与群間にスチューデント t-テストで有意差有り (significance level $p<0.05$)。

【発表原著論文】 83)

3. プルトニウムの生物影響

3.1 酸化プルトニウム吸入曝露ラットにおける肺腫瘍誘発に関する研究

核燃料物質プルトニウム（^{239}Pu）化合物の存在形態である不溶性酸化物の吸入被ばくによる肺がんリスクを実証的に解析評価するため、肺腫瘍の自然発生率が低く、線量算定・評価が可能なWistar系ラットに、酸化プルトニウムエアロゾルを吸入曝露し、生涯飼育して肺腫瘍発生率、肺細胞病態及びがん遺伝子の変異等を含む肺腫瘍誘発機構を検討するとともに、低LET（線エネルギー付与）放射線、X線を全身あるいは胸部局所照射した同系ラットにおける誘発肺腫瘍との比較を行った。

3.1.1 酸化プルトニウム吸入曝露ラットにおける肺腫瘍の線量効果

【目的】酸化プルトニウム吸入曝露により特異的に誘発される肺腫瘍、とくに悪性肺がんの発生率の線量効果関係を明らかにし、生涯リスク評価に資することを目的として、以下の実験を行った。

【方法】雌Wistar系ラット（80-150日齢）を用い、水酸化物を1,150 ℃で高温焼結した酸化物多分散エアロゾル（空気動力学的放射能中央径AMAD：0.3-0.4mm、標準偏差GSD:1.9-2.2）を1回、鼻部吸入曝露した。吸入曝露後7日目に麻酔下でNaIシンチレーターにて17 keVの特性X線を全身計測し、各個体の初期沈着量を推定し、蓄積肺線量は、吸入曝露時から死亡時までの吸収線量を初期沈着量と減衰曲線の積分によって求めた。全ての個体は死亡後病理解剖し、死因および肺腫瘍の病理組織学的検索を行った。

【結果および考察】未処置対照群ラット206匹に加え、吸入曝露ラット610匹を初期沈着量（initial lung deposition; ILD）および肺線量（lung dose）により9群に分け、それぞれの生存日数（吸入曝露後）、病理組織学的検索による良性（benign）および悪性（malignant）肺腫瘍の発生数を**表4**に示す。

表４　酸化プルトニウム吸入曝露ラットの生存時間と肺腫瘍誘発

実験群	動物数	初期沈着量* (Bq)	肺線量* (Gy)	生存時間* (日)	原発肺腫瘍発生数 (%)	
					良性肺腫瘍	悪性肺腫瘍
対照群	206	0	0	817±146	3 (1.5)	1 (0.5)
Pu 群 1	80	24±8	0.16±0.05	855±124	16 (20.0)	1 (1.2)
Pu 群 2	134	65±30	0.45±0.24	764±165	33 (24.6)	12 (8.9)
Pu 群 3	128	228±48	1.59±0.32	765±155	30 (23.4)	60 (46.9)
Pu 群 4	126	416±98	2.76±0.43	692±148	29 (23.0)	78 (61.9)
Pu 群 5	40	787±79	4.67±0.24	675± 98	5 (12.5)	32 (80.0)
Pu 群 6	31	948±76	5.43±0.29	622±105	3 (9.7)	27 (87.1)
Pu 群 7	31	1147±114	6.61±0.28	550± 82	1 (3.2)	28 (90.3)
Pu 群 8	30	1672±261	8.52±0.67	458± 95	0 (0)	27 (90.0)
Pu 群 9	10	2430±395	12.2±1.86	372±114	0 (0)	7 (70.0)

*平均値±標準誤差

結果は以下のようにまとめられる。

１）肺線量 0.45 Gy 以上の吸入曝露群で生存日数の有意な減少がみとめられ、これは悪性肺腫瘍の増加と相関している。

２）悪性肺腫瘍の大部分は癌腫で、肺線量 0.45 Gy 以上から急増して 6.6 Gy で約 90 % と最大値に達する。

３）肺腫瘍の組織型の違いによる線量反応の差がみとめられ、腺腫（adenoma）は比較的低線量域で、腺癌（adenocarcinoma）は中−高線量域で、腺扁平上皮癌および扁平上皮癌は高線量域で、それぞれ発生率のピークがみられた。

【発表原著論文】 62), 88), 122)

3.1.2 酸化プルトニウム吸入曝露ラットにおける肺腫瘍の誘発過程

【目的】酸化プルトニウム吸入曝露後、肺腫瘍発生に到るまでの期間、細胞レベルでみられる変化と病理過程を明らかにし、腫瘍病変形成に必要な線量と時間を推定することを目的として、以下の実験を行った。

【方法】雌 Wistar 系ラット（80-150 日齢）を用い、水酸化物を 1,150 ℃で高温焼結した酸化物多分散エアロゾル（空気動力学的放射能中央径 AMAD：0.3-0.4mm、標準偏差 GSD:1.9-2.2）を 1 回、鼻部吸入曝露した。吸入曝露後 7 日目に麻酔下で NaI シンチレーターにて 17 keV の特性 X 線を全身計測し、各個体の初期沈着量を推定し、蓄積肺線量は、吸入曝露時から死亡時までの吸収線量を初期沈着量と減衰曲線の積分によって求めた。吸入曝露後、経時的に殺処分し、肺洗浄細胞構成比、肺胞マクロファージ（PAM）の酸化窒素（NO）および腫瘍壊死因子（TNFα）放出活性、肺上皮細胞の DNA 合成能を調べるとともに、腫瘍を含む肺病変について病理組織学的に検討した。また全ての死亡動物は病理解剖し、死因、肺腫瘍の悪性度や組織型について病理組織学的検索を行った。

【結果および考察】吸入曝露後 1-24 ヶ月の各検査時点で、吸入曝露ラット 6-10 匹、未処置対照ラット最低 3 匹をそれぞれ殺処分した。また、一部の吸入曝露ラットは 155-804 日後に死亡したので、全て病理解剖・組織学的検索を行った。

結果は以下のようにまとめられる。

1）肺洗浄細胞数およびその中の肺胞マクロファージ（PAM）数は吸入曝露後 1-3 ヶ月で有意に減少したが、その後は未処置対照群レベルにまで回復した。

2）多核あるいは小核をもつ PAM 数は、吸入曝露後 1 ヶ月より有意に増加し、18 ヶ月までそれが持続した。

3）刺激 PAM より放出される NO および TNFα活性は、吸入曝露後 1-3 ヶ月で有意に増加したが、NO 活性は 6-18 ヶ月で減少するものの、TNFα活性は 12-18 ヶ月で再び増加した。

4）細気管支-肺胞上皮細胞の BrdU 標識率は、3-18 ヶ月まで有意に増加した。

5）病理組織学的には、吸入曝露後 1-3 ヶ月で滲出性の炎症が見られた後、細気管支肺胞上皮細胞の過形成・化成が 3-6 ヶ月でみられ、腺腫及び腺癌病変が 12 ヶ月で観察された。

6）原発腫瘍は、大部分腺腫・腺癌で、吸入曝露後12ヶ月で1-2 Gyに達したときにみとめられる。

【発表原著論文】 103)

3.1.3 酸化プルトニウム吸入曝露ラット肺腫瘍における分子レベルの変化

【目的】酸化プルトニウム吸入曝露後、発生肺腫瘍において最も起こりうるがん抑制遺伝子 *Tp53* の突然変異の有無を明らかにし、併せて肺腫瘍の起源となる上皮細胞を同定する目的で、以下の実験を行った。

【方法】雌Wistarラット（80-150日齢）を用い、水酸化物を1,150 ℃で高温焼結した酸化物多分散エアロゾル（空気動力学的放射能中央径AMAD：0.3-0.4mm、標準偏差GSD:1.9-2.2）を1回、鼻部吸入曝露した。吸入曝露後7日目に麻酔下でNaIシンチレーターにて17 keVの特性X線を全身計測し、各個体の初期沈着量を推定し、蓄積肺線量は、吸入曝露時から死亡時までの吸収線量を初期沈着量と減衰曲線の積分によって求めた。発生した肺腫瘍の組織標本を用いて、核内p53タンパクの免疫組織染色により、また抽出DNAのPCR-SSCP法およびシーケンサーによる *Tp53* 変異を検討するとともに、II型肺胞上皮細胞特異的なサーファクタント（SP-A）あるいはClara細胞特異的な抗原（CC-10）それぞれに対する抗体を用いた免疫組織染色により、肺腫瘍の起源となる細胞の同定を行った。

【結果および考察】核内p53タンパクの免疫組織学的検索には305例、*Tp53* 突然変異の検索には104例、起源となる細胞の免疫組織学的検索には146例の肺腫瘍をそれぞれ用いた。

結果は以下のようにまとめられる。

1）ラットp53タンパクに対する抗体（CM1）の陽性率はきわめて低く、9例（2.9%）が強陽性、48例（15.7%）が弱陽性、248例（81.3%）が陰性であった。

2）DNAが抽出できた98例中、13例（13.3%）のみがG to AまたはC to Tの置換型点突然変異を有していたが、これと肺腫瘍組織型との関連はみとめられなかった。

3）腺腫（75%）および腺癌（82%）の大部分がSP-A抗原陽性であり、腺腫（79%）お

よび腺癌（47%）がCC-10陽性であったことから、これらの肺腫瘍はいずれもII型肺胞上皮細胞あるいはClara細胞由来であることが明らかにされた。しかし、腺扁平上皮癌あるいは扁平上皮癌はこれらの抗原が陰性であった。

【発表原著論文】 88), 101), 117), 125)

3.1.4 X線照射ラットにおける肺腫瘍の線量効果と発生機構

【目的】全身あるいは胸部X線照射により誘発される肺腫瘍の線量効果と発生機構を明らかにし、酸化プルトニウム吸入曝露による肺腫瘍との比較を行う目的で、以下の実験を行った。

【方法】X線発生装置（Pantak HF320S、Shimadzu；管電圧200 kVp、管電流6-20 mA、照射野—線源間距離75-100 cm、0.5 mm Cuおよび0.5 mm Alフィルター使用）を用い、塩酸バルビタール麻酔下で雌Wistarラット（100-150日齢）の全身分割照射または胸部1回照射をそれぞれ行った。全身照射は、0.1 Gy/minの線量率で、2-3日毎0.5 Gy宛分割により、総線量0.5-10 Gyに達するまで行った。胸部照射は、胸部以外の体幹部・四肢・頭部を5 mm厚の鉛板でシールドし、0.6 Gy/minの線量率で、総線量1.0-10 Gyに達するまで行った。照射中、熱蛍光線量計（AE-1321型、Applied Engineering Inc.）に連結させたイオンチェンバー（0.6 ml C-110）により、線量測定を行い、この平均値を肺吸収線量とした。全ての個体は死亡後病理解剖し、死因および肺腫瘍の病理組織学的検索を行った。また発生した肺腫瘍の組織標本を用いて、核内p53タンパクの免疫組織染色により、また抽出DNAのPCR-SSCP法およびシーケンサーによる *Tp53* 変異を検討するとともに、II型肺胞上皮細胞特異的なサーファクタント（SP-A）あるいはClara細胞特異的な抗原（CC-10）それぞれに対する抗体を用いた免疫組織染色により、肺腫瘍の起源となる細胞の同定を行った。

【結果および考察】病理組織学的検索を行った合計150匹の非照射対照動物および600匹の照射動物をそれぞれ全身照射実験群（A-F）と胸部照射実験群（G-J）とに分け、生存日数（照射終了後）と、原発肺腫瘍（良性および悪性）発生率をそれぞれ**表5**に示す。また、肺腫瘍66例を核内p53タンパクの免疫組織学的検索に、33例をTp53

変異の検索に、さらに64例を起源となる細胞の免疫組織学的検索に用いた。

表５　X線照射ラットの生存時間と肺腫瘍誘発

実験群	動物数	線量 (Gy)	生存時間* (日)	原発肺腫瘍数 (%)	
全身照射					
対照群	99	0	812±125	1 (1.0)	0 (0)
照射群1	46	0.5	780±139	0 (0)	1 (2.2)
照射群2	47	1.0	800±163	2 (4.3)	1 (2.1)
照射群3	45	2.0	767±156	3 (6.7)	0 (0)
照射群4	47	3.0	711±140	3 (6.4)	3 (6.4)
照射群5	45	5.0	698±131	2 (4.4)	3 (6.7)
照射群6	45	10.0	584±150	3 (6.7)	4 (8.9)
胸部照射					
対照群	47	0	828±167	1 (2.1)	0 (0)
照射群1	70	1.0	803±142	3 (4.3)	3 (4.3)
照射群2	85	3.0	798±128	7 (8.2)	8 (9.4)
照射群3	84	5.0	687±168	11 (13.1)	11 (13.1)
照射群4	53	10.0	577±145	13 (24.5)	8 (15.1)

*平均値±標準誤差

結果は以下のようにまとめられる。

1）総線量2.0 Gy以上の全身照射ラットおよび5.0 Gy以上の胸部照射ラットで、それぞれ有意な生存日数の減少がみとめられたが、その死因の多くは肺腫瘍以外の悪性かつ転移性固形腫瘍によるものであった。

2）大部分の肺腫瘍は、腺腫あるいは腺癌であり、いずれも総線量5.0 Gy以上の胸部照射ラットでのみ、有意に増加していた。

3）胸部照射ラットおよび酸化プルトニウム吸入曝露ラットの悪性肺腫瘍（腺癌等）の線量効果曲線を比較すると、直線部分の勾配および50％発生率に相当する線量がそれぞれ約11倍異なっていた（**図４**）。

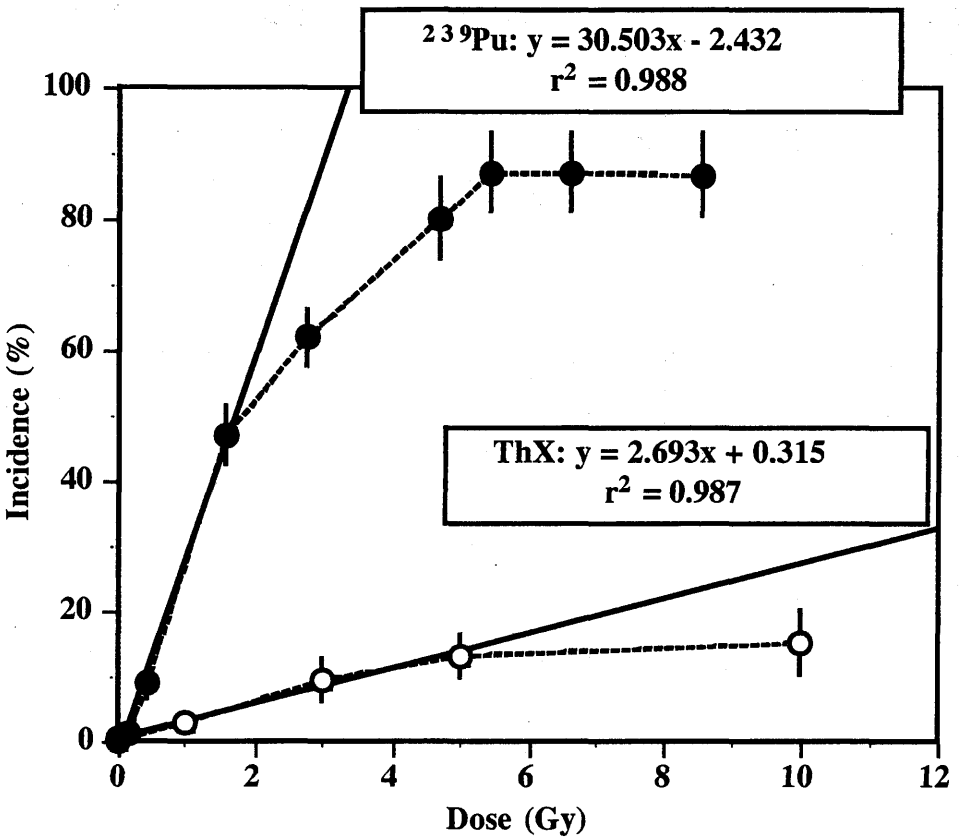

図４　酸化プルトニウム吸入曝露ラットおよびX線胸部照射ラットの肺がん発生率線量効果曲線比較

４）ラットp53タンパクに対するCM1抗体の陽性率は、きわめて低く、肺腫瘍66例中3例（4.5％）のみが弱陽性であり、肺腫瘍組織型との関連や、照射形式間での違い等はみとめられなかった。

５）DNAが抽出できた29例中、1例（3.4%）のみがC to Tの置換型点突然変異を有していた。

６）腺腫（80%）および腺癌（74%）の大部分がCC-10抗原陽性であり、腺腫（53%）および腺癌（74%）がSP-1陽性であったことから、これらの肺腫瘍はいずれもClara細胞あるいはII型肺胞上皮細胞由来であることが明らかにされた。しかし、腺扁平上皮癌あるいは扁平上皮癌はこれらの抗原が陰性であった。

【発表原著論文】 117), 122)

3.2　クエン酸プルトニウム注射投与マウスにおける発がんに関する研究

血中移行した核燃料物質プルトニウム（^{239}Pu）化合物の発がんリスクとその機構を実証的に解析評価するため、自然発生および放射線誘発腫瘍スペクトルの異なる3系統のマウスに可溶性クエン酸プルトニウムを注射投与し、生涯飼育して骨肉腫等腫瘍発生率および腫瘍誘発機構を検討するとともに、発がん剤投与あるいは低LET（線エネルギー付与）γ線を全身照射した同系マウスにおける誘発腫瘍との比較を行った。

3.2.1 クエン酸プルトニウム注射投与マウスにおける発生腫瘍スペクトル

【目的】クエン酸プルトニウムを注射投与した系統の異なるマウスにおける骨その他の腫瘍スペクトルと発生率の線量効果関係を明らかにし、生涯リスク評価に資することを目的として、以下の実験を行った。

【方法】雌C3H/HeN、C57BL/6J、およびその雑種B6C3F1マウス（70-140日齢）を用い、生理食塩水で希釈したクエン酸プルトニウム（^{239}Pu）水溶液（pH 6.8-7.2）を、1匹あたり100、500、1,000, 5,000および10,000 Bq宛それぞれ腹腔内注射し、生理食塩水のみ投与した対照群とともに生涯飼育した。全ての個体は死亡後病理解剖し、死因および発生腫瘍の病理組織学的検索を行った。別に同じクエン酸プルトニウムを1,000 Bq投与したマウスを経時的に殺処分し、灰化骨中の放射能を液体シンチレーション計測し、滞留曲線より求めた関数により死亡時までの平均骨吸収線量を計算した。

【結果および考察】予備的検討のため行ったC3H/HeNマウス（対照群100匹および投与群260匹）を用いた実験から、以下の結果が得られた。

1）骨線量2.93 Gy（投与量500 Bq）以上で、腫瘍死および非腫瘍死による生存日数の有意な減少がみられた。

2）発生腫瘍の多くは骨腫瘍（ほぼ全てが骨肉腫）で、対照群ではみられず、骨線量6.92 Gy（投与量1000 Bq）以上で96%の発生率を示した。

3）また少数ではあるが、対照群ではみられない非胸腺型でB前駆細胞型のリンパ腫が、骨線量10 Gy（投与量5,000 Bq）以上で最大36%の発生率まで増加した。

4）その他固形腫瘍は骨線量2.93 Gy（投与量500 Bq）以上では骨あるいはリンパ性腫瘍との競合によりむしろ減少し、骨髄性白血病は対照群・投与群とも全くみとめら

れなかった。

この結果をふまえ、次に3系統のマウス（対照群180匹、投与群467匹）を用いて骨腫瘍とリンパ性腫瘍等発生スペクトルの系統差について実験を行った。投与量（骨線量）により、5群に分け、それぞれ生存日数、腫瘍発生数を**表6**に示す。

表6　クエン酸プルトニウム注射投与マウスの生存時間と腫瘍誘発

実験群	動物数	投与量 (Bq)	骨線量* (Bq)	生存時間* (日)	腫瘍発生数（%）		
					骨腫瘍	リンパ性腫瘍	その他
C3H							
対照群	60	0	0	763±136	0 (0)	10 (16.7)	33 (55.0)
Pu群1	30	100	0.68±0.04	808± 81	4 (13.3)	0 (0)	11 (36.7)
Pu群2	30	500	2.71±0.35	592±105	19 (63.3)	0 (0)	3 (10.0)
Pu群3	30	1000	4.42±0.57	454± 72	14 (46.7)	0 (0)	0 (0)
Pu群4	32	5000	16.3± 2.2	314± 50	15 (46.9)	2 (6.3)	0 (0)
Pu群5	30	10000	32.2± 5.8	309± 67	8 (26.7)	3 (10.0)	0 (0)
C57BL							
対照群	60	0	0	675±183	0 (0)	20 (33.3)	11 (18.3)
Pu群1	30	100	0.63±0.06	727±100	3 (10.0)	8 (26.7)	6 (20.0)
Pu群2	31	500	2.66±0.43	580±117	7 (22.6)	8 (25.8)	2 (6.5)
Pu群3	32	1000	4.08±0.67	412± 84	16 (50.0)	2 (6.3)	0 (0)
Pu群4	31	5000	17.4± 3.5	343± 87	12 (38.7)	3 (9.7)	0 (0)
Pu群5	30	10000	41.9± 5.5	326± 68	4 (13.3)	4 (13.3)	0 (0)
BC3F1							
対照群	60	0	0	746±162	0 (0)	21 (35.0)	32 (53.3)
Pu群1	31	100	0.63±0.06	730±107	8 (25.8)	7 (22.6)	7 (22.6)
Pu群2	33	500	2.62±0.37	567±115	17 (51.5)	5 (15.2)	2 (6.1)
Pu群3	33	1000	4.38±0.50	449± 64	12 (36.4)	2 (6.1)	0 (0)
Pu群4	32	5000	15.4± 3.2	325±118	10 (31.3)	2 (6.3)	0 (0)
Pu群5	32	10000	41,5± 7.9	322± 95	11 (34.4)	4 (12.5)	0 (0)

*平均値±標準誤差

結果は以下のようにまとめられる。

1）全ての系統で500 Bq以上の投与群は、対照群に比し有意な生存日数の減少を示し、多くは骨腫瘍の早期発生によるものと考えられた。

2）全ての系統で骨腫瘍の大部分が骨肉腫で、2-3 Gyの骨線量域で、線量依存性に増加し、最大50-63%の発生率に達した。

3）リンパ性腫瘍は、5,000 Bq以上投与した全ての系統で早期に発生し、B前駆細胞型リンパ腫であることがわかった。

4）固形腫瘍は、500 Bq以上投与した全ての系統で減少しており、骨髄性白血病は、

対照・投与群すべてにみられないか、極少数しかみとめられなかった。

5）骨肉腫発生の分子機構を検討するため、解剖例の発生骨腫瘍のうち、新鮮または凍結未固定材料からのDNA抽出が可能であった11例について、*Tp53*腫瘍抑制遺伝子、*K-ras*、*H-ras*、*N-ras*それぞれの突然変異をPCR-SSCP解析により調べたところ、1例のみ*Tp53*遺伝子のエクソン7上でC to Aの転換点突然変異がみとめられた。

6）主要臓器に多様な変性、炎症等非腫瘍性病変がみられたが、対照群・実験群間に差はみられなかった。

【発表原著論文】 61), 84), 97), 120), 121)

3.2.2 クエン酸プルトニウム注射投与マウスにおける造血能

【目的】クエン酸プルトニウムを注射投与した系統の異なるマウスにおけるリンパ造血系腫瘍発生に関連する造血細胞系の変化を明らかにすることを目的として、以下の実験を行った。

【方法】雌C3H/HeN、C57BL/6J、およびその雑種B6C3F1マウス（90-110日齢）を用い、生理食塩水で希釈したクエン酸プルトニウム（^{239}Pu）水溶液（pH 6.8-7.2）を、1匹あたり5,000 Bq（急性造血系異常およびリンパ性腫瘍誘発量）宛それぞれ腹腔内注射後、生理食塩水のみ投与した対照群とともに1年間飼育し、経時的に末梢血白血球数、大腿骨骨髄および脾の有核細胞数並びに顆粒球・マクロファージコロニー形成細胞（GM-CFC）数を調べた。全ての個体はと殺ないし死亡後病理解剖し、死因および発生腫瘍の病理組織学的検索を行った。別に同じクエン酸プルトニウムを1,000 Bq投与したマウスを経時的に殺処分し、灰化骨中の放射能を液体シンチレーション計測し、滞留曲線より求めた関数により死亡時までの平均骨吸収線量を計算した。

【結果および考察】注射投与後30、90、180, 240および365日目に、プルトニウム投与マウス4匹および対照マウス2匹をそれぞれと殺して検討した結果は以下のようにまとめられる。

1）投与群の末梢血白血球数および骨髄細胞数は、全系統とも対照群に比し90日以降持続的減少がみられたが、脾細胞数は、逆に180日以降増加し、髄外造血によるも

のと考えられた。

2）投与群の骨髄 GM-CFC 数は、持続的に減少していたが、脾のそれは 90 日以降増加した。

3）造血系におけるこれらの変化は、放射線外部照射に対する応答とは異なるものであり、造血前駆細胞の持続的減少が、造血・リンパ系腫瘍の発生に影響を及ぼしているものと推察された。

【発表原著論文】 104)

3.2.3 化学発がん物質注射投与マウスにおけるリンパ腫

【目的】アルキル化化合物 N-methyl-N-nitrosourea (MNU) を注射投与した系統の異なるマウスに誘発されるリンパ性腫瘍を、クエン酸プルトニウム注射投与によるものと比較するため、以下の実験を行った。

【方法】雌 C3H/HeN、C57BL/6J、およびその雑種 B6C3F1 マウス (90-100 日齢) を用い、胸腺リンパ腫を誘導するとされる総量 5-6 mg／匹宛、MNU (40 mg/kg) を毎週 1 回計 5 回に分けて腹腔内投与後、飼育観察して、死亡後全個体の病理解剖を行い、発生するリンパ性腫瘍の組織学的および免疫組織学的検索を行った。

【結果および考察】各系統における生存日数、リンパ性腫瘍の組織型別発生数を**表 7** に示す。

表 7　MNU 注射投与マウスの生存時間とリンパ性腫瘍誘発

実験群 (系統)	動物数	生存時間* (日)	リンパ性腫瘍発生数 (%)			その他腫瘍発生数 (%)
			総数	T 芽細胞型	B 前駆細胞型	
C3H	60	106±64	20 (33.3)	18 (30.0)	2 (3.3)	11 (18.3)
C57BL	60	58±14	29 (48.3)	25 (41.7)	4 (6.7)	0 (0)
BC3F1	60	81±23	47 (78.3)	43 (71.7)	4 (6.7)	2 (3.3)

*平均値±標準誤差

結果は以下のようにまとめられる。

1）発生したリンパ性腫瘍は大部分T芽細胞型であり、全ての系統でそれぞれMNU投与後50-100日以内に出現する甚急性リンパ腫であった。

2）プルトニウム投与マウスで誘発されるB前駆細胞型リンパ腫とは、系統差も含めて出現時期、組織型等に大きな違いがあることが明らかであった。

3）その他の腫瘍発生数は少ないが、興味あることに、C3Hマウスの10例（16%）およびBC3F1マウスの2例（3%）でそれぞれ胃の扁平上皮癌がみとめられた。

【発表原著論文】 120)

3.2.4 γ線全身照射マウスにおける発生腫瘍スペクトル

【目的】低LET放射線（γ線）外部照射により誘発される腫瘍（とくにリンパ造血系腫瘍）スペクトルを、クエン酸プルトニウムおよびMNU投与によるものと比較するため、以下の実験を行った。

【方法】SPF雌C3H/HeN、C57BL/6J、およびその雑種B6C3F1マウス（85-88日齢）を用い、γ線（^{137}Cs線源；γセル）を、線量率0.6 Gy/minで、総線量1.0、2.0および3.0 Gyにそれぞれ達するまで全身照射後、生涯飼育して、死亡後全個体の病理解剖を行い、生存日数、死因、発生腫瘍等を病理組織学的に検索した。線量測定は、照射中熱蛍光線量計に連結したイオンチェンバーにより行い、平均値を吸収線量とした。

【結果および考察】各系統180匹の照射群および24匹の非照射対照群、総計612匹のマウスについて、生存日数、腫瘍（リンパ性、骨髄性、その他）発生数を**表8**に示す。

表８　γ線照射マウスの生存時間と腫瘍誘発

実験群	総線量 (Gy)	動物数	生存時間* (日)	腫瘍発生数 (%)		
				リンパ性腫瘍	骨髄性白血病	その他
C3H						
対照群	0	24	786± 72	2 (8.3)	0 (0)	4 (16.7)
照射群１	1.0	60	721± 95	2 (3.3)	0 (0)	39 (65.0)
照射群２	2.0	60	675±101	0 (0)	0 (0)	29 (48.3)
照射群３	3.0	60	591±137	0 (0)	0 (0)	36 (60.0)
C57BL						
対照群	0	24	739±137	6 (25.0)	2 (8.3)	5 (20.8)
照射群１	1.0	60	711±119	12 (20.0)	2 (3.3)	21 (35.0)
照射群２	2.0	60	702±123	13 (21.7)	2 (3.3)	17 (28.3)
照射群３	3.0	60	614±160	18 (30.0)	4 (6.7)	13 (21.7)
BC3F1						
対照群	0	24	857±149	12 (50.0)	1 (4.2)	10 (41.7)
照射群１	1.0	60	716±145	15 (25.0)	3 (5.0)	44 (73.3)
照射群２	2.0	60	659±155	18 (30.0)	2 (3.3)	50 (83.3)
照射群３	3.0	60	609±153	11 (18.3)	1 (16.7)	47 (78.3)

*平均値±標準誤差

主な結果は以下のようにまとめられる。

１）生存日数は、系統差があるが、2 Gy 以上照射群で減少する。

２）死因の多くは腫瘍死であり、非腫瘍死は少なかった。

３）発生腫瘍のうち、リンパ腫は C57BL と B6C3F1 照射マウスに多いが C3H マウスでは少ない。また線量効果に、系統差がある。

４）骨髄性白血病は少ないが、C3H マウスでは対照群・照射群とも皆無であった。

５）その他の腫瘍のうち、系統差はあるが、組織球肉腫、肝細胞癌、卵巣腫瘍（腺癌・顆粒膜細胞腫）、皮膚腫瘍（癌・線維肉腫）、肺腫瘍（腺腫・腺癌）、ハーダー腺癌等が多くみとめられた。線量効果はあるが、1 Gy 照射群の発生数が 3 Gy 照射群よりも多い傾向にある。これはリンパ腫発生との競合によるものと推察される。

６）主要臓器に多様な変性、炎症性病変等、非腫瘍性病変がみられたが、対照群との差、実験群間での違いは明らかではなかった。

5. 著書目録　(年代順：原著論文、および総説・プロシーディング)

原著論文

1990 年

1) Cheng, Y.S., Yamada, Y. and Yeh, H.C., Diffusion deposition on model fibrous filters with intermediate porosity. *Aerosol Sci. Technol.*, **12**, 286-299, (1990).

2) Cheng, Y.S., Yamada, Y., Yeh, H.C. and Su, Y.F., Size measurement of ultrafine particles (3 to 50nm) generated from electrostatic classifiers. *J. Aerosol Res. Jpn.*, **5**, 44-51 (1990).

3) Cheng, Y.S., Yamada, Y., Yeh, H.C. and Swift, D.L., Deposition of ultrafine aerosols in a human oral cast. *Aerosol Sci. Technol.*, **12**, 1075-1081, (1990).

4) Fukuda, S., Hseih, Y. and Chen, W., Toxicological study of DTPA as a drug (V). Toxicities of Ca-DTPA, Ca-EDTA and CBMIDA after intravenous injection in beagle dogs. *Hoken Buturi*, **25**, 115-119, (1990).

5) Fukuda, S. and Iida, H., Preventive effect of swimming on the reduction of bone mass in ovariectomized rats. *J. Bone Mineral. Metabolism*, **8**, 61-62, (1990).

6) Oghiso, Y., Yamada, Y. and Shibata, Y. Radiosensitivity of macrophege colony-forming cells-implications for their heterogeneity. *J. Radiat. Res.*, *31*, 324-332, (1990).

7) Takahashi, S., Kubota, Y. and Sato, H., The effect of external γ-irradiation on ^{59}Fe release in vitro from alveolar macrophages. Previously having ingested ^{59}Fe-iron hydroxide colloid. *J. Radiat. Res.*, **31**, 263-269, (1990).

1991 年

8) Fukuda, S., Iida, H., Hseih, Y. and Chen, W., Toxicological study of DTPA as drug (VI); Effects of intravenously injected Ca-DTPA, Ca-EDTA, CBMIDA and orally administered Zn-DTPA to bone metabolism in beagle dogs. *Hoken Butsuri*, **26**, 101-107, (1991).

9) Fukuda, S., Tsuchikura, S., Ikeda, K., Nara, Y., Horie, R. and Yamori, Y. Bone metabolism of SHRSP and its characteristics as a model for spontaneous osteoprosis. *Jpn. Heart. J.*, **32**, 586, (1991).

10) Ishigure, N., Nakano, T. and Enomoto, H., A device for in vitro irradiation with α-particles using an α-emitting radioactive source. *J. Radiat. Res.*, **32**, 404-416, (1991).

11) Oghiso, Y., Yamada, Y., Shibata, Y. and Yoshida, T., Maintenance of radioresistant alveolar colony-forming cells in mice bearing pulmonary foreign-body inflammation after ^{89}Sr-injection. *Regional Immunol.*, **3**, 318-322, (1991).

12) Takahashi, S., Distribution of ^{3}H in rat conceptus cultured in vitro following brief administration of [^{3}H] thymidine. *Radiat. Res.*, **128**, 59-63, (1991).

13) Takahashi, S., Kubota, Y. and Sato, H., Difference between C3H mice and Wistar rats in the effect of external γ-irradiation on ^{59}Fe release from alveolar macrophage ingested ^{59}Fe-iron hydroxide colloid. *J. Radiat. Res.*, **32**, 262-266, (1991).

14) Tsuchikura, S., Fukuda, S., Ikeda, K., Nara, Y., Horie, R. and Yamori, Y., Effect of dietary NaCl and calcium balance on bone mass in SHRSP as a model of spontaneous osteoporosis. *Jpn. Heart. J.*, **32**, 606, (1991).

15) Yamada, Y. and Koizumi, A., Simple method of size estimation of radioactive aerosols in air monitoring. *Hoken Butsuri*, **26**, 17-21, (1991).

16) 小木曽洋一, 山田裕, 柴田芳実, 吉田彪, マウス肺胞マクロファージ・コロニー形成細胞と気管内投与粒子の及ぼす影響. *日本網内系学会会誌*, **31**, 207-216, (1991).

17) 福田俊, 飯田治三, 加齢に伴う雌雄ラットの骨代謝と卵巣,精巣摘出年齢による影響の差. *日骨形態誌*, **1**, 89-94, (1991).

1992年

18) Fukuda, S. and Iida, H., Comparison of histomorphometric values in iliac trabecular bone of beagle dogs raised under different breeding systems. *Exp. Animal*, **41**, 131-137, (1992).

19) Fukuda, S., Iida, H., Hseih, Y. and Chen, W., Effects of CBMIDA [Catechol-3, 6-bis (methyleiminodiacetic acid)]on removal of plutonium in rats. *Hoken Butsuri*, **27**, 11-15, (1992).

20) Fukuda, S., Tsuchikura, S., Iida, H., Ikeda, K., Nara, Y. and Yamori, Y., Further study on osteoporosis in SHRSP : Quantitative analyses by bone histomorphometry and serum biochemical constituents related to bone. *Genetic Hypertension*, **218**, 421-423, (1992).

21) Inaba, J., Nishimura, N., Takeda, H. and Takahashi, S., Placental transfer of cerium in the rat with special reference to route of administration. *Radiat. Protect. Dosimetry*, **41**, 119-122, (1992) .

22) Ishigure, N., Nakano, T., Enomoto, H., Fukuda, S., Iida, H., Oghiso, Y., Yamada, Y. and Inaba, J., Assessment of initial alveolar deposition on rats exposed to plutonium aerosols using a whole body counter. *Hoken Butsuri*, **27**, 135-142, (1992) .

23) Kubota, Y., Sato, H. and Takahashi, S., The effect of γ-irradiation on the adherent capacity and iron metabolism of alveolar macrophages in mice and rats. *Environ. Health Perspect.*, **97**, 163-165, (1992) .

24) Oghiso, Y. and Yamada, Y., Heterogeneity of the radiosensitivity and origins of tissue macrophage colony-forming cells. *J. Radiat. Res.*, **33**, 334-341, (1992) .

25) Oghiso, Y., Yamada, Y. and Shibata, Y., Effects of instilled fibrogenic particles on the clonal growth of murine pulmonary alveolar macrophages. *Environ. Health Perspect.*, **97**, 159-161, (1992) .

26) Oghiso, Y., Yamada, Y. and Shibata, Y., Exudation of proliferative macrophages in local inflammation in the peritoneum. *J. Leukocyte Biol.*, **52**, 421-424, (1992) .

27) Takahashi, S., Kubota, Y. and Hatsuno, H., Effect of size on the movement of latex particles in the respiratory tract following local administration. *Inhalation Toxicol.*, **4**, 113-123, (1992) .

28) Takahashi, S., Sato, H., Kubota, Y. and Inaba, J., Transfer of plutonium to rat embryos in vivo and in vitro. *J. Radiat. Res.*, **33**, 301-308, (1992) .

29) Takahashi, S., Yamada, M., Kondo, T., Sato, H., Furuya, K. and Tanaka, I., Cytotoxicity of nickel oxide particles in rat alveolar macrophages cultured in vitro. *J. Toxicol. Sci.*, **17**, 243-251, (1992) .

30) Tsuchikura, S., Fukuda, S., Iida, H., Ikeda, K., Nara, Y. and Yamori, Y., Effects of antihypertensive agents on osteoporosis in SHRSP. *Genetic Hypertention*, **218**, 417-419, (1992).

31) Yamada, Y. and Koizumi, A., Particle coincidence error in pulse count mode of CNC. *J. Aerosol Res. Jpn.*, **7**, 240-244, (1992).

32) 石榑信人, 固体飛跡検出器のプルトニウム内部被曝研究への応用. *放射線*, **18**, 8-5, (1992).

33) 小泉彰, 山田裕司, 宮本勝宏, 高田雅元, 連続吸引型凝縮核カウンタ間の性能比較. *エアロゾル研究*, **7**, 2, 152-155, (1992).

34) 福田俊, 飯田治三, ビーグル犬における体重負荷が異なる部位の骨形態計測値の比較. *日骨形態誌*, **2**, 227-231, (1992).

35) 福田俊, 土倉覚, 飯田治三, 池田克巳, 奈良安雄, 堀江良一, 家森幸男, 脳卒中易発症高血圧自然発症ラットにおける加齢に伴う骨梁骨の形態変化。*日骨形態誌*, **2**, 93-98, (1992).

36) 山田裕司, 小泉彰, 宮本勝宏, 佐藤宏, 石榑信人, 仲野高志, 榎本宏子, 稲葉次郎, ネブライザで発生させた酸化プルトニウムエアロゾルの粒子性状. *保健物理*, **27**, 197-204, (1992).

1993年

37) Bulman, R.A., Sato, H., Takahashi, S. and Kubota, Y., ^{59}Fe release from alveolar macrophages by macromolecular forms of chelating agents. *J. Radiol. Protection*, **13**, 127-133, (1993).

38) Fukuda, S. and Iida, H., Histomorphometric changes in iliac trabecular bone during pregnancy and lactation in beagle dogs. *J. Vet. Med. Sci.*, **55**, 565-569, (1993).

39) Ishigure, N., Nakano, T. and Enomoto, H., Activity measurement of plutonium in solid samples by LX-ray counting with a phoswich detector. *Hoken Butsuri*, **28**, 195-201, (1993).

40) Kondo, T., Takahashi, S., Sato, H., Yamada, M., Kikuchi, T. and Furuya, K., Cytotoxicity of size-density fractionated coal fly ash in rat alveolar macrophages cultured in vitro. *Toxicol. in Vitro*, **7**, 61-67, (1993).

41) Kubota, Y., Sato, H., Koshimoto, C. and Takahashi, S., Transfer of ^{239}Pu to mouse fetoplacental tissues. *J. Radiat. Res.*, **34**, 157-163, (1993).

42) Oghiso, Y., Shao, F.-H. and Yamada, Y., Cytotoxicity of fibrogenic asbestos and silica on murine pulmonary alveolar macrophage colony-forming cells. *Inhalation Toxicol.*, **5**, 303-311, (1993).

43) Oghiso, Y., Yamada, Y., Ando, K., Ishihara, H. and Shibata, Y., Differential induction of prostaglandin E_2-dependent and -independent immune suppressor cells by tumor-derived GM-CSF and M-CSF. *J. Leukocyte Biol.*, **53**, 86-92, (1993).

44) Takahashi, S., Koshimoto, C. and Kubota, Y., Effect of γ-irradiation on the uptake and digestion of ^{125}I-labeled bovine serum albumin by rat visceral yolk sac cultured in vitro. *J. Radiat. Res.*, **34**, 171-176, (1993).

45) Takahashi, S., Kubota, Y., Sato, H. and Matsuoka, O., Retention of ^{133}Ba in the trachea of rabbits, dogs, and monkeys following local administration as $^{133}BaSO_4$ particles. *Inhalation Toxicol.*, **5**, 265-273, (1993).

46) Yamada, M., Takahashi, S., Sato, H., Kondo, T., Kikuchi, T., Furuya, K. and Tanaka, I., Solubility of nickel oxide particles in various solutions and rat alveolar macrophages. *Biol. Trace Element Res.*, **36**, 89-98, (1993).

47) 飯田治三，福田俊，ラットの加齢に伴う骨重量および含有成分量の変化. *Exp. Animal*, **42**, 349-356, (1993).

48) 小木曽洋一，肖慧娟，山田裕，肺胞マクロファージ・コロニー形成能に対する粉塵粒子の細胞毒性. *日本網内系学会誌*, **33**, 179-184, (1993).

49) 福田俊，飯田治三，骨梁骨の形態計測法による骨量とＤＸＡによる骨塩量との相関. *日骨形態誌*, **3**, 205-208, (1993).

1994年

50) Fukuda, S., Effects of active amino acid calcium : Its bioavailability on intestinal absorption, osteoporosis and removal of plutonium in animals. *J. Bone Mineral. Metabolism*, **2**, 47-51, (1994).

51) Fukuda, S., and Iida, H., Changes in histomorphometric values of iliac trabecular bone and serum biochemical constituents related to bone metabolism in beagle dogs during growth. *Exp. Animal*, **43**, 159-165, (1994).

52) Fukuda, S. and Iida, H., Effects of calcium on removal of plutonium in rats. Chelating agents in pharmacology. *Toxicology and Therapeutics*, **68**, 129-132, (1994).

53) Fukuda, S., Iida, H., Hseih, Y. and Chen, W., Removal of plutonium by CBMIDA in rats. Chelating agents in pharmacology. *Toxicology and Therapeutics*, **68**, 133-135, (1994).

54) Fukuda, S., Iida, H., Tsuchikura, S., Nara, Y., Ikeda, K. and Yamori, Y., Internal calcium abosorputionin spontaneously hypertensive rats. *Jpn. Heart J.*, **35**, 532, (1994) .

55) Fukuda, S., Tsuchikura, S., Iida, H., Ikeda, K., Nara, Y. and Yamari, Y., Intestinal calcium absorption and response of calcium regulating hormones in stroke pron spontaneously hypertensive rats(SHRSP)as a model of osteoporosis. *Clin. Exp. Pharmacol. Physiol.*, **1**, 87-88, (1994).

56) Inaba, J., Ishigure, N., Oghiso, Y. and Sato, H., Gastrointestinal absorption of americiumin rats : Effects of citrate concentration. *Radiat. Protect. Dosimetry*, **53**, 335-337, (1994) .

57) Ishigure, N., Nakano, T., Enomoto, H., Fukuda, S., Iida, H., Oghiso, Y., Sato, H., Takahashi, S., Yamada, Y., Koizumi, A., Yamada, Y., Miyamoto, K. and Inaba, J., Lung retention of Pu following inhalation of PuO_2 in rats measured using a whole body counter. *J. Radiat. Res.*, **35**, 16-25, (1994) .

58) Ishigure, N., Nakano, T., Enomoto, H. and Inaba, J., Longer lung retention of PuO_2 particles observed in rats measured using periodic in vivo counting. *Radiat. Protect. Dosimetry*, **53**, 195-198, (1994) .

59) Koshimoto, C., Takahashi, S., Kubota, Y., and Sato, H. Evaluation of the effect of gamma-irradiation on fetal erythropoiesis in rats using blood cell volume as the index. *J. Radiat. Res.*, 35, 74-82, (1994) .

60) Kubota, Y., Takahashi, S. and Sato, H., Effect of γ-irradiation on the function and viability of alveolar macrophages in mouse and rat. *Int. J. Radiat. Biol.*, **65**, 335-344, (1994) .

61) Oghiso, Y., Yamada, Y. and Iida, H., Differential induction of bone and hematopoietic tumors in C3H mice after the injection of ^{239}Pu citrate. *J. Radiat. Res.*, **35**, 236-247, (1994) .

62) Oghiso, Y. Yamada, Y., Ishigure, N., Fukuda, S., Iida, H., Yamada, Y., Sato, H., Koizumi, A. and Inaba, J., High incidence of malignant lung carcinomas in rats after inhalation of $^{239}PuO_2$ aerosol. *J. Radiat. Res.*, **35**, 222-235, (1994) .

63) Sato, H., Bulman, R.A., Takahashi, S. and Kubota, Y., Effects of macromolecular chelating agents on the release of ^{239}Pu and ^{59}Fe from rat alveolar macrophages after phagocytic uptake of ^{239}Pu- ^{59}Fe-iron hydroxide colloid. *Health Physics*, **66**, 545-549, (1994) .

64) Takahashi, S., Esaka, F., Sato, H., Kubota, Y., Kikuchi, T. and Furuya, K., Concentrations of metal elements in mouse lung after intratracheal administration of coal fly ash. *Inhalation Toxicol.*, **6**, 67-77, (1994).

65) Takahashi, S., Kubota, Y., Koshimoto, C., Sato, H. and Hatashita, S., Distribution of carbon-14 and associated radiation dose in rat fetal brain and liver after maternal injection of [^{14}C] thymidine. *Radiat. Res.*, **140**, 10-16, (1994).

66) Yamada, Y., Koizumi, A., Fukuda, S., Inaba, J., Cheng, Y.S., and Yeh, H.C., Deposition of ultrafine aerosol particles in a human tracheobronchial cast. *Hoken Butsuri*, **29**, 23-31, (1994).

67) 山田裕司, 小泉彰, 宮本勝宏, 稲葉次郎, Pu エアロゾルに対する HEPA フィルタの捕集性能. *保健物理*, **29**, 283-289, (1994).

1995 年

68) Esaka, F., Takahashi, S., Sato, H., Kubota, Y., Kikuchi, T. and Furuya, K., Concentration of metal elements in mouse organs after intratracheal administration of coal fly ash. *J. Toxicol. Sci.*, **20**, 103-108, (1995).

69) Fukuda, S., Iida, H., Hseih, Y. and Chen, W., Effects of CBMIDA and Zn-DTPA in drinking water on removal of plutonium in rats. *J. Health Physics*, **30**, 117-120, (1995).

70) Fukuda, S., Iida, H., Tsuchikura, S., Ikeda, K., Nara, Y. and Yamori, Y., Calcium regulating hormone with intestinal calcium absorption in stroke-prone spontaneously hyptertensive rat (SHRSP). *Jpn. Heart J.*, **36**, 508, (1995).

71) Fukuda, S., Tsuchikura, S., Iida, H., Ikeda, K., Nara, Y. and Yamori, Y., Intestinal calcium absorption and response of calcium regulating hormones in stroke-prone spontaneously hypertensive rat (SHRSP) as a model of osteoporosis. *Pathology and Physiology*, 240-241, (1995).

72) 石榑信人, 稲葉次郎, ＩＣＲＰ新呼吸気導モデルに基づく^{239}Ｐｕの内部被曝線量評価における粒子性状依存性. *保健物理*, **30**, 227-237, (1995).

73) 福田俊, 飯田治三, ラットにおける副甲状腺および甲状腺へのＸ線照射による後肢骨の障害. *日骨形態誌*, **5**, 47-51, (1995).

74) 福田俊, 飯田治三, 山崎一斗, 若林康夫, 食塩感受性ラット DIS/Eis(Inbred Dahl-Iwai Salt-sensitive rat)の骨形態計測学的検討. *日骨形態誌*, **5**, 135-139, (1995).

1996年
75) Ishigure, N. and Inaba, J., Analytical solution of the compartment model for respiratory tract clearance used in the new ICRP lung model. *J. Nucl. Sci. Technol.*, **33**. 179-186, (1996).

76) Sato, H., Takahashi, S., Suzuki, K., Esaka, F. and Furuya, K., Change in the concentrations of metal elements in various organs of the mouse following multiple intraperitoneal administration of Ca-DTPA. *J. Health Physics*, **31**, 41-48, (1996).

77) Yamada, Y., Koizumi, A. and Miyamoto, K., A model of aerosol penetration through fibrous filters with pinholes. *エアロゾル研究*, **11**, 35-43, (1996).

78) Yamada, Y., Park, M.S., Okinaka, R.T., Chen, D.J., Molecular analysis and comparison of radiation-induced large deletions of the *HPRT* locus in primary human skin fibroblast. *Radiat. Res.*, **145**, 481-490, (1996).

79) 石榑信人, 仲野高志, 榎本宏子, 稲葉次郎, ^{239}Ｐｕの吸入被ばくにおける線量の人体特性パラメータによる変動の試算. *保健物理*, **31**, 193-204, (1996).

80) 福田俊, 飯田治三, 重粒子線全身照射がラットの骨代謝に及ぼす影響. *日骨形態誌*, **6**, 287-291, (1996).

81) 宮本勝宏, 山田裕司, 小泉彰, 現場試験用 0.15μｍ単分散ＤＯＰエアロゾル発生装置の開発. *保健物理*, **31**, 33-39, (1996).

1997年
82) Fukuda. S., Iida, H., Yamada, Y., Koizumi, A. and Ishigure, N., Effects of DTPA therapy on removal of inhaled high-fired plutonium oxide in rats. *J. Health. Physics*, **32**, 383-386, (1997).

83) Kubota, Y., Takahashi, S. and Sato, H., Effect of a maternal injection of ^{239}Pu on the number of CFU-S in the foetal liver of the C3H and BDF1 mouse. *Int. J. Radiat. Biol.*, **72**, 71-78, (1997).

84) Oghiso, Y., Yamada, Y. and Iida, H., High frequency of leukemic lymphomas with osteosarcomas but no myeloid leukemias in C3H mice after ^{239}Pu citrate injection. *J. Radiat. Res.*, **38**, 77-86, (1997).

85) Yamada, Y., Koizumi, A. and Fukuda, S., Aerosolization of a chelating agent, Ca-DTPA, for emergent inhalation therapy. *J. Health Physics*, **32**, 167-172, (1997).

1998年
86) Fukuda, S., Iida, H., Xie, Y. and Chen, W., Effects of four CBMIDA analogues on removal of plutonium in rats. *J. Health Physics*, **33**, 331-336, (1998).

87) Ishigure, N., Enomoto, H., Nakano, T. and Inaba, J., Validity of ^{241}Am as a tracer of inhaled Pu in external chest counting. *Radiat. Protect. Dosimetry*, **79**, 133-136, (1998).

88) Oghiso, Y., Yamada, Y., Iida, H. and Inaba, J., Differential dose responses of pulmonary tumor types in the rat after inhalation of plutonium dioxide aerosols. *J. Radiat. Res.* **39**, 61-72, (1998).

89) Yamada, Y., Koizumi, A. and Inaba, J., A new casting method of human respiratory tract for aerosol deposition studies. *Radiat. Protect. Dosimetry*, **79**, 269-272, (1998).

90) Yamada, Y., Koizumi, A. and Miyamoto, K., Aerosol penetrations through filter media made of PTFE and/or glass fiber. *J. Aerosol Res. Jpn.*, **13**, 103-109, (1998).

91) 石榑信人, 仲野高志, 榎本宏子, 稲葉次郎, ICRPの内部被ばく線量評価モデルに基づく^{239}Puのモニタリング量の計算. *保健物理*, **33**, 415-423, (1998).

92) 榎本宏子, 石榑信人, 固体飛跡検出器CR-39におけるAgingとFadingの影響. *保健物理*, **33**, 407-413, (1998).

93) 小泉 彰, 山田裕司, 宮本勝宏, 下 道國, エアフィルタの目詰まりの季節変動. *エアロゾル研究*, **13**, 150-151, (1998).

1999年
94) Fukuda, S. and Iida, H., Removal of strontium by the chelating agent acetylamino propylidene diphosphonic acid in rats. *Health Physics*, **76**, 489-494, (1999).

95) Fukutsu, K., Yamada, Y., Koizumi, A. and Shimo, M., A statistical study on the design of particle count measurements. *J. Aerosol Res. Jpn.*, **14**, 55-62, (1999).

96) Ishigure, N., Calculation of retention and excretion of some selected radionuclides after acute intake by inhalation according to new ICRP dose estimation model. *J. Nucl. Sci. Technol.*, **36**, 830-838, (1999).

97) Oghiso, Y. and Yamada, Y., Carcinogenesis in mice after injection of soluble plutonium citrate. *Radiat. Res.* **152**, S27-S30 (1999).

98) Sato, H., Yamada, Y., Ishigure, N., Nakano, T., Enomoto, H., Takahashi, S., Kubota, Y. and Inaba, J., Retention, excretion and translocation of $^{239}PuO_2$ calcined at 1150 and 400℃. *J. Radiat. Res.*, **40**, 197-204, (1999).

99) Takahashi, S., Oishi, M., Takeda, E., Kubota, Y., Kikuchi, T., and Furuya, K., Physiochemical characteristics and toxicity of nickel oxide particles calcined st different temperatures. *Biol. Trace Element Res.*, **69**, 161-174, (1999).

100) Yamada, Y. Koizumi, A. and Miyamoto, K., Re-entrainment of $^{239}PuO_2$ particles captured on HEPA filter fibres. *Radiat. Protect. Dosimetry.*, **82**, 25-29, (1999).

101) Yamada, Y. and Oghiso, Y., Mutations in *Tp53* gene sequences from lung tumors in rats that inhaled plutonium dioxide. *Radiat. Res.* **152**, S107-S109 (1999).

2000年

102) Fukuda, S. and Iida, H., Effects of orchidectomy on bone metabolism in beagle dogs. *J. Vet. Med. Sci.*, **62**, 69-73, (2000).

103) Oghiso, Y. and Yamada, Y., Pathogenetic process of lung tumors induced by inhalation exposures of rats to plutonium dioxide aerosols. *Radiat. Res.* **154**, 253-260, (2000).

104) Oghiso, Y. and Yamada, Y., Strain differences in carcinogenic and hematopoietic responses of mice after injection of plutonium citrate. *Radiat. Res.*, **154**, 447-454, (2000).

105) Suzuki, K., Sekimoto, H. and Ishigure, N., Sensitivity analysis of dose coefficients for Pu-239 to transfer rates. *Radiat. Protect. Dosimetry*, **88**, 197-206, (2000).

106) Yamada, Y., Tokonami, S., Fukutsu, K. and Shimo, M., Improvement of the SDB/CNC aerosol sizing system for fast measurement at field. *Radiat. Protect. Dosimetry.*, **88**, 329-334, (2000).

2001年

107) Fukuda, S., Iida, H., Yamada, Y., Fukutsu, K. and Koizumi, A., Effective timing of initial administration of Ca-DTPA upon removal of inhaled plutonium nitrate in rats. *J. Health Physics.*, **36**, 25-30, (2001).

108) Ishigure, N., Electronic look-up tables on retention and excretion of radionuclides as a PC based support system for internal dosimetry, *Radiat. Protect. Dosimetry*, **93**, 161-165, (2001).

109) Ishigure, N. Nakano, T. and Enomoto, H., Am-241 as a metabolic tracer for inhaled plutonium nitrate in external chest counting, *Radiat. Protect. Dosimetry*, **97**, 271-273, (2001).

110) Fukuda, S. and Iida, H., DTPA treatment for removal of inhaled plutonium nitrate in rats. *Biomarkers and Environment*, **4**, 66-69, (2001).

111) Fukuda, S., Iida, H. Yamada, Y. Fukutsu, K. and Koizumi, A., Effective timing of initial administration of Ca-DTPA upon removal of inhaled plutonium nitrate in rats, *J. Health Physics*, **36**, 25-30, (2001).

112) Fukuda, S., Iida, H. Yan, X. and Xie, Y., Effects of CBMIDA on removal of uranium in rats. *Biomarkers and Environment*, **4**, 35-37, (2001).

113) Sato, H., Takahashi, S. and Kubota, Y., Effects of gadolinium on the retention and translocation of ^{239}Pu-hydroxide. *Health Physics*, **80**, 164-169, (2001).

114) Suzuki, K., Sekimoto, H. and Ishigure, N., Dependence of dose coefficients for Pu-239 on absorption parameters. *Radiat. Protect. Dosimetry*, **93**, 267-269, (2001).

115) 小泉彰、福田俊、山田裕司、飯田治三, 下道國, 緊急医療処置としてのＣａ－ＤＴＰＡの吸入投与法. *保健物理*, **36**, 45-50, (2001).

2002年

116) Fukuda, S. Yan, X. and Iida, H., Effects of human dose of Ca-DTPA on removal of plutonium in rats. *保健物理*., **37**, 158-161, (2002).

117) Oghiso, Y. and Yamada, Y., Immunohistochemical studay on cellular origins of rat lung tumors induced by inhalation exposures exposures to plutonium dioxide aerosols as compared to those by X-ray irradiation. *J. Radiat. Res.*, **43**, 301-311, (2002).

118) Yamada, Y., Oghiso, Y., Enomoto, Y. and Ishigure, N., Induction of micronuclei in a rat alveolar epithelial cell line by alpha particle irradiation. *Radiat. Protect. Dosimetry*, **99**, 219-221, (2002).

2003年
119) Fukuda, S., Iida, H., Yan, X., Xie, Y., Burgda, R. and Bailly, T., Efficacies of three chelating agents on removal of plutonium in rats: Comparison of CBIDA, 3,4,3-LIHOPO and Ca-DTPA. *保健物理*, **38**, 62-67, (2003).

120) Oghiso, Y. and Yamada, Y., Pre-B-cell lympholmas in mice following injection of ^{239}Pu Citrate: Comparison with MNU-induced T-lynphoblastic lymphomas , *J. Toxicol. Pathol.*, **16**, 93-102, (2003).

121) Oghiso, Y. and Yamada, Y., The specific induction of osteosarcomas in different mouse strains after injections of ^{239}Pu citrate, *J. Radiat. Res.*, **44**, 125-132, (2003).

122) Oghiso, Y. and Yamada, Y., Comparisons of pulmonary carcinogenesis in rats following inhalation exposure to pultonium dioxide or X-ray irradiation. *J. Radiat. Res.*, **44**, 261-270, (2003).

2004年
123) Fukuda, S., Iida, H., Yan, S. and Xie, Y., Effects of long-term orally administered Zn-DTPA and CBMIDA on plutonium-induced cancers and shortening of life span in rats., *Biomarkers and Environments*, **5**, 14-16, (2004).

124) Fukuda, S., Iida, H., Burgda, R. and Bailly, T., Effects of DTPP, CAP, LIHOPO and DTPA on removal of plutonium in rats. *Biomarkers and Environment*, **5**, 21-22, (2004).

125) Yamada, Y., Oghiso, Y., Morlier, J.-P., Guillet, K., Fritsch, P., Dudoignon, N. and Monchaux, G., Comparative study on *Tp53* gene mutations in lung tumors from rats exposed to ^{239}Pu, ^{237}Np and ^{222}Rn. *J. Radiat. Res.*, **45**, 69-76 (2004).

総説・プロシーディング

1989年

126) 福田俊, キレート剤DTPAの毒性研究. *放射線科学*, **32**, 73-78, (1989).

127) 福田俊, キレート剤DTPAの毒性研究. *放射線科学*, **32**, 115-118, (1989).

128) 福田俊, キレート剤DTPAの毒性評価. *保健物理*, **24**, 201-210, (1989).

1990年

129) 稲葉次郎, 年齢依存線量係数（Ⅰ）. *原案協だより*、 **117**, 7-10, (1990).

130) 稲葉次郎, 粒子状物質の吸入とその生物作用の発現機構. *放射線科学*, **33**, 123-126, (1990).

131) 福田　俊, 現状における除去剤の使用上の問題点と改善策の提案. *放射線科学*, **33**, 387-388, (1990).

132) 福田　俊, 飯田治三, ビーグル犬の成長に伴う骨代謝の変化. *骨の代謝と形態*, 86-91, 西村書店, (1990).

133) 山田裕司 ,エアロゾルを捉える　ー空気の濾過ー. *放射線科学*, **33**, 283-286, (1990).

1991年

134) 稲葉次郎, 内部被曝による線量当量の算定. *ISOTOPE NEWS*, **443**, 51-61 (1991)

135) 山田裕司, エアロゾルを観るー超微粒子計測ー.　*放射線科学*, **34**, 91—95, (1991).

1992年

136) Inaba, J., Takahashi, S., Sato, H., Ishigure, N., Nakano, T., Enomoto, H., Oghiso, Y., Fukuda, S., Yamada, Y., Iida, H., Koizumi, A., Yamada, Y. and Miyamoto, K., Biokinetics and biological effects of inhaled plutonium in rat. *Proc. Int. Conf. Radiat. Effects and Protection,* 247-249 (1992).

137) 稲葉次郎,　公衆のための体内被曝線量係数. *日本原子力学会誌*, **34**, 401-404, (1992).

1993年
138) Inaba, J., Fukuda, S., Takahashi, S., Sato, H., Kubota, Y., Ishigure, N., Nakano, T., Enomoto, H., Oghiso, Y., Yamada, Y., Iida, H., Koizumi, A., Yamada, Y. and Miyamoto, K., Plutonium inhalation toxicology studies in National Institute of Radiological Sciences. *Proc. Workshop Radiol. Biology Med. Protect.*, 146-152 (1993).

139) 石榑信人, 体内被曝線量評価コード専門研究会, 体内被ばく線量評価コード開発の現状, 4,3 LUDEP (Lung Dose Evaluation Program), *保健物理*, **28**, 72-74, (1993).

140) 小木曽洋一, マクロファージコロニー形成細胞の起源と放射線感受性. *医学のあゆみ*, **167**, 600, (1993).

141) 福田 俊, 実験動物における形態計測法とその応用ーラットおよびイヌの骨代謝の年齢変化を中心にー *骨代謝学会誌*, **11**, 194-198, (1993).

1994年
142) 稲葉次郎, プルトニウムの安全性の基礎 VI人体での観察. *日本原子力学会誌*, **36**, 1010-1012, (1994).

143) 小木曽洋一, プルトニウムの安全性の基礎 Vプルトニウムの生物影響(動物実験とそのリスク). *日本原子力学会誌*, **36**, 1006-1009, (1994).

144) 小木曽洋一, 放射性粒子吸入による生態影響 プルトニウム微粒子の発癌性. *エアロゾル研究*, **9**, 221-226, (1994).

145) 高橋千太郎, プルトニウムの安全性の基礎 Ⅳプルトニウムの生体内挙動と線量評価. *日本原子力学会誌*, **36**, 1003-1006, (1994).

146) 福田俊, 小泉彰, 放射性核種の生体内挙動と除去(4)プルトニウム. *放射線科学*, **37**, 7-9, (1994).

147) 福田俊, 小泉彰, 放射性核種の生体内挙動と除去(8). 鎖体の生成による放射性核種の除去、合成キレート剤によるプルトニウムの除去. *放射線科学*, **37**, 181-184, (1994).

1995年
148) 石榑信人, ICRP Publication 66 新呼吸気道モデル 概要と解説 *(日本保健物理学会 ICRP 新呼吸気道モデル専門研究会)*, 111-121, (1995).

149) 仲野高志, ICRP Publication 66 新呼吸気道モデル 概要と解説 (*日本保健物理学会 ICRP 新呼吸気道モデル専門研究会)*, 87-92, (1995).

150) 福田俊, NIRS ビーグル犬—1　体重と骨量. *放射線科学*, **38**, 312-313, (1995).

151) 福田俊, NIRS ビーグル犬—2　血液中テストステロンの変動. *放射線科学*, **38**, 368-369, (1995).

152) 福田俊, NIRS ビーグル犬－3　中年からの胸痛—助軟骨バンブー. *放射線科学*, **38**, 417-418, (1995).

153) 福田俊, NIRS ビーグル犬－4 黎明のドラマ. *放射線科学*, **38**, 464-465, (1995).

154) 山田裕司, エアロゾルを制する. *放射線科学*, **38**, 179-184, (1995).

155) 山田裕司, エアロゾルを操る. *放射線科学*, **38**, 419-423, (1995).

156) 山田裕司, プルトニウムエアロゾルーその性状と空気汚染管理. 空気清浄, **33**, 172-177, (1995).

1996 年

157) Ishigure, N., Nakano, T., Enomoto, H., Sato, H. and Inaba, J., Does initial lung burden affect the alveolar lung clearance of inhaled $^{239}PuO_2$. *Proc. Int. Cong. Radiat. Protect. (IRPA 9)*, Vol. 2, 470-472, (1996).

158) Fukuda, S., Iida, H., Yamada, Y., Koizumi, A., Sato, H., Ishigure, N., Nakano, T. and Enomoto, H., Chelating agent, DTPA, can not remove effectively inhaled-plutonium oxide in rats. *Proc. Int. Cong. Radiat. Protect. (IRPA 9)*, Vo. 2, 460-462, (1996).

159) Fukuda, S., Iida, H., Xie, Y. and Chen, W., Effects of new chelating agent, CBMIDA and its analogues, on removal of plutonium in rats. *Proc. Int. Cong. Radiat. Protect. (IRPA 9)*, Vo. 2 463-464, (1996).

160) 石榑信人, 新呼吸気道モデル. *放医研シンポジウムシリーズ* **No. 26**, 133-142, (1996).

161) 仲野高志, ＩＣＲＰの内部被ばく線量評価モデル. *放医研シンポジウムシリーズ* **No. 26**, 127-132, (1996).

162) 福田俊, NIRS ビーグル犬—5　妊娠哺乳期間の母犬のカルシウム代謝—骨肉の献身. *放射線科学*, **39**, 106-107, (1996).

1997年
163) 山田裕, アルファ線誘発突然変異の研究. *放射線科学*, **40**, 275-280, (1997).

1998年
164) Yamada, Y., Okinaka, R. T. and Chen, D. J., Molecular analysis of radiation-induced mutation in the HPRT of normal human skin fibroblasts. *Comparative Evaluation of Environmental Toxicants, Supplement* (ISBN 4-9389874-05-8), 173-180, (1998).

165) 石榑信人, 仲野高志, 榎本宏子:《特集:放医研におけるプルトニウムの生物影響評価研究》 5. 生物学的安全性評価研究におけるプルトニウムの線量評価, *保健物理*, **33**, 302-307, (1998).

166) 小木曽洋一, 山田裕, 飯田治三, 福津久美子, 福田 俊:《特集:放医研におけるプルトニウムの生物影響評価研究》 6. アルファ放射体内部被曝生物影響研究. *保健物理*, **33**, 308-313, (1998).

167) 小泉 彰, 福田 俊,《特集:放医研におけるプルトニウムの生物影響評価研究》2. プルトニウム動物実験施設の設計と管理経験. *保健物理*, **33**, 286-293, (1998).

168) 佐藤宏, 高橋千太郎, 久保田善久,《特集:放医研におけるプルトニウムの生物影響評価研究》4. プルトニウムの体内動態. *保健物理*, **33**, 298-301, (1998).

169) 下 道國,《特集:放医研におけるプルトニウムの生物影響評価研究》 1. プルトニウムの生物影響評価研究の目指すもの — 概要 —. *保健物理*, **33**, 283-285, (1998).

170) 福田 俊, 飯田治三:《特集:放医研におけるプルトニウムの生物影響評価研究》7. プルトニウム影響のリスク低減化に関する研究. *保健物理*, **33**, 314-320, (1998).

171) 山田裕司, 宮本勝宏, 小泉 彰,《特集:放医研におけるプルトニウムの生物影響評価研究》3. プルトニウムの吸入投与実験. *保健物理*, **33**, 294-297, (1998).

1999年
172) Oghiso, Y., Differential dose responses of pulmonary tumors in rats after inhalation of insoluble plutonium dioxide aerosols. *Indoor Radon Exposure and Its Health Consequences* (ISBN 4-906464-10-6), 155-161, (1999).

173) Oghiso, Y. and Yamada, Y., Lifespan animal studies on carcinogenesis following plutonium-exposures. *Proceedings of International Symposium on Biological effects of Low Dose Radiation* (ISBN 4-9980604-2-2), 80-86, (1999).

174) Yamada, Y. and Oghiso, Y., Mutagenesis in internal exposure of plutonium. *Proceedings of International Symposium on Biological effects of Low Dose Radiation* (ISBN 4-9980604-2-2), 87-92, (1999).

175) 小木曽洋一, 放射線の生体影響とその修飾—実験発がんを中心として— プルトニウムによる実験的内部被ばく発がん. *放射線科学*, **42**, 145-151, (1999).

176)久保田善久、高橋千太郎, 放射線の生体影響とその修飾—実験発がんを中心として— プルトニウムの胎児移行と造血障害. *放射線科学*, **42**, 152-161, (1999).

2000年

177) Akahane, K., Kai, M., and Oghiso, Y., Risk analysis of fatal and incidental lung tumors in Wistar rats after inhalation of plutonium dioxide. *Proc. Int. Cong. Radiat. Protect. (IRPA 10)*, P-2a-104, (2000).

178) Enomoto, H. and Ishigure, N., Change in the sensitivity of CR-39 for alpha-tracks after the storage at different temperatures. *Proc. Int. Cong. Radiat. Protect. (IRPA 10)*, P-1a-17, (2000).

179) Fukuda, S, Iida, H., Yamada, Y., Fukutsu, K. and Koizumi, A., Effects of early administration times of injected Ca-DTPA on removal of inhaled plutonium nitrate in rats. *Proc. Int. Cong. Radiat. Protect. (IRPA 10)*, P-2a-92, (2000).

180) Fukuda, S., Iida, H., Akahane, K., Ban, N. and Kai, M., Long term effects of injected plutonium-nitrate in rats. *Proc. Int. Cong. Radiat. Protect. (IRPA 10)*, P-2b-93, (2000).

181) Ishigure, N., Am-241 as a metabolic tracer for inhaled Pu nitrate in external chest counting. *Proc. Int. Cong. Radiat. Protect. (IRPA 10)*, P-3a-152, (2000).

182) Ishigure, N., Nakano, T. and Enomoto, H., Data file on retention and excretion of inhaled radionuclides calculated using ICRP dosimetric models. *Proc. Int. Cong. Radiat. Protect. (IRPA 10)*, P-3a-121, (2000).

183) Koizumi, A, Fukutus, S., Yamada, Y., Iida, H., Dosage of DTPA administration by inhalation. *Proc. Int. Cong. Radiat. Protect. (IRPA 10)*, P-3a-190, (2000).

184) Nakano, T. and Ishigure, N., Computer of Pu LX-rays generated in lung using various voxel size models. *Proc. Int. Cong. Radiat. Protect. (IRPA 10)*, P-3a-124, (2000).

185) Suzuki, K., Sekimoto, H. and Ishigure, N., Dependence of dose coefficients for Pu-239 on transfer rates and absorption parameters. *Proc. Int. Cong. Radiat. Protect. (IRPA 10)*, P-3a-122, (2000).

2001年
186) 小泉彰、福田俊、山田裕司、飯田治三、下道國, 緊急医療装置としてのCa-DTPAの吸入投与法. *保健物理*, **36**, 45-50, (2001).

2003年
187) Yamada, Y., Oghiso, Y., Nakamura, S., Morlier, J.-P., Guillet, K., Fritsch, P., Dudoignon, N. and Monchaux, G., Comparison of p53 mutations in radiation-induced rat lung tumors. *Molecular mechanisms for radiation-induced cellular response and cancer development* (ISBN 4-9980604-5-7), 131-135, (2003).

2004年
188) Ishigure, N., Matsumoto, M., Nakano, T. and Enomoto, H., Development of software for supporting internal dose estimation. *Proc. Int. Cong. Radiat. Protect. (IRPA 11)*, 3a16, (2004).

5. 報告書目録 （年次報告書・特別研究報告書等一覧）

1) 放射線医学総合研究所年報、平成元年度(1989) NIRS-AR-33, pp64-pp67

2) 放射線医学総合研究所年報、平成２年度(1990) NIRS-AR-34, pp62-pp65

3) 放射線医学総合研究所年報、平成３年度(1991) NIRS-AR-35, pp60-pp63

4) 放射線医学総合研究所年報、平成４年度(1992) NIRS-AR-36, pp49-pp51

5) 特別研究「公衆被曝のリスク評価に関する生物学的調査研究」最終報告書
昭和６３ー平成４年度 (1988ー1992) NIRS-R-24, pp85-pp135

6) 放射線医学総合研究所年報、平成５年度(1993)
NIRS-AR-37, ISSN 0439-5948, pp48-pp50

7) 放射線医学総合研究所年報、平成６年度(1994)
NIRS-AR-38, ISSN 0439-5948, pp58-pp60

8) 放射線医学総合研究所年報、平成７年度(1995)
NIRS-AR-39, ISSN 0439-5948, pp54-pp55

9) 放射線医学総合研究所年報、平成８年度(1996)
NIRS-AR-40, ISSN 0439-5948, pp63-pp64

10) 放射線医学総合研究所年報、平成９年度(1997)
NIRS-AR-41, ISSN 0439-5948, pp75-pp77

11) 特別研究「放射線被ばくのデトリメントとその修飾に関する生物学的調査研究」
最終報告書
平成５ー９年度 (1993ー1997) NIRS-R-37, ISBN 4-938987-07-4, pp35-pp50

12) 放射線医学総合研究所年報、平成１０年度(1998)
NIRS-AR-42, ISSN 0439-5948, pp81-pp83

13) 放射線医学総合研究所年報、平成１１年度(1999)
NIRS-AR-43, ISSN 0439-5948, pp87-pp89

14) Ishigure, N., Monitoring Data for Intake of Radionuclides -Acute Intake by Inhalation-. NIRS-M-131, ISBN 4-938987-06-6, (1999).

15) 放射線医学総合研究所年報、平成１２年度(2000)
NIRS-AR-44, ISSN 0439-5948, pp78-pp80

16) 石榑信人, 松本雅紀, 仲野高志, 榎本宏子, MONDAL/MONDES －内部被ばく線量評価支援システム－. NIRS-M-142 (CD-ROM), (2000)

17) 放射線医学総合研究所年報、平成１３年度(2001)
NIRS-AR-45, ISSN 0439-5948, pp71-pp73

18) 放射線医学総合研究所年報、平成１４年度(2002)
NIRS-AR-46, ISSN 0439-5948, pp43-pp45

19) 放射線医学総合研究所年報、平成１５年度(2003)
NIRS-AR-47, ISSN 0439-5948, pp45-pp49

20) 放射線医学総合研究所年報、平成１６年度(2004)
NIRS-AR-48, ISSN 0439-5948, pp48-pp49

21) Oghiso, Y. and Yamada, Y., Pathological Archives of Life-Span Animal Studies on Carcinogenesis Following Internal Exposures to Plutonium Compounds. NIRS-M-186, ISBN-4-938987-31-7, (2006).

プルトニウム内部被ばく研究報告書

平成１８年３月刊行

放射線医学総合研究所
放射線安全研究センター
内部被ばく影響研究グループ

〒263-8555　千葉県千葉市稲毛区穴川 4-9-1

NIRS-R-53
ISBN 4-938987-32-5

プルトニウム内部被ばく研究報告書

補　　遺
研究成果資料集

平成18年９月

放射線医学総合研究所

序　文

本研究資料集は、プルトニウム内部被ばく研究報告書の補遺として、本報告書の本文中に引用されている原著論文および特別研究報告書の抜粋を取りまとめて再掲載するものである。プルトニウム内部被ばく研究全体を概観するため、また本報告書中の内容をさらに詳細に理解するために参考にしていただければ幸いである。

目次

(3) 超ウラン元素による内部被曝のリスク評価に関する調査研究

1．超ウラン元素の代謝に関する比較毒性学的研究

① 超ウラン元素の呼吸器への沈着、代謝に関する研究

高橋千太郎、久保田善久、佐藤宏、山田裕司、小木曽洋一、稲葉次郎（内部被ばく研究部）

Deposition and Metabolism of Transuranic Radionuclides in the Respiratory Tract

Sentaro Takahashi, Yoshihisa Kubota, Hiroshi Sato, Yuuji Yamada, Youichi Oghiso, and Jiro Inaba
Division of Radiotoxicology

Alveolar macrophages play important roles on the retention and metabolism of inhaled radioactive particles deposited in the lung. In the present study, a new method was developed in order to evaluate the solubility of radioactive particles having phagocytosed by alveolar macrophages. By using this newly developed method, radiosensitivity of alveolar macrophages was investigated to estimate the effect of radiation emitted by radioactive particles on the functions of alveolar macrophages. This method was demonstrated to be a simple but useful method for the evaluation of the solubility of various particles in alveolar macrophages, compensating the disadvantages of the previous particle solubility tests performed in vivo and in vitro. The experiments on the radiosensitivity of alveolar macrophages showed that the alveolar macrophages of C3H mice were much more radiosensitive than those of the several other strains of mice and rats, with respect to the induction of apoptosis (a mode of interphase cell death). This suggests that the radiosensitivity of alveolar macrophages varies among animal species and / or strains, and that it is necessary to consider the species and strain differences in the radiosensitivity of alveolar macrophages for estimating the retention and metabolism of inhaled radioactive particles.

1．緒言

放射性物質の生体内摂取に起因する内部被ばくの影響を評価するためには、1）対象とする放射性物質の生体内での挙動（沈着、滞留、代謝および排泄）を明確にし、2）これをもとに、生体の各臓器が受ける放射線の線量を計算し、3）誘発された生体影響を線量との関係から明らかにすることが必要である。

この点から、対象とする放射性物質の生体内における挙動、代謝に関する知見は、内部被ばく影響評価の基礎をなすものである。過去、種々の放射性物質を対象として、その生体内挙動、代謝に関する研究が行われてきたが、それらの研究はイオン状の放射性核種を対象としたものが多く、生体内において粒子もしくはコロイドの状態で存在するいわゆる粒子状放射性物質の生体内挙動、代謝に関しては不明な点が多い。

生体内で粒子状物質として挙動する放射性核種の代表的なものは超ウラン元素である。原子力施設での使用量が増大し、放射線防護の観点から関心のもたれているプルトニウムなどの超ウラン元素は、空気中浮遊微粒子（エアロゾル）として呼吸にともなって生体に吸入され、呼吸器に沈着するという摂取経路がもっとも主要な経路と考えられている。さらに、これらの核種では、生体の体液中においては水酸化物重合体のような粒子状で挙動することが知られている。したがって、プルトニウムなどの超ウラン元素の生体内での挙動を明らかにするには、粒子状で吸入された物質の呼吸器での挙動、代謝に関する知見と、血液やリンパに吸収された後のコロイド粒子の生体内処理に関する知見が必要となってくる。この様な外因性異物粒子の処理を担当している細胞は、マクロファージ（貪食細胞）とよばれる血液細胞の一種である。たとえば、吸入によって呼吸器に沈着した粒子は、外来性の異物を排除し生体防御に重要な役割を担っている肺胞マクロファージにすみやかに貪食される。可溶性粒子は肺胞マクロファージ内で可溶化され、血液あるいはリンパ液を介して生体の他臓器に移行し、または糞尿中に排泄されるが、不溶性粒子の場合は肺胞マクロファージに貪食されたまま長期間肺深部に滞留し、肺組織を連続的に照射することになる。すなわち、放射線防護上重要な放射性核種「超ウラン元素」の内部被ばく影響評価においては、吸入後の体内挙動、代謝に深く関わっている肺胞マクロファージの異物粒子処理能に関する生理学的特性を明らかにし、さらに貪食した粒子から放出される

放射線に対する肺胞マクロファージの反応等の粒子との相互作用に関する知見を得ることが極めて重要である。

本研究では、吸入摂取された粒子状超ウラン元素の肺胞マクロファージによる貪食および可溶化、放射性粒子状物質が放出する放射線によって生ずる肺胞マクロファージの機能的変化に関する基礎的な知見を得ることを目的として、1）粒子状物質の肺胞マクロファージによる貪食、溶解能を評価するための新手法の開発、2）肺胞マクロファージによる粒子状物質溶解能に及ぼす放射線の影響、3）肺胞マクロファージの放射線感受性の種差、系統差、および4）放射線によって誘発される肺胞マクロファージの細胞死の様態について研究を実施し、以下の成果を得た。

2．研究方法

2－1．粒子状物質の肺胞マクロファージによる貪食、細胞内消化にともなう溶解を評価するための新しい手法の開発：

ウィスター系ラットをハロセンガス麻酔下で気管切開し、微細ナイロンカニューレを、先端が気管支第1分岐部に保持される状態で気管内挿管した。麻酔から覚醒した後、^{59}Fe－水酸化鉄コロイド溶解（Priestらの方法によって作製）、あるいは^{239}Pu－水酸化プルトニウムコロイド溶液（Lindenbaumの方法によって作製）0.5 mℓを、カニューレを介して肺内に投与した。投与後1日目、3日目、7日目に動物を麻酔下で放血死させ、リン酸緩衝生理食塩水（Ca^{++}, Mg^{++} free PBS）で肺洗浄を行った。得られた肺洗浄細胞を2～3回ハンクス緩衝液で洗浄した後、3時間培養した。培養終了後、培養液を遠心分離し、上清中に放出された放射活性をオートγカウンターおよび液体シンチレーションカウンターで測定した。培養開始時の全放射能に対する上清中放射能の割合から放出率を求めた。すなわち、この場合の放出率とは、肺胞マクロファージが粒子を貪食してから1、3、7日目において、細胞内消化され、短時間（3時間）で細胞から培養液中に放出される状態まで可溶化された粒子の量を意味している。

2－2．肺胞マクロファージによる粒子状物質溶解能に及ぼす放射線の影響：

^{59}Fe－水酸化鉄コロイド粒子を1）で述べた気管支挿管法でウィスター系ラット及びC3H系マウスの肺内に投与した。C3Hマウスの場合は、ラットの1/10量、0.05 mℓを投与した。投与後24時間目に動物を放血と殺し、肺洗浄によって得られた細胞浮遊液を^{137}Cs線源（線量率12.5Gy/min）で照射した後、10％のウシ胎児血清を含むイーグルMEM培養液で培養した。2時間後、プラスチックプレート非付着細胞を培養液で洗って除去した後、さらに同じ培養液で6－70時間培養した。培養後、細胞を遠心分離し、培養上清中に放出された^{59}Fe活性をオートγカウンターで測定した。また、一部の細胞では、0.5％トリパンブルーによる生存率の測定を行った。

2－3．肺胞マクロファージの生存率に及ぼす放射線照射の影響：

i）ウィスター系、SD系、フィシャー系、ルイス系ラット、およびC3H系、BALB系、C57Black系マウスから、上記の肺洗浄法を用いて肺胞マクロファージを採取した。非照射あるいは照射後一定期間培養した後、PBSで2回洗浄し、次に0.1％のクリスタルバイオレットで15～20分間染色した。染色が完了したプレートは水道水でよく洗浄したのち、乾燥させ、さらに0.5％ドデシル硫酸ナトリウム溶液を添加して染色細胞を溶解した。この染色細胞溶解液を一定倍率で希釈した後、分光光度計（波長540nm）で吸光度を測定した。非照射肺胞マクロファージの吸光度を100とした時の照射肺胞マクロファージの吸光度をその生存率とした。

ii）トリパンブルー色素排除能：非照射および照射肺胞マクロファージを24時間培養した後、PBSで洗浄して付着細胞と非付着細胞に分けた。非付着細胞数は直接コールターカウンターで測定し、付着細胞数は、5％のザッポグロビン（コールター社）で細胞壁を溶解した後、浮遊させた細胞核数をコールターカウンターで測定することにより求めた。非付着細胞のトリパンブルー色素排除能は、血球計算盤を使用して常法通り行い、付着細胞の色素排除能は、プレートに直接トリパンブルー色素液を滴下し、倒立顕微鏡下で観察することにより算定した。

2－4．放射線によって誘発される肺胞マクロファージの細胞死の様態：

i）マウス肺胞マクロファージのコロニー形成能：肺洗浄によって採取したマウスの肺胞マクロファージをX線照射後、10％の馬血清、300ユニット／mℓのリコンビナントGM－CSFを含むイーグルαMEM培地中で、7日間培養し、50個以上の細胞からなるコロニーの数を算定した。照射肺胞マクロファージのコロニー形成率は非照射肺胞マクロファージのコロニー数を100として表現した。

ii）照射肺胞マクロファージの形態：上記の方法で採取した肺胞マクロファージをγ線照射した後、さらに6時間培養した。培養後、細胞を酢酸メタノールで固定し、ギムサ染色した。光学顕微鏡を用いて観察し、核濃縮（ピクノーシス）あるいは核のフラグメンテーションをおこしている細胞の割合を算定した。

iii）照射肺胞マクロファージから抽出したDNAのアガロースゲル電気泳動：照射肺胞マクロファージを6時間培養したのち、ラウリル硫酸ナトリウムを含む細胞溶解液で溶解し、引き続きプロテナーゼKおよびRNAaseで処理した。さらに、フェノール／クロロホルム混合液を用いてDNAの抽出を2回行った後、0.2M NaCl，70％エタノールで沈降させ、最終的にトリスーEDTA溶液に溶解した。調製されたDNAサンプルは0.5μg/mℓのエチジウムブロマイドを含む1.2％アガロースに負荷し、15時間TBE（Tris borate EDTA buffer）溶液中で電気泳動を行った。泳動終了後、紫外線照射下でポラロイドカメラで写真を撮り、DNAのフラグメンテーションの有無を観察した。

3．結果および考察：

3－1．粒子状物質の肺胞マクロファージによる貪食および溶解能を評価するための新手法の開発：

表1は、^{59}Fe－水酸化鉄コロイドあるいは^{239}Pu－水酸化プルトニウムコロイドを気管挿管法によって肺内に投与されたウィスターラットから、投与後1日目、3日目、7日目に肺洗浄を行って得た肺胞マクロファージを3時間培養し、培養上清中に放出される放射活性を培養開始時の全放射活性のパーセンテージで表現したものである。投与後1日目の肺胞マクロファージでは3時間の培養で7.8％

Table 1 Rlease of ^{239}Pu or ^{59}Fe from alveolar macrophages having ingested ^{230}Pu- or ^{59}Fe-iron hydroxide colloids.

Radionuclides	Time after loading (h)		
	24	72	168
^{239}Pu	0.6±0.4* (100)**	1.2±0.3 (210)	2.5±0.8 (434)
^{59}Fe	7.8±5.3 (100)	5.4±2.1 (69)	3.9±2.8 (50)

* Values are mean±s.d. of triplicated assays in at least two experiments, and expressed as percentage of the initial activity in macrophages at the start of *in vitro* culture.

** Values in parentheses are percentages of the release rates to those at 24 h after loading of the colloids.

の^{59}Feを放出するが、投与後3日目では5.4％、7日目では3.9％と放出率の低下が認められる。一方^{239}Pu水酸化プルトニウムコロイドの場合は1日目0.6％、3日目1.2％、7日目2.5％と放出率が上昇した。^{59}Fe－水酸化鉄コロイドと^{239}Pu－水酸化プルトニウムコロイドの間で、コロイド貪食肺胞マクロファージから放出される割合が粒子投与後の時間経過で全く逆の傾向を示す機序については明らかでないが、個々の放射性核種およびその物理、化学的形態によって、生体内で肺胞マクロファージによる可溶化、細胞外への放出割合ならびにその時間的経過が大きく異なることを本実験は示唆している。従来、呼吸器に沈着した放射性粒子状物質の肺における可溶化を調べるためには、可溶化した放射性核種が他臓器へ再沈着し、また糞尿を介して体外に排出されるなど複雑な経路があるため、連続的な糞尿採取と動物の定期的な解剖、各臓器の採取、それらのサンプルの放射活性の測定が必要であり、多大な労力、動物数およびコストを要した。一方、in vitroで、培養肺胞マクロファージによる可溶化を定量化する実験が多くの研究者によって行われてきたが、この実験系の問題点は、長期にわたって肺胞マクロファージを培養することが不可能なため、長くても1週間程度の期間に限られること、また培養期間を延長すればするほど培養肺胞マクロファージの形態、機能が本来肺胞マクロファージが生体内で有しているものと異なってしまう可能性があることである。そのため、肺胞マクロファージの培養期間を延長できたとしても、それを使用した粒子状物質の可溶化試験の結果が、生体内での肺胞マクロファージによる粒子の可溶化及びその時間的変動を正確に反映するとは言い難いものであった。我々が考案した実験系でも肺から採取して培養することにより、肺胞マクロファージの生体内での本来の性質が変化する可能性を完全には否定できない。しかしながら、わずか3時間の培養であること、また図1の結果で、水酸化コロイドの溶解率が、コロイド投与後の時間経過によって変化する事実は、その時点での肺胞マクロファージの生体内における特性を正確に反映していることを示唆している。もし、肺胞マクロファージが、均一な培養条件によってその性質が固定化されるのならば、水酸化コロイドの投与後の時間経過によって肺胞マクロファージからの放出率の変動は認められないはずである。以上のことから、本実験系は、in vivoおよびin vitroの実験系の短所を補完し、肺胞マクロファージによる放射性粒子状物質の可溶化およびその時間的変動を比較的容易にスクリーニングしうる優れた方法であると思われる。

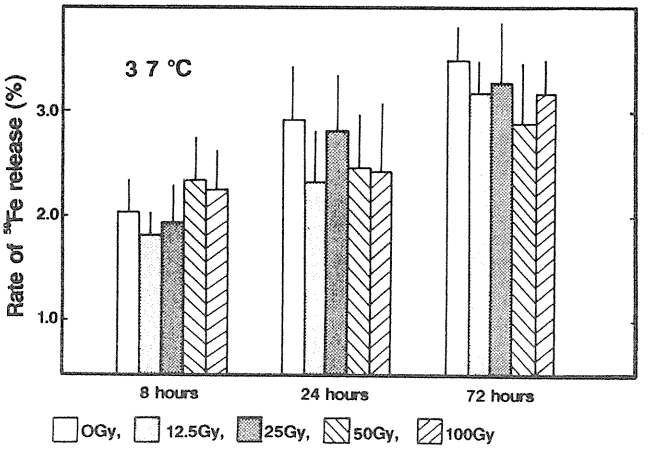

図1 The rate of ^{59}Fe release from AM which were loaded with ^{59}Fe-iron hydroxide colloid. Cell culture was carried out for 8-72 hrs after γ-irradiation at 37℃. Values are expressed as percentages of initial activity of ^{59}Fe in AM, and the vertical bar in each column shows the standard deviation.

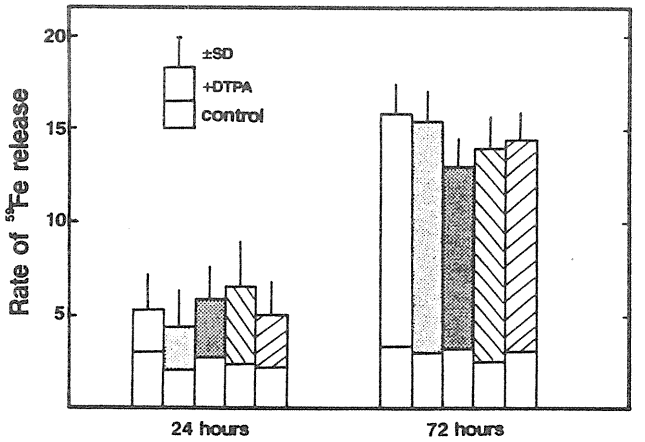

図2 The rate of ^{59}Fe release, expressed as percentages of initial activity of ^{59}Fe in AM, in AM cultured with 10 mM Ca-DTPA for 24 and 72 hrs after irradiation. The total length of each column denotes the ^{59}Fe release in AM cultured with Ca-DTPA and that of the blank column shows the release in control AM which were incubated in normal medium without Ca-DTPA.

3－2．肺胞マクロファージによる粒子状物質溶解能に及ぼす放射線の影響：

粒子状物質が吸入され、呼吸器に沈着すると粒子状物質の代謝に重要な役割を担っている肺胞マクロファージに貪食されるが、貪食された粒子が放射性粒子の場合、自身が放出する放射線によって肺胞マクロファージが機能的に変化し、非放射性粒子状物質と異なる挙動・代謝を示す可能

表2　Effect of γirradiation on ^{59}Fe release from AMs that had ingested ^{59}Fe-iron hydroxide colloid*1)

Animal	Time after irradiation (hr)	Radiation dose (Gy) 0	12.5	25	50	100
Mice	24	2.2±0.1*2)	2.9±0.3	4.3±0.6	16.8±3.9	23.4±4.9
	72	3.1±0.2	3.4±0.2	6.6±0.4	22.0±2.4	32.9±5.2
Rats	24	2.8±0.5	2.3±0.5	2.8±0.5	2.5±0.5	2.9±0.6
	72	3.2±0.3	3.4±0.3	3.3±0.6	2.9±0.6	3.8±0.3

*1) The rate of ^{59}Fe release is expressed as the percentage of the initial ^{59}Fe activity in AMs at the start of culture.
*2) Values are means ±s.d. of 6 to 9 culture dishes from 3 experiments.

表3　Effect of γirradiation on AM survival rate of C3H mice and Wistar rats*1)

Animal	Time after irradiation (hr)	Radiation dose (Gy) 12.5	25	50	100
Mice	24	76.2±15.8*2)	60.9±17.2	23.5±12.1	5.9± 6.0
	72	55.0±10.9	37.1±18.4	11.2±13.0	1.6± 1.5
Rats	24	101.1± 9.4	98.6±18.9	93.9±21.1	92.9±10.5
	72	78.6± 9.5	73.2±12.2	71.5±14.8	73.3±10.6

*1) The survival rate is defined as the ratio (%) of the optical density of crystal violet in the irradiated group to that in the non-irradiated controls.
*2) Values are means ±s.d. of 6 to 9 culture dishes from 3 experiments.

性がある。しかしながら、肺胞マクロファージの放射線に対する反応性、特に細胞内消化などの機能に対する放射線の影響についてはほとんど知られていない。そこで、^{59}Fe－水酸化鉄コロイドを気管内投与したウィスターラットから採取した肺胞マクロファージの^{59}Fe放出能に及ぼす放射線の影響を調べた（図1）。培養時間が8時間から72時間に長くなるにしたがい肺胞マクロファージから培養液中に放出される^{59}Feは増加したが、いずれの培養時間においても100Gyまでのγ線照射は^{59}Feの放出に全く影響を及ぼさなかった。肺胞マクロファージによって貪食された水酸化鉄コロイドは、ライソゾーム内に入りライソゾーム酵素によって加水分解され、鉄イオンとして細胞質内に移行し、さらに細胞内外の鉄イオン濃度差による受動的なトランスポートによって細胞外に放出されることが知られている。100Gyまでのγ線照射が、ラット肺胞マクロファージからの^{59}Feの放出に全く影響しないという事実は水酸化鉄コロイドの可溶化から鉄イオンの細胞膜透過までの過程がすべて非常に放射線抵抗性である可能性あるいは各過程が放射線によって影響をうけても、エンドポイントとしての^{59}Feの放出量は変化しない様に各過程が相互に補完している可能性を提起する。図2は培養液中に^{59}Feのキレート効果を有するカルシウム－DTPA10mM添加した実験の結果である。^{59}Feの肺胞マクロファージからの放出率はキレート剤によって顕著に増加し、特に培養72時間目で顕著であったが、100Gyまでのγ線照射を行っても、^{59}Feの放出率は非照射群と比較して有意な差を生じなかった。培地中にCa-DTPAを添加した場合細胞外に存在する鉄イオンはすみやかにCa-DTPAにキレーティングされるために、鉄イオンの細胞内外濃度平衡化のための細胞膜における受動的トランスポートは、一方的に鉄イオンの細胞外への放出を生じ、^{59}Feの肺胞マクロファージからの放出がこう進する状態にある。この様な状態においても、γ線照射の影響が認められないことから、γ線照射が、細胞のライソゾーム中での水酸化鉄コロイドの可溶化を促進又は抑制している可能性は考えにくい。そこでウィスターラットの肺胞マクロファージによる^{59}Fe－水酸化鉄コロイドの可溶化、細胞外放出の過程は極めて放射線抵抗性であると結論された。同様の実験をC3Hマウスの肺胞マクロファージを使用して行い、ウィスターラット肺胞マクロファージの結果と比較したのが表2である。非照射の肺胞マクロファージからの^{59}Feの放出量は、培養24時間で、ウィスターラット2.8％、C3Hマウス2.2％であり、培養72時間になると^{59}Fe放出率は両者共増加するがほぼ同レベルであった。ウィスターラットの肺胞マクロファージからの^{59}Fe放出は、100Gyまでのγ線照射によって全く影響を受けなかったのに対し、C3Hマウスの肺胞マクロファージからのFe放出は、線量依存性に増加した。この結果から、C3Hマウスの肺胞マクロファージはγ線照射によって細胞死、特に細胞膜の障害を誘発されやすく、細胞死によって貪食した^{59}Fe－水酸化鉄コロイドが漏出した可能性あるいは水酸化鉄コロイドのライソゾーム酵素による加水分解、それに続く^{59}Feの細胞外への放出という一連の過程のいずれかがγ線照射によってこう進した可能性が考えられた。そこでこれらの可能性を検討するために肺胞マクロファージの生存率に及ぼす放射線の影響を調べた（表3）。クリスタルバイオレットによる細胞の生体染色は、機能的に生存している細胞のみがこの色素を細胞内に取り込むことから、細胞の生存率を調べる簡単な方法として使用されてきた。本法によって肺胞マクロファージの生存率を評価した時、照射後24時間目で、ウィスターラットの肺胞マクロファージは100Gy照射されても92.9％の生存率を示すが、C3Hマウスの肺胞マクロファージでは5.9％と極端に減少していた。また72時間ではウィスターラットの100Gy照射された肺胞マクロファージの生存率は非照射コントロールの約70％であり、一方、C3Hマウスの肺胞マクロファージの生存率は、25Gyで37.1％、50Gyで11.2％、100Gyで1.6％と線量依存性に顕著に減少することが分かった。この結果は、C3Hマウスの肺胞マクロファージはウィスターラットの肺胞マクロファージと比べて放射線によって細胞死（膜障害）を生じ易いことを明確に示した。表2と表3を比較すると肺胞マクロファージに対する放射線の影響は、^{59}Fe－水酸化鉄コロイドを貪食した肺胞マクロファージからの^{59}Feの放出率より、クリスタルバイオレットによる細胞生存率試験の方が感度良く検出できることが分かる。例えばC3Hマウスの肺胞マクロファージを12.5Gy照射し72時間培養した時、クリスタルバイオレットによる細胞生存率は非照射コントロールの55％に低下するのに対し、^{59}Feの放出率は非照射コントロールと比べて有意な差が認められない。この傾向はウィスターラットの肺胞マクロファージにおいても、また使用したすべての線量で認められた。放射線によって重篤な膜障害を生じ、クリスタルバイオレットを取り込むことができなくなった肺胞マクロファージでも、照射以前に細胞内に取り込んだ水酸化鉄コロイドを放出せずに細胞内に蓄積し続けることが考えられるし、また^{59}Fe－水酸化鉄コロイド粒子が死滅した細胞から放出されても、まだ生残している肺胞マクロファージに再度取り込まれる可能性もある。いずれにせよ、この結果から^{59}Fe－水酸化鉄コロイドを貪食したC3Hマウスの肺胞マクロファージからの^{59}Feの放出に及ぼす放射線の影響は一義的に放射線による肺胞マクロファージの細胞死の誘発によって説明できる。

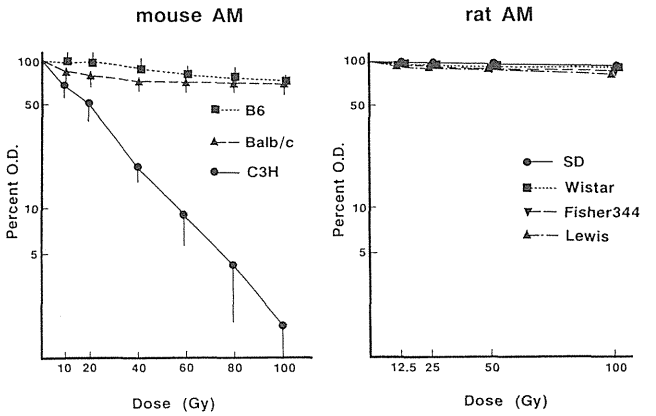

図3　The effect of γ− irradiation on the viability of mouse and rat alveolar macrophages determined by vital staining with crystal violet. Vertical bars indicate standard deviation of the means. There was no significant difference among rat alveolar macrophages of 4 strains at each dose-point.

表4　The viability of mouse and rat AM 24hrs after irradiation

Strain/ Species	Dose (Gy)	Percentage of initial cell number[a]		
		Adherent fraction[b]	Nonadherent fraction[c]	Total cell viability[f]
Wistar rat	0	89.3±4.7[d](98.7±0.8)[e]	9.7±1.4 (85.9±3.3)	95.9±4.5
	50	86.6±5.7 (96.1±5.7)	8.6±1.5 (80.2±4.6)	90.1±4.8
	100	80.3±7.6 (95.2±5.5)	12.9±2.5 (81.9±6.6)	87.2±5.7
SD rat	0	45.5±4.8 (97.1±5.3)	50.6±5.1 (93.4±5.8)	91.3±0.9
	50	46.5±6.3 (95.2±1.1)	48.7±2.9 (89.6±3.8)	87.8±5.5
	100	50.3±6.7 (94.7±1.5)	41.5±3.7 (95.6±1.2)	87.4±5.6
Fisher rat	0	66.5±6.7 (95.1±4.3)	31.9±3.2 (92.4±1.5)	92.9±4.6
	50	65.3±9.3 (98.4±5.7)	28.6±3.7 (89.7±7.2)	90.5±5.9
	100	56.2±5.8 (96.2±6.8)	35.4±6.8 (91.2±5.4)	86.4±5.7
Lewis rat	0	59.5±4.1 (97.9±6.1)	38.5±4.7 (87.9±7.2)	92.1±4.5
	50	65.5±8.3 (98.6±8.8)	33.2±7.2 (88.3±6.7)	93.4±8.5
	100	53.9±6.1 (97.6±7.4)	42.9±7.9 (86.4±9.9)	88.7±8.1
B6 mouse	0	74.6±9.4 (97.7±6.3)	24.2±5.2 (64.2±7.9)	89.0±9.7
	50	77.1±8.9 (86.2±3.4)	21.9±8.5 (55.8±6.6)	79.1±9.0
	100	66.2±7.5 (88.7±7.6)	18.4±3.6 (51.3±5.1)	68.2±8.1
C3H mouse	0	97.7±8.3 (99.3±2.6)	2.9±0.4 (77.6±3.9)	99.4±5.5
	50	48.0±5.2 (44.4±4.5)	26.7±6.2 (14.1±2.1)	25.1±3.6
	100	24.6±2.0 (13.1±3.1)	30.9±3.8 (5.2±3.0)	4.7±0.7
Balb mouse	0	89.1±5.2 (98.3±4.1)	8.9±1.1 (75.0±4.3)	93.5±5.3
	50	85.0±5.4 (89.5±5.0)	12.3±2.1 (57.3±4.0)	83.0±5.2
	100	82.2±3.5 (84.4±4.4)	12.0±1.5 (50.8±1.9)	75.6±3.1

[a] Initial cell number was that of AM adherent to dishes after 2hr of culture and was taken as 100%.
[b] Adherent fraction: AM still adherent to dishes after washing with PBS after 24hr in culture. The cell number in the adherent fraction was expressed as a percentage of the initial cell number.
[c] Nonadherent fraction: AM washed out with PBS after 24hr in culture and the cell number in the nonadherent fraction was expressed as a percentage of the initial cell number.
[d] The values are means of percent cell numbers and the standard deviations of the means in three separate experiments.
[e] The values in parentheses are the percent cell viabilities determined by trypan blue exclusion.
[f] Total cell viability expressed as a percentage of the initial cell number, was calculated from the percent cell number and the percent cell viability of both adherent and nonadherent fractions.

3－3．肺胞マクロファージの放射線感受性の種差、系統差および放射線によって誘発される肺胞マクロファージの細胞死の様態：

肺胞マクロファージの生存率に及ぼす放射線の影響がC3Hマウスとウィスターラットで異なることが明らかになったので、他の系統のマウスおよびラットの肺胞マクロファージについてもその放射線感受性を検討した（図3および表4）。図3はクリスタルバイオレットの生体染色による測定時においてプレートに付着している肺胞マクロファージの生存率を非照射コントロールを100％として表したものである。使用した4系統のラット、すなわち、ウィスター系、フィッシャー系、ルイス系およびSD系のラットの肺胞マクロファージはすべて放射線抵抗性であり、100Gyのγ線を照射されても、照射後24時間で非照射コントロールの90％以上の生存率を維持していた。またC57BlackおよびBalb系マウスの肺胞マクロファージも比較的放射線抵抗性であり、100Gyの照射でコントロールの70－80％の生存率であった。一方、調べたマウス、ラットの系統の中で、唯一C3Hマウスの肺胞マクロファージが顕著な放射線感受性を示し、100Gyの照射で生存率は非照射群の1－2％に低下していた。表4では測定時（照射後24時間）にプレート付着肺胞マクロファージと非付着マクロファージに分け、それぞれの細胞数とトリパンブルー色素排除能試験による生存率から全生存細胞数を計算し、培養開始時の生存細胞数に対するパーセンテージで表現した（表中のtotal cell viability）。その結果はクリスタルバイオレットの生体染色によるプレート付着肺胞マクロファージの生存率試験の結果と非常に良く一致した。すなわち4系統のラットの肺胞マクロファージおよびC57Black 、Balb系マウスの肺胞マクロファージは放射線抵抗性であるのに対し、C3Hマウスの肺胞マクロファージのみが特異的に顕著な放射線感受性を示した。インターロイキン－3やGM-CSF 、M-CSFなどのマクロファージを増殖させる因子を添加しない通常の培養条件下においては、肺胞マクロファージは全く増殖しないことが知られている。したがって、クリスタルバイオレットの生体染色およびトリパンブルー色素排除能試験によって明らかにされたC3Hマウスの肺胞マクロファージの放射線照射による生存率の低下は間期死（interphase cell death）によるものと考えられた。細胞の間期死には形態的にまた生化学的に全く異なる2つの様式すなわちネクローシスとアプトーシスが存在する。一般にネクローシスは細胞に激しい障害を与えることによって生じ、一方アプトーシスは生理的条件や非常にマイルドな刺激によって誘発されると言われている。放射線が胸腺細胞や腸管のクリプト細胞に比較的低線量で顕著なアプトーシスを誘発することはよく知られた事実である。アプトーシスは形態的には細胞核の濃縮、核の断片化、アプトーティックボディの出現等の特徴によって、また生化学的にはDNAのアガロースゲル電気泳動によって明らかにされるヌクレオゾームを単位とするDNAの断片化を指標として定義されてきた。C3Hマウスの肺胞マクロファージが放射線によって顕著な間期死を生ずることが明らかになったので、この間期死がいずれの様式によるものかを検討した。図4は50Gy照射後6時間目のC3Hマウスの肺胞マクロファージの光学顕微鏡写真である。濃縮して小さくなった細胞核や断片化した核が多くの肺胞マクロファージで認められる。また、図5は50Gy照射後6時間目の肺胞マクロファージから抽出したDNAのアガロースゲル電気泳動像である。50Gy照射されたC3Hマウスの肺胞マクロファージのみに顕著なDNAの梯子状の断片化が見られる。これらの結果から放射線照射によって誘発されるC3Hマウスの肺胞マクロファージの間期死はアプトーシスであると断定される。またデータには示さないが、アプトーシスにおいてDNAの

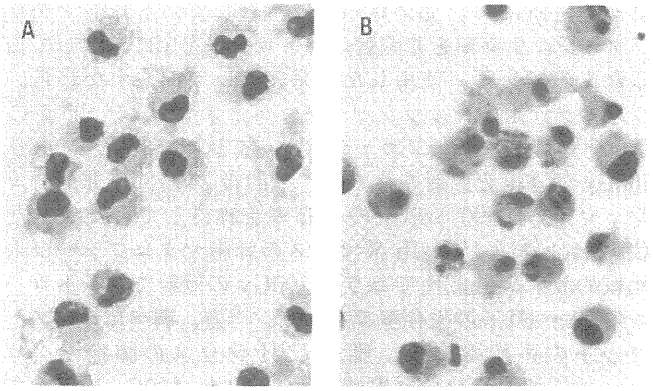

図4　Light microscopic photographs of C3H mouse alveolar macrophages 6hr after γ-irradiation. A, non-irradiated; B, 50Gy irradiated.

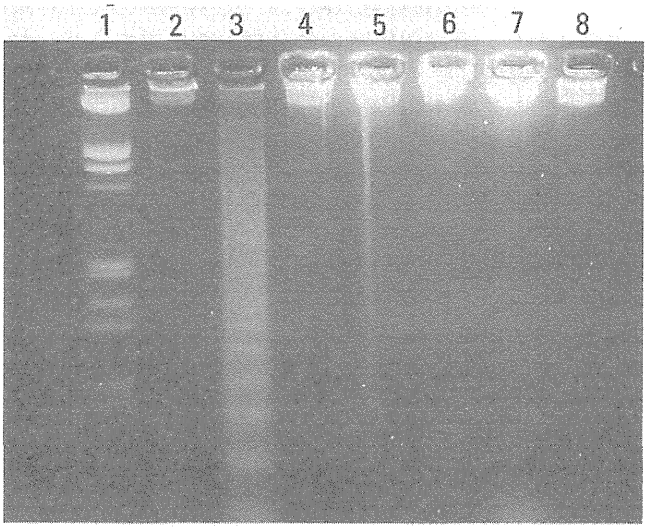

図5　DNA fragmentation of irradiated C3H mouse alveolar macro phages (AM). Lane 1, molecular size markers, Hind Ⅲ and Eco RI digests of lambda phage DNA; lane 2, non-irradiated C3H mouse AM; lane 3, 50Gy irradiated C3H mouse AM; lane 4, non-irradiated C57Black mouse AM; lane 5, 50Gy irradiated C57Black mouse AM; lane 8, C3H mouse AM treated with 0.33mM $ZnSO_4$ immediately after irradiation with 50Gy.

断片化に関与しているCa、Mg依存性DNAエンドヌクレアーゼの活性を阻害すると考えられている亜鉛イオンの照射直後の添加によってC3Hマウスの肺胞マクロファージの照射による細胞死は完全に抑制された。

放射線による肺胞マクロファージの間期死誘発にマウス、ラットの系統によって差があるので、放射線による増殖死（reproductive or proliferative cell death）にも系統差が存在するのか否かを調べた。ラットの肺胞マクロファージのコロニー形成能試験は、リコンビナントのインターロイキン－3、GM-CSF、M-CSFや優れたコンディションドメディウムが入手できないので行えず、マウスリコンビナントGM-CSFを使用してC3H、C57Black、Balb系マウスの肺胞マクロファージでコロニー形成能に及ぼす放射線の影響を調べた（図6）。平均のクローニング効率は3系統のマウスとも同レベルで約10％であった。肺胞

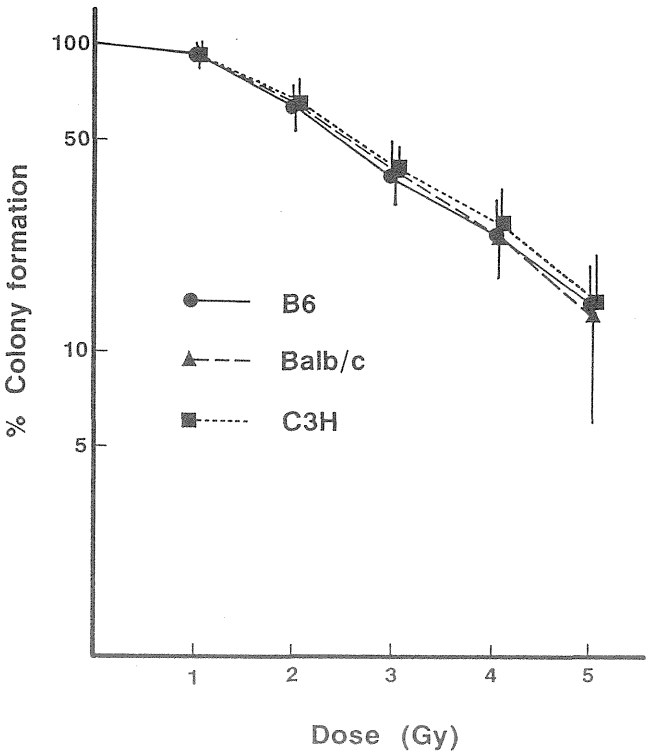

図6　The effect of X-irradiation on the colony forming ability of alveolar macrophages from 3 strains of mice. Vertical bars indicate the standard deviations of the means.

マクロファージのコロニー形成能の放射線感受性は図6に示すように比較的大きな肩をもつ直線になったが、3系統のマウスの間で全く差は認められなかった。マウスの肺胞マクロファージの放射線感受性に関して、増殖死では系統差が認められないのになぜ間期死の1様式であるアプトーシスの誘発ではC3Hマウスの肺胞マクロファージが特異的に高感受性なのだろうか。現在この問題に対する明確な答えはない。放射線による細胞の増殖死誘発の主たる原因は修復しえないDNAの2重鎖切断であることが培養株化細胞を使用して明らかにされてきている。マウスの肺胞マクロファージの放射線による増殖死も修復不能なDNAの2重鎖切断に依存していると考えれば図6の結果から3系統のマウスの肺胞マクロファージでは照射によって同レベルのDNA鎖切断が生じているはずである。放射線による肺胞マクロファージのアプトーシス誘発もDNA鎖切断に依存しているのならば、増殖死を誘発する線量（～5 Gy）に対してアプトーシスを誘発する線量（数10 Gy）によって生ずるDNA鎖切断の質や量にマウス系統差が存在するのかもしれない。また増殖因子存在下でコロニーを形成しえる肺胞マクロファージは全細胞の10％であり、他の肺胞マクロファージは増殖能を失い、より成熟した細胞と考えられるため、10％のコロニー形成可能な肺胞マクロファージの放射線感受性が3系統のマウス間で同一であっても肺胞マクロファージ全体としてアプトーシス誘発に関する放射線感受性が異なることも考えられる。さらに放射線によるDNA鎖切断の質や量が同じであっても最終的にアプトーシスを誘発するまでの細胞内で生ずる生化学的反応（例えば放射線によって胸腺細胞に誘導され、胸腺細胞のアプトーシスに必須であることが証明されている

p53 蛋白）に系統差が認められるかもしれない。一方、放射線照射によってC3Hマウスの肺胞マクロファージに顕著に誘発されるアプトーシスはDNA鎖切断に関係していない可能性もある。これらの可能性を検討することは今後の課題であるが、パルスフィールド電気泳動等を駆使した放射線による肺胞マクロファージのDNA鎖切断の定量化が解明の手がかりになると思われ、現在検討をすすめている。

4．結論

吸入によって呼吸器に沈着した放射線粒子状物質の生体内挙動、代謝に肺胞マクロファージが重要な役割を担っていることが知られている。本研究では肺胞マクロファージによって貪食された放射性粒子状物質の溶解性を評価するための新手法の開発および放射性粒子状物質の放出する放射線が肺胞マクロファージの機能に及ぼす影響を評価するために、数系統のマウス、ラットの肺胞マクロファージの放射線感受性に関して検討を行った。放射性粒子状物質の肺胞マクロファージによる溶解性を評価するために新しく開発された方法は、粒子の投与をin vivoで行い、その後の溶解性の評価をin vitroで行うものである。この方法は、今までに行われてきたin vivoおよびin vitroの粒子溶解性試験のそれぞれの短所を補完し、粒子状物質の呼吸器における溶解性を容易にスクリーニングすることを可能にする方法であり、今後、放射性物質を含め種々の粒子状物質の溶解性試験に広く利用できるものと期待される。

肺胞マクロファージの放射線感受性を調べた実験においては、検討した数系統のマウス、ラットのなかで、C3Hマウスの肺胞マクロファージが特異的に放射線感受性で、他の動物の肺胞マクロファージと比較して、放射線照射により間期死の一様式であるアプトーシスを生じ易いことが証明された。この結果は動物の種、系統によって肺胞マクロファージの放射線感受性がそれぞれ異なることを示唆しており、実際吸入によって肺に沈着した放射性粒子状物質の生体内挙動、代謝を評価する際には、肺胞マクロファージの放射線感受性の相違を考慮する必要のあることを示している。

［研究発表］

1） Kubota, Y., Sato, H. and Takahashi, S. : The effect of γ-irradiation on the function and viability of alveolar macrophages of mice and rats. Int. J. Radiat. Biol. 65, 335-344, 1994.

2） Takahashi, S., Esaka, F., Sato, K., Kikuchi, T., and Furuya, K. : Concentrations of metal elements in mouse lung after intratracheal administration of coal fly ash. Inhalation Toxicol., 6, 67-77, 1994.

3） Takahashi, S., Sato, H., Kubota, Y. and Matsuoka, O. : Retention of $^{133}BaSO_4$ in the trachea of rabbits, dogs, and monkeys following local administration as $^{133}BaSO_4$ particles. Inhalation Toxicol., 5, 265-272, 1993.

4） Kondo, T., Takahashi, S., Sato, H., Yamada, M., Kikuchi, T. and Furuya, K. : Cytotoxicity of size-density fractionated coal fly ash in rat alveolar macrophages cultured in vitro. Toxicol. In Vitro, 7, 61-67, 1993.

5） Yamada, M., Takahashi, S., Sato, H., Kondo, T., Kikuchi, T., Furuya, K. and Tanaka, I.: Solubility of nickel oxide particles in various solutions and rat alveolar macrophages. Biological Trace Element Research, 36,189-98, 1993.

6） Bulman, R. A., Sato, H., Takahashi, S. and Kubota, Y. : ^{59}Fe release from alveolar macrophages by macromolecular forms of chelating agents. J. Radiol. Prot., 13, 127-133, 1993.

7） 高橋千太郎、「呼吸器における大気中微粒子の挙動とその生体影響」、志賀健ら編「環境と健康」、HBJ出版、東京、1992.

8） Takahashi, S., Yamada, M., Kondo, T., Sato, H., Furuya, K. and Tanaka, I. : Cytotoxicity of nickel oxide particles in rat alveolar macrophages cultured in vitro. J. Toxicol. Sci., 17, 243-251, 1992.

9） Takahashi, S., Kubota, Y., and Sato, H. : Effect of size on the movement of latex particles in the respiratory tract following local administration. Inhalation Toxicol. 4, 113-123, 1992.

10） Kubota, Y., Sato, H. and Takahashi, S. : The effect of γ-irradiation on the adherent capacity and iron metabolism of alveolar macrophages in mice and rats. Environ. Health Perspect., 97, 163-165, 1992.

11） 高橋千太郎、生体における環境中微粒子の溶解性の評価、in vivoからin vitroまで。環境科学シンポジウム報文集、pp.178-179, 1991.

12） Takahashi, S., Kubota, Y. and Sato, H. : Difference between C3H mice and Wistar rats in ^{59}Fe release from alveolar macrophage ingested as colloidal form. J. Radiat. Res. 32, 262-269, 1991.

13） Takahashi, S. and Sato, H. : A new method to estimate the solubility of radioactive particles in the respiratory tract : Comparison of solubility between ^{59}Fe and ^{239}Pu-hydroxide colloid particles. Hoken Butsuri, 26, 351-353, 1991.

14） 高橋千太郎：「吸入粒子の呼吸器内挙動と代謝」、松岡ら編「粒子状物質の吸入とその生物作用の発現機構」、NIRS-M-78、実業公報社、1990.

15） Takahashi, S., Kubota, Y. and Sato, H. : The effect of external γ-irradiation on ^{59}Fe release in vitro from alveolar macrophages previously having ingested ^{59}Fe-iron hydroxide colloid. J. Radiat. Res., 31, 263-269, 1990.

16） Takahashi, S., Moriguchi, K. Kubota, Y. Sato, H. and Matsuoka, O.: The Deposition pattern of insoluble particles with different sizes in the rat trachea. Hoken Butsuri., 24, 19-24, 1989.

17） Kubota, Y., Takahashi, S., Sato,H. and Matsuoka, O.: Pulmonary deposition and clearance of inhaled or instilled ^{198}Au-colloid in the rat after the induction of pulmonary delayed type hypersensitivity reactions. Hoken Butsuri, 23, 295-302, 1988.

18) 高橋千太郎、久保田善久、佐藤宏：$^{133}BaSO_4$粒子のウサギ、イヌ、及びサル気管壁への沈着、第27回日本保健物理学会口頭発表、1992.5.（秋田）.

20) 高橋千太郎、久保田善久、佐藤宏：水酸化プルトニウムおよび水酸化鉄コロイドのラット肺胞マクロファージによる可溶化、第26回日本保健物理学会口頭発表、1991.5.（東京）.

21) 高橋千太郎、久保田善久、佐藤宏：呼吸気道に沈着した不溶性粒子の上行性クリアランスおよびリンパ節への移行における粒子径の影響、環境科学会1990年会口頭発表、1990.11.（東京）.

22) 高橋千太郎、久保田善久、佐藤宏：^{59}Fe－コロイド鉄貪食ラットマクロファージの鉄代謝に及ぼすγ線の影響、第32回日本放射線影響学会口頭発表、1989.9.（北九州）.

23) 高橋千太郎、久保田善久、佐藤宏：気道に沈着した不溶性粒子の上行性クリアランスにおよぼす粒子径の影響、第24回日本保健物理学会口頭発表、1989.5.（仙台）.

24) 高橋千太郎、久保田善久、佐藤宏：げっ歯類の気管壁への微細粒子の沈着と滞留、第23回日本保健物理学会、1988.5.（千葉）.

25) 佐藤宏、高橋千太郎、久保田善久：^{59}Fe－水酸化コロイドを気管に投与したラットに対するCa-DTPAの吸入の効果、第27回日本保健物理学会口頭発表、1992.5.（東京）.

26) 佐藤宏、高橋千太郎、久保田善久：酸化プルトニウム吸入ラットにおけるプルトニウムの糞尿中排泄、第26回日本保健物理学会口頭発表、1991.5.（大阪）.

27) 佐藤宏、高橋千太郎、久保田善久：培養肺マクロファージによる金属粒子の可溶化におよぼすキレート剤の効果、第26回日本保健物理学会口頭発表、1991.5.（大阪）.

28) 久保田善久、佐藤宏、高橋千太郎：マクロファージの腫瘍障害能に及ぼすγ線照射の影響、第32回日本放射線影響学会口頭発表、1988.10.（北九州）.

29) 久保田善久、佐藤宏、高橋千太郎：呼吸気道に沈着した径の異なるラテックス粒子の領域リンパ節への移行量、第24回日本保健物理学会口頭発表、1989.5.（名古屋）.

30) 佐藤宏、久保田善久、高橋千太郎：^{239}Pu・^{59}Fe－水酸化コロイドを取り込んだラット肺マクロファージからの^{239}Puおよび^{59}Fe放出に対するキレート剤の効果、第24回日本保健物理学会口頭発表、1989.5.（名古屋）.

1．超ウラン元素の代謝に関する比較毒性学的研究
②放射性エアロゾル粒子の肺沈着モデルに関する研究

山田裕司、久保田善久、高橋千太郎、福田俊、飯田治三、
小泉彰、宮本勝宏、稲葉次郎、（内部被ばく研究部）

Studies on Lung Deposition Model of Radioactive Aerosols

Yuji Yamada, Yoshihisa Kubota, Sentaro Takahashi, Satoshi Fukuda, Haruzo Iida,
Akira Koizumi, Katsuhiro Miyamoto and Jiro Inaba
Division of Radiotoxicology

In this study, we tried to develop a system for plutonium aerosol exposure and to clear aerosol deposition mechanism in a respiratory tract.

Our exposure system was specially designed for inhalation study of plutonium oxide, $^{239}PuO_2$, and two systems were developed for small rodents and dogs, respectively. Twenty rats or mice are exposed simultaneously in a nose-only exposure chamber, and for dog exposure a rubber death mask is used. Plutonium oxide aerosols were obtained by nebulizing of plutonium hydrate solution and calcinating the droplets in a high temperature furnace. Particle size of the generated aerosols was proportional to a cubic root of the plutonium concentration of the nebulizing solution. When the concentration was in the order of 10^6 Bq/cm³, AMAD(Activity Median Aerodynamic Diameter)was 0.4-0.5 μm and σ_g was approximately 2.0.

The activity size distribution was almost the same as the mass size distribution. It means that the specific activity of the plutonium aerosols is independent of the particle size. The ratio of americium to plutonium in aerosol particle, ^{241}Am / ^{239}Pu, was also found to be independent the particle size from the radiation analysis. And from electron microscopy the aerosols were observed to be spherical and non-coagulated particles.

Total depositions in human nasal and tracheobronchial casts were measured for ultrafine monodisperse aerosols below 0.2 μm in diameter. At 20 ℓ/min of constant flow, inspiratory nasal deposition efficiency reached approximately 40 % for 0.005μm. The efficiency increased with decreasing particle size and respiratory flow rate. Expiratory deposition was slightly higher than for inspiratory deposition. Inspiratory and expiratory deposition efficiencies were expressed as functions of the particle diffusion coefficient and respiratory flow rate derived from the turbulent diffusion theory for simple straight tube. Tracheobronchial deposition also increased with decreasing particle size and respiratory flow rate.

Deposition efficiencies under cyclic flow were found to be almost the same as those under constant flow having equivalent mean flow rate. It was also observed that varying the tidal volume, but keeping the minute volume constant (i.e., having the same mean flow rate), has little effect on deposition of ultrafine aerosols.

［はじめに］

放射性エアロゾルの呼吸気道内沈着様式を調べるためには、生体における粒子沈着解明のための実験動物を用いたin vivo実験と沈着機構解明のための気道模型を用いた工学実験という両方向のアプローチが必要である。このため本研究課題では、つぎの２つのテーマ、A：放射性エアロゾル吸入実験装置の開発、B：呼吸気道模擬キャストを用いたエアロゾル沈着様式の解明、に分けて実験的研究を実施した。

A：放射性エアロゾル吸入実験装置の開発

I　緒言

プルトニウムなどのアルファ放射体を取り扱う施設においては、吸入摂取による内部被曝影響が大きな問題である。吸入摂取の場合、吸入エアロゾルの化学形、粒度分布、粒子形状などの粒子性状が呼吸気道沈着部位、沈着率からの初期排泄、さらには、その後の生体影響に大きく作用する。つまり、吸入による生体影響を評価するためには、吸入摂取した放射能量のみならず粒子性状を知ることがこれに劣らず重要である。

本研究課題では、酸化プルトニウムエアロゾル吸入に係わる代謝・影響研究に必要な曝露動物を供給するための吸入実験装置の開発を行うとともに、吸入エアロゾルの性状

を明らかにするための諸計測を実施した。

Ⅱ　研究方法

吸入実験装置は、ラット・マウスなどの小動物用とイヌを対象とした中型動物用の２基を開発した。プルトニウムエアロゾルの吸入投与を可能とするため、運転制御部を除く装置本体は全てグローブボックスと呼ばれる密閉容器内に設置した。曝露方式としては、小動物用装置には20匹同時の鼻部曝露方式、中型動物用には１頭単独の頭部マスク曝露方式を採用した。エアロゾル発生方法など曝露方式以外の部分については、２基の吸入実験装置は基本的に同一である。Fig. 1には中型動物用の吸入実験装置の概略を、Photo. 1には曝露中のビーグル犬を示す。酸化プルトニウムエアロゾルの作成は、以下の方法で行った。硝酸塩の形の保存原液をエアロゾル化直前に水酸化物に転換した上で発生原液とした。これをシリンジポンプで一定量ずつネブライザに送り、ミスト化した。この水酸化プルトニウムミストを、300 ℃のプレヒータおよび1150 ℃の高温ヒータに通し２段階加熱を行うことにより、気相にて酸化プルトニウムエアロゾルを得た。

発生させた酸化プルトニウムエアロゾルの空気中放射能濃度、粒度分布、粒子形状などを調べるために用いた方法をつぎに示す。空気中放射能濃度測定については、エアロゾル発生実験中の濃度変動を監視するための光散乱方式のフォトメータを除いては、エアフィルタサンプリングを基本的とした。粒度分布測定にはカスケードインパクタを利用したが、ここでは、特に、QCM（Quartz Crystal Microbalance）型と呼ばれるインパクタを採用し、実時間で重量濃度データも得た。これにより粒子径別の濃度変動情報ばかりではなく、比放射能に関する情報も得ることができた。粒子状であることの確認およびその形状については走査型電子顕微鏡による観察の他、乾板法によるミクロレベル、イメージインテンシファイアによるマクロレベルのアルファ線飛跡観察などを実施した。

Ⅲ　結果および考察

開発した２基の吸入実験装置は基本的に同型であるので、発生エアロゾルの粒子性状については小動物用装置のデータを中心に示す。10^5～10^6 Bq／cm³のプルトニウム発生原液を用いた場合、吸入チャンバ部における空気中放射能濃度はおよそ0.1～1 Bq／cm³となり、最大１時間この濃度を持続することが可能であった。このときの発生原液使用量に対する吸入可能なエアロゾル量、つまり、有効エアロゾル化率は0.3～0.5 %であった。ただし、ここには再利用する発生廃液（補：廃液回収率＝90～95 %）の分が含まれていないので、この点を考慮すると実質的な有効エアロゾル化率は10 %近くに達する。

プルトニウムエアロゾルの粒度分布は、例えば、10^6 Bq／cm³のプルトニウム発生原液を用いた場合、空気力学的放射能中央径AMAD（Activity Median Aerodynamic Diameter）が0.4～0.5 μm、幾何標準偏差 σ_g（Geometric Standard Deviation）が～2.0であった。ただし、AMADは発生原液中のプルトニウム濃度に依存し、原液濃度が例えば10倍濃くなると粒子径は約$\sqrt{10}$≒2.2倍というように増大した。つぎに、粒度分布を放射能基準で評価した場合と重量基準で評価した場合とを比較してみると、Fig. 2に示すように、両者の分布曲線はかなりの部分で重なり、エアロゾルの比放射能が粒子径に依らず一定であることが示された。また、プルトニウムエアロゾルに不純物として混入しているアメリシウムの割合を粒子径別に求めたところ、Am／Pu比は0.04前後でほぼ一定であることも示された。これらの結果から、発生させたプルトニウムアエロゾルはほぼ均質な粒子であることが示唆された。

プルトニウムエアロゾルが粒子状であることの確認はつぎのようにして行った。捕集放射能が約400Bqのフィルタサンプルに対して、まず、そのマクロの捕集沈着面分布をアルファイメージングシステムで観察した。イメージインテンシファイアを通してアルファ線によるスポット像を

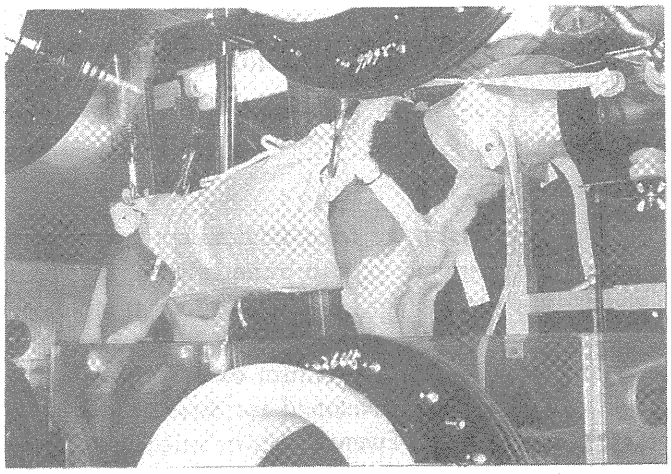

Photo.1 Beagle dog exposed to plutonium aerosols.

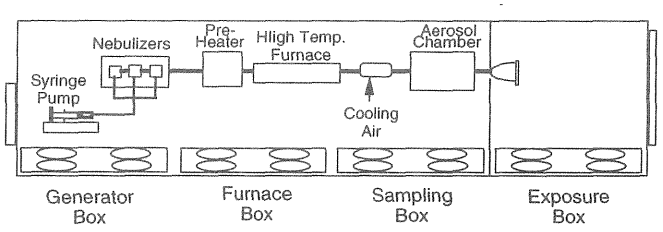

Fig.1 Schematic diagram of a radioactive aerosol exposure system for dogs.

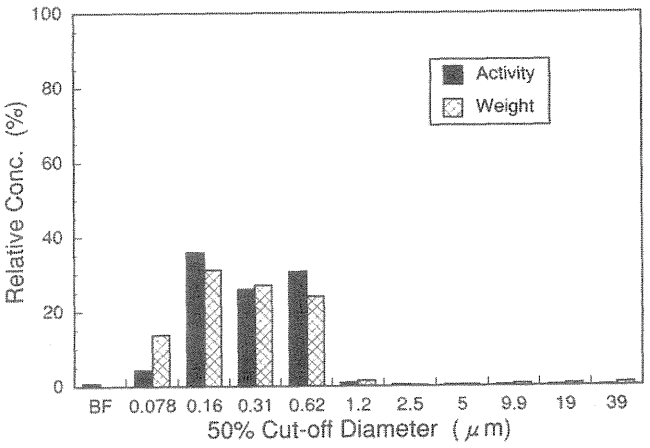

Fig.2 Activity and mass size distributions of plutonium aerosols.

強調しているため、短時間の露光にもかかわらず、有効直径37㎜のフィルタの全面から多数の像が得られた。このことは、大量の放射能をもった少数のプルトニウムエアロゾルが発生したのではなく、相当多数の微小エアロゾルであったことを推測させる。つぎに、ミクロレベルでの観察を行うためZnSシンチレータを介さずに、プルトニウムエアロゾルのアルファ線を飛跡の形で直接観察した結果をPhoto. 2に示す。飛跡の方向から判断して、この写真の中には少なくとも飛跡源が2点存在する。つまり、プルトニウムが粒子状で2粒存在することになる。この写真で見られる2つのスター状の飛跡は、偶然にも同一規模であったが、この他にもこれらとは大きさが異なるスター状の飛跡が別の観察場所で多数観察された。また、走査型電子顕微鏡では、ほぼ球形の粒子が凝集することなく、それぞれ単離して存在していたことが観察されている。

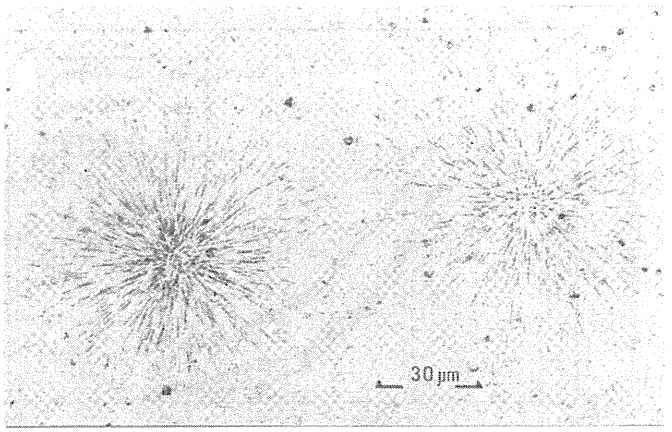

Photo.2 Star-like α trucks from plutonium aerosols.

Ⅳ　結論

プルトニウムをエアロゾル化し、これを実験動物に吸入投与するための実験装置を開発した。プルトニウムが主たる吸入対象物質ということで、装置の設計にかなりの制約を受け、また、装置の安全性を最優先したため、吸入装置としては必ずしも満足できるものにはならなかった。装置がグローブボックス内設置のため、実験条件の自由度、操作性などに問題があるものの、当初の目標であったラットの発ガンレベルの吸入投与がルーチンとして可能となったことは本研究課題の1つの大きな成果であると考える。

B：呼吸気道模擬キャストを用いたエアロゾル沈着様式の解明

Ⅰ　緒言

近年、ラドンの吸入被曝の問題、チェルノブイリ原発事故などから、原子力関係者のみならず、一般人の間にもエアロゾル吸入に対する関心が高まっている。また、ICRPの肺沈着モデルについても、現在、Pub.30モデルの改定作業が進められており、まもなく新しいモデルが公表されるようである。

現行の肺沈着モデルは、0.2 μm以上の比較的大きなエアロゾルを対象としており、火災事故で発生するような微細なエアロゾル、あるいは、ラドン娘核種のフリー成分などに対してはその適用が難しかった。そこで本研究では、従来、あまり検討されてこなかった0.2 μm以下のエアロゾルを中心にその呼吸気道内沈着様式を調べた。ただし、生体による沈着実験は制約が多く、また、沈着機構の解明に耐えられるデータが得難いので、ここでは呼吸気道を模擬した工学的模型（キャスト）による模擬沈着実験を試みた。

Ⅱ　研究方法

呼吸気道は大きく分けると、鼻咽頭（NP）部、気管－気管支（TB）部、肺胞（P）部の3つの部位に区分できる。本研究では、この中から、まず、鼻咽頭部および気管－気管支部についてそれぞれヒトの呼吸気道を模擬したキャストを作成した。鼻咽頭部キャストは、Fig. 3に示すように鼻孔から口腔を含め気管入口までである。一方、気管－気管支部キャストは気管から始まるが、気管支分岐次数はFig. 4に示すように一律ではなく4から10分岐ある。分岐から次の分岐までを1つの気道と数えると、気道総数は111本（気管を含む）あり、また、終端の気管支断面口は全部で56箇所ある。呼吸気道模擬キャスト内の空気の流れについては、一定速流で流れる定速呼吸と実際の呼吸のように吸気と呼気とが交互に現れ、しかも、流速がサインカーブのように刻々と変化する往復呼吸を模擬した。

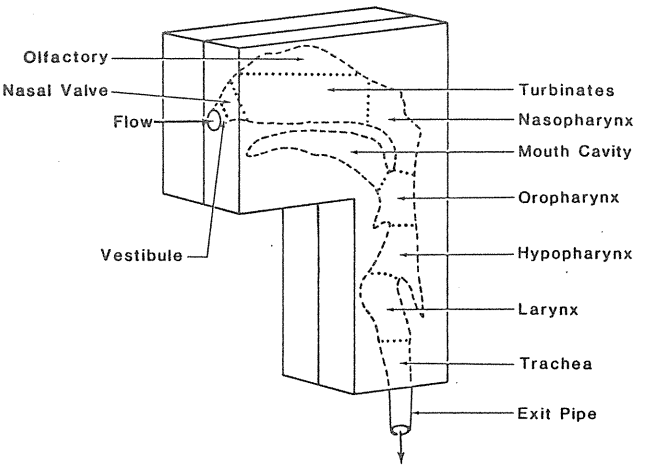

Fig.3 Human nasal cast

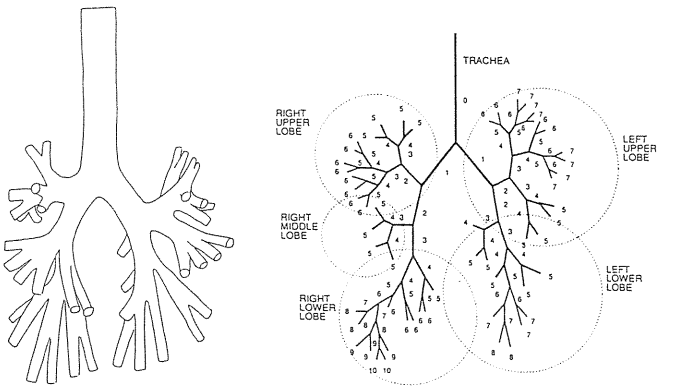

Fig.4 Branching pattern of a human tracheobronchial cast

沈着実験に用いる試験エアロゾルの作成は、まず、蒸発凝縮法により多分散のNaClエアロゾルを発生させ、これを静電分級法で単分散化することにより得た。エアロゾル粒子径は0.005 μmから0.2 μmまでの間で変化させた。模

擬気道内でのエアロゾル沈着率は、それぞれのキャストの上流および下流におけるエアロゾル濃度を凝縮核測定器ＣＮＣで計測することにより求めた。

Ⅲ　結果および考察

鼻咽頭部キャスト内でのエアロゾル沈着率を低速呼吸下で調べたところ、４～50 ℓ／min の何れの呼吸流量においても沈着率は０ではなく、かなりの沈着が認められた。特に、0.01 μm以下の超微小粒子径領域においてそれは顕著であった。結果の１例を Fig. 5 に示す。一般的傾向として、粒子径が小さいほど、また、呼吸流量が小さいほど沈着率は高かったが、呼吸流量への依存性は弱かった。低速呼吸ながら空気の流れが全く逆方向である吸気と呼気とを比べてみると、呼気時の方がわずかに沈着率が高かった。このような沈着傾向を示す鼻咽頭部沈着に対しその沈着機構を調べたところ、以下に示すような直円管に対する乱流拡散モデルでうまく説明できることが分かった。

$\eta = 1 - \exp(a \cdot Q^{-1/8} \cdot D^{2/3})$

ここで、η＝エアロゾル沈着率（－）、Q ：呼吸流量（ℓ／min）、D ：エアロゾル拡散係数（cm²／sec）、a ：装置定数（吸気時 a ＝－ 40.3 、呼気時 a ＝－ 48.7 ）である。

さらに、気管ー気管支部キャスト内でのエアロゾル沈着も、鼻咽頭部と同様に超微小粒子径領域にて高い沈着が認められた（Fig. 6）。粒子径が小さいほど、また、呼吸流量が小さいほど沈着率が高くなるという傾向も認められた。例えば、呼吸流量が 20 ℓ／min の低速呼吸の場合、粒子径が 0.1 μm では２～３％に過ぎなかった沈着率が、0.005 μm では 50 ％まで上昇している。つぎに、エアロゾル沈着性能がほぼ同一であることが確かめられた２体のキャストを人工胸郭中に吊し、さらに、特殊人工呼吸器を用いて往復呼吸時のエアロゾル沈着を調べたところ、呼吸流量が４ ℓ／min のとき Fig. 7 に示すような結果を得た。往復呼吸の場合、流速は絶えず変化しているので、呼吸流量は１回換気量と呼吸数との積で与えられる平均呼吸流量で表現されている。Fig. 7 の例では、同一の平均呼吸流量となる３種類の呼吸パターンについてエアロゾル沈着を調べたが、３者の沈着率曲線には明確な差は認められなかった。また、このときの沈着率曲線はちょうど呼吸流量が同じ定速呼吸時の曲線とほぼ重なった。この４ ℓ／min という呼吸流量はヒトの活動状態でいえば、安静時に相当する状態でかなり穏やかな呼吸といえる。図には示されていないが、呼吸流量がこれより多い 10 、 20 ℓ／min の場合においても、往復呼吸と定速呼吸との間には沈着率に明確な差は認められなかった。

Ⅳ　結論

ヒトの呼吸気道を模擬する鼻咽頭部キャスト、気管ー気管支部キャストを用いて 0.2 μm以下の微小エアロゾルの沈着様式を調べた。その結果、慣性あるいは重力による沈着だけで、0.1 μm以下のエアロゾルは通過してしまうと云われていた鼻咽頭部において、乱流拡散による微小粒子の多大な沈着を認めた。このことは、微小粒子の沈着はほとんど考えていなかった ICRP の沈着モデルにも大きな影響を与え、現在改訂作業中の新沈着モデルに反映されることが見込まれている。また、キャストのような工学的模

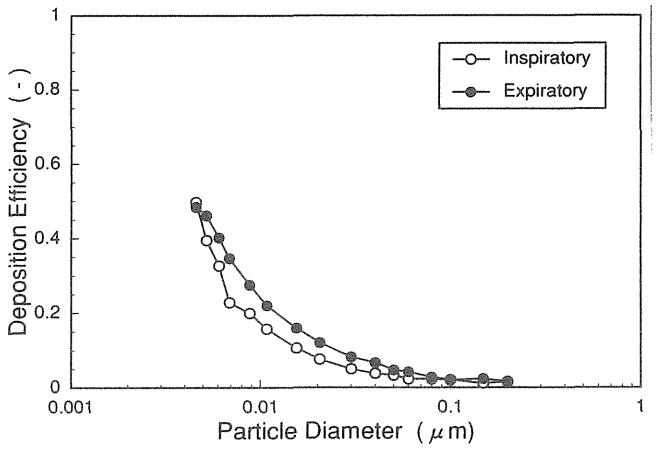

Fig.5 Aerosol deposition in a human nasal cast at 20 ℓ / min of constant flow.

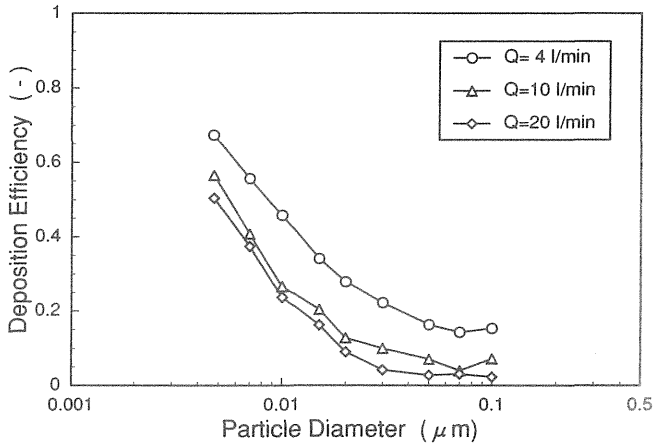

Fig.6 Expiratory deposition in a tracheobronchial cast under constant flow.

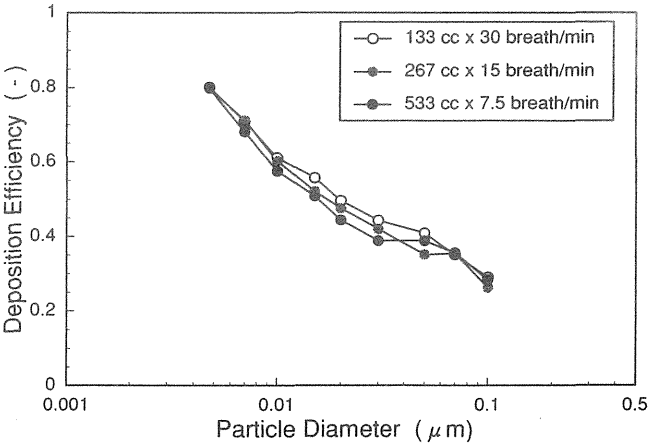

Fig.7 Effects of respiratory patterns on the tracheobronchial deposition.

型実験では、往復呼吸時の沈着を調べることが容易ではなかったが、新たな特殊人工呼吸器の開発によりこの方面の実験の可能性が拡がった。今回、実験を行った安静時から軽作業時の範囲では、１回換気量あるいは呼吸数で個別に評価するよりも、これらの積である呼吸流量で評価した方がエアロゾル沈着をうまく説明できることが分かった。ただし、呼吸流量がこれより大きい重作業あるいは中作業時には、呼吸気道内の流れの乱流度が高まり、エアロゾル沈

着に影響が現れる可能性がある。また、今回のキャストは何れも鋳型キャストであり、実際に近いという非常に大きな利点がある半面、形状が複雑すぎて理論的な解析が難しいという欠点もある。今後はこうした方面からのアプローチも考慮していく必要がある。

［研究発表］

1）山田裕司、Cheng, Y. S., Yeh, H. C., Swift, D. L. and McClellan, R. O. ：人体鼻咽頭部キャストへの微小エアロゾル粒子沈着、第23回日本保健物理学会、千葉、1988.

2）山田裕司、福田俊、飯田治三、宮本勝宏、小泉彰、鴇田和美、澤地邦宏：肺沈着モデルのためのビーグル犬肺の動的変移の解析、第23回日本保健物理学会、千葉、1988.

3）福田俊、山田裕司、飯田治三、宮本勝宏、小泉彰、鴇田和美、倉橋英治：犬気管支分岐に関する解剖学的特徴、第23回日本保健物理学会、千葉、1988.

4）山田裕司、Cheng, Y. S., Yeh, H. C., Swift, D. L. and McClellan, R. O. ：人体鼻咽頭部キャストへの微小エアロゾル粒子沈着、第6回エアロゾル科学・技術討論会、大阪、1988.

5）小泉彰、山田裕司、福田俊、飯田治三、宮本勝宏、倉橋英治、松下裕二：粒子沈着モデルのための犬気管支分岐の解剖学的解析、第6回エアロゾル科学・技術討論会、大阪、1988.

6）Yeh, H. C., Cheng, Y. S., Yamada, Y. and Swift, D. L. : Deposition of ultrafine particles in human nose and mouth, DOE contractors meeting on interactions of chemicals with living systems, Albuquerque (USA), 1988.

7）Yamada, Y., Cheng, Y. S. and Yeh, H. C. : Inspiratory and expiratory deposition of ultrafine particles in a human nasal cast, Inhalation Toxicol., Premier issue, 1-11, 1988.

8）Cheng, Y. S., Yamada, Y., Yeh, H. C. and Swift, D. L. : Diffusional deposition of ultrafine aerosols in a human nasal cast, J. Aerosol Sci., 19, 741-751, 1988.

9）山田裕司、久保田善久、松岡理：小動物用放射性エアロゾル吸入実験装置の開発とその基礎特性、第24回日本保健物理学会、名古屋、1989.

10）福田俊、山田裕司、小泉彰、澤地邦宏、圓谷誠司、松下裕二：肺沈着モデルを目的としたビーグル犬の呼吸生理学的機能に関する基礎的検討、第24回日本保健物理学会、名古屋、1989.

11）山田裕司、小泉彰、宮本勝宏、松岡理：小動物用放射性エアロゾル吸入実験装置の特性、第7回エアロゾル科学・技術討論会、嬬恋、1989.

12）山田裕司、久保田善久、小泉彰、松岡理：小動物用放射性エアロゾル吸入実験装置の開発とその基礎特性、保健物理、24, 331-336, 1989.

13）山田裕司、小泉彰、福田俊、稲葉次郎：ヒトの気管ー気管支キャストへの微小エアロゾル粒子沈着、第25回保健物理学会、つくば、1990.

14）藤田道郎、織間博光、清水幹子、本好茂一、福田俊、山田裕司、小泉彰、稲葉次郎：肺沈着モデルを目的としたビーグル犬の呼吸生理学的機能に関する基礎的検討(2)呼吸生理値の個体差、第25回日本保健物理学会、つくば、1990.

15）小泉彰、山田裕司、宮本勝宏、福田俊、飯田治三、石榑信人、佐藤宏、稲葉次郎：酸化Puエアロゾルの発生とラット気道への初期沈着、第33回日本放射線影響学会、仙台、1990.

16）串田尚隆、吉村竜一、藤田道郎、清水幹子、織間博光、本好茂一、友田勇、福田俊、山田裕司、小泉彰、稲葉次郎：犬の呼吸生理学的機能に関する基礎的研究、第110回日本獣医学会、宮崎、1990.

17）Cheng, Y. S., Yamada, Y. and Yeh, H. C. : Deposition of ultrafine aerosols in a human oral cast, Aerosol Sci. Technol., 12, 1075-1081, 1990.

18）山田裕司、小泉彰、宮本勝宏、佐藤宏、石榑信人、仲野高志、榎本宏子、稲葉次郎：ネブライザで発生させたPuエアロゾルの粒子性状、第26回日本保健物理学会、堺、1991.

19）福田俊、飯田治三、山田裕司、小泉彰、宮本勝宏、佐藤宏、吉田浩樹：無麻酔ラットにおける酸化プルトニウムの沈着量と初期体内挙動、第26回日本保健物理学会、堺、1991.

20）小泉彰、山田裕司、宮本勝宏、稲葉次郎：ラットへのプルトニウムエアロゾル吸入投与実験、第8回エアロゾル科学・技術討論会、東京、1991.

21）Yamada, Y., Koizumi, A., Fukuda, S., Inaba, J., Cheng, Y. S. and Yeh, H. C. : Deposition of ultrafine monodisperse particles in a human tracheobronchial cast, 7th Int. Symp. on Inhaled Particles, Edinburgh (UK), 1991.

22）山田裕司、小泉彰、福田俊、稲葉次郎：気管ー気管支部エアロゾル粒子沈着に対する呼吸様式の影響、第27回日本保健物理学会、秋田、1992.

23）山田裕司、小泉彰、福田俊：気管ー気管支部粒子沈着に対する呼吸様式の影響、第9回エアロゾル科学・技術討論会、太田、1992.

24）山田裕司、小泉彰、宮本勝宏、佐藤宏、石榑信人、仲野高志、榎本宏子、稲葉次郎：ネブライザで発生させた酸化プルトニウムエアロゾルの粒子性状、保健物理、27, 197-204, 1992.

25）Yamada, Y., Koizumi, A., Fukuda, S., Inaba, J., Cheng, Y. S. and Yeh, H. C. : Deposition of ultrafine aerosol particles in a human tracheobronchial cast, Hoken Butsuri (in press).

2．超ウラン元素の生物効果に関する比較毒性学的研究
①アルファ放射体による組織微細線量評価に関する研究

石榑信人、仲野高志、榎本宏子、小木曽洋一、
福田俊（内部被ばく研究部）

A Study on Microscopic Dose Distribution in Internal Exposure by α-Particle Emitters

Nobuhito Ishigure, Takashi Nakano, Hiroko Enomoto, Yoich Oghiso and Satoshi Fukuda
Division of Radiotoxicology

（A）Microscopic Dose Distribution in Parenchymal Lung Inhaled with Particulate Plutonium

The macroscopic quantity "absorbed dose" loses its validity to interpret the radiation-induced biological effects in the lung inhaled with particulate α-emitters like transuranic elements, because the doses to individual cells differ more widely than the range of doses over which the dose-response relationship can be regarded as linear. We intended to make up a three-dimensional model of parenchymal lung structure using a stack of actual histological sections in order to compute microscopic dose distribution around a particulate α-emitters instead of dose calculations given so far in which a mathematical model or two-dimensional models were employed. This theoretical dosimetric approach will provide a scientific basis to the extrapolation of results of animal experiments utilizing high doses to man exposed to relatively low level radioactivity and to the understanding of biological effects associated with "hot spots".

（B）*In Vivo* Counting of Pu in Experimental Animals and Its Application to Dosimetry

We have developed a method for *in vivo* counting of low energy LX-rays emitted from Pu. The minimum detectable activity was 90 Bq for 10% relative uncertainty. By this method, in contrast with serial-sacrifice study, a long term follow-up can be performed upon a specific exposed rat, which can reduce the number of animals required. This *in vivo* counting was applied to our dosimetric study: 1)the evaluation of initial lung burden of rats inhaled with PuO_2 particles, 2)the determination of our lung retention function of PuO_2 particles in rat lungs and 3) the examination of the behavior of ^{241}Am contained as a trace contaminant in PuO_2 particles.

（A）粒子状Puによる肺深部の微視的線量評価

Ⅰ．緒言

諸外国で行われた培養細胞の実験によれば、α粒子は細胞に致死的損傷を高い率で誘発し、その平均致死線量はα粒子１個の細胞通過に相当する場合もある。体内においてもこのような致死効果が事実であるならば、α粒子による細胞ヒットの回数分布は障害の発生確率を推定する上で重要な意味を持つ。

中課題「超ウラン元素・・・」では、Puの吸入被曝の生物影響が主要ターゲットであり、本小課題においても肺深部に沈着・滞留するα放射体の影響に強い関心を抱いている。

肺深部の構造を媒質とα粒子との相互作用という観点から区分した場合、空気で満たされた肺胞腔とそれを構築している肺胞壁等軟組織との２成分系と見なすことができる。従来の線量評価では、肺深部を、密度が一定の均質の無構造な媒質と仮定し、吸入されたPu粒子の回りの細胞のα粒子によるヒット数分布等を計算している。しかしながら肺胞のサイズや肺胞壁の厚みはα粒子の軟組織中の飛程と比べ充分小さいとは言えず、こうした均質無構造のモデルは良い近似を与えないと推察される。一方より複雑な数学モデルとして、肺胞の形状に偏五角十二面体を仮定するという構造モデルで線量評価が行われたこともある。

本小課題では、これら数学モデルではなく、可能な限り現実に近いモデルを作成すべく、最終的には、実験動物の肺の組織切片標本の２値化イメージと画像情報処理技術とによって肺深部のイマジナリーな立体構造を構築し、これを用いてヒット数分布、比吸収エネルギー分布等マイクロドシメトリーの諸量を求めようとするものである

Ⅱ．基本的な計算方法

１．フローチャート

計算のプロセスをFig.1のフローチャートに示す。実験動物の肺深部の多数枚の連続切片を作成し、その顕微鏡イメージをビデオカメラにより画像解析装置へ入力する。画

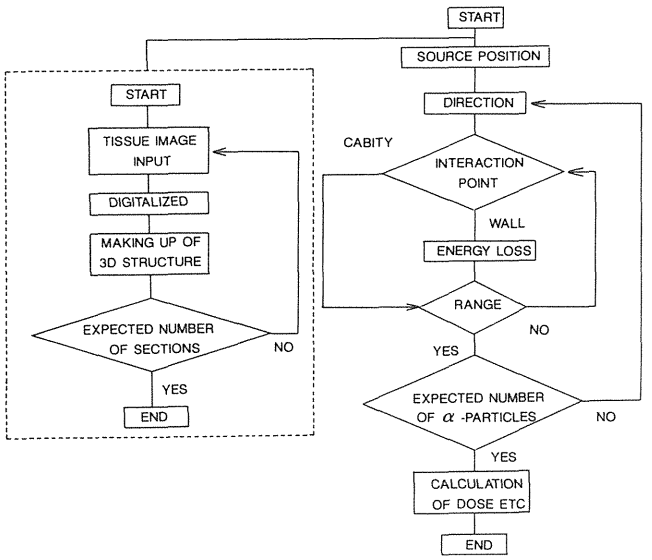

Fig.1 Flow chart of the procedures to calculate microscopic dose distribution using real lung tissues.

像の２値化等各種処理を施した後、画像記憶装置へ保存して肺深部の立体的な微細構造に関するファイルを作成する。これを利用して肺の中の線源粒子の位置や α 粒子の放出方向を乱数により選定し、その α 粒子が組織の無い空洞部を通過する時は何も相互作用を起こさず、組織部を通過する時はその部位にエネルギーを与え自身は減速してゆく、こうしたプロセスをその α 粒子が静止するまで追跡するというシミュレーションにより、 α 線の飛跡長さの分布や線源近傍の線量分布を求めようとするものである。

２．ハードウェア

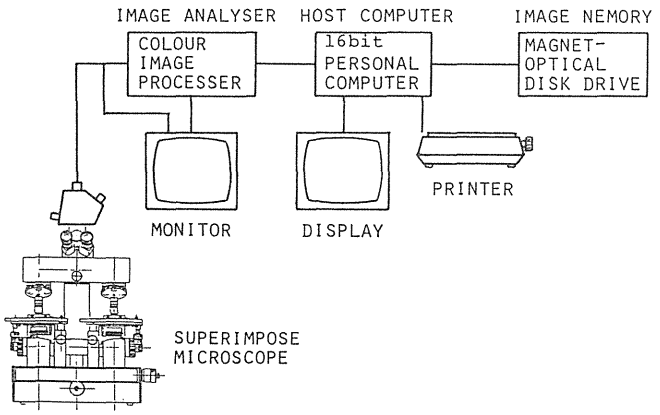

Fig.2 Block diagram of the image analyzing system used for the present dose calculation.

計算のために構成した装置を Fig.2 に示す。これは次の部品により構成されている。①組織切片の顕微鏡画像を入力するスーパーインポーズ顕微鏡、②画像の２値化や種々の補正を行う画像解析装置、③装置全体の制御や線量分布の計算を行うマイクロコンピュータ、④３次元の画像データや線量の計算結果を記憶する画像記憶装置。なお図の中のスーパーインポーズ顕微鏡は本研究において試作したものである。この装置は二つの独立したステージの各々に、隣合う切片を１枚づつ載せ両者からの合成像を観察しながら画像が一致するまで両方のステージの位置を独立に操作する顕微鏡である。

３．仮定

次の仮定を設けて計算を実行した。

①エネルギー損失の計算には Bethe-Bloch の理論式が解析的に与えられたものとして計算に使いやすい。しかし、この式は静止電子と高速荷電粒子とのクーロン相互作用のみを考えており、低エネルギー領域では荷電粒子の中性化の効果のため、エネルギー損失は過大評価となる。そこで、低エネルギー領域でより正しいと考えられる、実験経験を基にした Benton-Henke の式を使うこととした。

②肺を構成する組織の元素組成は次に示す Walsh のものを用いた。水素 63 %、炭素 9.5 %、窒素 1.4 %、そして酸素 26 %。なお、組織部分の密度を１とした。

③組織の無い空気の部分のエネルギー損失は組織中に比べ無視し得るものとした。

④線源や細胞は静止しているとした。

Ⅲ・計算結果

１．飛程分布

飛程計算時の CRT 画面の写真を Fig.3 に示す。図中、色の薄い部分が組織部、濃い部分が空洞部である。放射状の直線は模擬的に発生させた α 線の飛跡を表し、その長さは、各 α 線の飛程に対応している。

種々エネルギーの α 線について飛程分布を計算した。結果を Fig.4 に示す。これは、線源位置を 10 カ所とり各線源位置に関しては等角に 360 個（合計で 3600 個）の α 線を飛ばした結果である。

肺深部での実際の飛程は、均質無構造モデルに比べ大きく広がっており、遠くの組織を照射し得ることが示された。また、飛程の平均値と α 線の初期エネルギーとの間にはほぼ比例関係の成り立つことが示された。

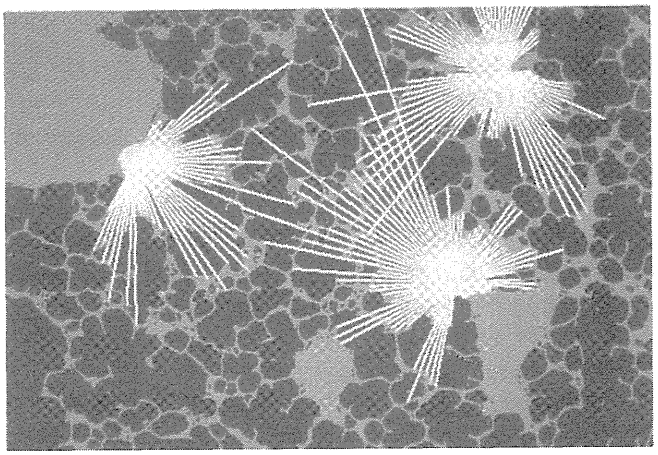

Fig.3 Digitized image of a lung section during the calculation of track length of αparticles in a parenchymal lung.

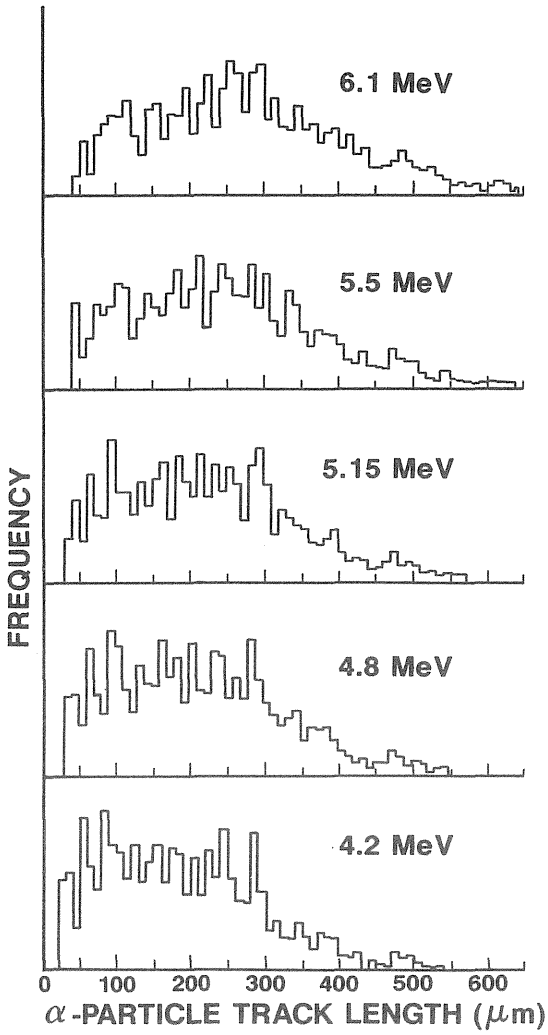

Fig.4 Calculated track length in a parenchymal lung for different α-particle energies.

2．ヒット数分布

(1)計算法

2次元の画像データを3次元へ敷衍するために肺深部の構造に等方性を仮定した。

線源から距離 r の点の α 粒子フルエンス $\phi(r)$ は、α 粒子放出数（線源粒子の α 放射能×積分期間）にその点への α 粒子到達確率 f(r) を掛け、これを半径 r の球の表面積で割ることにより得られる。即ち、

$\phi(r) =$ (α粒子放出数) × f(r) ／ (4 πr^2)

f(r) として、前節で述べた肺深部における飛程分布の計算結果を充てる。標的の幾何学的断面積 σ を上記 ϕ に掛けることにより平均のヒット数が得られ、次式に示すようにヒット数 n の関数としてポアッソン分布が計算できる。

$Pn = (\phi\sigma)^n \cdot \exp(-\phi\sigma) / n!$

この確率関数に半径 r 厚み dr の球殻内の細胞 N(r) を掛け、全空間に亘って積分すれば次式に示すように1個の線源粒子について、ヒット数を確率変数とする細胞の個数分布 n_n が得られる。

$n_n = \int P_n \cdot N(r)dr$

更に、個々の線源粒子の影響が独立と見なせる低レベル被曝の場合は、肺深部への沈着放射能 A を線源1個の放射能 a で割ったもの、即ち線源の個数をこの n_n に掛けることにより、肺全体で任意の回数ヒットを受ける細胞数 N_n を求めることができる。即ち、

$N_n = n_n \cdot (A / a)$

が得られる。

(2)1回ヒットされる細胞数

まず、1個の線源粒子の回りで1回だけヒットされる細胞の数を計算した。Fig.5 に計算結果を示す。これから分かるように、組織切片の2値化画像による場合と蜂の巣格子モデルによる場合とでは、粒子径依存性は比較的近い。一方、均質無構造モデルでは、0.8 μm をピークとしそれより大きい粒子では減少してゆき、2 μm 以上で殆ど0となるという他の二つのモデルとは著しく異なる粒子径依存性を示した。この結果は、均質無構造モデルを適用できる場合が限られていることを示唆している。

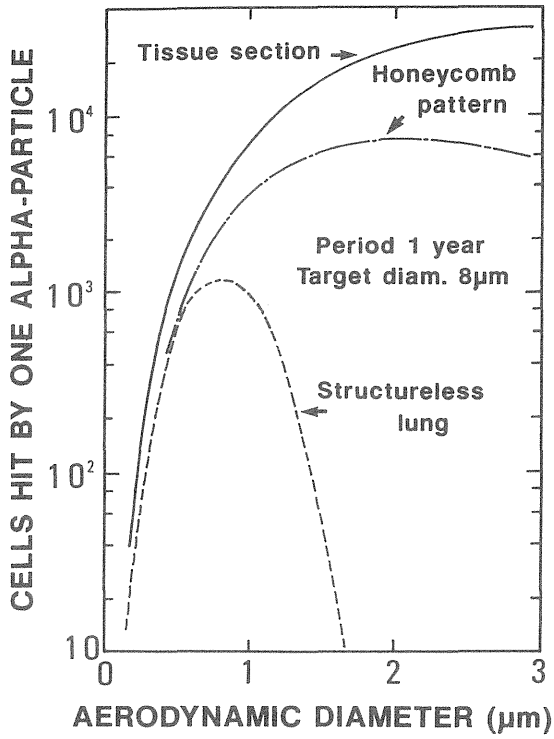

Fig.5 Number of cells hit by only one α-particle: dependence on particle diameter.

(3)ヒット後生存細胞数

冒頭で述べたように細胞は α 線にヒットされると高い確率で死ぬというデータがある。ここで、ヒットされてもなお生き残った細胞が障害の発生に深く関わっていると仮定する。また、細胞個々の悪性化への可能性はヒット回数に比例すると仮定する。すると、ヒット後生存細胞数 S（ヒット数による重み付け後）は1ヒット後の生存確率 p の n 乗にヒット回数を掛けさらに n 回ヒットされる細胞数 N_n を掛けて合計すれば得られる。即ち、

$S = \Sigma (N_n \cdot p^n \cdot n)$

p = 1 / 3 の場合の S の計算結果を Fig.6 に示す。3種のモデルとも粒子径1 μm に規格化した相対値である。この図より、いずれのモデルにおいても粒子径の増加に伴い S が減少した。そして減少の型はほぼ指数関数で近似できた。しかし、各々の傾きはモデルによって異なり、均質無構造モデルが最も大きい傾きを示し、このパラメータ

Sにおいても他の２種類のモデルとは大きく異なることが示された。

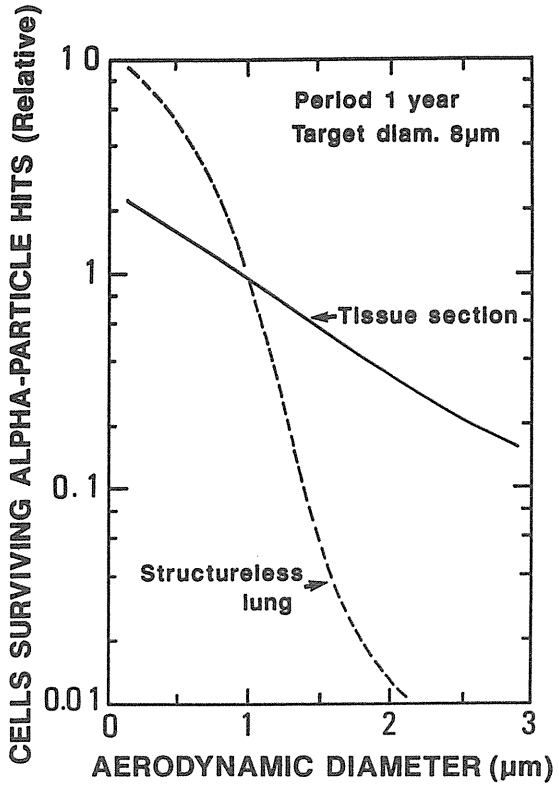

Fig.6 Number of cells surviving α-particle hits: dependence on particle diameter.

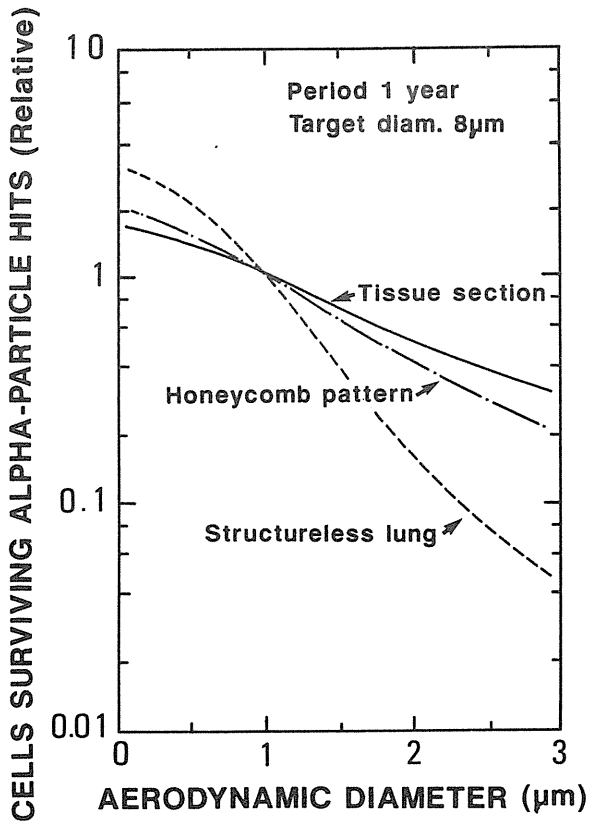

Fig.7 Number of cells surviving α-particle hits in the case that the space of the cells killed is occupied with reproduced cells.

(4)致死細胞の空間の取り扱い

次に、細胞がα線のヒットによって死に、処理された後その空間が、別の細胞の分裂の結果生まれた新たな細胞により短時間の内に補填されると仮定し計算した。紙面の制約上詳細は省くが、この場合Sは次式で表わされる。

$$S = N_1 \cdot p + \Sigma\ (N_n \cdot S_n)$$

なお、$S_n = \Sigma\ \{{}_{n-1}C_i \cdot p^i \cdot (1-p)^{n-1-i} \cdot p\ (i+1)\}$ である。

計算結果をFig.7に示す。粒子径依存性の傾きはFig.6に比べゆるやかとなった。このように致死細胞の空間のターンオーバーの実態はリスク推定の信頼性に強く影響すると推察され、この問題に関する知見の現在の到達段階を踏まえた上で、今後の計算に慎重に反映させる必要がある。

(5)標的サイズ及び積分期間の影響

ここまでの計算では、標的サイズと積分期間という２つのパラメータが使われていた。これらの値は、S（ヒット後生存細胞数）の線源粒子径依存性にどのように影響するのであろうか。粒子径依存性の指標として、Fig.6の傾き、即ち縦軸の値Sが1 μm粒子の場合の1/2に低下する粒子径をとることにした。結果をFig.8に示す。大きな標的では、また長い積分期間をとった場合には、線源粒子径依存性が若干弱くなることが示された。

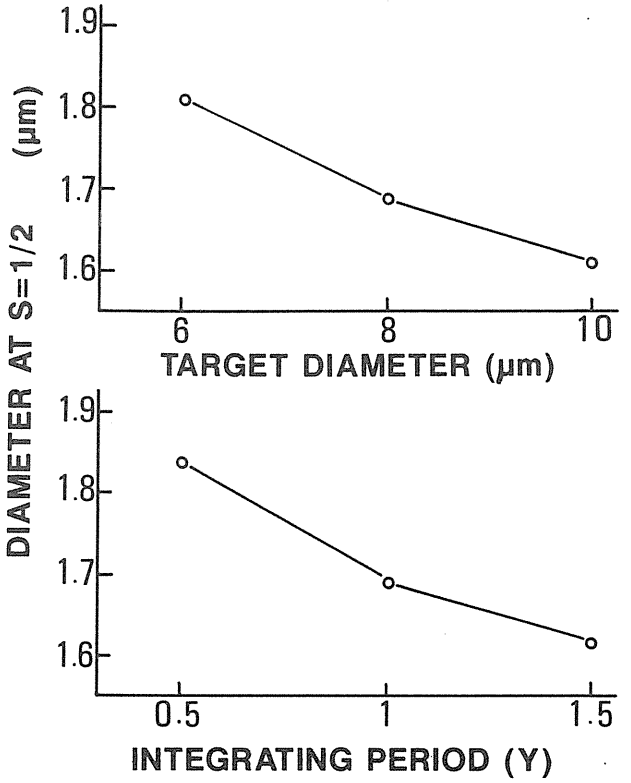

Fig.8 Effects of target size and integrating period on the size dependence of the calculated number of surviving cells.

Ⅳ. 結論

本研究で示唆された重要なポイントは次の通りである。

一定のα放射能が沈着した肺について線源の粒子径を変えてα線によるヒット数の分布を計算したところ、分布の型は、粒子径により大きく変化した。冒頭に述べた様に細胞は１回ヒットされると何割かは死に到る。従って

ヒットされなお生残する細胞は障害の発生に深い関わりがあると考えられる。この値を試算したところ、粒子径が大きい程減少する傾向が示された。ICRPの立場では、粒子のサイズをとりあえずは考慮しないとしている。今後、現在進めている計算の信頼性を高めることによって、粒子状α放射体の影響評価に関わるこうした重要課題に答える根拠を見つけることが期待される。

（B）体外計測法による動物体内Puの測定と線量評価への応用

Ⅰ．緒言

中課題「超ウラン元素・・・」は、プルトニウム（Pu）による内部被曝の生物影響の解明を固有の目的としている。この生物影響は原因量としてのPu体内量との関連で評価されて初めて量的見積りとして意味をなす。

諸外国では、実験動物5匹程度を一つの群とし、一群ごとに定期的に屠殺しながら体内Puの変化を見積ってきた。この方法では、同量のPuを吸入した動物を、群の数×5匹と多数用意しなければならず、この実施には大規模な設備と多大の労力を要する。本小課題では、こうした定期屠殺法に代わるものとして動物を生存状態で体外から計測する方法を開発した。本法によれば、個体別に長期間連続的に追跡できるため、少ない数の動物で目的とするデータが取得できる。また、動物の個体差に起因する誤差も除くことができ信頼性の高いデータが得られるといった長所があり、線量評価だけではなくPuの代謝や影響、その他内部被曝の多くの研究課題で共通に使われる基盤となる技術である。

この方法ではアルファ壊変の4％という低い放出率のしかも動物の組織自身による吸収減弱を強く受ける低エネルギーの微弱なX線を検出する必要がある。このため低バックグラウンドでかつ高い計数効率をもつ特殊な計測システムを構築する必要がある。さらに、試料が複雑な幾何学的形状のしかも生きた動物であることに起因する誤差の評価や作業者の安全を確保しながら実施するための技術的な困難も多い。

本研究では、試作した装置について、①種々計数ジオメトリに対する計数効率の依存性、②体表面汚染や肺以外の臓器に残留するPuの計数への影響、③放射能／計数率の校正係数の測定等を検討し、ラットの体内Puを正確に測定する具体的な実施手順を確立することを目的とした。ついで、線量評価に必要な初期沈着量の測定、及び残留特性の測定へ本方法を応用した。

Ⅱ．結果と考察

1．体外計測法の確立

(1)体外計測装置

Fig.9に試作した小動物用体外計測装置の概略図を示す。鉛製遮蔽箱は、厚さが5cm、外寸法は129cm（L）×74cm（W）×59cm（H）である。バックグラウンドの低エネルギー成分を低減するために、箱の内側に銅板とアクリル板とを内張りした。検出器は直径5cm、厚さ1mmの薄型NaI(Tl)シンチレーション検出器で、窓材は、0.025mmのAl薄膜である。このような検出器を動物の左右と腹側に各一本ずつ合計3本配置し、動物体外へ透過してくる低エネルギーX線を検出した。

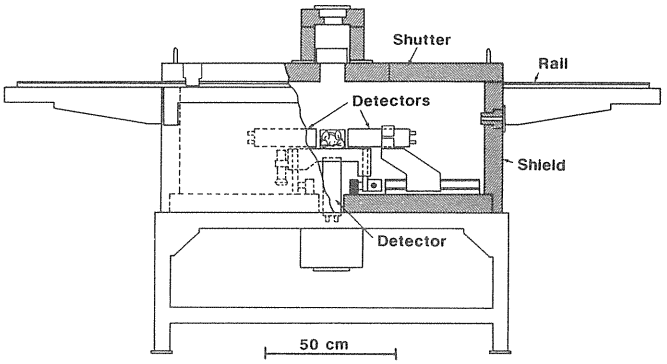

Fig.9 Schematic diagram of the whole body counter designed in the present study.

(2)体外計測の実施操作

グローブボックス（GB）やフードの外でPuを取り扱う場合、内部被曝の防止と作業環境の保全のために、原則として試料を密封することが要求される。しかし、この目的のために、生きた動物を生存に充分な容積をもつがっしりとした箱に密封することは許されない。検出する微弱な低エネルギーX線がその箱の構成材で著しく吸収減弱されたり、動物と検出器とが離れることによって幾何学的計数効率が低下するからである。

そこで本研究では、薄いアクリルの板（2mm厚）によりラットがようやく入る大きさの箱を作り、その中にラットを保定して、ついでその箱ごとラットを、呼吸用に空気をいれたファスナー付きのポリエチレン袋に密封するという方法によりこの問題の解決を図った。

Fig.10に体外計測の実施操作のフロー図を示す。

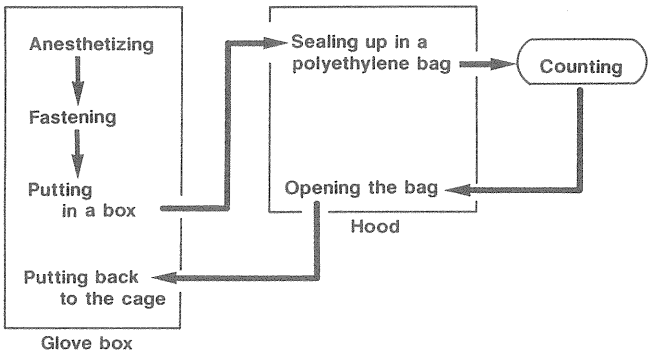

Fig.10 Flow chart of the whole body counting procedures.

1）GB内でラットを麻酔、

2）アクリル製保定板（2mm厚）の上に腹ばいにして載せ、前肢を伸ばした状態で保定、

3）保定箱に入れる、

4）この保定箱をGBからダブルカバーシステムによって取り出し、フードへ運搬、

5）フード内で保定箱をファスナー付きポリエチレン袋へいれ、低流量のポンプにより空気を入れる、

6）袋の口を閉じ、別の袋で包む、

7）体外計測を実施、

8）逆のルートでケージへ戻す。

なお、麻酔持続時間、袋の中の空気量、LX 線計数率等を考慮し計測時間を 1000 秒とした。

(2)ジオメトリ

検出する放射線が微弱なため、検出器をラットの体に可能な限り近付けて測定する必要がある。このため計数効率はジオメトリに強く依存することとなった。そこで計数効率のラットの位置依存性を検討し、再現性のよい計数効率の得られる最適なラットの位置の決定と、位置の不確かさがもたらす誤差の評価を行った。

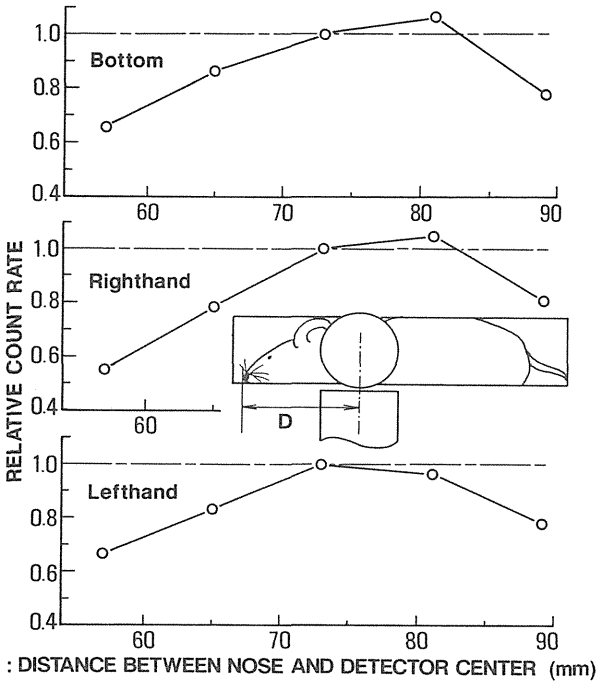

Fig.11 Dependence of count rate on the rat-detector geometry with different locations of the rat along its longitudinal axis.

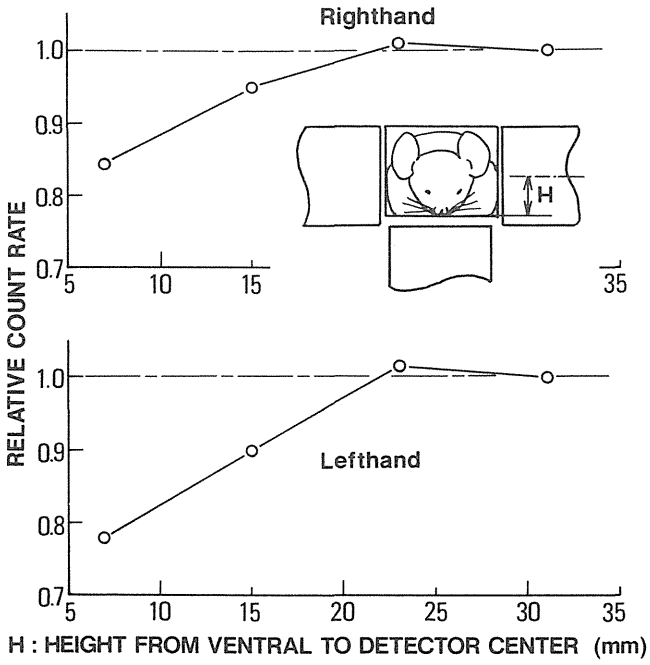

Fig.12 Dependence of count rate on the rat-detector geometry with different locations of the rat in the up / down direction.

Fig.11 にラットの位置を前後方向に動かした時の計数効率の変化を、Fig.12 には、上下方向に動かした時の変化を示す。

Fig.11 から、計数効率は前後方向の位置に応じてかなり敏感に変化し、5 mmの違いが計数効率に 10 %近い変動をもたらした。また、鼻先と検出器の中心が 70 ～ 80 mmの時に最も高い計数効率が得られた。

Fig.12 から、保定箱の底板が左右検出器の中心から 23 ～ 30 mm低い位置の時に最も高い計数効率が得られた。なお上下方向の場合は前後方向と異なり、設定の再現性が良好なので、計数効率の変動に注意する必要がない。

(4)肺以外の Pu の計数への影響

この体外計測法では、肺の中の Pu のみを評価したい。そこで体表面汚染や、肺以外の臓器に移行沈着した Pu がどの程度計数されるかを、次の方法により定量的に評価した。

まずラットを体外計測した。その後、ラットの肺のみを取り出し、残った死体を最初の体外計測と同じジオメトリで体外計測し、両者の計数率の比を求めた。

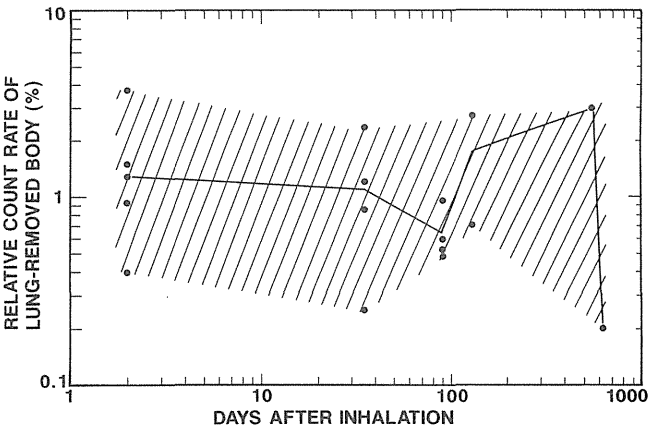

Fig.13 Effect of possible Pu content of the parts other than the lung on the count rate of the whole body counter.

結果を Fig.13 に示す。体表面汚染や胃腸管内 Pu の影響が懸念された吸入 2 日後に始まり、おもに骨と肝臓に沈着する Pu の影響が懸念された 600 日後に至る長期間、肺以外の部位の Pu は、体外計測値の 4 %以下であり、実際上は、無視しても構わないという結論が得られた。

(5)校正係数

体外計測の通常法では、体内放射能の定量は標準ファントムの計数率との比から求められる。しかし、Pu の場合は、検出する放射線が相互作用断面積の大きい低エネルギーの光子であるため、動物の体格のわずかの差が計数効率に強く影響する。このため、ファントム法を採用すると、体格の異なる非常に多くの標準ファントムを用意しなければならず、著者らは、これは現実的ではないと判断した。これに代わる校正方法として、次の方法を検討した。①まず、種々の体重のラットについて、体外計測の計数率と摘出した肺の放射能とから LX 線の計数効率を求める、②これを体重に関してプロットすることによって体重対計数効率の相関曲線を得る、③放射能を測定したいラットの体重

を体外計測時に測定し、相関曲線上で計数効率を読み取る。なお、摘出肺のPu放射能の測定には、筆者らが開発したフォスウィッチ検出器によるLX線計数法を用いた。

Fig.14に、このようにして得られた計数効率をラットの体重に対してプロットした結果を示す。体重増加に伴いLX線の吸収減弱がはなはだしくなり、計数効率が減少していることが示された。以上のように、両者の間にはきわめて強い相関関係が認められ、本方法により体内のPuの放射能を決定できることが明らかとなった。

以上の計数効率の検討とバックグラウンドの評価結果から、本装置の最小検出放射能を評価したところ、相対誤差10％を仮定した時90Bqが得られ、放医研における吸入放射能の範囲（100Bq～数1000Bq）をクリアしていた。

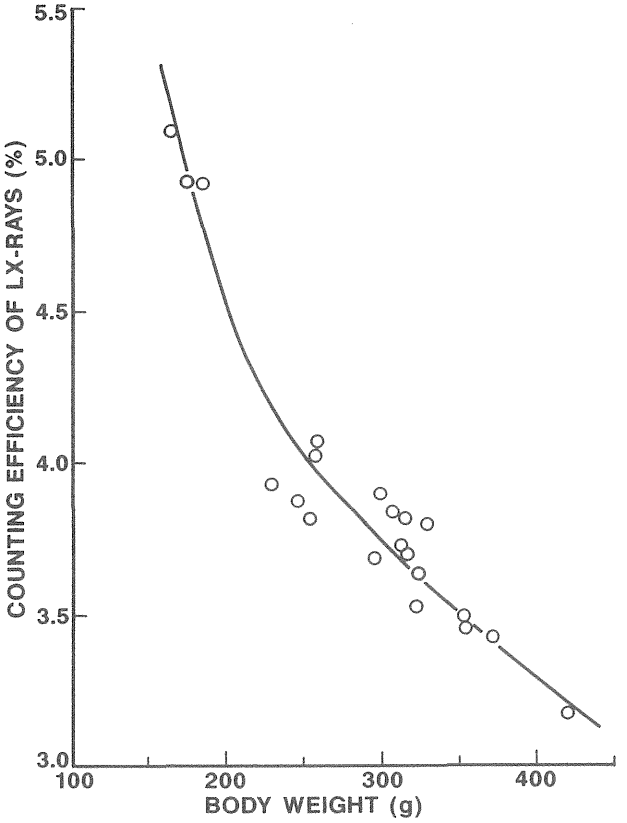

Fig.14 Counting efficiency of LX-rays for the rats of various body weights, which was used for the calibration of the whole body counter.

2．体外計測法の線量評価への応用

(1)肺深部初期沈着量の測定

肺への初期沈着量を決定することは内部被曝の影響の全ての研究の出発点となる。諸外国では、一緒に吸入投与した一群の動物から数匹をその群の代表として抽出し、屠殺後の肺の放射能分析結果をもってその群全体の初期沈着量としている。しかし、一緒に吸入させても実際に沈着する放射能は一般的に個体間で大きくばらつく。このため、屠殺した動物がその投与群を真に代表していたかどうかは不明である。本研究では、長期間飼育観察する動物そのものを全て一匹ごとに体外計測しPuの肺への初期沈着量を求めた。

放医研の吸入実験装置は20匹を同時吸入する装置であるが、例として、Fig.15に酸化Puの吸入実験5回分の

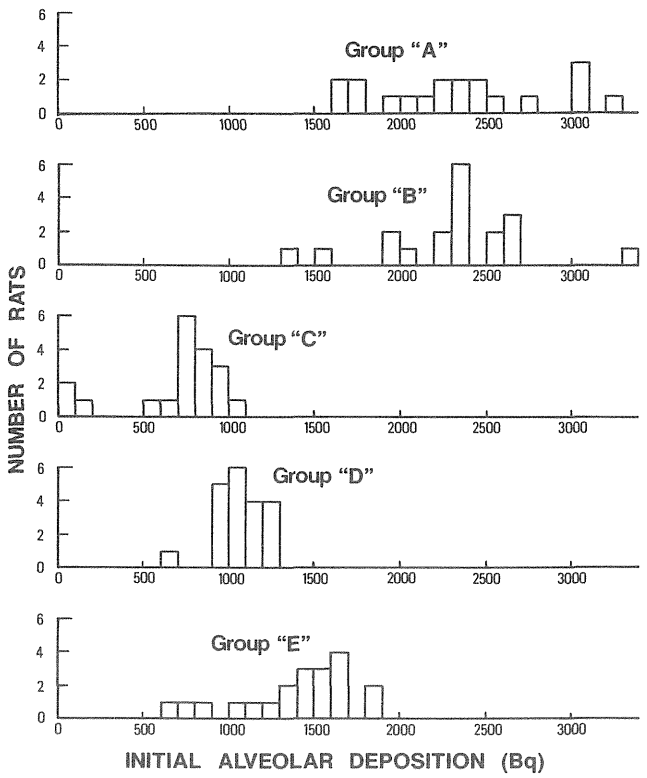

Fig.15 Distributions of initial lung burdens of PuO_2 particles for the five different batches of exposure.

Table 1 Deposition fractions of inhaled plutonium aerosols in alveolar region of rats

Batch	AMAD*1 (μm)	GSD	Exposure*2 (min·Bq/cc)	IAD (Bq)	Resp. Vol.*3 (cc/min)	Depos. Frac. (%)
A	0.48	2.0	69	2350	124	27
B	0.49	1.9	60	2310	128	30
C	0.42	2.1	38～45	800*4	99	18～21
D	0.39	1.9	46	1060	99	23
E	0.43	2.1	86	1390	97	17

*1 Activity median aerodynamic diameter.

*2 Time integral of air concentration of plutonium during exposure.

*3 Calculated values using the Guyton formula.

*4 Rejecting the three lowest IAD.

沈着量の頻度分布を示す。

このように測定した初期沈着量から初期沈着率を評価した。なお、ラットの呼吸量は吸入時にモニタできないので、Guytonが提唱している計算式により推定した。

得られた結果をTable 1に示す。これらを、珪酸塩粒子を用いて米国で測定された沈着率や密度が1の標準粒子に対する理論的計算値と比べたところ、酸化Puでは沈着率が高くなる傾向が観察された。この理由として、酸化Puは粒子の密度が大きいため、拡散機構による沈着率が高くなり、その結果、同じ空気力学径の標準粒子の場合よりも全体としての沈着率が高くなったものと推察された。

(2)酸化Puの肺残留特性

次に、酸化Puを吸入投与したラットについて、肺にお

ける残留率特性を本研究で開発した体外計測法により約500日間追跡した。こうしたデータは、ラットを用いた発がん実験において、吸収線量を正確に評価するために使われる。また、酸化Puの肺における挙動の理解に基礎的データを提供する。

吸入した酸化Pu粒子は、空気力学的放射能中央径0.47 μm、幾何標準偏差2.1の多分散エアロゾルである。肺深部初期沈着量は最も少ないラットが1990Bq、最も多いものが2960Bqであった。

この実験には、放医研で維持しているWistar系の雌ラット5匹を用いた。吸入時12週齢で、体重は平均230gであった。

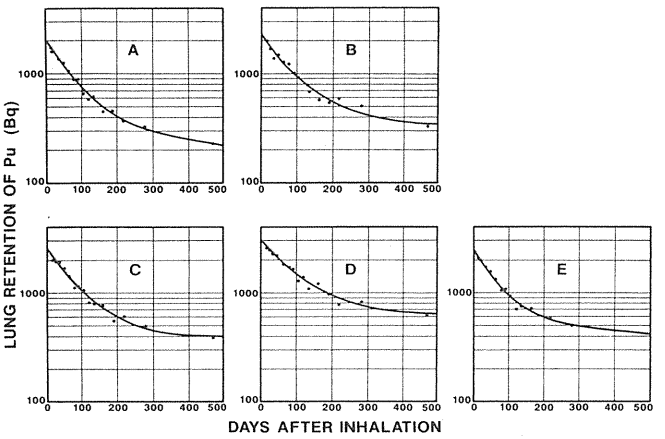

Fig.16 Lung retention of Pu of five rats following inhalation of PuO_2 particles.

Fig.16に5匹のラットの残留特性の測定結果を示す。残留率はいずれのラットにおいても2成分の指数関数でよく近似された。相互によく似た残留特性を示しているように思われる。

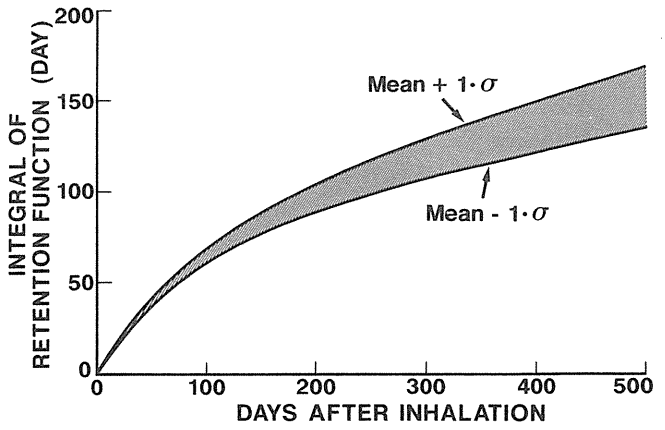

Fig.17 Time integral of retention function; the shadowed area indicates the range of the integral between [the mean] + [the standard deviation] and [the mean] − [the standard deviation] of the four rats.

残留率の時間積分は、蓄積線量のよい指標である。残留特性におけるこれら5匹の間の個体差を評価するために、この時間積分を計算した。5匹の平均値と標準偏差をFig.17に示す。この図が示すように標準偏差は小さく、個体差は比較的小さいことが明らかとなった。

これら5匹の残留率を平均し、母集団の残留率を推定した。結果を次式に示す。

$$Y(t) = 0.77\exp(-0.0136t) + 0.23\exp(-0.00084t)$$

ここでY(t)は、吸入後t日目における肺内Pu残留率である。これは、初期沈着量の77%は半減期51日で、一方残りの23%は長期間肺内に残留し、半減期825日でクリアランスされることを示している。

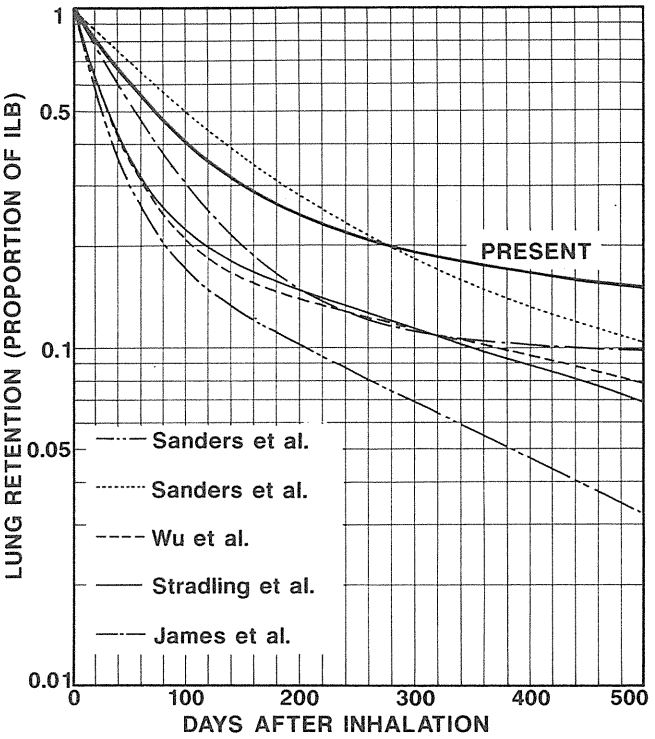

Fig.18 Comparison of the retention function with the other retention functions in a few literatures.

Fig.18に今回著者らが得た残留率曲線を諸外国のものと比較した。ここで注目されるのは、今回の結果が、バッテル研究所（USA）のSandersらの最近の結果とともに長い肺内残留を示している点である。

酸化Puのクリアランスを修飾する要因については従来いろいろな報告がなされてきた。その中のひとつに、沈着したPuのα線による肺の組織の照射効果が粒子の肺からのクリアランスを遅らせるという報告がある。

Sandersらの最近の方の実験も著者らのものも初期沈着量は比較的多い。このため照射効果がクリアランスを阻害した可能性も否定はできない。しかし、著者らは現在、より低い初期沈着量で残留特性を測定中であり、その途中経過を観察すると、必ずしも照射効果が今回の遅いクリアランスの主原因とは言えないということを示唆する結果が得られつつある。

放医研のエアロゾル発生法では、まず、水酸化Puの微小ミストを発生させ、これをエアロゾル状態のままで1150℃という高温で酸化することにより、酸化Puのエアロゾルを得ている。このため、Pu粒子は芯まで充分に酸化された球状の欠陥の少ない単結晶を形成しているものと推定される。一方、バッテル研等では、蓚酸Puの沈澱物を空気中で熱して酸化し、これを水に懸濁し、エアロゾル化している。このため、粒子は不整形であり、結晶として不完全である可能性が高い。このような粒子は表面積が

大きく、また結晶欠陥に起因する粒子の破砕も受け易いと思われる。これらは、クリアランスを早める原因となり得る。

以上のように、本研究においては、Puの防護を考える上で、酸化Puということだけではなしに、粒子の詳細な物理化学的性状にも留意しなければならないことが示唆された。また、Puの発がん研究における線量の評価に諸外国の残留率は適用できず、放医研の実験条件で実測された残留率をこそ使わなければならないことが実証されたことは、プロジェクト全体の成果の信頼性に少なからず寄与するものと考えられる。

(3)アメリシウム（Am）とPuとの随伴挙動

通常、Puには^{241}Puからβ壊変した^{241}Amが含まれている。現行のICRPの立場では、酸化PuはクラスY、つまり肺から年のオーダーで、AmはクラスW、つまり週のオーダーでクリアランスされるとしている。それでは、酸化Pu中で生成した^{241}Amはどのようなクリアランス特性を示すであろうか。本研究では^{241}Amを放射能比で4％含む酸化Puを吸入したラットの肺について、Am/Pu比を体外計測法で測定することによりこれら両元素のラットの肺における随伴性を検討した。

実験方法や材料は、前節と同じである。なお、^{241}Amの測定は、この核種から放出される60keVのγ線を計測することにより行った。

Am/Pu比を吸入後約500日間追跡した。その結果をFig.19に示す。これよりAm/Pu比は吸入後の時間経過によらず一定値を示すことが明らかとなった。つまり、Pu中に生成したAmは、ICRPのいうクラスWではなく、Puと随伴してクラスYとして挙動することが明らかとなった。この結果は酸化Puは大部分が肺の中で粒子状態のまま残留・クリアランスされることを示唆している。さらに本結果は、人体のように体が大きくてLX線の吸収を受け易くPuのモニタが困難な場合でも、測定の容易な^{241}Amを追跡することにより、Puの肺負荷量を推定できる可能性を示唆している。

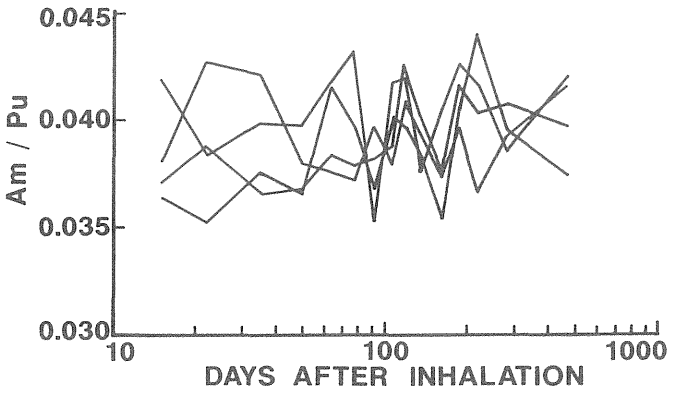

Fig.19 Ratio of Am/Pu in rat lung for long term follow-up.

Ⅲ．結論

本研究では、次のことが明らかにされた。

①開発した体外計測法の最小検出放射能は、相対誤差10％を仮定した時、90Bqであり、放医研における吸入放射能の範囲（100Bq～数1000Bq）をクリアした。

②本方法を用いて、.線量評価の基本情報であるPuO_2粒子の肺深部初期沈着量及び沈着率を評価した。

③本方法を用いて、PuO_2の肺深部残留特性を測定した。このデータは、発がん研究において吸収線量の正確な評価に使われている。初期沈着量の77％は半減期51日で、23％は825日でクリアランスされることが明らかとなった。これは、吸入毒性研究で有名なバッテル研の結果等と比較し、遅いクリアランスであった。この理由として、粒子の物理化学的性状の差異が示唆された。正確な理由を明らかにするためにはこの点に焦点を絞り、さらに検討を進める必要がある。

④^{241}Puのβ壊変により生じた^{241}Amは肺内でPuに随伴して挙動することが明らかにされ、ICRPの^{241}AmはクラスWであるという仮定はこのようなAmには適用できないことが示された。

〔研究発表〕

1）石榑信人，他：アルファ線測定用線源の固体飛跡検出器によるオートラジオグラフィ，RADIOISOTOPES, 38, 282-285, 1989.

2）Ishigure, N., Nakano, T. and Matsuoka, O.: An Investigation to Assess Which Component in the Air Is Concerned with the Vacuum Effect on Plastic Track Detector Sensitivity, Nucl. Tracks Radiat. Meas.(Int. J. Radiat. Appl. Instrum. Part D), 16, 57-59, 1989.

3）仲野高志：肺深部におけるα粒子の飛程分布，第21回放医研シンポジウム報文集，142-149, 1990.

4）石榑信人：肺深部における細胞のヒット数分布と粒子性，第21回放医研シンポジウム報文集，150-157, 1990.

5）Ishigure, N., Nakano, T., and Enomoto, H.: A Device for In Vitro Irradiation with α-Particles Using an α-Emitting Radioactive Source, J. Radiat. Res.,32, 404-416, 1991.

6）石榑信人：固体飛跡検出器のプルトニウム内部被曝への応用，放射線，18，8-15，1992.

7）Ishigure, N. et al.: Assessment of Initial Alveolar Deposition on Rats Exposed to Plutonium Aerosols Using a Whole Body Counter, 保健物理，27, 135-142, 1992.

8）Ishigure, N., Nakano, T. and Enomoto, H.: Activity Measurement of Plutonium in Solid Samples by LX-ray Counting with a Phoswich Detector, 保健物理，28, 195-201, 1993.

9）Ishigure, N. et al.: Lung Retention of Pu Following Inhalation of PuO_2 in Rats Measured Using a Whole Body Counter, J. Radiat. Res.,35, 16-25 1994.

2．超ウラン元素の生物効果に関する比較毒性学的研究
②超ウラン元素の生物効果とその発現機構に関する比較毒性学的研究

小木曽洋一、福田俊、山田裕、飯田治三、高橋千太郎、佐藤宏、石榑信人、
仲野高志、榎本宏子、山田裕司、小泉彰、稲葉次郎（内部被曝研究部）

Toxicological Studies on Biological Effects of Transuranium Elements

Yoichi Oghiso, Satoshi Fukuda, Yutaka Yamada, Haruzo Iida, Sentaro Takahashi, Hiroshi Sato, Nobuhito Ishigure, Takashi Nakano, Hiroko Enomoto, Yuji Yamada, Akira Koizumi and Jiro Inaba
Division of Comparative Radiotoxicology

For risk estimation of internal exposures of transuranium elements, especially plutonium, biologic parameters such as microdosimetory at tissue or cellular levels and factors modulating sensitivities of target cells remain to be elucidated. In this study, we focused on carcinogenic effects of plutonium either in inhalation exposures or the subsequent translocation to the liver, skeleton and hematopoietic organs. To investigate carcinogenesis of inhaled plutonium dioxide particles, approximately 120 rats were exposed to aerosols with 0.3 to 0.4 μm of AMAD, and were kept for life span periods. The results have shown that 97% of animals inhaled 1000 Bq or more died with lung tumors (mainly adenocarcinomas) within 600 days after inhalation, and that almost 60% of rats inhaled 500-1000Bq died with lung tumors from 500 to 700 days after inhalation, although the remaining animals are still survived. Estimated absorbed lung doses in these lung tumor-bearers were ranged from 3 to 8 Gy, depending on initial alveolar deposition and survival time. Carcinogenic effects of injected plutonium citrate were also examined in total 120 mice for life-span periods. Osteosarcomas were observed in approximately 60% of animals injected 1000 to 5000 Bq and 35% of animals injected 500 Bq, respectively, but only 17% of animals injected 10000 Bq had bone tumors, while no incidence of bone tumors has been noted in untreated control animals. Additionally, relatively higher incidence of lymphomas and lymphatic leukemias was observed in 17% of animals injected 5000-10000 Bq, as compared to 8% of control animals. Finally, to clarify biological parameters of α-ray exposures at cellular levels, preliminary assays for survival of colony-forming cells were performed by using *in vitro* exposure system of α-ray emitted from the source of ^{241}Am. As expected, both of pulmonary alveolar macrophages and bone marrow cells after α-ray exposures were more sensitive than those by γ-ray emitted from the source of ^{137}Cs, and the estimated RBE was approximately 1.5-2.1.

1．緒言

プルトニウム等超ウラン元素による内部被曝の生物効果で最も重要なものは、その発癌性であり、とくに骨肉腫については低LET放射線はもちろん、β線放出核種に比べてもきわめて誘発性が強く、プルトニウムはその最たるものとされている。一方、プルトニウムについてはその存在形態から、溶解度の極めて低い酸化プルトニウムエアロゾルの吸入被曝が最も危険度の高い被曝形式であり、その発癌性、すなわち肺腫瘍誘発性がリスクの対象となっている。プルトニウムによって誘発される骨肉腫あるいは肺腫瘍いずれにおいても、一定の線量効果関係がすでに米国等での大規模な動物実験で得られているが、低レベルでの発癌率やヒトでのリスク推定に必要とされる種々の生物学的パラメータ、すなわち標的細胞レベルの微細線量分布、標的細胞の感受性を決定する要因や微小環境要因などについてはまだ明らかにされていない。本研究では、以上のことを明らかにするために、まず酸化物エアロゾル吸入による肺腫瘍発生と吸収線量推定および体内移行して血液に侵入したプルトニウムが誘発する腫瘍のスペクトルについてそれぞれラットおよびマウスによる生涯飼育実験で病理学的に検索するとともに、α線をin vitroで標的細胞に照射したときの生物効果を検出して、生物学的パラメータのひとつであるRBEを推定する試みを行った。

2．方法

(1)酸化プルトニウムエアロゾルの吸入による肺腫瘍誘発と線量効果関係

すでに我々により開発されたエアロゾル吸入曝露装置を用い、硝酸塩から水酸化物に変換し、ジェネレータで発生させたミストを約1000℃で加熱・焼結により生じた酸化物（$^{239}PuO_2$）エアロゾル（AMAD：0.3-0.4μ、σ＝

2.0）を、雌のWistar系ラット（体重200-250g）に吸入した。吸入直後および一定期間毎に、LX線を検出する体外計測法により肺組織内沈着量を測定し、得られた滞留率曲線から初期沈着量（Initial alveolar deposition; IAD）を、また吸入後の時間（日数）までの肺組織全体に与えられた吸収線量を、滞留率と肺重量変化の関数の積分値とIADおよび諸係数によりそれぞれ計算した（アルファ放射体による組織微細線量評価に関する研究の項参照）。吸入動物は、同年齢の無処置対照群とともに終生飼育し、死亡個体について解剖と肺組織等の病理組織学的検索により、肺腫瘍誘発率を検討した。

(2)プルトニウム注射投与マウスにおける腫瘍誘発とそのスペクトル

硝酸塩からクエン酸塩に変換、pH 6-7に調整後、250nm poreサイズのミリポアフィルターを通過させ、生理食塩水で一定濃度に希釈した可溶性プルトニウム（^{239}Pu）をC3H / He系雌マウスの腹腔内に注射投与した。マウスは、同年齢の無処置対照マウスとともに終生飼育し、死亡個体について解剖と腫瘍組織等の病理組織学的検索により、腫瘍誘発率とスペクトルの違いを比較検討した。

(3) in vitro α線照射細胞による生物効果検出系の予備的検討

^{241}Am密封線源を用いてそのα線（3.2MeV、138KeV / μm、線量率0.1Gy / min）を薄膜（ダイヤホイル）上に付着・培養した細胞に照射し、生物効果を検出するシステム（アルファ放射体による組織微細線量評価に関する研究の項参照）を用い、予備的検討のため、マウス骨髄細胞および肺胞マクロファージによるコロニー形成能を生物学的パラメータとして、線量－生存率効果を検討し、^{137}Csのγ線（線量率1.0Gy / min）照射細胞のそれと比較した。コロニー形成能は照射直後の細胞をそれぞれ一定数、コロニー刺激因子（M-CSF）を含む0.5%アガロース培地を加えた径35㎜のプラスチックプレート上で7-21日培養し、固定・染色後生じたコロニー数を算定、比較した。

3．結果

(1)酸化プルトニウム吸入ラットにおける肺腫瘍誘発と線量効果関係

研究期間内に行った酸化プルトニウム吸入実験は、計8回、それぞれ20匹ずつ計160匹のラットに吸入させた。このうち約30匹は初期沈着量と滞留率測定のために定期的に処分され、残りを吸入量（Bq）の違いにより、次の4群および対照群に分けて終生飼育し、肺腫瘍誘発効果の検索に用いた。

グループ	吸入量（Bq）	動物数
対照	0	60
Level 1	< 740	18
Level 2	740 - 925	30
Level 3	925 - 1295	32
Level 4	1295 <	34

このうち、対照群の約70％と吸入量1000Bq以下（Level 1 および2）の動物の一部は現在（1993年10月）でも生存しているが、吸入量1000Bq以上（Level 3および4）の動物は全て吸入後約600日までに死亡した。それぞれの生存率の推移を図1に示すが、高レベル吸入群（Level 3および4群）は、250-300日より死亡が観察され、以後急速に死亡率が増加し、平均生存日数はそれぞれ454日（Level 4）および524日（Level 3）であった。これに対し低レベル吸入群（Level 1および2）は、500日以降より死亡が観察され、700-800日までに約40％および26％がそれぞれ死亡し、平均生存日数696日および593日であった。このように対照群の平均生存日数775日、生存率約70％と比較し、吸入群ではより早期の死亡が明らかではあるが、吸入レベルの低いものでは、死亡時期の遅延が明らかである。

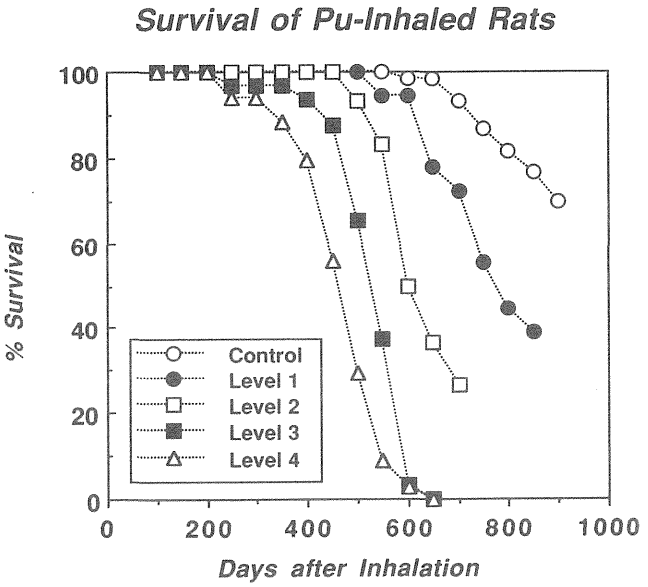

図1　酸化プルトニウム吸入ラットの生存率

この死亡の主要因は、肺腫瘍であるが、対照群においては、乳腺腫瘍、腎障害等他の原因が多く、肺腫瘍は現在のところ全くみられていない。プルトニウム吸入群の肺腫瘍発生率は、対照群と明らかに異なり、レベルに応じた累積増加率を示している（図2）。すなわち、高レベル（Level 3および4）群では、250日より増加し、最終的な肺腫瘍発生率は、それぞれ約97％であったが、低レベル（Level 1および2）群では、一部未だ生存中ではあるが、遅れて500日より増加し、現在それぞれ約55％および73％の発生率を示しており、今後さらに発生率が累積されるものと考えられる。肺腫瘍の病理組織型としては、これらの約80％以上が、深部細気管支－肺胞部より発生した腺癌（adenocarcinoma）で、一部化生して類表皮癌（epidermoid carcinoma）あるいは扁平上皮癌（squamous carcinoma）の形態を示した。なお肺腫瘍の組織型には吸入レベルによる大きな違いはないものの、低レベル吸入群では、腫瘍病巣が比較的限局されている傾向が強く、また、とくに高レベル吸入群では、線維化病変が顕著で、その周囲に腫瘍病巣がみられる場合が多かった。

次に、肺腫瘍により死亡した個体ごとに、肺吸収線量を計算し、その分布を吸入レベルごとに分類すると、図3に示すようにLevel 1では3-5Gy、Level 2では5-7Gy、Level 3では6-8Gy、Level 4では8Gy以上と吸入レベル

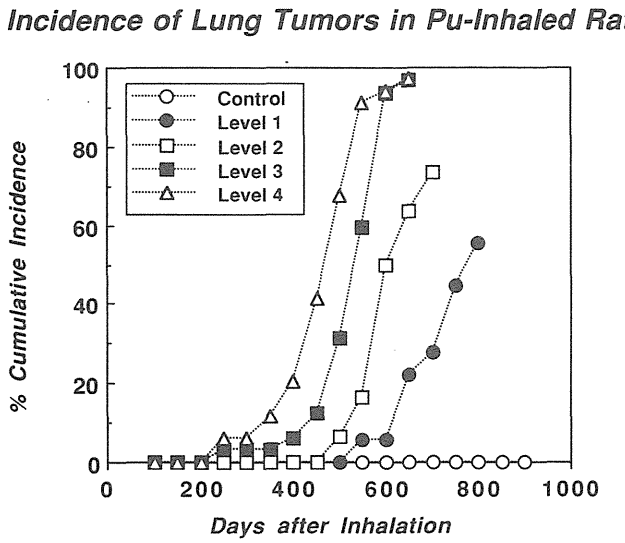

図２　酸化プルトニウム吸入ラットの肺腫瘍累積発生率

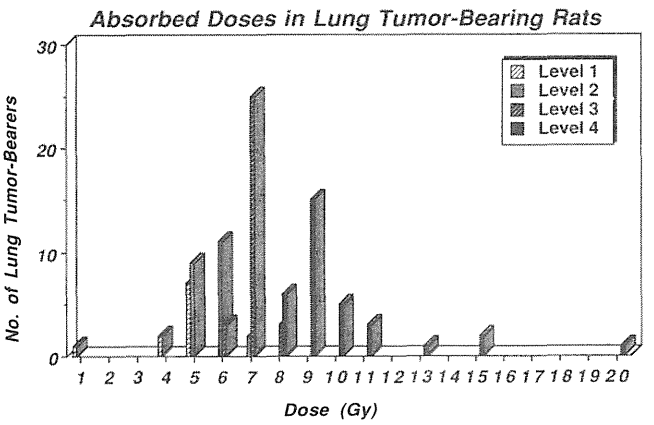

図３　酸化プルトニウム吸入ラット肺腫瘍例の肺吸収線量分布

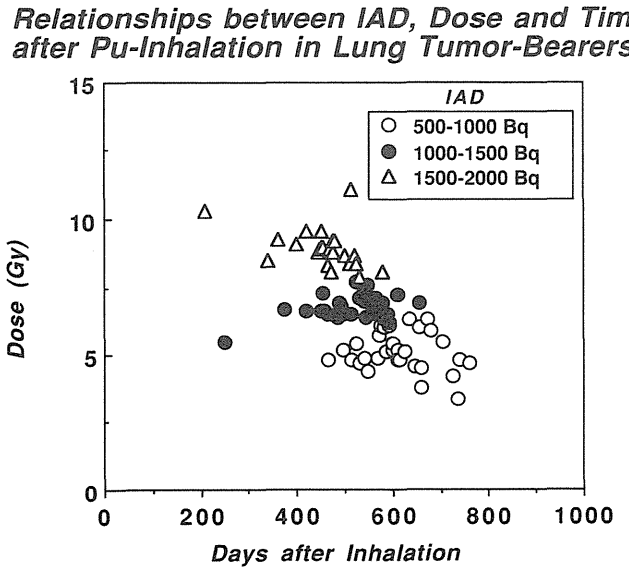

図４　酸化プルトニウム吸入ラット肺腫瘍例の肺吸収線量と初期沈着量（IAD）ならびに吸入後の時間との関係

の高低による差がみとめられ、高レベルほど大きかった。さらに、初期沈着量（IAD）、吸収線量および生存時間（日数）との関係をみたところ、IAD 500-1000Bq の個体の線量は、平均 5Gy で 600-800 日に、1000-1500Bq では平均 7Gy で 400-700 日に、また 1500-2000Bq では平均 8Gy で 300-600 日にそれぞれ最も多く分布し、初期沈着量レベルにより異なるが、肺腫瘍により死亡するまでの時間と吸収線量との間には一定の関係があることが推察される（図４）。しかしながら低レベル群の一部個体の検索では、1Gy 以下でも肺腫瘍が発生しており、今後肺腫瘍誘発の線量効果関係が詳細化されると思われる。

(2)プルトニウム注射マウスにおける腫瘍誘発とそのスペクトル

可溶性プルトニウムを、投与レベルの異なる次の４群のマウスに分けて注射投与し、無処置対照群とともに、終生飼育して腫瘍誘発率およびそのスペクトルを比較・検討した。

グループ	投与量（Bq）	動物数
対照	0	60
Level 1	500-600	30
Level 2	1000-1500	30
Level 3	5000-6000	30
Level 4	10000-11000	30

このうち対照群の動物は現在約 60 %が生存中であるが、プルトニウム投与群の動物のほとんど全てが 700 日までに死亡した。生存率の推移は図５に示すとおりで、高レベル（Level 3 および 4）群は、約 200 日から死亡が観察され、500 日までにほぼ全例が死亡し、平均生存日数は 350-360 日であったのに対し、中レベル（Level 2）群はやや遅れて 300 日から 600 日に全てが死亡、平均生存日数は 430 日であった。低レベル（Level 1）群は、さらに時期が遅れて 400 日から 700 日までに 95 %が死亡し、平均生存日数 530 日であった。いずれのプルトニウム投与群もレベルによる差が明らかであるが、対照群の平均生存日数 750 日と比較して、早期の死亡が特徴であった。この早期の死亡の主要因としては腫瘍発生以外に、高レベル群（とくに Level 4）においては急性造血器障害によるものが多かった。腫瘍による累積死亡率の推移を図６に示すが、対照群では 600 日以降に腫瘍死が観察され、現在（1993 年 10 月）までに約 30 %に達しているのに比べて、Level 1 では 400 日から約 45 %、Level 2 では 300 日から約 67 %に、また Level 3 では 200 日から 63 %に、それぞれ腫瘍死がみられた。しかし最もレベルの高い Level 4 群では 200 日よりみられるものの最終的な累積腫瘍死は約 34 %にしか達しなかった。これは急性死によるためと考えられる。

発生した腫瘍を病理組織学的に分類すると、対照群では肝癌（hepatocellular carcinoma）、リンパ腫（lymphoma）、卵巣腫瘍（granulosa cell tumor あるいは adenocarcinoma）および肺腫瘍（adenoma あるいは adenocarcinoma）がほとんどであったが、プルトニウム投与群では、骨肉腫（osteosarcoma）、リンパ腫ならびにリンパ性白血病（lymphoma / lymphatic leukemia）が大部分を占めていた。各群におけるこれら腫瘍の発生率を骨肉腫、リンパ腫・白血病およびその他の腫瘍（肝癌等）に分けて比べ

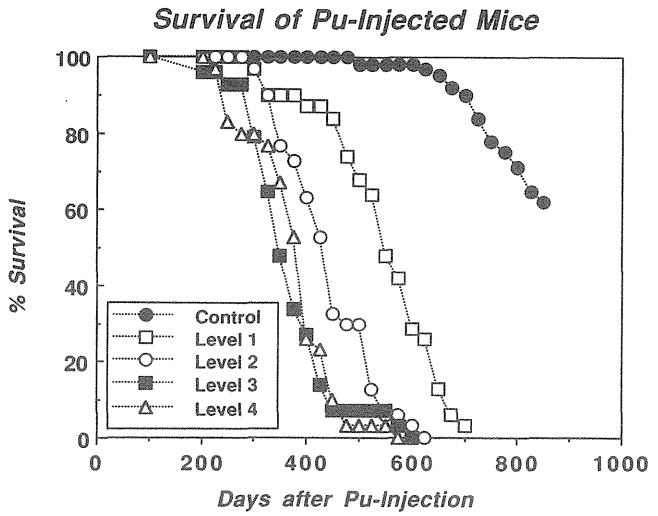

図５　プルトニウム注射投与マウスの生存率

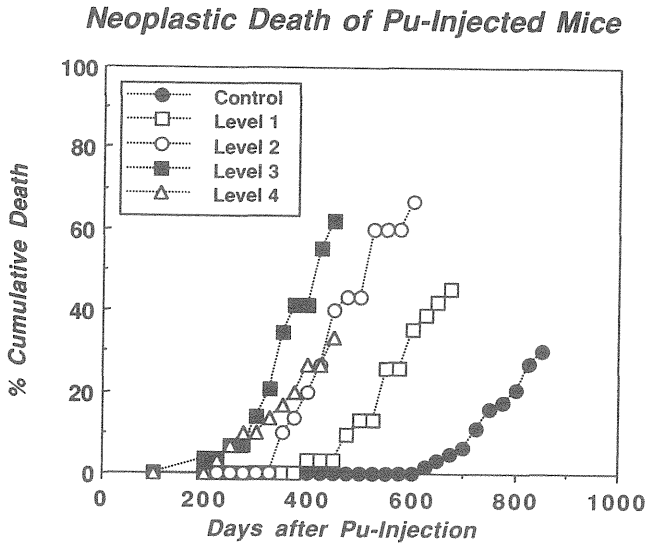

図６　プルトニウム注射投与マウスの腫瘍による累積死亡率

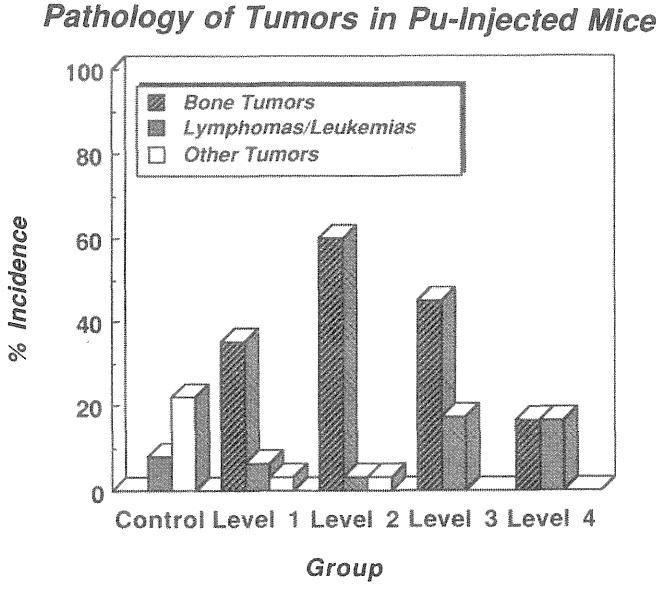

図７　プルトニウム注射投与マウスに誘発された腫瘍の発生率

ると、図７に示すように、骨肉腫は対照群で全くみられないのに対し、投与群ではLevel　1で35％、Level　2で60％、Level 3で45％、Level 4で17％と投与レベルに依存した増減を示した。リンパ腫・白血病は、高レベルのLevel　3および4で約17％であり、対照群の約８％と比べて有意に高いが、低レベル群（Level 1および２）では６％以下であり、有意差はみられなかった。その他の腫瘍については高レベル投与群では全くみられず、低レベル群で約３％であり、対照群の24％に比べて低かった。これは対照群の腫瘍（とくに肝癌）が700日以降にみられるのに対し、プルトニウム投与群ではそれより早期に骨肉腫あるいはリンパ腫・白血病等で死亡してしまうためと考えられた。このことは、実際に腫瘍の発生時期を比較してみると、プルトニウム投与群での骨肉腫は300-400日より、またリンパ腫・白血病は200-300日よりそれぞれ出現するのに対し、対照群の全ての腫瘍は600-700日から出現することからも明らかである。

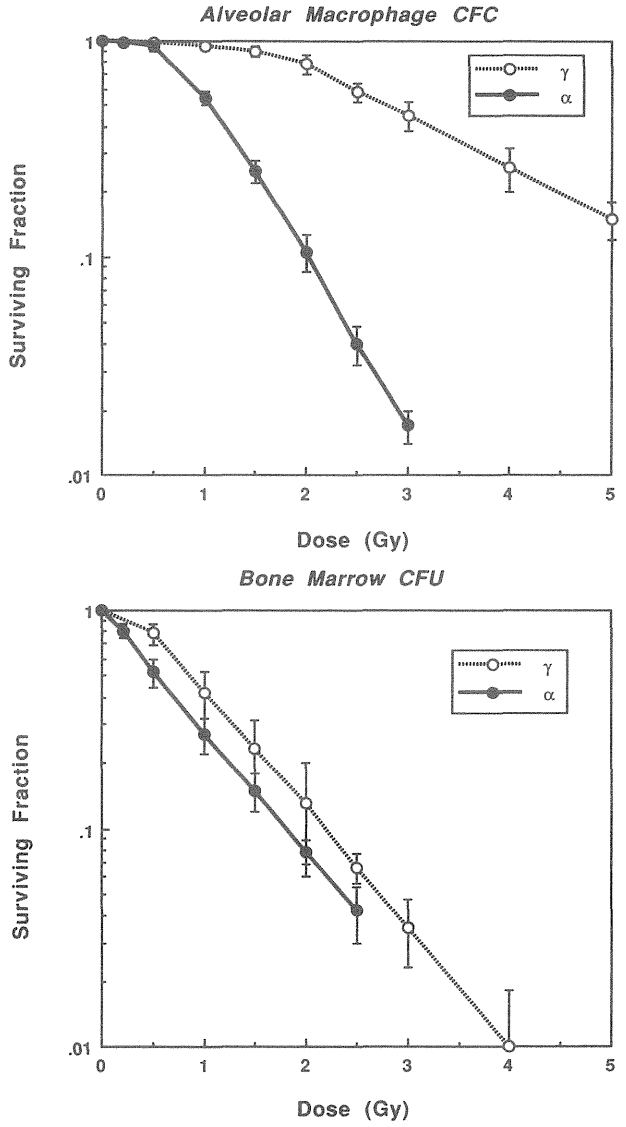

図８　α線およびγ線照射肺胞マクロファージ・コロニー形成細胞（上）および骨髄CFU（下）の生存率曲線

(3)肺胞マクロファージおよび骨髄細胞のコロニー形成に対するα線照射の効果

コロニー形成能を指標としたα線およびγ線照射肺胞マクロファージの生存率曲線はきわめて異なり、線質による放射線感受性の違いが明らかであった（図8）。この場合のD_0値は、それぞれ0.5および2.0となり、D_{37}値で比べた生物学的効果比（RBE）は約2.1と推定された。一方、造血コロニー形成能を指標としたα線照射骨髄細胞の生存率曲線は、肩のほとんどない直線となり、γ線照射の場合と比べると、D_0値は0.8と同じであるが、D_{37}値で比較したRBEは約1.5となり、肺胞細胞との放射線感受性の違い（骨髄細胞の方が高い）が明らかであった（図8）。

4．考察

プルトニウムは、超ウラン元素のうち最も毒性の強いα放射性核種に位置付けられているが、人体障害例についての報告は未だなく、従って人体でのリスク評価は、動物実験による詳細な線量ー効果関係によって導き出さざるを得ない。プルトニウムの発癌性に関する動物実験データは、米国等でのイヌを用いての大規模実験がすでに行われ、とくに注射投与等により、血液に移行したプルトニウムが閾値のない直線的線量効果関係で骨肉腫を誘発することが知られているものの、これをヒトに外挿するために必要な動物種差、標的細胞レベルでの線量分布や感受性の差等様々な生物学的パラメータは十分明らかにされていない。さらに骨肉腫以外の腫瘍、例えば白血病などがプルトニウムの内部被曝により誘発されるとされているが、その線量効果関係やスペクトルについての情報は乏しい。一方、特異的ではあるが重要な被曝形式である吸入被曝に関しても、イヌを用いた大規模実験により、化学形やエアロゾル粒子径等による発癌（肺腫瘍誘発）の線量効果関係がある程度明らかにされているが、低レベル酸化物エアロゾルの吸入による発癌率等についてのデータはほとんどないのが現状である。このような観点から、我々はラット、マウスのような小動物におけるプルトニウムの発癌性について、注射投与による腫瘍誘発のスペクトルおよび吸入投与による肺腫瘍誘発の低線量域での発癌率にそれぞれ焦点を絞り、研究を行った。また同時に、プルトニウムの生物学的効果比を推定するために、α線による標的細胞レベルでの生物学的効果とその線量効果関係を検出する実験系の確立を試みた。

不溶性酸化物プルトニウム・エアロゾルのラットへの吸入実験は、全てsubmicronサイズの粒子径（AMAD：0.3-0.4μm）で行われたが、これは大部分肺深部に沈着し得る大きさのエアロゾルであり、実際にデータには示さなかったがミクロオートラジオグラフィーにより肺胞部への沈着を確認しており、誘発された肺腫瘍も全て細気管支ー肺胞部の上皮細胞より生じた腺癌、類表皮癌あるいは扁平上皮癌であり、上部気道粘膜等より生じた腫瘍はなかった。さらに今回の実験では、大部分の動物の吸入量（初期沈着量）が1000-2000Bqで、これまでにラットで報告されている吸入レベルの内でも比較的低い範囲にあったが、発癌率（肺腫瘍誘発率）はきわめて高く、1000Bq以上の2群では、97％にも達した。また、1000Bq以下の群ではこれより死亡時期が遅れ、一部生存中ではあるが、約60％以上で比較的高く、死亡個体の90％以上は肺腫瘍であるため、今後さらに発生率の累積増加が期待される。従って、肺腫瘍発生率と吸入量との関係を明らかにするためには、これら比較的低レベル吸入群での最終的な結果に加えて、さらに極低レベル、例えば100-500Bqあるいは100Bq以下の群における発生率に関する検討が必要と思われる。現在この極低レベル群の吸入実験を施行中である。

吸入による肺腫瘍発生についての線量効果関係の確立のためには、肺全体および組織微細部分における線量評価が不可欠である。これまでに報告されているプルトニウム吸入動物での肺吸収線量は、比較的大きく8Gy以上と推定されるものが多いが、今回我々が体外計測法により推定した吸収線量は、3Gyから8Gyのものが多かった。これは粒子径の違い、肺深部における分布の均等性等様々な物理学的要因を考慮する必要があろうが、1Gy以下のものでも肺腫瘍誘発がみとめられているので、肺腫瘍誘発に必要な線量は、おそらくさらに低いと推定される。そのためには、低レベルあるいは極低レベル群についての十分なデータが必要であろう。しかしながら、今回推定された肺腫瘍例での吸収線量は、初期沈着量にもよるが、平均ほぼ5-8Gyのものが最も多く分布しており、死亡するまでの時間と吸収線量の大きさとの間には一定の関係があり、単に線量の蓄積だけでなく、それに達するまでの時間が腫瘍誘発に必要であることも考えられる。

次に血液移行したプルトニウムによる腫瘍誘発のスペクトル検討のため行った注射投与マウスでは、予想したとおり骨肉腫が多発し、しかも投与レベルにより発生率に差がみられた。この場合、高レベル（5000-10000Bq）投与群においては、骨肉腫の出現する以前に急性造血障害あるいは早期のリンパ腫・白血病により死亡する割合が高いため、みかけ上の発生率が低くなると考えられる。また、肝癌や卵巣腫瘍など対照群で600日以降出現するその他の腫瘍についてもプルトニウム投与群ではきわめて低かったが、これも同様であると考えられる。骨肉腫以外の腫瘍として、高レベルのプルトニウム投与動物ではリンパ腫・白血病が対照群に比べて有意に高く、かつ早期に出現したが、低レベル群では対照群よりも低かった。マウスにおけるリンパ腫発生はプルトニウム投与動物でもこれまで報告されているが、いずれもかなり高レベル投与においてのみ対照レベルより高い値を示している。我々の場合、すべてのリンパ節・リンパ組織を侵襲するタイプのものがほとんどであり、プルトニウムの沈着は胸部以外みとめられなかったので、このリンパ腫の誘発にプルトニウム（のα線）が直接関わっているとは考えにくい。このメカニズムについては、外部照射によるリンパ腫発生と比較したとき興味深いものがあるが、現在のところ不明である。なお、骨に沈着したプルトニウムが、骨細胞のみならず骨髄細胞にもそのα線の効果を及ぼすことは、よく知られているものの、今回の実験では、いずれの群（対照群も含めて）でも骨髄性白血病は観察されていない。他報告にもあるように、骨髄性白血病はきわめて低い線量でしか起こり得ず、今回の投与量ではむしろ細胞死のほうが先行してしまうためと考えられるが、標的細胞によっては放射線感受性の差が腫瘍誘発の違いを決定するひとつの要因であると思われ、極低レベル、例えば100Bq以下のような投与量による実験を現在遂行中である。

α線を直接標的細胞に in vitro 照射し、その生物効果を検出し、線量効果あるいはRBE等を明らかにすることは、プルトニウムの生物影響評価を補完するうえで重要である。このため、我々は^{241}Am線源を用いた照射・培養装置を開発して、実験を開始した。今回は、コロニー形成を指標とした生存率に関する実験のみ行っただけであるが、肺および骨髄細胞における線量効果の違い、およびこれら標的細胞の放射線感受性とα線による致死効果がγ線による反応とかなり異なることが明らかにされた。今後は、このシステムを用いて、例えば突然変異の出現率など生物学的パラメータと線量評価の検討を行ってゆく予定である。

5．まとめ

プルトニウムによる内部被曝のリスク評価において重要な生物学的パラメータを明らかにするため、重要な被曝形式である酸化物エアロゾルの吸入によって誘発される肺腫瘍、血液移行したプルトニウムによる腫瘍誘発、および標的細胞レベルでのα線照射による生物効果をそれぞれ検討した。プルトニウム吸入ラットにおける肺腫瘍誘発率は、きわめて高く1000Bq以上で97％、1000Bq以下で60-70％に達した。また、吸収線量は初期沈着量により異なるが、平均で5-8Gyのものが多く、死亡するまでの時間との間には一定の関係がみとめられた。プルトニウム注射マウスにおいて誘発された腫瘍のうち、骨肉腫は最も多く、投与レベルにより17-60％の発生率を示したが、このほかリンパ腫・白血病が高レベル投与群において17％と有意に高い発生率で、かつ早期に出現した。α線を照射した肺胞細胞および骨髄細胞のコロニー形成能を指標とした生存率はいずれもγ線と比較して低く、線質による違いおよび細胞の放射線感受性の違いが明らかとなった。

6．研究発表

1）Oghiso, Y., Yamada, Y., and Shibata, Y. : Radiosensitivity of macrophage colony-forming cells. Implications for their heterogeneity. J. Radiat. Res., 31, 324-332, 1990.

2）Ishigure, N., Nakano, T., Enomoto, H., Fukuda, S., Iida, H., Oghiso, Y., Yamada, Y., and Inaba, J. : Assessement of initial alveolar deposition on rats exposed to plutonium aerosols using a whole body counter. Hoken Butsuri, 27, 135-142, 1992.

3）Inaba, J., Takahashi, S., Sato, H., Ishigure, H., Nakano, T., Enomoto, H., Oghiso, Y., Fukuda, S., Yamada, Y., Iida, H., Koizumi, A., Yamada, Y., and Miyamoto, K. : Biokinetics and biological effects of inhaled plutonium in rat. Proceedings of International Conference on Radiation Protection, 247-249, 1992.

4）Oghiso, Y. and Yamada, Y. : Heterogeneity of the radiosensitivity and origins of tissue macrophage colony-forming cells. J. Radiat. Res., 33, 334-341. 1992.

2．超ウラン元素の生物効果に関する比較毒性学的研究
③　骨代謝ならびにプルトニウムの骨に対する効果に関する研究

福田俊、飯田治三（内部被ばく研究部）

Bone Metabolism and Effects of Injected Plutonium in Rats and Beagle Dogs

Satoshi Fukuda and Haruzo Iida
Division of Comparative Radiotoxicology

Bone metabolism and some regulation factors related to bone were examined in rats and beagle dogs in order to be useful of carrying out the experiments on the effects of injected plutonium-nitrate to bone and other organs, and evaluating the results obtained from experiments for human damages.

The results examined on the age-related changes in bone metabolism of Wistar-Mishima (WM) rats by histomorphometry and analyses of bone strength, mineral contents, serum biochemical constituents related to bone showed that bone mass and surface area, strength and mineral contents in bone increased with development and reached to the peak at the age of 12 months both sexes, thereafter these parameters decreased with age, indicated that the age of 12 months in rats would correspond to the age of 30-40 years in human and the age of 2-4 years in beagle dogs when the bone mass and bone mineral density were highest. Some factors occurring the reductions of bone mass and fragility of bone such as the loss of sex hormone by ovariectomy and orchidectomy, decrease of stimulation to bone by reductions of body burden and exercise in fixed of hind limb with the body, x-ray irradiation to whole body, locally to hind limb or neck including parathyroid and thyroid in WM rats, osteoporosis and decrease of intestinal calcium absorption in the stroke-prone spontaneously hypertensive rats, and some beneficial factors of preventing loss of bone mass such as exercise by swimming, calcium supplement were examined.

Plutonium contents (Bq / kg) in bone, liver, spleen, kidney in rats were highest at the age of 12 months compared to those at the age of 3 or 24 months both sexes, and were higher in female than male, and higher in ovary than in testes. These results suggested that the contents of plutonium deposited in bone and other organs were highest at the middle age (30-40 years) in human that might correspond to the age of 12 months in rats. Plutonium nitrate of 0.185-3.7 $\times 10^5$ Bq / kg was injected peritoneally to rats in order to examine the long term effects, up to now the shortening of average of life span and decrease of body weight, bone tumor were found out. In dogs injected intravenously plutonium nitrate, about 18 % of administered dose was excreted in urine and feces 4 weeks later, and remaining 82 % including 20 % in liver retained in the body. Plutonium content was highest in trabecular bone, subsequently cortical bone and bone marrow, tended to increase in the trabecular bone but decrease in cortical bone and bone marrow. The observation of plutonium-oxide inhaled beagle dogs was initiated.

X-ray irradiation to whole body (1.25-5.0Gy), hind limb (1.25-15.0Gy), and neck (1.25-15.0Gy), and neck (1.25-15 Gy) of 4 week-old rats caused not only the shortening of length of bones in hind limb induced by damage of growth plate, but also decrease of bone mass, mineral density and fragility, and the magnitudes of these bone damages were strongly in whole body > hind limb > neck irradiated groups in order. The damages of bone by neck irradiation were induced by loss or decrease of calcium regulating hormone such as parathyroid hormone and calcitonin.

Plutonium nitrate was injected immediately or 7 days after whole body (2.5 and 5.0 Gy), hind limb (15Gy) or neck (15Gy) irradiation to examine the effects of combinations of x-ray external and Pu internal irradiation. Plutonium contents (Bq / kg) of bone immediately after x-ray irradiation did not change but decreased 7 days post-plutonium injection in whole body irradiated group, while those decreased both immediately and 7 days after plutonium injection in

hind limb or neck irradiated group. All results on plutonium deposition and bone metabolism obtained in this study can be available to assess the risk by plutonium intake in human. In this study, the anatomical and physiological analyses of the trachea-bronchi and respiratory exercise in beagle dogs, and pathological examinations of rats and beagle dogs were also done.

1．緒言

骨親和性核種であるプルトニウム（Pu）の人の、とりわけ骨に対する影響を評価するために、これまでに進めているビーグル犬に加えてラットの骨代謝に関する基礎的およびその修飾因子に関する検索を先行させながら、これらの結果に基づいて注射投与した硝酸Puの初期沈着および効果について検討を進めた。とくに、Puの沈着や効果に対する年齢、雌雄差、骨代謝に影響を及ぼす生理的な種々の要因について、また放射線感受性や線量評価を行うために外部被曝の影響、外部被曝との複合被曝の影響について検索した。さらに犬に関しては、Puの吸入実験における実験条件の設定および影響評価のために、気管ー気管支の解剖学的な特徴および呼吸の生理的運動について、またビーグル犬およびラットにおけるPuの効果を評価するために自然発がんに注目した病理学的な基礎データの集積も実施した。

2．方法

1）骨代謝の検索方法

骨の形態および代謝の検索は、骨標識した非脱灰組織標本による骨形態動態計測法、骨強度試験法、骨含ミネラル分析法、骨代謝に関連した血清生化学成分の分析法、走査電子顕微鏡観察法などを用いて行った。

(1) 骨形態動態計測法：ビーグル犬およびラットの骨組織の動態を解析するために、骨標識剤であるテトラサイクリンとカルセインを一定間隔で投与して骨二重標識を行なった。犬の生検採取した腸骨やラットの脛骨をVillanueva's bone stainで染色、アルコール脱水、メチルメタクリレート樹脂包埋、薄切、研磨して非脱灰骨組織標本を作製した。また、必要に応じてToluidine blue染色を行った。犬の腸骨の海綿骨部分、ラットの脛骨の近位骨幹端の海綿骨（secondary spongiosa）部分を対象に、蛍光顕微鏡で観察しながら骨組織形態計測用の半自動画像解析装置を用いて、形態および動態の計測を行った。

(2) 骨強度試験：ラットの大腿骨の強度（破断力および変位）は骨強度試験装置によって測定した。測定部分の下方の2点の支柱に大腿骨を置き、上方から1点の支柱が下方の2点の中央に位置するように加重を加え、骨が破断した時の加重力と変位（しなりの距離）を測定した。

(3) 骨含有ミネラル量の測定：ラット大腿骨の生重量、乾燥重量（24時間、100℃）、灰化重量（24時間、600℃）を測定した。灰化した骨は硝酸で溶解した後、カルシウム量はCresolphthalein conplexone法で、リン量はMolybdenum blue法でそれぞれ測定した。これらの結果から、生骨重量に対する水分含有量（生骨重量ー乾燥重量）、有機成分重量（乾燥骨重量ー灰化重量）、灰分量、カルシウム量、リン量の比率を求めた。

(4) 骨代謝関連血清生化学成分の測定：血清中のParathyroid hormone, Calcitonin, Vitamin D metabolites, Alkaline phosphatase activity, Total and ionized calcium, Phosphorusなどを測定した。

2）硝酸Puの注射投与および濃度測定

硝酸Pu原液をクエン酸でpHおよび濃度調整後、(1)ラットを用いた長期（終生）飼育による発がんおよび障害の検索（Pu投与群：0.37-3.7x10^5 Bq / kgの4段階、合計255頭）、(2)ラットにおけるPu沈着量の年齢差、雌雄差および初期挙動の検索、③ラットにおける外部照射と組み合わせた場合の骨へのPu沈着量に及ぼす影響、④ビーグル犬（6頭）における初期の臓器沈着量と体内挙動の検索を目的として、静脈あるいは腹腔内投与した。また、成犬（6頭）に酸化Puを吸入させ、肺への初期沈着と糞尿中への排泄の経時変化の測定を開始した（一部は長期実験中）。

各実験で採取した臓器や糞尿中のPu濃度は、灰化処理後、液体シンチレーションカウンターで測定した。

3）外部照射

成長および成熟ラットの全身あるいは局所（後肢、頸部）にX線照射を1回行った。線量は、全身照射群では0-15Gy, 局所照射群では0-25Gyとした。

4）犬の気管一気管支の解剖生理学的および呼吸機能の生理学的検討

成犬から摘出した肺にシリコン樹脂を流し込んだ後、肺組織を苛性ソーダで溶解して気管一気管支キャストを作製した。麻酔した成犬の肺に造影剤を注入し、生理的な呼吸運動と判断される範囲における最大呼気と吸気時、および強制的に拡大した時（最大拡張）の気管一気管支のX線造影写真を撮影した。気管一気管支キャストおよびX線造影写真から、犬の気管一気管支の分岐図の作製と呼吸運動に伴う気管支の伸縮率（長さおよび直径）や動態を計測した。さらに、麻酔した犬に気管カテーテルを挿入しポリグラフを用いて呼吸曲線を測定した。

5） ビーグル犬およびラットの病理学的検索

ビーグル犬およびラットを長期飼育しながら、生存年齢や発生腫瘍など臨床病理学的検索を行った。

3．結果

1）ラットおよび犬の骨代謝とその修飾因子

雌雄Wistar-Mishima（WM）ラットの海綿骨の骨量や骨表面積は成長に伴って増加し、12カ月齢でピークに達した後、加齢が進むにつれて減少した。（Fig.1）。石灰化速度や骨形成速度は成長に伴なって急速に減少し、12カ月齢以降ほぼ一定になった。骨強度やカルシウム、リン含有量は12カ月齢まで増加し、6-12カ月齢まで水分含有率は減少、灰分含有率は増加した後それぞれ一定になったが、24-27カ月齢以降に雄の水分含有率の増加、灰分含有率の減少がみられた。すなわち、WMラットにおける骨の形態および代謝の年齢変化は、生後から12カ月齢までの骨組織量、骨塩量、強度が増加し続けてピークに達する急速な成長およびそれに続く成熟過程と、12カ月齢から老齢に至るまでの全身的な加齢の進行に伴った骨組織や代謝活性の減少過程に分かれることが認められた。

骨代謝に及ぼす修飾要因である性ホルモンの消失の影響を卵巣あるいは精巣摘出して検索した結果、骨代謝は

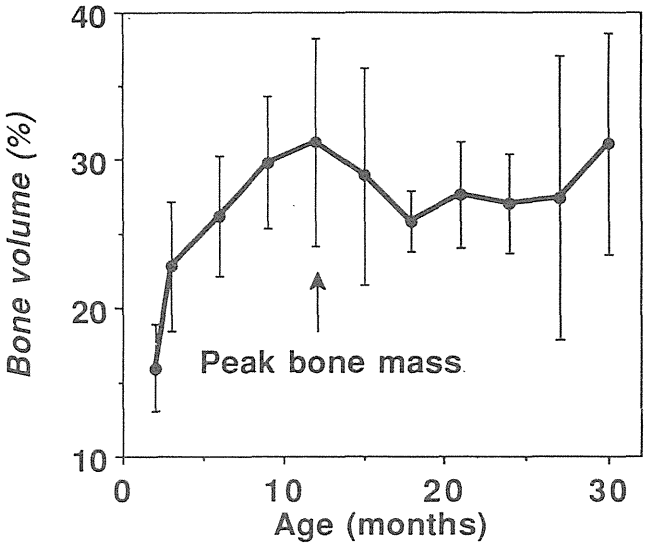

Fig.1 Age-related changes in bone volume in female Wistar-Mishima rats. There is the peak bone mass at the age of 12 months.

high turnoverになり、骨量が減少したが、その減少速度は12カ月齢以降の方が3ヶ月齢よりも著しかった。すなわち、性ホルモンが消失すると若い年齢では骨成長や形成障害による骨の組織量や骨塩量の減少および脆弱化が起こり、成熟および老齢期では骨代謝の維持機能の消失、減少が全身的な加齢変化も加わって著しく起こることが示唆された。高血圧自然発症ラット（spontaneously hypertensive rat; SHR）および脳卒中易発症SHR（stroke-prone SHR;SHRSP）の骨の形態および代謝の年齢変化を、正常血圧のWistar Kyoto（WKY）およびWMラットと比較した結果、とりわけSHRSPの骨代謝はLow turnoverを示し、5ヵ月齢以降から骨量の減少や脆弱化（骨粗鬆症化）が著しく進むことを初めて確認し、その原因が従来報告されている腎臓からのカルシウム多量排泄だけでなく、Vitamin Dの低代謝、高血圧および腸管からのカルシウム吸収機能の低下にもあることを認めた。WMラットにおける片側の後肢を体躯に固定して体重や運動の骨に対する負荷重による刺激を除いた結果、骨粗鬆症化がみられた。このような骨粗鬆症化に対して、水泳運動による骨刺激やカルシウム補給を行うと予防および回復効果が認められた。

2）骨代謝の加齢性変化とPuの初期沈着量の関係

(1) Pu注射投与ラットの長期観察実験は現在も継続中であるが、これまでに得られた結果では、平均寿命は対照群では雄：687±166日（n＝201）、雌：806±222日（n＝248）であったが、0.37Bqx10^5 Bq/kg投与群では436±65日（n＝11）、0.925x10^5 Bq/kg投与群では498±145日（n＝26）、1.85x10^5 Bq/kg投与群では466±147日（n＝24）、3.7x10^5 Bq/kg投与群では345±175日（n＝6）であった。骨腫瘍の発生は後肢骨、腰椎に認められている。

(2) 3, 12, 24カ月齢に硝酸Puを腹腔内投与した2週間後の雌雄ラットの骨、肝臓、脾臓、腎臓の1g当りのPu濃度は、骨量および骨表面積が最大になる12カ月齢で最も高く、各臓器のPuの濃度は雌の方が雄よりも、また卵巣の方が精巣よりも高かった（Fig.2）。4週間後の各臓器濃度は、2週間後の結果と大きな差はみられなかった。

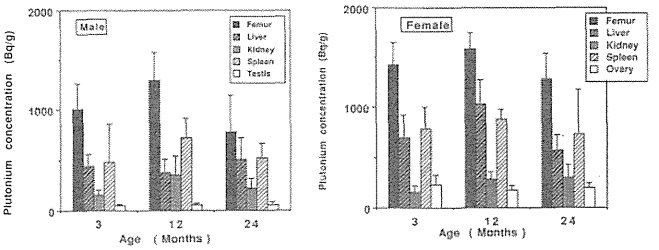

Fig.2 Plutonium contents in bone and other oragans 2 weeks after X-ray irradiation and Pu injection on various ages of male and female rats.

(3) 2歳齢の雌ビーグル犬に投与した硝酸Puの4週間後までの糞尿排泄は、投与4日後までは急速に、続く9日までは緩徐になり、その後一定となった。糞と尿への排泄割合は投与1日後では尿＞糞、2-15日後では糞＞尿、16日以降は尿＞糞であった。投与14日および28日後の糞尿中へ総排泄率はほとんど差がなく投与量の約18％で、体内に残った82％のうち約20％が肝臓に、その残りは骨やその他の臓器に沈着した。すなわち、Pu投与14日以降では体内からの排泄率は変化がみられないことを示した。各臓器のPu濃度（Bq/g）は、骨と肝臓が最も高く、続いて腎、脾、リンパ節、腸管、膵、血清の順に低かった。骨の各部分の濃度は、骨梁骨が最も高く、次に皮質骨、骨髄の順であった。骨梁骨への沈着を骨標識を用いて観察した結果、骨形成面への沈着が著しかった。2週間後と4週間後の濃度を比較すると、骨梁骨、肝臓、骨髄で増加がみられ、その他の臓器では減少傾向にあった（Table 1）。

Table 1 Plutonium contents in various organs 2 and 4 weeks after plutonium injection in beagle dogs

Organs	2 weeks after Pu injection	4 weeks after Pu injection
Liver	128.96±14.81 Bq/g	175.45±49.50 Bq/kg
Spleen	31.33±20.47	23.43±6.90
Kidney	37.97±15.73	24.94±3.86
Lung	8.74±2.57	6.45±2.87
Small intestine	5.39±0.92	2.76±0.36
Lymp node	18.84±4.37	15.49±5.35
Pancreas	4.63±2.25	2.15±0.24
Bone (Femur)		
Trabecular bone	159.00±45.00	301.00±93.00
Cortical bone	39.28±7.60	31.90±8.50
Bone marrow	14.13±4.30	16.36±10.81
Serum	2.17±0.42	0.88±0.36

3）X線による外部照射の骨代謝に及ぼす影響

骨の成長が最も激しい4週齢に1.25, 2.5, 5.0GyのX線を1回全身照射すると、照射線量の増加に対応して、増体重の減少、骨端軟骨の形成障害による骨長の短縮、骨形成量の減少、脆弱化の重度化が認められた。1.25-25.0Gyを後肢骨のみに照射した時にも同様な障害が線量の増加に応じて認められたが、同一の線量における障害の程度は全身照射よりも軽度であり、また同一個体の非照射側の骨では、ほとんど障害はみられなかった。1.25-25.0Gyを頭部のみに照射した時の後肢骨にも同様な骨障害がみられたが、その障害の程度は全身照射および後肢の局所照射に比べて軽度であった。すなわち、外部照射による骨障害は少なくとも1.25Gy以上で起こり、その障害の重度は同一線量では

全身照射が最も大きく、次に骨、頸部の順であった（Fig.3）。

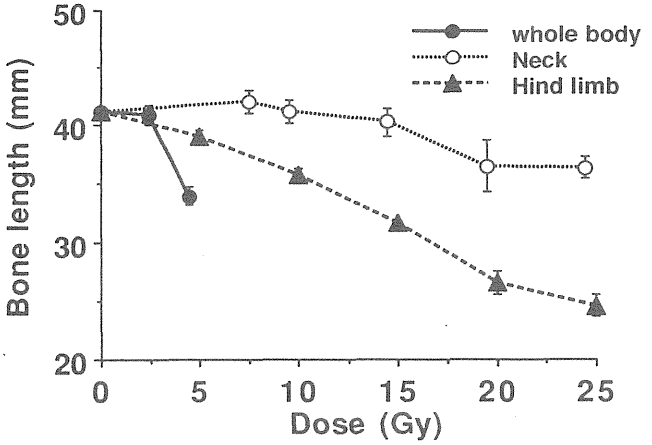

Fig.3 Longitudinal lengths of tibia 18 weeks after single irradiation to whole body, neck and hind limb at the age of 4 weeks in rats.

4）外部照射とPuの内部被曝の複合被曝

全身（2.5, 5.0 Gy）、片側の後肢（15 Gy）、頸部（15Gy）にX線を照射した直後および7日後に硝酸Puを投与して、それぞれ7日後の骨のPu濃度（Bq/g）を測定した結果、照射直後にPuを投与した場合の全身照射群では対照群に較べて変化はみられなかった。頸部照射では対照群に比べてPu濃度の減少が、後肢照射した骨では非照射側の骨および対照群に比べて減少がみられた。照射7日後のPu濃度は、全身照射では線量の増加に反して減少がみられた。局所照射では頸部、後肢の照射側と非照射側のいずれも対照群に比べていずれも同程度の減少を示した。（Fig.4）。

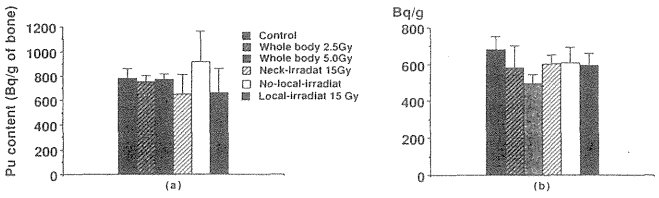

Fig.4 Plutonium contents in tibia 7 days (a) after x-ray irradiation and plutonium injection and (b) after plutonium injection 7 days post irradiation in rats.

5）犬の気管ー気管支の解剖および動態ならびに呼吸機能の解析

ビーグル犬の気管ー気管支の分岐マップを作製した。その結果、気管支の分岐は気管分岐部から非対称分岐を繰り返しながら細くなり、気管終末に近い部分から対称分岐が増加した。気管の分岐回数も部位によって著しい差が認められた。呼吸運動による胸腔内における呼気時の位置から最大拡張時の尾部方向および腹側方向への移動距離は、それぞれ気管分岐部が11.5, 13,5 mm, 後葉の終末に近い部分が15.5, 19.0 mm、また呼気時に対する最大拡張時の気管支の断面積は気管分岐部では1.31倍，後葉の終末に近い部分では1.59倍であった。すなわち、気管支が終末に向って細くなるにつれて、伸縮率は大きくなり、呼気時に対する最大拡張期の増加割合は50％以下であった。

呼吸曲線から分析した呼吸運動の特徴として、各呼吸間には長い静止期がある、吸気より呼気の時間の方が長い、最大流速は吸気より呼気時の方が大きい、呼吸数や一回換気量は年齢により異なるが分時換気量は一定であることが認められた。このような、呼吸の特徴は腹臥位および横臥位では一定であるが、背臥位では変化した。

6）犬およびラットの病理学的な検索

犬における悪性腫瘍の発生は8-12歳で高く、乳腺、肺、腎、脾、消化管（胃、小腸）の腫瘍、リンパ腫、血管肉腫などが観察されたが、骨腫瘍はみられていない。悪性腫瘍を発生しなかった個体の寿命はおおよそ15歳であった。詳細な病理学的な検索は検討中である。ラットでは、乳腺、肺、骨に腫瘍が認められた。

4．考察

ラットの骨量、骨強度、ミネラル含有量が雌雄ともに成長に伴って増加して12カ月齢にピークを示す様相は、人の骨量あるいは骨塩量のピークが30-40歳代にみられる様相と一致しており、骨形態や代謝を基準に比較するとラットの12カ月齢と人の30-40歳代が年齢対応し、それぞれの年齢とこれまでに検索した犬の2-4歳齢が対応していることが認められた。この成果は異なる年齢のラットに硝酸Puを投与した結果において骨の最大沈着量が12カ月齢に認められたのと一致した。すなわち、人がPuを摂取した場合、骨におけるPuの初期沈着量はいわゆる骨梁骨の表面積や量、骨塩量が最大になるmiddle ageが最も多いことを示唆した。骨内におけるPu沈着量は、犬の骨の検索から海綿骨が皮質や骨髄に比べてはるかに多く、骨梁骨の石灰化面に集中することが確認された。さらに、ラットにおいて観察された骨以外の肝臓、脾臓、腎臓へのPuの沈着量が12カ月齢で最も多かった結果は、これらの臓器においても加齢に伴ってPuの沈着量が増加するような新陳代謝速度や含有成分の変化が起こっていると推定された。本結果とビーグルのjuvenile、young adult, adultの各年齢に硝酸Puを投与すると、young adultやadultの方がjuvenileよりも寿命が短い研究報告と合わせると、Pu摂取による内部被曝の影響評価では幼若期の方が細胞の放射線感受性が高いために骨肉腫や重要な障害が発生すると説明されているが、Puの臓器沈着量の年齢による相違および沈着後の挙動も、重要な要因であることが示唆された。

Puを注射投与したラットの長期観察実験において得られた結果からは、対照群の平均寿命に比べて、Pu投与群では投与量が増加するにしたがって短くなり、多くの例で削痩が顕著である。ラットの骨腫瘍発生率に関しては人やビーグル犬に比べて低いとの報告があるが、この点については本実験で得られたラットの骨代謝と犬あるいは人との詳細な比較、あるいは平均寿命の短縮や骨以外の臓器にみられる障害を含めて、臓器中のPu濃度と病理組織検索を進めながら現在観察中の動物の最終的な検査結果が得られた時点でまとめたい。

外部被曝を全身に受けた場合の骨代謝の影響が骨へ直接被曝を受けた場合よりも重度であった結果は、骨代謝に関連した臓器だけでなくその他の全身の臓器の機能障害の影響が加わったためと推察された。とりわけ、骨およびカル

シウム代謝調節ホルモンであるParathyroid hormoneを分泌する副甲状腺およびcalcitoninを分泌する甲状腺のある頸部の局所照射によって、全身の骨代謝障害が生じることは、チェルノブイリ事故において問題とされる甲状腺がんの発生だけでなく、外部被曝や甲状腺に沈着した放射性ヨードによる副甲状腺や甲状腺の被曝による副甲状腺ホルモンやカルシトニン分泌の機能低下、および治療処置として副甲状腺を含めた甲状腺摘出に起因したこれらのホルモンの消失は、骨の発育障害や形成障害を起こす可能性が十分にあることを示唆している。

本実験において全身被曝と同時にPuを摂取した場合には骨へのPu沈着量は非被曝群と変わらないが外部被曝7日後にPuを摂取すると減少した結果は、上述した外部被曝の骨代謝への影響が遅れて現れたことを示した。後肢骨や頸部へ外部被曝を受けた場合には直後から骨のPu沈着濃度が減少した結果は、全身照射よりも照射線量が大きいために早期に重度な障害が発現したためであるが、少なくとも1.25Gy以上の局所照射を受けると全身照射群と同様な骨障害が認められることから、骨へのPu沈着量は減少すると推定された。しかし、外部被曝とPu摂取を同時に受けた場合の骨へのPu沈着量の減少は総合的な放射線障害の発生の軽減を示すものではない。したがって、放射線事故における外部被曝と内部被曝の複合被曝の影響に関する研究が今後も必要と考えられた。

Puの内部被曝の評価を行う場合、年齢によって臓器の沈着量に著しい相違が認められ、とくに骨に注目すれば成長期、成熟期、老年期の影響は、骨代謝を修飾する性ホルモン、運動、高血圧、腸管のカルシウム吸収機能などによって大きな影響を受けることが示唆される一方、障害リスクの軽減にもこれらの修飾要因の関与が重要であると判断された。

ビーグル犬の気管一気管支の解剖学特徴や動態および呼吸の波形や運動生理学的な検討によって得られた結果は、犬へのPuの吸入実験の条件設定だけでなく、Pu吸入量の算定、吸器系への吸入粒子状物質の沈着分布やその後の挙動の評価に有用であった。とくに、放射性物質の吸入被曝に用いられている人工モデルにおける呼吸の波形は連続運動する台形波や正弦波であったが、実験によって実測したこれらとは異なる波形や呼吸運動の成果は、シミュレートによるより精度の高い評価を得るために重要な成果であった。

ビーグル犬やラットに関する腫瘍に注目した病理学的な検索や種々の臓器や血液成分などに関する加齢性変化などの基礎研究の成果は、本研究において実施しているPuの代謝や影響実験の結果およびこれまでに外国で発表された研究論文の内容を評価するために有用であると判断された。

5．結論

本研究の結果から、人における骨や肝臓などの主要臓器のPuの沈着量は若年および老年に比べて、骨量や骨塩量がピークとなる中年期（30-40歳代）に、また男性よりも女性の方が多いことが認められた。骨では骨梁骨への沈着が最も多く、時間の経過につれてさらに骨梁骨の骨形成面に集まること、外部被曝を同時に受けた場合には全身被曝あるいは骨への局部被曝だけでなく、骨代謝やカルシウム代謝ホルモンの調節臓器である副甲状腺や甲状腺被曝の影響が重要であること、Pu摂取に伴う影響は寿命の短縮だけでなく、骨代謝を大きく修飾する年齢、性別、生活様式などの種々の要因を、人におけるPuの障害リスクを評価する場合に考慮しなければならないことが示唆された。

〔研究発表〕

1） Fukuda, S., Kawashima, N., Iida, H., Aoki, J. and Tokita, K: Age dependency of hematological values and concentrations of serum biochemical constituents in normal beagle from 1 to 14 years of age. Jpn. J. Vet. Sci., 51, 636-641, 1989.

2） Fukuda, S.: Circadian rhythm of serum testosterone levels in male beagle dogs. -Effects of lighting zone-. Exp. Anim., 39, 65-68, 1990.

3） 飯田治三、福田俊、川島直行、山崎友吉、青木純二、鴇田和実、森岡一憲、宝田奈美、添田照子：ビーグル仔犬の犬パルボウイルス、犬ジステンパーウイルスおよび犬伝染性肝炎ウイルスに対する移行抗体価の推移とワクチン摂取に対する応答について、実験動物、39, 9-19, 1990.

4） Fukuda, S. and Iida, H. : Effects of swimming in ovariectomized rats. Bone Morphometry. 157-160. Nishimura, Smith-Gordon, 1990.

5） 福田　俊、飯田治三：ビーグル犬の成長に伴う骨代謝の変化、骨の代謝と形態。86-91 , 西村書店、1990 .

6） 家森幸男、堀江良一、奈良安雄、池田克巳、福田　俊、飯田治三、土倉　覚、織間博光：骨粗鬆症自然発症ラットの確立とそれを用いた微小重力による骨量減少メカニズムおよび予防法に関する提案。第7回宇宙利用シンポジウムプロシーディング。286-290, 1990.

7） Fukuda, S. and Iida, H.: Preventive effects of swimming on the reduction of bone mass in ovariectomized rats. JBMM, 8, 61-62, 1990.

8） 百武衆一、後藤澄雄、山県正庸、神山知典、小林康正、福田　俊：運動負荷に対する骨変化に関する研究、日整会誌、7, 65, 1991.

9） Yamori, Y., Fukuda, S., Tsuchikura, S., Ikeda, K., Nara, Y. and Horie, R.: Stroke-prone SHR(SHRSP) as a model for osteoporosis. Clinical and Experimental Hypertension, 13, 755-762, 1991.

10） Fukuda, S., Iida, H., Miyamoto, T., Tanabe, M. and Takahashi, H. : Quantitative analysis of radiation damage in growth cartilage of rat using histomorophometric measurements. Radiation Research, Vol.l, 163, 1991.

11） 福田　俊、飯田治三：加齢に伴う雌雄ラットの骨代謝と卵巣、精巣摘出年齢による影響の差、日骨形態誌、1, 89-94, 1991.

12） Fukuda, S., Tsuchikura, S., Ikeda, K., Nara, Y., Horie, R. and Yamori, Y.: Bone metabolism of SHRSP and its characteristics as a model for spontaneous osteoporosis. Jpn. Heart J. 32, 586, 1991.

13） Tsuchikura, S., Fukuda, S., Nara, Y., Ikeda, K. and Yamori, Y.: Effect of dietary NaCl and calcium balance on bone mass in SHRSP as a

model for spontaneous osteoporosis. Jpn. Heart J., 32, 606, 1991.
14) Fukuda, S. and Iida, H.: Comparison of histomorphometric values in iliac trabecular bone of beagle dogs raised different breeding system. Exp. Anim., 41, 131-137, 1992.
15) Fukuda, S., Tsuchikura, S., Iida, H., Ikeda, K., Nara, Y. and Yamori, Y.: Further study on osteoporosis in SHRSP: Quantitaive analyses by bone histomorphometry and serum biochemical constituents related to bone. Genetic Hypertension. 218, 421-423, 1992.
16) Tsuchikura, S., Fukuda, S., Iida, H., Ikeda, K., Nara, Y. and Yamori. Y.: Effects of antihypertensive agents on osteoporosis in SHRSP. Genetic Hypertension. 218, 417-419, 1992.
17) 福田　俊、土倉　覚、飯田治三、池田克巳、奈良安雄、堀江良一、家森幸男：脳卒中易発症高血圧自然発症ラットにおける加齢に伴う骨梁骨の形態変化、日骨形態誌、2, 93-98, 1992.
18) 福田　俊、飯田治三：ビーグル犬における体重負荷が異なる部位の骨形態計測値の比較、日骨形態誌、2, 227-231, 1992.
19) 飯田治三、福田　俊：ラットの加齢に伴う骨重量および含有成分量の変化、実験動物、42, 349-356, 1992.
20) Fukuda, S. and Iida, H.: Histomorphometric changes in iliac trabecular bone during pregnancy and lactation in beagle dogs. J. Vet. Med. Sci, 55, 565-569, 1993.
21) 福田　俊：実験動物における形態計測法とその応用－ラットおよびイヌの骨代謝の年齢変化を中心に－。骨代謝学会誌、11, 194-198, 1992.
22) 福田　俊、飯田治三：第105回日本獣医学会、東京、1988, 4.
23) 福田　俊、山田裕司、飯田治三ら：日本保健物理学会第23回研究発表会，千葉，1998, 5.
24) 倉橋英治、松下裕二、福田　俊ら：日本実験動物技術者協会第22回総会，東京，1988, 7.
25) 永島　博、森岡一憲、福田　俊ら：日本実験動物技術者協会第22回総会，東京，1988, 7.
26) 宝田奈美、斎藤紀子、福田　俊ら：日本実験動物技術者協会第22回総会，東京，1988, 7.
27) Fukuda, S. and Iida, H.: The Fifth International Congress on Bone Morphometry. Niigata, 1988, 7.
28) Haba, T., Takahashi, H. and Fukuda, S.: The Fifth International Congress on Bone Morphometry. Niigata, 1988, 7.
29) 福田　俊、飯田治三：第107回日本獣医学会、東京、1989, 4.
30) Yamori, Y., Fukuda, S., Tsuchikura, S., et al.: Sixth International Symposium on SHR and Related Studies. Mishigan. 1989, 5.
31) 福田　俊、澤地邦宏、永島　博ら：日本保健理学会第23回研究発表会，名古屋、1989, 5.
32) 福田　俊、山田裕司、小泉　彰ら：日本保健理学会第23回研究発表会，名古屋、1989, 5.
33) 飯田治三、福田　俊：日本実験動物技術者協会第23回総会，鹿児島、1989, 7.
34) 福田　俊、飯田治三：第7回日本骨代謝学会，東京，1989, 7.
35) 土倉　覚、福田　俊、池田克巳ら：第25回高血圧自然発症ラット学会総会，東京，1989, 9.
36) 福田　俊、飯田治三：第5回日本獣医畜産大学学会，東京，1989, 11.
37) 福田　俊、土倉　覚、池田克巳ら：第9回骨粗鬆症研究会，静岡，1989, 11.
38) 福田　俊、飯田治三：第109回日本獣医学会、東京、1990, 4.
39) 福田　俊、家森幸男：第44回日本栄養食糧学会、仙台、1990, 5.
40) 福田　俊、飯田治三：第10回日本骨形態計測学会、大阪、1990, 6.
41) 福田　俊、土倉　覚、池田克巳ら：第8回日本骨代謝学会、東京、1990, 7.
42) 福田　俊、土倉　覚、池田克巳ら：第6回ビタミンDワークショップ、横浜、1990, 9.
43) 福田　俊、土倉　覚、池田克巳ら：第26回高血圧自然発症ラット学会総会、大阪、1990, 9.
44) 土倉　覚、福田　俊、池田克巳ら：第26回高血圧自然発症ラット学会総会、大阪、1990, 9.
45) 福田　俊、飯田治三、山田裕司ら：第33回日本放射線影響学会、仙台、1990, 10.
46) 福田　俊、飯田治三、宮本忠昭ら：第33回日本放射線影響学会、仙台、1990, 10.
47) 福田　俊、飯田治三：第10回骨粗鬆症研究会、浜松、1990, 11.
48) 飯田治三、福田　俊：日本実験動物技術者協会第24会総会、東京、1991, 2.
49) 土倉　覚、福田　俊、池田克巳ら：第80回日本病理学会総会、大阪、1991, 4.
50) 福田　俊、飯田治三：日本保健物理学会第26回研究発表会、大阪、1991, 5.
51) 福田　俊、飯田治三、山田裕司ら：日本保健物理学会第26回研究発表会、大阪、1991, 5.
52) 福田　俊、飯田治三、土倉　覚ら：第11回日本骨形態計測学会、つくば、1991, 6.
53) 土倉　覚、福田　俊、飯田治三ら：第27回高血圧自然発症ラット学会総会、札幌、1991, 6.
54) Fukuda, S., Iida, H., Miyamoto, M., et al. : Ninth ICRR, Tronto, 1991, 7.
55) Fukuda, S., Tsuchikura, S., Iida, H., et al: Seventh International Symposium on SHR and Related Studies. Lyon, 1991, 10.
56) Tsuchikura, S., Fukuda, S., Iida, H., et al: Seventh International Symposium on SHR and Related Studies. Lyon, 1991, 10.
57) Fukuda, S.: International Conference on Osteoporosis. Kobe, 1991, 11.
58) Fukuda, S., Tsuchikura, S., Iida, H., et al.: International Conference on Osteoporosis. Kobe, 1991, 11.
59) Fukuda, S. and Iida, H.: International Conference

on Osteoporosis. Kobe, 1991, 11.
60) 福田　俊、飯田治三：第113回日本獣医学会、東京、1992, 4.
61) Hori, M., Fukuda, S., Uzawa, T., et al.: ICCRH, Italy, 1992, 4.
62) 飯田治三、福田　俊：第39回日本実験動物学会、東京、1992, 5.
63) 福田　俊、飯田治三：日本保健物理学会第27回研究発表会、秋田、1992, 5.
64) 福田　俊、飯田治三：第12回日本骨形態計測学会、京都、1992, 7.
65) 福田　俊：第10回日本骨代謝学会、東京、1992, 7.
66) 福田　俊、飯田治三：第10回日本骨代謝学会、東京、1992, 7.
67) 福田　俊、飯田治三：第1回日本骨粗鬆症研究会、大阪、1992, 10.

3．内部被曝リスクの低減化に関する研究
①　キレート剤による生体除染とリスク低減に関する研究

佐藤宏、福田俊、飯田治三、稲葉次郎（内部被ばく研究部）

Studies of the Removal of Plutonium and the Reduction of Biological Effects by Chelating Agents

Hiroshi Sato, Satoshi Fukuda, Haruzou Iida and Jiro Inaba
Division of Comparative Radiotoxicology

（A）肺胞マクロファージからの^{59}Feおよび^{239}Pu放出に対する高分子キレート剤の効果

Effect of Macromolecular Chelating Agents on the Release of ^{239}Pu and ^{59}Fe from Rat Alveolar Macrophages

The effect of macromolecular chelating agents (MCAs) on the release of ^{59}Fe from rat alveolar macrophages (AMs) ingested ^{59}Fe-iron hydroxide colloid was studied. Six MCAs were tested. Each MCA and Ca-DTPA were added into the culture medium at the concentration which is not toxic for AMs. The activity of ^{59}Fe released into culture medium was determined 8 hr after the addition of MCA or Ca-DTPA. The most increase of ^{59}Fe release was shown by Si-DTPA. It was about 15 times of Ca-DTPA. Amyl-DTPA is effective more than 10 times of Ca-DTPA. The intensive effect was also shown by AEC- and O-AEC-DTPA. The extracellular release of ^{239}Pu and ^{59}Fe from AMs after ingestion of ^{239}Pu-^{59}Fe-hydroxide colloid is determined by the degree of aggregation of colloids. It is assumed that the dissolution of and redistribution of ^{239}Pu and ^{59}Fe from the lung after instillation of hydroxide colloid of these radionuclides are affected by the degree of their aggregation. The efficacy of chelating agents differed between Fe and Pu, suggesting a significant difference in the dissolution of the colloids and subsequent metabolism of these radionuclides in AMs. Except for Si-DTPA, the chelating agents at removing intracellular ^{59}Fe also showed a significant effectiveness for ^{239}Pu. On the release of ^{239}Pu from AMs ingested ^{239}Pu hydroxide, the effect of chelating agents was tested in AMs obtained 24, 72 and 144 or 168 hr after the instillation of Pu. Ca-DTPA was the most effective in each experiment.

1．緒言

吸入されたPu粒子は気道内に沈着するが、肺深部に達した粒子は肺胞に存在するマクロファージ（alveolar macrophage、AM）の貪食により細胞内に取り込まれる。これらの粒子はlysosomeにより消化、可溶化されたものは血液中へ移行し全身へ分布する。しかし、未消化のものは細胞内に残留する。生体内へ取り込まれたPuの除去にはキレート剤の投与が考えられているが、すでに臨床に応用されたCa-DTPAは水溶性であるために細胞内のPuには効果がないかまたは弱い。この点を改良して効力増強するために、疎水基を結合させて膜透過性を良くする方法や、liposomeとして投与する方法、また、AMを活性化する物質との併用等、種々の方法が報告されている。本研究ではその1つとして英国NRPBのDr. Bulmanとの共同でAMに貪食されうる物質にDTPAを結合させた高分子DTPAについて^{59}Fe-水酸化コロイド、^{239}Pu－^{59}Fe－水酸化鉄コロイド、水酸化Puの3種類の粒子を使用してCa-DTPAとの効力比較を検討した。

2．実験方法

a．キレート剤

高分子DTPAはaminoethylcellulose-DTPA (AEC-DTPA)、AEC-DTPA oxidized with periodic acid (O-AEC-DTPA)、amino-propyl silica-DTPA (Si-DTPA)、dextran hexylamio-DTPA (Dx-DTPA)、amylose-NH. PEG.NH-DTPA (amyl-DTPA)、alginic trien-DTPA (alg-DTPA)、polyvinyl alcohol-DTPA (PVA-DTPA)、polyethylene glyclo-DTPA (PEG-DTPA)の8種、さらに高分子DTPAの効果比較の対照としてCa-DTPAを使用した。濃度は、Si-DTPA 0.12mg / ml、PVA-DTPA 3.9、PEG-DTPA 13、Ca-DTPA 1.8、他はすべて1.2mg / mlとした。

b．^{59}Fe-水酸化鉄コロイド溶液（Fe-コロイド）の調製

Priestらの方法に若干の変更を加え以下の通り調製し

た。^{59}Fe-塩化鉄（NEN製）の0.5M塩酸溶液に2％（W/V）塩化鉄水溶液0.5mlを加えた後、沸騰水浴中で加温しながら蒸留水を加えて水酸化鉄コロイドを生成させた。冷却後、2％（W/V）デキストランでコロイドを安定化させて蒸留水に対する透析を行って鉄イオンを除去した。グルコースを添加して等張とし、投与液とした。

c．^{239}Pu-^{59}Fe-水酸化鉄コロイド溶液（PuFe-コロイド）の調製

^{59}Fe-水酸化鉄コロイドの調製法とほぼ同様にして調製した。硝酸Pu（11kBq）および^{59}Fe-塩化鉄（348kBq）を含む溶液に塩化鉄溶液を加え、加温しながら蒸留水3mlを加えて生成させたコロイドに、安定化剤としてデキストランを加え、グルコースにより等張とした。

d．水酸化Pu溶液の調製

硝酸Puの8 $NHNO_3$溶液（54MBq/ml）を0.1$NHNO_3$溶液に希釈しNaOH溶液でpH7.4に調製して水酸化Puを生成させた。ゼラチンで安定化しグルコースで等張とした。凝集度の違うコロイドを調製し、コロイド1およびコロイド2とした。

e．AMの回収

ウィスター系雌性ラット（3～5か月齢）にハロセン麻酔下でFe-コロイド、PuFe-コロイド、水酸化Puを気管内挿管法により肺へ投与し、24時間後、水酸化Puについてはさらに72、144時間後に肺洗浄を行いAMを回収した。

f．^{239}Pu、^{59}Fe放出率の算定

回収したAMをイーグルのMEM（EMEM）無血清培地で洗浄して細胞表面に吸着した^{239}Pu、^{59}Feを除去した後10％牛胎児血清を含むEMEM培地に懸濁し96穴マイクロプレートに$5X10^4$/0.2ml/穴の割合でまいた。5％CO_2気相下37℃でインキュベーションした。Fe-コロイドの場合は8時間、PuFe-コロイド、水酸化Puの場合は3時間後に0.22μmφのフィルター付き遠心チューブ（ウルトラフリーC3）を使用して遠沈し培養液上清を得た。上清中の^{239}Puの放射能は液体シンチレーションカウンター（1219RACKBETA）、^{59}Feはオートウェルγ-カウンター（Gamma 5500）でそれぞれ計測した。一方細胞は0.2％SDS溶液で溶解し、同様に放射能を計測し、以下の式より放出率を算定した。

$$\text{放出率（％）}=\frac{\text{培養液上清中の放射能}}{\text{プレートの各穴に含まれる総放射能}}\times 100$$

3．結果

a．細胞毒性

キレート剤の濃度はAMに対する細胞毒性を色素排除法により検討した。表1に示したようにCa-DTPA 1.8mg/ml、AEC-DTPA、O-AEC-DTPA、Dx-DTPA、alg-DTPA、amyl-DTPAはそれぞれ1.2～1.3mg/ml、PVA-DTPA 3.9mg/ml、PEGDTPA 13mg/ml、Si-DTPA 0.12mg/mlいずれにおいても生残率は81～96％で、細胞に対する毒性はほとんど見られなかった。

b．Fe-コロイドを取り込んだAMからのFe放出

表2に示したようにFe-コロイドを取り込んだAMから8時間の培養で2.95％の^{59}Feが放出された。Ca-DTPA1.8mg/ml存在下では3.6％の放出が見られ統計的に有意差はなかったが、約20％の放出増加傾向がみられた。これに対し高分子キレート剤を添加した群でCa-DTPA以上の効果が認められた。AEC-DTPA、O-AEC-DTPAではそれぞれ対照の6.5、5.3倍に放出率が増加し、alg-DTPA存在下では10.3倍、Si-DTPAでは約15倍の放出促進が認められた。これらの効果はCa-DTPAと比較しても4～12倍に相当する。Dx-DTPA、alg-DTPAについては放出促進はみられなかった。

表1　AM生残率に対するキレート剤の影響

キレート剤	生残率(％)
対　照	91.9±3.3
Ca-DTPA	93.3±0.8
AEC-DTPA	86.5±1.3
O-AEC-DTPA	87.5±2.2
Si-DTPA	93.3±0.8
Dx-DTPA	96.0±1.2
amyl-DTPA	81.3±3.5
PVA-DTPA	86.3±3.1
PEG-DTPA	90.9±3.4

表2　Fe-コロイドを取り込んだAMからの^{59}Fe放出に対するキレート剤の効果

キレート剤	放出率(％)
対　照	2.95±0.52　(100)
Ca-DTPA	3.60±0.05　(122)
AEC-DTPA	19.2 ±0.23*　(651)
O-AEC-DTPA	15.7 ±1.4*　(532)
Si-DTPA	43.6 ±2.4*　(1478)
Dx-DTPA	2.16±0.68　(73)
amyl-DTPA	30.3 ±0.44*　(1027)
alg-DTPA	2.21±0.41　(75)

( )対照を100とした場合の値．　* P＜0.005

c．PuFe-コロイドを取り込んだAMからのPu、Fe放出

1）コロイド1とコロイド2の違い：コロイド1とコロイド2の投与液中の10kDa以下の割合を見ると、コロイド1が47％に対しコロイド2が3.3％でコロイド2の凝集度が高いのは明らかであり、コロイド2を投与したラットの肺洗浄液中の細胞画分に含まれる^{239}Puの割合はコロイド1の2.1倍高く、細胞画分と洗浄液上清画分に含まれる^{239}Puの割合はコロイド1の2.1倍高く、細胞画分と洗浄液上清への分布の比率では6.2倍で凝集度の高いコロイドがAMに取り込まれやすい（表3）。

表3　PuFe-コロイドを投与したラット肺洗浄液中のPu分布

	投与液に含まれる10kDa以下の割合	肺洗浄液		
		細胞画分	上清	細胞画分/上清
コロイド1	47.2	3.4	16.0	0.21
コロイド2	3.3	7.3	5.7	1.3

数値は投与したPu量に対する割合を百分率で表した.

2）コロイド1に対する効果：結果は表4にまとめた。コロイド1を取り込んだAMからの^{239}Puおよび^{59}Feの培養3時間の放出率は対照ではそれぞれ1.15、1.13％で同程度であった。しかし、キレート剤の効力には大きな違いが見られた。Si-DTPA以外のキレート剤について、いずれも^{239}Puと^{59}Feの放出率を比較するとCa-DTPAで^{239}Puの方が4.1倍高い放出促進を示し、高分子キレート剤で1.7-3.8倍高い効果を示した。^{239}Puについて見るとCa-DTPA、O-AEC-DTPA、PVA-DTPAでそれぞれ11.3、11.7、28.3％でPVA-DTPAはCa-DTPAより高い放出促進を示し、O-AEC-DTPAでCa-DTPAと同程度の効果が認められた。他のキレート剤も対照の4倍以上の促進効果を示した。^{59}FeではPEG-DTPAの1.5倍からPVA-DTPAの13倍までの範囲で放出促進がみられた。一方、Si-DTPAは^{59}Feの放出に対してのみ効果がみられた。

表4　PuFe-コロイドを取り込んだAMからの^{239}Pu、^{59}Fe放出に対するキレート剤の効果（コロイド1）

キレート剤	^{239}Pu放出率(%)	^{59}Fe放出率(%)
対　照	1.15±0.62　(100)	1.13±0.26　(100)
Ca-DTPA	11.3 ±0.71** (983)	2.68±0.18** (237)
AEC-DTPA	4.54±0.41** (395)	2.59±0.37* (229)
O-AEC-DTPA	11.7 ±1.0** (1017)	5.07±0.24** (449)
Si-DTPA	1.17±0.41　(102)	4.29±0.37** (380)
PVA-DTPA	28.3 ±0.35**(2457)	14.9 ±0.72**(1319)
PEG-DTPA	6.97±1.0** (606)	1.78±0.16　(158)

( )対照を100とした場合の値. * P<0.01, ** P<0.005

表5　PuFe-コロイドを取り込んだAMからの^{239}Pu、^{59}Fe放出に対するキレート剤の効果（コロイド2）

キレート剤	^{239}Pu放出率(%)	^{59}Fe放出率(%)
対　照	0.24±0.07　(100)	0.03±0.02　(100)
Ca-DTPA	0.44±0.05* (183)	0.09±0.02* (300)
AEC-DTPA	0.24±0.03　(100)	0.09±0.01* (300)
O-AEC-DTPA	0.52±0.03** (217)	0.20±0.04** (667)
Si-DTPA	0.16±0.01　(67)	0.07±0.01　(233)
PVA-DTPA	3.66±0.50**(1525)	0.42±0.02**(1400)
PEG-DTPA	0.36±0.04　(150)	0.03±0.01　(100)

( )対照を100とした場合の値. * P<0.01, ** P<0.005

3）コロイド2に対する効果：表5に示したように凝集度の高いコロイド2の場合は、コロイド1の場合と比較して大きく異なった点は対照の^{239}Pu放出が^{59}Feより高かったこと、キレート剤による放出促進が^{59}Feの方が大きかったことである。すなわち、^{239}Puに対する放出促進はCa-DTPA、O-AEC-DTPAがそれぞれ対照の1.8、2.2倍であったのに比較して^{59}Feでは3.0、6.7倍であった。Si-DTPAは^{59}Feに対してのみ効果がありPVA-DTPAでは^{239}Puと^{59}Feに対して同程度の効果を示した。

d．水酸化Puを取り込んだAMからの^{239}Pu放出

1）凝集度の低い水酸化Puに対する効果：水酸化Puを投与して24、72、144時間後に回収したAM(AM24、AM72、AM144)の3時間培養で放出される^{239}Puは対照でそれぞれ1.2、2.9、5.6％で、Pu投与後の時間経過にともない増加した（表6）。AM24ではCa-DTPAで4.2％に放出が増加し、試験した高分子キレート剤全てが有意な放出促進を示し、放出率は1.6-3.6％であった。AM72の場合はSi-DTPA以外の放出率は3.6-7.1％の範囲で放出促進効果が見られ、AM144ではAEC-DTPA、Si-DTPAを除きいずれも効果が認められた。放出率は7.7-13％であった。AM24、AM72、AM144いずれもCa-DTPAが最も効果が強かった。

表6　凝集度の低い水酸化Puを取り込んだAMからのPu放出に対するキレート剤の効果

キレート剤	Pu投与後の時間		
	24時間	72時間	144時間
対　照	1.22±0.06　(100)	2.87±0.14　(100)	5.56±0.34　(100)
Ca-DTPA	4.16±0.10** (341)	7.13±0.30** (248)	13.2 ±0.40** (237)
AEC-DTPA	1.60±0.16$ (131)	3.58±0.12# (125)	5.73±0.25　(103)
O-AEC-DTPA	3.39±0.13** (278)	4.09±0.05** (143)	8.52±0.13** (153)
Si-DTPA	1.56±0.07# (128)	2.53±0.07　(88)	5.70±0.32　(103)
Dx-DTPA	3.21±0.22** (263)	5.48±0.61** (191)	13.0 ±1.51** (234)
alg-DTPA	2.58±0.15** (211)	4.69±0.60** (163)	8.95±0.51** (161)
amyl-DTPA	3.59±0.10** (294)	4.83±0.12** (168)	7.74±0.45# (139)

( )対照を100とした場合の値. $ P<0.05, # P<0.025, * P<0.01, ** P<0.005

2）凝集度の高い水酸化Puに対する効果：AM24、AM72、AM144の放出率は対照でそれぞれ0.31、1.2、1.6％で凝集度の高い水酸化Puでも Pu投与後の時間経過にともない増加した（表7）。amyl-DTPAが最も効果が高く、ついでO-AEC-DTPA、次に効果の高かったのは、Si-DTPAであった。

表7　凝集度の低い水酸化Puを取り込んだAMからのPu放出に対するキレート剤の効果

キレート剤	Pu投与後の時間		
	24時間	72時間	168時間
対　照	0.31±0.04　(100)	1.22±0.07　(100)	1.64±0.09　(100)
Ca-DTPA	0.53±0.02# (171)	1.65±0.01* (136)	2.36±0.17** (144)
AEC-DTPA	0.45±0.05　(146)	1.84±0.11** (151)	1.58±0.06　(96)
O-AEC-DTPA	0.65±0.01** (208)	2.29±0.09** (188)	2.36±0.09** (144)
Si-DTPA	0.59±0.09# (191)	1.75±0.09** (144)	2.46±0.14　(150)
Dx-DTPA	0.60±0.06* (195)	1.59±0.18　(131)	1.61±0.11　(98)
alg-DTPA	0.55±0.05* (177)	1.37±0.06　(112)	1.49±0.05　(90)
amyl-DTPA	0.83±0.07** (268)	2.43±0.03** (199)	3.20±0.25** (195)

( )対照を100とした場合の値. # P<0.025, * P<0.01, ** P<0.005.

4．考察

Fe-コロイドが取り込んだAMをキレート剤存在下で8時間培養するとAEC-DTPA、O-AEC-DTPA、Si-DTPA、amyl-DTPAで高い放出率が認められたが、いずれもAMの生存率は81～93％で毒性は認められない濃度であり細胞死による放出ではなく、膜を介した放出が促進された結果と推測される。使用した高分子キレート剤には、Si-DTPA、amyl-DTPA、O-AEC-DTPA、AEC-DTPAでそれぞれ0.13、25、30、124μg/mlの

DTPAが含まれ、Si-DTPAが他の3種と比較して1/200以下であること、また、Si-DTPAのみは不溶性で粒子として存在していること等から他のキレート剤とは作用機序が異なることが推測される。Si-DTPAではSiによりAMが活性化されることにより細胞内での可溶化が促進されたために、他に比べ促進効果が高くあらわれたものと考えられる。

次にPuFe－コロイドの場合のPuとFeに対する効力の違いについて。コロイド1とコロイド2それぞれの粒子径は測定していないが、コロイド1が水溶液中で長時間安定であるのに対しコロイド2は2、3時間内に一部が沈降してくる。これからみても粒子径の違いは明らかであり、コロイド2は正確にはコロイドとは言えないがここではコロイド2としてコロイド1と区別した。肺洗浄液において細胞画分に存在するPuの洗浄液上清中のPuに対する比率がコロイド2で約6倍高いことから、コロイド2がAMに取り込まれやすいことを示している。（表3）また、3時間培養で培養液中に放出されるPuの割合はコロイド1が約5倍高く、コロイド1が可溶化されやすいことを示唆している。Feではさらに違いが大きくコロイド2ではコロイド1に比して著しく可溶化されにくい。PuとFeの違いの原因は不明であるが、Feが必須元素であることのほかにPuFe－コロイドにはキャリアーとしてFeの安定同位体が多く含まれていることが考えられる。キレート剤の効力の点からみて大きな違いは、PuについてSi-DTPA以外のキレート剤でコロイド1が395～2457％、コロイド2が100～1525％と、凝集度が高いと効果が弱くなること、FeではPuと異なり凝集度の違いは効果にあまり影響しないこと、Si-DTPAはFeの放出に対してのみ促進効果がみられた点である。Si-DTPAがPuに対して効果がない点についてその原因は不明であるが、PuとFeに対するキレート剤の効果の違いは、細胞内で可溶化された後の細胞内での存在形態の違いによるのかも知れない。Feはフェリチンと結合して細胞内に貯蔵され、Puもフェリチンと結合すると考えられるが、フェリチンーPuの解離にはFeにみられるような価数の変化は必要ないことが報告されており、これが内因性キレート剤であるフェリチンとDTPAとの間でPu、Feに対する競合的結合する際に差が生じキレート剤の効力の違いとして現れたと考えられる。一方、水酸化Puについては、Pu投与後AM回収までの時間が長くなるにしたがってAMの3時間培養で放出されるPuの割合は、凝集度の高い水酸化Pu、凝集度の低いPuのいずれにおいても高くなり時間と共に細胞内可溶化が進行していることを示唆するものである。各種キレート剤の効果については、AM24、AM72、AM144いずれにおいてもCa-DTPAが最も効果が強く、凝集度の低い水酸化Puではamyl-DTPAがCa-DTPA以上の効果を示したが、全体としては時間経過と共にキレート剤の効果は弱くなる傾向がみられた。これは、Pu摂取後初期の段階でのキレート剤治療が効果的であるとする従来のin vivo実験の結果を支持するものである。

5．結論

DTPAの効力増強を目指して開発した種々の高分子DTPAについて、FeとPuに対する効果をin vitro系でCa-DTPAと比較検討してきた。Feに対してはCa-DTPA以上の効果が認められた高分子DTPAが2、3あったがPuに対してはCa-DTPA以上に効果的なものはほとんど見つからず、本研究においては、Puに対しCa-DTPAが最も有効であるとの結論に達した。

（B）Ca-DTPA吸入投与による生体除染

Decorporation of ^{59}Fe and ^{239}Pu by the Inhalation of Ca-DTPA

The inhalation of Ca-DTPA is effective on the removal of ^{59}Fe and ^{239}Pu. On the other hand, it was not shown by the intraperitoneal injection. The urinary exclusion of ^{239}Pu was 100 times of ^{59}Fe in content. This may be due to the difference of characteristics of two elements, but it was increased about 3 times of the control in both ^{239}Pu and ^{59}Fe. The inhalation was carried out by the neblizer on the market, which is very convenient, and it confirmed that the inhalative Ca-DTPA is effective on the removal of accidental inhalation.

1．緒言

実際に吸入により生体内に取り込まれた粒子状放射性金属の除去方法としては、肺洗浄の他にキレート剤による除去が考えられる。前特研ではキレート剤を気管内挿管法により肺へ投与することにより除去効果が得られることを報告した。しかし、臨床応用を考慮すると気管内挿管法は非現実的であり、実用性を考慮した場合の吸入摂取金属粒子の除去には以下の点で吸入法が適している。1）摂取者自身による投与が可能、2）摂取後迅速な処置が可能、3）効果の持続性が期待できる。本研究では市販されている簡便かつ安価な吸入装置を使用して吸入投与法の効果を調べ、臨床面での応用の可能性について検討した。in vitro系の結果との比較も考慮して対象金属粒子として水酸化鉄コロイドを選択したが、実際に原発で事故が発生した場合に想定される摂取金属であるPuは必須金属である鉄とは体内動態が異なることから粒子状水酸化Puに対するキレート剤吸入投与の効果についても検討し、効力比較を行った。

2．実験方法

a．^{59}Fe水酸化鉄コロイドおよび水酸化Puの投与

（A）2．b．およびd．により調製した^{59}Fe－水酸化鉄コロイドおよび水酸化Puをハロセン麻酔下で気管内挿管法によりラット肺に投与した。

b．Ca-DTPAの吸入投与

^{59}Fe－水酸化鉄コロイドおよび水酸化Puを投与し、粘液繊毛運動による上部気道沈着分の初期排泄が終了する2日目からCa-DTPAを吸入投与した。発生原液の10％(W／V)水溶液とし、超音波式ネブライザー（オムロンNE-U12型）でエアロゾル化し1回15分、週2回全身曝露した（図1）。Ca-DTPAの投与の比較対照として7 mg／kgを腹腔内投与した。

c．試料中の放射能計測

Ca-DTPA吸入投与開始後、糞尿は週3－4回分別採取し、^{59}Fe投与群は30日目、^{239}Pu投与群は38日目に放血屠殺後、臓器を摘出した。得られた試料中の放射活性は

^{59}Feについてはオートウェル γ-カウンターにより^{239}Puについては尿は未処理のまま、糞、臓器は灰化後硝酸とフッ化水素酸の混合酸に溶解し液体シチレーションカウンターによりそれぞれ計測を実施した。

曝露条件

Ca-DTPA溶液の濃度：10%(w/v)
流量：17L/ml
エアロゾル化率：0.7ml/分
粒子径：1～5μm
曝露時間：15分

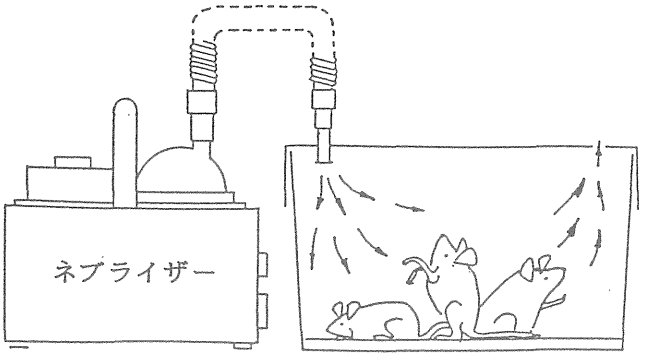

図1　DTPA吸入投与の概略

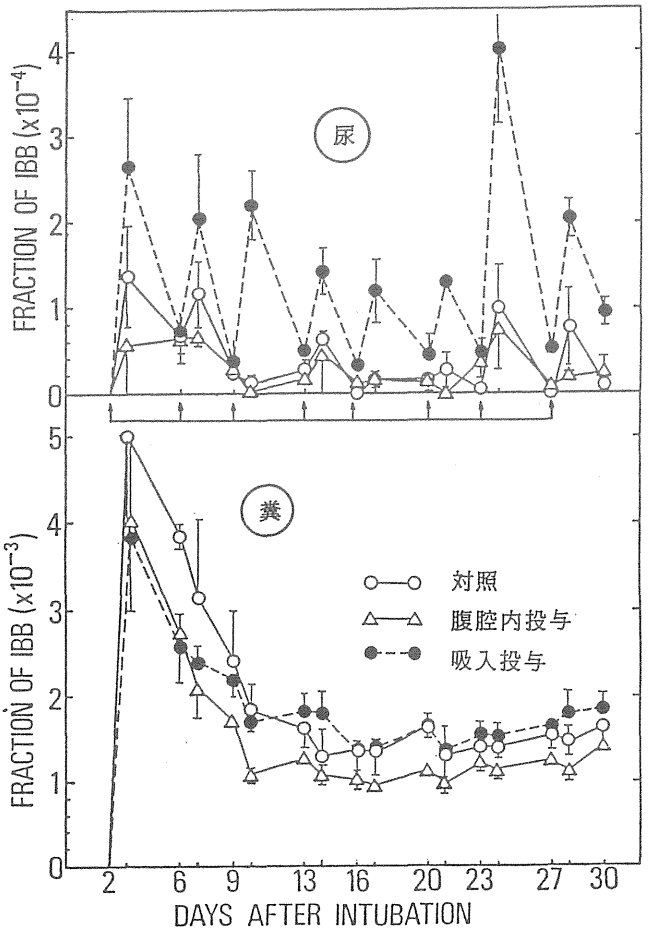

図2　^{59}Fe投与ラットにおける糞尿排泄の経日変化

表8　Fe-コロイドを投与したラットの臓器分布に対するCa-DTPAの効果

処置方法	肺	肝	脾	腎	大腿骨
対　照	87.1±1.71	2.60±0.29	0.04±0.01	0.09±0.03	0.04±0.03
腹腔内投与	89.2±0.76	2.32±0.13	0.03±0.00	0.03±0.00	0.01±0.00
吸入投与	88.6±1.21	2.31±0.16	0.03±0.01	0.04±0.01	0.01±0.00

表9　Fe-コロイドを投与したラットの排泄に対するCa-DTPAの効果

	尿		糞	
処置方法	総排泄率	排泄率/日	総排泄率	排泄率 /日
対　照	0.10±0.04	0.005±0.001	5.59±0.79	0.20±0.03
腹腔内投与	0.08±0.02	0.003±0.001	4.25±0.21	0.15±0.02
吸入投与	0.28±0.05$^{\$}$	0.013±0.003	5.28±0.49	0.19±0.02

$ P<0.05

3．結果

a．^{59}Feの体内分布、排泄への効果

未処置対照群の各臓器への残留率は^{59}Fe投与2日目の体内残留量を100％とした場合肺87％、肝2.6％、脾0.04％、腎0.09％、大腿骨0.04％で、大部分が肺に残っていた。肺、肝、脾についてはCa-DTPA投与による影響は見られず、腎、大腿骨では有意差は認められなかったが、残留率が低下する傾向が認められた（表8）。排泄への影響についてみると表9に示されたように糞への排泄にはCa-DTPA投与による影響はなかった。また、腹腔内投与による尿中排泄増加も見られなかった。しかし、Ca-DTPA吸入投与により尿中への排泄は約3倍に増加した。すなわち、吸入投与により1日当りの尿中排泄率が対照の0.0045％が0.013％に、吸入投与開始後28日間の総排泄量でも対照の0.10％から0.28％に増加した。Ca-DTPA吸入投与による尿中排泄の変化を図2に示したが、吸入投与後24時間の排泄率が高くなっているのがわかる。

b．^{239}Puの体内分布、排泄への効果

表10に示したように^{239}Puを投与したラットでは投与38日後の肺への残留量は投与2日目の体内残留量の21％に減少した。Ca-DTPA吸入投与では20％で対照と差はなかった。しかし、肺から全身への移行、排泄に差が見られた。Ca-DTPA投与群の肝への残留は15％に低下し、脾では有意差はなかったが40％に低下した。腎、大腿骨ではそれぞれ対照の37、22％が残っていた。糞中への排泄には影響はほとんど認められなかったが、尿への総排泄量は2.8倍に増加し、1日当りの平均で比較しても2.7倍高い排泄率を示した（表11）。図3には糞尿中への排泄の変化を示した。

表10　水酸化Puを投与したラットの臓器分布に対するCa-DTPA吸入投与の効果

処置方法	肺	肝	脾	腎	大腿骨
対　照	21.4±2.53	1.19±0.32	0.040±0.022	0.15 ±0.024	0.45 ±0.10
Ca-DTPA	20.0±4.35	0.18±0.011$^{\$}$	0.016±0.010	0.056±0.003*	0.098±0.012*

$ P<0.05, * P<0.025

表11　水酸化 Pu を投与したラットからの排泄に対する Ca-DTPA 吸入投与

	尿		糞	
処置方法	総排泄率	排泄率/日	総排泄率	排泄率 /日
対　照	10.0±1.14	0.28±0.032	58.1±3.09	1.62±0.086
Ca-DTPA	27.5±3.15*	0.76±0.087$	50.3±2.48	1.40±0.069

$ P<0.05,　* P<0.01

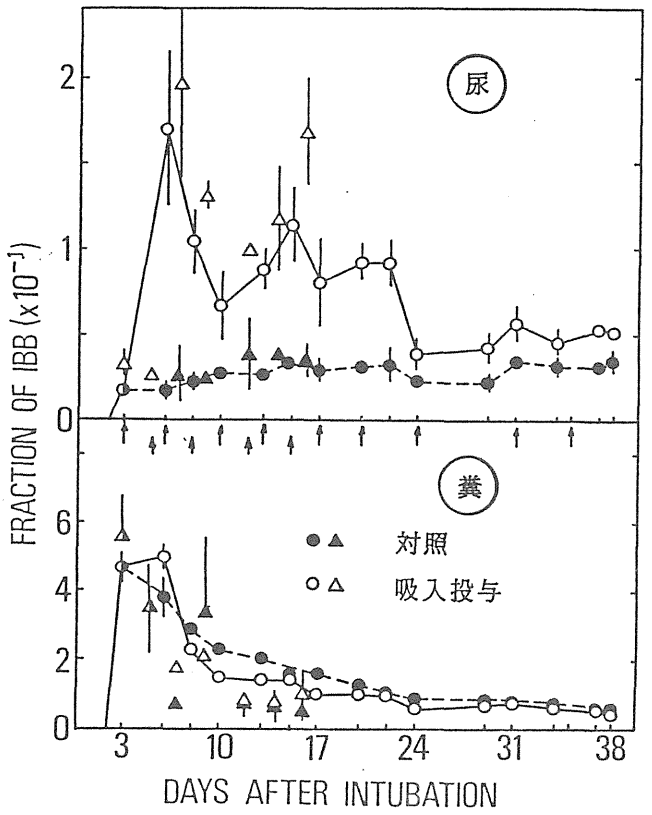

図3　^{239}Pu 投与ラットにおける糞尿排泄の経日変化

4．考察

^{59}Fe の体内分布についてみると、Ca-DTPA による影響はほとんど見られない。1カ月後においても肺への残留は 87 %と依然高い残留率を示しており、全身への移行が少ない。鉄は必須元素であるため、投与した^{59}Fe が肺組織内に貯蔵され全身へ移行しにくいと考えられる。移行した^{59}Fe の分布を見ると肝への移行率が高いがこれは肺から移行した^{59}Fe はすべてイオン状ではなく微細粒子状の^{59}Fe も移行系に含まれそれらが肝へ沈着したためと考えられる。一方、排泄については尿に比べ糞への排泄率が高いが糞への排泄は胆汁を介する経路のほかに2日目以降も気道から上行性にクリアランスされる経路があり、それらが消化管を経て排泄されたものが含まれたためと考えられる。DTPA 投与群の尿中排泄を比較すると腹腔内投与では効果がないのに対し吸入投与で約3倍の排泄増加が見られたが、DTPA の投与方法による効果の違いが如実に現れた。すなわち、Stather らの報告に示されたように、吸入投与では^{59}Fe の存在する肺局所に一時的に滞留し、徐々に血液中に移行するために静脈内投与（腹腔内投与もほとんど同程度の血中保持時間）の様に投与後急速に血液中濃度が低下することなく一定のレベルが比較的長く保たれる。この違いが尿中排泄率の増加として反映されたと考えられる。図2に糞尿排泄の経日変化を示したが、吸入投与24時間の排泄が強く促進され、さらに72時間までの排泄も促進される傾向がみられ、腹腔内投与ではほとんどが体外へ排泄されてしまう24時間以降も効果が持続していることが示唆された。

Pu の体内分布については38日後の肺への残留率は21 %、データは示さなかったが16日目では31 %であった。硝酸 Pu の気管内投与では7日目で31 %との報告があり、硝酸 Pu が生体内で水酸化 Pu に変化することを考慮すると本研究での結果はその報告にほぼ合致する。Fe の30日目の肺への残留率が87 %であるのに対し Pu は21 %と低い。化学形態が同一でないことが大きな原因と考えられるが、Pu が Fe と異なり必須元素でないために組織的へ貯蔵されにくく、全身へ移行しやすいためとも考えられる。移行した Pu の臓器分布を見ると、Fe との大きな違いがあるが、大腿骨への残留率が Fe で 0.04 %、Pu が 0.45 %で10倍の差がある。これは Pu が bone seeker といわれるように骨に沈着しやすいことを示唆している。糞尿排泄については Pu、Fe が対照でそれぞれ 68 %、5.7 %と大きな差があり、DTPA 投与で78、5.6 %と Fe では差がなく Pu で10 %の排泄増加がみられたように DTPA は Pu に対しては有効性が示唆された。また、in vitro で Pu に対しての効果が強いことが示されたが、in vivo でもそれが裏付けられた。

5．結論

Ca-DTPA の吸入は市販のネブライザーを使用し、15分間ラットに全身曝露することにより行ったが、水酸化 Pu のように酸化 Pu と比較して比較的可溶性の粒子状 Pu に対しては効果が認められた。事故による被曝においては被曝者自身がマウスピースによる吸入もしくは鼻部曝露による吸入となり、全身曝露より効果的な投与が可能と考えられるので効果はさらに高いと考えられる。しかも携帯が可能なので被曝直後の投与ができ操作も非常に簡便であることから、臨床応用の面からも十分に価値があると思われる。

［研究発表］

1）佐藤：キレート剤による体内摂取金属の除去．放射線科学、33, 386-387, 1990.

2）佐藤：重金属のキレート剤による追い出し。第21回放医研シンポジウム「粒子状物質の吸入とその生物作用の発現機構」報文集 (NIRS-M-78)：　pp.222-228, 1991.

3）Bulman, R. A., Sato, H., Takahashi, S. and Kubota, Y.: ^{59}Fe release from alveolar macrophages by macromolecular forms of chelating agents. J. Radiol. Prot., **13**, 127-133, 1993.

4）Sato, H., Bulman, R.A., Takahashi, S. and Kubota, Y.: Effects of macromolecular chelating agents on the release of ^{239}Pu and ^{59}Fe from rat alveolar macrophages after phagocytic uptake of ^{239}Pu-^{59}Fe-iron hydroxide colloid. Health Phys., **66**, 545-549, 1994.

3．内部被曝リスクの低減化に関する研究
②キレート剤のプルトニウム除去効果と毒性

福田　俊、飯田治三（内部被ばく研究部）
Hsieh Yuyuan（中国科学院上海薬物研究所）

Effects of Chelating Agents DTPA, CBMIDA, and Calcium supplement on Removal of Plutonium, and the Assessments of Their Toxicities in Experimental Animals

Satoshi Fukuda, Haruzo Iida and Hsieh Yuyuan*
Division of Comparative Radiotoxicology, *Shanghai Institute of Materia Medica

In this study, the overall assessments on toxicity of DTPA (Diethylenetriaminpentaacetic acid) were summarized, and the effects of new chelating agent CBMIDA [Catechol-3,6-bis (methyleiminodiacetic acid)] on removal of plutonium and its toxicity, and calcium supplement to help the Ca-DTPA effect were examined.

The overall results obtained from our many toxicological studies on DTPA concluded that the recommended human dose(30μmol / kg)of DTPA has very low toxicities but the devised administration routes, such as intravenous injection of Ca-DTPA at early period after accident and the following oral administration of Zn-DTPA for a long term treatment could lower the toxicities, in addition to raise the effect on removal of plutonium from body.

The effects of new chelating agent CBMIDA on removal of plutonium were higher than those of Ca-DTPA and Zn-DTPA in bones, and almost the same as those of DTPAs in liver of rats. The toxicity of CBMIDA was almost the same as those of DTPA, rather lower than the intravenous injection of Zn-DTPA. Therefore, CBMIDA can be regarded as a most beneficial chelating agent to remove plutonium from human body.

Pre- and post-supplement of calcium-oxide, showing high calcium absorption from small intestine, against plutonium intake, had beneficial effects to decrease plutonium deposition and help to enlarge the effect of Ca-DTPA on removal of plutonium.

1．緒言

プルトニウムの体内摂取に伴う内部被曝の障害リスクを低減する方法として、除去効果が高いとされる合成キレート剤DTPA（diethylenetriaminepentaacetic acid）の使用が推奨されている。しかし、その毒性に関しては十分な安全性の評価が得られておらず、除去効果も十分とはいえないことから、さらに高い除去効果かつ低毒性のキレート剤の開発が望まれている。

本研究では緊急医療および保健物理学的な観点から、前特研において得られた成果を合わせたDTPAの総合的な毒性評価、および新しいキレート剤CBMIDA［Catechol-3, 6-bis（methyleiminodiacetic acid）］のPuの除去効果と毒性の検索、およびDTPAの除去効果の向上と低毒性化について検討した。

2．研究方法

（1）キレート剤の毒性

① Ca-DTPA、Ca-EDTAおよびCBMIDAの静脈注射による一般急性毒性および骨毒性を検索するために、ビーグルの成犬9頭を3群に分け、Ca-DTPA、Ca-EDTAおよびCBMIDA（150μmol / kg）を0.06-0.08ml / sの速度で静脈注射した15、30、45、60分後に採血して、血清中のカルシウム濃度を測定した。その後、同量の各キレート剤を1日1回、1カ月間連続して静脈注射した。投与0、1、2、3、4週後に採血を行い、GOT、GPT、ALP、BUN、Creatinineの測定を行った。また、骨代謝への影響を検索するために、テトラサイクリンとカルセインを投与して骨二重標識を行った。実験終了時に解剖して、主要臓器および腸骨を採取した。各臓器の検索はパラフィン包埋した病理組織標本を作製して行った。骨の検索は非脱灰組織標本を用いた形態計測法によって行った。

CBMIDAは中国科学院上海薬物研究所のHsieh Yuyuan博士によって、合成されたキレート剤である（図1）。

② Zn-DTPAの経口投与による骨毒性を検索するために、ビーグル成犬8頭に30μmol／kg、3頭に150μmol／kg、5頭に300μmol／kgを1日1回、1カ月間連続投与した。実験①と同一の方法で骨標識を行い、骨形態計測法を用いて検索した。

（2）CBMIDAとDTPAのPu除去効果の比較

Fig.1 Catechol-3,6-bis(methyleimino diacetic acid)
CBMIDA

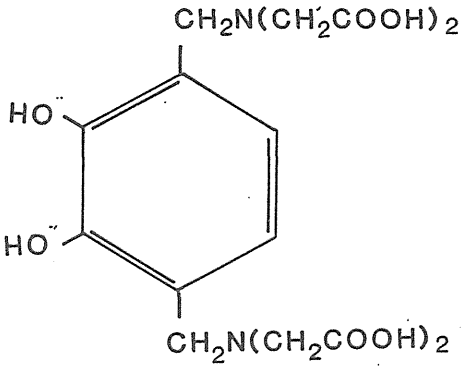

ラット（3カ月齢、雄）の20頭に硝酸Pu(1.85×10^4 Bq／kg）を静脈投与した後に4群（5頭／群）に分け、3群にはCBMIDA、Ca-DTPA、Zn-DTPAのそれぞれ150 μmol／kgを2週間連続して腹腔内注射した。残りの1群はPu対照群とした。動物は糞尿分離ケージで飼育し、24時間置きに糞尿を採取した。大腿骨、肝臓、糞尿中のPu濃度は、灰化した後、硝酸で溶解して液体シンチレションカウンターで測定した。

（3）酸化カルシウムによる除去効果とCa-DTPAとの併用投与の効果

ラット（3カ月齢、雄）の25頭を、①Pu投与1週間前からカルシウム飼料を投与した群、②Pu投与直後からカルシウム飼料を投与した群、③Pu投与後にカルシウム飼料と腹腔内にCa-DTPA（150 μmol／kg）を投与した群、④Ca-DTPA（150 μmol／kg）と通常の飼料を投与した群、⑤Pu対照（通常の飼料を投与）群に分けた。投与した硝酸Puの量は1.85×10^4 Bq／kgであった。カルシウム飼料は、貝がらを焼成して得た酸化カルシウム（1%）を通常の飼料に加える炭酸カルシウムと入れ換えて作製した。動物の飼育および大腿骨、肝臓、糞尿中のPu濃度は、実験（2）と同様な方法を用いた。

3．結果

（1）キレート剤の毒性

ビーグル犬にCa-DTPA、Ca-EDTA、CBMIDAを点滴の速度で静脈投与した後には、血清カルシウム濃度の変化は認められなかった。1カ月間連続静脈注射投与した結果、骨毒性以外の観察においてCa-DTPA投与群では、平均体重の有意な減少、GOT、GPT、BUN、Creatinineの上昇がみられた。Ca-EDTA投与群では、有意な変化はみられなかった。CBMIDA投与群では、GPT、ALP、Creatinineの上昇がみられた。すべての群で、軽度の小腸粘膜の充血とリンパ球の浸潤、腎臓の近位尿細管のリンパ球の浸潤、肝臓の変性がみられた。

骨毒性を検索した結果、Ca-DTPA、Ca-EDTA、CBMIDA静脈投与群およびZn-DTPAの経口投与群のいずれにおいても、骨量や骨梁幅に変化はみられなかった。CBMIDA投与群では類骨量や類骨幅の有意な増加がみられたが、石灰化速度や骨形成速度は骨標識の不全のため計測できなかった。Zn-DTPA150 μmol／kg投与群で類骨量や類骨幅の有意な減少、石灰化速度や骨形成速度の増加が、300 μmol／kg投与群では類骨量の増加がみられた。血清成分については、Zn-DTPA30 μmol／kg投与群ではリン濃度の低下、Parathyroid hormone濃度の上昇、150 μmol／kg投与群ではParathyroid hormone濃度の低下がみられた。

前特研および本特研において検索したDTPAの毒性をまとめ、結果を表1および図2に示した。また、人への安全な投与方法を図3に示した。

Table 1 Damages in various organs and clinical signs induced by DTPA

Blood or organs (Intestine, Kidney, Liver)	RBC↓, Ht↓, GOT↑, GPT↑, ALP↑, BUN↑ Zn-deficiency, Inhibition of DNA, RNA synthesis Ca-deficiency, Hemorrhage, Congestion,
Clinical signs	Loss of appetite, Dehydration, Sore mouth and throat, Decrease of body weight, Abdominal tenderness Nausea, Vomiting, Hematemesis, Melena, Diarrhea, Hemafecia, Hematuria, Hair loss,

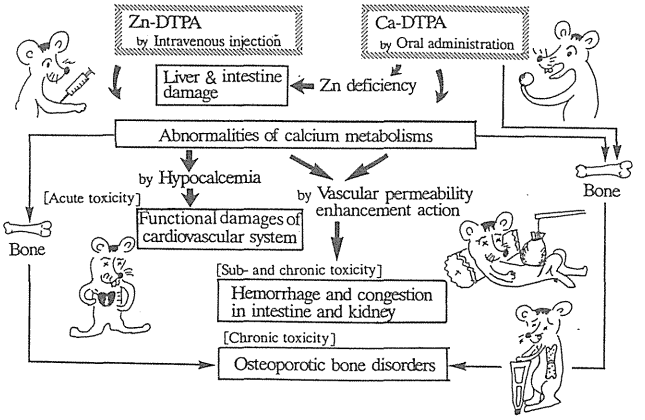

Fig.2 Summary of DTPA toxicity

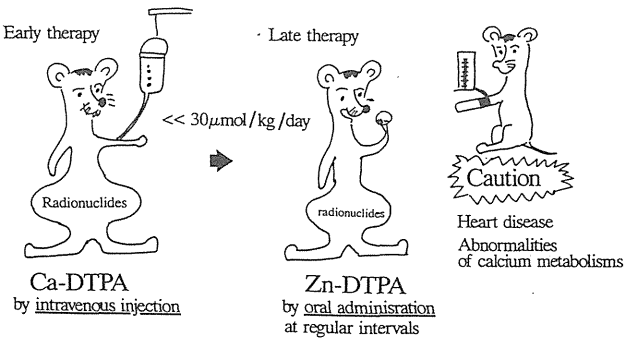

Fig.3 Administration routes for use in safety

（2）CBMIDAとDTPAのPu除去効果の比較

Pu投与量に対する骨および肝臓含有率の測定結果を図4に示した。骨に対するCBMIDAの効果は、Ca-DTPAとZn-DTPAに比べて高く、とりわけZn-DTPAとは有意な差がみられた。肝臓に対する効果は、いずれも同程度で投与量の0.35-0.62%であった。尿中へのPu排泄は、すべてのキレート剤とも対照群よりも高かった。糞中への排泄は、Pu投与5日後までは対照群よりも高かったが、

それ以降低くなった。

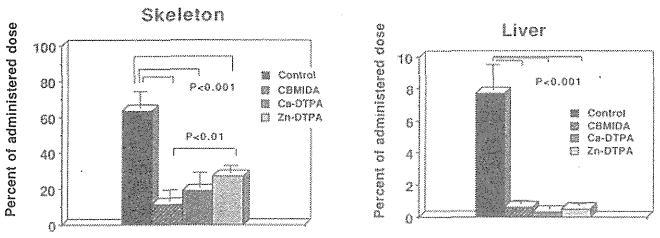

Fig.4 Plutonium content of skeleton and liver (percent of administered dose) in the CBMIDA, Ca-DTPA, Zn-DTPA and control groups on day 14 after plutonium injection.

（3）酸化カルシウムによる除去効果とCa-DTPAとの併用投与の効果

酸化カルシウムの経口投与およびCa-DTPAの注射投与との併用効果の結果を図5に示した。骨および肝臓ともにPuの沈着率は、Pu投与前および後のいずれの場合にも酸化カルシウム投与の効果がみられ、Pu投与前の場合の方が効果的であった。これらの効果は、Ca-DTPA注射投与と併用すると著しく高まり、Ca-DTPAのみの投与より効果的であった。

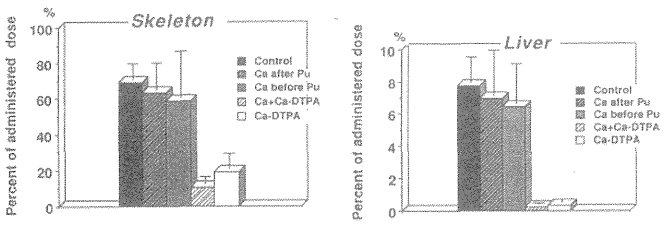

Fig.5 Plutonium contents of skeleton and liver in the pre- and post-calcium supplement groups, calcium supplement and Ca-DTPA injected group, Ca-DTPA injected group and control group on day 14 after plutonuim injection.

4．考察

前特研および本特研において実施したDTPAの毒性研究は、催奇形性試験、長期毒性試験、急性毒性、薬理試験である。催奇形性試験では、妊娠ラットにCa-DTPAを投与すると460μmol／kg以上の投与量で無眼球症、小眼球症、脳露出症、肋骨融合などの胎児の奇形が発現したが、Zn-DTPAは1,080μmol／kgまで奇形はみられなかった。すなわち、Ca-DTPAの毒性はZn-DTPAよりも強いことが認められた。Tayor, GNら（1978）の研究では30μmol／kgのCa-DTPAを妊娠ビーグル犬に投与すると、重度な奇形や毒性が認められることから、人体推奨量である30μmol／kgであっても妊婦あるいはその可能性のある女性へのDTPAの投与はできないと結論している。Ca-DTPAおよびZn-DTPAを長期間投与すると、表1に示すような種々の毒性が臨床的あるいは病理学的にみられる。この一連の研究において、Ca-DTPAよりも安全であるとされたZn-DTPAを静脈注射すると、血液中のカルシウム濃度が低下し、その結果血圧の上昇や心機能の亢進などの循環器系の異常が認められることから、とくに静脈注射によるZn-DTPAの投与は慎重に行うべきであること、さらに被曝者が高血圧などの循環器系の疾患を有する場合にはこの副作用が増大すること、DTPAの薬理作用として血管の拡張作用があり、Pu等の物質の透過性亢進によって組織への沈着が増加すること、骨における石灰化障害による骨の脆弱化やカルシウム代謝異常が起こることを新たに指摘した。CBMIDAおよび高投与量のDTPAによって見られた類骨や石灰化速度、骨形成度の変化は、同時にPuの骨沈着阻止作用が強いことを表していると判断された。

DTPAの毒性に関する結論として、人の推奨量である30μmol／kgの毒性は非常に低いが、とくに長期投与を行う場合には十分に安全な量とはいい難い。事故直後にはCa-DTPAの点滴投与、その後はZn-DTPAの経口投与によって、副作用を軽減できることが確認された。このDTPAの適用方法は、これまでの報告によって同時にPuの除去効果を高めることができることが知られている。

中国科学院上海薬物研究所と共同研究したCBMIDAのPu除去効果は、Ca-DTPAおよびZn-DTPAのいずれに比べても、Puが親和性を持つ骨の沈着を有意に減少でき、また肝臓の沈着もDTPAと同等の効果を有することから、さらに副作用もDTPAと同等あるいは注射投与では低い結果を合わせて判断すると、現時点では最もPu摂取事故において除去効果が高く、かつ安全な合成キレート剤であるといえる。

Puの除去効果は天然キレート剤に比べて合成キレート剤の方が高いが、その使用は副作用の発現によって大きく制限される。また、被曝者の状態によっても使用制限が生じる。この詳細な内容については、放医研シンポジウムシリーズNo.23, 129-137, 1992.に述べた。事故直後の被曝者自身によるPuの体内沈着量の減少および長期治療における除去対策、さらにCa-DTPAの効果の上昇と副作用低減化（低投与量化）を目的として検討した、酸化カルシウムの摂取は単独投与ではわずかであるが骨や肝臓への沈着阻止の効果がみられた。Pu投与前から酸化カルシウムを摂取しておくとより高い効果がみられた結果は、酸化カルシウムには毒性がないのでPu取り扱い作業前の服用による実用性がある。また酸化カルシウムの投与はCa-DTPAとの併用によって、Ca-DTPA単味の投与よりも骨や肝臓へのPu沈着阻止効果を高めた。酸化カルシウムによるPuの骨沈着阻止の増加率は、骨梁骨の形成割合とほぼ同等であった。したがって、酸化カルシウムの効果は、酸化カルシウムの腸管吸収率が高いため、急速に血液中へ入ったカルシウムが骨の石灰化表面に結合し、Puの沈着を阻止するためと推察された。しかし、酸化カルシウムの使用は、合成キレート剤のあくまでも補助手段であり、本質的には合成キレート剤の使用が重要である。現在人体への使用が推奨されているDTPAは、その除去効果と毒性を総合判断すると必ずしも満足できるキレート剤ではなく、さらに高い除去効果と低毒性のキレート剤の検討が必要である。

5．結論

本研究において、現在人体への使用が推奨されているDTPAの毒性の総合評価、新しい合成キレート剤である

CBMIDA の Pu の除去効果と毒性、酸化カルシウムの補助効果について検討した。その結果、次のような成果が得られた。

1） Ca-DTPA および Zn-DTPA ともに、人体投与推奨量である 30 μmol ／kgは毒性は非常に低い。事故直後に Ca-DTPA を点滴投与、その後に Zn-DTPA を経口投与することによって、除去効果だけでなく、毒性を低減できることが認められた。しかし、とくに循環器系の疾患あるいはその恐れのある被曝者に対しては、投与に際して慎重な対策が必要である。

2） 新合成キレート剤 CBMIDA の Pu 除去効果は、DTPA に比べてとりわけ骨への Pu 沈着阻止に有意な効果があり、毒性も同等あるいはやや低いことから、最も有用な薬物であると判断された。

3） 酸化カルシウムの経口投与は Pu の体内沈着阻止効果、とくに Ca-DTPA との併用適用によって除去効果の増大が認められ、被曝直後あるいは長期摂取における合成キレート剤の効果が期待された。

〔謝辞〕

本研究の遂行にあたり、CBMIDA の合成および使用に関して技術的な協力および指導を頂きました中国科学院上海薬物研究所長 Hsieh, Yuyuan 博士に深謝いたします。また、Ⅲ International Chelation Conference（Georgetown University, Washington, DC, 1989）の講演への招待および有意義な指導を頂きました International Chelation Research Foundation 理事長、Martin Rubin 博士に深謝いたします。

〔研究発表〕

1） Fukuda, S.:Toxicity of DTPA administered intravenously or orally in rats and beagles. Chelating Agents in Pharmacology, Toxicity and Therapeutics. Suppl., 56, 41-43, 1988.

2） 福田　俊：キレート剤 DTPA の毒性評価、保健物理、24, 201-210, 1989.

3） Fukuda, S., Iida, H., Hsieh, Y. and Chen, W.: Toxicological study of DTPA as a drug(V). Toxicities of Ca-DTPA, Ca-EDTA and CBMIDA after intravenous injection in beagle dogs. Hoken Butsuri, 25, 115-119, 1990.

4） 福田　俊：キレート剤の生体機能への影響と人における DTPA の安全性評価、NIRS-M-78(放医研シンポジウムシリーズ No. 21), 229-236, 1991.

5） Fukuda, S., Iida, H., Hsieh, Y. and Chen, W.: Toxicological study of DTPA as a drug(VI). Effects of intravenously injeceted Ca-DTPA, Ca-EDTA, CBMIDA and orally administered Zn-DTPA to bone metabolism in beagle dogs. Hoken Butsuri, 26, 101-107, 1991.

6） Fukuda, S., Iida, H., Hsieh, Y. and Chen, W.: Effects of CBMIDA [Catechol-3,6-bis (methyleiminodiacetic scid)] on removal of plutonium in rats. Hoken Butsuri, 27, 11-15, 1992.

7） 福田　俊：プルトニウムの沈着阻止と体外除去、NIRS-M-86 （放医研シンポジウムシリーズ No. 23), 129-137, 1992.

8） Fukuda, S. and Iida, H.: Removal of plutonium by a new type calcium and combination of the calcium and Ca-DTPA in rats. Hoken Butsuri, 28, 167-172, 1993.

9） 福田　俊、飯田治三：日本保健物理学会第 23 回研究発表会、千葉、1988, 5.

10） 福田　俊、飯田治三：日本保健物理学会第 24 回研究発表会、名古屋、1989,5.

11） Fukuda, S.:IIIrd International Chelation Conference. Washington D.C., 1989, 7.

12） Fukuda, S, Ikeda,K., Tsuchikura, S., et al.: IIIrd International Chelation Conference. Washington D.C., 1989, 7.

13） 福田　俊：第 21 回放医研シンポジウム、千葉、1989,12.

14） 福田　俊、土倉　覚、池田克巳ら：日本保健物理学会第 25 回研究発表会、つくば、1990, 5.

15） 福田　俊、飯田治三、稲葉次郎：日本保健物理学会第 25 回研究発表会、つくば、1990, 5.

16） 福田　俊、飯田治三：日本保健物理学会第 26 回研究発表会、大阪、1991, 5.

17） 福田　俊：第 23 回放医研シンポジウム、千葉、1991, 12.

3．内部被曝リスクの低減化に関する研究
③内部被曝個人モニタリングの改善に関する研究

小泉　彰、山田裕司、宮本勝宏、福田　俊、飯田治三（内部被ばく研究部）

Studies on Improvements of Protection Techniques for Inhalation of Radioactive Aerosols

Akira Koizumi, Yuji Yamada, Katsuhiro Miyamoto, Satoshi Fukuda and Haruzo Iida
Division of Radiotoxicology

In this series of study, three investigations were carried out independently as follows;

1) Estimation of dispersal rates for non-volatile radioactive nuclides under some operations with experimental animals

The dispersal rates of non-volatile radioactive nuclides were determined with a view to obtaining a basic information, which will be applicable to safety handling of experimental animals administered radioactive nuclides like as Pu. Under injection of RI to rats, the dispersal rates detected during the injection operation, housing in cages, anatomical operation were the order of 10^{-7}/ h. But the dispersal rates from contaminated surface of animals were very high values, the order of 10^{-7} per one operation. Air contamination dispersed from 20 rats administered Pu by inhalation and animal surface contamination decreased rapidly, and were not detectable after 2 weeks from administration.

2) Calibration method for alpha counting of Pu on an air filter paper

It is important to know the over-all counting efficiency of alpha measurements of air filter in radiation protection. In this study, the counting efficiencies of ZnS(Ag) scintillation counting were measured for three types of sample as follows;

sample A:filter paper collected Pu aerosols.

sample B:plate source which Pu solution was dropped on and dried.

sample C:filter paper which Pu solution was dropped on and dried.

Pu activities on each sample were decided by characteristic X-rays counting. Each counting efficiency for sample A,B,C were 6.6%, 35%, 6.8%. Alpha spectrum of sample A was quite different from that of sample C, it was clear that sample C was not pertinent as a standard source. These results show that using sample B as a standard source causes a large under-estimation of air concentration.

3) Size estimation method of radioactive aerosols in air monitoring

New simplified method for particle size estimation of radioactive aerosols was proposed for air monitoring. It does not need any new instruments but a traditional aerosol sampling device with a multistage filter system. The method is based on the particle size dependency of penetration for air filter. Decontamination factor data measured in each filter stage is inverted to a size distribution of aerosols. When air filter for a dust sampler such as Toyo HE-40T is used, the method can be applied for a size estimation of aerosols ranging from 0.2 to 10 μm in which ICRP is interested for lung deposition model. In a size measurement of ^{198}Au aerosols, it was shown that the size distribution estimated by the present method was in a good agreement with the distribution by the existent method using a cascade impactor.

緒言

放射性物質の吸入による内部被曝の問題は核燃料再処理事業の民営化などの推移もあり、年々その重要性を増している。特にプルトニウムに代表されるアルファ核種による内部被曝においては、摂取量に比して被曝線量（預託線量当量）が大きく、そのため各種のモニタリング技術の精度、感度、迅速性などはベータ核種、ガンマ核種よりも高度なものが要求される。しかし、プルトニウムのようなアルファ核種のエアロゾルの吸入摂取に伴う内部被曝を想定すると様々な問題が残されている。まず第１の問題はアル

ファ核種が取り扱う操作によって空気中へどの程度舞い上がるか、すなわち飛散率はどの程度かという点である。この飛散率が各作業者個人の内部被曝評価の基本となるが、これまで飛散率の知見は極めて少ない。第２の問題はエアロゾルの濃度を計測する方法である。通常放射性エアロゾルはエアフィルタによってサンプリングされ、そのフィルタの放射能を計測することによって濃度が決定されるが、アルファ核種のエアロゾルの場合ではこの放射能計測が容易でない。その理由はアルファ線の透過力が非常に小さいことと、エアロゾル粒子がフィルタに捕捉される際フィルタ繊維層内に潜り込むためにアルファ線の吸収あるいはエネルギーロスが生じることから、定量的な計測が困難になるためである。第３の問題はエアロゾルの粒子径分布が通常不明であるため、内部被曝線量の計算による評価で大きな誤差（不確定要因）を生じることである。エアロゾルが吸入摂取される際、粒子が肺気道内壁に沈着する場所と沈着率はその粒子径によって異なる。沈着部位によって粒子のその後の代謝・挙動は大きく異なる。そのため被曝線量の評価値に大きな不確定性が生じる。粒子径分布が通常不明なためICRP Publ.30[1]では１ μm に仮定することを勧告しているが、0.1 μm と１ μm では被曝線量の評価値には約５倍の差が生じると考えられる。

本研究は上記のような内部被曝防護上の種々の問題を研究課題としたが、内部被曝実験棟におけるプルトニウムの内部被曝影響研究プロジェクトの安全性研究としても位置付けられた。従って、安全性を検討する対象は種々の実験研究の作業、及びこれらに対する安全管理技術に限定した。そのため具体的な研究課題は次の３点とした。

１）プルトニウムを投与した実験動物の実験上の種々の取り扱い操作におけるプルトニウムの空気中への飛散量の評価
２）プルトニウムエアロゾルを捕集したフィルタ試料の校正方法の開発
３）日常的なモニタリング手法としてのプルトニウムエアロゾルの粒子径分布の評価方法の開発

研究１．動物実験における投与RIの飛散率の評価

実験の概要と結果

動物に投与されたRIの飛散の程度は核種と取り扱い操作によって異なる[2]。核種は揮発性か非揮発性かに大別され、プルトニウムは非揮発性核種の代表である。また取り扱い操作はその内容によって飛散率が大きく異なるが、動物実験での各種操作における飛散率のデータは揮発性核種を除いて皆無であった。そこで、非揮発性核種の^{99m}Tcをプルトニウムの代わりに用い、代表的な動物実験操作である注射投与、飼育、解剖の３つの操作について^{99m}Tcの飛散量を実測した。飛散量の測定方法は、アクリル製ボックス（図１）の中で各実験操作を行い、その間に発生した空気汚染の全量をフィルタで採取し、投与量とフィルタの放射能から求めた。その結果、従来から提唱されてきた飛散率概算法[3]で得られる飛散率より高い値が観察された。この結果が生じる理由を検討した結果、動物の体毛が汚染した時空気汚染が発生し易くなることが考えられた。そこで注射投与操作をさらに分割し、注射器へのRIの分取・注射投与の操作と体毛を汚染させた動物（ラット）に触れる操作について飛散率を測定した。その結果、表１に

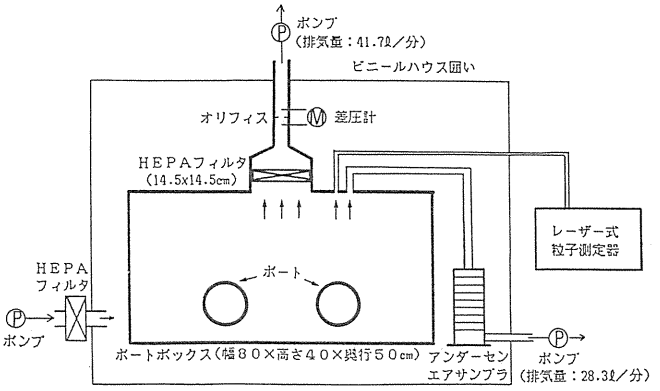

図１　飛散率実験用ボックスの概略図

表１　飛散率測定結果

回 / 操作	注射投与（分割）		注射投与（総合）
	分取・注射	接触・摩擦	
１回目	$<5.5 \times 10^{-10}$ (ND)	7.0×10^{-5}	1.2×10^{-6}
２回目	$<5.5 \times 10^{-10}$ (ND)	1.1×10^{-4}	6.1×10^{-7}
３回目	$<5.5 \times 10^{-9}$ (ND)	1.2×10^{-4}	3.6×10^{-7}
平　均	——	1.0×10^{-4}	7.2×10^{-7}

(ND)：BG値にBG値の標準偏差の3倍を加算した値を検出限界とした。

示す通り動物の体毛が汚染した時空気汚染が発生し易くなるという予測が実証された。

さらにプルトニウムを吸入投与したラット（20匹）について、飼育中の空気汚染濃度および空気汚染の源になると考えられるラット体表面のプルトニウム汚染量を投与直後から経時的に測定した。また吸入投与直後のラットの鼻先と吸入投与の際に用いる吸入ホルダ（吸入投与中ラットを固定する治具）の表面汚染を測定した。測定方法の概略は次の通りであった。

１）飼育中の空気汚染濃度

プルトニウムを投与された動物はケージごとグローブボックスのなかに収納され飼育管理される。このグローブボックスの排気の一部を投与後38日までサンプリングし、フィルタ試料にプルトニウムを捕集した。フィルタ試料の放射能量にはホスウィッチ検出器による特性X線計測（数Bq以上）またはSSD半導体検出器によるアルファ線計測（数Bq以下）を用いた。

２）ラット体表面のプルトニウム汚染量

投与後２時間後、２日後、36日後および３カ月後に麻酔下でラットの腹部、背部、鼻先上部および鼻先下部の４箇所の体表面をZnSサーベイメータで測定した。

３）鼻先、吸入ホルダの表面汚染

湿式スメアガーゼによってスメアし、ガーゼ試料をホスウィッチ検出器によって特性X線を計測した。

表２　Pu吸入投与ラット飼育時の空気汚染測定結果

試料No.	採取期間（吸入後）	検出Pu量 (Bq)	空気汚染濃度 (Bq/cc)	飼育装置内作業
RS-1	0～4 h	2.4×10^{-3}	2.7×10^{-10}	ホルダ搬入・解剖
RS-2	4～28h	1.2×10^{-3}	1.7×10^{-11}	ケージ交換
RS-3	1～3 日	ND	$\leqq3.9\times10^{-12}$	ケージ交換・解剖
RS-4	3～4 日	8.8×10^{-4}	1.1×10^{-11}	ケージ交換
RS-5	4～6 日	ND	$\leqq3.2\times10^{-12}$	ケージ交換
RS-6	6～9 日	ND	$\leqq1.9\times10^{-12}$	ケージ交換・解剖
RS-7	9～16日	ND	$\leqq9.4\times10^{-13}$	ケージ交換
RS-8	16～27日	ND	$\leqq4.8\times10^{-13}$	ケージ交換
RS-9	27～38 h	9.0×10^{-4}	1.2×10^{-12}	ケージ交換・解剖

ND：5～7 $\times10^{-4}$ Bq

表３　Pu 吸入ラットの体表面汚染測定結果

ラットNo.	背面	腹面	咽—鼻先	頭部—鼻先	合計
吸入２時間後(cpm)					
B-1	10.5	23.0	17.0	120	170.5
B-2	3.5	1.5	9.2	32	45.2
B-3	6.0	1.3	33.8	89	130.1
B-4	8.0	4.0	21.0	58.2	91.2
B-5	1.0	4.5	4.5	33	43.0
				平均	77.8
吸入後　２日(cpm)					
B-6	2.0	1.0	0	10.0	13.0
B-7	2.0	1.0	4.0	7.0	13.0
B-8	3.0	0	1.0	0	4.0
B-9	0	0	1.0	17.0	18.0
B-9	0	0	1.0	17.0	18.0
B-10	0	0	0	7.0	7.0
				平均	77.8
吸入後　36日(cpm)					
B-11	0	0	0	0	0
B-12	0	0	0	0	0
B-13	1.0	0	0	0	1.0
B-14	1.0	0	0	0	1.0
				平均	0.5
吸入後　3カ月(cpm)					
B-11	1.0	0	0	0	1.0
B-12	1.0	0	0	0	1.0
B-13	0	0	0	0	0
B-14	0	0	0	0	0
				平均	0.5

表４　吸入ホルダとラット鼻先のスメアガーゼの Pu 量（Bq）

試料No.	吸入ホルダ	鼻先
HSF-1	2250±200	17±2
HSF-2	2630±250	12±1
HSF-3	3590±390	47±3
HSF-4	4110±410	62±5
HSF-5	3340±290	47±3
HSF-6	2050±370	22±2
HSF-7	3280±410	43±3
HSF-8	2420±260	11±1
HSF-9	5020±630	37±3
HSF-10	5250±450	22±2
HSF-11	5490±540	49±4
HSF-12	5570±550	109±8
HSF-13	5330±660	59±4
HSF-14	6930±600	11±1
HSF-15	4360±540	------
HSF-16	6710±720	25±2
HSF-17	6510±1100	123±9
HSF-18	7400±500	5±1
HSF-19	3760±470	10±1
HSF-20	4550±90	14±1
平均	4528 Bq	38 Bq
合計	90550 Bq	725 Bq

表２にプルトニウム吸入投与ラット飼育時の空気汚染濃度の経時的な測定結果を示す。表３にプルトニウム吸入ラットの体表面汚染の経時的な測定結果を示す。また表４に吸入投与直後のラットの鼻先と吸入ホルダのスメア想定結果を示す。

考察

動物実験の代表的な実験操作での非揮発性核種（^{99m}Tc）の飛散率は比較的高く、プルトニウムのようなアルファ核種の使用の際には注意を要することがわかった。この飛散率が高くなる理由は表１の結果が示す通り、体毛が密生している動物体表面が汚染し、そこに実験者の手等による接触・摩擦が加わったとき飛散し易くなることであった。このときの飛散率は約 10^{-4}であり、RI の注射器への分取・注射投与の操作での飛散率はほぼ無視し得るレベルであった。測定された飛散率から注射投与時の動物体毛を汚染させた RI 溶液の量は 1×10^{-3} ml 程度と計算される。注射時にこの程度の量が動物体毛を汚染させることは充分に考えられる。これらのことは空気汚染を可能な限り低く抑えるためには動物体毛を可能な限り汚染させないようにする、という安全対策に結び付く。

表２、表３に示したプルトニウムの空気汚染濃度、動物体毛の汚染の経時的変化の結果は両者とも約２週間後にはほぼ無視できるレベルまで時間と共に低下することを示す。このことは発ガン性研究のような長期間飼育において、グローブボックスより開放的な飼育方法が可能であることを意味する。

プルトニウムを吸入投与されたラットの飼育時の空気汚染レベルは投与直後でも約 10×10^{-10} Bq / cc と極めて低く、このレベルでも法規制値の１／100 以下であった。空気汚染を低レベルに保つことができた理由には、吸入投与方法に鼻部曝露方式を採用し、体表面の汚染部を鼻先のみに限定したこと、および吸入投与直後に鼻先の汚染を拭き取ったことが大きく働いていると考えられる。

結論

プルトニウムを投与し、その安全性を研究する実験を念頭に置き、動物実験の際の非揮発性核種の空気中飛散率を検討した。その結果、次のことがわかった。

①動物体毛が汚染すると空気中への飛散率が大きくなり、その飛散率は約 10^{-4}であった。

②動物体毛、および飼育時の空気汚染レベルは時間と共に低下し、約２週間後にはほぼ無視できるレベルまで低下した。

本研究で得られた上記の知見は現在内部被曝実験棟におけるプルトニウム投与動物および各種試料の取り扱いに対する安全管理に反映され、利用されている。しかし、種々のケースでの飛散率のデータはまだ少なく、今後とも多くの事例で飛散率データを積み重ねていく必要があると思われる。

研究２．プルトニウム粒子を捕集したフィルタ試料の校正方法

実験の概要と結果

放射性エアロゾルによる空気汚染は通常エアスニッファ設備でフィルタに粒子を捕集し、そのフィルタの放射能の測定から求められる。このときアルファ核種については ZnS シンチレーションカウンタの用いられることが多い。この ZnS シンチレーションカウンタの計数効率は適当な

標準線源が無いため、アルファ核種の電着試料あるいは既知濃度溶液をフィルタに滴下した試料から求められる。これらの標準試料での計数効率と実サンプル（プルトニウム粒子を捕集したフィルタ試料）での計数効率にどの程度の差異があるかを次の方法で測定した。

プルトニウムエアロゾルを捕集したHE-40Tフィルタ試料（実サンプル）、プルトニウム溶液をステンレス板に滴下し、蒸発乾固した試料（標準乾固試料）、およびプルトニウム溶液をHE-40Tフィルタに滴下し、蒸発乾固した試料（標準含浸試料）の３種類の試料を作製し、それぞれのプルトニウム量を特性X線計測によって求めた。３種類の試料を日常モニタリングに用いられるZnSシンチレーションカウンタでアルファ線を計測した。さらに３種類の試料のアルファ線スペクトルをシリコン半導体検出器で測定した。

３種類の試料のアルファ線スペクトルを図２～図４に示す。このスペクトルから標準乾固試料ではプルトニウムアルファ線スペクトルのみが観察されるが、実サンプルおよび標準含浸試料ではフィルタ内部への潜り込みに起因する低エネルギー成分が見られ、その割合は多かった。３種類の試料のZnSシンチレーションカウンタでの計数効率は実サンプルが6.6％、標準乾固試料が35％、標準含浸試料が6.8％であった。

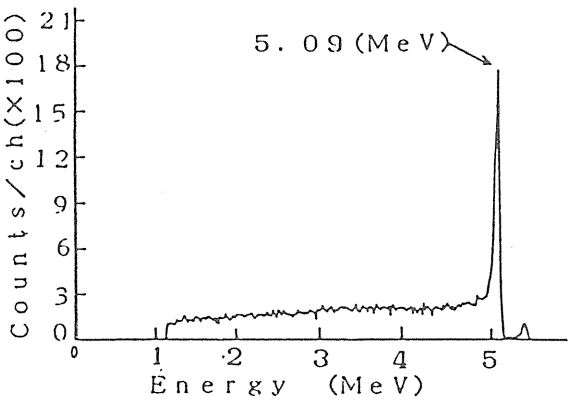

図２　サンプルのα線スペクトル

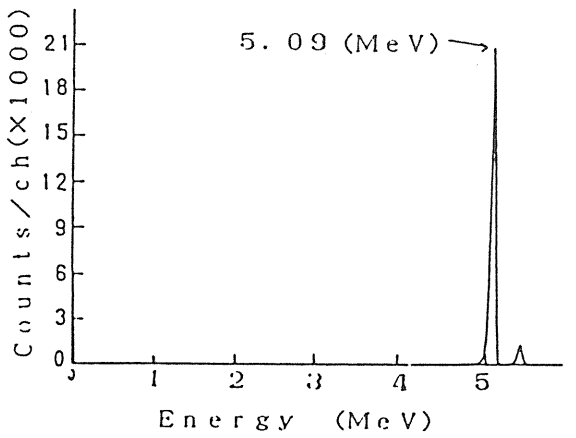

図３　標準乾固試材のα線スペクトル

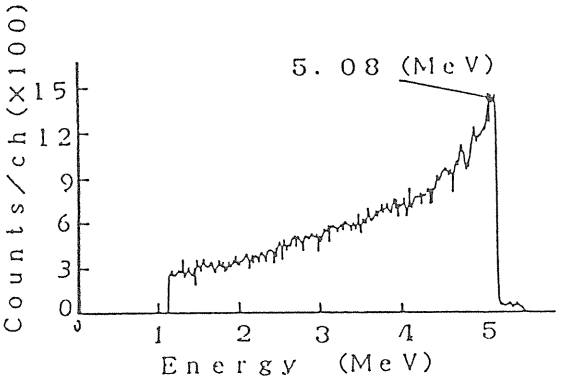

図４　標準含浸試材のα線スペクトル

考察

実サンプルと標準含浸試料の計数効率は近い値を示したが、アルファ線スペクトルを比べると全く異なっており、ZnSシンチレーションカウンタのディスクリレベルが不明な点を考慮すると標準含浸試料が標準線源としては不適当なことは明らかである。一方、実サンプルと標準乾固試料とでは計数効率に約５倍の差があり、またこの差は空気汚染濃度を１／５に過少評価することを意味する。安全管理上かなりの注意を要すると考えられる。しかし、今回得られた実サンプルの計数効率は、汚染空気のサンプリング流量すなわち面風速が異なるとフィルタの捕集効率、フィルタ内部への潜り込みの程度が変わってくるため変化すると考えられる。さらに放射性エアロゾルの粒子径分布が異なると同様に計数効率は変化すると考えられる。

結論

①アルファ核種のエアロゾルを捕集したフィルタのアルファ線計測における標準線源として、電着線源、蒸発乾固試料、あるいはフィルタへ溶液を滴下し、蒸発乾固した試料はそれぞれが不適当である。

②電着線源、蒸発乾固試料から求めた計数効率を用いると、空気汚染濃度を１／５程度に過少評価する可能性がある。

③アルファ核種のエアロゾルを捕集したフィルタのアルファ線計測における計数効率は、既知量のエアロゾルを捕集したフィルタを用いて求める必要がある。

研究３．放射性エアロゾルの粒子径分布評価法の開発

実験の概要と結果

プルトニウム等のアルファ核種を取り扱う事業所では通常エアスニッファなどによって常時空気中の放射性エアロゾルをフィルタに採取し、空気中放射能濃度を監視している。しかし、この方法では空気中濃度の情報は得られるが、内部被曝線量評価の際有用なエアロゾル粒子の中央径、分散の情報は得られない。そこで事故的な吸入摂取時の内部被曝における線量評価の精度向上を目的とし、通常１段フィルタのエアスニッファを多段にする多段フィルタサンプリングによって得られる各段のフィルタの放射能値から空気汚染濃度のみならず、粒子径分布も評価する方法を考案した。

多段フィルタ法の原理は次のとおりである。フィルタの上流側と下流側のエアロゾル分布を測定した例を図５に示す。上流側と下流側ではエアロゾル分布の形が変化している。このデータから粒子径ごとに透過率＝下流側濃度÷上

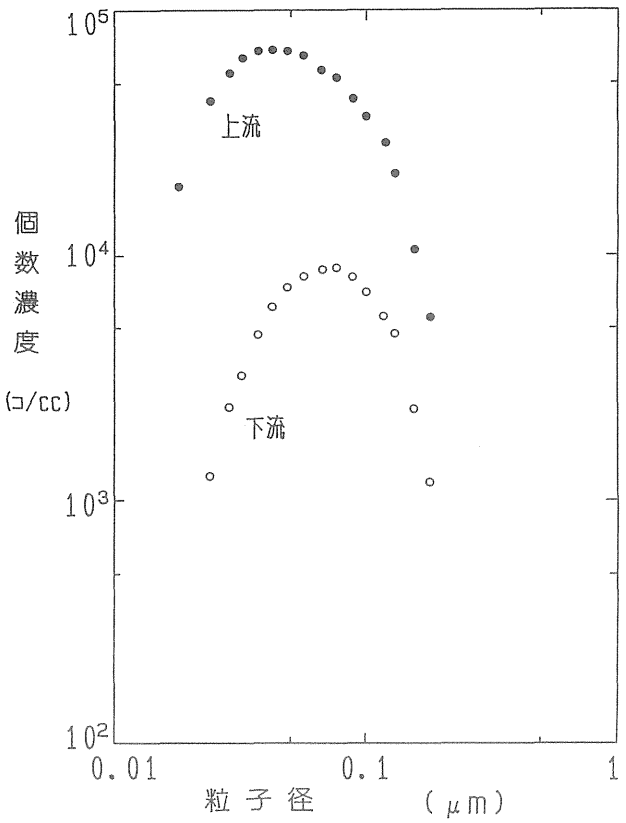

図5　フィルタ上流・下流の粒子径分布

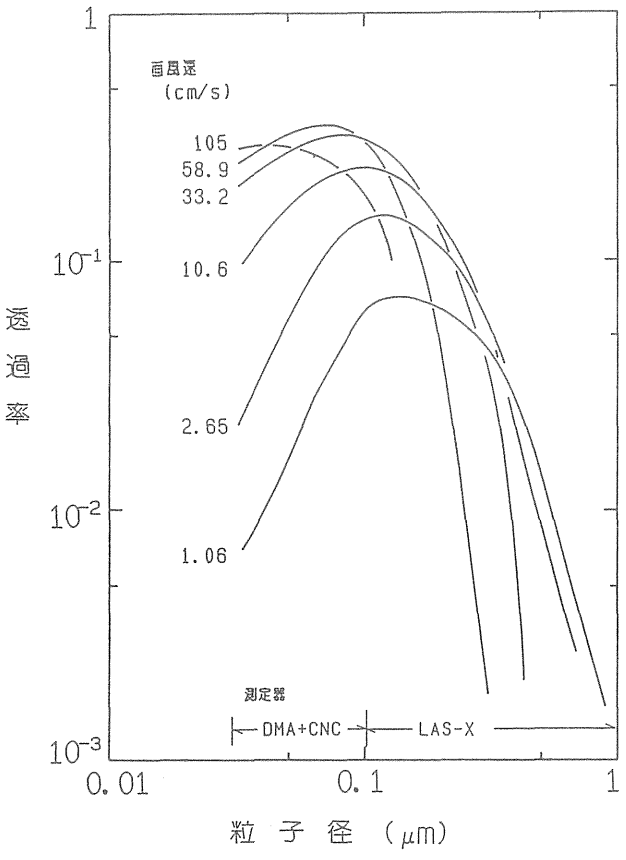

図6　HE-40T フィルタの透過率曲線（面風速依存性）

流側濃度、を計算すると一つの曲線となり、これを透過率曲線という。図6に空気汚染サンプリング用フィルタの透過率曲線の測定例を示す。フィルタのエアロゾル透過率曲線はフィルタ繊維および粒子の帯電が無い場合1つの曲線となる。すなわち透過率曲線はそのフィルタ固有の性能であり、2段、3段に用いても変化せず、またエアロゾル粒子の種類が異なっても変化しない。一定の面風速での透過率曲線が得られれば1段目フィルタの上流側の粒子径別濃度分布から下流側の粒子径別濃度分布が計算できる。1段目フィルタの下流側の粒子径別濃度分布は2段目フィルタの上流側の粒子径別濃度分布であるから2段目フィルタの下流側の粒子径別濃度分布も計算できる。同様に3段目フィルタの下流側の粒子径別濃度分布も計算できる。この計算結果から各段のフィルタの除染計数（DF）が求められる。この計算を様々な粒子径分布（中央径と分散）について行い、粒子径分布ごとに各段の DF の組み合せを予め計算しておく。多段フィルタ各段の放射能実測値から各段の DF を計算し、この DF に最も近い組み合せとなる粒子径分布を選び出す。この粒子径分布が汚染空気のエアロゾルの粒子径分布である。

ダストサンプリング用ろ紙（東洋、HE-40T）について面風速 1.33 cm／sec での透過率曲線を測定し、数値計算に用いる関数として次の近似関数を得た。

$$\log P = -2.25\ \{\log dp\}^2 - 4.12\ \{\log dp\} - 2.71$$

ただし、Pは透過率、dp は粒子径（μm）である。この近似関数を用い、中央径（MD）が 0.1 から 10μm の範囲、および幾何標準偏差（GSD）が1～5の範囲の、812 通りの粒子径分布における各段の DF を計算機で予め計算した。次にカスケードインパクタで粒子径分布が測定されている ^{189}Au の放射性エアロゾルを HE-40T フィルタの3段フィルタでサンプリングし、各段の放射能実測値から各段の DF を算出した。算出された DF の組み合せに近い組み合せを 812 通りの粒子径分布から計算機によって選出させた。その結果を表5に示す。選出された粒子径分布はどれもカスケードインパクタによる実測値と極めて良い一致を見た。

表5．多段フィルタ各段の DF の実測値と計算値の比較

Filter	Decontamination Factor (DF)			
	Experiment*	Calculation		
	MD =1.2 GSD=2.0	MD =0.9 GSD=1.8	MD =1.0 GSD=1.9	MD =1.2 GSD=2.0
First Stage	94.1±3.9	89.6	99.3	130.6
Second Stage	20.7±1.1	21.4	20.2	20.4
Third Stage	13.9±3.1	13.1	12.4	12.2

*；Size distribution determined by a cascade impactor and DFs measured in the three stage filer.

考察

今回の実験結果は考案した多段フィルタ法が放射性エアロゾルの粒子径分布評価法として妥当であることを示している。またその評価精度は内部被曝線量の評価には充分であった。多段フィルタ法によって得られる粒子径は内部被曝線量計算で必要となる放射能基準中央径（AMAD）であり、エアロゾル粒子の種類の違いにおける粒子密度の差を考慮する必要が無い利点がある。また最大の利点は事故時のような通常粒子径分布の情報が得られないケースに対しても、エアスニッファの1段フィルタを3段フィルタシステムに替えることのみで対応でき、カスケードインパク

タのような特別な装置を必要としないことである。ただし、フィルタを多段に用いるため通気抵抗（圧量損失）が高くなるので、従来のエアスニッファにそのまま適用するには問題があると考えられる。

今回の実験では粒子の体積に放射能量が比例するケースを検討した。しかし、ラドン、トロンの娘核種の吸入摂取の場合のように非放射性粒子の表面にRIが付着している、すなわち放射能が粒子表面積に比例するケースも考えられる。このようなケースでも種々の粒子径分布について予めDFを計算する段階で粒子表面積に比例する計算をしておけば対応できると考えられる。

結論

放射性エアロゾルの粒子径分布評価法として多段フィルタ法を考案し、その妥当性を実験的に確認できた。多段フィルタ法は特別な装置を必要とせず、日常的なモニタリング手法として採用でき、予め予測できない事故的な空気汚染の発生にも対応できる。

［参考文献］

1）ICRP,Publication 30 Part 1.(日本アイソトープ協会).p55.1980.

2）高田　茂、他　RADIOISOTOPES、32、260-269、1983.

［研究発表］

1）山田裕司、宮本勝宏、小泉　彰：HEPAフィルタの捕集効率と除染係数、保健物理、21、237-244、1986.

2）宮本勝宏、山田裕司、福田　俊、飯田治三、小泉彰：第23回日本保健物理研究発表会口頭発表、1988.5.（千葉）.

3）小泉　彰、宮本勝宏、山田裕司：第24回日本保健物理研究発表会口頭発表、1989.5.（千葉）.

4）山田裕司、福田　俊、小泉勝三、飯田治三、小泉彰：第24回日本保健物理研究発表会口頭発表、1989.5.（愛知）.

5）小泉　彰、山田裕司、宮本勝宏：集塵用フィルタの粒子捕集効率の面風速依存性、保健物理、24、123-127、1989.

6）小泉　彰、山田裕司：第25回日本保健物理研究発表会口頭発表、1990.5.（つくば）.

7）福田　俊、飯田治三、山田裕司、小泉　彰、宮本勝宏、佐藤　宏、吉田浩樹：第26回日本保健物理研究発表会口頭発表、1991.5.（大阪）.

8）Yamada, Y. and Koizumi, A.: Simple method of size estimation of radioactive aerosols in air monitoring, J. Jpn. Health Phys. Soc., 26,17-21,1991.

9）吉田浩樹、津浦伸次、小泉　彰、山田裕司：第27回日本保健物理研究発表会口頭発表、1992.6.（秋田）.

10）小泉　彰、山田裕司、宮本勝宏、陳　淑恵：第28回日本保健物理研究発表会口頭発表、1993.5.（福岡）.

Ⅲ. アルファ放射体による内部被ばくの生物学的影響とその修飾因子に関する研究

1. 吸入放射性物質の気道内沈着と体内動態に関する研究

佐藤　宏、山田裕司、宮本勝宏、小泉　彰(内部被ばく・防護研究部)、
稲葉次郎(研究総務官)

Deposition of Inhaled Radionuclides in the Respiratory Tract and Metabolism

Hiroshi Sato, Yuji Yamada, Katsuhiro Miyamoto,
Akira Koizumi (Division of Radiotoxicology and Protection),
and Jiro Inaba (Deputy Director-General)

A. Modeling of larynx and tracheo-bronchial regions for aerosol deposition study

New cast models of larynx and tracheo-bronchial (TB) regions were developed for aerosol deposition study. Stereo-lithography method was applied to the modeling. Geometrical shape and dimensions of the larynx were originally determined based on a human anatomical data. Those of the TB region were given by Weibel's bifurcation model data. Total depositions in the cast were measured for monodisperse aerosols ranging from 0.01 to 0.3 μm in diameter. Deposition efficiency increased with decreasing particle size and flow rate.

B. Effects of firing temperature on the metabolism of plutonium inhaled into the rats

Wistar rats were inhaled PuO_2 produced by firing Pu hydroxide at 1150 and 400℃ and the difference in lung retention, excretion and translocation of Pu between the both firing temperature were studied. The clearance of Pu from lung was relatively faster in rats exposed to PuO_2 fired at 400℃ (low temperature group) than in the rats exposed to PuO_2 fired at 1150℃ (high temperature grouop). The fecal excretion of Pu was larger in the low temperature group than high temperature group and the ratio of fecal excretion to urinary excretion was higher for low temperature group than high temperature group. The amounts of Pu, although, translocated from lung the organs, even liver, were very small, the re-distribution of Pu to liver was higher in the low temperature group. This study suggests that the lung retention of Pu is slightly affected by the firing temperature of PuO_2 in rats.

A. 呼吸気道模擬モデル

1. 緒　言

国際放射線防護委員会ICRPにおいて検討されていた呼吸気道モデルがPub.66(1994)として発表された。本モデルはPub.30(1979)に替わるもので、その中でエアロゾル粒子沈着モデルも大幅に手直しされるなど、呼吸気道内における沈着問題は今、大きな関心を集めている。しかしながら、呼吸気道における沈着現象を実験的に調べ、これを理論的に解析・解明することは容易ではなく未だ十分な知見が得られているとは言えない状況にある。

沈着実験研究には、ヒトからデータを直接得る方法から動物実験、あるいは全くの工学的実験までいろいろなアプローチ法があるが、何れも1つでは十分ではなく、それぞれに限界がありお互いに補完しあっていく必要がある。これらの中で著者らはこれまで工学的手法で生体に如何に近づけるかということで、呼吸気道の鋳型というキャストモデルを用いた実験的アプローチをしてきた。しかし、今回は沈着機構の解明に焦点を絞るため、「生体に近いモデル」を目指すのではなく「解析し易いモデル」による沈着実験を追い求めた。ここでは、この目的のため呼吸気道模擬キャスト作成法の新提案とこれを用いて得られたエアロゾル沈着データを示す。

2. 実験方法

呼吸気道内エアロゾル沈着機構解明にとって「解析し易いモデル」ということで、形態学的に幾何モデル化し易い部位、つまり、喉頭部及び気管－気管支部をまず選んだ。気管－気管支部についてはWeibelの対称2分岐モデルを基本に分岐構造を持った直円管で表現した。喉頭部については解剖学的所見を参考に直円管・放物球・楕円球などを組み合わせて出来るだけ単純に表現した。こうしてできた幾何表現モデルの具現には3次元光造形法を利用した。呼吸気道模擬キャストの作成にはFig.1に示したような方法に

て行った。まず、Weibelの対称２分岐モデルの数値データを３次元CADデータに展開した。これを基にレーザービームで光硬化樹脂に照射し、0.178mmの厚みで100層にも積層して気管ー気管支部模擬キャストを作成した。分岐次数が８分岐の気管ー気管支部模擬キャストをFig.2に示した。エアロゾル沈着実験は、胸郭を模擬したチャンバ内にキャストを吊して行った。実験には蒸発ー凝縮法により発生させたNaClエアロゾルを静電分級器で単分散化したエアロゾルを用い、0.01～0.3μm径範囲でキャスト内粒子径別沈着率を凝集核測定器CNCで調べた。なお、沈着実験に先立ちキャスト表面には静電気防止剤を塗布し、静電気による沈着影響を防止した。

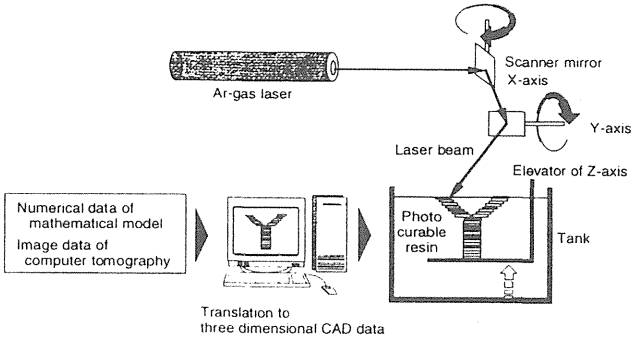

Fig.1 Casting method for the respiratory tract model by stereo-lithography.

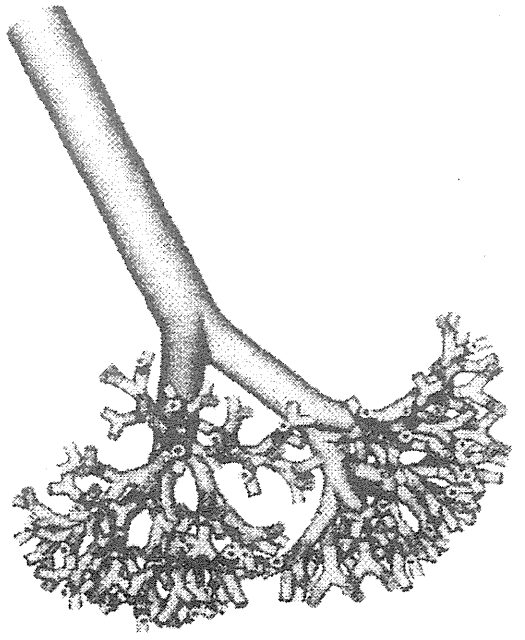

Fig.2 Tracheobronchial cast model of photo-curable resin.

3．実験結果及び考察

７分岐モデルを用いたエアロゾル沈着実験の結果をFig.3に示した。空気の流れは気管から気管支末端へという吸気の方向で、流量は1.5、4、10l/mの定速流である。粒子径が0.01～0.3μmで1%以下であった沈着率は粒子径が小さくなるにつれて上昇し、0.01μmでは10%以上になった。特に流量が少ない1.5l/mにおいては40%に達した。このように分岐次数が比較的浅い７分岐までの気管支部においても、粒子径が小さく、流量が少ない場合はかなりの高率で粒子沈着が生じることがわかった。図中に示した理論曲線は単純な直円管の連結体を仮定し、拡散沈着のみを考慮した場合の沈着予測である。予測値は実験値に近いところもあるが、これだけで沈着を説明することは困難である。次に気道分岐次数の違いによる沈着率の差異を調べた。Fig.4には７分岐モデルと４分岐モデルの沈着率を示した。分岐次数が少ない場合には、当然の結果ながら沈着率は低く観察された。両モデルにおける沈着率の差がちょうど５、６、７分岐目までにおいて沈着した成分となる。今回用いたような実験系では0分岐からn分岐までの気道全域における全沈着率しか測定できないが、分岐次数が異なるモデルを組み合わせることにより各分岐次数毎の沈着率を評価できる。

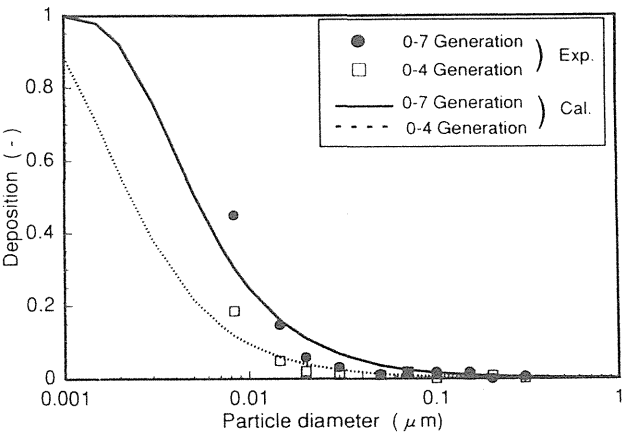

Fig.3 Aerosol deposition effciencies within the tracheobronchial cast with 0-7 generations.

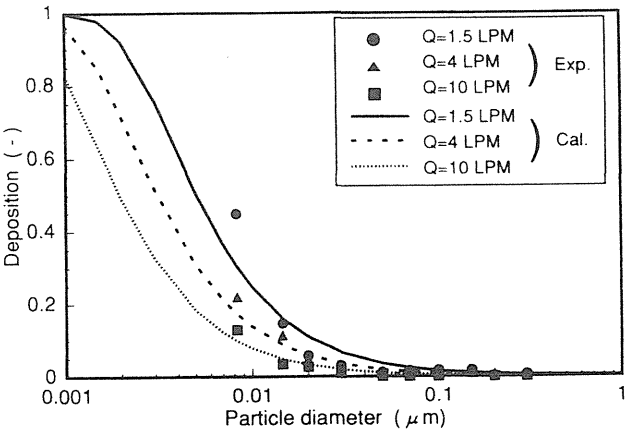

Fig.4 Comparison of aerosol deposition efficiencies at an air flow rate of 1.5 liter/min for casts with 0-7and 0-4 generations.

4．結論

従来の気道モデルは樹脂を体内に注入するなどして鋳型を作成。これを沈着実験に使用していたが、形状が複雑な肺深部に対しては鋳型法は適用できないという背景があった。しかし今回、3次元光造形法による気道モデルを世界で初めて実用化し、これを沈着実験に適用できることを実証した。また、超微小サイズ（ナノメートル）エアロゾルの高強度沈着現象を鼻咽頭部に続いて気管ー気管支部でも観察できた。ICRPの肺沈着の旧モデル（Publ.30モデル、1979）と新モデル（Publ.66モデル、1994）との大きな違いの1つが鼻咽頭部における超微小サイズエアロゾルの高強度沈着を認めたことである。これはラドンのように超微小サイズエアロゾル（ラドン分野では通例、フリー成分あるいは非付着成分と呼ばれる）が存在する場合の吸入被曝線量の算定に大きな差異をもたらすことを意味する。

B．ラットに吸入されたPuの体内動態に及ぼす焼結温度の影響

1．緒言

吸入されたPuの体内動態に影響を与える因子としてはPuの化学形、粒子状Puの粒子径、酸化Pu生成時の焼結温度、初期沈着量などが考えられる。特にPuの化学形はその溶解性に大きく関わってくるため、肺に沈着後の代謝に大きな影響を及ぼすと考えられる。Pu化合物としてはクエン酸塩、硝酸塩、水酸化物、酸化物等があるが、本研究では水酸化物の焼結により化学変換した酸化物と未焼結の水酸化物の粒子状Pu 2種類についてラットへの吸入実験を実施した。酸化Puの吸入実験に関して、犬では焼結温度の違いにより肺でのretentionが大きく異なるが、マウスでは全く影響を受けないとの報告がある。しかし、マウスと犬の中間に位置するラットでは焼結温度の違いによる肺でのretentionへの影響についての報告はない。中課題「アルファ放射体による内部被ばくの生物学的影響とその修飾因子に関する研究」では高温の1150℃で焼結させた酸化Puのラットへの吸入実験を中心に行っているが、本研究では低温の400℃で焼結させた酸化Puについても同様の実験を行い、2種類の温度で焼結させた酸化Puの肺でのretention、肺から全身への移行、糞尿への排泄が焼結温度により異なるのか否かを検討した。また、吸入後に沈着した肺において、肺の細胞内の微細分布に違いがあるのか、違いがあるならばそれがretentionにどのように関わっているのかを検討する目的で2カ月までの短期吸入実験を行った。

2．実験方法

2－1．体内動態に対する焼結温度の影響：ウィスター系雌ラットに無麻酔下で焼結温度の異なる2種類の酸化Puを吸入させ、また、比較の意味で未焼結の水酸化Puを吸入させた。吸入2日後、体外計測法により肺への沈着量を算定し初期肺沈着量（initial alveolar deposition,IAD）とした。吸入直後よりラットを1匹ずつ個別のケージで飼育し、糞尿を分別採取した。肺でのretentionは経時的に体外計測法により求めた。摘出した臓器中および糞中のPu量は600℃で灰化後に試料を硝酸とフッ化水素酸の混合酸に溶解し、液体シンチレーションカウンター（液シン）で計測することにより求めた。尿中のPu量は直接、液シンで測定して求めた。

2－2．細胞内分布に対する焼結温度の影響：2－1と同様にPuを吸入させたラットより肺を摘出、4匹分をまとめて0.25Mショ糖液中ワーリング・ブレンダーにてホモジナイズし、通常の細胞分画法により以下の画分に分けた。750gで10min遠心分離後の沈渣を核画分、3,000g、12minおよび30,000g、25minの沈渣をそれぞれミトコンドリア、リソゾーム画分とした。30,000g上清を更に105,000gで60min遠心分離して得られた沈渣をミクロゾーム、上清を可溶画分とした。各画分を精製後、0.25Mショ糖液に懸濁し、液シンで放射活性を測定してPu量を求めた。

3．実験結果及び考察

3－1．体内動態に対する焼結温度の影響：ラットに吸入されたPuの粒子径（activity median aerodynamic diameter, AMAD）、吸入量、IAD、沈着率（吸入量に対するIADの割合）をTable 1に示した。沈着率は高温で焼結させた酸化Pu（以下、高温酸化物）の35%に対し低温で焼結させた酸化Pu（以下、低温酸化物）では52%で1.5倍、水酸化Pu（以下、水酸化物）では1/2の17%であった。2種類の酸化物は吸入量がほぼ同じにも関わらずIADに差が生じた。AMADは低温酸化物の方が25%小さいが、ICRPの報告書によると0.3～0.4 μmの範囲では沈着率にあまり差がないことからAMADの関与は考えにくい。したがって、原因としては焼結温度の違いが考えられるが、現段階では沈着率の違いの真の原因は不明である。水酸化物のAMADは高温酸化物とほぼ同じであるがIADは1/2であり、これは化学形の違いに起因したものであろう。2種類の酸化物

Table 1. Initial alveolar deposition of plutonium dioxide and hydroxide

Chemical form	Firing temp.(℃)	AMAD (μm)	σ_g	Inhaled	IAD	IAD/Inhaled
dioxide	1150	0.38	1.7	4102±581*	1398±88	0.35±0.043
dioxide	400	0.29	2.1	3873±660	2005±498	0.52±0.070
hydroxide		0.40	2.2	7131±1330	1193±498	0.17±0.051

AMAD: activity median aerodynamic diameter, IAD: initial alveolar deposition.
*: mean ± SD.

Table 2. Translocation of Pu from the lung to the other organs 1 month after inhalation of Pu dioxides and hydroxide

Organ/Excreta	Oxide (1150℃)	Oxide (400℃)	Hydroxide
Lung	79.2±6.78*	58.3±4.01	6.10±6.72
Liver	0.044±0.020	0.075±0.037	0.207±0.025
Spleen	0.0047±0.0028	0.0019±0.0090	0.017±0.0024
Kidney	0.0065±0.001	0.0028±0.0010	0.045±0.0057
Femur	0.0015±0.0021	0.0004±0.0004	0.040±0.0025

*The values are mean ± SD of 4 rats, and expressed as % IAD.

の肺でのretentionを水酸化物を対照としてFig. 5に示した。高温酸化物を吸入されたラットのlung retentionは吸入後いずれの時期においても水酸化物より大きく、肺から全身への移行速度は水酸化物の方が速い（Fig. 5A）低温酸化物は水酸化物よりlung retentionがやや小さい時期もあったが概して類似のretention curveを描く（Fig. 5B）。排泄についても同様の傾向が見られた。Fig. 6は1日当たりの排泄率の経時変化をに示したものであるが、糞および尿中への排泄率は水酸化物の方が高温酸化物より高く、特に尿中への排泄率が水酸化物では0.1－0.3%で酸化物の0.05－0.1%に対し数倍高い値を示した（Fig. 6A）。一方、

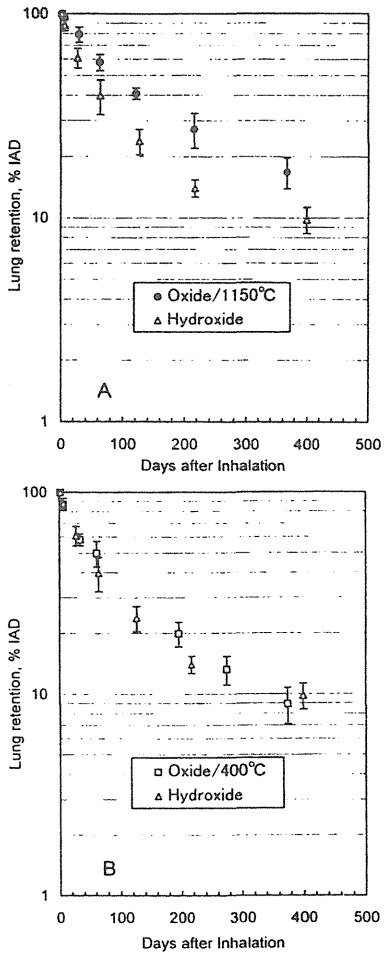

Fig.5 Ling retention of Pu following inhalation of PuO_2 fired at 1150℃(A) and 400℃(B)

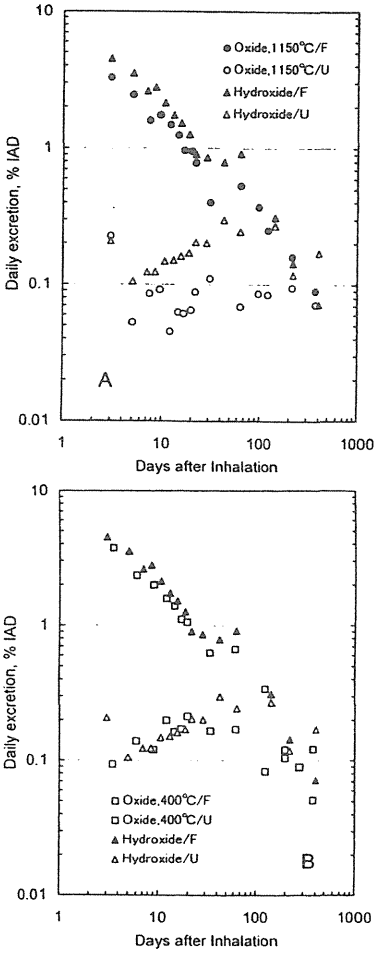

Fig.6 Daily fecal and urinary excretion of Pu following inhalation of PuO_2 fired at 1150℃(A) and 400℃(B)

低温酸化物では糞中への排泄率が水酸化物よりやや低い傾向が見られたが尿中への排泄はほとんど同じ様に推移し、非常によく似た排泄パターンを示した（Fig. 6B)。肺から全身へ移行したPuの吸入１カ月後の臓器分布をTable 2に示した。各臓器中のPu存在量はいずれも１％未満で少なかったが、酸化物と水酸化物で分布率に違いが見られた。すなわち、２種類の酸化物の臓器分布はほぼ同レベルであったが、水酸化物では数倍高い割合で存在していた。特に骨への分布率の違いが大きく、1桁以上の差が見られた。以上のように、焼結温度の異なる２種類の酸化物をラットに吸入させた場合lung retentionに差が生じるが、その差はイヌの場合ほどは大きくない。しかし、マウスの場合のように全く差がないという結果でもない。一般に小さい動物ほど物質の代謝速度が速いと考えられるが、マウス、ラット、イヌ３種類の動物のデータの違いは代謝速度の違い、すなわち動物種差によるものと考えられる。

また、酸化Puと水酸化Puを吸入させたラットについて、IADが異なる吸入群において吸入沈着後のPuの臓器分布がどのように異なるか、IADと臓器分布との関連性を検討した。比較したのは、低温酸化物でIADが500Bq（低IAD群）と2000Bq（高IAD群)、水酸化物で200Bq（低IAD群）と1000Bq（高IAD群）である。対象臓器は肝、脾、腎、大腿骨。Fig. 7は低温酸化物の吸入１カ月後における対象臓器の分布率を個体毎に示したものである。いずれの臓器においても高IAD群の方が臓器への分布率は小さい。特に腎、大腿骨で差が大きく、大腿骨では約40倍の差がある。Fig. 8は水酸化物の吸入１カ月後の結果を示したものであるが、肝、大腿骨でやや違いが見られる程度で全体としてはあまり差は見られない。酸化物ではIADが１桁ないし２桁違う場合に臓器分布が異なると報告されている。確かに低温酸化物ではIADが数倍違っても臓器分布に差が見られたが、水酸化物では酸化物の場合のような違いが見られなかったことから化学形の違いによることは容易に推測できる。しかしそのメカニズムは不明である。酸化物でのIADによる臓器分布の違いはlung retentionの違いによると思われる。肺では酸化物の溶解がある速度で少しずつ進むとすると高IAD群では単位時間当たりに可溶化される割合が低IAD群に比べて小さくなる。このようなことがIADの違いによって臓器分布が異なる原因になっているのではないかと思われる。

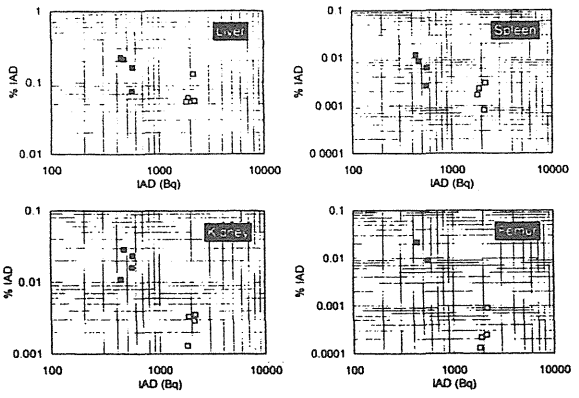

Fig.7 Effect of IAD on the tissue distribution of Pu following inhalation of PuO_2 fired at 400℃

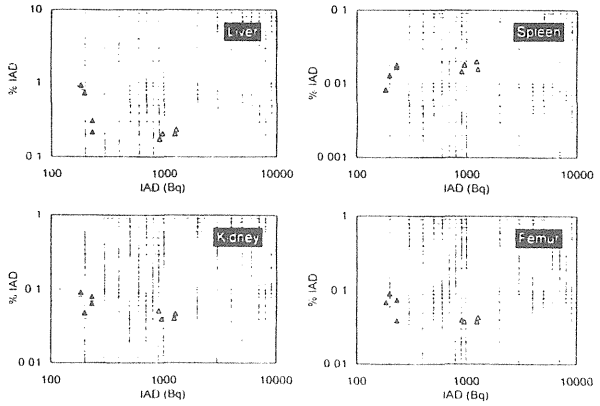

Fig.8 Effect of IAD on the tissue distribution of Pu following inhalation of Pu hydroxide.

3－2．細胞内分布に対する焼結温度の影響：Fig. 9に示したように、高温酸化物では1週間後、約60%がミトコンドリアに存在し、残りはリソゾームと核に存在していた。ミトコンドリア画分のPu量は徐々に増加し、9週間後には80%がミトコンドリアに存在していた。リソゾーム中のPu量は投与後の時間により多少の変動はあるが、実験期間中を通してほぼ20%であった。核画分のPuはリソゾームと1週目に約20%であったが、2週目に数%に減少した後は実験期間中を通してほぼ同じレベルであった。水酸化物の場合は1週目に80%がミトコンドリアに存在し、2週目に60%に減少した後は大きな変動は見られなかった。リソゾーム中のPu量は高温酸化物の場合と同様のレベルで推移したが、4週目から9週目にかけて逆に増加する傾向が見られた。核では、1週目が数%でその後4週目まで徐々に増加したが、9週目では1週目のレベルまで減少した。ミクロゾーム、可溶画分にはPuはほとんど存在しなかった。細胞内のPuはリソゾームに存在するといわれている。本実験においてもPuはリソゾームに存在した。しかしミトコンドリアには更に数倍に達する量のPuが存在していて、ミトコンドリアがPuの細胞内での代謝に大きく関わっていることを示唆する結果が得られた。ただ、肺を構成する種々の細胞を一緒にして細胞分画しているためにどの細胞がPuの代謝に大きく関わっているかは不明である。また、実施した細胞分画法ではリソゾームとミトコンドリアをクリアに分画できないためリソゾームの中でも重い成分（heavy lysosome）はミトコンドリア画分に含まれていたことが十分に考えられる。もしそれが事実ならば、細胞内のPuはやはりリソゾームに存在することになるが、これを明らかにするには更なる検討が必要である。

4．結　論

焼結温度の異なる2種類の酸化Pu及び水酸化Puをラットに吸入させて肺への沈着、沈着したPuの肺から全身臓器への移行、糞尿中への排泄について検討し、焼結温度により何れも違いが見られた。マウスでは焼結温度の影響がなく、イヌでは焼結温度によりlung retentionが異なることは知られていたが、ラットでの報告はなかった。今回の一連の実験でラットでもイヌほど顕著ではないが差が見られたことより、体重がラットの1/10ほどのマウスでは差がなく、ラットの約30倍のイヌでは顕著な違いが見られていることを考慮すると、マウスとイヌでの違いは動物種差によるものである可能性が高いことが示唆された。しかし、酸化Puのlung retentionがどうして焼結温度により異なるのかは未だ不明である。酸化Puの物理化学的性状が焼結温度により異なるためではないかと考えられるが現時点では推測の域を脱しない。また、焼結温度差によるlung retentionの違いと肺の細胞内の微細分布との関連を裏付ける結果は得られず、細胞内分布がPuのlung retentionに関与しているか否かは明らかではない。

[研究発表]

1．Yamada, Y., Koizumi, A., Fukuda, S., Inaba, J., Cheng, Y.S., Yeh, H.C. : Hoken Butsuri, 29, 23-31, 1994.
2．Inaba, J., Ishigure, N., Oghiso, Y., Sato, H. : J. Radiat. Prot. Dosim., 53, 335-337, 1994.
3．佐藤，高橋，久保田，越本：日本放射線影響学会第37回研究発表会，福岡，1994.10.
4．Esaka, F., Takahashi, S., Sato, H., Kubota, Y., Kikuchi, T., Furuya, K.: J. Toxicol. Sci., 20, 103-108, 1995.
5．山田，小泉，稲葉：日本保健物理学会第30回研究発表会，水戸，1995.5.
6．山田，小泉，稲葉：第12回エアロゾル科学・技術研究討論会，八王子，1995.8.
7．佐藤，山田，石榑，仲野，榎本，小泉，宮本，小木曽，福田，飯田，高橋，久保田，稲葉： 日本放射線影響学会第38回研究発表会，千葉，1995.11.
8．Sato, H. : The 1st Japan-France Workshop on Radiobiology, Chiba, 1996.9.
9．Yamada, Y., Koizumi, A., Inaba, J. : Workshop : Intakes of Radionuclides, France, 1997.9
10．Yamada, Y., Koizumi, A., and Inaba, J. : J.Radiat. Prot. Dosim., 79, 269-272, 1998.

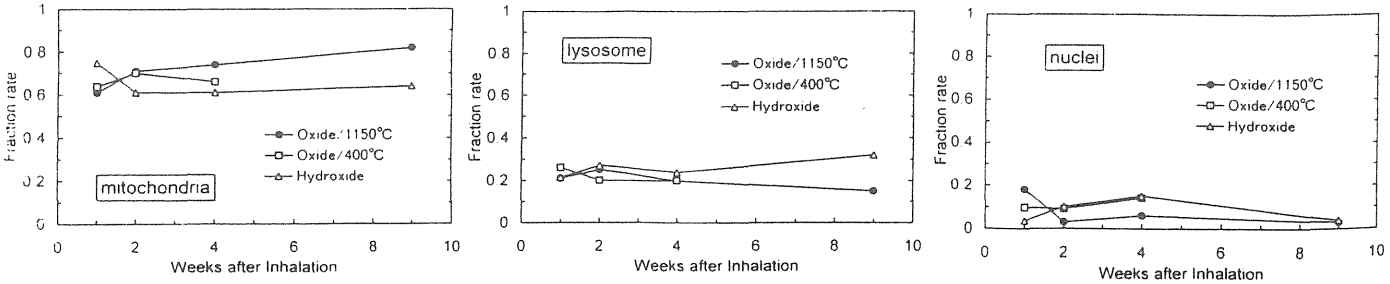

Fig.9 Sub-cellular distribution of Pu following inhalation of PuO_2 fired at 1150 and 400℃ and Pu hydroxide.

Ⅲ. アルファ放射体による内部被ばくの生物学的影響とその修飾因子に関する研究

2. アルファ放射体による内部被ばくのバイオドシメトリに関する研究

石榑信人、仲野高志、榎本宏子、小木曽洋一、山田　裕（内部被ばく・防護研究部）、
稲葉次郎（研究総務官）

Studies on Biodosimetry in the Internal Exposure by Alpha-particle Emitters

Nobuhito Ishigure, Takashi Nakano, Hiroko Enomoto, Yoichi Oghiso,
Yutaka Yamada (Divison of Radiotoxicology and Protection)
and Jiro Inaba (Deputy Director-General)

A basic study has been carried out to develop a biologically based method for estimating alpha doses (biodosimetry) in animal exposure experiment in our institute. In the biodosimetric method, alpha dose to the cells sampled from the exposed animals is estimated by comparing the cytotoxic or cytogenetic response observed in the cells with the response of the cells exposed to alpha-particles *in vitro*, where the dose is known.

A device to irradiate a monolayer of cultured cells with alpha-particles *in vitro* using Am-241 source (3.3×10^7Bq) was designed. This device can be used conveniently in a common laboratory by a small number of researchers. The device performs as follows: (1) The energy of alpha-particles at the entrance of the cell layer is 3.2 MeV with a standard deviation of 0.25 MeV, (2) the incident angle to the cell layer is 82.8 degrees with a standard deviation of 3.2 degrees, (3) the fluence rate is 4.7×10^5 cm^{-2} min^{-1}, (4) the average LET for a cell layer 5μm thick is 138 keV/μm, (5) the average dose rate for a cell layer 5μm thick is 0.10 Gy/min. and (6) a temperature and CO_2 concentration conductive to cell cultivation are maintained during irradiation.

V79 Chinese hamster cells were irradiated normally with alpha-particles using the device mentioned above. The survival curve was exponential with a D_{37} of 0.97Gy, which corresponds to the cross section of 22μm^2. The dose response for micronucleus induction using a cytocharasin B blocking technique fitted well to a linear relationship: $Y=0.019+0.111D$, where Y is the number of micronuclei per binucleated cell and D is the alpha-particle dose in Gy. This result supports the validity of the micronucleus induction rate as the endpoint index of cell doses.

Ⅰ. 緒言

1. 意義と目的

ICRPの新しい呼吸気道モデルでは、器官の平均線量ではなく細胞の線量を精密に評価するよう求められている。こうした細胞の線量が臓器平均線量以上にリスクの有効な目安たり得るためには、放射毒性学の基礎としての実験動物における発がんデータも、臓器や組織の平均線量ではなく、細胞の線量を基準にして再評価されなければならない。ベータ・ガンマ放射体への被ばくでは、臓器平均線量と細胞の線量との差異は小さい。しかし、アルファ放射体の内部被ばくでは、アルファ線の飛程がきわめて短いため、細胞の線量は臓器平均線量から大きく隔たって分布する。こうした細胞の線量を正しく評価するためには、組織の微細形態や放射体の沈着微細分布が定量的に正確に決定されなければならないが、これは決して容易な作業ではない。そこで、本研究においてはアルファ放射体に被ばくした動物の細胞に生じる細胞遺伝学的変異等を測定することにより、物理学的手法のみでなく、生物学的指標からアルファ線線量を評価する“バイオドシメトリ”の開発に必要な基礎的検討を行う。

2. バイオドシメトリの基本的考え方

動物への吸入投与実験におけるバイオドシメトリの基本的な考え方は次の通りである。まず、線量を評価する組織から採取した細胞、たとえば気管支上皮細胞等を初代培養する。この細胞に、アルファ線エネルギー、入射方向、線量等のよく制御されたアルファ線を照射する。次にアル

ファ線照射により細胞に生じる細胞遺伝学的変異等を定量し、これを細胞線量に対してプロットする。この線量反応曲線は、バイオドシメトリのいわばレファレンススケールとなる。アルファ放射体を吸入投与したラットから同じ種類の細胞を採取し、そこに生じている生物学的な変化を定量する。これを、すでに作成してある線量反応曲線、すなわちレファレンススケールと比較・参照することによって、その細胞が実際に受けた線量を推定しようという考え方である。

Ⅱ．アルファ線インビトロ照射装置

緒言で述べたバイオドシメトリのレファレンススケールを作成するためには、培養細胞に、線量等のよく制御されたアルファ線を照射する装置が不可欠である。本研究では、こうした目的に使用するアルファ線インビトロ照射装置を試作した。

1．装置の概要

概略図をFig.1に示す。装置全体は炭酸ガスインキュベータの中に格納され、照射中も培養条件が保持される。パルスモーターで駆動されるステージの上にコリメータ付きのアルファ線源を載せ培養細胞に下から垂直に照射する。なお、細胞は薄いマイラー膜を底面にもつ特殊なガラス製培養皿で培養される。ステージをマイコン制御により左右・前後にat randomに動かすことにより、照射面におけるアルファ線のフルエンスを一様にする。培養皿は、リモート

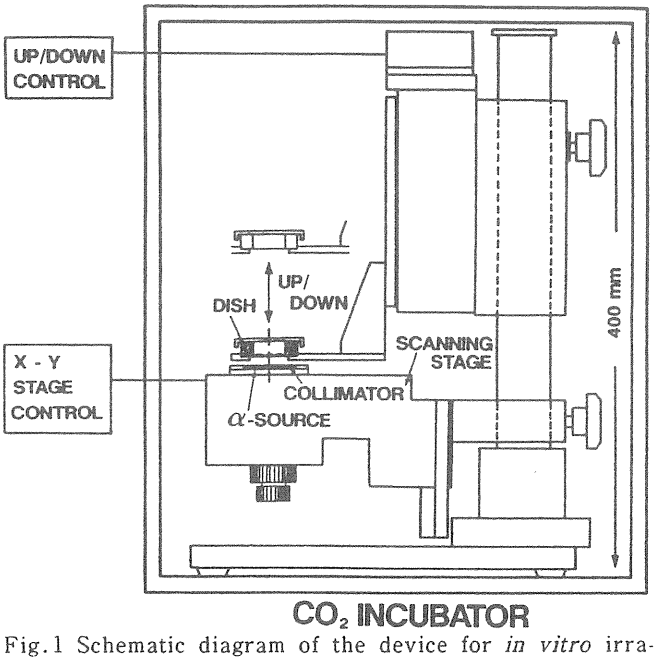

Fig.1 Schematic diagram of the device for *in vitro* irradiation with alpha-particles designed in the present study.

操作により迅速に上下させられるステージの上に載せる。このステージをコリメータぎりぎりまで下げて照射を開始し、終了する時は同じくリモート操作で培養皿を一気に上げアルファ線の飛程よりも遠くへ離すことによって終了させる。

線源は市販の^{241}Amの密封線源であり、その表面はごく薄い白金の箔により覆われている。放射能は3.3×10^{7}Bqであった。

コリメータは、空気層によるアルファ線エネルギーの低下を防ぐため、薄いものにする必要がある。試作した装置では、厚さ0.8mmのセラミック板に直径0.2mmの小ホール10000個を、中心間隔3mmでレーザー光によりあけたものである。

2．入射方向

コリメータを用いた時のアルファ線の入射角の分布をモンテカルロ法によりシミュレーションした。その結果をFig.2に示す。入射角分布は、平均値が82.8度で標準偏差3.2度の広がりをもつと推定された。パスレングスの分布もシミュレーション計算したが、垂直入射を1とした時の平均パスレングスは1.008となり、ほとんど1に揃っていると推定された。

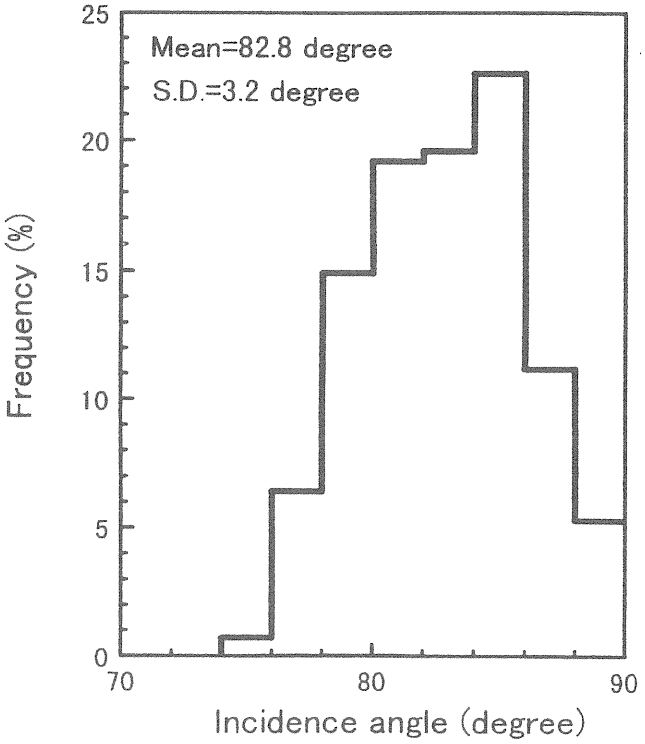

Fig.2 Distribution of the incident angles, which was calculated by Monte-Carlo simulation.

3．粒子束密度

細胞照射面におけるアルファ粒子の平均粒子束密度とその一様性を調べた。培養皿の位置に固体飛跡検出器CR-39を置き、記録されるアルファ粒子飛跡の密度分布を計数した。即ち、照射後のCR-39をエッチング処理すると、アルファ粒子飛跡一個一個はFig.3に示すように小さな黒点として光学顕微鏡による観察が可能となる。一定面積の微小エリアを照射範囲全域から無作為に抽出し、その中の飛跡の計数値に関する頻度分布を求めた。その結果をFig.4の白いヒストグラムで示す。なお、微小エリア内の平均飛跡数は8.8であった。比較のため、同じ平均飛跡数に対するポアソン分布を計算し、同図に黒のヒストグラムで示した。カイ2乗適合度検定の結果、この両者はよく一致しており、粒子束密度の一様性を確認できた。また粒子束密度の値そのものは4.7×10^{5} cm^{-2} min.$^{-1}$であった。

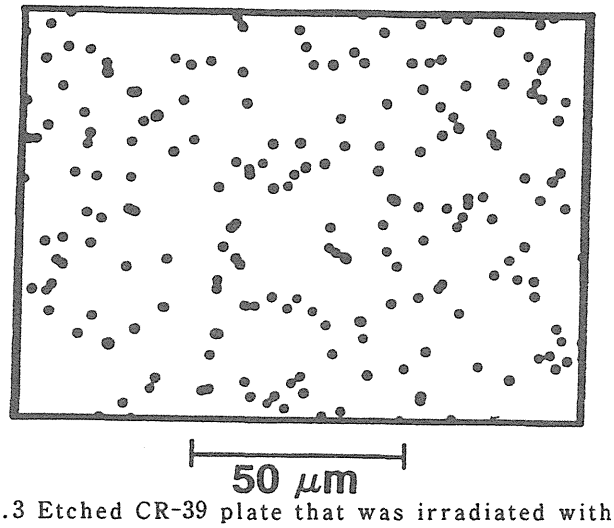

Fig.3 Etched CR-39 plate that was irradiated with alpha-particles at the cell layer position.

4．アルファ粒子のエネルギー分布

シリコン半導体検出器によるアルファ粒子エネルギー分布の測定結果をFig.5に示す。吸収体が無い場合、同図の白丸に示すように平均値4.14MeV、標準偏差0.20MeVであった。一方、細胞照射面では、培養皿底面のマイラー膜および線源－薄膜間の3mmの空気層によりエネルギーが吸収されるため、平均値3.20MeV、標準偏差0.25MeVとなった。

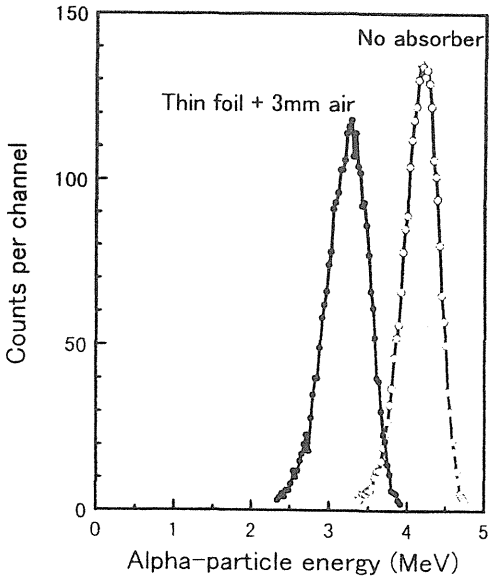

Fig.5 Measured energy spectra of alpha-particles: (○) in vacuum and (●) after the traversal of both a base thin foil and 3 mm in air space, which is the distance between the source surface and the base foil of the culture dish.

5．線量率およびLET分布

前記第3節の粒子束密度および第4節のアルファ線エネルギー分布の実測値と阻止能の文献値（ICRU Report 36）とを用い、LETおよび線量率の細胞内深さ分布を計算した。その結果をFig.6とFig.7にそれぞれ示す。細胞の厚みを5 μmと仮定すると、平均線量率は0.10 Cy/min.、平均LETは138 keV/μmと評価される。

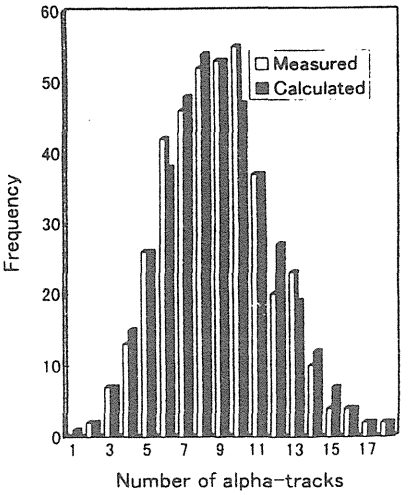

Fig.4 Uniformity of fluence rate at the cell layer position: Frequency distribution of the number of tracks counted in each 25 μm×25 μm square on the irradiated CR-39 plate. Randomness of the spatial distribution of incident positions of alpha-particles was verified as a result of the closeness of the fit between the measured frequency distribution and the calculated Poisson distribution.

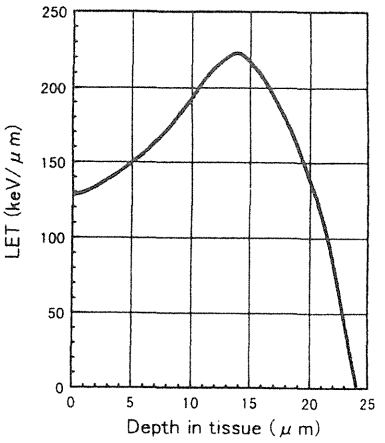

Fig.6 Dependence of LET on the depth of soft tissue for the beam available in the present device, by approximating the values tabulated in ICRU REPORT 36 by a polynomial function of alpha-particle energy.

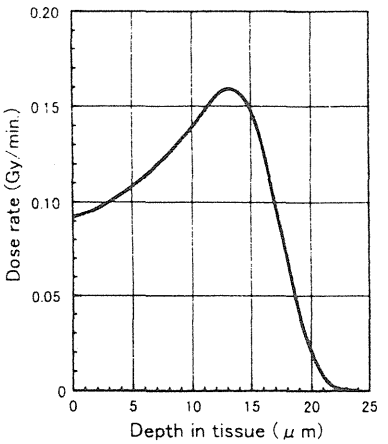

Fig.7 Dependence of absorbed dose on the depth of soft tissue for the beam available in the present device, by approximating the values tabulated in ICRU REPORT 36 by a polynomial function of alpha-particle energy.

Ⅲ．培養細胞に対するアルファ線照射効果

アルファ放射体を投与した実験動物からの生物学的試料を用いた実験を行う以前に、アルファ線被ばくのバイオドシメトリとして要求される諸条件（最小検出線量、感度、線量の計測可能範囲、再現性、測定の簡便性など）について、種々の細胞応答に対して検討しておく必要がある。そのために、培養細胞系として、放射線生物研究でしばしば用いられるチャイニーズ・ハムスターV79 細胞を導入して、アルファ線照射に対する線量反応関係に関する基礎データを得た。

1．実験方法

チャイニーズ・ハムスターV79 細胞をマイラー膜を貼った特製の培養皿を用いて、CO_2インキュベーター内で培養した後、第Ⅱ章で述べた^{241}Amを線源にもつアルファ線照射装置によりアルファ線照射を行った。

照射後、トリプシン処理により細胞をマイラー膜から剝がし、一部は、コロニー形成法による細胞生存率を測定するために適当に希釈の後培養皿（ファルコン）に再播種した。他の一部は小核形成頻度の測定のために培養皿内のカバーグラス上に再播種した。

CO_2インキュベータ内で再培養し、1週間後に形成されたコロニーの数を計数し、生存率を求めた。

また、小核数の測定を2核細胞法で行うために、再播種後、サイトカラシンB（5 μg/mℓ）を添加した。サイトカラシンBは、核分裂は阻害しないが、細胞質の分裂を阻害するので、照射後細胞分裂期を通過した細胞は2核細胞として容易に同定できる。10時間培養後、細胞をカルノア液で固定し、アクリジン・オレンジによる核酸染色を施し、蛍光顕微鏡下で小核数を計数した。

2．細胞の生存率

アルファ線照射後の細胞生存率の測定結果をFig.8に示す。生存率は照射された線量の増加に伴い指数関数的に減少し、生存率曲線は片対数プロットで肩の無い直線となり、高 LET放射線に典型的にみられる線量反応関係を示した。同図より、LD_{50}は0.68 Gyであり、D_{37}は0.97 Gyであることが分かった。0.97 Gyの時のアルファ粒子フルエンスは、0.0454 μm^{-2}であり、この値から反応断面積を算出すると、22.0 μm^2となる。つまり、ターゲットのサイズは5.3 μm円相当径と推定された。

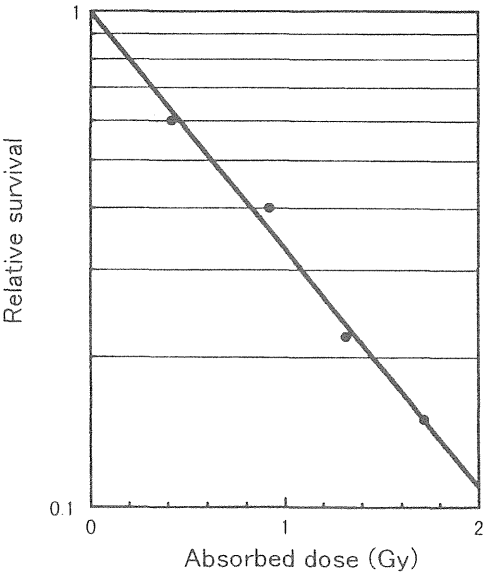

Fig.8 Survival curve for the V79 Chinese Hamster cells exposed to alpha-particles with the energy of 3.2 MeV. The line represents the fit of exponential model with the D_{37} of 0.97 Gy

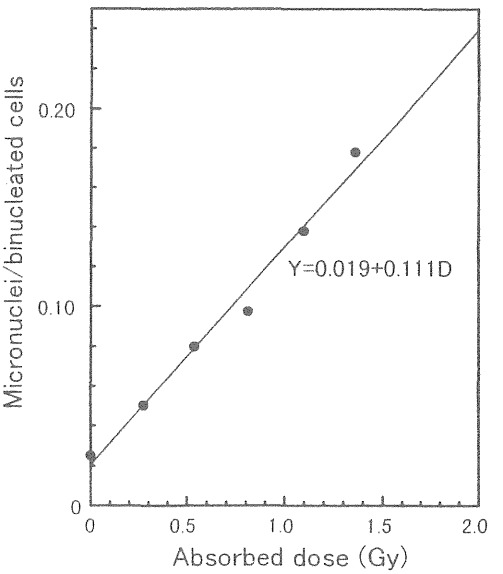

Fig.9 Dose response curve for micronucleus induction, which fitted well to a linear relationship: $Y=0.019+0.111D$, where Y is the number of micronuclei per binucleated cell and D is the alpha-particle dose in Gy.

3．小核形成率

小核形成の測定結果をFig.9に示す。この図から分かるように、線量が低いあいだは明らかに直線モデルに適合する線量反応関係が得られた。その関係式を最小2乗法で求めたところ

$$Y=0.019+0.111D$$
$$(\gamma=0.989)$$

となった。但し、上式においてYは2核細胞当たりの小核数を、DはGyで表した細胞線量を表す。この結果から小核形成率の倍加線量は0.17Gyと評価され、0.1Gy 程度の低線量でもバックグラウンドレベルと比べ、有意な小核頻度の上昇が期待される。それ故、小核形成率は、アルファ線被ばくにおけるバイオドシメトリの指標として有望な候補の一つであると判断された。

4．数理解析

本章第3、4節の実験結果に対し、以下のような数理解析を行った。

I個のトラックが通過した後の細胞の生存率$S(I)$は、シングルトラック当たりの致死確率をpとすると、

$$S(I)=(1-p)^I$$

で表される。

また、I個のトラック通過後の小核誘発率$N(I)$はシングルトラック当たりの小核誘発率をm、自然の誘発率をm_0とすると次式で表すことができる。

$$N(I) = 1 - (1 - m)^I (1 - m_0)$$

一方、前述したように、生存率の測定結果から細胞不活化に対する反応断面積が22 μm^2と評価された。したがって、アルファ粒子フルエンスがfの時、細胞核を通過するトラック数の平均値Mは、p（シングルトラック当たりの致死確率）と細胞不活化断面積とから次の式のように表すことができる。

$$M = \frac{22}{p} f$$

この平均値Mより、ポアソン統計の式を用いてI個のトラックが通過する確率$F(I)$は

$$F(I) = \left(\frac{M^I}{I!}\right) \exp(-M)$$

と表される。

以上より、アルファ粒子フルエンスがfの時の小核誘発率$N(f)$は、I個のトラックが通過する確率に生存率と小核誘発率を掛け、Iに関してサメンションすることにより得られる。すなわち、

$$N(f) = \sum F(I) \cdot S(I) \cdot N(I)$$

$$= \sum \left\{ \frac{(22f/p)^I}{I!} \right\} \exp\left(\frac{-22f}{p}\right) (1-p)^I \left\{ 1 - (1-m)^I (1-m_0) \right\}$$

となる。

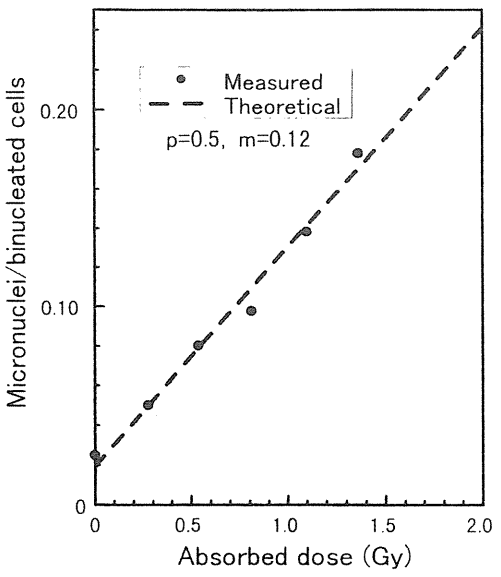

Fig.10 Theoretical prediction for micronucleous induction where p (number of lethal lesion per single track) is 0.5 and m (probability for micronucleous induction) is 0.12, which showed a good fitness to the observed dose response curve for micronucleous induction.

ここで、測定から得られる変数は、小核細胞の割合Nと、アルファ粒子フルエンスfであるから、p即ちシングルトラック当たりの致死確率とm即ちとシングルトラック当りの小核誘発率との関係は実験値にフィッティングすることにより知ることができる。

例えば、pを0.5と仮定した時、mの最適値として0.12が得られる。実験値と重ねあわせるとFig.10のようになり、直線というよりは若干上に凸の曲線になってはいるが実験値とかなり良好な一致を示していると言える。

Fig.11は、pをいろいろに仮定し、こうしたフィッティングを行った時のpとmとの関係を示したものである。この図よりpの増加に伴いmも単調増加を示すと言うこと、ほとんどの領域でmはpよりかなり小さいということが示されている。このように別の実験でpを求めることができればmも決められる。

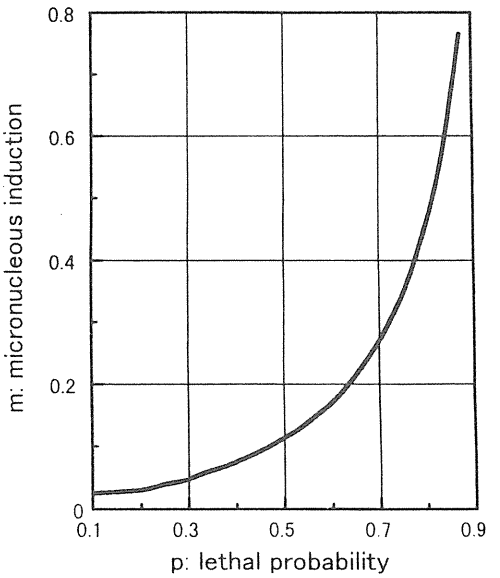

Fig.11 Theoretical prediction for the relationship between p (number of lethal lesion per single track) and m (probability for micronucleous induction).

Ⅳ. 結　言

アルファ線照射によるチャイニーズハムスタV79の細胞生存率および小核形成率を求める実験から、小核形成率は、アルファ放射体吸入投与実験におけるバイオドシメトリの指標として有力な候補の一つであることが示された。また、既存の気道上皮細胞株(SV40T2)を用いた予備的検討から、小核形成効果はV79細胞よりも高いことが示唆され、吸入被ばくで問題になる気道上皮細胞の線量の評価に小核形成率を指標としたバイオドシメトリが適用できる可能性が強く支持された。

小核形成率の測定自体には格段の新奇性があるわけではないが、アルファ線照射による効果を定量的に評価した例は他になく、本特別研究で得られたデータは独自のものと考えられる。

生物学的指標から細胞のアルファ線線量を評価することは、プルトニウムのみならず、ラドンの生物影響研究においてもたいへん重要であり、今回の特研の成果を踏まえ、平成10年度に開始された特別研究小課題「ラドンの線量評

価及び生物学的指標に関する研究」として継続発展が見込まれる。

[研究発表]

1) Ishigure, N., Nakano, T. and Enomoto, H.: Activity Measurement of Plutonium in Solid Samples by L X-ray Counting with a Phoswich Detector, 保健物理, 28, 195-201, 1993.
2) Ishigure, N., Nakano, T., Enomoto, H. and Inaba, J.: Longer Lung Retention of PuO_2 Particles in Rats Measured Using Periodic In Vivo Counting, Radiat. Prot. Dosimetry, 53, 195-198, 1994.
3) Ishigure, N., Nakano, T., Enomoto, H, Fukuda, S., Iida, H., Oghiso, Y., Sato, H., Takahashi, S., Yamada, Y., Koizumi, A., Yamada, Y., Miyamoto K. and Inaba, J.: Lung Retention of Pu Following Inhalation of PuO_2 in Rats Measured Using a Whole Body Counter, J. Radiat. Res., 35, 16-25, 1994.
4) Inaba, J., Ishigure, N., Oghiso, Y. and Sato, H.: Gastointestinal Absorption of Americium Administered with Large Amount of Sodium Citrate in Rats, Radiat. Prot. Dosimetry, 53, 335-337, 1994.
5) Ishigure, N. and Inaba, J.: Analytical Solution of the Compartment Model for Respiratory Tract Clearance Used in the New ICRP Lung Model, J. Nucl. Sci Technology, 33, 179-186, 1996.
6) Ishigure, N., Enomoto, H., Nakano, T. and Inaba, J.: Validity of Am-241 as a Tracer of Inhaled Pu in External Chest Counting, Radiat. Prot. Dosimetry, 79, 133-136, 1998.
7) 石榑、仲野、榎本、稲葉: 日本保健物理学会第28回研究発表会, 福岡, 1993.5.
8) Ishigure, N., Nakano, T. Enomoto, H. and Inaba, J.: CEC Workshop on Intakes of Radionuclides, Bath, UK, 1993.9.
9) 石榑、佐藤、仲野、榎本、稲葉: 日本保健物理学会第29回研究発表会, 敦賀, 1994.5.
10) 仲野、石榑: 日本保健物理学会第29回研究発表会, 敦賀, 1994.5.
11) 石榑、稲葉: 日本放射線影響学会第37回大会, 福岡, 1994.10.
12) 石榑、稲葉:日本保健物理学会第30回研究発表会, 水戸, 1995.5.
13) 石榑、稲葉: 日本原子力学会1995年秋の大会, 東海, 1995.10.
14) 石榑、稲葉: 日本放射線影響学会第38回大会, 千葉, 1995.11.
15) Ishigure, N., Nakano, T. Enomoto, H., Sato, H. and Inaba, J.: 1996 Int. Cong. Radiat. Prot., Vienna, 1996.4.
16) 石榑、榎本、稲葉、生島* (京都教育大) : 日本保健物理学会第31回研究発表会, 札幌, 1996.5.
17) 仲野、石榑: 日本保健物理学会第31回研究発表会, 札幌, 1996.5.
18) 石榑、榎本、稲葉、生島* (京都教育大) : 日本放射線影響学会第38回大会, 大阪, 1996.11.
19) 仲野、石榑: 日本保健物理学会第32回研究発表会, 奈良, 1997.5.
20) Ishigure, N., Enomoto, H., Nakano, T. and Inaba, J.: CEC Workshop on Intakes of Radionuclides, Avignon, France, 1997.9.

Ⅲ. アルファ放射体による内部被ばくの生物学的影響とその修飾因子に関する研究

3. アルファ放射体による内部被ばく発がんとその生物学的修飾因子に関する研究

小木曽洋一、山田　裕、飯田治三、福津久美子、石榑信人、仲野高志、榎本宏子、
佐藤　宏、山田裕司、小泉　彰、稲葉次郎（内部被ばく・防護研究部）

Studies on the Carcinogenesis Induced by Internal Alpha-emitters and Its Biological Modifiers

Yoichi Oghiso, Yutaka Yamada, Haruzo Iida, Kumiko Fukutsu,
Nobuhito Ishigure, Takashi Nakano, Hiroko Enomoto,
Hiroshi Sato, Yuji Yamada, Akira Koizumi, and Jiro Inaba
(Division of Radiotoxicology and Protection)

The carcinogenic effects of an alpha-emitter, ^{239}Pu, were investigated by animal experiments as focused on both pulmonary tumors after inhalation exposures to insoluble oxide aerosols and tumor spectra induced by injection of soluble citrate. The life-span study using Wistar strain rats exposed to Pu dioxide aerosols has shown differential dose-related responses of malignancies and histopathological phenotypes of lung tumors, suggesting a threshold dose around 1.0 Gy of the lung dose. As abnormality of tumor-related genes could be supposed for the background of pulmonary carcinogenesis, the mutations of p53 tumor suppressor gene were examined by PCR-SSCP analysis using DNA fragments extracted from lung tumors. While mutations were detected in 23 cases (about 28%) among 82 lung tumors, their relations to either malignancies, histological phenotypes, dose, or oncogenesis are not yet to be elucidated. The life-span study using C3H strain mice injected with Pu citrate has shown contrast dose responses between osteosarcomas and lymphoid tumors around 10 Gy of the skeletal dose, and further indicated specific tumor spectra differed from low LET radiation exposures as shown by much more frequency of B cell type leukemic lymphomas and none of myeloid leukemias.

緒　言

アルファ放射体のうち、長半減期で体内滞留率が大きく、発がん性が最大とされるが未だ不明確なプルトニウム（^{239}Pu）の人体における発がんリスクを科学的に推定し、その防護・低減化をはかるためには、動物実験による実証解析が必要である。本研究では、プルトニウム化合物の物理化学的性状と被曝形式に依存した体内挙動・線量分布・発がん効果の特異性とそれを修飾する生物学的要因や機構について明らかにすることを目的として、以下のように、最も可能性の高い被曝様式としての不溶性酸化物エアロゾルの吸入曝露および体内移行成分の効果を考慮した可溶性クエン酸塩の注射投与により、それぞれ生涯飼育動物実験と発がん効果に関する種々の検討を行った。

実験方法

(1) 酸化物エアロゾルの吸入曝露実験では、硝酸溶液から水酸化物に変換し、約1150℃に高温焼結して発生させた多分散$^{239}PuO_2$エアロゾル（空気動力学的中央径 AMAD: 0.3-0.4μm、幾何学的標準偏差 GSD: 1.8-2.0）を、我々が開発したグローブボックス型小動物吸入曝露チェンバー内でWistar雌ラット（体重140-160g、10-15週齢）に鼻部吸入曝露させた。吸入曝露後6-7日目に、各動物を麻酔下で体外計測装置（ホスウィッチ型NaIシンチレーション検出器）を用いてLX線（17keV）を測定することにより、肺における初期沈着量（Bq）を推定し、蓄積肺線量（Gy）は既に得られている肺滞留率曲線から求めた。このようにして作成した吸入曝露動物約500匹（初期沈着量20-3000Bq）を無処置対照群約200匹とともに生涯飼育し、死亡後病理解剖と組織学的検索を行ない、生存率、死因、線量効果等を解析した。また発がん過程と機構を明らかにするため、別に100匹の吸入曝露群（初期沈着量300-500Bq）と無処置対照群60匹を長期飼育して肺腫瘍発生・発育過程、潜伏期、線量との関係を経時的に検討した。さらにこれらの吸入曝露動物で発生した肺腫瘍におけるがん関連遺伝子の発現とその役割を検討するため、とくにがん抑制遺

伝子p53の突然変異について、肺腫瘍組織の免疫組織染色および抽出DNAのPCR-SSCP解析による検討を試みた。
(2)クエン酸塩の注射投与実験では、硝酸溶液からクエン溶液に変換・滴定し、pH6.8-7.0に調整した単量体クエン酸^{239}Pu溶液を、C3H雌マウス（体重25-28g、10-12週齢）計360匹に1匹あたり10-12000Bq宛て腹腔内注射投与して、生理食塩水投与対照群100匹とともに生涯飼育し、死亡後病理解剖と組織学的検索を行ない、生存率、死因、線量効果等を解析した。骨線量（Gy）は別に作成した注射投与動物を漸次殺処分して全身の骨組織における沈着量（Bq）を灰化後液体シンチレーション計測して求めた滞留率曲線により計算した。また系統差を明らかにするため、C3Hに加えてC57BL/6およびBC3F1の3系統雌マウス合計550匹（1匹あたり100-5000Bq宛て腹腔内注射投与）と生理食塩水投与対照群合計250匹の生涯飼育実験を行うとともに、一部発がん過程と血液病理学的動態について経時的検討を加えた。

結果および考察

(1)酸化プルトニウム・エアロゾル吸入曝露ラットにおける肺腫瘍誘発とその線量効果

生涯飼育群のうち、これまでにその約8-9割にあたる約600匹が死亡し、病理組織検査を終了しているが、その結果から以下のような所見が得られた。

①対照群と比較して吸入曝露動物の平均生存日数は、肺線量1.0 Gy以下までは有意差をみとめないが、1.5 Gy以上から有意に減少し、これと並行して原発肺腫瘍発生率は1.0 Gy以下の約40%から、1.5 Gyで約66%、さらに5.4 Gyで約97%にまで急増する（Fig.1A）。またこれらの肺腫瘍のうち、腫瘍病巣が限局され、周囲への浸潤・転移のない良性腫瘍は1.0 Gy以下では約35%と大部分を占めているが、1.5 Gy以上から減少し、代わって多発性で浸潤・転移の顕著な悪性腫瘍発生率が急増して6.6 Gyで約90%に達する。このように1.0 Gy近辺での生存期間および悪性度による肺腫瘍発生率の線量効果の差が明らかであるが、悪性腫瘍の発生は、吸入後300日以上から増加して600日目までに最高に達するのに対して、良性腫瘍は600日以上から増加して900日目までに最高に達するように、早期死因の多くはこの悪性肺腫瘍発生によるものであり、遅い時期に発生する良性腫瘍は直接の死因に結び付かないものと考えられた。

②発生した原発肺腫瘍の大部分（99%）は、気管支-細気管支から肺胞部にかけての気道被覆上皮細胞より生じた上皮性腫瘍で、病理組織学的に良性の腺腫（adenoma）と、悪性の腺癌（adenocarcinoma）、腺扁平上皮癌（adenosquamous carcinoma）および扁平上皮癌（squamous cell carcinoma）の4型に分類された。このうち最も多くを占める組織型は腺癌（全体の44%）であり、次いで腺腫（同27%）、腺扁平上皮癌（同22%）、扁平上皮癌（同6%）であったが、この割合はこれまでに米国で報告されている同様な実験結果と比べ、かなり異なっており、各々の発生率の線量効果にも違いがみとめられた。すなわち、腺腫は0.6 Gyで最大（約35%）の発生率を示し、1.5 Gy以上では減少するが、代わって腺癌が増加して2.8 Gyで最大（約47%）の発生率を、また腺扁平上皮癌および扁平上皮癌が4.7 Gy以上から増加して5.4-8.5 Gyの線量域で最大の発生率をそれぞれ示すことが明らかであった（Fig.1B）。このことは肺腫瘍組織型による誘発線量域が異なることを示すものであり、さらに組織標本上で腫瘍病変の程度・出現数を算定すると、初期化生・増殖病変が0.6-1.5 Gy、腺腫・腺癌病変が1.5-2.8 Gy、扁平上皮癌病変が5.4-6.6 Gyでそれぞれ出現・顕在化するように、腫瘍病変形成にも異なる線量域が存在していることが明らかであった。

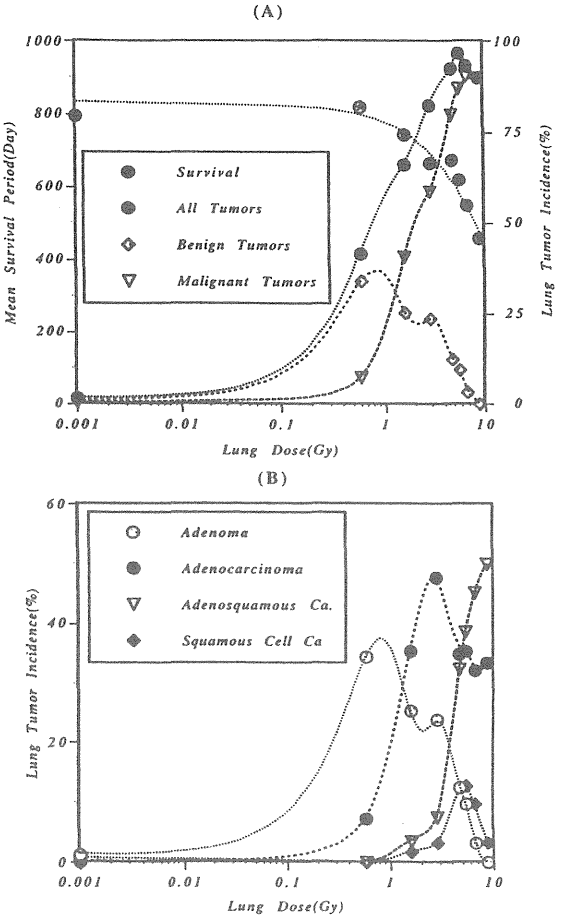

Fig.1. Dose Effect Relationships on Survival and Lung Tumor Induction of $^{239}PuO_2$-Exposed Rats
(A) Lung dose vs. mean survival perriod and benign or malignant tumor incidences.
(B) Lung dose vs. incidences of lung tumor types.

③このように発生肺腫瘍の悪性度・組織型・病変形成により線量域が異なること、一定の閾値線量域が存在する背景には、様々な要因が考えられる。このうち最も考えられる要因として、吸入エアロゾル粒子の物理化学的性状、とくに粒子径の差にもとづく呼吸気道内沈着・線量分布・線量率および標的気道上皮細胞の感受性の違いがあげられるが、腫瘍発生・悪性化および癌化等発がんの分子機構、とりわけがん関連遺伝子とその産物の異常発現も深く関わっているものと考えられる。このうち、悪性化・癌化に関わるとされるp53癌抑制遺伝子の突然変異について検討を試みた。まず306例の肺腫瘍について核内p53タンパクの蓄積程度を特異抗体による免疫染色により調べてみると、良性の腺腫全てを含む約83%の腫瘍例が陰性であり、残り約17%の癌腫が弱陽性ないし陽性を示し、陽性例の多くは腺扁平上皮癌および扁平上皮癌であった（Table 1）。次いで

Table 1 Intranuclear p53 Protein Accumulation and Lung Tumor Types in $^{239}PuO_2$-Exposed Rats

Histological Types	No. Examined	p53 Protein Accumulation*		
		Negative	Slight	Positive
Adenoma	84	84	0	0
Adenocarcinoma	136	121	14	1
Adenosquamous Carcinoma	68	41	25	2
Squamous Cell Carcinoma	18	9	5	4
Total	306	255	44	7

* Criteria for positivity by immunohistochemistry: negative, not detectable in all nuclei; slight, detectable in 10% or less of all nuclei; positive, detectable in 30% or more of all nuclei of tumor cells

これらのうち、82例の肺腫瘍標本からDNAを抽出し、ラットのp53エクソン5～8ごとに作成したプライマーを用いたPCR-SSCP解析を試みたところ、23例（約28%）でいずれかのエクソンに異常が検出されたが、正常（野性型）と比較して腫瘍組織型および核内タンパク陽性度との間に特別な違いはみとめられなかったものの、変異例のうち大部分にあたる20例でエクソン5あるいは6に異常がみとめられたことが特徴であった（Fig.2）。さらにこれら23例について突然変異部位のシーケンスを行ったところ、エクソン5および6に異常をみとめた11例でコドン141～219にわたるG→AまたはC→Tの置換点突然変異がみとめられたものの、他の12例では正常な塩基配列を示すという結果が得られた。従って、現在のところp53突然変異の肺腫瘍発生・悪性化・癌化との関連については明らかでない。

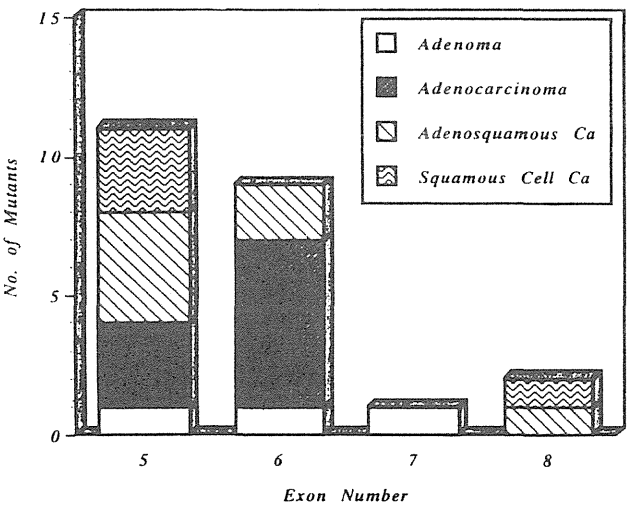

Fig.2. PCR-SSCP Analysis on p53 Mutations of Lung Tumors from $^{239}PuO_2$-Exposed Rats
Distribution of mutants and lung tumor types in each exon.

④吸入曝露によって誘発される肺腫瘍の発生時期・病変形成過程および線量・時間との関係を明らかにするため、新たに作成した吸入曝露動物について経時的検討を行ったところ、吸入後1-3カ月目までに惹起される炎症病変と肺胞マクロファージの形態・機能変化、3-6カ月目までに生じる線維化病変および気道上皮細胞の増殖・化生病変という過程の後、1年目から肺線量1-2Gyに達した動物において、腺腫および腺癌病変が出現・増加してくる傾向が明らかにされている。引続き吸入後2年目までの経時的検索とp53等がん関連遺伝子異常に関する解析を施行中である。

(2) クエン酸プルトニウム注射投与マウスにおける発がんとその線量効果

体内摂取された可溶性プルトニウムの最終沈着臓器である骨の腫瘍に加えて、骨髄幹細胞の照射によって生じるであろう造血・リンパ系腫瘍の発生について、生涯飼育マウスによる検索の結果、以下のような所見が得られた。

①C3Hマウスの生涯発がん実験においては、対照群と比較して骨線量2.9 Gy（投与量500 Bq）以上で、平均生存日数および50%生存日数の有意な減少が明らかにみとめられ、これらの実験群では投与後200日前後より腫瘍性病変および白血球減少、貧血、循環器・肝・腎障害等非腫瘍性病変による累積死亡率が急増していることから、早期の腫瘍死ないし非腫瘍死による生存期間の短縮と考えられた。

②誘発された腫瘍のうち、最も高率に発生する骨腫瘍は大部分が椎骨および四肢骨の骨肉腫であり、骨線量1 Gy（投与量100 Bq）以上から急増し、6-8 Gy（投与量1000-5000 Bq）で最高の発生率（96%）に達するが、10 Gy（投与量5000 Bq）以上から漸次減少した（Fig.3）。一方、対照群の約20%にみとめられるリンパ性腫瘍は、投与群では骨線量1-8 Gy（投与量100-5000 Bq）ではほとんどみられず、10 Gy（投与量5000 Bq）以上から増加して、25 Gy（投与量5000-10000 Bq）で最高（36%）に達した。このことから、骨線量10 Gy近辺での骨腫瘍とリンパ性腫瘍の対比的線量効果が明らかであった。

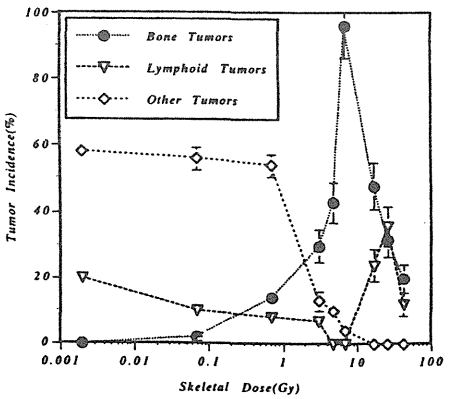

Fig.3. Dose Effect Relationships on Tumor Incidences of Citrate-Incidences Mice
Skeletal dose vs. incidence of each tumor

③さらに肝細胞癌、卵巣癌、肺癌等その他の固形腫瘍の発生率は、骨線量1 Gy（投与量100 Bq）以上から著減し、10 Gy（投与量5000 Bq）以上では発生率ゼロとなったが、これは骨腫瘍およびリンパ性腫瘍との競合によるものと考えられた。なお、低LET放射線の外部照射等でしばしば誘発される骨髄性白血病等造血系腫瘍は、対照群・投与群全て

において全くみとめられなかったので、線質あるいは線量率と骨髄幹細胞の感受性等の差が示唆された。
④上記の高線量域で有意の発生がみとめられたリンパ性腫瘍は、対照群と投与群との間に発生時期および組織形態の違いがみられた。すなわち対照群では700日以上の遅い時期に発生するのに対し、投与群では多くが150-200日の早期に発生する傾向が明らかであり（Fig.4)、その組織型も対照群で多くみられる胸腺リンパ腫は少なく、B細胞性白血病ないし悪性リンパ腫が増加していることが特徴であった（Table 2)。これらの結果は、低LET放射線の外部照射で誘発される胸腺リンパ腫の発生機構とは異なり、骨髄前駆細胞から胸腺を介することなく発生・増殖するB細胞リンパ腫の発病機構の存在する可能性を示唆している。

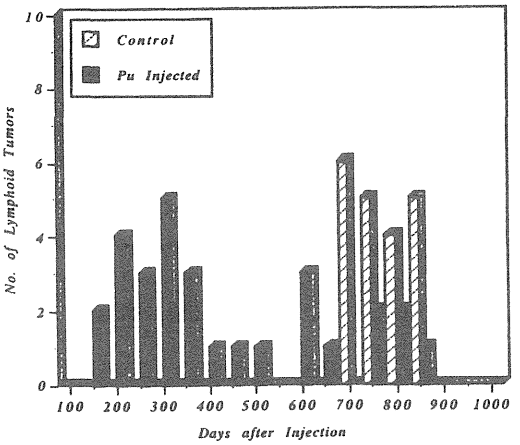

Fig. 4. Onset Time of Lymphoid Tumors from ^{239}Pu Citrate-Injected Mice

Numbers of lymphoid tumors appeared after injection

Table 2. Histological Phenotypes of Lymphoid Tumors in ^{239}Pu Citrate-Injected Mice

Experimental Group	No. Lymphoid Tumors	Histological Phenotypes* Thymic Lymphoma	B Cell Lymphoma	T Cell Leukemia	B Cell Leukemia	Malignant Histiocytoma
Control	20	5	8	0	0	7
Pu Injected	29	1	13	2	13	0

* Differential diagnosis by immunohistochemistry using Thy1.2 and B220 monoclonal antibodies

⑤このような外部照射と異なる発生腫瘍スペクトルの違いが、線質・線量分布・線量率等物理学的要因のみならず、マウス感受性の遺伝的背景によるものであるのかを明らかにするため、自然発生腫瘍スペクトルの異なる3系統（肝腫瘍が多いC3H、胸腺リンパ腫の多いC57BL/6、およびそれらの雑種BC3F1）の雌マウスによる生涯発がん効果の比較検索を施行中である。現在までに、約6割の動物の病理検索を終えており、骨腫瘍発生率はいずれの系統でもほぼ同様な線量効果を示すが、リンパ性腫瘍はC57BL/6およびBC3F1の2系統において低線量域でも比較的高率に発生すること、さらに骨髄性白血病発生率はいずれの系統でも極めて低いこと等の傾向がみとめられている。

結　論

不溶性の酸化物エアロゾル吸入曝露により、粒子径・線量率・気道内線量分布あるいは標的細胞の感受性に依存した高率の肺腫瘍発生率と悪性度・組織型による線量効果の違いが明らかにされた。また、可溶性塩の注射投与により、骨腫瘍およびリンパ性腫瘍の対比的・競合的線量効果と、低LET放射線照射の場合と異なるリンパ・造血系腫瘍等誘発腫瘍スペクトルの違いが明らかにされた。これらはいずれもアルファ核種による発がんの特異性を示すものであるが、その背景や機構については明らかでなく、吸入曝露による肺腫瘍誘発に関しては、粒子径・化学形・線量率等、また注射投与による発がんに関しては、種差・系統差・年齢差等の比較をそれぞれ重点項目としながら、それぞれ発がんの特異性と分子機構についてさらに解析を加える必要がある。

研究発表

（原著論文）

1．Oghiso,Y., Yamada,Y., Ishigure,N., Fukuda,S., Iida,H., Yamada,Y., Sato,H., Koizumi,A., and Inaba,J.: J.Radiat.Res., 35, 223-236, 1994.
2．Oghiso,Y., Yamada,Y., and Iida,H.: J.Radiat.Res., 35, 237-248, 1994.
3．Oghiso,Y., Yamada,Y., and Iida,H.: J.Radiat.Res., 38, 77-86, 1997.
4．Oghiso,Y., Yamada,Y., Iida,H., and Inaba,J.: J.Radiat.Res., 39, 61-72, 1998.

（総説・プロシーディング等）

1．小木曽:エアロゾル研究、9、221-226、1994.
2．小木曽:日本原子力学会誌、36、1006-1009、1994.
3．Oghiso,Y., Ishigure,N., Yamada,Y., Sato,H., Fukuda,S., and Inaba,J.: Proc.10th Intl.Congress Radiat.Res., Wutzburg, Germany, 315, 1995.
4．小木曽、山田、飯田、福津、福田:保健物理、33、308-313、1998.

（学会口頭発表等）

1．小木曽、山田、飯田、福田、石榑、稲葉: 日本放射線影響学会第36回大会、広島、1993.10.
2．山田、小木曽、飯田、佐藤: 日本放射線影響学会第36回大会、広島、1993.10.
3．小木曽、山田、石榑、福田、山田、飯田、稲葉: 日本放射線影響学会第37回大会、福岡、1994.10.

4．小木曽、山田、飯田:日本放射線影響学会第38回大会、千葉、1995.11.
5．山田、Okinaka、Chen:日本放射線影響学会第38回大会、千葉、1995.11.
6．Oghiso,Y., Yamada,Y., Ishigure,N., Fukuda,S., Iida,H.,Yamada,Y.,Sato,H.,Koizumi,A.,Nakano,T.,Enomoto,H.,and Inaba,J.: 2nd Japan-Italy Workshop on Radiation Effects and Biomedical Applications, Rome, 1995.12.
7．小木曽、山田:日本放射線影響学会第39回大会、大阪、1996.11.
8．小木曽:日本放射線影響学会第39回大会、大阪、1996.11.
9．小木曽:日本原子力学会第35回大会、東京、1997.3.
10. 山田、福津、小木曽: 日本放射線影響学会第40回大会、京都、1997.11.
11. Oghiso,Y.: Intl.Workshop on Indoor Radon Exposure and Its Health Consequences, Chiba, 1997.10.
12. Oghiso,Y.,and Yamada,Y.: 2nd Japan-France Workshop on Radiobiology and Isotopic Imaging, Paris, 1998.2.

保健物理，**33**(3)，283（1998）

特集：放医研におけるプルトニウムの生物影響評価研究

放射線医学総合研究所　内部被ばく・防護研究部

昨今，環境や情報関連分野が世上の注目を浴びるにつれ，相対的に原子力全般に対する関心の度合いが，事故などの場合を除いて，減少しているように見受けられる。それは一面では社会的な暗黙の受容を示しているのかもしれない。つまり，医療や工業，研究などの分野での加速器や放射性同位元素の開発・利用は社会的におおむね容認され，よりいっそうの利用に向けての活発な活動が少なくないことと対応している。しかしながら，現在のわが国の総発電量の30%以上を担っている原子力発電，将来の利用が意図されている新型炉やそれにともなう核燃料サイクルの開発については，実に厳しい目があるのも事実である。周知のことであるが，その大きな理由の一つがプルトニウムである。このプルトニウム問題とは，それの核兵器への転用と摂取時の生体の安全性（影響評価）につきる。

プルトニウムについては，これまでに学会誌等の専門誌上いく度か解説や特集が組まれた。また，啓蒙書などでもその有用性から生体への影響と安全性や工学・管理上の安全性まで幅広く紹介され，専門家のみならず広く一般の理解に供されている。ここでは取り上げ方を少し変えて，放射線医学総合研究所（放医研）内部被ばく・防護研究部に的を絞ることとする。すなわち，生体への影響評価に関する研究とその研究を遂行する上で，どうしても避けることのできない関連研究と諸課題に焦点を当て，わが国におけるプルトニウムの生体影響評価に関する研究を一つのシナリオとして系統的に解説する。

プルトニウムの生体への安全性評価に関する研究は，単に生物・医学・獣医学だけではなく，工学・物理・化学の分野まで含んだいわば総合科学であり，これら相互の連係と理解がなければ進展はあり得ない。このことが十分に理解していただけるよう，著者一同念願している。

なお，本特集は以下の章立てになっている。

1. 放医研のプルトニウムの生物影響評価研究の目指すもの―概要―
2. プルトニウム動物実験施設の設計と管理経験
3. プルトニウムの吸入投与実験
4. プルトニウムの体内動態―難溶性放射性粒子の呼吸気道内挙動ならびにプルトニウムの胎児移行を中心にして―
5. 生物学的安全性評価研究におけるプルトニウムの線量評価
6. アルファ放射体内部被曝生物影響研究―プルトニウム発がん実験を中心に―
7. プルトニウム影響のリスク低減化に関する研究

保健物理，33(3)，284～285（1998）

≪特集：放医研におけるプルトニウムの生物影響評価研究≫

1. プルトニウムの生物影響評価研究の目指すもの

——概要——

下　道　國[*1]

放射線医学総合研究所（放医研）内部被ばく・防護研究部における，これまでのプルトニウムに関する研究の流れを経時的にかつ全体的に概観することによって，研究担当者のプルトニウムの生体への安全性に関する研究に対するスタンスとその手法を紹介する。

はじめに，内部被ばく・防護研究部には，プルトニウムの生体への影響を評価する唯一の国立研究機関として，次のような認識がある。すなわち，わが国において，原子力政策が堅持される限り，今後も発電炉等においてプルトニウムが生産され，蓄積され，そして保存される。しかも本格的な操業はまだ先であるものの，核燃料サイクルの工程ではプルトニウムの取り扱いが主要な過程を占めることが予定されている。したがって，起こり得るかもしれない職業被曝だけでなく公衆被曝としての吸入被曝とその影響評価ならびに低減化について，必要にして十分な知識と技術を取得し，かつそれらを高いレベルで維持しなければならない。また，この一朝一夕には達成しえない生体（誤解なくいえば人間）への影響評価研究を永く遂行することも国立研究機関の責務である，といった認識である。

さて，放医研におけるプルトニウム研究の源流は1966年頃まで遡ることができる。丁度このころは原子力が“光”を浴びている時で，将来の電力の大部分を原子力発電で賄うという政策が押し進められている時期であった。それゆえに，プルトニウムの生物影響研究の重要性が関係者の間でよく認識されていたのは当然といえる。しかしながら，プルトニウムであるがために，慎重にかつ細心に計画は運ばれ，内部被曝研究部の発足はそれから16年後の1982年である。その数年前から新たに開発された諸設備を備えた内部被曝実験棟で実験が始められるようになったが，それは構想が打ち上げられてから実に20年後の1985年である。1985年からいよいよ動物吸入曝露実験がラットによって開始された。はじめの約3年は，コールドランも兼ねた非放射性粒子を用いた研究が行われ，次いで放射性粒子での実験が2年ほど行われた。1987年になって，日本原子力研究所からプルトニウム5.0gの譲渡を得ることができ，ようやくプルトニウムを使った吸入曝露実験が開始された。現在(1997年末)まで，一定粒径の酸化プルトニウムをラット・マウス合せて2,500匹以上に，吸入あるいは注射で投与され，大部分は生涯飼育の後に解剖され多くのデータが得られたが，一部は現在なお飼育中である。なお，イヌについては，予備実験が終了した段階である。

ところで，プルトニウムの人間への影響を知ることが目的であるにもかかわらず，人体を使った直接的な検証実験はできない。そこで，ラット・マウス・イヌといった動物にプルトニウムエアロゾルを含んだ空気を吸入させ，それを生涯飼育した後の解剖所見から発癌固体数を数え，それから人間のリスク評価のための知見を得るという手段が採用されたのである。動物実験結果をそのままヒトに外挿する点の危うさ（これはどの動物実験にもある）を念頭に置きつつも，である。この目的達成のために考えられた放医研の研究とその成果を逐一紹介するには膨大なスペースを必要とするので，この特集では，次のような章立てと内容にして，放医研内部被ばく・防護研究部での主要な研究に限ることとした。

第2章では，動物実験施設の設計と管理経験を記したが，それは，研究方針を本当に理解した上で実験施設を設計し，運転し，維持・管理するという業務が研究を進めることと同様あるいはそれ以上に，重要かつ困難な仕

[*1] 放射線医学総合研究所内部被ばく・防護研究部；千葉県千葉市稲毛区穴川 4-9-1（〒263-8555）
National Institute of Radiological Sciences；4-9-1, Anagawa, Inage-ku, Chiba 263-8555, Japan.

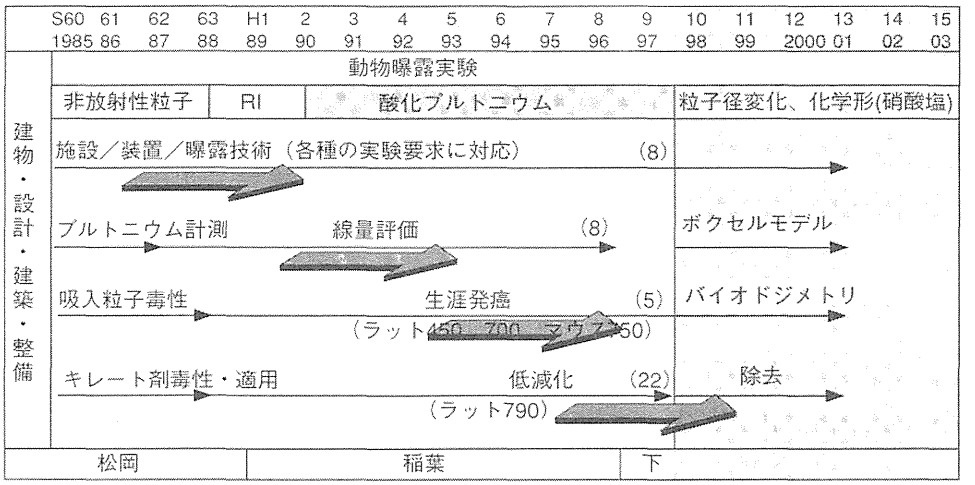

第1図　プルトニウム研究の推移

事であるという位置付けである。

第3章は，吸入曝露技術・装置の開発，吸入粒子の発生と特性の把握および制御といった技術課題である。これがクリアされない限り，以後の研究は進展しない。これら2つの章の保健物理学的・工学的過程は，この研究プロジェクトの先行部分として極めて重要な位置を占める。

第4章は，プルトニウムの体内での挙動で，吸入したプルトニウムの気道内沈着，肺からの移行と胎児への移行とその解析である。この体内での挙動の解明は，線量（次章）の正確な評価と発癌機構の解明に必要な知見である。

第5章は，吸入プルトニウム試料の曝露量（あるいは体内沈着量）の定量，ならびにそれからの線量の算定といった計測学・線量学の課題である。影響研究では線量が指標とされることから，線量評価がこの研究プロジェクト上極めて重要な位置を占めることはいうまでもない。

第6章では，本プロジェクトの中心ともいえる発癌実験である。ここでは腫瘍・癌の発生率のほかその種類が，線量および線量率の関係で論じられる。

第7章は，体内に取り込まれたプルトニウムの速やかな除去についてである。そのためにはキレート剤を開発し，その特性を知り，かつ使用法を明らかにしなければならない。安全評価上，リスク係数を求めたり発癌機構を明らかにすることはもちろん重要であるが，プルトニウムの体内からの除去に関する研究・技術はそれに劣らず重要である。

これら一連の技術開発・実験研究から得た多くの知見は原著論文としてまとめられ，このプロジェクトに直接関係した論文だけで40編以上，関連論文を含めると197編にのぼる。ここでは，全体像を摑む便宜のために，研究の流れを示すきわめて単純化した図を**第1図**に示した。以下の章では，大枠の課題（章のタイトルに対応）が理解されやすいように記述に留意した。なお，個別の詳細な研究成果については，読者において各論文に目を通されることを期待する。

保健物理，33(3)，286～293（1998）

≪特集：放医研におけるプルトニウムの生物影響評価研究≫

2. プルトニウム動物実験施設の設計と管理経験

小泉　彰*1，福田　俊*1

1. はじめに

核燃料物質を取り扱う工学的施設は数多く存在するが，放医研がプルトニウム（Pu）の安全性研究プロジェクトをスタートさせようと計画していた頃にはプルトニウムを用いた本格的な動物実験施設は我が国にはなかった。そのため，さまざまな問題，特に動物実験に由来する問題に対して，原子力工学がそれまでに集積してきた貴重な技術，ノウハウをどのように取り入れるかが大きな課題であった。

ここでは，放医研内部被ばく実験棟（以下，本施設という）について，動物実験を行う核燃料施設としての特殊性を中心に施設の設計および管理の実状を報告する。核燃料施設としては極めて特殊な施設であるが，参考になれば幸いである。

2. 施設設計の条件・方針

2.1 設計条件としての実験計画

施設設計の条件となる実験計画のうち，設計に最も影響するものは，やはり動物実験であった。その概要は次の通りであった。

① 用いる実験動物はラット，マウス，ビーグル犬であり，他に若干のサルを使用できること。

② 使用する放射性物質は，生物影響が観察できるレベルで投与するPuと，トレーサーレベルで使用する若干のRIである。Puは^{239}Puの割合が96%以上の，核分裂生成物を含まない純粋なPuである。

③ Puの投与方法は，吸入投与，注射投与とする。

④ Puを投与した動物のうち，影響研究の対象の動物は生涯飼育（死亡するまで飼育）し，その臓器・組織の病理検索を行う。なお，生涯飼育とは，ラット，マウスで3年，イヌで15年を意味する。

⑤ Puを投与した動物のうち，代謝研究の対象の動物は，適宜安楽死させ，その臓器・組織のPu分析等の処理を行う。

これらの条件から，Pu投与動物の排泄物処理，Puエアロゾル（高濃度汚染空気）の制御，生涯飼育のスペース確保，Pu混入試料（臓器，組織切片など）のグローブボックス（GB）外での安全取扱法，などの問題が生じてくる。

また，使用する動物の数についても，設計当初には計画した匹数が条件として存在したが，実際の設計段階での検討において，「施設建設予算を考慮し，可能な限り飼育スペースを多くとり，その中で飼育できる匹数を用いる」ことにした。その最大の理由は，発ガン性などを調べるための生涯飼育のスペースが非常に大きくなってしまうからであった。結果として得られた動物飼育スペースは，小動物1800匹，ビーグル犬200頭，となった。

2.2 設計方針について

本施設の設計に関していくつかの重要な方針があった。そのうちのいくつかを紹介し，若干の評価を述べる。

① 施設の耐震性

本施設のPu使用量（許可量）はわずか10 gである。しかし，核燃料使用施設である以上，建設完了までの過程で安全審査等の審議を経なければならない。そこで問題となったのが施設の耐震性をどこまで持たせるか，ということであった。それまでの我が国の核燃料施設はすべて工学施設であり，本施設のような生物学的研究施設のための判断例，判断基準がなかった。そのため，原子力発電所建設時の考え方から，耐震Bクラスとすることにした。従って，建物の軀体のみならず，動物飼育装置も含め，すべての設備を耐震Bクラスで設置することとした。しかし，運転開始後10余年の現在，施設・設備の維持管理経験から耐震Bクラスはオーバースペックだったのではないかという気がしている。我が国のPu施設で行われている厳しい種々の管理，例えば，グローブ

*1 放射線医学総合研究所内部被ばく・防護研究部；千葉県千葉市稲毛区穴川 4-9-1（〒263-8555）
National Institute of Radiological Sciences；4-9-1, Anagawa, Inage-ku, Chiba 263-8555, Japan.

ボックスの管理や作業管理がなされている限り，本施設のような生物学的研究施設の潜在的危険性は高くないという感触を得ているからである。

② 負圧管理

Pu施設に必ず求められる設備機能に負圧管理がある。潜在危険度の高い区域ほど気圧を低くして，万が一，汚染空気が発生しても危険度の低い区域から高い区域に風が流れ，その結果，汚染空気の拡大を防止する安全対策機能のことである。しかし，実験動物施設では全く逆の，陽圧管理の考え方がある。これは，実験動物への疾病の空気感染を防止するためである。この相矛盾する設計理念に対して，動物飼育室と他の区域の境界に緩衝区域を設け，負圧バランスを吸収する方法と，換気のための給気にフィルタを使用し，雑菌の流入を防止するという2つの方法で対処した。

施設運転開始後，この給気フィルタは思わぬメリットをもたらすことが分かった。給気中の大気塵が除かれるため，排気フィルタの寿命が5〜10倍に延び，使用済みフィルタという放射性廃棄物の排出量が予想よりはるかに少なかったことである。ガラス繊維が使われているため焼却処理のできない使用済みフィルタは，廃棄物保管の点で大きな問題である。この経験から，他の原子力施設でも給気にフィルタを使用することは十分採算のとれることと思われる。なお，給気フィルタには，HEPAフィルタのような高い性能は必要ない。

本施設の負圧管理設計にはひとつの反省点がある。それは，負圧を実験室ごとに設定し，設備機能を設計したため，いったん崩れた負圧バランスを再度初期の設定に戻す給排気量調整に多くの時間を要することである。他のPu施設では管理区域をゾーンに区分し，ゾーン間で負圧管理を行っている例が多い。この方が負圧管理がはるかに容易であったと思われる。

③ 廃棄物処理

原子力施設の設計においては排水の排出量を少量にすることがひとつの常識となっている。その理由は，排水処理設備は建設費，ランニングコストが大きいこと，維持管理，すなわちメンテナンスが重要な設備であること，などである。しかし，実験動物の飼育・管理ではし尿処理や飼育環境の滅菌作業など，多量の水を使う作業が多い。そのため，動物飼育に伴う作業一つ一つについて水を使わない方法，使用量を減らす方法を検討した。その結果，現在の動物飼育管理技術には水を使わない，あるいは少量で済ませるノウハウはない，という結論に達し，専門の排水処理設備の導入を決定した。この検討の中で，最も重要視しなければならなかったことは，動物の疾病防止が研究プロジェクトの死命を制する，ということであった。

排水処理の基本方針として，まず，し尿有機物を微生物の活動によって分解する浄化槽で除去した後に，放射性物質を除去することとした。排水中の放射性物質を除去する技術は，日本原子力研究所や動力炉核燃料開発事業団などの永年の開発によって確立されたさまざまな技術があったが，し尿有機物の含まれる多量の排水にはどれも適用できなかったからである。また，汚水浄化処理では余剰汚泥の排出が避けられないため，当初は，有機物を高温・高圧下の水中で酸化・分解させるZIMMERMANNプロセスを検討したが，高温・高圧運転の危険性と高いBOD，COD成分を含む二次排水の排出があることから断念した。さらに排水中の放射性物質を除去するプロセスを考えるうえで，処理対象核種をPuに限定した。その理由は，他の核種はトレーサーレベルで使用量が少なく，排水量が多いことから高い濃度にはならないと評価できたからである。

また，排水放出時のPu濃度は法規制濃度の1/1000にすることを，除去設備の設計目標とした。この値は，当初のゼロリリースにしたい，という心情的な方針を，1/1000ならほぼゼロリリースと言えるだろうという，かなり感覚的な判断によって具体的な目標値としたものである。最大量のPuを取り扱う実験を想定し，総排水予想量から計算された処理前の排水中Puはおおよそ法規制値の濃度と同等であった。従って，Pu除去設備の除染係数は1000を設計目標とした。

一方，Puなどの核燃料物質を含む放射性廃棄物は，アイソトープ協会等に引き渡すことなく，施設内に永久保管（保管廃棄）することになる。従って，保管する廃棄物は永年にわたって安定性が確保されなければならない。この意味で，本施設から排出される廃棄物のうち，最も考慮しなければならない廃棄物は動物の死体と汚水処理から排出される汚泥であった。これらの廃棄物の減容，安定化を図るためには焼却処理しか選択できなかった。焼却炉設備は設備投資が高価になることと，慎重な維持管理が必要なことから，導入が最も躊躇された設備であったが，研究プロジェクトが長期間を要するという特質を考慮すると導入を決定せざるを得なかった。また，廃棄物をさらに減容することを考え，焼却灰のマイクロ波溶融処理も検討したが，将来決定されるであろう廃棄物の処分技術に対応する余地を残すため，焼却灰の形で保管廃棄することとした。

なお，施設建設に先立ち，諸外国の同様の施設を調査したが，たとえPuであっても放射性廃棄物の処理に対

する社会通念が全く異なるためか，参考になる設備や設計理念は見いだせなかった。

3. 施設・設備の概要

本施設の特色となっている部分をいくつか紹介する。

3.1 建物の構造

通常の施設では，ダクト・配管類は天井裏に設置される。しかし，本施設ではこの天井裏に相当する部分を一フロアとした。従って，2，4，6階の実験用フロアの間にサンドウィッチ状にダクト・配管類のためだけのフロアが挟まっていて，このフロアを著者らはメカニカルフロアと呼んでいる。これは，Pu施設にとってメンテナンスがきわめて重要との認識の結果である。想定した通り，現在このフロアによって各種の点検，修理などが容易に，的確に行えている。このフロアのメリットはこれだけではなかった。本施設は実験研究施設であり，実験研究はその進展に伴って，フードがほしい，流しがいらない，といったように設備機能の要求が変化する。この要求の変化に対する対応をメカニカルフロアは容易にしてくれる。実験研究施設はしばしば使用目的の変化に追随できず，施設としての寿命が来てしまうことが多いが，メカニカルフロアはその意味でも施設の寿命を延ばす効果があると考えられる。

3.2 負圧管理システム

本施設の各実験室における負圧管理には**第1図**に示すような3つのパターンがある。第1のパターンはフードのない部屋の最も単純なシステムで，定風量ダンパー（CAV）で制御された給気量と排気量の差で負圧を生じさせている。部屋と廊下との間に設置した微差圧調整ダンパーは，負圧によって扉の開閉が重くなることを防ぐためである。GBの設置してある部屋も，グローブボックスの排気量が部屋の換気量に比べて小さいため，このパターンに含まれる。

第2のパターンは，通常のフードが設置された場合のシステムである。微量のPuを含むすべての生物学的試料をGBの中で取り扱うことは困難である。その対応策として，本施設ではフードが多用されている。フードの排気量は大きいため，フード使用時には室内排気量を可変風量ダンパー（VAV）で自動的に低下させる。

第3のパターンは，エアカーテン式フードを設置したケースである。このフードは，作業者の頭上からエアカ

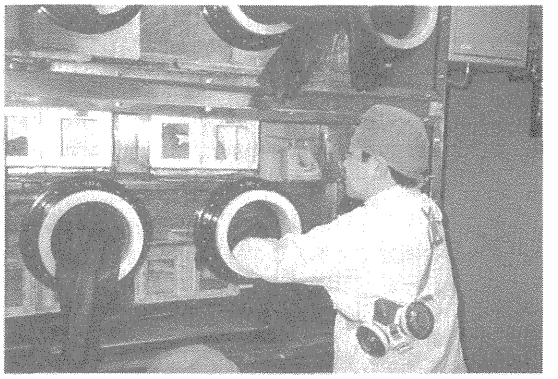

第2図 プルトニウム投与直後の動物のためのGB型飼育装置の写真

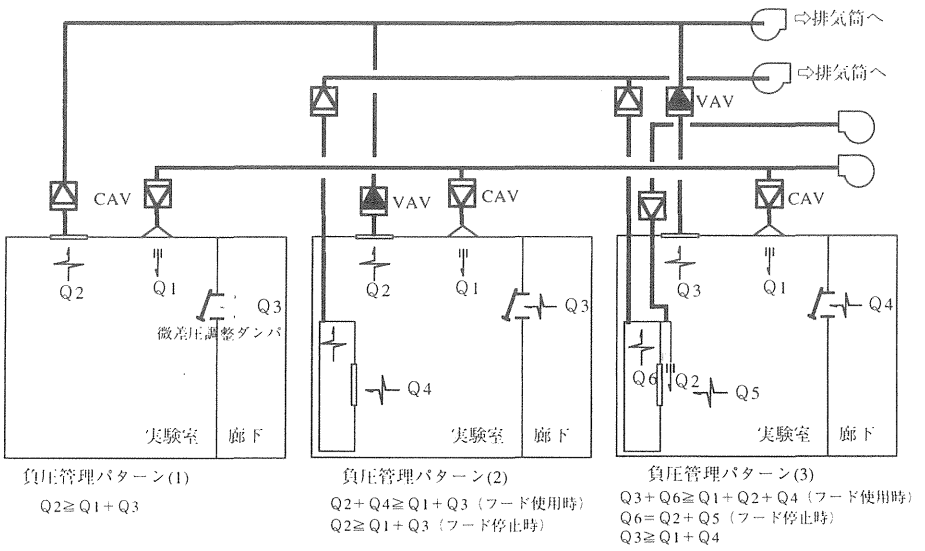

第1図 内部被ばく実験棟における負圧管理パターン

ーテン状に新鮮空気を流し，汚染空気の乱流による舞い戻りを防止する方式で，より安全性が高い。しかし，そのために給排気量制御に複雑なシーケンスを組まなければならない。

3.3 動物飼育設備

Puを投与された動物の飼育装置にはその密閉性において3つの方式を用いている。3つの飼育方式の使い分けについては後述する。

① GB型飼育装置：Puを投与した直後の動物は初期排泄量が多いため，ほぼGBと同等の密閉性を有する箱の中に飼育装置を納めている(**第2図**参照)。この中の動物に対するケア作業（給餌，ケージ交換・洗浄，給水など)はすべてグローブ越しの作業となる。GB間の動物の移動には，二重扉式搬出入装置（ダブルカバーシステム）を用いている。GB型飼育装置の中での動物飼育には，ケア作業が長時間になる，十分な健康管理ができない，単位面積当たりに飼育できる動物数が限られる，などの問題がある。

② フード型飼育装置：各ケージの前に小窓があり，この窓を開けて作業できる。GB型より密閉性は低く，フード程度である。ケア作業は若干楽になるが，単位面積当たりに飼育できる動物数はGB型と同じである。

③ 開放型飼育装置：棚飼育と呼ばれる通常の飼育方法で，汚染空気の閉じ込め機能はない。しかし，単位面積当たりに飼育できる動物数は数倍になる。

3.4 グローブボックス

本施設で使用しているGBは小型のものが多く，最も大きいPu吸入実験用GBが約5 m^3で，他は1 m^3前後である。その他，GBとしての仕様は，原子力分野におけるGB仕様で製作され，管理されている。

3.5 廃棄物処理設備

a) 排水処理設備

本施設の放射性排水処理設備のフロー図を**第3図**に示す。排水処理の系統は，し尿有機物を含む汚水系排水と含まない実験室系排水の2系統あるが，濃度レベルによって系統分けはしていない。実験室系排水は汚水系排水の浄化処理の後に合流させている。

汚水系排水は処理工程に入る前に，沈砂槽でポンプ等を傷める砂を除去し，水に浮いてしまう飼料を破砕し，バルブ等を閉塞させる動物体毛をスクリーンで除去する，動物管理で使用される消毒薬を中和する，という前処理がある。

し尿有機物を微生物によって分解する浄化槽技術には，回転円板式接触酸化法を採用した。この浄化槽技術は，下半分が汚水に浸かりながらゆっくりと回転する円板集合体の表面にさまざまな微生物コロニーを付着・繁殖させ，彼らの活動によって有機成分を除去する技術である。この浄化槽技術には，放射性排水の処理に用いられた実績はなかったが，

① 実験に伴う動物数の変化によるし尿成分の変動に自動的に浄化能力が追随するので人為的に制御する必要がない，

② バルキングと呼ばれる，微生物が一斉に死滅する現象が発生し難い，

③ 余剰汚泥の発生量が，他の浄化槽技術（活性汚泥法，散水露床法など）に比べて少ない，

④ ほぼ，メンテナンスフリーで運転できる，

といった利点があった。汚水系排水を直列3段のこの浄化槽を通過させることによって，汚水排水中の有機成分(BOD, COD)は，JIS規格による測定法の検出限界付近まで除去されている。

汚水浄化処理を経た排水は実験室系排水と合流し，凝集沈殿処理と活性炭吸着処理によってPu除去される。活性炭処理を選択した理由は，水素イオン濃度が中性領域にある排水の中でPuはイオン化しておらず，水酸化物あるいは酸化物の形で溶存していると考えられたからである。活性炭の寿命は，排水中のBOD, COD成分の濃度に依存する。従って，前述の浄化槽技術の高い浄化能

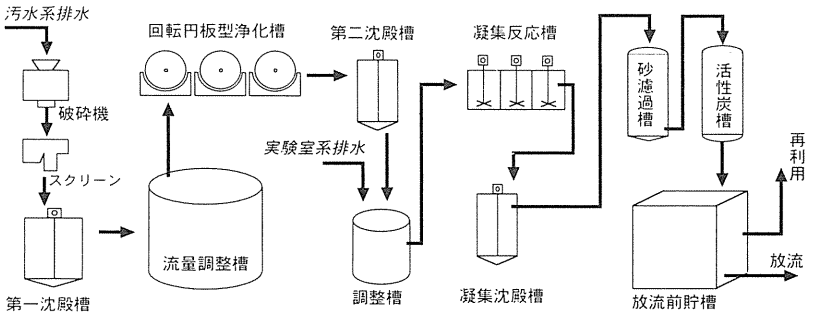

第3図　内部被ばく実験棟の放射性排水処理フロー図

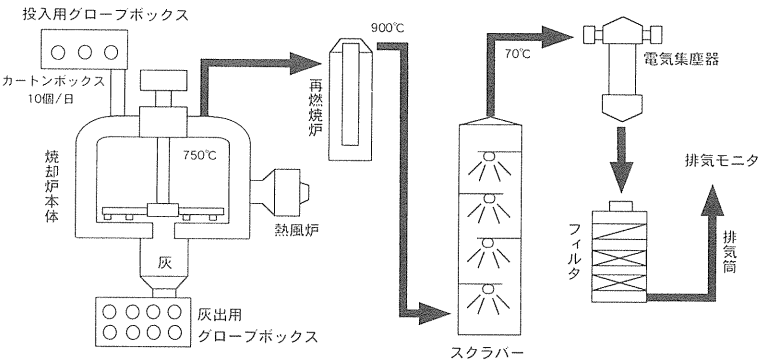

第4図 内部被ばく実験棟の放射性廃棄物焼却設備の概要

第1表 平成8年度年間焼却処理量

廃棄物の種類	カートン数（個）	重量（kg）
可燃物	1064	1,789
廃活性炭	431	2045
動物死体	22	47.8
回収毛	231	755.6
有機廃液	293	422.7
脱水汚泥	—	17,828
合計	2041	22,888
焼却灰排出量	—	1,115

力と安定な運転が極めて重要となっている。

排水処理設備の処理量は現在ほぼ一定状態に達しており，約50 m³/日である。また，1週間当たりでは約100 m³で，実効容積100 m³（3基）に貯留，モニタリングの後，市下水道に放流している。なお，排水処理量の約65～70%を動物し尿を流す水として，再利用している。

b) 焼却炉設備

放射性廃棄物処理を永久保管までのシステムとして考えると，焼却設備は不可欠な，システムの要となる。特に本施設のように動物由来の廃棄物を毎日多量に排出する施設では廃棄物処理対策が完結しない。本施設の焼却設備のフロー図を**第4図**に示す。また，**第1表**に種類別の年間処理量を示す。

この焼却炉の熱源は，灯油バーナー式熱風炉であり，炉内温度は700～750℃で維持される。炉床は直径2.6 mの円形で，焼却物は円周付近に投入される。炉床には灰が3 cmの厚さで堆積していて，6本のアームの下についている攪拌板（スクレーパ）が灰と焼却物をゆっくりと攪拌する。焼却物は円周部から中心に向かってラセンを描きながら移動する間に，乾燥-炭化-灰化のプロセスを経て灰になり，炉床の中心にある灰出し口から落下，排出される。

この焼却炉の最大の特徴は，炉内を低酸素状態にして燃焼させる，乾留灰化運転が可能なことである。この運転では炉内風速を非常に低く保つことができるため，汚泥焼却時のフライアッシュの発生を低く押さえることができる。同時に，燃焼速度が焼却物の種類にあまり影響されず，極めて安定な燃焼状態が得られる。この安定な燃焼は，炉の安全性，耐久性を高めている。

焼却炉の排ガスは，再燃焼炉，スクラバー，電気集塵器，HEPAフィルタ，の順で処理される。再燃焼炉は，焼却燃焼時の未燃ガス，未燃焼煤塵を完全燃焼させるための二次燃焼室に相当する。炉内温度は，900℃に保たれている。スクラバーは，排ガスの温度を低下させることと同時に，煤塵の除去を目的にしているが，スクラバー廃液という二次廃棄物が発生する。この廃液には，動物由来のハロゲン化物，硫黄化合物，燐酸類，カルシウム成分などが多く含まれ，腐食性が高く，スケールの発生しやすい性質を有する。

焼却炉の排ガスは，最終段階でHEPAフィルタによる浄化処理をしているが，それまでの再燃焼炉，スクラバー，電気集塵器による処理で十分に煤塵を除去できている。その結果，HEPAフィルタの寿命は1年以上となっている。

4. 放射線管理

4.1 施設管理

本施設における空気中濃度，空間線量当量率および表面汚染密度の管理の内容には，他の核燃料施設における管理と差異はなく，大きな特徴はない。過去10年間のモニタリング結果はすべてネガティヴである。放射線管理の対象として，本施設は「面白み」のない現場である。参考として，それぞれの管理の本施設における管理基準

第2表　内部被ばく実験棟における空気中放射能モニタリングの管理基準

測定核種	法規制値（Bq/cm³）	管理基準値（Bq/cm³）	管理目標値（Bq/cm³）
アルファ核種	8×10^{-8} （3カ月平均濃度）	8×10^{-8} （1カ月平均濃度）	8×10^{-8} （1週間平均濃度）
非アルファ核種	4×10^{-6} （3カ月平均濃度）	4×10^{-6} （1カ月平均濃度）	5×10^{-8} （1週間平均濃度）

第3表　内部被ばく実験棟における空間線量当量率モニタリングの管理基準

測定場所	法規制値	管理基準値	管理目標値
管理区域	1 mSv/w	25 μSv/h	12.5 μSv/h
周辺監視区域	250 μSv/3 mon	0.5 μSv/h	0.25 μSv/h

第4表　内部被ばく実験棟における表面汚染モニタリングの管理基準

測定核種		法規制値（Bq/cm²）	管理基準値（Bq/cm²）	管理目標値（Bq/cm²）
アルファ核種	管理区域	4	0.4	0.2
アルファ核種	搬出基準	0.4	0.2	0.1
非アルファ核種	管理区域	40	4	2
非アルファ核種	搬出基準	4	2	1

とモニタリング方法を**第2〜4表**に示す。

4.2　個人被ばく管理

前にも述べたように，本施設で使用されている非密封放射性物質は純粋なPuとトレーサーレベルのRIであり，これらによる外部被ばくは問題とならない。外部被ばくの可能性のある主要な作業は，X線発生装置（診断用X線装置，実験用軟X線装置など）の取扱作業である。

内部被ばくの定常的な評価方法は，エアスニッファによる作業環境中のPu空気汚染モニタリング結果からの算出である。しかし，空気汚染が検出されたことはなく，従って，定常モニタリングに基づいて，より詳細な内部被ばく線量評価を行ったことはない。一方，個人管理の対象としての登録時と登録抹消時には肺モニタによる体内汚染のモニタリングを行っている。

4.3　作業管理

本施設における放射線管理の中で最も重要なものが作業管理である。作業管理では，危険性の高いと考えられる作業や初めての作業に対して，事前に協議し，作業方法，防護手段，モニタリング方法等を予め定めて実行する。さらに，作業に立ち会い，作業中にモニタリング（特殊モニタリング）を行い，作業および管理が適正であったことを確認しながら，作業を完了させる。繰り返して行われる作業については，管理データが得られ，安全性が確認された時点で作業管理の対象から外される。

本施設のホットラン開始当初は，さまざまな実験手法，特に動物実験に関連する実験手法が作業管理の対象として検討されたが，現在では多くの作業が定常化していて，作業管理の対象となる実験操作の件数は少なくなっている。その代わりに施設の老朽化に伴う更新・改修工事が増加している。

4.4　環境モニタリング

本施設がホットランに入る3年前から四半期ごとに次のPu分析を（財）日本分析センターに委託している。

① 大気浮遊塵：敷地境界付近5点（約10,000 m³/点）
② 排水：所排水口2点（100 l/点）
③ 表面土壌：敷地境界付近6点（地表3 cm厚さ）

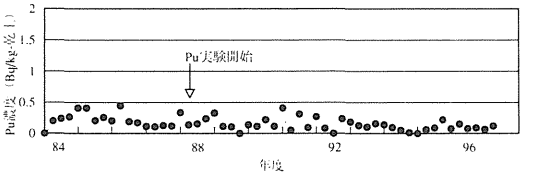

第5図　環境モニタリングの例：敷地内表面土壌中のプルトニウム濃度

第5表 プルトニウム吸入投与ラットの体表面（鼻先）汚染の経時変化

吸入後1日	吸入後7日	吸入後1カ月	吸入後3カ月
4.0×10^{-1} Bq/cm²	ND	ND	ND
4.2×10^{0} Bq/cm²	8.6×10^{-2}	ND	ND
ND	ND	ND	ND
1.2×10^{0} Bq/cm²	3.2×10^{-1}	ND	ND
3.2×10^{-1} Bq/cm²	ND	ND	ND

ND：検出限界以下

④ 排水・汚泥：千葉市中央下水処理場の排水と汚泥，各1点

これらの環境試料のPu分析は，法律に基づいた業務ではない。現在，さまざまな環境試料中に，これまでの大気圏内核実験やPu電池搭載衛星の落下などに起因するPuが検出されている。このPuの濃度レベルの推移を把握して，本施設の管理の適正を確認することが環境モニタリングの目的である。

これらの試料のうち，定常的にPuが検出されるのは表面土壌と下水処理場の汚泥である。参考に，ある地点での表面土壌中のPu濃度（Bq/kg乾土）の，10数年にわたるモニタリング結果を**第5図**に示す。

5. 施設維持・管理の経験

本施設を運転し，管理するなかで，さまざまな管理データが集積されている。その中から保健物理学的に意義のあるものをいくつか紹介する。

5.1 吸入実験の排気処理

特殊な動物実験設備である吸入実験装置については，本稿では割愛するので他稿を参照されたい。しかし，Puの微細エアロゾルを動物に吸入させるということから懸念されたことは，放出基準の10^6倍程度に達する高濃度のPu汚染空気を確実に制御できるか，であった。このことがエアフィルタの性能を評価し直す研究[1~3]のきっかけとなった。その結果，① フィルタを最も通過しやすい粒子径（最透過粒子径）が0.15 μm付近にあること，② 多段フィルタの捕集性能は最透過粒子径での透過率の積とすると，安全側に評価できること，などの知見を得た。これらの結果から，Pu吸入実験装置から排出されるPuの濃度は，ULPAフィルタ2段，HEPAフィルタ3段のエアフィルタによって，安全側に見ても$1/10^{17}$にまでに除去・低減できていると評価している。さらに，この装置からの排気は施設の換気に伴う排気によって約10^6倍に希釈されるので，放出基準の$1/10^{17}$以下まで低減できていると評価できる。

5.2 動物の移動（投与直後の排泄物）

実験動物の飼育装置は前に述べたように，その気密性で3段階に分けられ，投与直後には最も気密性の高いグローブボックス型の飼育装置を用いる。投与後1カ月以上を経てから，次の3項目の基準を満足すると，フード型飼育装置に動物を移動させる。

① 排泄物中Pu濃度が，4 Bq/g-wet以下

② 動物体表面汚染が，4 Bq/cm²以下

③ 飼育装置内空気汚染レベルが，1×10^{-9} Bq/cm³以下

これらの管理基準を定める際には，体表面汚染および排泄物のPu濃度の経時的変化を測定し，1～2週間でPuの排泄がほぼ完了し，検出されなくなること，動物の体表面汚染も同様に短期間に消失すること（**第5表**参照），飼育装置内の空気汚染レベルは，投与直後には検出されるが，管理基準値を越えることはない，などの知見を実験的に確認した[4,5]。動物に投与されたPuは，初期代謝の時期を過ぎるときわめて排泄され難く，生体が強固なバリアとなっていると考えられる。

5.3 焼却炉の改修

本施設の放射性廃棄物用焼却炉は運転開始後約10年を経て，灰掻き寄せアームを覆っている耐火物（キャスタブル）の亀裂，一部脱落が生じ始めた。この現象は設計当初から予想された経年劣化であった。このまま症状が進行すると炉の正常な運転に支障をきたす可能性が考えられた。そのため，6本のアームを更新する改修工事を実施した。

炉内にはPuを含む灰が堆積しているため，厳重な安全性の検討が行われ，作業計画と安全管理計画が立案された。その中で，これまでに提唱されてきた再浮遊係数[6]を用いて防護対策を決定し，この作業時での再浮遊係数を実測[7]した。その結果，飛散を生じやすいと考えられる焼却灰の取り扱い作業に対しても，提唱されてきた再浮遊係数が妥当な値であって，安全確保のための実用性が確認された。

6. おわりに

本実験施設の特殊性の一端を紹介したが，核燃料取扱施設であると同時に動物実験施設であることの特殊性の一端がご理解いただけたであろうか。1979年に米国の研究施設を調査のために訪れた際，Dr. J.L. BAER がPu施設の設計指針書[8]とともに，「Pu施設で，設計よりも放射線管理よりも難しいことは，施設の品質管理(Quality Control) だよ」という言葉をプレゼントしてくれた。今，実感として彼の言葉が理解できる。事故時の対応など，いわゆる危機管理の問題が議論されている現在，施設の維持・管理の健全性を維持することが今後の重要課題と考えている。Puに関する安全性研究プロジェクトは幸いにも順調に成果を揚げつつあるが，建設後10年余りを経た現在の最も考えるべき問題は，施設の維持・管理業務を担当する者とそれを支援する技術役務集団の技術力維持であると考えている。関係者および諸先輩のご指導を今後とも期待したい。

本稿を終えるにあたり，著者らは動力炉核燃料開発事業団の故小泉 勝三氏に感謝の意を強く表したい。氏には，安全管理技術の専門家として本施設における安全管理システム[9]のレールを敷いていただいたばかりでなく，さまざまな実験手法や施設管理業務に対しても，Pu施設としてのやり方，考え方を植え付けていただいた。今日，無事に施設が運転されているのは，氏の努力のおかげであると考えている。

参考文献

1) Y. YAMADA, K. MIYAMOTO, T. MORI and A. KOIZUMI；Penetration of submicron aerosols through high-efficiency air filters, *Health Physics*, **46**, 543-547 (1984).
2) 山田裕司，宮本勝宏，高橋千太郎，小泉 彰；^{198}Auエアロゾル粒子に対するエアフィルタの除染係数，保健物理，**22**, 403-410 (1987).
3) 山田裕司，小泉 彰，宮本勝宏，稲葉次郎；Puエアロゾルに対するHEPAフィルタの捕集性能，保健物理，**29**, 283-289 (1994).
4) 金岩祥子，小泉 彰，福田 俊，鈴木信夫；Pu投与動物のし尿中Pu濃度の放射線管理を目的とした測定法の検討，日本保健物理学会第29回研究発表会 (1994).
5) 辺見敏彦，吉田浩樹，横山和昭，小泉 彰，福田 俊；プルトニウム吸入ラットの汚染モニタリングと飼育管理レベルの判断，日本保健物理学会第30回研究発表会 (1995).
6) “高放射性物質取扱施設設計マニュアル，”(社)日本原子力学会，東京 (1985).
7) 横山和昭，小泉 彰，児玉浩一，古川敏夫，吉田浩樹；プルトニウム廃棄物用焼却炉の炉内改修における放射線管理経験，日本保健物理学会第31回研究発表会 (1996).
8) “A Guide to Good Practises at Plutonium Facilities,” BNWL-2086, UC-41, Battelle Pacific Northwest Laboratories (1997).
9) 小泉勝三，小泉 彰；核燃料物質取扱施設の放射線管理，KURRI-TR-308, 51-57 (1987).

保健物理，33(3)，294～297（1998）

≪特集：放医研におけるプルトニウムの生物影響評価研究≫

3. プルトニウムの吸入投与実験

山田裕司[*1]，宮本勝宏[*1]，小泉　彰[*1]

1. はじめに

放医研の実験施設，予算規模，管理基準などを考えるとプルトニウムの動物実験，特に吸入実験の規模は相当限定されたものになることが予想された。したがって，諸外国のように大量の吸入投与群を作成するのではなく，1個体ずつのデータを重要視するいわゆる少数精鋭主義で考えざるを得なかった。そこで，吸入も可能な限り1個体ずつのデータを得るため，吸入曝露時においてもその呼吸生理状態を監視し呼吸数・呼吸量等を個体別に収集することが計画された。また，プルトニウム初期沈着量を曝露群からの抜き取り方式で知るのではなく，専用の体外計測法を開発することで殺処分せず個別データを得ることが計画された。ただし，このような制約の下でも動物の曝露は可能な限り自然な形である，つまり，無麻酔下での曝露が求められた。

ところで，プルトニウムという理由で，その吸入投与法に何か特殊性があるかというと，実は基本的には差異は何もない。しかし，実験の安全確保については極めて厳しいものがあり，その象徴はグローブボックスであった。装置自身のハードウェア性能よりも装置の安全運転・排ガス処理の方が重要であったことは言うまでもない。

このような状況の下で実施されたプルトニウム吸入実験についてその概略を，実験装置というハードウェアの紹介，プルトニウムエアロゾルの特徴，吸入投与の実例の紹介の順で記述した。

2. プルトニウムエアロゾル吸入実験装置

放医研のプルトニウムエアロゾル吸入実験装置は，小動物用[1]およびイヌ用にそれぞれ1基製作された。グローブボックス内に設置された小動物用装置の外観写真を**Fig. 1**に示す。装置は，エアロゾル発生部，加熱酸化部，濃度調節部，吸入チャンバ部，排気処理部で構成されている。基本的には酸化プルトニウム用装置であるが，発生原液の前処理の有無，加熱処理の有無などにより硝酸塩，水酸化物の形態での曝露も可能である。

酸化プルトニウムエアロゾルの作成はRAABE *et al.*[2]の方法に従った。エアロゾル発生は，発生原液を定量ポンプで供給し，これを圧縮空気による霧吹き方式のネブライザ3台でミスト化するものである。なお，浮遊できなかった大きな液滴はドレン廃液として回収される。発生するエアロゾルの大きさは，発生原液の溶質重量濃度に依存するので，粒子径の制御はこれを利用するが，その感度はあまり良くない(溶質重量濃度の1/3乗に比例)ので粒子径を大きく変動させることは事実上困難である。加熱酸化は加熱温度300°Cのプレヒータと1150°Cのメインヒータの2段加熱法を採用することにより，均質で強固な酸化物粒子を得ている。ここまでのプロセスが吸入曝露チャンバの状態（動物の有無，圧力，流量）の影響を受けることがないように，曝露チャンバの上下流に緩衝用エアロゾルチャンバを設け，バランス運転をしている。

曝露チャンバは2重円筒型で20匹同時に鼻部曝露できるものである。全身曝露に比べ鼻部曝露は，一般的には困難な点が多々あるが，放医研のプルトニウム吸入実験にとってはメリットも少なくない。その最大の恩恵は，体表面汚染を防止し動物個体の体外計測を容易にしていることである。それはさらに，投与レベルについて群別管理から個体管理へと結びつき，少ない動物数で実験精度を高めることに貢献している。鼻部曝露のための動物ホルダ（**Fig. 2**参照）は被検動物の呼吸機能測定用ボディプレシスモグラフボックスの機能も持たせているため，曝露中動物の呼吸を個体ごとに監視することも可能である。ボディプレシスモグラフ法による吸入投与中動物の呼吸測定システムについては，BOECKER *et al.*[3]が

[*1] 放射線医学総合研究所内部被ばく・防護研究部；千葉県千葉市稲毛区穴川 4-9-1（〒263-8555）
National Institute of Radiological Sciences；4-9-1, Anagawa, Inage-ku, Chiba 263-8555, Japan.

Fig. 1 Plutonium exposure system for small rodents.

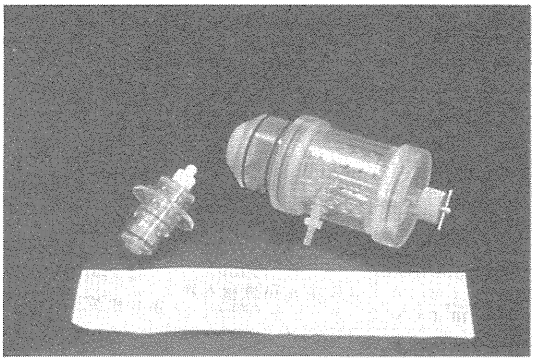

Fig. 2 Animal holder for rats and mice.

恒圧型のプレシスモで既に実用化を果たしていたが，放医研では，グローブボックス対応とするため恒容積型のプレシスモで実用化を試みた[4]。鼻部曝露方式のデメリットとしては，投与匹数の少数化と曝露前の馴致飼育の大変さが上げられる。イヌの場合には，曝露チャンバこそないものの，鼻孔部のみを露出させたイヌ用デスマスクを介して同様の曝露を受ける。

最後に，排気処理であるが，吸入実験装置の排気は，2列2段の超高性能ULPAフィルタを経て濾過された後，装置が設置されているグローブボックス内の排気系へ処理空気が放出される。装置の運転・制御はグローブボックス外にある制御盤から遠隔操作で行われる。

3. プルトニウムエアロゾルの粒子性状

エアロゾル化したプルトニウムについては，空気中濃度，粒度分布，形状などを中心にその粒子性状が調べられた。

プルトニウムエアロゾルの空気中放射能濃度は吸入チャンバからのエアサンプリングにより求めた。使用した濾紙は捕集効率[5]・アルファ線遮蔽効果・扱い易さなどを考慮して，ダストモニタリング用濾紙ではなくHEPAフィルタ用濾紙を用いた。放射能測定は表面障壁型SSDによる平均5.15 MeVのアルファ線計測法とNaI(Tl)/CsI(Tl)フォスウィッチ検出器による平均17 keVのLX線計測法とを放射能強度に応じて適宜使い分けられた。SSDによる計測は既存のシステムをそのまま用いたが，フォスウィッチによる計測は新たに開発された動物用体外計測システム[6]が利用された。通常の吸入実験における空気中濃度はおよそ1 Bq/cm³である。

プルトニウムエアロゾルの粒度分布はインパクタ法による空気力学的粒子径で評価された。使用したインパクタはQCM (Quartz Crystal Microbalance) 型と呼ばれるカスケードインパクタで，サンプリング装置としての機能のみならず各捕集ステージの捕集粒子重量もngの感度で測定できる。同一サンプルに対して放射能基準での粒度分布と重量基準での粒度分布とを同時に知ることができる[7]。現在，放医研で進められている吸入曝露実験はAMAD (Activity Median Aerodynamic Diameter)＝0.3～0.5 μm，GSD (Geometric Standard Deviation)＝2.0の多分散エアロゾルが中心となっている。

プルトニウムエアロゾルの可視化については，走査型電子顕微鏡による粒子形状の直接観察が試みられ，直径0.1～0.2 μmの球形の粒子像が得られている[7]。粒子の幾何学的な大きさとAMADとの間にはこのような差が認められるのは，プルトニウムエアロゾルは粒子密度が大きいためである。プルトニウムのアルファ線の可視化についても，手元の写真用フィルム等を利用すれば，特別の準備や前処理することなく容易にそのスター状の飛跡を観ることができる[7]。

エアロゾル発生に用いたプルトニウムの保存原液には僅かではあるがアメリシウム^{241}Am（アルファ放射能として）が含まれている。この比率はエアロゾル化の過程でも変化することはなく，粒子中のPu/Am比は粒子径に依存せずほぼ一定であり，均質な粒子であることの1つの証となった。

4. プルトニウムエアロゾル吸入実験

プルトニウムエアロゾルをラットに吸入投与したとき，プルトニウムがどの程度均一に肺内に沈着するかを調べた実験がある。プルトニウムエアロゾルの大きさはAMAD＝0.48 μm，GSD＝2.0で，これを0.96 Bq/cm³の空気中濃度で1時間だけ鼻部曝露させたときの各肺葉毎の初期沈着量を調べた結果の一部を**Table 1**に示す。放射能の絶対値では，例えば，2倍以上の差があった左葉（平均667 Bq）と右中葉（平均270 Bq）も，臓器重量

Table 1 Initial burden per lung weight (Bq/lung-g) of rats exposed to plutonium aerosols.

	Rat-#1	Rat-#2	Rat-#3	Rat-#4	Rat-#5	Ave.
Trachea	213	270	171	700	81	287
Left Lobe	1409	1664	1830	1626	1604	1627
R. Anterior L.	2107	1933	2291	2438	2350	2224
R. Middle L.	1720	1756	2100	1985	1635	1839
R. Posterior L.	1466	2010	1739	1846	1833	1779
Median L.	1915	2750	2333	1900	2292	2238
Whole Lung	1723	2023	2059	1959	1943	1941

Fig. 3 Beagle dog exposed to plutonium aerosols.

当たりの放射能で比べると 1627, 1839 Bq/lung-g となりかなり接近する。この他の葉の臓器重量当たりの放射能もこれらの値と大きく違わないことがこの表から分かる。つまり，少なくとも肺の分葉ごとのマクロな分布においては，プルトニウムは均一に沈着していたことが分かった。ラットホルダが置かれる吸入チャンバの位置によって，曝露物質の空気中濃度が最大 20%程度ばらつく[1]ことが予測されていた。**Table 1** の例では，全肺中のプルトニウム沈着量のばらつきは予測よりも小さかったが，ばらつきが 50%以上になる場合も少なくなかった。その原因の多くは，ラットの大きさがホルダに不適合で，あるいは，馴致不足であったことによる。ただし，このような場合でも，個体別に吸入沈着量が評価できたことから，1 匹のラットも無駄な棄却データとすることなく全数を実験投与群として扱うことができた。

1990 年から開始されたラットへのプルトニウム吸入投与実験は 1997 年末までに 940 匹に昇った。当初は，代謝実験・高投与レベル影響実験が中心であったが，次第に低投与レベル影響実験・影響低減化実験へと比重が移ってきているようである。イヌについては，ラットより 2 年遅れてスタートし，直ぐに，6 頭の吸入投与実績（参考：**Fig. 3** はマスク方式で吸入曝露中のビーグル犬）を上げたが，先行していたラットでの実験が優先となり，現在は中断したままとなっている。

5. おわりに

放医研の内ばく棟でのプルトニウム吸入実験計画が立案されていた時，外国では既に大規模な動物曝露実験が進んでいた。このため，曝露装置の早急な完成が求められていた。そこで，装置開発においては必ずしも 100%のオリジナリティに拘ることなく利用できるものは利用するという考えで開発期間の短縮を図ることになった。新規導入が出来ず日の目を見なかった幾つかのアイデアもあるが，その分，余裕が出来た予算は安全確保に重点配備し，時間は運転習熟に充てることができた。プルトニウムホットラン前の非汚染状態での運転経験は実に貴重なノウハウを与えてくれた。

吸入実験は特定の専門分野の研究者が可能とするものではなく，工学・理学・医学・農学とあらゆる領域の研究者・技術者が知恵を寄せ集めて初めて実現するものである。放医研の吸入実験も所内外の応援を得て今日成立していることは言うまでもない。この場を借りて御礼申し上げる。

参考文献

1) 山田裕司，久保田善久，小泉　彰，松岡　理；小動物用放射性エアロゾル吸入実験装置の開発とその基礎特性，保健物理，**24**, 331 (1989).

2) O.G. RAABE, H.A. BOYD, G.M. KANAPILLY, C.J. WILLKINSON and G.J. NEWTON；Development and use of a system for routine production of monodisperse particles of $^{238}PuO_2$ and evaluation of gamma emitting labels, *Health Phys.*, **28**, 665

(1975).

3) B.B. BOECKER, F.L. AGUILAR and T.T. MERCER ; A canine inhalation exposure apparatus utilizing a whole body plethysmograph, *Health Phys.*, **10**, 1077 (1964).

4) 久保田善久，山田裕司，高橋千太郎，松岡　理；ラット吸入実験における吸入量の算定，*Exp. Anim.*, **33**, 535 (1984).

5) 小泉　彰，山田裕司，宮本勝宏；集塵用フィルタの粒子捕集効率の面風速依存性，保健物理，**24**, 123 (1989).

6) N. ISHIGURE, T. NAKANO, H. ENOMOTO, S. FUKUDA, H. IIDA, Y. OGHISO, H. SATO, S. TAKAHASHI, Y. YAMADA, A. KOIZUMI, Y. YAMADA, K. MIYAMOTO and J. INABA ; Assessment of initial alveolar deposition on rats exposed to plutonium aerosols using a whole body counter, *Hoken Butsuri*, **27**, 135 (1992).

7) 山田裕司，小泉　彰，宮本勝宏，佐藤　宏，石榑信人，仲野高志，榎本宏子，稲葉次郎；ネブライザで発生させた酸化プルトニウムエアロゾルの粒子性状，保健物理，**27**, 197 (1992).

保健物理，33(3)，298～301（1998）

≪特集：放医研におけるプルトニウムの生物影響評価研究≫

4. プルトニウムの体内動態

——難溶性放射性粒子の呼吸気道内挙動ならびにプルトニウムの胎児移行を中心として——

佐藤　宏[*1]，高橋千太郎[*1]，久保田善久[*1]

1. はじめに

超ウラン元素による内部被ばくにおいて重要な体内摂取経路の一つに吸入摂取がある。本研究の目的は，呼吸器に沈着した粒子状超ウラン元素により呼吸器ならびに身体各部が受ける線量を計算し，その影響を評価するために必要な代謝データ，特に，いわゆる気道内粒子代謝モデルの策定に必要な基礎データを得ることである。すでにこの種のモデルはICRP等により策定，勧告がなされているが，これらのモデルは単純な数学的モデルであり生理学的見地からは矛盾する点も多かった[1]。したがって，既存の肺モデルによる線量評価の精度を向上させ，さらに幼児等をも含めた一般公衆へ適用できる包括的肺モデルの策定が必要とされ，ICRPは近年，新しい呼吸器モデルを勧告した[2]。本研究では，比較生理学，毒性学的見地から気道内粒子挙動の機序を再検討し，放射性粒子に対する既存肺モデルを基礎に，より適用範囲の広い高精度代謝モデルの策定に必要なデータを提示していくことを目的に，粒子状物質の気道内沈着，沈着した粒子の肺での挙動および肺から全身への移行について検討を進めた。また，胎児へのプルトニウムの移行に関してはあまり報告がなく不明な点が多いことから，胎児移行に関する検討も行ってきた。ここでは，プルトニウムの体内動態，特に酸化プルトニウムやそのモデルとなる各種の難溶性放射性粒子の呼吸気道内での挙動や代謝，ならびにプルトニウムの胎児移行に関して，これまでに我々の研究室で得られたデータを中心に概説する。

[*1] 放射線医学総合研究所内部被ばく・防護研究部；千葉県千葉市稲毛区穴川 4-9-1（〒263-8555）
National Institute of Radiological Sciences；4-9-1, Anagawa, Inage-ku, Chiba 263-8555, Japan.

2. 粒子状物質の気道内沈着

吸入された粒子状物質の一部は，気管や気管支といった，いわゆる上部呼吸気道に沈着するが，沈着後，直ちに粘液繊毛運動によって上行性に除去され，沈着部位には長く滞留しないものと考えられてきた。しかし，ヒトでのデータなどで，上部気道にも粒子の長期的な滞留が認められたとの報告があり，また，この部位で吸入毒性物質による発ガンが認められることから，詳細な研究が必要と考えた。そこで$BaSO_4$粒子を難溶性粒子のモデルとして用い，上部気道における滞留，リンパ系への移行に関する検討を行った。

実験は，呼吸器の他の部位へ沈着した粒子の影響を避けるため，微細なカニューレーションを経気管的に行い，極微量の$^{133}BaSO_4$粒子を気管第1分岐部付近に投与し，経時的に滞留量を外部計測により求めた。また，定期的にラットを屠殺し，呼吸器および領域リンパ節への移行量を測定した。その結果，ラットにおいては，投与量の約1%が投与後1週間でもこの部位に滞留し，さらに従来の知見と大きく異なることには投与後24週を経ても投与量の0.5%程度が依然この部位に認められた[3]。さらに，著者らはこのような不溶性粒子の上部気道壁への長期的滞留が，ウサギ，犬，サルで認められること[4]，$^{133}BaSO_4$以外の不溶性粒子でも認められることなどを明らかにした[5,6]。本知見は，酸化プルトニウムなどの不溶性または難溶性粒子の上部気道における代謝・挙動と線量評価に関して重要な知見であり，ICRPの新しい呼吸器モデル[7]において，上部気道における放射性粒子の代謝モデルの基礎的知見として引用されている。

3. 放射性粒子のマクロファージによる溶解

^{59}Fe-コロイドおよび^{239}Pu-重合体コロイドの肺マクロファージによる可溶化，細胞外放出の時間依存性につ

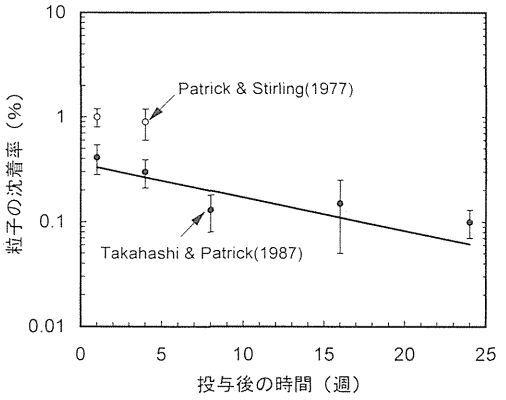

第1図　ラット気管における $^{133}BaSO_4$ の沈着

第1表　肺マクロファージのPuとFeの細胞外放出の違い

核種	水酸化コロイド投与後の時間（h）		
	24	72	168
^{239}Pu	0.6±0.4*(100)	1.2±0.3(210)	2.5±0.8(434)
^{59}Fe	7.8±5.3 (100)	5.4±2.1 (69)	3.9±2.8 (50)

*：投与量に対する割合

いて検討した。トレーサー粒子を気管内挿管法によりラットの肺深部に投与した後1，3，7日目に粒子を貪食した肺マクロファージを肺洗浄法により採取し，ハンクス平衡塩類溶液中で一定時間培養して細胞外へ放出される ^{239}Pu および ^{59}Fe の量を測定した。その結果，^{239}Pu では負荷後の時間経過に比例して細胞外放出量は増大したが，^{59}Fe ではほぼ一定の細胞外放出率が認められ，肺マクロファージによる粒子の細胞内溶解，細胞外放出の経時変化が粒子の種類により異なることを示唆する知見が得られた[8]。この知見は，肺深部における粒子の溶解に伴うクリアランスが摂取後の時間に依存せず一定と仮定しているICRP等の既存肺モデルと異なっており，今後の詳細な検討の必要がある。

このようなマクロファージによる粒子の溶解に大きな影響を与える要因の一つは粒子自身の溶解性である。溶解性の異なる2種類の水酸化鉄コロイドを使用してこの点を検討した。すなわち，^{59}Fe と ^{239}Pu で二重に標識した水酸化鉄コロイドをラットの肺深部に投与，24時間後に肺洗浄により回収した水酸化鉄コロイドを貪食した肺マクロファージを培養系に移して ^{59}Fe および ^{239}Pu の細胞外放出率について検討した。限外濾過により10

第2表　焼結温度による酸化プルトニウムの代謝の違い

焼結温度（℃）	吸入後の時間	臓器分布		排泄	
		肺	肝	糞	尿
1150	1カ月	79*	0.04	20	3.2
	12カ月	17	0.12	52	31
400	1カ月	58	0.08	32	3.8
	12カ月	8.9	0.17	68	23

*：初期沈着量に対する割合

kDa以下の粒子を約50%含む比較的溶解性の高い水酸化鉄コロイド（コロイド1）と大部分が10 kDa以上の粒子からなる難溶性の水酸化鉄コロイド（コロイド2）の細胞外放出率を比較すると，約5倍の違いが認められた[9]。^{239}Pu で標識された水酸化鉄コロイドの物理化学的性状が肺における溶解性，肺からの移行にどのような影響を与えるかは明らかではないが，微粒子状の酸化プルトニウムはミクロン程度の酸化プルトニウムより速く，肺から血液中へ移行することが知られており，コロイド1のマクロファージによる溶解が速いことはこれを支持するものである。一方，プルトニウム等の放射性物質の吸入毒性以外にも，吸入摂取された粒子の呼吸器における溶解は種々の面で重要である。その一例として環境中の有害微粒子の吸入毒性をあげることができる。著者らは，そのような観点から，石炭フライアッシュ，酸化ニッケル等のマクロファージにおける溶解や呼吸器における溶解性に関する研究を行い，実質的に酸化プルトニウムと同一の機序による呼吸器内挙動・代謝を認めた[10~12]。

4. 吸入Puの肺からの移行

粒子状プルトニウムが吸入により肺へ沈着した後の動態はプルトニウムの化学形，粒子径，肺への初期沈着量等，種々の要因により変化することはすでに多くの報告がある。一般に溶解性の高いプルトニウムは肺から他の臓器への移行，体外への排泄が高い。放医研では酸化プルトニウムのラットへの吸入実験を中心に行っているが，焼結温度により生成される酸化プルトニウムの物理化学的性状は異なると考えられる。事実，ビーグル犬を使用した米国の報告では低温で焼結させた酸化プルトニウムの方が肺から他臓器への移行が速い[13]。しかし，マウスでは焼結温度が肺沈着後の他臓器への移行に影響しないことが報告されている[14]。動物種差によるのかもしれない。では，ラットの場合はどうであるか。そこで著

者らは，高温（1150℃）と低温（400℃）で焼結させた2種類の酸化プルトニウムをラットに吸入後，肺に沈着したプルトニウム量を体外計測により求めた。1カ月後，高温および低温焼結酸化プルトニウムを吸入させたラットの肺残留率はそれぞれ初期沈着量の79および58%で，低温焼結の方が肺から他臓器への移行が速いという結果を得た。1年後の肺残留率も，高温および低温焼結酸化プルトニウムでそれぞれ17，9%で，低温焼結の方が高温焼結の約半分まで減少した。肝のプルトニウムは吸入1カ月および1年後で0.04～0.17%で量としては少ないが，低温焼結の方が高い傾向を示した。一方，体外へのプルトニウムの排泄率は肺からの移行が速い低温焼結酸化プルトニウム吸入ラットの方が高い。吸入後1カ月間に糞および尿へ35%が排泄され，高温焼結酸化プルトニウム吸入ラットの約1.5倍であった。実験はいまだ継続中で確定的なことは言えないが，ラットでは焼結温度の違いによりプルトニウムの体内動態にやや違いが見られるものの，ビーグル犬ほど顕著な違いはなく，また，焼結温度による差がほとんど見られないマウスとも異なっているようである。放医研では水酸化プルトニウムを焼結させて酸化プルトニウムに変換しているが，高温焼結と比較して低温焼結ではすべて酸化プルトニウムに変換されていないかあるいは変換された酸化プルトニウムの溶解性に違いがあるためではないかと思われる。また，このような粒子側の要因に加えて，動物種差が関与している可能性もあり，詳細は今後の検討課題として残されているが，プルトニウムの体内での代謝の機序解明の鍵が隠されているかもしれない。

5. Puの胎児移行

母体側要因の影響を受けることなく解析するため，ラット全胚培養系を用いてプルトニウムの胚および胎児への移行量，移行経路，移行機序を検討した。はじめに全胚培養系における培養胚の生存性を確認するために，^{3}H-チミジンの妊娠12.5日齢のラット器官形成期胚への移行，蓄積について検討した。その結果，従来のような100%ラット血清を使用しなくても，牛胎児血清をイーグルMEMで30～70%に希釈した比較的単純な培養液で旋回培養法により最長6時間，胎児の生存を維持できること，卵黄嚢による^{3}H-チミジンの選択的取り込みが行われること，卵黄腔液にも比較的多量の^{3}Hの蓄積が見られることが明らかになった[15]。

以上の培養系を使用してプルトニウムの胎児移行について検討した。まず，プルトニウムの胎盤通過の機序を推定するために *in vitro* 全胚培養系と妊娠12.5日齢のラット胚におけるプルトニウムの分布を比較した。*in vitro* 培養系では，胎児に対する卵黄嚢のプルトニウム存在比がイオン状のクエン酸プルトニウムでは18-27，粒子状の水酸化プルトニウムでは67-84で粒子状プルトニウムのほうが高く，また，投与後の時間に関係なくその値はほぼ一定であった。一方，*in vivo* では投与後5分および60分でそれぞれ15と62で，経過時間により存在比が増加した。生体内ではクエン酸プルトニウムとして投与されたプルトニウムが重合体を形成して水酸化プルトニウムのような粒子状プルトニウムに変化するためと考えられる。いずれにしても卵黄嚢中のプルトニウム量は *in vitro*，*in vivo* 共に胎児より多いことから卵黄嚢はプルトニウムの胎児移行においてバリアーの役目を果たしていることが示唆された[16]。

第3表 胎児・胎盤の平均線量

妊娠時期（日）	各組織の平均線量（cGy/日）			
	受胎産物	卵黄嚢	胎児	母体肝
10.5	0.77	6.02	0.02	16.4
11.5	0.75	6.86	0.03	16.3
12.5	0.80	7.95	0.03	15.9
13.5	0.88	7.22	0.06	12.0
14.5	1.35	12.4	0.11	11.9
15.5	1.43	15.1	0.12	9.74
16.5	1.44	20.4	0.12	8.47

プルトニウム投与後の母体と胎膜・胎児へのプルトニウムの分布が妊娠期間中にどのように変化するかを妊娠10.5日から16.5日のマウスで調べたところ，クエン酸プルトニウム投与24時間後の受胎産物中のプルトニウムは妊娠後期で高く，10.5日齢で投与量のわずか0.12%であったのが，16.5日齢では10倍の1.3%に増加した。妊娠期間全般にわたり受胎産物のプルトニウムの90%は卵黄嚢と脱落膜に存在し，また，妊娠前期から後期へ移行するにしたがって受胎産物中のプルトニウム濃度は増加するため妊娠後期の卵黄嚢の平均線量は母体の肝より高くなった[17]。

プルトニウムが胎児の初期造血器官である卵黄嚢に移行・沈着し，比較的高線量を付与することから，母体に投与されたプルトニウムの胎児造血器系への影響について検討した。その結果，妊娠末期の胎児肝臓における造血幹細胞数を指標とすると，プルトニウム投与群で有意な低下が認められること，ならびにマウスの系統によってその影響に差があることを見いだした[18]。本結果は，α線によるゲノムの不安定性誘発とも関連している可能

性があり，きわめて興味深い知見である。

6. おわりに

プルトニウムの生体内での挙動・代謝に関する報告は数多く，吸入に限らず，注射，経口，経皮等の摂取経路や硝酸塩，クエン酸塩，酸化物などの化学形の違いが生体内代謝に及ぼす影響に関しても報告されている。放医研では酸化プルトニウムの吸入を主として実施しているが，諸外国の研究機関が行った酸化プルトニウムの吸入実験では粒子径が1 μm前後であるのに対し，放医研では0.4 μm前後と半分以下の粒子径を使用している。肺に沈着したプルトニウムの肺からの移行に粒子径は関与しないとの報告もあるが，放医研のデータとすでに報告されているデータとの比較は粒子径の差違を念頭に置くべきである。放医研では酸化プルトニウムを初期肺沈着量200～2000 Bqの範囲でラットに吸入させているが，初期沈着量により肺に沈着後の代謝が変化することが報告されており，200 Bqより低いレベルでの代謝データを集積する必要がある。また，肺から全身への移行の機序を知る上で肺を構成する細胞内の微細分布，マクロファージのみならず，上皮細胞におけるプルトニウムの溶解，放出についてのデータを集積する必要があり，今後の検討課題として残されている。

参考文献

1) ICRP Publication 30 (1979).
2) ICRP Publication 72 (1996).
3) S. TAKAHASHI and G. PATRICK ; Long-term retention of ^{133}Ba in the rat trachea following local administration as barium sulfate particles, *Radiat. Res.*, **110**, 321-328 (1987).
4) S. TAKAHASHI, Y. KUBOTA, H. SATO and O. MATSUOKA ; Retention of ^{133}Ba in the trachea of rabbits, dogs, and monkeys following local administration as ^{133}Ba SO_4 particles, *Inhalation Toxicol.*, **5**, 265-573 (1993).
5) Y. KUBOTA, S. TAKAHASHI, H. SATO, Y. YAMADA and O. MATSUOKA ; Pulmonary deposition and clearance of inhaled or instilled ^{198}Au-colloid in the rat after the induction of pulmonary delayed type hypersensitivity reactions, *Hoken Butsuri*, **23**, 295-302 (1988).
6) S. TAKAHASHI, K. MORIGUCHI, Y. KUBOTA, H. SATO and O. MATSUOKA ; The deposition pattern of insoluble particles with different sizes in the rat trachea, *Jpn. J. Radiat. Protec.*, **24**, 19-24 (1989).
7) ICRP Publication 67 (1994).
8) S. TAKAHASHI and H. SATO ; A new method to estimate the solubility of radioactive particles in the respiratory tract : Comparison of solubility between ^{59}Fe- and ^{239}Pu-hydroxide colloid particles, *Hoken Butsuri*, **26**, 351-353 (1991).
9) H. SATO, R.A. BULMAN, S. TAKAHASHI and Y. KUBOTA ; Effects of macromolecular chelating agents on the release of ^{239}Pu and ^{59}Fe from rat alveolar macrophages after phagocytic uptake of ^{239}Pu-^{59}Fe-iron hydroxide colloid, *Health Phys.*, **66**, 545-549 (1994).
10) M. YAMADA, S. TAKAHASHI, H. SATO, T. KONDO, T. KIKUCHI, K. FURUYA and I. TANAKA ; Solubility of nickel oxide particles in various solutions and rat alveolar macrophages, *Biol. Trace Element Res.*, **36**, 89-98 (1993).
11) T. KONDO, S. TAKAHASHI, H. SATO, M. YAMADA, T. KIKUCHI and K. FURUYA ; Cytotoxicity of size-density fractionated coal fly ash in rat alveolar macrophages cultured *in vitro*, Toxicol. *In Vitro*, **7**, 61-67 (1993).
12) S. TAKAHASHI, F. ESAKA, H. SATO, T. KIKUCHI and K. FURUYA ; Concentration of metal elements in mouse lung after intratracheal administration of coal fly ash, *Inhalation Toxicol.*, **6**, 67-77 (1994).
13) J.A. MEWHINNEY, B.A. MUGGENBURG, R.O. McCLELLAN and J.J. MIGLIO ; The effect of varying physical and chemical characteristics of inhaled plutonium aerosols of metabolism and excretion, *In* "Diagnosis and Treatment of Incorporated Radionuclides," IAEA-SR-6/29, pp. 87-97 (1976).
14) A. MORGAN, A. BLACK, D. KNIGHT and S.R. MOORES ; The effect of firing temperature on the lung retention and translocation of Pu following the inhalation of $^{238}PuO_2$ and $^{239}PuO_2$ by CBA/H mice, *Health Phys.*, **54**, 301-310 (1988).
15) S. TAKAHASHI ; Distribution of ^{3}H in rat conceptus culture *in vitro* following brief administration of [^{3}H] thymidine, *Radiat. Res.*, **128**, 59-63 (1991).
16) S. TAKAHASHI, H. SATO, Y. KUBOTA and J. INABA ; Transfer of plutonium to rat embryos *in vivo* and *in vitro*, *J. Radiat. Res.*, **33**, 301-308 (1992).
17) Y. KUBOTA, H. SATO, C. KOSHIMOTO and S. TAKAHASHI ; Transfer of ^{239}Pu to mouse feto-placental tissues, *J. Radiat. Res.*, **34**, 157-163 (1993).
18) Y. KUBOTA, S. TAKAHASHI and H. SATO ; Effect of a maternal injection of ^{239}Pu on the number of CFU-S in the foetal liver of the C3H and BDCF1 mouse, *Int. J. Radiat. Biol.*, **72**, 71-78 (1997).

保健物理，33(3)，302～307（1998）

≪特集：放医研におけるプルトニウムの生物影響評価研究≫

5. 生物学的安全性評価研究における プルトニウムの線量評価

石榑信人*1，仲野高志*1，榎本宏子*1

1. 緒　　言

プルトニウム（Pu）の生物学的安全性評価研究プロジェクトの中で，線量評価研究としてまず求められたのは，動物実験で線量効果関係を求める際の一方の軸としてのPu投与動物の線量を評価することであった。この目的のために，動物用のPu体外計測装置が試作され，Puを吸入投与された動物の初期沈着放射能および肺残留率の測定が実施された[1~5]。

また，Puの体内分布を観察し，線量評価の基礎データを得る方法として，固体飛跡検出器CR-39を撮像媒体とするα線オートラジオグラフィが開発された[6~9]。

Puは体内で偏った分布を示し，放出されるα粒子も線源近傍の微小体積の中へ大きいエネルギーを与えるので，マクロな組織平均線量は，生物影響の原因の量として必ずしも適切ではないと考えられている。これまでに，Puの線量を細胞レベルで評価する試みの一つとして，肺に沈着したPu粒子の周りの細胞のα粒子によるヒット数分布等が理論的に検討された[10,11]。

また，細胞レベルの線量評価に関する別の試みとして，α放射体を投与した実験動物の細胞等に生じた細胞遺伝学的変異等の評価に基づくいわゆるバイオドシメトリの開発のための基礎的検討も開始された[12]。

放射線防護の実務に関連する線量評価研究としては，ICRPの新しい呼吸気道モデルおよび新しい体内動態モデルを取り込んだPuの内部被ばく線量計算コードが作成され，年齢，体格等の人体特性パラメータやエアロゾル性状パラメータによる線量の変動特性が検討された[13~15]。また，肺モニタ等の校正に用いる数学ファントムの高度化の検討も進められている[16~18]。

以上をまとめると，当研究プロジェクトにおけるPuの線量評価研究は，（イ）動物実験の基盤としての線量評価，（ロ）リスクの推定精度の向上のための細胞レベルの線量評価，および（ハ）放射線防護の実務に関連した線量評価，の3種類に分類される。

拙稿においては，本特集の主題を重視し，紙幅の制約も考慮しながら，以上の中から，Pu吸入動物における線量評価および肺深部に沈着した粒子状Puによる細胞レベルの線量評価を取り上げ，その概略を紹介する。

2. Puの動物体外計測法と線量評価

2.1 小型動物用体外計測装置

実験動物の体内のPuを，生存状態で体外より測定する技術は，マクロなレベルではあるが，1匹の個体を連続的に追跡できる長所があり，代謝研究，生物影響研究等，多くの研究課題で共通に使われる基盤となる技術である。これには，放出率が低い上に動物自身による自己吸収を受けやすい低エネルギーの微弱なX線を検出する必要があり，低バックグラウンドでかつ計数効率の高い計測システムの開発が必要となる。

本研究で試作された小型動物用体外計測装置の概略図を**Fig. 1**に示す。

しゃへい箱の外寸は，幅1290 mm，高さ590 mm，奥行き740 mmである。主しゃへい材として厚さ50 mmの鉛が用いられ，その内壁は，バックグラウンドの低エネルギー成分を減衰させるため銅板とアクリル板とが各5 mmずつ内張りされている。

検出器は直径50 mm，厚さ1 mmの薄型NaI(Tl)シンチレーションカウンタである。これが左右上下各1本ずつ最高で4本セットすることができ，動物体外へ透過してくる低エネルギーX線（LX線）を検出する。

この装置で観察されるLX線ピークの見かけのエネル

*1 放射線医学総合研究所内部被ばく・防護研究部；千葉県千葉市稲毛区穴川 4-9-1（〒263-8555）
National Institute of Radiological Sciences；4-9-1, Anagawa, Inage-ku, Chiba 263-8555, Japan.

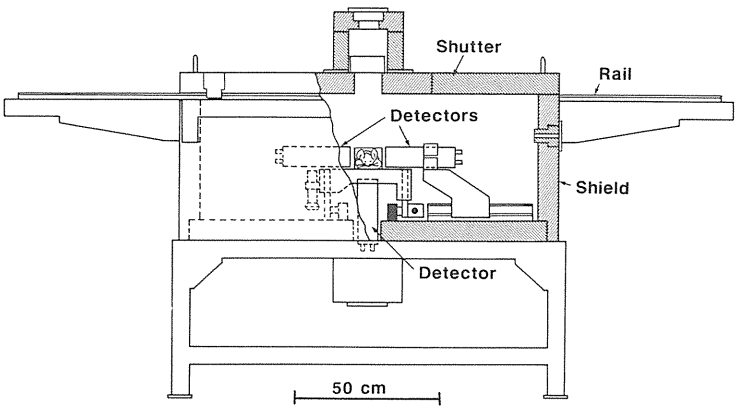

Fig. 1 Schematic diagram of the whole-body counter for rats.

ギー分解能は40%であり，Puを吸入していないラットのLX線計数領域のバックグラウンド計数率は0.26 cpsを示した。

ラットの計測時間は1000秒を基本とし，麻酔，保定，運搬等も含め1匹当たり約25分かかっている。

2.2 計数効率

LX線の計数効率は動物のサイズに敏感なため，体外計測装置の校正係数は個体ごとに異なる値をとる。本研究では，種々の体重のラットを選び，摘出肺の放射能と体外計測値とから計数効率を測定し，体重対計数効率の相関曲線を求めておき，体内量を測定したいラットの体重を体外計測時に測定し，その相関曲線上で計数効率の値を読み取ることによって，その動物個体に対する計数効率を求めるという方法がとられた。

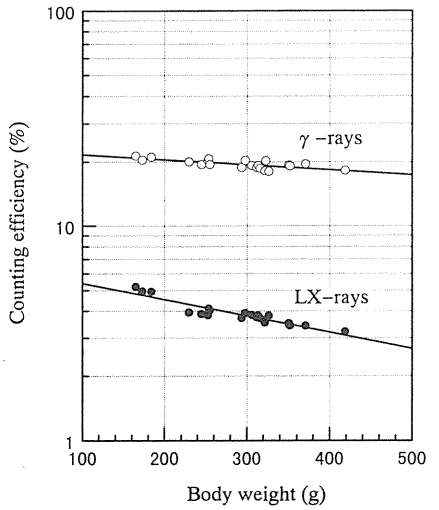

Fig. 2 Counting efficiency of LX rays and γ-rays for the rats of different weights.

LX線およびγ線の計数効率を**Fig. 2**に示す。γ線と比べLX線の計数効率は体重の増加に伴い著しく減少することが示されている。

計数効率の検討とバックグラウンドの評価結果から，本装置の最小検出放射能として，計数誤差10%で91 Bq，33%では23 Bqが得られた。

2.3 体外計測法によるPuの初期沈着放射能の測定

Puを吸入投与された動物の初期沈着放射能を求めることは線量評価に不可欠である。本研究では，吸入投与1週間後にすべてのラットを体外計測し，次節で述べる残留率曲線を用いて0日，つまり吸入当日へ外挿し，初期沈着放射能が決定されている。なお，ここで初期沈着放射能とは長期残留成分のみの沈着量をさしている。主に気道の上部に沈着し，沈着直後から短期間にクリアランスされる成分は線量にほとんど寄与しないので本研究の対象とはされていない。

Pu発がんの大規模な研究を行ってきた米国のPacific Northwest Laboratory (PNL)では，直接Puを測定するのではなく，^{169}Ybを同時に吸入投与し，^{169}Ybのγ線測定の結果から間接的にPuの初期沈着放射能を決定している[19]。

このように，トレーサーを使うことなく，動物体内のPuが直接測定される点が本プロジェクトの特徴である。

2.4 体外計測法によるPuの肺残留率の測定

投与されたPuの肺残留率の経時変化の測定は線量評価に不可欠である。

PNL等では，Puを投与した動物を数匹ずつ経時的に解剖し，肺のPuを測定して残留率を求めている。この方法では，同量のPuを投与した動物を数10匹用意する必要があり，また，別個体の残留率を同一の時間軸に並べ

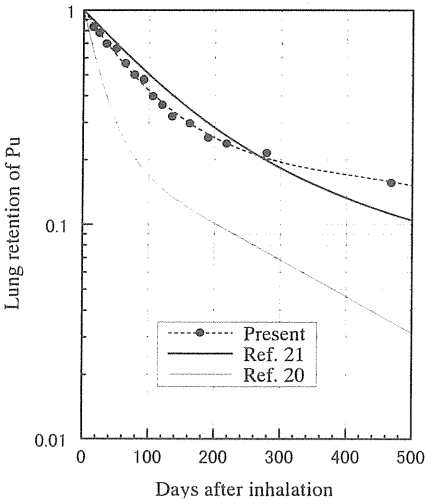

Fig. 3 Lung retention of Pu in rats following inhalation of aerosols of PuO_2.

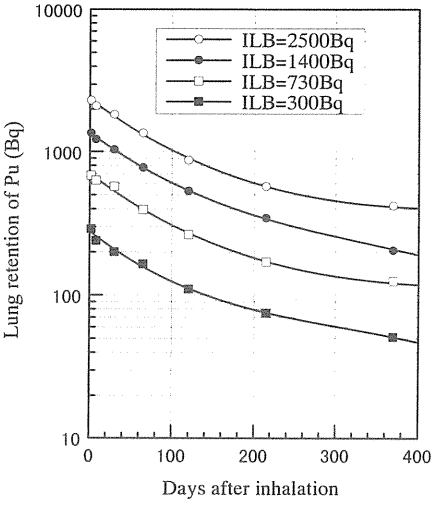

Fig. 4 Lung retention of Pu in rats for different initial lung burdens (ILB) of PuO_2.

るため，不確実さも問題になろう。

本研究では，同一個体の肺内 Pu を体外計測法により長期間追跡することによって Pu の肺残留率が求められた。この方法により得られた PuO_2 の残留率曲線を **Fig. 3** に示す。なお，この図は5匹のラットから得られた値の平均を表わしている。

吸入後 t 日目における肺残留率 $Y(t)$ は，次式に示す2成分の指数関数で近似された。

$$Y(t)=0.77\exp(-0.0131\,t)+0.23\exp(-0.000873\,t)$$

つまり，初期沈着放射能の77%が半減期53日で，残りの23%は半減期794日でクリアランスされることを示している。同じ図に PNL のデータも示した。両者の比較より放医研の方が残留率が高いことが分かる。つまり，初期沈着放射能が同じとき，放医研のラットの方が線量が高くなる。

最近，PNL により，残留率の沈着量依存性が報告され，その理由として α 粒子によるダメージがクリアランスを遅らせる可能性が示唆された[20,21]。本研究では，この効果の有無を明らかにするため，いろいろな初期沈着量における残留率が検討された。その結果を **Fig. 4** に示す。

同図が示すように，少なくともここで検討された範囲では，残留率の沈着量依存性が観察されず，したがって，線量を評価するに当たりすべての吸入投与レベルの動物に同一の残留率曲線を適用してもよいことが確かめられたと考えている。

その他残留特性を修飾する要因の詳しい議論は別の稿にゆずるが，放医研で投与されてきた PuO_2 の粒子径は諸外国のものよりかなり小さく，肺内の沈着分布も異なっている可能性もあり，このことが高い残留率の原因の一つとも考えられる。

2.5 アメリシウム（Am）と Pu との随伴挙動

Pu には，再処理等化学分離直後の新鮮なものを除き ^{241}Pu から生成する ^{241}Am が含まれている。ICRP の

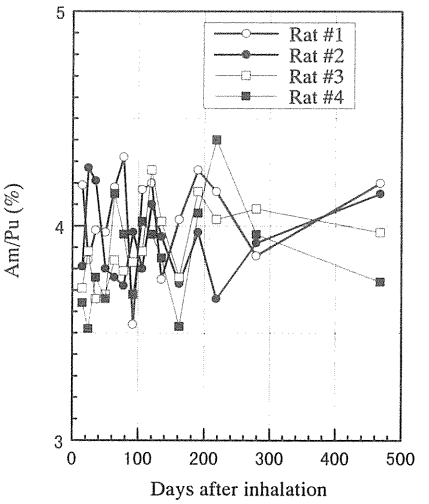

Fig. 5 Ratio of lung burdens of ^{241}Am and Pu in rats following inhalation of aerosols of PuO_2. containing ^{241}Am with 4% of the proportion of Pu.

仮定では，PuO_2 はタイプS，Am はすべての化合物がタイプMに指定されている。それでは，PuO_2 の中で生成した ^{241}Am はどのような挙動を示すのであろうか。本研究では，^{241}Am を4%含む PuO_2 をラットに吸入し，^{241}Am と Pu ともに体外計測法で長期間追跡してこれら両元素の肺における挙動が調べられた。

Am/Pu 比の追跡結果を **Fig. 5** に示す。同図は，Am/Pu 比が長期間変わらないことを示している。つまり，PuO_2 中に生成した Am は，ICRP の言うようにタイプMではなく，Pu と随伴してタイプSとして挙動することが明らかとされた。この結果は，人体のように LX 線の吸収を受けやすく Pu の肺計測が困難な場合でも，測定の容易な ^{241}Am をトレーサーとすることにより，Pu の肺負荷量を推定できる可能性を示している。

3. Pu 粒子による肺胞部の微視的線量評価

3.1 はじめに

もしも，α 粒子にヒットされなおかつ生き残った細胞が，がん化の起源となるのであれば，α 粒子によるヒット数の分布は障害の発生確率の指標として重要な意味を持つ。

肺胞部の構造を物質と α 粒子との相互作用という観点から区分すると，空気で満たされた肺胞腔とそれを構築している肺胞壁等軟組織の2成分系と考えることができる。ヒット数の分布を計算しようとする場合，このような構造をどこまで精密にモデル化できるかが計算結果の信頼性を左右する。本研究では，可能な限り現実に近いモデルを作成すべく，最終的には，実験動物の肺の組織切片標本の2値化画像と画像情報処理技術とによって肺深部のバーチャルな立体構造を構築し，これを用いてヒット数の分布等線量評価に関わる種々統計量を求めようとするものである。

3.2 飛程分布

ラットの肺の組織切片の2値化画像と，その画像上で発生させた α 粒子の飛跡のシミュレーションを **Fig. 6** に示す。この図で白い部分が空洞部，灰色の部分が組織部，直線が α 粒子の飛跡を表わしている。

肺に沈着した ^{239}Pu から放出される α 粒子の飛程分布が上記シミュレーションにより計算された。その結果を **Fig. 7** に示す。この図が示すように肺深部での実際の飛程は，均質無構造の肺モデルに比べ大きく広がっており，遠くの組織にもヒットし得る。

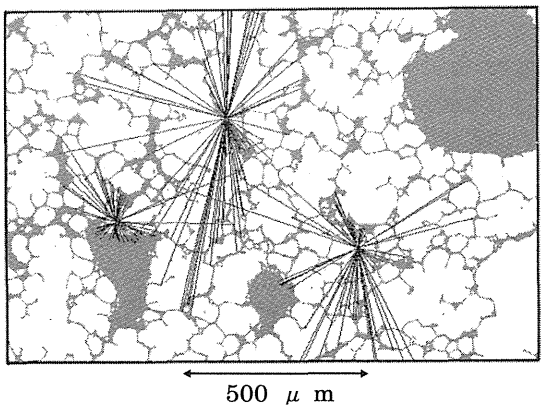

Fig. 6 Digitized image of a histological section of rat parenchymal lung superimposed with alpha-particle tracks generated in a computer.

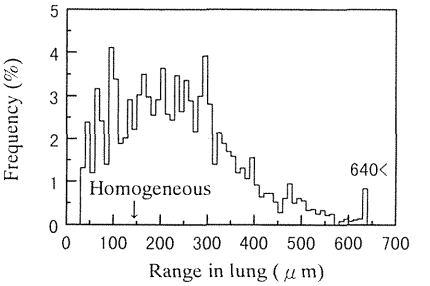

Fig. 7 Distribution of simulated track lengths of alpha-particles in a parenchymal lung.

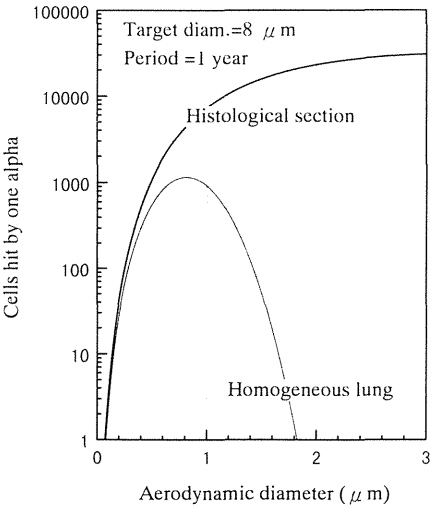

Fig. 8 Calculated number of cells traversed by one alpha-particle emitted from particulate PuO_2 with different diameters assuming that the target diameter is 8 micrometer and exposure period is one year.

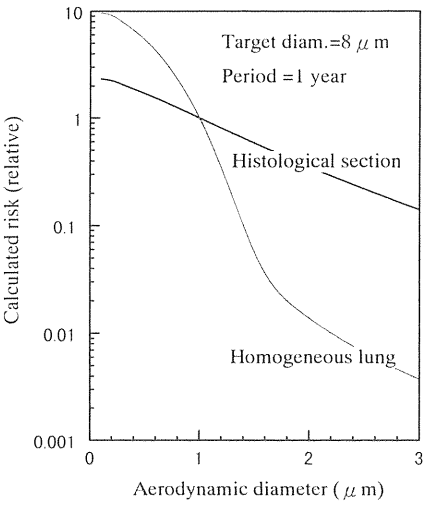

Fig. 9 Calculated risk in lungs burdened with the same total activity of particulate PuO_2 with different diameters assuming that the target diameter is 8 micrometer and exposure period is one year.

3.3 ヒット数分布

線源から，ある距離の標的へのα粒子のヒットは，ポアッソン分布に従うので，前節で述べられた飛程分布の相対累積度数を用いることにより，ヒット数を確率変数とする細胞の個数分布を計算することができる。

1個の線源粒子の周りの細胞で1回だけヒットされるものの数の計算結果を **Fig. 8** に示す。これは，標的直径8μm，被ばく期間1年を仮定し計算されたものである。

この図が示すように，組織切片画像による計算と均質無構造の肺モデルとでは粒子径依存性が著しく異なり，従来からの均質無構造モデルの適用は計算が容易ではあるが，実際の被ばくを正しく反映していないと言える。

3.4 ヒット後生存細胞数のリスク

細胞はα粒子にヒットされると高い確率で死ぬ。ここで，ヒットされてもなお生き残る細胞が障害の発生に深く関わっており，その細胞個々の悪性化への可能性はヒットの回数に比例すると仮定する。すると，ヒットされた後の生存細胞でヒット数による重み付けをされたものの個数の合計（以下「リスク」と記す）は，障害の発生確率の指標の候補の一つと考えることができる。

一例として，1ヒット当たりの致死率を2/3と仮定した場合の「リスク」を **Fig. 9** に示す。なお，どの粒子径の場合も，肺に沈着している総放射能を一定としているので，線源粒子の個数は大きい粒子ほど少なくなっている。また，縦軸には粒子径1μmに規格化された相対値が示された。この図より，いずれのモデルにおいても，粒子径が大きいほど「リスク」が小さくなっており，粒子状Puによる障害の発生確率は粒子径にかなり依存する可能性が示唆された。

放医研で用いられている PuO_2 粒子はAMAD 0.3～0.5μmであり，ICRPのデフォルト値5μmと比べ，メディアンサイズで比較すると粒子1個当たりの放射能は，数千分の1と小さい。

ICRPは，確率的影響の発生確率の評価に当たり，当面，粒子のサイズを考慮しないとしている。今後，こうした計算の信頼性が高められ，また，異なる粒子径を用いた実験研究が行われるならば，Puの生物学的安全性に関し，いろいろと新しい知見が得られる可能性がある。

4. 結　び

放射性物質の生物学的安全性評価は，物質の量や濃度直接によってではなく，モデル等を介していったん線量に変換された上で評価されるという特徴がある。したがって，明示的な研究目的が安全性評価であるならば，毒性が未知のものは別として，Puのようにある程度分かっているものについては，生物学的研究においても，得られた結果が線量評価に生かされなければあまり意味がない。誤解を恐れずに言うならば，「Puの生物学的安全性評価の研究」は，広い意味で「Puの線量評価の研究」である。

代謝研究の場合，その成果が体内動態モデルに直結しており，また微視的な線量評価の基礎データともなることから，上記の事情は理解しやすい。

一方生物影響研究の場合，線量を修飾するいろいろな因子，たとえばRBE，第3章で紹介した粒子サイズの影響，等々は実験動物や培養細胞を用いた生物影響研究を待たずしては明らかにし得ないものであることから，生物影響研究もまた線量評価研究に緊密に繋がっていることは理解されるであろう。

以上のことから，今後進められるべき「Puの生物学的安全性評価の研究」においては，その成果が「線量評価」に反映されるくっきりとした道筋が今まで以上に強く意識されたものとなることが望まれる。

参 考 文 献

1) N. Ishigure, T. Nakano, H. Enomoto, S. Fukuda, H. Iida, Y. Oghiso, Y. Yamada and J. Inaba; Assessment of initial alveolar deposition on rats exposed to plutonium aerosols using a whole body counter, 保健物理, **27**, 135-142 (1992).

2) N. ISHIGURE, T. NAKANO and H. ENOMOTO ; Activity measurement of plutonium in solid samples by L X-ray counting with a phoswich detector, 保健物理, **28**, 195-201 (1993).
3) N. ISHIGURE, T. NAKANO, H. ENOMOTO, S. FUKUDA, H. IIDA, Y. OGHISO, H. SATO, S. TAKAHASHI, Y. YAMADA, A. KOIZUMI, Y. YAMADA, K. MIYAMOTO and J. INABA ; Lung retention of Pu following inhalation of PuO_2 particles in rats measured using periodic *in vivo* counting, *J. Radiat. Res.*, **35**, 16-25 (1994).
4) N. ISHIGURE, T. NAKANO, H. ENOMOTO and J. INABA ; Longer lung retention of PuO_2 particles in rats measured using periodic *in vivo* counting, *Radiat. Prot. Dosimetry*, **53**, 195-198 (1994).
5) N. ISHIGURE, T. NAKANO, H. ENOMOTO, H. SATO and J. INABA ; Does initial lung burden affect the alveolar lung clearance of inhaled $^{239}PuO_2$?, Proc. 1996 Int. Con. Radiat. Protection, Vol. 2, p. 470 (1996).
6) N. ISHIGURE ; Application of CR-39 plastic to rapid and quantitative macroautoradiography of α-emitters in a whole body section of an experimental animal, *RADIOISOTOPES*, **34**, 101-102 (1985).
7) N. ISHIGURE and O. MATSUOKA ; Property of TS-16N solid state nuclear track detectors as an imaging medium for macroautoradiography of α-emitters in biological specimens, *RADIOISOTOPES*, **37**, 63-68 (1988).
8) N. ISHIGURE and O. MATSUOKA ; Factors affecting the etching properties of CR-39 detectors for α-particles, *J. Nucl. Sci. Technol.*, **25**, 404-409 (1988).
9) 石榑信人；固体飛跡検出器のプルトニウム内部被曝研究への応用，放射線，**18**, 8-15 (1992).
10) 仲野高志；肺深部におけるα粒子の飛程分布，“NIRS-M-78：粒子状物質の吸入とその生物作用の発現機構，” p. 142 (1991).
11) 石榑信人；肺深部における細胞のヒット数分布と粒子性，“NIRS-M-78：粒子状物質の吸入とその生物作用の発現機構，” p. 150 (1991).
12) N. ISHIGURE, T. NAKANO and H. ENOMOTO ; A device for *in vitro* irradiation with α-particles using an α-emitting radioactive source, *J. Radiat. Res.*, **32**, 404-416 (1991).
13) 石榑信人，稲葉次郎；ICRP 新呼吸気道モデルに基づく ^{239}Pu の内部被曝線量評価における粒子性状依存性，保健物理，**30**, 227-237 (1995).
14) N. ISHIGURE and J. INABA ; Analytical solution of the compartment model for respiratory tract clearance used in the new ICRP lung model, *J. Nucl. Sci. Technol.*, **33**, 179-186 (1996).
15) 石榑信人，仲野高志，榎本宏子，稲葉次郎；^{239}Pu の吸入被ばくにおける線量の人体特性パラメータによる変動の試算，保健物理，**31**, 193-204 (1996).
16) 関口昌道，福田信男，飯沼　武；磁気共鳴映像法を用いた Pu 肺モニタ校正用個人ファントムの作成，保健物理，**20**, 389-392 (1985).
17) 関口昌道；低エネルギー光子肺計測における散乱線の影響のモンテカルロ法による解析，保健物理，**21**, 179-183 (1986).
18) 関口昌道，遠藤真広，飯沼　武，松岡　理；人体ファントムの X 線 CT 画像データを用いた Pu 肺計測のモンテカルロ・シミュレーション，保健物理，**21**, 185-189 (1986).
19) C.L. SANDERS, K.E. McDONALD, B.W. KILLAND, J. A. MAHAFFEY and W.C. CANNON ; Low-level inhaled-$^{239}PuO_2$ life-span studies in rats, “Life-span radiation effects studies in animals : What can they tell us?,” p. 429 (1986), US DOE, Virginia.
20) C.L. SANDERS, K.E. McDONALD and J.A. MAHAFFEY ; A lung tumor response to inhaled Pu and its implications for radiation protection, *Health Phys.*, **55**, 455-462 (1988).
21) C.L. SANDERS, K.E. McDONALD, K.E. LAUHALA and G.A. SANDERS ; Lifespan studies in rats exposed to $^{239}PuO_2$ aerosol, *Health Phys.*, **64**, 509-521 (1993).

保健物理，33(3)，308～313（1998）

≪特集：放医研におけるプルトニウムの生物影響評価研究≫

6。アルファ放射体内部被曝生物影響研究

——プルトニウム発がん実験を中心に——

小木曽洋一*1，山田裕　*1，飯田治三*1，福津久美子*1，福田　俊*1,*2

1. はじめに

プルトニウム等核燃料物質の内部被曝影響を動物実験により研究するためのプロジェクトがスタートして20年近い年月が経過した。この間，わが国で唯一の内部被曝実験棟の設計と竣工(1982年)，研究実施の中心母体としての内部被曝研究部の設立(1983年)，プルトニウム線源の入手・化学変換（1986年），および吸入曝露等動物実験の本格的開始（1990年）を経て現在に到るまで，我々はアルファ放射体内部被曝による発がん等生物効果研究をすすめてきた。本稿では，そのうちプルトニウムを吸入あるいは注射投与した生涯飼育動物における実験的発がん研究を中心にその概要と将来展望・計画について記述する。

2. 酸化プルトニウム・エアロゾル吸入曝露ラットにおける肺腫瘍

その存在形態・発生・被曝様式・体内挙動の特異性から重要な，酸化物プルトニウムの吸入被曝による発がん（肺がん）リスクを動物実験により実証するため，高温（1150°C）で焼結して発生させた不溶性の多分散 $^{239}PuO_2$ エアロゾル（AMAD：0.3～0.5 μm，GSD：1.8～2.1）をWistar系雌ラットに鼻部吸入曝露して生涯飼育し，その肺腫瘍発生率と，LX線(17 keV)の体外計測により得られた初期肺沈着量・滞留率関数から求めた肺吸収線量との線量効果関係を検討する実験を1990年から開始した。**第1表**に現在までに吸入曝露された動物の総数，生涯飼育数，死亡および検索数を初期肺沈着量・推定肺線量ごとに列記したが，吸入曝露実験群，無処置対照群とも約7割の動物がすでに病理学的検索を終えており，これにもとづく成績を以下紹介する。

(1) 生存率・肺腫瘍発生率・腫瘍組織型の線量効果

対照群では，原発肺腫瘍の発生率は約2.0%ときわめて低いが，平均肺吸収線量が1 Gy以下の吸入群では，良性肺腫瘍の増加（35%）はあるものの対照群と比較した平均生存日数に差はみられず，1 Gyを越えると有意に減少し，それに伴って悪性肺腫瘍が急増，6～7 Gyで最高（97%）となる線量効果関係（**第1図A**）が，また吸入曝露動物の死亡数と悪性肺腫瘍の発生・増加時期はほぼ一致し，良性腫瘍は吸入後700～800日の後期に増加する（**第1図B**）ことがそれぞれ明らかであり，肺線量1 Gy近辺における悪性肺腫瘍の早期発生と生存率の減少との相関が示唆された[1~3]。

また，肺腫瘍の大部分は上皮性の腺腫(adenoma)，腺癌(adenocarcinoma)，腺扁平上皮癌(adenosquamous carcinoma)，および扁平上皮癌(squamous cell carcinoma)であったが，これらの組織型による線量効果関係の違いも明らかにされた(**第2図**)。すなわち，良性腫瘍の大部分を占める腺腫は，肺線量1 Gy以上では減少するが，悪性癌のうち腺癌は2.9 Gy，腺扁平上皮癌は8.5 Gy，扁平上皮癌は5.4 Gyで，それぞれピークとなることが明らかであり，腫瘍性病変の程度も初期化生から腺腫性化生が1～1.5 Gy，腺癌化生が1.5～2.9 Gy，腺扁平上皮ないし扁平上皮化生が5.4～6.6 Gyでそれぞれ顕著となるように，線量に依存した異なる腫瘍病変出現と増減が示された[4]。

このような酸化プルトニウム吸入曝露ラット肺腫瘍発生率の線量効果関係は，これまでに米国で公表されている実験成績[5~7]と比べ，発がん線量域・発生腫瘍の組織型

*1 放射線医学総合研究所内部被ばく・防護研究部；千葉県千葉市稲毛区穴川 4-9-1（〒263-8555）
National Institute of Radiological Sciences；4-9-1, Anagawa, Inage-ku, Chiba 263-8555, Japan.
*2 放射線医学総合研究所宇宙環境生物医学および粒子線生物学グループ；千葉県千葉市稲毛区穴川 4-9-1（〒263-8555）
National Institute of Radiological Sciences；4-9-1, Anagawa, Inage-ku, Chiba 263-8555, Japan.

第1表　酸化プルトニウム吸入曝露ラット発がん実験規模

初期肺沈着量（Bq）	推定肺線量（Gy）	動物（ラット）数		
		吸入曝露	生涯飼育	死亡・検索
0	0	270	206	147
20-150	＜1.0	135	111	52
160-350	＜2.0	165	123	89
400-700	＜4.0	165	125	81
700-900	＜5.0	40	40	40
950-1000	＜6.0	35	31	31
1000-1300	＜7.0	35	31	31
1400-1800	＜9.0	35	30	30
2000-3000	10.0＜	30	10	10
小　計		910	707	511

（注）平成10年3月15日現在のもの。吸入曝露動物の一部は中途処分・死亡等により生涯飼育数に含められていない。

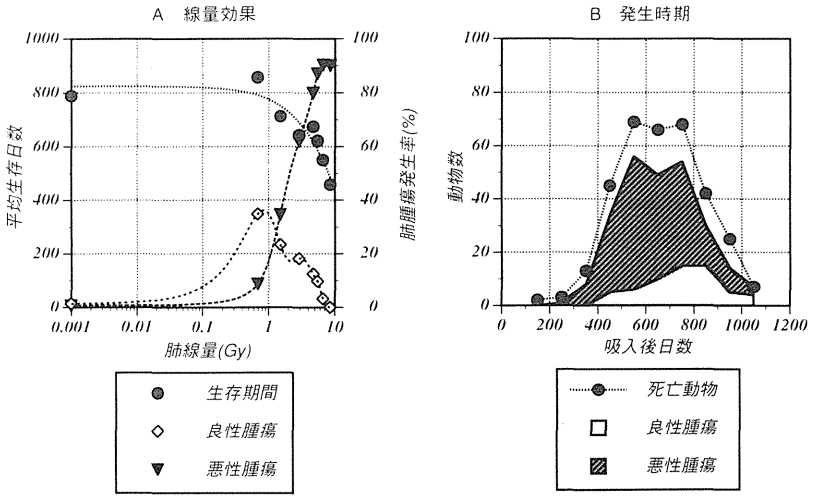

第1図　酸化プルトニウム吸入曝露ラットの生存率・肺腫瘍発生率

等の点でかなり異なっており，ラット系統差や性差はごく小さいことから，最も考えられる要因として発生エアロゾルの粒子径分布とそれにもとづく呼吸気道各部位への沈着率・標的気道上皮細胞の感受性と表現型の違いが強く示唆されるので，粒子径差による発がん効果の比較検討を行う計画である。

(2)　肺腫瘍発生過程と発がん機構

酸化プルトニウム吸入曝露ラットに誘発される肺腫瘍の潜伏期・発生時期・病変形成過程と発がん線量域を明らかにするため，初期沈着量150～500 Bq（推定肺線量1～4 Gy）の吸入群（計100匹）を対照群（計60匹）とともに1カ月から2年間までの期間飼育・観察し，一次標的である肺胞マクロファージの多核・小核形成率およびサイトカイン産生能，BrdU標識による気管支･肺胞上皮細胞のDNA合成能，化生・腫瘍性病変の出現およびがん関連遺伝子発現等を経時的に検索する実験を1997年から開始した。またこれと並行して，アルファ線発がんの特異性を明らかにするため，低線量率X線分割照射を施したラット（総線量0.5～10 Gy，計450匹）における生涯発がん効果を比較検索する実験も1996年からす

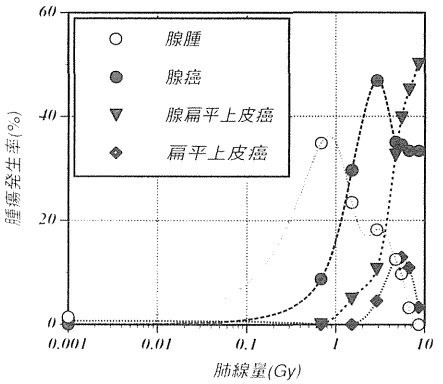

第2図　酸化プルトニウム吸入曝露ラットの肺腫瘍組織型による線量効果

第2表　酸化プルトニウム吸入曝露ラット肺腫瘍の核内 p53 タンパク発現

肺腫瘍組織型	検索数	核内 p53 発現例数		
		陰性	弱陽性	陽性
腺　腫	64	64	0	0
腺　癌	107	95	11	1
腺扁平上皮癌	68	41	25	2
扁平上皮癌	16	8	4	4
計	255	208	40	7

すめているところである。

次に，発がん機構におけるがん関連遺伝子の活性化・突然変異等の役割を明らかにするため，これまでにみとめられた肺腫瘍の組織標本について分子病理学的検索を試みた。そのうち腫瘍発生と悪性化に深く関わるとされるがん抑制遺伝子 p53 の突然変異により生じる核内 p53 タンパクについて腫瘍部位の免疫染色を行ったところ，**第2表**に示すように腺腫全てを含む約 81%の肺腫瘍が陰性で，癌腫のみ（とくに扁平上皮化生を伴う腫瘍）が弱陽性ないし陽性を示した[4]。

さらに，肺腫瘍部位の組織標本から DNA を抽出し，ラットの p53 遺伝子の Exon 5 から 8 をそれぞれプライマーとして PCR-SSCP 法で増幅し，電気泳動を行ったところ，DNA が抽出できた 82 例の肺腫瘍中，23 例（28%）から突然変異を示す異常バンドがとくに Exon 5 および 6 で検出されたが，腫瘍組織型と核内 p53 発現との関係では，いずれの Exon からも突然変異が検出できなかった野性型と比較して差はみられていないのが他の研究[8]と異なっている（**第3表**）。今後さらに検索例数を増やして突然変異率および突然変異部位の詳細な解析を行うとともに，ras 等他のがん関連遺伝子についても検討する計画であり，将来的には他の放射線源によって誘発される腫瘍との比較を行って，アルファ線特異的発がん機構を明らかにしてゆく予定である。

3.　可溶性プルトニウム注射投与マウスにおける発がん効果

血液等体液を介して体内移行したプルトニウムによる発がんの線量効果および特異性を動物実験で実証するため，硝酸塩から変換した可溶性の ^{239}Pu クエン酸塩を，マウスに注射投与して生涯飼育によりみとめられる腫瘍の発生率と骨線量にもとづく線量効果を検討する実験を 1990 年から開始した。**第4表**にその実験規模を示すが，このうち 1 匹あたり 10 Bq から 10,000 Bq までを投与した C3H 雌マウス 365 匹についての実験は全て終了しており，以下にその成績を中心に紹介する。

(1)　クエン酸プルトニウム注射投与 C3H 雌マウスの発がん効果

骨線量 3 Gy 以上から対照群と比較して平均生存日数の有意な減少と，早期の腫瘍死および非腫瘍死がみとめられた。発生腫瘍は，骨腫瘍(大部分が骨肉腫)，リンパ性腫瘍，および肺・肝・卵巣等軟組織にみられるその他の固形腫瘍であったが，骨髄性白血病等血液腫瘍は全くみとめられなかった[9,10]。これらの腫瘍のうち，骨腫瘍は対照群ではみとめられず，骨線量 1 Gy 以上から急増して 6〜8 Gy で最高 (96%) となり，10 Gy 以上では減少するのに対し，リンパ性腫瘍は対照群で約 20%の発生率を

第3表　酸化プルトニウム吸入曝露ラット肺腫瘍の p53 遺伝子突然変異

	突然変異 Exon 部位				腫瘍組織型				核内 p53	
	5	6	7	8	腺　腫	腺　癌	腺扁平上皮癌	扁平上皮癌	陰性	弱陽性陽性
突然変異 (23)	11	9	1	2	3	9	7	4	11	12
野生型 (59)	0	0	0	0	6	16	28	9	30	29

第4表　クエン酸プルトニウム注射投与マウス発がん実験規模

マウス系統		投与量（Bq）	動物数
C3H		0	100
		10	50
		100	50
		500	30
		1000	55
		5000	50
		10000	30
	C3H	0	60
		100	30
		500	30
		1000	30
	C57BL/6	0	60
		100	30
		500	30
		1000	30
	BC3F1	0	60
		100	30
		500	30
		1000	30
計			815

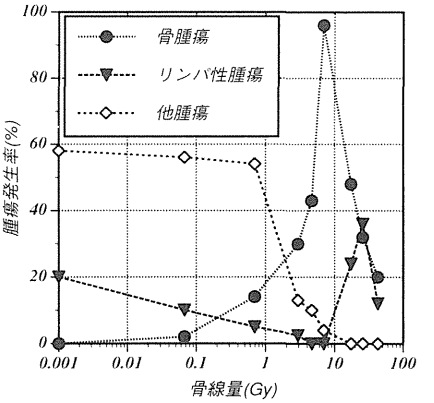

第3図　クエン酸プルトニウム注射投与C3Hマウスに発生する腫瘍の線量効果

示すものの，骨線量1～8 Gyで著減し，10 Gy以上から増加して最高（36%）に達する対照的な線量効果関係が明らかにされた(**第3図**)。また，その他の腫瘍は，骨線量1 Gy以上から著減し，10 Gy以上ではみとめられないことから，これら発生腫瘍間の競合が示唆された。

なお，プルトニウム投与マウスにみられたリンパ性腫瘍は，対照群に比較して早期に発生し，その組織形態も大部分がB細胞リンパ腫ないし白血病であり，対照群やγ線・X線・中性子線照射マウスでみられる胸腺（T細胞）リンパ腫[11~13]はほとんどみられない等の違いが明らかにされた（**第5表**）。

(2)　発がん効果の系統差および発がん機構

クエン酸プルトニウムを注射投与したC3H雌マウスでは，外部照射による場合と比べて発がん効果に大きな違いがみられたことから，被曝様式・線質・線量率等の違いに加えて，放射線感受性・発がんスペクトルを支配する遺伝的背景の異なるマウス系統差等の修飾要因が考えられる。このことを明らかにするため，C3H系以外に，胸腺リンパ腫好発系であるC57BL/6系およびC3HとC57BL/6の雑種であるBC3F1系の雌マウスをそれぞれ用いて，注射プルトニウムによる発生腫瘍スペクトルとその線量効果を比較する実験を1996年より開始し，現在対照群を含め各系統150匹ずつ計450匹規模での生涯飼育を継続しているところである。

また，注射プルトニウムによる骨肉腫やリンパ・造血系腫瘍を中心に各腫瘍の発生時期・形成過程およびがん関連遺伝子の活性化・突然変異等発がん機構を明らかにするため，クエン酸プルトニウムを5000 Bq注射投与したマウスを約2年間長期飼育して，経時的観察と検索を行う実験を1997年より新たに開始した。上記系統差に関する検討と併せて，将来的にはアルファ放射体内部被曝による発がんとその機構の特異性が明らかにされると

第5表　クエン酸プルトニウム注射投与マウスのリンパ性腫瘍組織型

	リンパ性腫瘍総数	リンパ性腫瘍組織型内訳			
		胸腺リンパ腫	B細胞リンパ腫	リンパ性白血病	組織球性リンパ腫
対照群	20	5	8	0	7
注射投与群	29	1	13	15	0

思われる。

4.　アルファ線誘発突然変異・形質転換

プルトニウム，アメリシウム等核燃料関連核種あるいはラドンのようなアルファ放射体は，低 LET 放射線と比較して，細胞死や遺伝子突然変異等標的的細胞レベルでの反応において，高い生物学的効果比（RBE）を示すといわれているが，これらの比較的初期の放射線損傷とその修復過程において生じてくる染色体・遺伝子の異常さらには細胞形質転換のような反応の蓄積が上述したような放射線発がん機構に密接に関連していると考えられるため，アルファ線特異的な細胞・分子損傷とその誘発機構を明らかにすることはきわめて重要である。

しかしながら，アルファ放射体内部被曝の人体障害例あるいは動物実験のような個体・集団レベルでの検索には限界があるため，均一な細胞集団を標的として線質・エネルギー・線量分布・線量率等を制御された条件で *in vitro* 照射して生じる突然変異・染色体異常・形質転換等の反応を比較検討する必要がある。このような観点からこれまでにさまざまな *in vitro* 照射実験が行われてきているが，とくに標的細胞・生物反応指標の選択や線源・線量・線量率の違いが大きく，未だ明確な知見に乏しいのが現状である。**第 4 図**は，米国ロスアラモス国立研究所で実施した共同研究成果の一部で，^{238}Pu 密封線源からの α 線をヒト皮膚線維芽細胞に照射して生じた *hprt* 遺伝子突然変異率を ^{60}Co 線源の γ 線照射と比較したところ，RBE は約 10 と推定された[14]。さらに得られた *hprt* 遺伝子突然変異株すべて（非照射自然誘発 23 株，γ 線誘発 101 株，α 線誘発 172 株）について，9 個の Exon ごとの PCR 増幅により詳細な変異スペクトル解析を行ったところ，全 Exon 欠失突然変異率および一部の Exon 欠失突然変異率とも，非照射自然誘発突然変異株に比べて放射線誘発突然変異株で有意に高かったが，γ 線あるいは α 線誘発突然変異株との間に有意の差はみられず（**第 6 表**），また全欠失のサイズ分布を比較すると，いずれも数 10 k 塩基対からメガ塩基対までさまざまなサイズの欠失が生じており，統計的有意差はみられなかった。従って，ヒト線維芽細胞におけるアルファ線誘発 *hprt* 遺伝子突然変異率の RBE は高いが，全欠失あるいは部分欠失とそのサイズ分布において線質差はみられないという結果が得られた[15]。

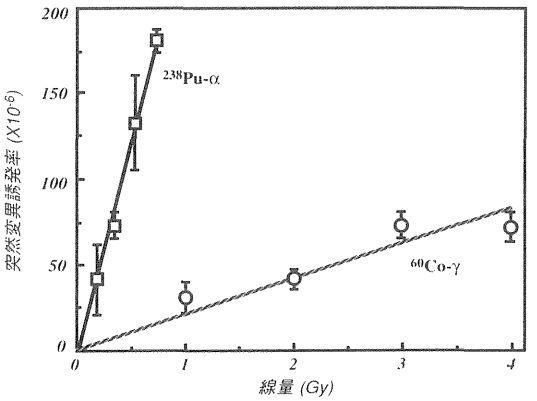

第 4 図　ヒト皮膚線維芽細胞の *hprt* 遺伝子突然変異の線量効果

我々はさらに，吸入性プルトニウムあるいはラドン等による肺がんの発生機構におけるアルファ線誘発突然変異と形質転換について明らかにし，またこれらを指標とする生物学的線量評価（バイオドシメトリー）の確立を目的として，実験動物（主にラット）の気道上皮細胞を標的とするアルファ線 *in vitro* 照射とそれによる生存率・小核形成・染色体異常・遺伝子突然変異等を検討する実験を 1996 年より開始した。現在そのために必要な，^{238}Pu 密封線源および照射装置の作製と，正常ラットより分離・精製した気管・気管支上皮細胞あるいはII型肺胞上皮細胞の初代培養系の確立をすすめながら，ヒトを含めた気道上皮細胞の樹立株や SV40 による不死化細胞株を用いた放射線感受性の比較検討を行っているところである。将来的には，これら気道上皮細胞レベルでの放射線感受性の比較や *hprt*, *ras*, *p53* 等の遺伝子突然変異および形質転換の分子機構が明らかにされることになると思われる。

第 6 表　ヒト皮膚線維芽細胞 *hprt* 遺伝子突然変異スペクトル比較

放射線照射	突然変異株総数	突然変異スペクトル数（%）		
		正　常	全欠失	部分欠失
非照射	23	21（91）	1（4）	1（4）
γ 線	101	55（54）	26（26）	20（20）
α 線	172	93（54）	62（36）	17（10）

5. おわりに

プルトニウムの内部被曝による発がんの動物実験を中心に，ラドンも含めたアルファ放射体による突然変異等に関する細胞・分子生物学的実験まで，現在我々の研究室員が取り組んでいる生物影響研究を紹介した。それぞれの課題ごとにも記したが，将来展望として吸入プルトニウムの発がん研究は，粒子径，化学形あるいはウランとの混合酸化物（MOX）の成分比による比較検討へと，さらには新たな対象として線量率・半減期・気道内分布の異なるラドン娘核種エアロゾル吸入曝露による発がん研究へと発展させてゆくことになるであろう。また，体内移行したプルトニウムその他のアルファ放射体の発がん効果の比較，細胞・分子レベルでの放射線感受性・突然変異の比較等を通じて，アルファ放射体内部被曝生物影響の特異性とリスクをより明らかにしてゆきたい。

稿を終えるにあたり，とくにプルトニウムエアロゾル発生・吸入曝露や体外計測等実験技術面での当研究部スタッフならびに動物飼育や放射線管理等技術支援部門スタッフの多大な協力に深謝するとともに，このように貴重な紹介の場を提供していただいた日本保健物理学会誌編集委員会および事務局の方々に謝辞を表したい。

参考文献

1) Y. Oghiso, Y. Yamada, N. Ishigure, S. Fukuda, H. Iida, Y. Yamada, H. Sato, A. Koizumi and J. Inaba ; High incidence of malignant lung carcinomas in rats after inhalation of $^{239}PuO_2$ aerosol, *J. Radiat. Res.*, **35**, 222-235 (1994).
2) 小木曽洋一；放射性粒子吸入による生体影響．プルトニウム微粒子の発癌性，エアロゾル研究，**9**, 221-226 (1994).
3) 小木曽洋一：プルトニウムの生物影響．動物実験とそのリスク，日本原子力学会誌，**36**, 1006-1009 (1994).
4) Y. Oghiso, Y. Yamada, H. Iida and J. Inaba ; Differential dose responses of pulmonary tumor types in the rat after inhalation of plutonium dioxide aerosols, *J. Radiat. Res.*, **39**, 61-72 (1998).
5) C.L. Sanders, K.E. Lauhala and K.E. McDonald ; Lifespan studies in rats exposed to $^{239}PuO_2$ aerosol. III. Survival and lung tumors, *Int. J. Radiat. Biol.*, **64**, 417-430 (1993).
6) D.L. Lundgren, P.J. Haley, F.F. Hahn, J.H. Diel, W.C. Griffith and B.R. Scott ; Pulmonary carcinogenicity of repeated inhalation exposure of rats to aerosols of $^{239}PuO_2$, *Radiat. Res.*, **142**, 39-53 (1995).
7) C.L. Sanders and D.L. Lundgren ; Pulmonary carcinogenesis in the F344 and Wistar rat after inhalation of plutonium dioxide, *Radiat. Res.*, **144**, 206-214 (1995).
8) G. Kelly, B.L. Stegelmeier and F.F. Hahn ; p53 alterations in plutonium-induced F344 rat lung tumors, *Radiat. Res.*, **142**, 263-269 (1995).
9) Y. Oghiso, Y. Yamada and H. Iida ; Differential induction of bone and hematopoietic tumors in C3H mice after the induction of ^{239}Pu citrate, *J. Radiat. Res.*, **35**, 236-247 (1994).
10) Y. Oghiso, Y. Yamada and H. Iida ; High frequency of leukemic lymphomas with osteosarcomas but not myeloid leukemias in C3H mice after ^{239}Pu citrate injection, *J. Radiat. Res.*, **38**, 77-86 (1997).
11) S. Sasaki and T. Kasuga ; Life-shortening and carcinogenesis in mice irradiated neonatally with X rays, *Radiat. Res.*, **88**, 313-325 (1981).
12) M. Seki, K. Yoshida, M. Nishimura and K. Nemoto ; Radiation-induced myeloid leukemia in C3H/He mice and the effect of predonisolone acetate on leukemogenesis, *Radiat. Res.*, **127**, 146-149 (1991).
13) J.R. Maisin, A. Wambersie, G.B. Gerber, G. Mattelin, M. Lambiet-Collier, B. Decoster and J. Gueulette ; Life-shortening and disease incidence in C57Bl mice after single and fractionated γ and high-energy neutron exposure, *Radiat. Res.*, **113**, 300-317 (1988).
14) Y. Yamada, M.D. Park, R.T. Okinaka and D.J. Chen ; Molecular analysis and comparison of radiation-induced large deletions of the HPRT locus in primary human skin fibroblasts, *Radiat. Res.*, **145**, 481-490 (1996).
15) 山田　裕；アルファ線誘発突然変異の研究，放射線科学，**40**, 275-280 (1997).

保健物理，33(3)，314～320（1998）

≪特集：放医研におけるプルトニウムの生物影響評価研究≫

7。プルトニウム影響のリスク低減化に関する研究

福田　俊[*1,*2]，飯田治三[*1]

1. はじめに

プルトニウム（Pu）摂取による影響リスクの低減化に関する研究は，動物実験によるPuの体内挙動および影響研究を基礎にして，体内摂取されたPuを体外へ迅速かつ効果的に除去する方法の確立と同時に薬物としての安全性を検討し，さらにその除去効果によって得られる影響リスク低減の評価を行い，最後に得られた成果を本研究の目的である緊急医療処置において人へ適用できるようにすることに意義がある。

この目的を達成するために，まず本プロジェクトに不可欠な国内で初めてのPuの生物影響研究を目的とした内部被ばく実験棟の設計・建設，実験遂行のための種々の技術的検討や支援体制の確立に多大な労力と時間が払われた。一方，本研究を開始するための情報が少ない状況にあったことから，多くの基礎研究を先行させる必要があった。これまで本研究は計画に沿って進めてきたが，実験内容にはプロジェクト運営上の区々によって前後した内容もある。ここでは，それらを整理しながら，すでに文献の項に記した論文や印刷物の内容は最小限にとどめ，主に保健物理学会で発表した内容を中心に述べる。

2. 実験技術および基礎研究

1) 動物実験のための技術的開発

Puの厳しい取扱い制限と研究者や技術支援者の安全性を確保するために，作業効率や操作性の悪いグローボックス（GB）内で動物の飼育や実験を行うことは日本独特の方法である。そのため，ラットの糞尿を効率的に分離採取するための代謝ケージ，洗浄や移動が容易な多頭数飼育ケージ，ビーグル犬用の代謝兼飼育ケージ，Pu吸入用GBと飼育用GB間のラットや犬の移動システムなどの種々の飼育および実験装置の開発，Puをラットに自然呼吸によって吸入させるために無麻酔で鼻部暴露できるように独自に開発した吸入用ホルダーの小穴からラットが自ら鼻部のみを出すための馴致などの実験手法，GB内でラットや犬へPu溶液を静脈注射するための訓練，多量の生物試料中のPu測定技術，などの多くの技術的な解決が必要であった。詳細な内容は省略。

2) 動物実験のための基礎研究

(1) 動物の骨代謝に関する研究

実験に使用するラットおよびビーグル犬の骨代謝の研究は，Puが骨親和性核種であるので骨内の挙動や影響を検討するために必要であったが，それだけではなく成長や加齢に伴う骨の形態や代謝の変化を比較することによって動物と人の年齢対応ができるので，実験開始時期（被曝年齢）の選択や得られた結果を人へ外挿して影響評価を行う上でも重要である。しかし，ラットやビーグル犬の骨代謝に関する基礎知見は乏しく，とりわけ生涯研究を目的とするための知見はほとんどなかったことから，これらの動物の骨代謝に関する研究が先行して行われ，これまでに多くの研究成果を得た。ここではその関連成果は省略するが，その成果を利用してPuの影響やリスク低減研究を進め，また得られた結果の評価に利用してきた。

(2) キレート剤の毒性試験手法の導入

Puの体外除去剤であるDTPAやCBMIDAの安全性（毒性）に関する研究は，プロジェクトの当初から人体適用を念頭におき医薬品の開発指針に定められている催奇形性試験，薬理試験，急性および慢性毒性試験などの方法に準じて進めた。

(3) ビーグル犬の呼吸および気管-気管支の分岐の生理学的・解剖学的研究

Puの吸入実験に供するビーグル犬の選択基準や吸入

[*1] 放射線医学総合研究所内部被ばく・防護研究部；千葉県千葉市稲毛区穴川 4-9-1（〒263-8555）
National Institute of Radiological Sciences；4-9-1, Anagawa, Inage-ku, Chiba 263-8555, Japan.
[*2] 放射線医学総合研究所宇宙環境生物医学および粒子線生物学グループ；千葉県千葉市稲毛区穴川 4-9-1（〒263-8555）
National Institute of Radiological Sciences；4-9-1, Anagawa, Inage-ku, Chiba 263-8555, Japan.

後の障害評価に利用する目的で，ポリグラフを用いて呼吸の生理学的解析を行い，個体差や年齢変化などの検討を行った。

吸入摂取された粒子状Puの気管-気管支内の挙動やそのシミュレーション研究に利用するために，肺造影技術を用いて，呼吸の最大拡大時，生理的拡大時，最小収縮時の気管支造影X線写真像を用いて，気管分岐部からの各分岐区々ごとの長さ，直径などの計測を行い，そのデータを三次元構築し，呼吸運動に伴う動的モデルの作成を試みた。

3. Puの生体内挙動と影響研究

1) 体内挙動に関する研究とこれまでの成果

Puのリスク低減方法を検討する上で，Puは酸化物，硝酸塩，粒子状あるいは溶解度などの物理化学的性状によって大きな相違が見られる摂取後の体内挙動や影響を明らかにしておくことが重要である[1,2]。本プロジェクトでは，吸入実験装置の安全性維持や計画的運営などの条件から，酸化Puの吸入投与を先行させ，硝酸Puは注射投与によって進められた。

(1) 酸化Puの吸入摂取後の呼吸器系における分布と挙動

ラットに吸入投与された酸化Pu（焼結温度：1150°C，AMAD：約0.2 μm）は，約20分後には肺マクロファージに取り込まれ，3日後の組織観察では肺胞表面に不均一に分布していた。吸入後から少量ずつ（肺沈着量の0.35～0.20%）血液中へ移行し糞尿中へ排泄される[3]。吸入投与1か月後における肺の各分葉の沈着量はその大きさに依存して差がみられたが，単位g当たりにするとほぼ一定で，解剖学的な位置による分葉間の差はなかった。肺に対する他の器官の沈着量の比率は気管：0.1%，全骨格：2.0%，肝臓：1.63%，腎臓：0.23%，脾臓：0.18%で，親和性の高い骨や肝臓で高かったが，いずれにしても粒子状の酸化Puが肺から移行しにくいことは明確であった。少数例のビーグル犬を用いた実験でも，ラットとほぼ同様な結果であった。

(2) 硝酸Puの静脈投与後の体内挙動

ラットに硝酸Puを静脈注射すると，血液中の濃度は投与15分後の値に対して1時間後では約50%，6時間後では約40%，1日後では約15%，2日後では10%以下となり，血液中から急速に消失し，一方肝臓や骨では急速に増加することが認められた。この結果から，Ca-DTPAなどのキレート剤は血液中のPuと強く結合することによって除去効果を示すが，臓器沈着後のPuに対してはほとんど無効になるので，影響リスクの低減化を高めるには，事故後のキレート療法の開始時期がいかに重要性であるかを示唆している。

ビーグル犬に静脈投与した1日後にはPuは糞中よりも尿中へ多く排泄されるが，2日以降では逆に糞中への排泄が多くなることから，短時間で肝臓へ沈着することを示している。投与14日後の臓器濃度は，骨，肝臓が最も高く，腎臓，脾臓，リンパ節，肺，腸管，膵臓の順で続いた。骨では海綿骨が最も高く，皮質骨，骨髄と続く。28日後の沈着濃度は14日後に比べて海綿骨，肝臓，骨髄で増加し，他の臓器や血液では低下していたことから，親和性の高い骨や肝臓への再沈着が起っていることが認められた。

ラットとビーグル犬の骨内の組織1g当たりのPu沈着量を比較（ラット/イヌ）すると，海綿骨では1.03，皮質骨では5.25，骨髄では7.81で，海綿骨以外では大きな種差がみられた。海綿骨表面に沈着したPuが骨内に埋め込まれる速度を推定するために，人の石灰速度に対するこれらの動物の比を求めるとラットでは1.6倍，イヌでは1.3倍，turnoverの割合はラットでは4倍，イヌでは2倍で，人に比べて骨内の挙動が激しいことが推察された。

(3) 静脈内投与による硝酸Puの臓器分布の年齢差

前項の結果から，Puは骨の表面積の大きい海綿骨に多量に沈着し，その代謝によって挙動が変化することが認められた。人の骨量は20歳代まで急速に増加し，20～40歳代で最大となり，その後徐々に減少する年齢変化を示すことが明らかになっている。これはPuの沈着量や挙動が，年齢によって異なることを表わしている。骨代謝の基礎実験で，ラットでは骨量が12か月齢で最大になり，人の20～40歳代に相当することを認めているので，3，12および24か月齢の雌雄ラットに硝酸Puを静脈投与して，投与2および4週後における臓器沈着量の年齢差を検討した。いずれの年齢でも雌雄ともに沈着率(Bq/g)は骨が最も高かったが，次には多くの観察時点で肝臓よりもむしろ脾臓が続いた。各臓器の年齢差をみると，骨では12か月齢で最も高くなると同時に，肝臓，腎臓，脾臓でも高くなる傾向を示したが，雌雄や投与後の観察時期によって変動がみられた。

この結果から，Puの臓器沈着やその後の挙動は年齢によって差がみられることが明らかになった。とくに骨の沈着量がラットでは12か月齢に最高になる結果は，人では骨量が最大になる20～40歳代に高率に沈着することを示唆していることが注目された。従来，放射線影響研究では放射線感受性が高い若齢時の被曝を対象としてきている。ラットの12か月齢では3か月齢に比べ骨量の増加に反して骨代謝は低下しており，おそらく骨細胞

の数や活性，また放射線感受性も低下すると考えられる。一方，骨代謝が低いことは骨表面のPuが同一部位に長期に沈着し続けることによる骨や骨髄の細胞が受ける線量が増加することを意味しており，影響リスク評価において年齢による細胞の感受性とPu沈着量や被曝量の関係を考慮する必要性があることを示唆している。

(4) 外部被曝との複合汚染による臓器の沈着差

放射線事故においてはPu摂取と外部被ばくとの複合汚染の可能性が考えられるが，このような事態を想定した研究は非常に少なく，Puの体内挙動等についても不明な点が多い。そこで，外部被ばくと同時にPuを摂取した場合と遅れて摂取した場合の相違について検討した。外部被ばくは特に骨への沈着の影響を検索するために，X線を用いて全身（2.5，5.0 Gy），頸部（骨代謝調節機能を持つ副甲状腺と甲状腺がある）あるいは頸部の臓器障害による影響を受けない例として後肢の局所（いずれも15 Gy）に1回照射した直後と7日後に，それぞれ硝酸Puを投与して1週後の臓器濃度を測定した。

その結果，全身照射直後にPuを投与した群の骨沈着量は照射線量に関わらず差がみられなかったが，照射7日後投与群では線量の増加に反して沈着量は減少した。肝臓と脾臓のPu沈着量は，照射直後投与群では線量による差はないが，照射7日後投与群では線量増加に伴って増加した。腎臓では照射直後投与群で減少が，卵巣では照射直後および7日後投与群とも線量増加に伴う沈着量の増加がみられた。頸部への局所照射直後および7日後投与群ともにPu沈着量の減少傾向が，後肢への局所照射直後群の骨沈着量はやや増加，7日後では減少傾向にあった。すなわち，全身照射では外部被曝7日後ではPu沈着量は骨では減少，軟臓器では増加し，局所的な大線量被曝でも骨障害に伴う沈着量の減少や変化が起ることから，複合被ばくにおける影響評価が極めて困難になることを表わしている。

2) 注射投与した硝酸Puの影響研究

注射投与した硝酸Puの影響研究は，投与量と発癌や寿命短縮などの影響，長期滞留による各臓器の濃度分布や線量との関係を明らかにすること，また得られた結果と，除去剤を用いた場合のリスク低減効果の評価および吸入投与した酸化Puや硝酸Pu実験の結果を比較し，投与経路や物理化学性状による相違を明らかにすることを目的として進められている。

実験規模は雌雄ラットのそれぞれ240頭で，1群40頭からなる6投与量（0.185～7.4×10^5 Bq/kg）群に分け，飼育スペースの制限から先行させた雄はほとんど終了間近になっている。これまでに投与量に応じた寿命短縮と，0.37～1.85×10^5 Bq/kg群で骨腫瘍の有意な増加がみられ，また雌雄差もみられている。骨腫瘍の骨格における好発部位は上腕骨，大腿骨，脛骨，椎骨などで，椎骨以外の長骨では骨端の表面積が大きい海綿骨部にみられる。椎骨のPu濃度は全身骨格に対して明らかに高く，他の部位については骨端の骨量とPu濃度との詳細な関係について検索を進めている。また，大腿骨の骨強度はPu濃度に比例して弱く，脆弱化が起ることを認めている。この研究では，肺，肝臓，腎臓，脾臓，精巣あるいは卵巣の濃度も測定し，基礎データの蓄積が進んでいる。

4. Puの体外除去法に関する研究

1) 除去方法に関する研究の経過

体内摂取されたPuの影響リスクを低減化する最大の問題は，Pu摂取後いかに迅速に体外除去あるいは臓器沈着阻止の処置を行うかにあり，そのためには除去効果が高くかつ副作用の低い体外除去剤を開発し，事故後直ちに投与できる体制を確立することにある。

Puの摂取事故時に国外で人体適用が推奨されている除去剤として，Ca-DTPAとZn-DTPAがある。2種類のDTPAが準備されている理由として，DTPA自体は不溶性で体内のカルシウム欠乏による副作用を起すためCa-DTPAがまず開発されたが，その後Ca-DTPAを経口投与すると腸管の亜鉛欠乏による障害を起すことからZn-DTPAが安全な化合物として追加された。我々がDTPAの研究に着手した時期は内部被ばく実験棟の設計建設前で，欧米でも安全性が明確に確認されていなかったことから，まず前述した医薬品開発の基準を参考にしながら安全性（副作用）試験に着手した。

DTPAは最も人体投与に適した除去剤として広く使用されているが，開発当初から終局的なキレート剤ではなく，さらに除去効果が高く，副作用の少ないキレート剤の開発の必要性が唱えられていた。欧米ではDTPA以後も試行錯誤を繰り返しながらいくつかのキレート剤の開発研究が進められているが，原子力政策の転換やDTPA開発世代に続く研究者の減少によって，この分野の研究は停滞気味になり現在に至っている。我々は欧米とは異なる化合物である新しいキレート剤の開発を中国上海薬物研究所との共同研究によって進め，これまでにCBMIDAおよびその類似物の検討を行ってきた。CBMIDAは，Puの親和性が高い骨への沈着を抑制する効果が高いこと，経口投与による毒性が低いことなど，DTPAよりも優れていることを確認している。すでに，中国では使用目的は異なるが薬物として人体適用経験があるとのことから，安全性に関しても期待ができる。

しかし，現在に至るまで日本ではDTPAもCBMIDA

のいずれも汚染事故に対して人体投与できる医薬品や治験薬として認められておらず，欧米のような投与や監視体制も整っているとはいえない状態が続いている。このような状況から，万一の事故時には緊急処置薬としてDTPAを使用することは困難であると判断し，人体投与が問題にならず，かつ簡単に入手できる応急的方法として，Puの骨沈着阻止を目的としたカルシウム剤の投与効果について検討した。健康食品や医薬品，あるいは食物として簡単に入手できるカルシウム剤をPu投与直後のラットに与えると，骨のPu初期沈着を防止する効果が認められた。すなわち，カルシウムの摂取は事故時に摂取量の測定や影響評価などDTPAの投与決定までに時間がかかるときに，また事故直後の被災者の自己防御手段として有用であり，その後のDTPA療法にも大きな妨害にはならず，むしろ骨沈着阻止効果によりDTPAの除去効率を高める可能性も期待できる実用的な応急手段となるのではないかと考えられる[4~9]。以下にこれまでに得られた成果の概略を述べる。

(1)　除去効果

欧米のキレート剤研究においてDTPAではPuを完全にあるいは充分に満足できる除去効果が得られないことが問題になった。この問題に対して，我々はCa-DTPAとZn-DTPAともに，とくにCa-DTPAの方が強い薬理学的作用として血管透過性亢進作用があることを明らかにし[10]，その後これらのDTPAと粒子状物質を静脈投与すると，粒子状物質が血管から結合織へ漏れ出ることを確認し，これがDTPAによって完全にPuを除去できない理由として報告した。

酸化Puに対するDTPAの除去効果は，事故で摂取されたPuの物理化学的性状やDTPAの適用方法が一定していないために報告によって相違がみられる。そこで，我々は実験的に高温（1,150°C），低温（300°C）で焼結した酸化物および焼結しないコロイド状の水酸化物をラットに吸入させて，Ca-DTPAの注射投与とそれに続くZn-DTPAの経口投与によるキレート療法を30日間行った結果，除去効果はまったく認められなかった。この時，Puの性状によっては体液で溶解する可能性があり，吸入後でもDTPAの効果が期待できる場合があることが示唆されているので，Pu吸入後からのキレート療法の開始時期を遅らせて検討したが，効果は認められなかった。さらに，1年半以上にわたって，一定間隔でCa-DTPAの投与を続けている実験でも効果はまったく認められていない[11]。

吸入摂取したPuに対して，事故後被災者が直ちにDTPAを摂取できる方法としてCa-DTPAをネブライザーでエアロゾル化あるいはスピンヘラー（簡易型粉末飛散器）によって発生させて直接肺へ吸入投与する方法の効果が期待されている。この方法は，呼吸器系に摂取されたPuに吸入投与したDTPAを直接結合させる効果と呼吸器系の粘膜からのDTPAの吸収による効果の両方が期待できる。除去効果に関しては，2種類の投与方法とも少なくとも酸化Puに対する効果は現在までの検討では明確にできていない。DTPAの投与方法としての検討は現在検討中であるが，吸入時間により投与量を調節できることを確認し，さらに副作用の検索を進めており，今後除去効果の結果とあわせて実用性について総合的な検討を行う予定である。

新しく開発したCBMIDAの注射投与による硝酸Puの除去効果をDTPAと比較した結果，とりわけ骨沈着阻止効果が優れていることを明らかにした[12~15]。CBMIDAの経口投与による効果はZn-DTPAと比べた結果，やはり優れており，投与量を増量しても副作用が低いことが認められた[16]。しかし，CBMIDAは腎臓へのPu蓄積を増加させる傾向があり，この点の改善とさらに高い除去効果を得ることを目的として10種類のCBMIDAの類似物質を試した結果，このうち2種類の類似物質に腎臓への蓄積増加に対する改善効果がみられた。今後，骨と肝臓の沈着阻止に優れたCBMIDA，肝臓や腎臓の沈着阻止効果が優れたDTPAの組み合わせによる効果などについて，検討を進める予定である。

(2)　薬物としての安全性の検討

DTPAの安全性（副作用）研究に関しては[17]，ラットの経口投与による慢性毒性試験[18]，ラットとイヌを用いた毒性の比較[19]，犬の経口投与毒性試験[20]など一般的な検討を行った[21,22]。さらに，DTPAの特異的な副作用として，Zn-DTPAを静脈注射すると血液中のカルシウム濃度を低下させ，心機能低下あるいは停止が起こり，高血圧症など循環器系疾患を有する場合にはリスクが高まる可能性があること[23~25]，キレート剤が金属と結合作用を持つ性質により，とくに長期投与すると石灰化阻害などの骨代謝障害を起すこと[26]などを明らかにした。1989年までの成果は保健物理学会論文賞の受賞をきっかけに総説としてまとめた[27]。その後も，EDTA，DTPA，CBMIDAの副作用の比較[28]，DTPAの毒性と放射線影響（外部照射）の比較，DTPAの吸入投与による毒性や代謝などについて継続して検討している[29,30]。

(3)　キレート剤研究に関する国際的活動

Puの体内摂取に伴う影響リスクの低減化を目的としたキレート剤の開発研究は，その重要性を認めている欧米では影響研究と並行して正面から進め，その成果とし

てDTPAがドイツや米国では医薬品や治験薬として人体適用が許可され，さらに緊急医療体制が整ったREACTSのような施設が稼働している。キレート剤の開発研究は，一般の医薬品開発と同様に除去効果(薬効)と安全性（副作用）の両面を同時に満足しなければならない厳しい研究であり，専門分野の幅も広いため，欧米では国境を越えて研究者が分担して開発を進めたきた。その成果であるDTPAは金属中毒や金属代謝異常の治療にも使用され，放射線事故時以外の治療にも役だっている。一方，日本におけるキレート剤の開発研究に対する認識は低く，1980年頃以前にはキレート剤に関連した実験はほとんど行われていず，1983年に保健物理学会に初めて発表した以降も研究者はほとんどいない状態が続いたので，最近の放射線事故で関心が高まってくるまでは，目が国外へ向くのは必然的な結果である。

1983年に米国におけるDTPA研究推進の第1人者であったMAYS博士の依頼によりUtha大学のセミナーで毒性試験の結果を発表したのが最初で，当時はDTPAの安全性に関しては十分ではなかった状況から，その後の研究や欧米での動向などの情報交換のきっかけとなった。1987年に，その後得られた毒性や薬理試験の成果を，第2回International Symposium：Chelating agents in Pharmacology, Toxicology and Therapeutics（現在のチェコ，以下チェコ学会と略す）で発表。この学会を機に，上海薬物研究所所長のDr. XIEと新しいキレート剤CBMIDAの共同研究を，また欧米におけるDTPA研究推進の権威であるDr. VOLF（ドイツ）との情報交換も開始された。さらに，この学会の課題として取り上げられたキレート剤研究の臨床応用への確立を主題に，キレート剤研究の世界的権威者であるDr. RUBIN（米国，Georgetown大学）によって，1989年に開催された第3回International Chelation Research (Washington, D.C.) において招待講演を行った。

1990年の第3回チェコ学会ではDr. VOLFによって，それまで安全性が高いとされたZn-DTPAは静脈注射によってCa欠乏を起し，循環器系へ強い障害を及ぼすことを我々が指摘した内容に対する追認の発表が行われ，訪日した際の講演でも取り上げられた。1991年には上海薬物研究所との共同で，除去効果と安全性を高めることを目的としたCBMIDAのアナログの開発が進められた。1993年の第4回チェコ学会でCBMIDAの成果について発表した。同時に，Vandenbilt大学のDr. JONESとの共同研究のきっかけとなった。1996年のIRPA 9および第5回チェコ学会ではCBMIDAの成果と同時に，上海薬物研究所との共同で始めたストロンチウムの除去剤の成果も注目を浴びた。

国際的な学会において絶えず受ける印象は別に述べたとおり，日本での事故対策に関する認識の低さと実用体制の遅れであり，実際に国外から緊急医療体制の不備が指摘されている[31~34]。

(4) 肺洗浄の医学的リスクに関する研究

不溶性の酸化Puが肺に摂取された場合，キレート剤の効果はみられないことはすでに述べた。また，その粒子は非常に早い時期に肺マクロファージに取り込まれたり，肺胞表面に沈着し，肺からの移行は非常に緩やかである。

このような粒子状のPuを体外へ除去する方法として肺洗浄法がある。この方法の医学的リスクについてビーグル犬を用いて検討した。先端が2又に分かれたダブルルーメンカテーテルを左右の気管支に挿入し，一方は呼吸確保に使い，もう一方に生理食塩水を注入して肺洗浄を行った。その結果，洗浄によって$10^{6\sim7}$個の肺マクロファージが採取できることから，マクロファージに取り込まれたPuと遊離性の粒子を除去できる可能性が期待できた。医学的リスクに関しては，肺洗浄中は麻酔管理，血液ガス値や心電図の変化を，洗浄処置後は呼吸機能監視とX線写真による肺機能の回復を検討した。その結果，医学的リスクは肺洗浄の各操作や監視を的確に行えば，それほど高いものではないと判断された。実際にPuが混入する場合には，二次汚染の可能性を防ぐための洗浄液や血液サンプルの取扱や手袋の汚染など，実際の場で解決すべき問題があることが知られた。

5. 現状と今後の課題

国内でも原子力関連施設において汚染事故が発生し，単に緊急医療の体制の見直しや強化の必要性が強調されるだけでなく，原子力の安全政策は実動的な緊急医療体制の確立と運営によって完成されると考えられるので，具体的な対策の確立が求められるのは必然であろう[35]。このような状況を踏まえて，平成10年度から第三次医療機関である放射線医学総合研究所では緊急医療対策総合研究プロジェクトを進めPuを含む汚染事故に伴う基礎から臨床までの医療や緊急連絡対応などの総合的な体制確立に向けてスタートする。これまでに本研究や関連活動において得られた成果は学会発表等にとどまらず，研究所内外の緊急医療対策に関する多くの委員会において生かす努力をしてきたが，残された課題も多い。今後，総合研究プロジェクトに合わせて本研究の残された課題である硝酸Puの吸入に対するリスク低減だけでなく，他の核種についても実証的な研究を進める予定である。

参 考 文 献

1) 福田 俊, 小泉 彰；"人体内放射能の除去技術—挙動と除染のメカニズム,"p. 24-30, 講談社サイエンティフィク, 東京 (1996).
2) 福田 俊, 小泉 彰；放射性核種の生体内挙動と除去—プルトニウム, 放射線科学, **37**, 7-9 (1994).
3) S. FUKUDA, H. IIDA, Y. YAMADA, A. KOIZUMI and N. ISHIGURE；Effects of DTPA therapy on removal of inhaled high-fired plutonium oxide in rats, *J. Health Physics*, **32**, 383-386 (1997).
4) 福田 俊；プルトニウムの沈着阻止と体外除去, NIRS-M-86, p. 129-137 (1992).
5) S. FUKUDA and H. IIDA；Removal of plutonium by a new type calcium and combination of the calcium and Ca-DTPA in rats, *J. Health Physics*, **28**, 167-172 (1993).
6) S. FUKUDA；Effects of active amino acid calcium：Its bioavailability on intestinal absorption, osteoporosis and removal of plutonium in animals, *J. Bone Miner, Met.*, **II**, S47-51 (1994).
7) S. FUKUDA and H. IIDA；Effects of calcium on removal of plutonium in rats, *Chelating Agents in Pharmacol. Toxic. and Therap.*, Suppl. **68**, 129-132 (1993).
8) 福田 俊；現状における除去剤の使用上の問題点と改善策の提案, 放射線科学, **33**, 387-388 (1990).
9) 福田 俊；内部被曝事故に対する機能性食品を用いた予防対策の提案, 放射線科学, **34**, 105-108 (1991).
10) S. FUKUDA, H. IIDA and Y. OGISO；The enhancement of vascular permeability by DTPA, *J. Health Physics*, **20**, 13-18 (1985).
11) S. FUKUDA, H. IIDA, Y. YAMADA, A. KOIZUMI, H. SATO, N. ISHIGURE, N. NAKANO and H. ENOMOTO；Chelating agent, DTPA, can not remove effectively inhaled-plutonium oxide in rats, 1996 ICRP Proceedings 2, p. 460 (1996).
12) S. FUKUDA, H. IIDA, Y. HSEIH and W. CHEN；Effects of CBMIDA [Catechol-3,6-bis(methyleiminodiacetic acid)] on removal of plutonium in rats, *J. Health Physics*, **27**, 11-15 (1992).
13) S. FUKUDA, H. IIDA, Y. HSEIH and W. CHEN；Removal of plutonium by CBMIDA in rats, *Chelating Agents in Pharmacol. Toxic. and Therap.*, Suppl. **68**, 133-135 (1993).
14) S. FUKUDA, H. IIDA, Y. XIE and W. CHEN；Effects of new chelating agents, CBMIDA and its analogues, on removal of plutonium in rats, 1996 ICRP Proceedings 2, p. 463 (1996).
15) S. FUKUDA, Y. YAN, H. IIDA, W. CHEN and Y. XIE；Removal of plutonium by chelating agent, CBMIDA analogues in rats, *Plzen Med. Report*, Suppl. **71**, 91-92 (1996).
16) S. FUKUDA, H. IIDA, Y. HSEIH and W. CHEN；Effects of CBMIDA and Zn-DTPA in drinking water on removal of plutonium in rats, *J. Health Physics*, **30**, 117-120 (1995).
17) S. FUKUDA and H. IIDA；Toxicological studies on the safety of DTPA as a drug, (I) Teratological study in the rat, *J. Health Physics*, **18**, 37-42 (1983).
18) S. FUKUDA, H. IIDA and J. YAMAGIWA；Toxicological study of DTPA as a drug, (II) Chronic side effects of orally administered DTPA to rats, *J. Health Physics*, **19**, 119-126 (1985).
19) S. FUKUDA；Toxicity of DTPA administered intravenously or orally in rats and beagles, *Chelating Agents in Pharmacol. Toxicol. and Therap.*, Suppl. **56**, p. 41 (1988).
20) S. FUKUDA and H. IIDA；Toxicological study of DTPA as a drug, (III) Side effects of orally administered Zn-DTPA to beagles, *J. Health Physics*, **22**, 439-444 (1987).
21) 福田 俊；キレート剤DTPAの毒性研究(1), 放射線科学, **32**, 73-78 (1989).
22) 福田 俊；キレート剤DTPAの毒性研究(2), 放射線科学, **32**, 115-118 (1989).
23) S. FUKUDA, J. YAMAGIWA and H. IIDA；Effects of intravenously injected DTPA on cardiovascular system in rats, *J. Health Physics*, **21**, 245-250 (1986).
24) S. FUKUDA and H. IIDA；Toxicological study of DTPA as a drug, (IV) Effect of intravenously injected DTPA on cardiovascular system in beagle dogs, *J. Health Physics*, **23**, 99-104 (1988).
25) 福田 俊；キレート剤の生体機能への影響と人におけるDTPAの安全性評価, NIRS-M-78, p. 229-236 (1991).
26) S. FUKUDA, H. IIDA, Y. HSEIH and W. CHEN；Toxicological study of DTPA as a drug (VI)；Effects of intravenously injected Ca-DTPA, Ca-

EDTA, CBMIDA and orally administered Zn-DTPA to bone metabolism in beagle dogs, *J. Health Physics*, **26**, 101-107 (1991).
27) 福田 俊；キレート剤DTPAの毒性評価，保健物理，**24**, 201-210 (1989).
28) S. FUKUDA, H. IIDA, Y. HSEIH and W. CHEN；Toxicological study of DTPA as a drug (V), Toxicities of Ca-DTPA, Ca-EDTA and CBMIDA after intravenous injection in beagle dogs, *J. Health Physics*, **25**, 115-119 (1990).
29) 福田 俊，小泉 彰；合成キレート剤によるプルトニウムの除去，放射線科学，**37**, 181-184 (1994).
30) 福田 俊，小泉 彰；“人体内放射能の除去技術―挙動と除染のメカニズム，” p. 49-55，講談社サイエンティフィク，東京 (1996).
31) 福田 俊；第3回国際キレーション会議，放射線科学，**32**, 323-324 (1989).
32) 福田 俊：第4回薬理学，毒性学，治療学におけるキレート剤に関する国際シンポジウムに参加して，保健物理，**28**, 453-456 (1993).
33) 福田 俊：「こう兎三窟」の結論は温泉の効果？第4回薬理学，毒性学，治療学におけるキレート剤に関する国際シンポジウムに思う，放射線科学，**37**, 25-28 (1994).
34) 福田 俊：隔靴掻痒―第5回キレート剤の薬理学，毒性学および治療学における国際シンポジウムに参加して―，放射線科学，**39**, 439-441 (1996).
35) 福田 俊：緊急被ばく医療の現状と展望―内部被ばくリスク低減化に関する研究から実用体制の充実に向けて―，原安協だより，**161**, 3-6 (1998).

保健物理，33(3)，321（1998）

≪特集：放医研におけるプルトニウムの生物影響評価研究≫

特集を終えるにあたり

放射線医学総合研究所　内部被ばく・防護研究部

放医研内部被ばく・防護研究部におけるプルトニウムの生体への影響評価に関する研究について，その全体的な意義が理解されることを期待して，これまでに得られたいくつかの成果を中心に紹介した。もとより，これは放医研内部被ばく・防護研究部で行われてきたプルトニウム研究の一断面であり，切り口は多々あるはずである。この中で解決されたり，明らかにされた課題も多いものの，まだまだ多くの未解決の問題が残っている。たとえば，重要な課題として一例を挙げれば，線量-影響関係についてこれまでの諸外国のデータとは異なるデータが得られているのであるが，その解釈がまだついていないことがある。このような点の解決も視野に入れ，放医研における当面の課題として，吸入粒子径や化学形の違い（これまでの酸化プルトニウムとは異なる，核燃料サイクルの途中工程で発生する硝酸プルトニウム）に由来する影響の差異の評価があり，あるいは，新しい線量評価モデルであるボクセルモデルの開発やより有効な新しいキレート剤の開発などがある。

このような状況にあって，この特集の冒頭で述べたように，放医研ではプルトニウム生物影響評価の研究が今後も続けられる。同時に，施設完成から10年以上がたって諸設備の更新時期を迎えつつあること，研究の進展に伴った新しい吸入技術の開発，さらには後継者の育成など，純粋な研究面以外にも多くの課題が山積している。また，プルトニウム以外に，超ウラン核種のアルファ放射核種はもとより，主要なベータ放射核種に対象を広げていくこと，施設の利用機会の拡大など，将来を見て長期的視点に立った展開も考えていくべき時にきている。

本特集を組むに当って，プルトニウムの生体への影響評価研究を行う研究機関がわが国には他にないとはいえ，一研究機関（厳密には一研究部門）にこのような機会を与えて頂いた本学会に感謝したい。放医研内部被ばく・防護研究部での研究遂行に関して，設備の設計・建設の段階から運転・保守管理の現在に至るまでに，所外の多くの方々にご支援いただいてきた（いる）ことに深くお礼申上げる。また，歴代の所長・科学研究官はじめ所内の多数の研究者および関連部局の暖かい理解と励ましに深謝するとともに，研究の立ち上げから現在まで，直接の担当者として多くの困難を解決し，いまある姿と成果を導いてこられた松岡　理元部長ならびに稲葉次郎前部長のご尽力を多としたい。

J. RADIAT. RES., 33, 301–308 (1992)

Transfer of Plutonium to Rat Embryos *in vivo* and *in vitro*

SENTARO TAKAHASHI, HIROSHI SATO, YOSHIHISA KUBOTA AND JIRO INABA

Division of Comparative Radiotoxicology, National Institute of Radiological Sciences, 4-9-1, Anagawa, Inage-ku, Chiba-shi, Chiba 263, Japan

(Received April 13, 1992)
(Revision recevied July 10, 1992, Accepted July 14, 1992)

Plutonium/Cross-placental transfer/Rat embryo/Yolk sac

The ^{239}Pu distribution in the 12.5-day-old rat conceptus was compared between *in vivo* and *in vitro* experimental systems to establish a possible mechanism of cross-palcental transfer of this radionuclide. In the *in vivo* study, plutonium citrate solution was injected intravenously to pregnant Wistar rats. In the *in vitro* study, either plutonium citrate or plutonium hydroxide colloid was administered, as a solution of Eagle MEM and FCS containing ^{239}Pu at the concentration used in the maternal serum in the *in vivo* experiments, to rat conceptuses maintained by the whole-embryo culture method. The concentration of ^{239}Pu in the yolk sac (^{239}Pu activity per gram wet weight) were much higher than in the embryo in both the *in vivo* and *in vitro* experiments, suggesting that the yolk sac may be an effective barrier against the transfer of plutonium to the embryos. The ratios of the ^{239}Pu concentration in the yolk sac to that in the embryo were relatively constant with time after administration in the *in vitro* system; 18–27 for plutonium citrate and 67–84 for plutonium hydroxide. In the *in vivo* experiment, these ratios changed with time after injection; 15 at 5 min and 62 and 60 min after injection. This suggests that in the *in vivo* system, the chemical form of ^{239}Pu changed with time after injection, probably to a macromolecular form such as the hydroxide colloid or plutonium-protein complex although ^{239}Pu was injected to the maternal blood as citrate.

INTRODUCTION

Actinides, particularly plutonium, are among the most toxic radioactive materials. Cross-placental transfer of plutonium administered to pregnant rodents and its distribution and retention in the embryo or fetus have been investigated extensively for the purpose of dose estimation[1–7]. Little, however, is known about the actual mechanism for the transport of plutonium across the placenta.

In rodents, the transfer of materials across the placenta, which consists of the yolk sac and chorioallantoic placenta, is done mainly by three mechanisms: simple diffusion, active transport, and pinocytosis. In general, ions are transferred by the first two mechanisms, and macromolecular materials by the third mechanism. At present, there is no published information about the mechanism of plutonium transfer to the embryo or fetus. Even when ionic plutonium is injected

高橋千太郎：放射線医学総合研究所　内部被曝研究部，千葉市稲毛区穴川4-9-1　〒263

into pregnant animals, as in a number of previous studies, it is transferred from the maternal blood to the fetus not only by simple diffusion and active transport as the ionic form, but by pinocytosis as macromolecular material as well because ionic plutonium is known to change its chemical form readily to the polymer in body fluid[8-9]. In these conventional *in vivo* experiments, in which the activity of plutonium in the fetus was measured after administration of plutonium to pregnant females, it was impossible to determine the detailed mechanism of plutonium transfer across the placenta.

The whole embryo culture method recently has become popular for teratological studies. With this method, rat embryos on day 9.5 of gestation could be maintained *in vitro* for up to 95 hrs[10-11]. The whole embryo culture method may prove useful for studying the mechanism of plutonium transfer across the placenta without interference from changes in the chemical form of plutonium during its passage through the maternal blood to the yolk sac placenta. We here compare the kinetics of plutonium transfer to the embryo in converntional *in vivo* experiments and in *in vitro* experiments in which the embryo is cultured by the whole embryo culture method and discuss possible mechanisms of plutonium transfer to rat embryos.

MATERIALS AND METHODS

The animals used were Wistar strain rats that were housed in a controlled environment (22 $\pm 1^{\circ}$C, 14 hrs light) and given food and water *ad libitum*. Nulliparous females, 12–18 weeks old, weighing 170–240 g, were caged nightly with males; the occurrence of mating was determined the following morning by the presence of a vaginal plug.

^{239}Pu-citrate and ^{239}Pu-hydroxide colloid were prepared from plutonium nitrate by the procedure described by Lindenbaum, with slight modification[12]. The ^{239}Pu-citrate solution was prepared by the addition of a stock solution of ^{239}Pu-nitrate (52.5 MBq per ml of 5 N HNO_3) to tri-sodium citrate to obtain a final molecular ratio of Pu to citrate of 1:100. This solution was adjusted to pH 4 with 1N NaOH then filtered through a 0.22 μm Milipore filter. The ^{239}Pu-hydroxide colloid was prepared similarly by an addition of the stock solution of plutonium nitrate to tri-sodium citrate to give a final molecular ratio of Pu to citrate of 1:1. It then was adjusted to pH 8 with 1N NaOH. The ^{239}Pu-citrate and hydroxide colloid solutions were made one day before the experiment in order to avoid chemical change with time after preparation.

In the *in vivo* study, pregnant rats on day 12.5 of gestation were anesthetized with pentobarbital (40 mg per kg of body weight), after which the plutonium citrate solution (0.5 ml, 43.2 kBq per rat) was injected intravenously. At 5, 15, 30, and 60 min after injection, animals were killed by bleeding them under anesthesia, after which the uteri were removed and washed with chilled saline. The uterine wall was excised onto absorbant paper, and the conceptuses (including the decidua) were placed in small dishes. Under a dissection microscope, each conceptus was divided into three samples, care being taken to avoid cross contamination. The samples were the embryo with circulating blood and amniotic fluid, the embryonic membrane containing the visceral yolk sac and aminion, and the decidua including the parietal yolk sac and Reichert's membrane. The plutonium activity in two to three conceptuses per litter was

determined, at least three litters being used for each time point.

The experimental protocol used for the whole embryo culture was similar to that reported elsewhere[13]. In brief, the conceptuses (including the decidua) were collected from pregnant rats on day 12.5 of gestation and placed in culture medium that was a mixture of fetal calf serum (Lot No. 1811, Cell Culture Lab.) and Eagle MEM (Nissui Pharmacy) at the volume ratio of 3:1. The Reichert membrane of each embryo was torn open in the medium before incubation, but the visceral yolk sac, amnion, and allantoic placenta were left intact. Each embryo then was transferred gently to a 50 ml culture bottle which contained 15 ml of the culture medium. The bottles previously had been filled with 5% CO_2 and 95% air. They were warmed at 37°C and rotated at about 30 rpm throughout the culture peirod. Four to six embryos explanted from the same dam were cultured in one bottle. The embryos first were incubated for 15 min, after which ^{239}Pu-citrate or ^{239}Pu-hydroxide colloid was intraduced into the culture bottle to give a concentration of 3.2 kBq ml^{-1} (the same as the average concentration of ^{239}Pu in the maternal serum in the *in vivo* study). At scheduled times after the addition of Pu, two or three embryos were taken from the culture bottle, washed twice with cold medium, then dissected into two samples; the embryo with circulating blood and amniotic fluid, and the embryonic membrane consisting of the visceral yolk sac and amnion. Six to nine conceptuses from at least three litters were used for each time point.

The samples were dissolved with 50 μl of tissue solubilizer (Protosol, New England Nuclear) at 60°C for 1 hour, then, neutralized with 1 N HCl. Radioactivity was measured in a scientillation cocktail (Aquasol-2, New England Nuclear) with a liquid scintillation spectometer (LKB, RackBeta 1219). The activity concentration of ^{239}Pu in the culture medium, measured before and after the experiment, did not change significantly during the experiment, which indicates that the plutonium was not absorbed and immobilized on the surface of the culture dish. The viability of embryos cultured by the present method has been reported elsewhere[13]. Almost all the embryos could be well maintained for up to 2 hrs by the present culture method. Viability was more than 95% 2 hrs after incubation, as assessed by direct microscopic observations of the heart-beat, blood circulation, and expansion of the yolk sac.

RESULTS

The concentration of ^{239}Pu in the maternal serum was 3.7 kBq ml^{-1} 5 min after injection, decreasing thereafter to 2.8 kBq ml^{-1} 60 min after injection (Fig. 1). The change in the serum ^{239}Pu concentraiton was expressed approximately by the equation $C(t)=3.74 \exp(-0.0047t)$, in which C(t) is the concentration of ^{239}Pu (kBq ml^{-1}) and t the time in min after injection. The average concentration of ^{239}Pu calculated from the equation was approximately 3.2 kBq ml^{-1} for the 60-min experimental period. This value was used the concentration of Pu in the culture medium in the *in vitro* study as detailed in Materials and Methods.

In the *in vivo* experiment, the respective concentrations of ^{239}Pu in the embryos were 5, 13, 16 and 18 Bq g^{-1} at 5, 15, 30 and 60 min after injection. The respective ^{239}Pu concentrations in the yolk sac were much higher than those in the embryos, being 69, 198, 681 and 1083 Bq g^{-1} at

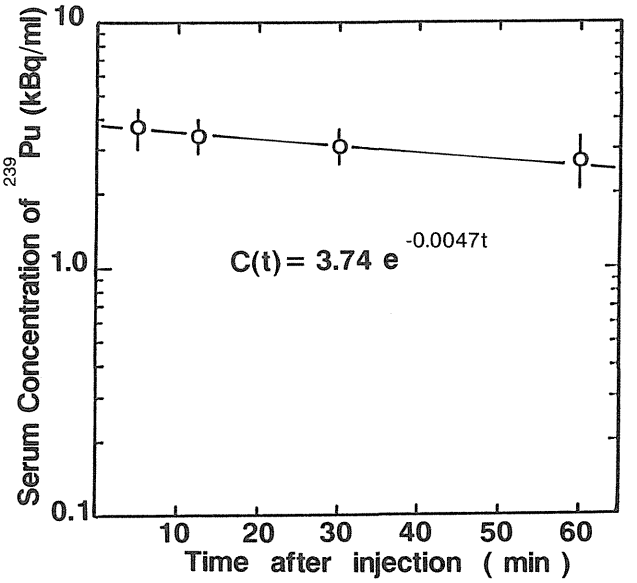

Fig. 1. Concentration of ^{239}Pu in maternal serum after an intravenous injection of ^{239}Pu-citrate. The ^{239}Pu concentration is expressed approximately by the equation $C(t)=3.74 \exp(-0.0047 t)$, in which C(t) is the concentration of ^{239}Pu (kBq ml^{-1}) and t the time in minutes after injection.

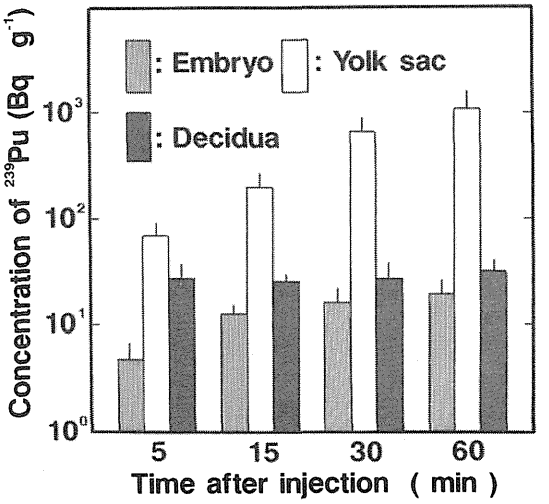

Fig. 2. Concentrations of ^{239}Pu (Bq g^{-1}) in the embryo, yolk sac and decidua in the *in vivo* experiments. Vertical bars denote the standard deviation (n=at least 6).

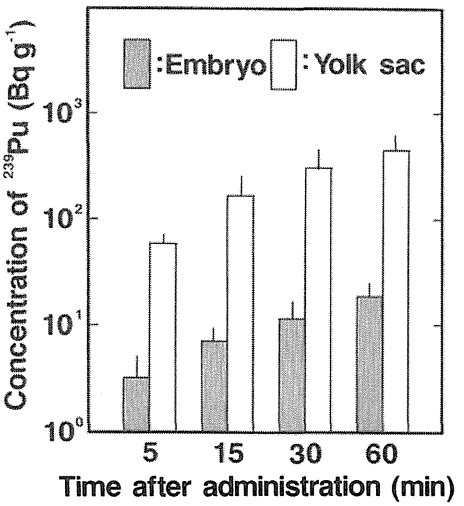

Fig. 3. Concentrations of ^{239}Pu (Bq g^{-1}) in the embryo and yolk sac in the *in vitro* experiment after administration of ^{239}Pu citrate. Vertical bars denote the standard deviation (n=at least 6).

5, 15, 30 and 60 min after injection. The concentrations of ^{239}Pu in the decidua were relatively constant, in the range of 26–32 Bq g^{-1} throughout the experimental period (Fig. 2).

In the *in vitro* experiment, either Pu-citrate or Pu-hydroxide colloid was administered to the cultured embryos. In the experiment with Pu-citrate, the embryo and yolk sac concentrations of ^{239}Pu were relatively smaller than the values in the *in vivo* experiment (Fig. 3). The respective ^{239}Pu-concentrations in the embryo were 3, 7, 11, and 18 Bq g^{-1} at 5, 15, 30 and 60 min after injection. The yolk sac concentrations of ^{239}Pu were 60, 160, 304 and 467 Bq g^{-1} for the same time points.

In contrast to the Pu-citrate, the concentration of Pu in the embryo was much smaller when Pu-hydroxide was loaded to the cultured embryo (Fig. 4). The respective concentrations of Pu in the embryo were approximately 0, 2, 7 and 11 Bq g^{-1} at 5, 15, 30 and 60 min after injection. In contrast, the Pu concentrations in the yolk sac were relatively larger than those for Pu-citrate.

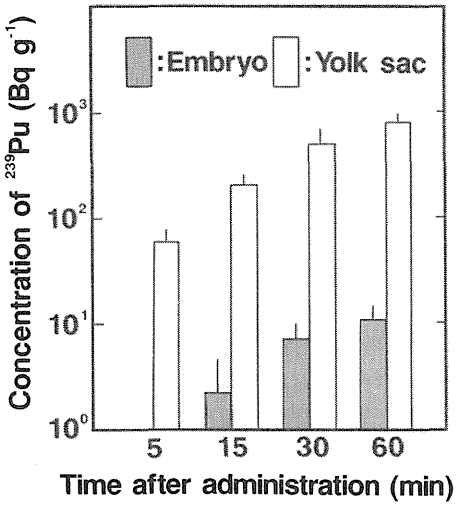

Fig. 4. Concentrations of ^{239}Pu (Bq g^{-1}) in the embryo and yolk sac in the *in vitro* experiment after administration of ^{239}Pu hydroxide colloid. Vertical bars denote the standard deviation (n=at least 6).

DISCUSSION

Under optimal culture conditions, 9.5-day-old rat embryos have been cultured for 95 hrs by the whole embryo culture method, when fresh rat serum prepared from the same animals immediately before embryo explantation was used as the culture medium, and the gas phase during the culture was monitored and strictly controlled[10–14]. In our study, fetal bovine serum diluted with Eagle MEM was used as the culture medium in place of rat serum in order to simplify the procedure, and the gas phase was not monitored and controlled during the culture period. The present culture method, however, is sufficient for examining the mechanism that transfers plutonium to the embryo across the yolk sac for short-term periods, as the 60 min used here, because we previously found that viability and ^{3}H-thymidine uptake were maintained for 2 hrs in embryos cultured by the method used here[13]. The uptake of ^{239}Pu by the embryo in the *in*

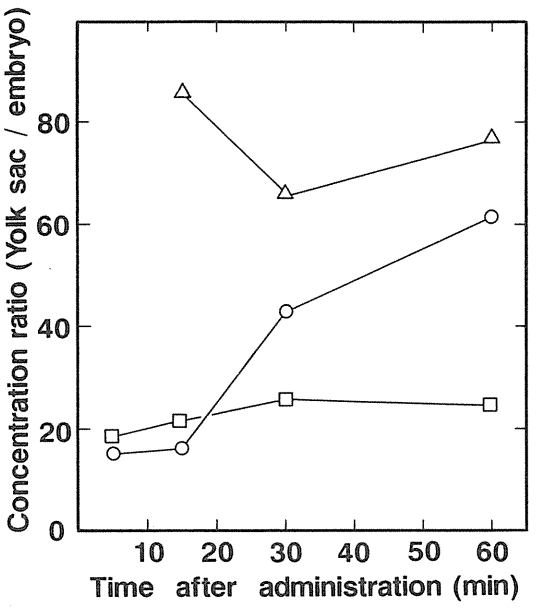

Fig. 5. Ratios of ^{239}Pu concentration in the yolk sac to that in the embryo in the *in vivo* and *in vitro* experiments. Circle (○): *in vivo* experiment. Square (□): *in vitro* experiment with ^{239}Pu citrate. Triangle (△): *in vitro* experiment with ^{239}Pu hydroxide colloid.

vitro experiment with ^{239}Pu citrate was slightly lower than that in the *in vivo* experiment, but the difference was small and did not interfere with the normal transfer mechanism of plutonium across the yolk sac placenta.

In both the *in vitro* and *in vivo* experiments, the concentration of ^{239}Pu in the yolk sac was much higher than that in the embryos, suggesting that the yolk sac acts as a barrier against the transfer of plutonium to the embryo or fetus. This observation is consistent with a number of previous reports: the accumulation of actinide elements, including plutonium, in the yolk sac has been observed in autoradiographic studies and radiochemical analyses[2–7,14–16]. The Pu-concentration in the yolk sac in the *in vitro* experiment with Pu-citrate was significantly lower than that in the *in vivo* experiment, and in the *in vitro* experiment with Pu-hydroxide as well. This indicates that the uptake of plutonium by the yolk sac is influenced by the chemical form of the element to which the yolk sac membrane is exposed.

The ratios of the ^{239}Pu concentration in the yolk sac to that in the embryo were calculated and are plotted in Fig. 5. In the *in vivo* experiment, the yolk sac/embryo concentration ratio of plutonium was about 15 at 5 and 15 min after injection, increasing thereafter to 62 at 60 min after injection. In previous *in vivo* studies, the raitos were reported to be 386 and 469 respectively in the rat conceptuses on the 11.5 and 15th day of gestation, 1 day after injection[3,7]. No previous data has been published on the concentration ratios of the yolk sac and embryo for such a short time after injection as the 60 min used in our study.

In contrast to the *in vivo* experiment, in the *in vitro* experiment the ratios of the yolk sac/embryo Pu concentrations were relatively constant with time after administration. The ratios were 18–27 in the *in vitro* experiment with ^{239}Pu-citrate throughout the experimental period. When ^{239}Pu was introduced to the culture medium as hydroxide colloid, the yolk sac/embryo concentration ratios were 67–84 between 15 and 60 min after administration (the ratio at 5 min

could not be calculated because the ^{239}Pu activity in the embryos was undetectable). There is much evidence that both the chorioallantoic and yolk sac placentas act as efficient barriers between the dam and embryo. This barrier function is especially marked for macromolecular or colloidal materials[17–21]. In our *in vitro* experiments, the ^{239}Pu concentation ratios for the yolk sac to the embryo were significantly higher for the Pu-hydroxide colloid as compared to Pu-citrate. This suggests that for plutonium transfer of the colloidal or macromolecular form is blocked more efficiently by the yolk sac placenta than is the ionic form, as also has been reported for other materials.

In the *in vivo* experiments, the Pu concentration ratios of the yolk sac to embryo increased with time after injection. At 5 and 15 min after injection, the ratios were similar to those in the *in vitro* experiment with Pu-citrate. At 30 and 60 min, they approached values similar to those in the *in vitro* experiment with Pu-hydroxide colloid. This indicates that the chemical form of ^{239}Pu may change with time after injection in the *in vivo* system although ^{239}Pu was administered as citrate to the maternal blood. Previous reports have shown that ionic plutonium, such as the citrate, changes its chemical form to a macromolecule which is similar to the hydroxide colloid or plutonium-protein complex in the living body[8,12]. We have no available data on the actual chemical form of the plutonium in the culture medium; but, the molar ratio of citrate to plutonium continued to be relatively high, about 100 : 1 because the citrate was metabolized very little in the *in vitro* system. This suggests that most of the plutonium introduced into the culture medium as citrate remained in the ionic state.

In conclusion, our results are strong evidence that the well known phenomenon of the concentrated accumulation of plutonium in the rodent yolk sac following intravenous injection of ionic plutonium as Pu-citrate may be attributable to, at least in part, the change in its ionic form to a macromolecular or colloidal form during passage through the maternal blood to the yolk sac. This finding also suggests that the mechanism of plutonium transfer may involve not only active or passive transport but pinocytic uptake by the yolk sac placenta as well.

REFERENCES

1. Finkel, M. P. (1947) The transmission of radiostrontium and plutonium from the mother to offspring in laboratory animals. Physiol. Zool. **20**: 405–421.
2. Ullberg, S., Nelson, A., Kristoffersson, H. and Engstrom, A. (1962) Distribution of plutonium in mice. An autoradiographic study. Acta Radiol. **58**: 459–471.
3. Sikov, M. R. and Mahlum, D. D. (1968) Cross-placental transfer of selected actinides in the rat. Health Physics. **14**: 205–208.
4. Weiss, J. F. and Walburg, H. E. (1978) Influence of the mass of administered plutonium on its cross-placental transfer in mice. Health Physics. **35**: 773–777.
5. Green, D., Howells, G. R. and Watts, R. H. (1979) Plutonium in the tissues of foetal, neonatal and suckling mice after Pu-administration to their dams. Int. J. Radiat. Biol. **35**: 417–433.
6. Mason, T. M., Humphreys. E. R. and Lord, B. I. (1991) Alphaparticle irradiation of haemopoietic tissue in pre- and postnatal mice 1: Distribution of plutonium-239 after mid-term contamination. Int. J. Radiat. Biol. **59**: 467–478.
7. Morgan, A., Haines, J. W. and Harrison, J. D. (1991) The incorporation of plutonium by the embryos

and fetuses of rats and guinea-pigs. Int. J. Radiat. Biol. **59**: 1395–1413.
8. Nenot, J. C. and Stather, J. W. The toxicity of plutonium, americium and curium: A report prepared under contract for the commission of the European Communities within its research and development program on "Plutonium Recycling in Light Water Reactors", pp. 3–6 Pergamon Press, Oxford.
9. Lindenbaum, A. and Westfall, W. (1965) Colloidal properties of plutonium in dilute aqueous solution. Int. J. Appl. Radiat. Isotop. **16**: 545–561.
10. New, D. A. T., Coppola, P. T. and Terry, S. (1973) Culture of explanted rat embryos in rotating tubes. J. Reprod. Fertil. **35**: 135–138.
11. New, D. A. T., Coppola, P. T. and Cockroft, D. L. (1976) Improved development of head-fold rat embryos in culture resulting from low oxygen and modifications of the culture serum. J. Reprod. Fertil. **48**: 219–222.
12. Lindenbaum, A., Lund, C., Smoler, M. and Rosenthal, M. W. (1968) Preparation, characterization and distribution in mouse tissues of graded polymeric and monomeric plutonium. In Diagnosis and Treatment of Deposited Radionauclides, eds. Kornberg, H. A. et al., pp. 56–64. Excerpta Medica Foundation, Amsterdam.
13. Takahashi, S. (1991) Distribution of ^{3}H in rat conceptus cultured in vitro following brief administration of [^{3}H] thymidine. Radiat. Res. **128**: 59–63.
14. Ovcharenko, E. P. (1972) An experimental evaluation of the effects of transuranic elements on reproductive ability. Health Physics. **22**: 641–646.
15. Maskalev, J. I., Buldakov, L. A., Lyaginskaya, A. M., Ovcharenko, E. P. and Egorov, T. M. (1969) Experimental study of radionuclide transfer through the placenta and the biological action on the fetus. In Radiation Biology of the Foetal and Juvenile Mammal, eds. M. R. Sikov and D. D. Mahlum (US AEC DTI), 153–160.
16. Hisamatu, S. and Takizawa, Y. (1983) Placental transfer and distribution of ^{241}Am in the rat. Radiat. Res. **94**: 81–88.
17. Roberts, A. V. S., Williams, K. E. and Lloyd, J. B. (1977) The pinocytosis of ^{125}I-labelled poly (vinylpyrrolidone), (^{14}C)sucrose and colloidal (^{198}Au)gold by rat yolk sac cultured in vitro. Biochem. J. **168**: 239–244.
18. Takahashi, S., Kubota, Y. and Matsuoka, O. (1983) Placental transfer of ^{59}Fe in rats after intravenous injection of ^{59}Fe-iron dextran at near term. J. Radiat. Res. **24**: 137–147.
19. Schultz, R. L. (1970) Placental transport: A reivew. Obstet. Gynecol. Surv. **25**: 979–1020.
20. Takahashi, S. and Matsuoka, O. (1982) Placental deposition and transfer of iron dextran to fetuses in mice at near term. Exp. Anim. **31**: 253–258.
21. Takahashi, S. and Matsuoka, O. (1982) Placental uptake and transfer of coloidal carbon in near term mice. Jpn. J. Ani. Reprod. **28**: 96–99.

J. RADIAT. RES., 34, 157–163 (1993)

Transfer of ^{239}Pu to mouse fetoplacental tissues

YOSHIHISA KUBOTA, HIROSHI SATO, CHIHIRO KOSHIMOTO AND SENTARO TAKAHASHI

Division of Comparative Radiotoxicology, National Institute of Radiological Sciences, 4-9-1, Anagawa, Inage-ku, Chiba-shi, Chiba 263, Japan

(*Received November 16, 1992*)
(*Revision received January 11, 1993*)
(*Accepted January 14, 1993*)

Plutonium/Cross-placental transfer/Mouse fetus/Yolk sac

Cross-placental transfer of ^{239}Pu from the mother to fetus was studied in C3H mice. The activity of ^{239}Pu in the conceptus was measured 24 hrs after the intravenous injection of ^{239}Pu citrate on days 10.5 to 16.5 of gestation. More ^{239}Pu was transferred to the conceptus when the plutonium was administered in the later stages of gestation; 0.12% of the injected dose per conceptus on day 10.5 and 1.3% on day 16.5. In all the gestational stages examined, the yolk sac and decidua contained more than 89% of the total activity distributed in the conceptus. The concentration of ^{239}Pu in the yolk sac was about two orders of magnitude greater than that in the fetus. The ^{239}Pu concentration in the maternal liver decreased with the gestational stage. In the early gestational stages the concentration in the maternal liver was greater than that in the yolk sac; but, this relationship was reversed in the later stages.

INTRODUCTION

The embryo and fetus are considered to be more sensitive than the adult to ionizing radiation with regard to many biological aspects including cancer induction[1]. This conclusion is based on data for external radiation exposure to animals and humans[1–3]. In comparison to the estimation of external radiation doses, the assessment of fetal doses from maternal intake of radionuclides is more complex, requiring information both on the uptake and the distribution of radionuclides in the rapidly growing fetus.

Investigations into possible links between childhood leukemias and radionuclide exposure in the vicinity of nuclear sites have demonstrated the uncertainty of calculations of *in utero* doses and the risks from radionuclides such as the isotopes of Pu and Am[4–6]. Moreover, recent studies have shown impaired bone marrow hemopoietic functions in the offspring of mice injected with Pu or Am mid-term in gestation[7,8]. The necessity of more accurate estimations of *in utero* doses, especially to fetal hemopoietic cells, was stressed in these reports.

Previous animal studies, primarily in rats and mice, have showed that the general tendency

久保田善久：放射線医学総合研究所，内部被ばく研究部，千葉市稲毛区穴川4-9-1　〒263

for ^{239}Pu to be transferred from the mother to the fetus increases with gestation and that substantially higher amounts accumulate in the yolk sac and placenta[9–18]. The experimental designs for these studies, however, vary markedly, mainly as to the tissue assayed, the amount of plutonium administered, and the gestational stages at which the radionuclides were administered and the tissues sampled. As a result, it is difficult to compare the data in those studies and to reach a reasonable conclusion. Recently, Morgan et al.[19] reported that the placental transfer of ^{239}Pu took place in rats and guinea pigs throughout most of the gestational stages. We know of no previous studies, however, in which the placental transfer of plutonium in mice was investigated in all the gestational stages. Dysfunction of hemopoietic cells in offspring after maternal contamination with plutonium, however, has been found in mice[7,8]. We have investigated the cross-placental transfer of plutonium administered to mice during different stages of pregnancy to obtain more detailed data for making accurate estimations of *in utero* doses; in particular in such primary fetal hemopoietic tissues as the yolk sac and fetal liver.

MATERIALS AND METHODS

The C3H/HeN mice used were housed in a controlled environment ($22 \pm 1^{\circ}$C, 14 hrs light) and had access to food and water *ad libitum*. Nulliparous females, 12–18 weeks old, were caged nightly with males, mating being confirmed the following morning by the presence of a vaginal plug. As ovulation and fertilization were assumed to have taken place at about midnight, midday of the following day being considered to be 0.5 days after conception.

^{239}Pu-citrate was prepared from plutonium nitrate by the procedure described by Lindenbaum, with slight modification[20]. A ^{239}Pu-citrate solution was prepared by adding a stock solution of ^{239}Pu-nitrate (52.5 MBq/ml of 5 N HNO_3) to trisodium citrate to give a final molecular ratio of Pu to citrate of 1 : 100. This solution was adjusted to pH 4 with 1 N NaOH, then diluted with saline to 40 kBq/ml and filtered through a 0.22 μm Milipore filter. This procedure was carried out on the day of injection to avoid chemical change with time after preparation.

On days 10.5–16.5 of pregnancy groups of mice were anesthetized with pentobarbital (40 mg/kg of body weight) then injected intravenously with ^{239}Pu-citrate at 400 kBq per kg of body weight. The animals were anesthetized 24 hrs after injection then killed by bleeding them, after which their uteri were removed and washed with saline. The uterine wall was excised, after which the couceptuses (including the decidua) were placed in small dishes. Each conceptus was divided into four samples under a dissection microscope, care being taken to avoid cross contamination. The samples assayed were the fetus; the fetal fluid consisting of the amniotic fluid and fetal circulating blood which flowed out during dissection; the yolk sac that included the visceral yolk sac and amnion; and the decidua that included the parietal yolk sac, Reichert's membrane and the chorioallantoic placenta. Plutonium activity in three conceptuses per litter was determined, at least two litters being used for each gestational age. Activity in the maternal liver and blood plasma also were measured. Samples were dissolved in 0.5–1 ml of tissue solubilizer (Protosol, New England Nuclear) at 60°C for 12–24 hrs, after which the solution was

neutralized with 1 N HCl. The radioactivity in a scintillation cocktail (Aquasol II, New England Nuclear) was measured in a liquid scintillation spectrometer (LKB, Rack Beta 1219).

RESULTS

The retention and concentration of ^{239}Pu in the maternal liver and plasma 24 hrs after injection are shown in Table 1. They both decreased in the liver gradually as gestation advanced, but there was no significant change in the plasma ^{239}Pu concentration. Table 2 shows that ^{239}Pu retention increased in the conceptuses with gestational age; from 0.12% of the injected activity on day 10.5 of gestation to 1.30% on day 16.5. The yolk sac had more than 50% of the ^{239}Pu activity in the conceptus, and more than 30% of this percentage was distributed in the decidua. The total ^{239}Pu activity reaching the fetus on day 16.5 of gestation was 0.080% of the injected activity; 80-fold that on day 10.5 of gestation (0.001%). In contrast, ^{239}Pu activity in the decidua, yolk sac and fetal fluid increased approximately 10-fold during the same period (from 0.049% on day 10.5 to 0.49% on day 16.5 in the decidua). Table 3 shows ^{239}Pu concentrations in the fetoplacental tissues. They were markedly higher in the yolk sac than in the other tissues; about two orders of magnitude that in the fetus but the same order of magnitude as in the maternal liver. The plutonium concentration increased in all fetoplacental tissues as gestation advanced. ^{239}Pu activity reaching the fetus increased markedly with gestation, but the concentration in the day-16.5 fetus was only 3–4 times that in the day-10.5 fetus because fetal weight increased 25-fold (from 30 mg on day 10.5 to 732 mg on day 16.5). The concentrations of plutonium in the decidua, yolk sac and fetal fluid on day 15.5 or 16.5 also were 2- to 5-fold the values on day 10.5 (e.g., 7.68% on day 10.5 and 21.20% on day 16.5 for the yolk sac). The mean dose rates of α-irradiation to fetoplacental tissues 24 hrs after injection are given in Table 4. The rates were calculated from the values in Tables 1 and 3 and the mean α-energy of ^{239}Pu per disintegration (0.834 pJ)[21]. The mean dose rates to the yolk sac were between 6 and 20 cGy per day from day 10.5 to 16.5 of gestation, much higher than in the fetal liver (0.2–0.3 cGy per day on days 15.5–

Table 1. ^{239}Pu distribution in the liver and plasma of pregnant mice 1 day after intravenous administration of plutonium citrate

Days of pregnancy at injection	Number of dams	Percentage injected activity (% IA) Liver	Concentration (%IA per g tissue) Liver	Plasma
10.5	3	25.52±5.33*	21.08±6.44	0.41±0.16
11.5	2	24.74±7.57	20.36±2.55	0.43±0.03
12.5	2	24.39±4.28	18.95±1.27	0.43±0.19
13.5	4	22.82±5.91	14.34±5.41	0.54±0.28
14.5	4	24.66±4.59	13.17±3.13	0.58±0.19
15.5	3	18.94±5.54	10.47±2.23	0.65±0.27
16.5	2	17.23±2.87	8.85±2.46	0.57±0.18

* Values are means±s.ds for 2–4 dams, expressed as percentages of injected activity.

Table 2. ^{239}Pu distribution in conceptuses 1 day after intravenous administration of plutonium citrate to pregnant mice

Days of pregnancy at injection	No. of dams	Percentage of injected activity in conceptus	Percentage of injected activity* (Percentage distribution of activity in conceptus)**				
			Decidua	Yolk sac	Fetal fluid	Fetus	Fetal liver
10.5	3	0.124±0.012	0.049±0.009	0.069±0.010	0.006±0.002	0.001±0.000	n.d ****
			(39.2± 5.3)	(55.5± 5.5)	(4.7±1.9)	(0.6±0.1)	n.d
11.5	2	0.183±0.046	0.061±0.017	0.114±0.030	0.005±0.002	0.003±0.001	n.d
			(33.1± 4.6)	(62.6± 3.9)	(2.9±0.6)	(1.5±0.3)	n.d
12.5	2	0.306±0.030	0.093±0.022	0.199±0.015	0.008±0.004	0.006±0.001	n.d
			(30.2± 6.0)	(65.3± 4.9)	(2.6±1.4)	(1.8±0.4)	n.d
13.5	4	0.446±0.137	0.151±0.074	0.264±0.082	0.017±0.009	0.014±0.006	n.d
			(32.9± 7.9)	(59.9± 7.6)	(4.2±2.6)	(3.1±0.5)	n.d
14.5	4	0.905±0.103	0.303±0.031	0.514±0.129	0.046±0.024	0.042±0.012	n.d
			(34.3± 8.4)	(56.0± 8.8)	(5.2±2.9)	(4.6±1.0)	n.d
15.5	3	1.097±0.181	0.395±0.132	0.582±0.197	0.057±0.036	0.063±0.007 ***	0.019±0.007
			(36.5±12.9)	(52.4±14.0)	(5.3±3.2)	(5.7±0.5)	(1.7±0.5)
16.5	2	1.304±0.040	0.494±0.119	0.731±0.086	n.d	0.080±0.010 ***	0.013±0.001
			(37.8± 8.4)	(56.1± 7.6)	n.d	(6.1±0.9)	(1.0±0.1)

* Values are means±s.ds for 6–12 conceptuses.
** Values in parentheses are percentages of total activity in conceptuses.
*** Values for the fetus, including fetal liver.
**** not determined.

Table 3. ^{239}Pu concentration in conceptuses 1 day after intravenous administration of plutonium citrate to pregnant mice

Days of pregnancy at injection	^{239}Pu Concentration (% IA/g tissue)					
	Conceptus	Decidua	Yolk sac	Fetal fluid	Fetus	Fetal liver
10.5	0.98±0.27	1.19±0.47	7.68±3.61	0.13±0.05	0.03±0.01	n.d **
	(125± 16)*	(41± 12)	(9± 2)	(45± 8)	(30± 6)	
11.5	0.94±0.17	0.94±0.23	8.55±0.86	0.15±0.08	0.04±0.01	n.d
	(196± 36)	(65± 13)	(14± 5)	(45± 23)	(72± 8)	
12.5	0.95±0.05	1.29±0.17	9.43±2.23	0.09±0.04	0.04±0.01	n.d
	(323± 21)	(72± 13)	(22± 4)	(95± 11)	(134± 9)	
13.5	1.05±0.29	1.71±0.77	8.62±3.34	0.17±0.08	0.07±0.02	n.d
	(426± 28)	(88± 10)	(32± 7)	(99± 14)	(207± 19)	
14.5	1.48±0.09	3.04±0.48	13.69±3.44	0.38±0.16	0.12±0.02	n.d
	(608± 45)	(101± 15)	(38± 4)	(120± 20)	(350± 36)	
15.5	1.53±0.20	3.49±1.17	16.07±3.99	0.62±0.38	0.13±0.02 ***	0.24±0.15
	(721±117)	(117± 26)	(36± 6)	(111± 52)	(457± 71)	(33±13)
16.5	1.50±0.08	4.76±0.38	21.20±2.71	n.d	0.12±0.02 ***	0.27±0.05
	(869± 38)	(103± 17)	(35± 4)		(732± 43)	(50±11)

* Values in parentheses are tissue weights(mg).
** not determined.
*** Values for fetuses including fetal liver.

Table 4. Mean dose rates in fetoplacental tissues 24 hrs after ^{239}Pu injection

Days of pregnancy at injection	Mean dose rates (cGy per day)*						
	Conceptus	Decidua	Yolk sac	Fetal fluid	Fetus	Fetal liver	Maternal liver
10.5	0.77	0.93	6.02	0.10	0.02	n.d.**	16.44
11.5	0.75	0.75	6.86	0.12	0.03	n.d	16.30
12.5	0.80	1.09	7.95	0.08	0.03	n.d	15.93
13.5	0.88	1.43	7.22	0.14	0.06	n.d	12.00
14.5	1.35	2.76	12.43	0.34	0.11	n.d	11.90
15.5	1.43	3.27	15.05	0.58	0.12	0.22	9.74
16.5	1.44	4.58	20.40	n.d	0.12	0.26	8.47

* Values were calculated from the mean values in Tables 1 and 3 and the mean α-energy of ^{239}Pu per disintegration (0.834 pJ).

** not determined.

16.5). On days 14.5–16.5, the dose rate to the yolk sac always was higher than that to the maternal liver.

DISCUSSION

To make a detailed evaluation of radiation accumulated in the embryo or fetus following maternal contamination with radionuclides, it is essential to have accurate information on the movement of radionuclides across the placenta because this movement changes greatly with advancing gestation[19]. We have determined the daily change in the tranfer of a plutonium isotope across the placenta, and the retention and distribution of the isotope in the maternal and fetoplacental tissues of mice on days 10.5 to 16.5 of gestation. We know of no previous studies on daily change in the transfer and retention of plutonium in the mouse fetoplacental unit. Morgan et al.[19], however, recently reported the placental transfer of ^{238}Pu to rat fetuses from day 3.5 to 14.5 of gestation. Considering the difference in the animal species used, in the day on which the animals were killed (24 hr after injection in our study, 3 days after in the study of Morgan et al.), the rate of transfer of plutonium to the conceptus (0.905% of the injected activity in mice, 0.858% in rats at injection on day 14.5 of gestation); the plutonium concentration in fetoplacental tissues (e.g., 13.69% and 11.50% respectively in the yolk sacs of mice and rats at injection on day 14.5); and plutonium distribution patterns in the conceptus were very similar. Using mice, Weiss et al.[17] and Mason et al.[21] obtained data on the transfer and distribution of ^{239}Pu in fetoplacental tissues at mid-term in gestation. The pattern of plutonium distribution in the fetoplacental tissues found in our study is consistent with their report. But the rates of transfer of plutonium to the fetus and fetal membrane are somewhat lower in our study. This may be because of the dose of ^{239}Pu injected; 30 kBq per kg body weight in the study reported by Mason et al.; less than one-tenth the dose used in our study. An inverse relationship between the percentage of activity transferred across the placenta and the level of contamination

in the mother also has been reported[12].

The accumulation of plutonium in rodent yolk sacs is a well known phenomenon. A number of studies show a higher plutonium concentration in the yolk sac as compared with other fetoplacental tissues[9–12,14–18]. We found plutonium hydroxide colloid was concentrated in the yolk sac than was plutonium citrate, which suggests that change in the chemical characteristics of plutonium (from an ionic to a macromolecular or protein-binding form) may be the mechanism of this phenomenon[22]. In our study, the plutonium concentration in the yolk sac ranged from 114-(13.69%/0.12% at injection on day 14.5 of gestation) to 256-fold (7.68%/0.03% at injection on day 10.5) that in the fetus. Ratios of the plutonium concentration in the yolk sac to that in the fetus have been reported[10,12,14,19,21]. In the literature we reviewed, the highest ratio reported was by Morgan et al. who found a yolk sac/fetus concentration ratio of plutonium about 575 in HMT rats administered ^{238}Pu citrate on day 14.5 of gestation and killed on day 17.5[19]. The lowest ratio reported was 73 in mice injected with ^{239}Pu citrate on day 13.5 of gestation and killed 3 days later[21]. Although direct comparison is difficult because of such differences in experimental conditions as animal species, the dose injected and the gestational stage at which radionuclides were administered and tissues sampled, the yolk sac/fetus plutonium concentration ratios reported in our study are reasonable values. The accumulation of plutonium in the yolk sac may be important with respect to the element's effect on fetal hemopoietic cells because the blood island of the yolk sac is the initial site of fetal hemopoiesis[23]. Van Den Heuvel et al.[7] reported that the number of bone marrow hemopoietic stem cells decreased in offspring of pregnant mice administered ^{241}Am on day 14.5 of gestation. Mason et al.[8] also reported a decrease in the spleen colony forming unit in offspring of pregnant mice given ^{239}Pu on day 13.5 of gestation. These researchers speculated that the observed dysfunctions of hemopoietic cells are attributable to exposure of the fetal liver and neonatal bone marrow to radiation. Fetal hemopoiesis in the yolk sacs of mice continued up to day 12 of gestation; whereas, progressive hemopoiesis in the fetal liver began on day 10–11[23]. As shown in Table 4, the average radiation dose rates were much higher in the yolk sac than in the other fetoplacental tissues at all the stages of gestation examined from day 10.5; therefore, doses of radiation to the yolk sac would be important early in gestation. It is necessary to investigate whether hemopoietic dysfunctions are present in the offspring of pregnant mice contaminated with plutonium during early gestation. If so, it would be because of α-irradiation to the yolk sac. This must be determined in the future studies.

REFERENCES

1. Brent, R. L., Beckman, D. A. and Jensh, R. P. (1987) Relative radiosensitivity of fetal tissue. Adv. Radiat. Biol. **12**: 239.
2. UNSCEAR (1988) Genetic and somatic effects of ionizing radiation. Report to the general assembly, with annexes. United Nations, New York, 306–419.
3. Kato, H., Yoshimoto, Y. and Schull, W. J. (1989) Risk of cancer among children exposed to atomic bomb radiation *in utero*. In Perinatal and Multigeneration Carcinogenesis, eds. N. P. Napalkov, J. M. Rice, L. Tomati and H. Yamasaki, pp 365–374. IARC Scientific Publications, No. 96, Oxford.

4. Stather, J. W., Wrixon, A. D. and Simmonds, J. R. (1984) The risks of leukemia and other cancers in Seascale from radiation exposure. NRPB-R171, HMSO, London.
5. Stather, J. W., Dionian, J., Brown, J., Fell, T. P. and Muirhead, C. R. (1986) The risks of leukemia and other cancers in Seascale from radiation exposure. NRPB-R171 Addendum, HMSO, London.
6. Stather, J. W., Clarke, R. H. and Duncan, K. P. (1988) The risks of child leukemia near nuclear establishments. NRPB-R215, HMSO, London.
7. Van Den Heuvel, R. L. (1990) Bone marrow from Balb/c mice radiocontaminated with ^{241}Am *in utero* shows a deficient in vitro haemopoiesis. Int. J. Radiat. Biol. **57**: 103–115.
8. Mason, T. M., Lord, B. I., Molineux, G. and Humphreys, E. R. (1992) Alpha-irradiation of haemopoietic tissue in pre- and postnatal mice: 2. Effects of mid-term contamination with ^{239}Pu *in utero*. Int. J. Radiat. Biol. **61**: 393–403.
9. Finkel, M. P. (1947) The transmission of radio-strontium and plutonium from mother to offspring in laboratory animals. Physiol. Zool. **20**: 405–421.
10. Sikov, M. R. and Mahlum, D. D. (1976) Comparative cross-placental transfer and fetoplacental distribution of plutonium-237, -238, -239. Pacific Northwest Laboratory Annual Report for 1975 to DOE, BNWL-2000, part 1, 83–84.
11. Sikov, M. R. and Andrew, F. D. (1979) Fetal and juvenile radiotoxicity. Pacific Northwest Laboratory Annual Report for 1978 to DOE, PNL-2850, part 1, 3.75–3.76.
12. Green, D., Howells, G. R. and Watts, R. H. (1979) Plutonium in the tissues of fetal, neonatal and suckling mice after plutonium administration to their dams. Int. J. Radiat. Biol. **35**: 417–432.
13. Hackett, P. L., Sikov, M. R., Mahlum, D. D., Andrew, F. D. and Hess, J. O. (1979) Strain defferences in the embryotoxicity of ^{239}Pu. Pacific Northwest Laboratory Annual Report for 1978 to DOE, PNL-2850, part 1, 3.77–3.80.
14. Sikov, M. R. and Mahlum, D. D. (1968) Cross-placental transfer of selected actinides in the rat. Health Physics **14**: 205–208.
15. Moskalev, J. I., Buldakov, L. A., Lyaginskaya, A. M., Ovcharenko, E. P. and Egorov, T. M. (1969) Experimental study of radionuclides transfer through the placenta and their biological action on the fetus. Radiation Biology of the Foetal and Juvenile Mammal, eds. M. R. Sikov and D. D. Mahlum, pp 153–160. US AEC DTI.
16. Ovcharenko, E. P. (1972) An experimental evaluation of transuranic elements on reproductive ability. Health Physics **22**: 641–646.
17. Weiss, J. F. and Walburg, H. E. (1978) Influence of mass of administered plutonium on its cross-placental transfer in mice. Health Physics **35**: 773–777.
18. Sikov, M. R., Mahlum, D. D. and Howard, E. B. (1970) Localisation and effect of ^{239}Pu in the prenatal rat and the placenta. Radiat. Res. **43**: 250.
19. Morgan, A., Haines, J. W. and Harrison, J. D. (1991) The incorporation of plutonium by the embryo and fetus of rats and guinea-pigs. Int. J. Radiat. Biol. **59**: 1395–1413.
20. Lindenbaum, A., Lund, C., Smoler, M. and Rosenthal, M. W. (1968) Preparation, characterization and distribution in mouse tissues of graded polymeric and monomeric plutonium. In Diagnosis and Treatment of Deposited Radionuclides, eds. H. A. Kornberg et al. pp 56–64. Excerpta Medica Foundation, Amsterdam.
21. Mason, T. M., Humphreys, E. R. and Lord, B. I. (1991) Alpha-particle irradiation of haemopoietic tissue in pre- and postnatal mice. 1: Distribution of plutonium-239 after mid-term contamination. Int. J. Radiat. Biol. **59**: 467–478.
22. Takahashi, S., Sato, H., Kubota, Y. and Inaba, J. (1992) Transfer of plutonium to rat embryos in vivo and in vitro. J. Radiat. Res. **33**: 301–308.
23. Tavassoli, M. (1991) Embryonic and fetal hemopoiesis: An overview. Blood Cells. **1**: 269–281.

J. RADIAT. RES., 35, 236–247 (1994)

Differential Induction of Bone and Hematopoietic Tumors in C3H Mice after the Injection of ^{239}Pu Citrate

YOICHI OGHISO, YUTAKA YAMADA, and HARUZO IIDA

Division of Radiotoxicology, National Institute of Radiological Sciences,
9-1, 4-chome, Anagawa, Inage-ku, Chiba 263, Japan

(Received, August 25, 1994)
(Revision received, October 17, 1994)
(Accepted, November 4, 1994)

Osteosarcomas/lymphomas/myeloid leukemia/mice/plutonium

Although alpha-emitting plutonium is easily distributed in the skeleton via circulation and subsequenlty induces bone tumors, there is little evidence that hematopoietic neoplasias are highly induced even though bone marrow stem cells are irradiated internally by alpha particles. We injected groups of female C3H strain mice with doses of ^{239}Pu citrate from 500 to 10000 Bq to investigate the dose-related spectrum of tumor types induced during a lifetime. Survival time was reduced strikingly in all the injected mice due to much earlier induction of bone and lymphoid tumors as compared to the control animals that showed a variety of soft tissue tumors after a longer period of survival. Induction of osterosarcomas was dose-dependent, being maximal in 70% of the animals that received a mean skeletal dose of 10 Gy or less, but was 48% or less at 20 Gy or more. Non-thymic lymphomas accompanied by lymphocytic leukemia were observed in only 4–6% of the animals that received a dose of 10 Gy or less whereas it was maximal in 17–19% at 20 Gy or more. In contrast, there were no bone tumors in the control animals, rather thymic lymphomas or histiocytic lymphomas were found very late in 20% and other soft tissue tumors, including lung, liver and ovary tumors, were noted in 60%. Neither myeloid leukemia nor other myelogenous neoplasias were found in the control and ^{239}Pu-injected animals that received a mean skeletal dose of 3 Gy or more. These results indicate that the differential induction of bone tumors and hematopoietic tumors in mice depends on the dose range and the time after the injection of plutonium.

INTRODUCTION

Because of its high linear energy transfer (LET) radiation of alpha-particles and its long half-life, plutonium is recognized as the most toxic and carcinogenic radionuclide. Once plutonium compounds in a soluble form, such as nitrate or citrate, enter the body, they are readily distributed in the skeleton through blood circulation, and are deposited on endosteal bone surfaces where they are retained for a long time and finally induce bone tumors, osteogenic sarcomas (1, 2). Results of life span animal studies strongly suggest that bone carcinogenicity for injected ^{239}Pu is the highest among a variety of alpha- or beta-emitting radionuclides, whether

小木曽洋一：放射線医学総合研究所内部被ばく研究部，千葉市稲毛区穴川4-9-1　〒263

bone surface-seekers or volume-seekers, being about 15–16 times the value for ^{226}Ra in both mice and dogs (3, 4). There is little evidence, however, whether such hematopoietic neoplasia as myeloid leukemia are highly induced in animals after the injection of plutonium, even though alpha particles distributed initially in the endosteal and trabecular bone surfaces could irradiate internally bone marrow stem cells (1), which are suspected progenitor cells for leukemogenesis. In fact, the incidence of myeloid leukemia reported in experimental carcinogenesis is much lower for the injection of ^{239}Pu (5, 6), ^{224}Ra (7), or ^{90}Sr (8) as compared to the incidence due to external irradiation of low LET radiations (9). In contrast, lymphoid neoplasias, including lymphomas and lymphocytic leukemia, which also might be derived from lymphoid precursors that originate in the bone marrow, have been reported to be induced in CBA/H strain mice by injections of relatively high doses of ^{239}Pu (10). The reasons for the differences in the spectrum of tumor types induced by plutonium, as well as their ontogeny, have yet to be clarified.

We here report the current summary of experimental carcinogenesis caused by ^{239}Pu citrate injected to female C3H strain mice which, in our experience, have spontaneously lower incidences of bone tumors and myeloid leukemia. Results indicate that non-thymic lymphomas accompanied by lymphocytic leukemia are differentially induced by higher cumulative skeletal doses than are osteosarcomas, whereas no myeloid leukemia was found. Differences also were noted in the frequencies of bone tumors and lymphoid tumor types that are related to the skeletal dose range.

MATERIALS AND METHODS

Experimental animals

Six- to eight-week-old specific-pathogen-free (SPF) female C3H strain mice were purchased from our animal breeding facility, maintained on a commercial diet with water *ad libitum* and kept under a barrier-filtered air before and after the experiments.

Preparation of ^{239}Pu citrate solution

In the alternative method used (11), part of the stock solution of ^{239}Pu nitrate (10.2 mM) was added to trisodium citrate solution (100 mM) to obtain a molecular ratio of 1 : 50, after which the mixture was titrated by the careful addition of droplets of 1N NaOH solution to a final pH of 6.8–7.2. Immediately before administration, part of the plutonium solution was diluted with physiological saline then passed first through a 0.2 μm-pore size milliporefilter and next through a 0.025 μm-pore size milliporefilter to obtain the monomeric ^{239}Pu solution, the activity of which was about 10^5 Bq/ml as counted in a liquid scintillation spectrometer.

Injection of ^{239}Pu and animal care

Four groups of mice weighing 25–28 g were injected intraperitoneally (ip) with different amounts of ^{239}Pu solution: 500 Bq/animal (Level 1), 1000 Bq/animal (Level 2), 5000 Bq/animal (Level 3), and 10000 Bq/animal (Level 4). As the vehicle controls, groups of age-matched animals were injected ip with 0.1 ml of saline. These animals were housed ten per polycarbonate cage and kept in a closed hood rack during their lifetimes. The animal rooms and hood racks

were maintained on a 12 hr-daylight cycle with an air temperature of $23\pm1.0^{\circ}C$ and a humidity of $55\pm5.0\%$. Animal care consisted of exchanging new clean cages weekly and checking the animal conditions daily for survival and pathological examinations.

Calculation of the cumulative skeletal dose

A separate group of mice that received 1000 Bq/animal was used for measuring the concentration of ^{239}Pu deposited in the ashed bones in a liquid scintillation spectrometer from 1 to 9 months after injection. The skeletal retention curve for our female C3H mice showed a single exponential component with a half-time of 739 days ($\lambda=0.000938$/day) and an initial skeletal deposition of 0.343. The resulting skeletal retention function is given as follows;

$$R(t)=0.343e^{-0.000938t}$$

where t is the number of days after injection.

If the total bone mass is 7.5% of body weight (mean $25g\times0.075\%=1.875g$), and the energy delivered by the disintegration of ^{239}Pu is 5.15 MeV as described elsewhere (3), then the mean skeletal dose rate for 1 Bq ^{239}Pu injected is given as follows;

$$\left(\frac{dD}{dt}\right)t=\frac{(1\ Bp/sec)(8.64\times10^{4}\ sec/day)(5.15\ MeV/dis)}{(6.24\times10^{5}\ MeV/erg)(100\ erg/g.rad)(1.875\ g)}R(t)\ (rad/day)$$

where R(t) is the retention rate of the initial concentration in the skeleton at t days after injection.

The cumulative mean skeletal dose for each animal until death therefore could be calculated by the following function;

$$D(T)=3.8\times10^{-5}\times A\times\int_{0}^{T}R(t)dt$$

where T is the survival time (day), A is the injected dose (Bq) per animal, and D(T) is expressed as gray (Gy).

Pathological examinations

Of the total 120 mice injected with ^{239}Pu and the 62 control animals used at the start of experiments, 3 of the injected and 2 of the control animals were deleted from the analysis for such compelling reasons as loss of main organs due to the cannibalism and severe autolysis due to delayed discovery. A total of 117 injected mice (31 in Level 1, 30 in Level 2, 27 in Level 3, 29 in Level 4) and 60 control animals therefore were available for pathological examinations. At autopsy, gross lesions were examined carefully, in particluar as to the onset and distribution of tumors, then the main organs (liver, kidneys, spleen, pancreas, alimentary tract, ovaries, uterus, adrenal glands, salivary glands, thyroid glands, thymus, heart, lungs, lymph nodes, and all of the bones) were fixed in 10% phosphate-buffered formalin. The bones and bone tumors were decalcified with 10% formic acid in 10% formalin after fixation. All of the organs and tissues were dissected into small pieces, then processed with graded ethanol in an automatic tissue processor and embedded in paraffin. Five to six μm-thick sections were stained with hematoxylin and eosin for light microscopic examinations.

Statistics

Student's T test was used to ascertain wheter there were significant differences between the groups of control and injected mice.

RESULTS

Survival and neoplastic death

As shown in Table 1, the control mice had a mean survival time of 836 days overall, 825 days for non-neoplastic death and 839 days for neoplastic death, which suggests that most of the control mice died spontaneously of senile or neoplastic disorders. As compared to the control values, all the groups of mice injected with ^{239}Pu (Levels 1–4) showed a reduction of survival time whether or not there were neoplasias, each mean survival time clearly being reduced to 540 through 360 days as mean skeletal doses increased from 3.1 to 40.2 Gy. A similar dose-effect on survival and the appearance of neoplasias also was found in the survival curves and the cumulative incidence curves of the neoplasias in each group (Fig. 1). The earliest death occurred 190 to 200 days after the injection of a higher dose (Level 3 and 4), and survival dropped sharply between 450 and 680 days with an increase in dose, as compared to the control group in which the first death was noted at 650 days and survival gradually decreased up to 1000 days (Fig. 1A). Similarly, the cumulative incidence curves of the neoplasias showed that tumors appeared much earlier in the injected groups 200 to 400 days after injection and that the incidence increased rapidly between 300 and 500 days with the increase in dose as compared to the control group which showed an increase of tumors much later, between 650 and 1000 days (Fig. 1B). In the highest dose group (Level 4), however, the cumulative incidence of tumors was lower than that of the next highest dose group (Level 3) or lower dose group (Level 2) because of higher mortality due to non-neoplastic disorders, including bone marrow aplasia and anemias. In contrast, non-neoplastic death in the lowest dose group (Level 1) and in the control group frequently was accompanied by chronic hepatosis and nephritis. These results indicate that the survival of plutonium-injected mice was greatly reduced by the acute neoplasias that occurred in most of the groups or by acute hematopoietic disorders, especially in the highest skeletal dose

Table 1. Survival Time and Skeletal Dose in ^{239}Pu Citrate-Injected Mice

Experimental Group	No. of Mice	Injected Dose (Bq/animal)	Survival Time for			Skeletal Dose (Gy)
			All	Non-neoplasias	Neoplasias	
Control	60	0	836± 90 (60)	825± 96 (12)	839±88 (48)	0 (60)
Level 1	31	500	539±106 (31)	510±121 (15)	567±80 (16)	3.1±0.6 (31)
Level 2	30	1000	463± 83 (30)	404± 85 (10)	452±78 (20)	5.9±1.2 (30)
Level 3	27	5000	350± 59 (27)	343± 40 (9)	354±67 (18)	19.4±3.1 (27)
Level 4	29	10000	360± 75 (29)	377± 63 (19)	329±85 (10)	40.2±6.9 (29)

Values indicate mean±SD of survival time (day) and cumulative mean skeletal dose±SD. The number of animals is given in parenthesis.

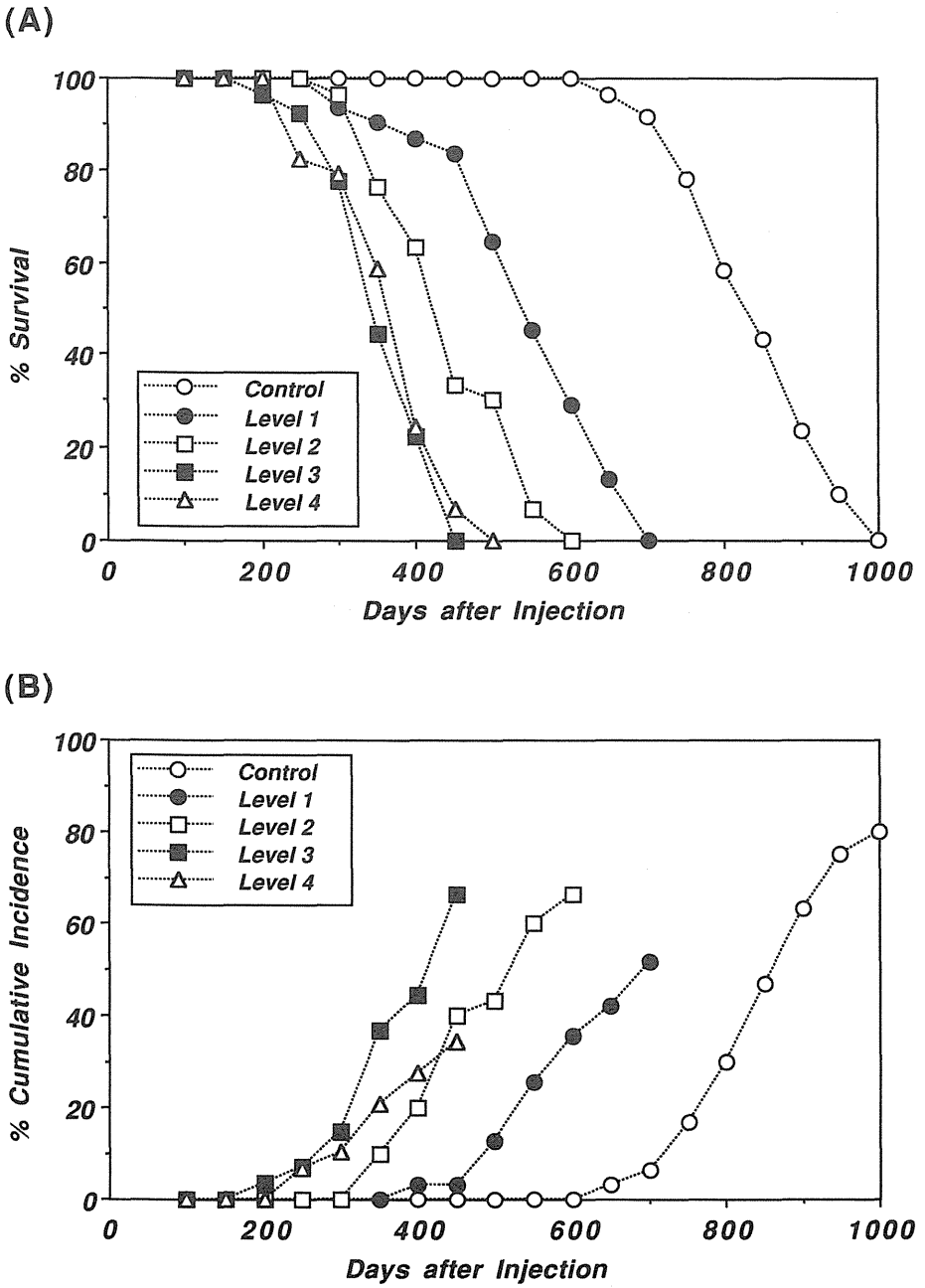

Fig. 1. Survival curves (**A**) and cumulative incidence of neoplasias (**B**) in the controls and mice that received 500 Bq/animal (Level 1), 1000 Bq/animal (Level 2), 5000 Bq/animal (Level 3) or 10000 Bq/animal (Level 4) of ^{239}Pu citrate.

group, as compared to the findings for chronic, non-neoplastic or neoplastic death that occurred among the controls.

Types of tumors and incidence

As shown in Table 2, tumors of the control and ^{239}Pu-injected mice differed in histologic type and frequency. Control mice had a variety of tumors that affected various organs and tissues: adenomas and adenocarcinomas in the lung; hepatocellular or chollangiocellular carcinomas in the liver; lymphoid tumors, including thymic lymphomas and histiocytic lymphomas; cystadenomas or adenocarcinomas and granulosa cell tumors in the ovary; subcutaneous fibrosarcomas and histiocytomas; and miscellaneous tumors, including stomach carcinomas and pancreatic adenomas, but no bone tumors were found. In contrast, there were many bone tumors, mostly osteosarcomas, in all the groups of ^{239}Pu-injected mice, and their crude incidences appeared to depend on the injected dose: 35% in the lowest dose group (Level 1),

Table 2. Types of Tumors in ^{239}Pu Citrate-Injected Mice

	Group				
	Control	Level 1	Level 2	Level 3	Level 4
No. of animals	60	31	30	27	29
All tumors					
No. of animals (%)	48 (80.0)	16 (51.6)	20 (66.6)	18 (66.6)	10 (34.5)
Mean survival±SD	839±85	567±80	452±78	354±67	329±85
Lung tumors					
No. of animals (%)	10 (16.6)	0 (0)	0 (0)	0 (0)	0 (0)
Mean survival±SD	818±84	—	—	—	—
Liver tumors					
No. of animals (%)	13 (21.6)	1 (3.2)	1 (3.3)	0 (0)	0 (0)
Mean survival±SD	801±95	538	583	—	—
Lymphoid tumors					
No. of animals (%)	12 (20.0)	2 (6.4)	1 (3.3)	5 (18.5)	5 (17.2)
Mean survival±SD	820±66	558	461	310±65	254±46
Ovary tumors					
No. of animals (%)	23 (38.3)	9 (29.0)	4 (13.3)	0 (0)	0 (0)
Mean survival±SD	867±80	562±97	491±95	—	—
Subcutaneous tumors					
No. of animals (%)	10 (16.6)	0 (0)	0 (0)	0 (0)	0 (0)
Mean survival±SD	858±55	—	—	—	—
Bone tumors					
No. of animals (%)	0 (0)	11 (35.5)	18 (60.0)	13 (48.1)	5 (17.2)
Mean survival±SD	—	550±76	444±75	371±59	403±35
Miscellaneous tumors					
No. of animals (%)	7 (11.6)	0 (0)	0 (0)	0 (0)	0 (0)
Mean survival±SD	790±77	—	—	—	—

Values indicate the incidence of tumors (% in parenthese) and the survival time (day) in each group.

60% in a low dose group (Level 2), 48% in a high dose group (Level 3), and 17% in the highest dose group (Level 4). Lymphoid tumors also were found in ^{239}Pu-injected mice, but the crude incidence was much lower (3–6%) in lower dose groups (Levels 1 and 2) and were similar (17–18%) to the incidence for the control (20%) in both higher dose groups (Level 3 and 4). Of the lymphoid tumors, thymic lymphomas, however, were not found in all the groups of ^{239}Pu-injected mice, rather lymphocytic lymphomas and lymphocytic leukemia were particularly increased in higher dose groups (Levels 3 and 4) as compared to the control group. Other soft tissue tumors such as ovary cystadenomas and hepatocellular carinomas, were noted only in lower dose groups (Levels 1 and 2)(Table 2). The major types of tumors commonly observed in ^{239}Pu-injected mice therefore were osteosarcomas and lymphoid tumors, both of which occurred much earlier than in the controls, whereas other soft tissue tumors are suspected to occur spontaneously in both the control group and lower dose groups of ^{239}Pu-injected mice. Moreover neither myeloid leukemia nor such other myelogenous tumors as myelomas were found in the control and ^{239}Pu-injected mice.

Skeletal dose in relation to the incidence of bone and lymphoid tumors

Although all of the animals with bone tumors or lymphoid tumors are within the wide range of cumulative mean skeletal doses from 2.4 to 46 Gy, the crude incidences appeared to be dose-dependent (Fig. 2). No bone tumors occurred at 0 Gy (control), the incidence being 36% at 3 Gy and maximum level (70%) at 10 Gy, after which it decreased to 48% or less at 20 Gy or more. In contrast, the incidence of lymphoid tumors was much lower (4–6%) at 3–5 Gy than for the controls (20%), increasing to the maximum of 17–19% at 20 Gy or more. The occurrence of

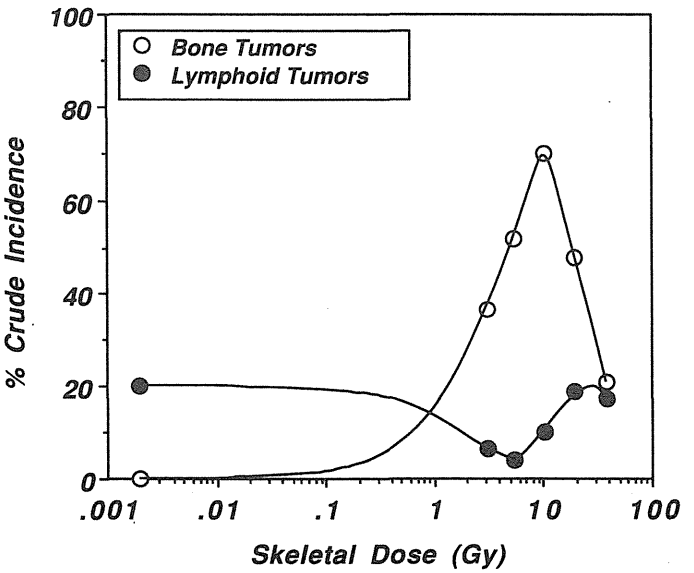

Fig. 2. Crude incidence of bone tumors (open circles) and lymphoid tumors (closed circles) in mice as a function of the cumulative mean skeletal dose (Gy) after the injection of ^{239}Pu citrate.

bone tumors therefore appeared to be maximal at a dose of less than 10 Gy, whereas lymphoid tumors appeared to be decreased at a dose of less than 10 Gy, and to increase to almost the same value as that of the controls at a dose of more than 20 Gy. Differences in the dose vs. crude incidence between bone and lymphoid tumors also were demonstrated by characterizing their distributions, types of malignancies, and occurrence sites or histologic types for different skeletal dose ranges (Table 3). Of the 47 osteosarcomas, 29 (62%) were distributed in the cumulative skeletal dose range of less than 10 Gy, 13 (27%) at 15–25 Gy, and only 5 (10%) at 40 Gy or more. Although osteosarcomas that occurred at a single bone (single occurrence) mainly were distributed in the dose range of 10 Gy or less, those that occurred at two or more places of the bones (multiple occurrence) were mainly in the range of 15–25 Gy. Malignancies of osteosarcomas, based on size (microscopic or macroscopic) and metastasis to other organs and tissues including the lung and liver, were the highest in mice that received 5–10 Gy as this range showed the most cases of macroscopic size and metastasis. Although no differences in the occurrence sites of osteosarcomas were found between the dose ranges, most of the tumors were located at the vertebrae (especially the thoracic and lumbar vertebrae), femurs, tibiae, humeri and scapulae and not so frequently at the ischium, pelvis, sternum, and ribs. No osteosarcomas

Table 3. Distributions of Malignancies or Histologic Types of Bone and Lymphoid Tumors in ^{239}Pu Citrate-Injected Mice that Received Different Skeletal Doses

	Cumulative Skeletal Dose Range (Gy)					
	0	<5	5–10	15–25	30–40	40<
Osteosarcomas						
Total	0	12	17	13	0	5
Single occurrence	0	8	9	3	0	4
Multiple occurrence	0	4	8	10	0	1
Microscopic size	0	4	5	5	0	1
Macroscopic size	0	8	12	8	0	4
Metastasis	0	0	3	0	0	0
Site at femur and tibia	0	4	7	8	0	2
humerus and scapula	0	2	4	6	0	4
vertebra	0	7	8	7	0	0
ischium and pelvis	0	2	1	1	0	0
sternum and rib	0	1	3	0	0	0
Lymphoid tumors						
Total	12	3	0	7	3	0
Thymic lymphoma	5	0	0	0	0	0
Lymphocytic lymphoma	3	2	0	5	2	0
Histiocytic lymphoma	4	1	0	0	1	0
Lymphocytic leukemia	1	2	0	6	0	0

Values indicate the number of tumors per mean skeletal dose as shown in each category, characterizing the distribution and malignancies for bone tumors and distribution of histologic types for lymphoid tumors.

were found at the cranium or radii. The osteosarcomas in ^{239}Pu-injected mice therefore mostly occurred at the vertebral and long bone sites, showing single occurrence and more malignant features at a dose of 10 Gy or less.

In contrast, 10 (77%) of the 13 lymphoid tumors were distributed in the dose range of more than 15 Gy, only 3 (23%) being found at 10 Gy or less (Table 3). The most frequent histologic types were lymphocytic lymphomas and leukemias in the dose range of 15–25 Gy (average 19.8 Gy). No thymic lymphomas and only a few histiocytic lymphomas, however, were found for any dose range. Lymphoid tumors in ^{239}Pu-injected mice therefore were mostly non-thymic lymphomas accompanied by lymphocytic leukemia and were most frequently distributed in mice that received 20 Gy or more.

DISCUSSION

Our findings show that life-shortening associated with acute occurrence of bone tumors and lymphoid tumors predominated after the injection of relatively higher doses of ^{239}Pu citrate estimated as being between 3 and 40 Gy for the cumulative mean skeletal dose, as compared to the control mice that molstly died much later due to spontaneous neoplasias, such as lymphoid tumors and other soft tissue tumors, but not bone tumors. Whereas non-neoplastic but acute hemopoietic dysplasias also appeared to be related to life-shortening in the highest dose group (Level 4) injected with 10000 Bq/animal, a skeletal dose of 40 Gy, in the lowest dose group (Level 1) injected with 500 Bq/animal, a skeletal dose of 3 Gy, non-neoplastic disorders such as chronic hepatosis and nephritis as well as other soft tissue tumors are considered to have been mostly spontaneous, incidental disorders as in the controls. As a result in combination with the neoplastic and non-neoplastic disorders, survival time was reduced markedly in a dose-dependent manner by ^{239}Pu-injection. Although the magnitude of the reduction of survival time is much greater in our experiments than that reported elsewhere (3, 5, 12), we could not determine from these results whether survival would be protracted at much lower doses than the injected amount of 500 Bq/animal, a skeletal dose of 3 Gy, used.

The crude incidence of osteosarcomas increased, reaching a maximum at the mean skeletal dose of 10 Gy or less, but it decreased at 20 Gy or more; whereas, the crude incidence of lymphoid tumors was much lower than that of the controls at 5–10 Gy but increasing almost to the same level as that of the controls at 20 Gy or more. The induction of lymphoid tumors in other strains of mice by injection of ^{239}Pu has been reported, but the incidence of reticular tumors in CF-1 mice did not exceed the spontaneous level of the controls at any of the doses injected (12), and generalized (non-thymic) lymphoma has been found but at a lower incidence in CBA/H strain mice that received a high cumulative bone marrow dose of 25–75 Gy, which could not induce significantly more bone tumors (10). These and our findings show that bone and lymphoid tumors are induced by different skeletal ^{239}Pu dose ranges. Otherwise, the induction of lymphoid tumors would be overwhelmed by bone tumors; for example, the incidence of lymphoid tumors in our study which appeared to be suppressed in the dose range of 5–10 Gy by a high incidence of bone tumors, in as much as the lymphoid tumors occurred

spontaneously with a relatively higher incidence (20%) in the controls. Even though the crude incidence of lymphoid tumors did not exceed that of the controls in our experiments, their histologic types as well as the time of occurrence after ^{239}Pu-injection differed. Lymphomas accompanied by lymphocytic leukemia, classified as non-thymic or generalized lymphomas (10), were more acutely and highly induced in mice that received a mean skeletal dose of 15–20 Gy, whereas thymic lymphomas and histiocytic lymphomas were more frequent at later periods in the lefetime of the control mice. As the external irradiation by X- or γ-radiation induces thymic lymphomas and leukemias more frequently and more effectively if given in fractionated exposures to C57BL strain mice (13) and high LET neutrons induce leukemias and other tumors more rapidly if given as single or fractionated exposures (14), the differences in the frequencies and types of lymphoid tumors induced by low LET radiations as compared to by high LET radiations, including alpha-particle, may reflect underlying mechanisms which differ in dose- and dose rate-effectiveness for radiation-induced carcinogenesis.

Finally, neither myeloid leukemia nor such myelogenous neoplasias as myelomas were found in our experimental mice after the injection of 500 Bq/animal or more of ^{239}Pu, skeletal doses of more than 3 Gy. Because osteosarcomas predominated at vertebral and long bone sites which are rich in trabecular bones and bone marrow, as shown in the studies done on beagle dogs (15, 16), bone marrow stem cells, the progenitors for leukemogenic cells, located near the surrounding trabecular bone surfaces should be exposed internally to alpha-particles from ^{239}Pu deposited (1). Significant but small yields of myeloid leukemia have been found in CBA/H strain mice injected with much lower doses of ^{239}Pu than we used (5), although even protraction of the alpha-dose by multiple injections of smaller amounts of ^{239}Pu did not significantly increase the incidence of myeloid leukemia in comparison to a single injection. Myeloid leukemia also has been induced in the rat by a single or multiple injections of relatively high doses of ^{239}Pu, but the incidences for both types of injections were very low (6, 17). Therefore, myeloid leukemia seems not to be induced by ^{239}Pu, whether as a single, low dose injection or multiple injections of a lower dose rate. Although it has not been determined what radiation dose or dose rate from ^{239}Pu is essential for the induction of myeloid leukemia, our and other results (5, 10) suggest that very low doses would be required for significant yields of myeloid leukemia, whereas relatively high doses would induce osteosarcomas or non-thymic leukemic lymphomas in a dose-dependent manner but competitively. The mechanisms that underly the onset of hematopoietic tumors induced differentially from osteosarcomas by different doses of ^{239}Pu have yet to be fully elucidated. As reported in a review on the molecular basis of radiation-induced carcinogenesis (13), thymic lymphomas proceed through an indirect mechanism and frequently are associated with the expression of recombinant proviruses as well as osterosarcomas, whereas myeloid leukemia is characterized by a very early initiating event, the rearrangement and/or deletion of chromosome 2, which leads to leukemogenesis. One plausible explanation for much lower frequencies of myeloid leukemia produced by ^{239}Pu is that proleukemic cells, if initiated, might subsequently be sterilized by high LET alpha-radiation as supposed elsewhere (5). The frequency of chromosomal abberations in bone marrow cells, however, has been shown to increase early after ^{239}Pu-injection and to tend to decrease at later periods (18), whereas bone marrow hemopoietic progenitor cells (CFU-S) persistently decrease in number during the longer period

of 1–2 years, except for a recovery 3–6 months after exposure to ^{239}Pu (19). These findings indicate the possibility that bone marrow stem cells, at least in part receive sublethal damage that leads eventually to malignancies rather than their receiving lethal damage and subsequent sterilization. The mechanisms for the induction of myeloid leukemia by alpha-particles are complicated ones, but could indirectly involve interaction with stromal cells leading to the full development of leukemia as shown with external low LET radiations (20).

Although of too limited size to be able to estimate the dose-response for carcinogenesis caused by injected ^{239}Pu, our study indicates the differential induction of osterosarcoma and non-thymic lymphoma, but not myeloid leukemia, is dependent on cumulative skeletal doses in C3H mice. Further studies are needed to investigate differences in the spectrum of tumor types that occur at very low doses of injected ^{239}Pu.

ACKNOWLEDGEMENT

This work was supported by a grant from the Research Fund for Project Research on Risks Due to Low Level Radiation Exposure to the General Population of Japan Science and Technology Agency. The authors greatly appreciate Animal Cares, Co. and Tokyo Nuclear Services, Co., respectively for the help of animal cares and radiation protections.

REFERENCES

1. Bleaney, B. (1969) Plutonium deposition on bone surfaces and in bone marrow following intravenous and intramuscular injections. *In* Delayed Effects of Bone-Seeking Radionuclides, eds. C. W. Mays, W. S. S. Jee, R. D. Lloyd, B. J. Stover, J. H. Dougherty and G. N. Taylor, The University of Utah Press, Salt Lake City, Utah, pp. 125–135.
2. Mays, C. W., Dougherty, T. F., Taylor, G. N., Lloyd, R. D., Stover, B. J., Jee, W. S. S., Christensen, J. H., Dougherty, J. H., and Atherton, D. R. (1969) Radiation-induced bone cancer in beagles. *In* Delayed Effects of Bone-Seeking Radionuclides, eds. C. W. Mays, W. S. S. Jee, R. D. Lloyd, B. J. Stover, J. H. Dougherty and G. N. Taylor, The University of Utah Press, Salt Lake City, Utah, pp. 387–408.
3. Taylor, G. N., Mays, C. W., Lloyd, R. D., Gradner, P. A., Talbot, L. R., McFarland, S. S., Pollard, T. A., Atherton, D. R., van Moorhem, D., Brammer, D., Brammer, T. W., Ayoroa, G., and Taysum, D. H. (1983) Comparative toxicity of ^{226}Ra, ^{239}Pu, ^{241}Am, ^{249}Cf and ^{252}Cf in C57BL/Do black and albino mice. Radiat. Res. **95**, 584–601.
4. Mays, C. W., Taylor, G. N., and Lloyd, R. D. (1986) Toxicity ratios: their use and abuse in predicting the risk from induced cancer. *In* Life-Span Radiation Effects Studies in Animals: What Can They Tell Us? eds. R. C. Thompson and J. A. Mahaffey, US DOE CONF-830951, pp. 299–310.
5. Humphreys, E. R., Loutit, J. F., and Stones, V. A. (1987) The induction by ^{239}Pu of myeloid leukemia and osteosarcoma in female CBA mice. Int. J. Radiat. Biol. **51**, 331–339.
6. Taylor, D. M. (1986) The comparative carcinogenesis of ^{239}Pu, ^{241}Am and ^{244}Cm in the rat. *In* Life-Span Radiation Effects Studies in Animals: What Can They Tell Us? eds. R. C. Thompson and J. A. Mahaffey, US DOE CONF-830951, pp. 404–412.
7. Humphreys, E. R., Issacs, K. R., Raine, T. A., Saunders, J., Stones, V. A., and Wood, D. L. (1993)

Myeloid leukemia and osteosarcoma in CBA/H mice given ^{224}Ra. Int. J. Radiat. Biol. **64**, 231–235.
8. McClellan, R. O. and Jones, R. K. (1969) ^{90}Sr-induced neoplasia: a selective review. *In* Delayed Effects of Bone-Seeking Radionuclides, eds. C. W. Mays, W. S. S. Jee, R. D. Lloyd, B. J. Stover, J. H. Dougherty and G. N. Taylor, The University of Utah, Salt Lake City, Utah, pp. 293–322.
9. Mole, R. H., Papworth, D. G., and Corp, M. J. (1983) The dose-response for X-ray induction of myeloid leukemia in male CBA/H mice. Brit. J. Cancer **47**, 285–291.
10. Loutit, J. F. and Carr, T. E. F. (1978) Lymphoid tumors and leukemia induced in mice by bone-seeking radionuclides. Int. J. Radiat. Biol. **33**, 245–263.
11. Lindenbaum, A. and Westfall, W. (1965) Colloidal properties of plutonium in diluted aqueous solution. Int. J. Appl. Radiat. Isotop. **16**, 545–553.
12. Finkel, M. P. and Biskis, B. O. (1962) Toxicity of plutonium in mice. Health Phys. **8**, 565–579.
13. Janowski, M., Cox, R., and Strauss, P. G. (1990) The molecular biology of radiation-induced carcinogenesis: thymic lymphoma, myeloid leukemia and osteosarcoma. Int. J. Radiat. Biol. **57**, 677–691.
14. Maisin, J. R., Wambersie, A., Gerber, G. B., Mattelin, G., Lambiet-Collier, M., DeCoster, B., and Gueulette, J. (1988) Life-shortening and disease incidence in C57B1 mice after single and fractionated γ and high-energy neutron exposure. Radiat. Res. **113**, 300–317.
15. Wronski, T. J., Smith, J. M., and Jee, W. S. W. (1980) The microdistribution and retention of injected ^{239}Pu on trabecular bone surfaces of the beagle: implications for the induction of osteosarcoma. Radiat. Res. **83**, 74–89.
16. Smith, J. M., Miller, S. C., and Jee, W. S. S. (1984) The relationships between bone marrow type and microvasculature to the microdistribution and local dosimetry of plutonium in the adult skeleton. Radiat. Res. **99**, 324–335.
17. Bensted, J. P. M., Chir, B., Taylor, D. M., and Sowby, F. D. (1965) The carcinogenic effects of americium 241 and plutonium 239 in the rat. Brit. J. Radiol. **38**, 920–925.
18. Svoboda, V., Sedlak, A., Kypenova, H., and Bubenikova, D. (1987) Long-term effects of low-level ^{239}Pu contamination on murine bone-marrow stem cells and their progeny. Int. J. Radiat. Biol. **52**, 517–526.
19. Lord, B. I., Molineux, G., Humphreys, E. R., and Stones, V. A. (1991) Long-term effects of plutonium-239 and radium-224 on the distribution and performance of pluripotent hemopoietic progenitor cells and their regulatory microenvironment. Int. J. Radiat. Biol. **59**, 211–227.
20. Naparstek, E., Fitzgerald, T. J., Sakakeeny, M. A., Klassen, V., Pierce, J. H., Woda, B. A., Falco, J., Fitzgerald, S., Nizin, P., and Greenberger, J. S. (1986) Induction of malignant transformation of cocultivated hematopoietic stem cells by X-irradiation of murine bone marrow stromal cells in vitro. Cancer Res. **46**, 4677–4684.

J. RADIAT. RES., 35, 222–235 (1994)

High Incidence of Malignant Lung Carcinomas in Rats after Inhalation of $^{239}PuO_2$ Aerosol

YOICHI OGHISO, YUJI YAMADA, NOBUHITO ISHIGURE, SATOSHI FUKUDA, HARUZO IIDA, YUTAKA YAMADA, HIROSHI SATO, AKIRA KOIZUMI and JIRO INABA

Division of Radiotoxicology, National Institute of Radiological Sciences, 9-1, 4-chome, Anagawa, Inage-ku, Chiba 263, Japan

(*Received, August 1, 1994*)
(*Revision received, September 19, 1994*)
(*Accepted, October 11, 1994*)

Inhalation/carcinogenesis/$^{239}PuO_2$/aerosol/lung dose

Female Wistar strain rats were exposed to a single inhalation of a submicron-size aerosol of high-fired $^{239}PuO_2$ to investigate pulmonary carcinogenesis during lifespan periods. The absorbed lung doses of the exposed anmals ranged from 0.6 to 12 Gy and were well correlated with the initial lung deposition (ILD) of 0.1 to 2.3 kBq. Survival and induction of primary lung tumors in 116 exposed rats were compared with those in 56 untreated control rats in respect to lung doses received. Mean survival time was greatly reduced, and the cumulative incidence of total lung tumors was markedly increased to 90–100% in rats that received more than 4 Gy, whereas of the controls only one animal (1.8%) died of primary lung tumors. Primary but benign adenomas were present in exposed animals given 1.0 Gy or less, and the incidence of adenomas was 22–25% at 4–5 Gy, but decreased sharply to 3–5% at 6–8 Gy. In contrast, no malignant carcinomas, including adenocarcinomas, adenosquamous carcinomas and squamous cell carcinomas, developed at a dose of less than 1.0 Gy, whereas they were present in 75% or more of the rats given 4–10 Gy, but only in 55% at 12 Gy. Although there were no clear differences in the dose and time required for induction among the carcinoma types, all tended to develope in earlier periods after inhalation than adenomas. Despite the limited number of exposed animals that received lower doses, results suggest that malignant lung carcinomas are highly and early induced and have a different dose-effect relationship than benign adenomas at doses of more than 1 Gy after inhalation exposure to $^{239}PuO_2$.

INTRODUCTION

In relation to radiation protection, it has been proposed that some linear dose-effect relationships are without a threshold in radiation-induced carcinogenesis (1). A number of studies on experimental carcinogenesis induced by internally deposited radionuclides, however, indicate the presence of some threshold-like dose ranges which would not be needed to induce

小木曽洋一：放射線医学総合研究所内部被ばく研究部，千葉市稲毛区穴川4-9-1　〒263

significant or excessive increases in the incidence of tumors in exposed animals as compared to that of the spontaneous tumors found in sham-exposed or vehicle controls. For example, in beagle dogs by injection or ingestion of ^{90}Sr, a beta-emitting bone-seeking radionuclide, induces bone tumors at a threshold skeletal dose of more than 20 Gy (2, 3). Another bone-seeker, alpha-emitting ^{226}Ra, also induces bone tumors but at a threshold skeletal dose of 1.1 Gy for mice and 0.5 Gy for dogs (4). Other alpha-emitting radionuclides such as ^{241}Am and ^{228}Th produce much higher incidences of bone tumors than ^{226}Ra, and their dose responses would most likely fit a quadratic model with a threshold (2). For bone tumor induction in beagle dogs by injection of ^{239}Pu, the most toxic transuranic alpha-emitter (5), however, there is no evidence that a threshold actually is present even at doses much lower than 0.1 Gy (6).

Inhalation exposure to various alpha-emitting radionuclides after occupational accidents or environmental contamination would result in the highest risk for lung cancer induction in people. Experiments using rats indicate that the inhalation of high-fired transuranic compounds such as $^{244}CmO_2$ (7) and $^{241}AmO_2$ (8) or environmentally air-borne radon daughters (9) induce lung tumors with a stochastic dose-responsiveness but with a threshold-like dose range. The estimated lung cancer risk for high-fired $^{239}PuO_2$ obtained from lifespan studies in beagle dogs, was assumed to be about 12-fold less than that for $^{239}Pu(No_3)_4$ but 4-fold higher than that for $^{238}PuO_2$ and fit a pure quadratic model rather than a pure linear one (10, 11). Sanders et al. (1993) have proposed a "practical" threshold at the low dose of 1 Gy or more for the induction of malignant lung tumors in rats after inhalation of high-fired $^{239}PuO_2$ aerosol (12). In as much as risk assessments for lung carcinogenesis caused by inhaled radionuclides are based on dose-effect ralationships without extrapolation, most results of lifespan animal studies suggest some quadratic dose-responses with a threshold in the low dose ranges.

We report summarized data obtained from lifespan studies of lung tumor induction in rats after inhalation exposure to high-fired $^{239}PuO_2$ aerosol to clarify the relationship between lung doses and lung tumor incidence. Although the sizes of our experimental groups are insufficient for estimating dose-effect ralationships at dose levels much lower than 1.0 Gy, data on the incidence of lung tumors in rats that received a dose of 1 to 10 Gy are available for comparison with values reported elsewhere (12). Our results indicate that there are differences in the incidence and occurrence of malignant carcinomas and benign adenomas induced in this dose range.

MATERIALS AND METHODS

Experimental animals and cares

Young adult (60-to 70-day-old), female Wistar strain (W/M) rats, purchased from our breeding facility, were fed with a commercial diet and water *ad libitum* under the condition of barrier-filtered air before and after the experiments described below. All the animals were trained daily for at least 2 weeks prior to inhalation exposure to breathe air from a hole of plastic hand-made holders for nose-only inhalation exposure without anesthesia. Twenty healthy, tame rats (100- to 150-day-old, weighing 180–210 g) were selected for each experiment and exposed

once for a maximum of 60 min to $^{239}PuO_2$ aerosol in a multiport nose-only inhalation chamber device. Immediately after inhalation, all the exposed animals were wiped around the nose with wet gauze to decontaminate any radioactivity on the skin, after which they were housed five per cage and kept in a glove-box type closed hood rack during their lifetimes. Unexposed, age-matched animals, the lifespan controls, also were housed five per cage and kept in a closed hood rack. Totally 130 exposed and 60 control animals were used in the study. The animal rooms were maintained on a 12 hr-daylight cycle with an air temperature of $23\pm1.0^{\circ}C$ and a humidity of $55\pm5.0\%$. The animals were changed to new clean cages weekly and their daily conditions were monitored for survival and immediate pathological examinations.

Aerosol generation and assessment

Part of a stock solution of plutonium nitrate was treated chemically to obtain a colloidal suspension of plutonium hydroxide in HCl solution. This solution was nebulized in a compressed air-driven nebulizer and passed through a tube heated at 300°C to dry the droplets in air then conducted into a high temperature furnace heated to 1150°C to oxidize the dried particles. An air flow containing the high-fired $^{239}PuO_2$ particles was introduced through negative pressure by an exhaust air-pump into a multiport inhalation chamber in which 20 animals in a nose-only holder had been settled. Aerosol samples were collected simultaneously on 10-stage plates by a cascade impactor in order to determine the particle size distribution and to measure the radioactivity by counting the low energy LX-ray (17 keV in average) emitted from ^{239}Pu as described elsewhere (13). The activity median aerodynamic diameter (AMAD) ranged from 0.3 to 0.5 μm with a geometric standard deviation of 1.9–2.0 in a total of 6 experiments, indicative of the generation of polydispersed, but submicron-size, aerosol particles.

Determinations of initial lung deposition and lung dose

As previously reported (13), the initial lung deposition (ILD) was determined individually from the whole-body count of the low energy LX-rays (17 keV) emitted from ^{239}Pu present in the lung 6–8 days after inhalation, and by correcting the whole-body count values to the day 0 values by multipling by a factor of 1.07 or 1.08 in accordance with the lung retention curve obtained from the long-term and follow-up counting. Actual lung retention (R(t), where t is days after inhalation) is given by:

$$R(t)=0.766e^{-0.0131t}+0.234e^{-0.000873t}$$

The cumulative dose absorbed in the entire lung mass was calculated at death, based on ILD (Bq); the above lung retention function R(t), where t is days after inhalation; the lung weight (kg) given by the function below (L(t), where t is days after inhalation); and the survival time (day). Lung dose at death (D(T), where T is survival time) for individual exposed animal is given by;

$$D(T)=7.119\times10^{-8}\times ILD\times\int_0^T R(t)/L(t)dt$$

$$L(t)=-1.5197\times10^{-8}t^2+9.30967\times10^{-6}t+0.00102806$$

Pathological examinations

Gross and histological examinations were done to analyze the cause of death, lung tumor incidence, and tumor types. Of the 130 exposed animals, the 14 were omitted from the analysis for compelling reasons. These include six rats that died by choking immediately after the cessation of inhalation exposure, four that died accidentally due to aspiration pneumonitis and clearly not due to plutonium-related disorders 80–90 days after inhalation, and four that lost their lungs due to cannibalism after lifespan death. Four of the 60 control rats also were omitted from the analysis because severe autolysis rendered them unavaiable for histologic observations. A total of 116 exposed and 56 control animals were therefore given pathological examinations. At autopsy, a search for gross lesions was made on the trachea, bronchi, all the lung lobes, and tracheobronchial lymph nodes (TBLN), as well as thymus, heart, liver, spleen, kidneys, pancreas, alimentary tracts, ovaries, uterus, adrenal glands, salivary glands, superficial and mesenteric lymph nodes, femoral and vertebral bones including bone marrow, and mammary glands, if mammary tumors were grossly observed. Each tissue in which gross lesions were present was fixed in 10% phosphate-buffered formalin then dissected into small pieces. After being processed with graded ethanol in an automatic tissue processor and embedded in paraffin, 5–6 μm-thick sections were stained with hematoxylin and eosin for light microscopic examination.

In the diagnosis of lung tumors, a careful distinction between primary and metastatic tumors, especially the mammary gland tumors, was made. In the case of primary lung tumors, they were assessed as benign or malignant according to the WHO criteria (14). As a result, a few of the controls showed metastatic lung tumors from such tissues as mammary glands, but no metastatic lung tumors were noted in exposed rats based on the definition of histologic types different from those of the other tissues. The primary lung tumors classified in this study were benign adenomas and malignant tumors such as adenocarcinomas, adenosquamous carcinomas, squamous cell carcinomas, fibrosarcomas, and hemangiosarcomas.

RESULTS

Survival time and lung dose

As shown in Table 1, the 116 exposed rats were divided into eight groups based on different mean lung doses form 0.64 to 20.3 Gy together with 56 controls (0 Gy). Of these groups, only two animals were included in the lowest group (0.64 Gy), and only one animal in the highest group (20.3 Gy), the remaining exposed rats being distributed in six groups with mean doses of 4.54–12.0 Gy. The mean values of the initial lung deposition (ILD), ranged from 93 Bq to 2.3 kBq, are well correlated with the mean lung doses ($r=0.992$; Fig. 1). As compared to the mean survival time for all the control rats (849 ± 116 days), the survival time for the exposed animals with the lowest dose did not differ, whereas the survival times for the exposed rats at doses of 4.54–12.0 Gy were greatly reduced to about 400–650 days, which correlated well with the increased doses ($r=0.982$; Fig. 2). The mean survival time for the exposed rats that received doses of more than 4.54 Gy and had primary, malignant or benign lung tumors did not differ

Table 1. Lung Doses, Initial Lung Deposition (ILD), Survival Time and Lung Tumors in $^{239}PuO_2$-Inhaled Rats

Dose (Gy)	ILD (Bq)	No. of Rats	Survival Day for Cases of									
			Total	Primary LT		Metastatic LT		Malignant LT		Benign LT		Others	
0	0	56	849±116	(56)	777	(1)	934±89	(4)	903±102	(5)		904±81	(11)
0.64±0.03	93±5	2	798±27	(2)	771	(1)					771	(1)	
4.54±0.34	756±93	24	654±89	(24)	654±89	(24)			664±84	(18)	624±97	(6)	653±78 (4)
5.36±0.27	938±83	18	595±101	(18)	595±101	(18)			594±103	(15)	598±86	(3)	
6.54±0.25	1140±123	28	537±81	(28)	549±74	(25)			548±76	(24)	576	(1)	535±137 (3)
7.71±0.51	1438±201	18	501±90	(18)	518±58	(17)			519±59	(16)	499	(1)	587±22 (2)
9.06±0.26	1829±204	16	433±86	(16)	454±40	(14)			454±40	(14)			477 (1)
12.0±1.80	2360±351	9	399±140	(9)	483±65	(6)			483±65	(6)			557 (1)
20.3	3065	1	630	(1)	630	(1)			630	(1)			630 (1)

Values indicate mean±SD for the number of animals in parenthese. LT: lung tumors, including primary or metastatic ones from other sites, Others: tumors, including mammary gland tumors other than primary lung tumors.

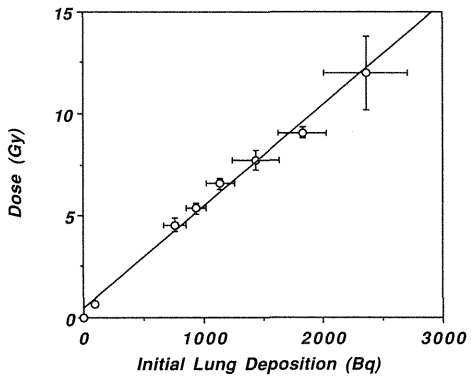

Fig. 1. Relationship between the mean initial lung deposition (ILD) of inhaled $^{239}PuO_2$ and the mean lung dose received during the survival time for all exposed rats. Bars: ±SD.

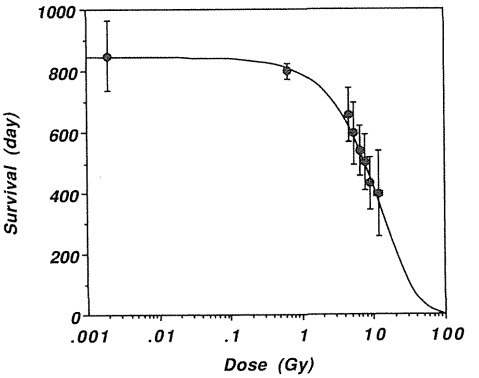

Fig. 2. Relationship between the mean survival time and the mean lung dose received for all exposed rats after inhalation of $^{239}PuO_2$. Bars: ±SD.

much from that for the total exposed animals, but it showed a significant decrease than the value for the control group in which only one animal died later (at 777 days) of primary, malignant lung tumor, and four animals died much later (at 934 days) due to malignant lung tumors that had metastasized from other organs such as the mammary glands (Table 1). Of the two exposed animals that received 0.64 Gy, one died of primary lung tumors, the other due to pulmonary fibrosis. Only a few of the exposed animals given a dose of more than 6.54 Gy died early of severe pulmonary edema or pneumonitis, none of lung tumors. None of the exposed rats had

metastatic lung tumors. The mean survival time for 11 control animals (19%) that had tumors other than primary lung tumors (eg., mammary gland tumors) was much longer than that for total 12 exposed animals (10%) that had other tumors (Table 1). These results strongly suggest that the significant decrease in the survival times of exposed rats given lung doses of 4.5 Gy or more was mainly due to the occurrence of primary lung tumors, not of the other tumors that were incidental and non-fatal. This was confirmed by the survival curves and the cumulative incidence curves for primary lung timors that were obtained from the controls and each group

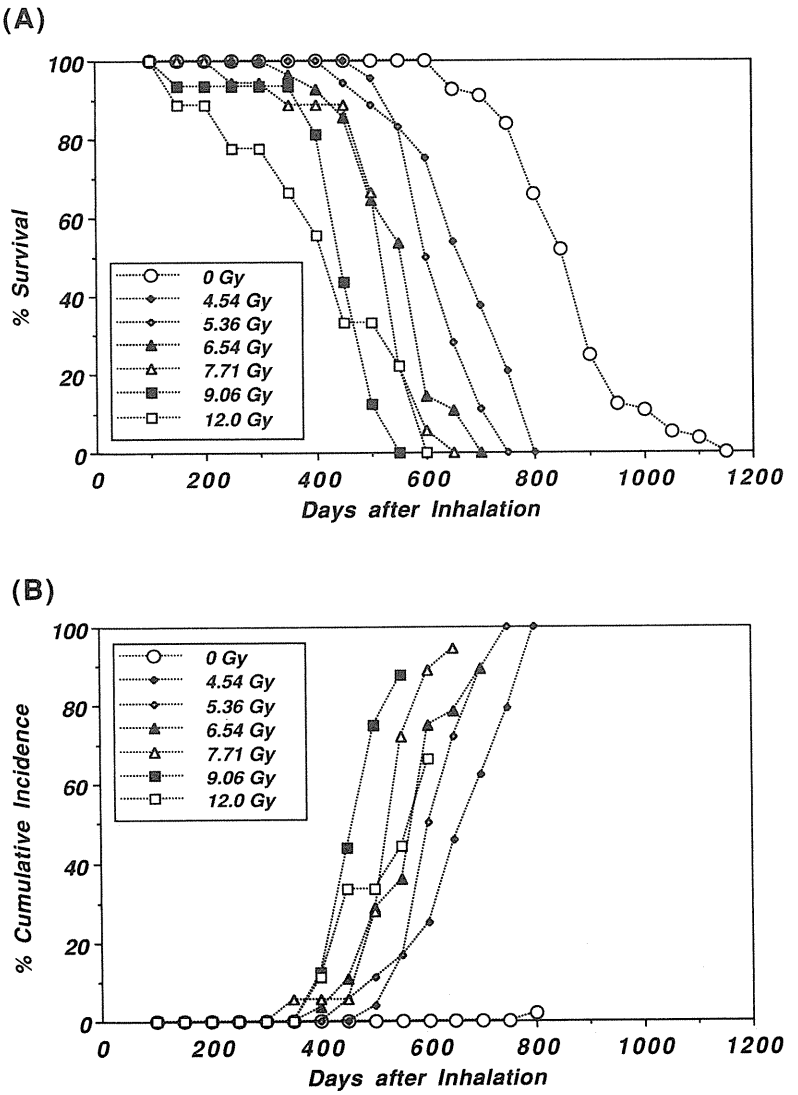

Fig. 3. Survival curves (**A**) and cumulative incidences of all lung tumors (**B**) for the control and the exposed groups of rats that received different doses as a function of days after inhalation of $^{239}PuO_2$.

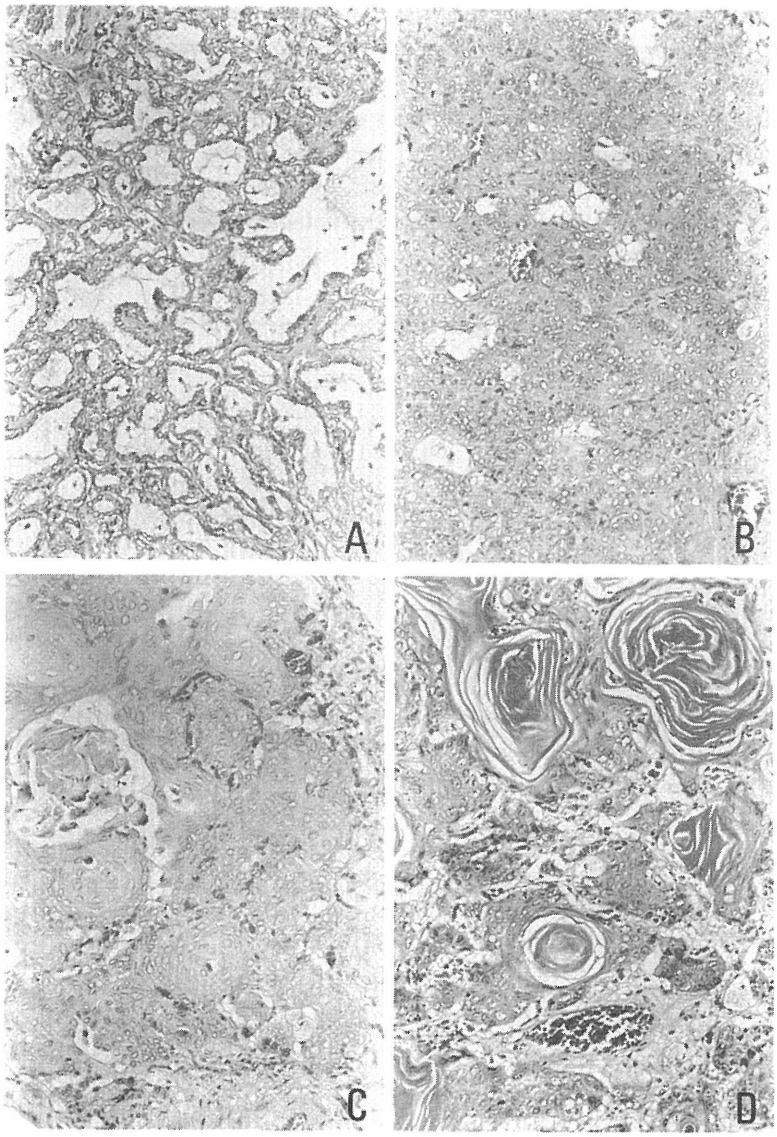

Fig. 4. Photomicrographs of representative histologic types of primary lung tumors found in exposed rats after inhalation of $^{239}PuO_2$. Hematoxylin and eosin stain at lower power magnification of $\times 100$. (**A**) adenoma with papillary growth in a bronchioloalveolar region of a rat given 5.47 Gy and died at 706 days, (**B**) adenocarcinoma with invasive growth in a bronchioloalveolar region of a rat given 6.53 Gy and died at 580 days, (**C**) adenosquamous carcinoma with non-keratinized epidermoid cells of a rat given 4.67 Gy and died at 761 days, (**D**) squamous cell carcinoma with keratinized epithelial pearl structure of a rat given 14.8 Gy and died at 562 days.

within the mean doses from 4.54 Gy to 12.0 Gy (Fig. 3). Thus, animal death first occurred approximately 150 to 500 days after inhalation, and the length of survival dropped sharply between 550 and 750 days as the doses increased in comparison to the control curve in which the first death was noted at 650 days and the survival dropped gradually up to 1150 days (Fig. 3A). Similarly, the cumulative incidence curve for primary lung tumors in the exposed groups showed a rapid increase to 90–100% between 300 and 750 days after inhalation as the doses increased, whereas the controls showed only a 1.8% increase at about 800 days (Fig. 3B).

Types of primary lung tumors and lung dose

Primary lung tumors in the control and exposed rats were classified mainly into the four histological types, as shown in Fig. 4: 1) adenomas consisting of one or a few layers of relatively well differentiated cuboidal or columnar epithelium lining the terminal and respiratory bronchioles or alveoli, and associated with papillary growth and a variety of differentiations such as into secretory and ciliated epithelium (Fig. 4A); 2) adenocarcinomas which consisting of multilayers of large, irregular-shaped epithelium lining the bronchiolar and alveolar spaces and growing invasively into the bronchioloalveolar or surrounding connective tissue stromas (Fig. 4B) ;3) adenosquamous carcinomas having adenocarcinoma structures with non-keratinized epidermoid cells (Fig. 4C); 4) squamous cell carcinomas consisting multilayers of stratified and squamous epithelium associated with keratinization and epithelial "pearl" structures and lining the bronchial or bronchiolar spaces of relatively upper respiratory tracts (Fig. 4D). In some instances, there were metaplastic variations between these types of carcinomas, as in adenomas accompanied by adenocarcinomatous metaplasias, adenocarcinomas accompanied by adenosquamous metaplasias, or adenosquamous carcinomas accompanied by squamous metaplasias. In most cases, pulmonary fibrosis and the inflammatory exudation of macrophages, granulocytes and lymphocytes were observed around these tumor lesions. In addition to these four types of epithelial-origin tumors, a few of the exposed rats had tumors of non-epithelial origin such as fibrosarcomas and hemangiosarcomas, which we classified as other types of malignant lung tumors.

On the basis of the histological criteria described above, the primary lung tumors found in the different dose groups as well as in the controls were divided into five types. The crude incidence of each tumor type is shown in Table 2. Although the crude incidence of all primary lung tumors in the control group (0 Gy) was only 1.8% (squamous cell carcinoma), it increased to 100% in both the groups of 4.54 and 5.36 Gy, and was substantially higher (88–94%) in the groups of 6.54, 7.71 and 9.06 Gy, but slightly reduced to 66% in the group of 12.0 Gy. Primary lung tumors were markedly induced in exposed rats that received doses of less than 10 Gy, but among them the crude incidence of benign adenomas in each dose group differed from that of malignant carcinomas that included adenocarcinomas, adenosquamous carcinomas, and squamous cell carcinomas. Benign adenomas were found even at a dose of 0.64 Gy, and the crude incidence was 22–25% at 4.54 or 5.36 Gy, but this decreased sharply to 3–5% at 6.54 Gy or more. In contrast, none of the types of malignant carcinomas were found at a dose of less than 1.0 Gy, but were about 75–87% at 4.54–9.06 Gy, being decreased to 55% at 12.0 Gy. No clear differences in incidence vs. dose were found among the carcinoma types in the exposed

Table 2. Doses and Primary Lung Tumor Types in $^{239}PuO_2$-Inhaled Rats

Mean Dose (Gy)	No. of Rats	No. of LT(%)											
		All LT		Adenoma		AC		ASC		SC		All Carcinomas		Others	
0	56	1	(1.8)	0	(0)	0	(0)	0	(0)	1	(1.8)	1	(1.8)	0	(0)
0.64	2	1	(50.0)	1	(50.0)	0	(0)	0	(0)	0	(0)	0	(0)	0	(0)
4.54	24	24	(100)	6	(25.0)	8	(33.3)	9	(37.5)	1	(4.1)	18	(75.0)	0	(0)
5.36	18	18	(100)	4	(22.2)	5	(27.8)	7	(38.9)	2	(11.1)	14	(77.8)	0	(0)
6.54	28	25	(89.3)	1	(3.6)	7	(25.0)	13	(46.4)	3	(10.7)	23	(82.1)	1	(3.6)
7.71	18	17	(94.4)	1	(5.5)	6	(33.3)	9	(50.0)	0	(0)	15	(83.3)	1	(5.5)
9.06	16	14	(87.5)	0	(0)	7	(43.7)	6	(37.5)	1	(6.2)	14	(87.5)	0	(0)
12.0	9	6	(66.6)	0	(0)	3	(33.3)	1	(11.1)	1	(11.1)	5	(55.5)	1	(11.1)
20.3	1	1	(100)	0	(0)	0	(0)	1	(100)	0	(0)	1	(100)	0	(0)

Values indicate the number of animals with the percentage in parenthese. LT: lung tumors, AC: adenocarcinoma, ASC: adenosquamous carcinoma, SC: squamous cell carcinoma, Others: other LT, including fibrosarcoma and hemangiosarcoma.

animals, whereas either adenocarcinomas or adenosquamous carcinomas increased to about 50% in the dose range of 6.54–9.06 Gy as compared to the low incidence (11%) of squamous cell carcinomas (Table 2). The incidences of the other types of malignant tumors including fibrosarcomas and hemangiosarcomas were much lower at doses of more than 6.54 Gy.

A comparison of the cumulative incidence of the tumor types showed that all of carcinomas in the groups that received doses of more than 5.36 Gy appeared at earlier time (from 250 to 400 days after inhalation) and increased more rapidly as the doses increased than did benign adenomas which were seen first between 500 and 550 days after inhalation only in the groups given a dose of 4.54 or 5.36 Gy (Fig. 5). No clear differences in incidence vs. time, however, were found among the carcinoma types, although adenocarcinomas seemed to appear slightly earlier and to increase gradually in the groups given 4.54 or 5.36 Gy (data not shown). These results indicate that both the dose and time after inhalation are associated with the induction and phenotypic expression of primary lung tumors.

DISCUSSION

Lifespan animal studies are required to estimate the risk of radiation-induced carcinogenesis because direct evaluations from epidemiological studies can not be made in human cases (15). Uncertainties exist even in animal studies because the experimental designs for radiation exposures are far from those for human, and differences in the responses or sensitivities to ionizing radiation exist among the animal species used. Despite that inhalation of high-fired $^{239}PuO_2$ represents one of the highest risks for pulmonary carcinogenesis (16), there has been no evidence of significantly increased lung cancers shown by results of human studies in nuclear workers with and without occupational exposures (17, 18). After inhalation exposure to ^{239}Pu

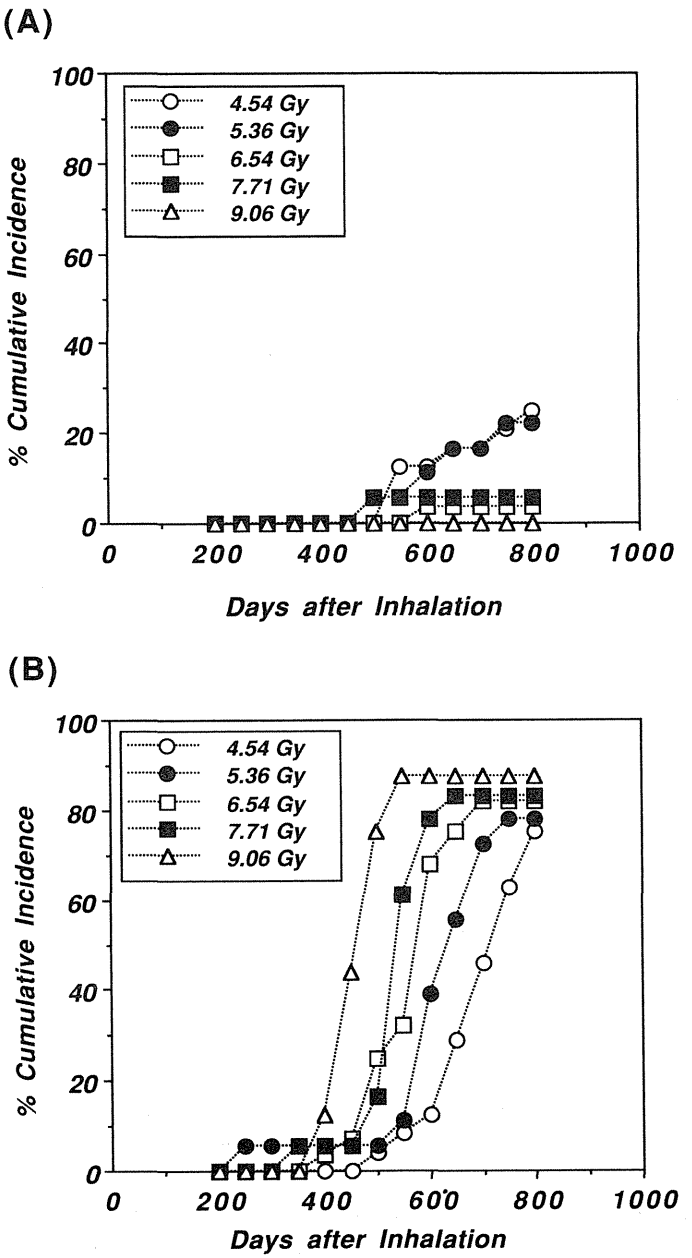

Fig. 5. Cumulative incidence of benign adenomas (**A**) and malignant tumors, including adenocarcinomas, adenosquamous carcinomas and squamous cell carcinomas (**B**) in the groups of rats received different doses as a function of days after inhalation of $^{239}PuO_2$.

aerosol, lung tumors have been induced in most experimental animals, but their incidences vary, being very low in both hamsters (19) and monkeys (20), and relatively higher in mice (21) on repeated inhalation of protracted higher doses. As spontaneous lung tumors are frequently observed in the mouse, it is difficult to estimate the dose-effect relationships. In contrast, the rat (7, 8) is recognized as having a very low incidence of spontaneous lung tumors and a high sensitivity to the induction of lung tumors by inhaled radioactive particles, as do beagle dogs (11, 22). Therefore, the rat and dog would be the most useful experimental animals for lifespan studies on lung carcinogenesis by inhaled $^{239}PuO_2$.

Our report summarizes the current data obtained from lifespan studies in rats for carcinogenesis due to inhaled $^{239}PuO_2$, which are on-going in our laboratory in order to clarify the dose-effect relationships, being focused on the low dose range below 1.0 Gy. Although the sizes of the control and lower-dose groups are not yet sufficient to estimate lifetime risks, our present results indicate there are some differences in both induction and the dose-effect relationships of lung tumors from those reported elsewhere (12). The survival time for all the exposed rats received a dose of 4.54 Gy or more was greatly reduced as compared to the controls, and did not differ much from the values for exposed animals with primary lung tumors given doses of more than 4.54 Gy. This dose which produced a reduction of survival time was almost 7-fold lower than that in the other lifespan study which showed 30 Gy or more either for all the exposed rats or for the exposed rats with primary lung tumors (12). It differed from the value for the control animals that showed a very low incidence of primary lung tumors and mostly died late of other causes such as senile disorders or tumors outside the lung, whereas the exposed animals mostly died of primary lung tumors but not metastatic tumors.

The crude incidence of all the primary lung tumors in our experiments was the highest (100%) at a dose of less than 5 Gy, which is assumed to be approximately 8- or 9-times lower as compared to the dose (44 Gy) for the highest incidence (88%) of primary tumors found by the other lifespan study using female Wistar strain rats (12). In addition, the primary lung tumors in our exposed rats were mostly being adenomas and such malignant carcinomas as adenocarcinomas, adenosquamous carcinomas and squamous cell carcinomas, all of which have been frequently observed in rats and dogs following inhalation of $^{239}PuO_2$ (11, 12). The dose range for the highest incidence of these tumor types, however, differed as benign adenomas occurred at a dose of less than 1 Gy but not at doses of more than 5 Gy, whereas the incidence of malignant carcinomas increased only in the dose range of 4–10 Gy. Among the carcinoma types, the crude incidence of squamous cell carcinomas was lower than the values for adenocarcinomas and adenosquamous carcinomas. In contrast to our study, Sanders et al. (12) showed that the crude incidence of either adenomas, adenocarcinomas or adenosquamous carcinomas was much lower than that of squamous cell carcinomas which had the highest incidence at 44 Gy. Squamous metaplasia and its severity also increased much more in the high dose ranges than did adenomatous metaplasia (23). Taken together, the results show that adenoma or adenomatous metaplasia would be induced at doses lower than 1 Gy but that malignant phenotypes would increase significantly at doses higher than 1 Gy.

All of the carcinomas tended to occur in earlier periods after inhalation than did adenomas in our study. This would reflect anaplastic processes from benign to malignant phenotypes

leading to death rather than the appearance of carcinomas independent of adenomas from target cells. The target cells for carcinogenesis by inhaled $^{239}PuO_2$ have been shown in both the rat (24) and mouse (25) to be Type II alveolar epithelial or Clara cells which show hypertrophy or hyperplasia associated with increased DNA synthesis in early periods after inhalation, and metaplastic but pre-neoplastic changes followed by the onset of neoplastic change to adenocarcinomas or squamous cell carcinomas in later periods. Carcinogenic processes after inhalation of $^{239}PuO_2$ therefore are dose- and time-dependent as it is assumed that adenomatous metaplasias appeared in the early stages at much lower doses that would not result in death, but neoplastic change to various malignancies would be promoted by higher doses, leading to death faster than benign adenomas.

Finally, it must be referred to whether there exists a threshold-like dose for the induction of malignant carcinomas as shown in the study of Sanders et al. (12). A threshold-like response frequently has been noted in the experimental carcinogenesis induced either by local irradiations or by fractionated and repeated irradiations at a low dose rate of low linear energy transfer (LET) radiations, as shown in mouse lung tumors at a single dose of X-rays (26), in mouse skin tumors by repeated beta irradiations at a low dose rate (27), and in mouse leukemias by fractionated gamma irradiations (28). These studies suggest that radiation-induced carcinogenesis is a complex process involving not only DNA damage which presumably leads to the initiation of genetic mutations, but also repairs or deletions of DNA damage to down-regulate the promotion of neoplastic sequela. We conclude that malignant lung carcinomas are induced markedly in female Wistar rats that received doses of more than 1 Gy following inhalation of submicron-size $^{239}PuO_2$ aerosol, but benign adenomas would appear even at the doses much lower than 1 Gy. Further lifespan studies are needed to estimate the differences in the dose-effect relationships of benign and malignant lung tumors, in which a larger cohort of control and exposed animals would receive doses much lower than 1 Gy.

ACKNOWLEDGEMENT

This work was supported by the Research Fund for Project Research on Risks Due to Low Level Radiation Exposure to the General Population from Japan Science and Technology Agency. We greatly appreciate the help of Animal Cares, Co. for their services on animal care and that of Tokyo Nuclear Services, Co. for radiation protection.

REFERENCES

1. BEIR V (1990) Health effects of exposure to low levels of ionizing radiation. ed. National Research Council Committee on the Biological Effects of Ionizing Radiations, Board of Radiation Effects Research, Commission on Life Sciences, National Academy of Sciences, National Academny Press, Washington, D. C.
2. Wrenn, M.E., Taylor, G.N., Stevens, W., Mays, C.W., Jee, W.S.S., Lloyd, R.D., Atherton, D.R., Bruenger, F.W., Miller, S.C., Smith, J.M., Shabestari, L.R., Woodburr, L.A., and Stover, B.J. (1986)

DOE life-span radiation effects studies in experimental animals at University of Utah Division of Radiobiology. In Life-Span Radiation Effects Studies in Animals: What Can They Tell Us? eds. R.C. Thompson & J.A. Mahaffey, US DOE CONF-830951, pp. 35–52.
3. Goldman, M., Rosenblatt, L.S., and Book, S.A. (1986) Lifetime radiation effects research in animals: an overview of the status and philosophy of studies at University of California-Davis Laboratory for energy-related health research. In Life-Span Radiation Effects Studies in Animals: What Can They Tell Us? eds. R.C. Thompson & J.A. Mahaffey, US DOE CONF-830951, pp. 53–65.
4. Raabe, D.G., Book, S.A., and Parks, N.J. (1983) Lifetime bone cancer dose-response relationships in beagles and people from skeletal burdens of ^{226}Ra and ^{90}Sr. Health Phys. 44 (suppl. 1), 33–48.
5. Mays, C.W., Taylor, G.N., and Lloyd, R.D. (1986) Toxicity ratios: their use and abuse in predicting the risk from induced cancer. In Life-span Radiation Effects Studies in Animals: What Can They Tell Us? eds. R.C. Thompson & J.A. Mahaffey, US DOE CONF-830951, pp. 299–310.
6. Mays, C.W., Lloyd, R.D., Taylor, G.N., and Wrenn, M.E. (1987) Cancer incidence and lifespan vs. α-particle dose in beagles. Health Phys. **52**, 617–624.
7. Sanders, C.L., and Mahaffey, J.A. (1978) Inhalation carcinogenesis of high-fired $^{244}CmO_2$ in rats. Radiat. Res. **76**, 384–401.
8. Sanders, C.L., and Mahaffey, J.A. (1983) Inhalation carcinogenesis of high-fired $^{241}AmO_2$ in rats. Radiat. Res. **94**, 66–80.
9. Lafuma, J., Chmelevsky, D., Chameaud, J., Morin, M., Masse, R., and Kellerer, A.M. (1989) Lung carcinomas in Spague-Dawley rats after exposure to low doses of radon daughters, fission neutrons, or γ rays. Radiat. Res. **118**, 230–245.
10. Fisher, D.R., Cannon, W.C., Hadley, R.T., and Park, J.F. (1986) Preliminary evaluation of lung doses for dogs exposed to $^{239}PuO_2$ In Life-span Radiation Effects Studies in Animals: What Can They Tell Us? eds. R.C. Thompson & J.A. Mahaffey, US DOE CONF-830951, pp. 683–696.
11. Dagle, G. E., Parks, J. F., Gilbert, E. S., and Weller, R. E. (1989) Risk estimates for lung tumors from inhaled $^{239}PuO_2$, $^{238}PuO_2$, and $^{239}Pu(NO_3)_4$ in beagle dogs. Radiat. Protect. Dosimetry **26**, 173–176.
12. Sanders, C.L., Lauhala, K.E., and McDonald, K.E. (1993) Lifespan studies in rats exposed to $^{239}PuO_2$ aerosol. III. Survival and lung tumors. Int. J. Radiat. Biol. **64**, 417–430.
13. Ishigure, N., Nakano, T., Enomoto, H., Fukuda, S., Iida, H., Oghiso, Y., Sato, H., Takahashi, S., Yamada, Y., Koizumi, A., Yamada, Y., Miyamoto, K., and Inaba, J. (1994) Lung retention of Pu following inhalation of PuO_2 in rats measured using a whole body counter. J. Radiat. Res. 35, 16–25.
14. WHO (1992) International Classification of Rodent Tumors, Part I The Rat, 1. Respiratory System, ed.-in-chief, U. Mohr, IARC Scientific Publications No. 122, Lyons.
15. NCRP (1993) Research Needs for Radiation Protection, NCRP Peport No. 117, Bethesda.
16. ICRP (1980) Biological effects of inhaled radionuclides, Annals of ICRP 4, 22–108.
17. Tietjen, G.L. (1987) Plutonium and lung cancer. Health Phys. **52**, 625–628.
18. Gilbert, E.S., Fry, S.A., Wiggs, L.D., Voelz, G.L., Cragle, D.L., and Petersen, G.R. (1989) Analyses of combined mortality data on workers at the Hanford site, Oak Ridge National Laboratory and Rocky Flats Nuclear Weapons Plant. Radiat. Res. **120**, 19–35.
19. Sanders, C.L. (1977) Inhalation toxicology of $^{238}PuO_2$ and $^{239}PuO_2$ in Syrian golden hamsters. Radiat. Res. **70**, 334–344.
20. Brooks, A.L., Guilmette, R.A., Hahn, F.F., Haley, P.J., Muggenburg, B.A., Mewhinney, J.A., and McClellan, R.O. (1992) Distribution and biological effects of inhaled $^{239}Pu(NO_3)_4$ in Cynomolgus monkeys. Radiat. Res. **130**, 79–87.
21. Lundgren, D.L., Gillett, N.A., Hahn, F.F., Griffith, W.C., and McClellan, R.O. (1987) Effects of protraction of the α dose to the lungs of mice by repeated inhalation exposures to aerosols of $^{239}PuO_2$. Radiat. Res. **111**, 201–224.
22. Hahn, F.F., Muggenburg, B.A., Boecker, B.B., Cuddihy, R.G., Griffith, W.C., Guilmette, R.A., McClellan, R.O. and Mewhinney, J.A. (1986) Insights into radionuclide-induced lung cancer in people

from life-span studies in beagle dogs. In Life-Span Radiation Effects Studies in Animals: What Can They Tell Us? eds. R.C. Thompson & J.A. Mahaffey, US DOE CONF-830951, pp. 521–534.
23. Sanders, C.L., McDonald, K.E., and Mahaffey, J.A. (1988) Lung tumor response to inhaled Pu and its implications for radiation protection. Health Phys. **55**, 455–462.
24. Herbert, R.A., Gillett, N.A., Rebar, A.H., Lundgren, D.L., Hoober, M.D., Chang, I.Y., Carlton, W.W., and Hahn, F.F. (1993) Sequential analysis of the pathogenesis of plutonium-induced pulmonary neoplasms in the rat: morphology, morphometry, and cytokinetics. Radiat. Res. **134**, 29–42.
25. Taya, A., Black, A., Baker, S.T., and Humphreys, J.A.H. (1993) Proliferation of mouse lung epithelial cells after inhalation exposure to $^{239}PuO_2$. Radiat. Res. **136**, 366–372.
26. Ullrich, R.L., Jernigan, M.C., and Adams, L.M. (1979) Induction of lung tumors in RFM mice after localized exposures to X-rays and neutrons. Radiat. Res. **80**, 464–473.
27. Ootsuyama, A., and Tanooka, H. (1991) Threshold-like dose of local beta irradiation repeated throughout the life span of mice for induction of skin and bone tumors. Radiat. Res. **125**, 98–101.
28. Maisin, J.R., Wambersie, A., Gerber, G.B., Mattelin, G., Lambiet-Collier, M., and Gueulette, J. (1983) The effect of fractionated gamma irradiation on life shortening and disease incidence in BALB/c mice. Radiat. Res. **94**, 359–373.

EFFECTS OF MACROMOLECULAR CHELATING AGENTS ON THE RELEASE OF ^{239}Pu AND ^{59}Fe FROM RAT ALVEOLAR MACROPHAGES AFTER PHAGOCYTIC UPTAKE OF ^{239}Pu-^{59}Fe-IRON HYDROXIDE COLLOID

H. Sato,* R. A. Bulman,† S. Takahashi,* and Y. Kubota*

Abstract—**The chelation-mediated mobilization of ^{239}Pu and ^{59}Fe from rat alveolar macrophages which had engulfed ^{239}Pu-^{59}Fe-hydroxide colloids was studied by exposing the macrophages to diethylenetriaminepentaacetic acid and macromolecular weight forms of diethylenetriaminepentaacetic acid. The release of ^{239}Pu and ^{59}Fe by these macromolecular weight chelating agents and diethylenetriaminepentaacetic acid was assessed in monolayer culture and shown to be dependent upon the nature of the engulfed colloids. Whereas calcium-diethylenetriaminepentaacetic acid, aminoethylcellulose-diethylenetriaminepentaacetic acid, and aminoethylcellulose-diethylenetriaminepentaacetic acid oxidized with periodic acid (aminoethylcellulose-diethylenetriaminepentaacetic acid(I_2) exhibited some effectiveness at releasing ^{239}Pu and ^{59}Fe from macrophages which had engulfed the low aggregative colloid, they were less effective in the release of these radionuclides from the high aggregative colloid. The efficacy of these chelating agents on the removal of radionuclides from alveolar macrophages differed between iron and plutonium, suggesting the significant difference in the dissolution and subsequent metabolism of these radionuclides in alveolar macrophages. From the similarities of the percentage increases in ^{239}Pu mobilized from the low aggregate colloid by aminoethylcellulose-diethylenetriaminepentaacetic acid (I_2) and diethylenetriaminepentaacetic acid, it would appear that both forms of diethylenetriaminepentaacetic acid could be accessing the same deposits of ^{239}Pu; however, for ^{59}Fe the percentage increases are quite different for the two forms of diethylenetriaminepentaacetic acid. SiO_2-diethylenetriaminepentaacetic acid, an insoluble macromolecular weight chelating agent, was ineffective at releasing ^{239}Pu but was slightly effective at releasing radioiron.**

Health Phys. 66(5):545–549; 1994

Key words: chelation; ^{239}Pu; rat; iron

INTRODUCTION

IT IS now well established that inhaled particles are engulfed by pulmonary alveolar macrophages (Silverstein et al. 1977; Valberg et al. 1982) and that many engulfed particles are digested within the lysosome with, in some cases, the release of metal ions into the bloodstream (Robinson and Schneider 1980; Lundborg et al. 1984, 1985; Kreyling et al. 1990; Yamada et al. 1993). Enhancement of the clearance of released metal ions largely involves administration of chelating agents such as salts of diethylenetriaminepentaacetic acid (DTPA). As DTPA is a highly hydrophilic chelating agent, its penetration of cell membranes is likely to be low as it cannot mobilize intracellular metal ions. A variety of procedures—ranging from administration of liposomally entrapped DTPA (Stather et al. 1976) through lipophilic derivatives (Markley 1963; Bulman and Griffin 1981a) and phagocytizable forms (Bulman and Griffin 1981b) to coadministration with macrophage-activating glucans (Rosenthal et al. 1973; Sato et al. 1986)—have been examined for enhancing the effect of the chelating agents such as DTPA.

As glycoconjugates have been used with some success to target drugs to cells (e.g., Bonfils et al. 1992), we have examined in this account and elsewhere (Bulman et al. 1993) the potential of DTPA bound to polysaccharide derivatives as a pro-drug delivery procedure. DTPA immobilized upon aminopropylsilica has been used as a phagocytizable form of DTPA. We found that some macromolecular chelating agents were more effective than Ca-DTPA at doses nontoxic for alveolar macrophages when the efficacy was determined from release of ^{59}Fe from alveolar macrophages after phagocytic uptake of ^{59}Fe-iron hydroxide colloids (Bulman et al. 1993). Although we used ^{59}Fe to evaluate the efficacy of chelating agents in those studies, because ^{59}Fe is easy to obtain and safe to handle, transuranic radionuclides, such as ^{239}Pu, are more important for the chelation therapy as a counter measure for accidental intakes. It is well known that soluble forms of Pu(IV), such as citrate or nitrate, change to colloidal forms on hydrolysis at physiological pH in the airways after inhalation (ICRP 1972). Although the degree of polymerization of Pu(IV) has not been quantitatively clarified, it is reasonable to assume that the size of colloidal Pu(IV) and the degree of aggregation varies with several factors such as the time after inhalation, the concentration of

* Division of Comparative Radiotoxicology, National Institute of Radiological Sciences, 9–1, Anagawa 4-chome, Inage-ku, Chiba-shi 263, Japan; † National Radiological Protection Board, Chilton, Didcot, Oxon OXll 0RQ, United Kingdom.

(*Manuscript received* 19 *February* 1993; *revised manuscript received* 26 *October* 1993, *accepted* 9 *November* 1993)

0017-9078/94/$3.00/0

acid inhaled with Pu(IV), and so on. The engulfment of colloids and subsequent solubilization by the macrophages might vary with the size and degree of aggregation of colloids.

In the present study, therefore, three macromolecular chelating agents, which had been proven more effective than Ca-DTPA in our previous experiments with ^{59}Fe, have been examined for their ability to mobilize ^{239}Pu and ^{59}Fe from alveolar macrophages that had ingested ^{239}Pu-^{59}Fe-iron hydroxide colloidal particles. In addition, the effect of the aggregation of colloid particles on the efficacy of these chelating agents were investigated, since in practical situations such as accidental inhalation of plutonium, alveolar macrophages may engulf Pu(IV)-hydroxide colloids with different degrees of aggregation.

MATERIALS AND METHODS

Chemicals

^{59}Fe-ferric chloride (480 MBq mg^{-1}Fe) was purchased from New England Nuclear.‡ ^{239}Pu nitrate was prepared by the procedure described by Black and Drummond (1965) with a slight modification. Briefly, 1 g of $^{239}PuO_2$ was added to 40 mL of 8 M HNO_3 in a Teflon® flask and heated for 6 h at 70°C after the addition of 0.15 mL of concentrated hydrogen fluoride. After complete dissolution, the solution was dried by gentle heating and then redissolved to 8 M HNO_3 in order to remove the hydrogen fluoride. This procedure was repeated two times and the resultant solution (54 MBq mL^{-1}) was used as a stock solution in the following experiment.

Aminoethylcellulose (AEC) and aminopropylsilica were obtained from Sigma Chemical Co. Ltd.‖ and Fluka Chemicals Ltd.,¶ respectively. Ca-DTPA was purchased from Dojin Chemical Laboratories.# Fuller experimental details of the preparation of the macromolecular weight chelating agents (MCAs) are given elsewhere (Andersen et al. 1989), but basically DTPA was immobilized on AEC and aminopropylsilica with the reaction of DTPA-bisanhydride. The silica-immobilized DTPA, henceforth SiO_2-DTPA, was micronized as a suspension in ethanol in an agate bead mill.** As AEC-immobilized DTPA is insoluble in water, it was solubilized to yield AEC-DTPA after paraperiodic acid oxidation (Nieuwenhuizen 1985) for 36 h and AEC-DTPA(I_2) after 96 h. The macromolecular form of DTPA, if insoluble, was recovered by retention on a Buchner funnel. The retentate was washed with distilled water, typically 3 L, to around 10 g of retentate. Soluble forms of DTPA conjugates were freed of reactants by overnight dialysis against running distilled water and the retentate recovered by freeze-drying. The association of DTPA with the macromolecules was established by acid hydrolysis and the amount of DTPA released determined by isotachophoresis (Bulman et al. 1993).

‡ New England Nuclear, 549 Albany Street, Boston, MA 02118.
‖ Sigma Chemical Co. Ltd., Poole, Dorset BH17 7NH, England.
¶ Fluka Chemicals Ltd., The Old Brickyard Gillingham, Dorset BH17 7NH, England.
# Dojin Chemical Laboratories, 2025-5, Tarbaru, Mashiki, Kumamoto 861-22, Japan.
** McCrone Research Associates Ltd., 2 McCrone Mews, London, England.

Preparation of radiolabeled colloids

^{239}Pu-^{59}Fe-iron hydroxide colloids were used in the present study in order to load simultaneously alveolar macrophages with colloidal plutonium and iron. The ^{239}Pu-^{59}Fe-iron hydroxide colloids stabilized with dextran were prepared by a slightly modified procedure previously described (Priest and Haines 1982). Briefly, 3 mL of hot distilled water was added to 1 mL of 2% (w/v) ferric chloride solution containing ^{59}Fe-ferric chloride (348 kBq, 1.1×10^{-3} mg^{-1}Fe) and ^{239}Pu nitrate (11 kBq) of the previously mentioned stock solution. The solution was heated at about 90–95°C by placing the tube in a beaker of boiling water. During this heating process, the color of the initial solution changed from yellow (the color of ferrous ions) to dark red (the color of ferric hydroxide colloid) over a period of ~5 min. When the dark red sol colloid of ferric hydroxide had formed, the heating was continued for 60 s to yield the low aggregative colloid, *Colloid 1*. To prepare the more highly aggregative colloid, *Colloid 2*, the same procedure was used but final heating was carried out at a higher temperature (more than 95°C) and for a longer period (5 min). In both cases the colloid suspension solutions were cooled and dialyzed against distilled water by using conventional cellophane dialysis tubes (exclusion limit: 3–4 kDa) until no free ^{239}Pu and ^{59}Fe could be detected in the dialyzate. Finally the colloids were stabilized with 2% (w/v) dextran (40 kDa) and made isotonic with glucose (0.25 M). The pH of the final colloid suspension solution was 5.5–6.2 and the concentrations were 5 kBq mL^{-1} for ^{239}Pu and 210 kBq mL^{-1} for ^{59}Fe in both colloids.

Preparation of alveolar macrophages loaded with ^{239}Pu-^{59}Fe-colloid

Female Wistar rats, 3–5 mo old and weighing 280–329 g, were obtained from the animal facility at our institute. All animals were kept under barrier conditions and had no apparent pulmonary disorders on pathological examination after lung lavage. The animals were anesthetized with halothane and 0.3 mL of *Colloid 1* or *Colloid 2* solution (^{239}Pu: 1.5 kBq, ^{59}Fe: 63 kBq) was instilled into the whole lung via an intratracheal canulae (Takahashi and Patrick 1987). Instillation, i.e., *in vivo* loading of the colloidal particles to the alveolar macrophages, was used because it allows the macrophages to take up colloidal particles under a relatively physiological condition rather than by an *in vitro* method in which the colloidal particles were administered *in vitro* to the cultured macrophages.

Twenty hours after the instillation of ^{239}Pu-^{59}Fe-colloid, the rats were killed by exsanguination under anesthesia with diethylether and the lungs were lavaged three times with sterilized Dulbecco's calcium-free and magnesium-free phosphate buffered saline (PBS). The

lavage fluids were pooled and centrifuged to separate the cell pellet (bronchoalveolar cells) from the supernatant. The cells were washed twice with Eagle's minimum essential medium (EMEM) and finally suspended in EMEM containing 10% fetal calf serum. The type of recovered cells, determined by light microscopy with Giemsa stain, was alveolar macrophages (more than 80%), polymorphonuclear leukocytes (approximately 15%), and lymphocytes and monocytes (less than 5%).

Cell viability

Cell suspensions containing 2×10^5 cells mL^{-1} were incubated at 37°C for 8 h in a 35-mm-diameter dish with or without addition of the chelating agents at various concentrations. At the end of culture, a supernatant of the culture medium was removed and 2 mL of 0.5% trypan blue in saline was added. The cell viability of the control group which was not administered the chelating agents was 91.9%. The maximum concentrations of the chelating agents which did not show the significant decrease in the cell viability were 1.8, 1.3, 1.3, and 0.12 mg mL^{-1} for Ca-DTPA, AEC-DTPA, AEC-DTPA(I_2), and SiO_2-DTPA, respectively (Table 1).

Measurement of ^{239}Pu and ^{59}Fe release from macrophages

The cell suspension was poured into a 96-well microplate [5×10^4 cells $(0.2\ mL)^{-1}$ $(well)^{-1}$], and Ca-DTPA, AEC-DTPA, AEC-DTPA(I_2) in PBS or SiO_2-DTPA suspended in PBS was added to be 1.8, 1.3, 1.3, and 0.12 mg mL^{-1}, respectively. PBS was added to nontreated controls. The cells were then incubated at 37°C under 5% CO_2 and 95% air for 3 h. After the incubation, the culture medium was collected and passed through a filter with a pore diameter of 0.22 μm by centrifugation. The amount of ^{239}Pu and ^{59}Fe in the filtrates was measured by liquid scintillation counter[††] (for ^{239}Pu) and gamma well counter[‡‡] (for ^{59}Fe). The adherent cells in the residual bottom-medium were lysed by addition of 0.1 mL of 0.2% sodium dodecylsulphate, and the lysed cell solution was collected. The well of the culture plate was then washed with distilled water. The lysed cell solution and washing solution were pooled and the radioactivity in these solutions was also measured. The release of ^{239}Pu and ^{59}Fe was calculated by the following equation:

$$\text{release } (\%) = \frac{\text{activity in filtrates}}{\text{total activity in well}} \times 100. \quad (1)$$

RESULTS AND DISCUSSION

An important consideration in this kind of study is the cytotoxicity of the chelating agent on the cultured alveolar macrophages. If the chelating agents were cytotoxic at the concentrations used, the radionuclide leakage might occur through the damaged cell membrane; therefore, the amount released would not indicate the actual effect of the chelating agents on the extracellular release of dissolved radionuclide. In the present study we used the maximum concentrations of the chelating agents which did not impair the cell viability after 8 h exposure in culture (Table 1). The trypan blue dye exclusion test used for the assessment of viability is a sensitive index of membrane damage of cells. Furthermore, we used the shorter incubation period (3 h) for evaluating the efficacy of chelating agents, compared with that for cell viability test (8 h); therefore, we believe there was no radionuclide leakage through damaged cell membranes in these experiments.

The differences in the physicochemical state of the two types of colloids used here were quite marked in their stability in aqueous media: whereas *Colloid 1* stayed suspended in water for several weeks, *Colloid 2* precipitated within a few hours. The amounts of ^{239}Pu in the ultrafiltrate (Millipore Ultrafree C3, exclusion limit: 10 kDa) were 47 and 3.3% of the injected radioactivity for *Colloids 1* and *2*, respectively (Table 2). It is clear that *Colloid 2* was a particulate material which had formed from an aggregation of colloidal hydroxides. The distribution of the particles in the lung also differed between *Colloid 1* and *Colloid 2*. In the lung lavage fluid, the ratio of the radioactivity in the bronchoalveolar cells (BAC) to that in supernatant is 0.21 and 1.3 in *Colloids 1* and *2*, respectively (Table 2).

Tables 3 and 4 show the percentage releases of ^{59}Fe and ^{239}Pu from the alveolar macrophages. The extracellular release of both radionuclides was much higher from the macrophages that ingested *Colloid 1* than those that ingested *Colloid 2*, and was not affected by the types of chelating agents used. This difference in

Table 1. Viability of alveolar macrophages incubated with some chelating agents for 8 h in monolayer culture.

Treatment		Viability (%)
Control		91.9 ± 3.3[a]
Ca-DTPA	1.8 mg mL^{-1}	93.3 ± 0.8
AEC-DTPA	1.3 mg mL^{-1}	86.5 ± 1.3
AEC-DTPA(I_2)	1.3 mg mL^{-1}	87.5 ± 2.2
SiO_2-DTPA	0.12 mg mL^{-1}	93.3 ± 0.8

[a] Values are expressed as mean ± standard error of the mean (SE) of four cultures.

Table 2. Distribution of ^{239}Pu activity in lavage fluid.

	Administered solution	Lavage fluid			
	Administered activity	<10 kDa	BAC	Sup.[a]	BAC/Sup.[a]
Colloid 1	100	47.2[b]	3.4	16.0	0.21
Colloid 2	100	3.3	7.3	5.7	1.3

[a] Supernatant.
[b] Denotes percentage of ^{239}Pu activity contained in the ultrafiltrate (exclusion limit: 10 kDa).

[††] 1219 Rackbeta, Wallac Oy, P.O. Box 10, SF-20101, Turku, Finland.
[‡‡] Gamma 5500, Beckman Instruments, Inc., 2500 Harbor Blvd., P.O. Box 3100, Fullterton, CA 92634-3100.

Table 3. Percentage release of ^{239}Pu and ^{59}Fe from alveolar macrophages which had ingested *Colloid 1*.

Treatment		Plutonium	Iron
Control		1.15 ± 0.62[a] (100)[b]	1.13 ± 0.26 (100)
Ca-DTPA	1.8 mg mL^{-1}	11.3 ± 0.71[c] (983)	2.68 ± 0.18[c] (237)
AEC-DTPA	1.3 mg mL^{-1}	4.54 ± 0.41[c] (395)	2.59 ± 0.37[d] (229)
AEC-DTPA(I_2)	1.3 mg mL^{-1}	11.7 ± 1.0[c] (1,017)	5.07 ± 0.24[c] (449)
SiO_2-DTPA	0.12 mg mL^{-1}	1.17 ± 0.41 (102)	4.29 ± 0.37[c] (380)

[a] Mean ± SE.
[b] Percentage of control.
[c] Denotes significant difference from the control group at $p < 0.005$.
[d] $p < 0.01$.

Table 4. Percentage release of ^{239}Pu and ^{59}Fe from alveolar macrophages which had ingested *Colloid 2*.

Treatment		Plutonium	Iron
Control		0.24 ± 0.07[a] (100)[b]	0.03 ± 0.02 (100)
Ca-DTPA	1.8 mg mL^{-1}	0.44 ± 0.05[c] (183)	0.09 ± 0.02[c] (300)
AEC-DTPA	1.3 mg mL^{-1}	0.24 ± 0.03 (100)	0.09 ± 0.01[c] (300)
AEC-DTPA(I_2)	1.3 mg mL^{-1}	0.52 ± 0.03[d] (217)	0.20 ± 0.04[d] (667)
SiO_2-DTPA	0.12 mg mL^{-1}	0.16 ± 0.01 (67)	0.07 ± 0.01 (233)

[a] Mean ± SE.
[b] Percentage of control.
[c] Denotes significant difference from the control group at $p < 0.05$.
[d] $p < 0.005$.

the release from the colloids may be attributable to the different physicochemical properties of the colloids, such as surface area and stability of colloid. Although there are no available data on effect of physicochemical properties of Pu(IV)-hydroxide colloids on the dissolution or transportability in the lung, it is known that ultrafine particles of PuO_2 of colloidal size redistribute more rapidly from the lung to the blood than submicron size PuO_2 particles (Smith et al. 1977).

It is clear from a consideration of the percentage increases (Tables 3 and 4) of the amount of ^{239}Pu and ^{59}Fe released by the water-soluble chelating agents from macrophages that the chelating agents exhibit significantly different effects upon the release of intracellularly accumulated ^{239}Pu and ^{59}Fe. For *Colloid 1*, chelating agents other than SiO_2-DTPA were more effective for plutonium than for iron. On the other hand, for *Colloid 2*, all chelating agents used were less effective for plutonium than iron. Furthermore, the percentage increase in ^{239}Pu released by the water-soluble chelating agents from ingested *Colloid 1* is much higher (range 395–1,017%) than the percentage increase (range 183–217%) in ^{239}Pu released from ingested *Colloid 2*.

In contrast, the diversity of the percentage increase in ^{59}Fe released from both ingested colloids by the water-soluble chelating agents is much less than that observed for ingested ^{239}Pu. These differences in the release of the radionuclides might reflect the degree of lysosomal digestion of the engulfed radionuclides and the stability of dissolved radionuclides in the cell. Although it was not evidenced experimentally, it is assumed that the stabilities of the binding of these radionuclides to the intracellular sites, such as ferritin, are different and that there will be significant differences in the desorption of ^{239}Pu and ^{59}Fe from such intracellular binding sites by the water-soluble chelating agents. In the blood it is well known that the stability constant of plutonium-transferrin is lower than that of iron-transferrin (Stevens et al. 1968; Stover et al. 1968). This assumption may be indirectly supported by the previous findings, whereas chelating agents, such as DTPA, fail to release iron from ferritin unless it is reduced to the ferrous state (Crichton et al. 1987), there are no such restrictions for the release of $^{239}Pu(IV)$.

The release of ^{239}Pu by DTPA and AEC-DTPA(I_2) from macrophages that ingested *Colloid 1* was similar, about 11%, and this might indicate that both forms of DTPA are able to reach the same forms of ^{239}Pu. The contribution of extended oxidation of AEC-immobilized DTPA to the action of AEC-DTPA(I_2) remains unknown. Whereas intracellular DTPA arising from phagocytized forms of AEC-DTPA might be bringing about the release of intracellular radionuclides, it is difficult to conjecture the same role for Ca-DTPA, a highly hydrophilic molecule. Such high hydrophilicity and, therefore correspondingly low lipophilicity, should suppress its penetration of the cell membrane.

In this study, insoluble SiO_2-DTPA was ineffective at releasing intracellular ^{239}Pu but was slightly effective at releasing intracellular ^{59}Fe. In other studies we have shown that SiO_2-DTPA is effective at releasing intracellularly accumulated ^{59}Fe (Bulman et al. 1993) but this might have been a reflection of the longer monolayer culture time of 8 h as opposed to 3 h in this study.

As described in the Introduction, the macromolecular chelating agents used here were more effective than Ca-DTPA in our preliminary experiments with ^{59}Fe-hydroxide colloids. In the present study we confirmed that AEC-DTPA(I_2) was as effective as Ca-DTPA for the release of plutonium and iron from alveolar macrophages after their ingestion as plutonium-iron-hydroxide colloids. Although it is generally difficult to predict the efficacy of drugs in animal experiments from *in vitro* experiments, the results of the present study

indicate that AEC-DTPA(I_2) may be a possible macromolecular chelating agent for the treatment of accidental inhalation of plutonium.

CONCLUSIONS

The extracellular release of ^{239}Pu and ^{59}Fe from alveolar macrophages after ingestion of ^{239}Pu-^{59}Fe-hydroxide colloid is determined by the degree of aggregation of colloids. It is assumed that the dissolution and redistribution of ^{239}Pu and ^{59}Fe from the lung after inhalation of hydroxide colloid of these radionuclides are affected by the degree of their aggregation. The efficacy of chelating agents differed between iron and plutonium, suggesting a significant difference in the dissolution of the colloids and subsequent metabolism of these radionuclides in alveolar macrophages. Except for SiO_2-DTPA, the chelating agents that were effective at removing intracellular ^{59}Fe also showed a significant effectiveness for ^{239}Pu; therefore, ^{59}Fe can be used for assessing the efficacy of chelating agents for ^{239}Pu in such an *in vitro* screening test as the present study. The success of AEC-DTPA(I_2) at releasing intracellular radionuclides indicates that this macromolecular chelating agent should be further evaluated in other *in vivo* experiments.

REFERENCES

Andersen, O.; Bulman, R. A.; Nielsen, J. B. Effects of macromolecular chelates on intestinal cadmium absorption in mice. Pharmacol. Toxicol. 64:216–221; 1989.

Black, R. M.; Drummond, J. L. A comparison of procedures for dissolving ignited plutonium oxides for analysis. In: The reactor group report. Warrington, Lancaster; TRG Report 1072(D); 1965: 1–9.

Bonfils, E.; Mendes, C.; Roche, A. C.; Monsigny, M.; Midoux, P. Uptake by macrophages of a biotinylated oligo-alpha-deoxythymidylate by using mannosylated streptavidin. Bioconjug. Chem. 3:277–284; 1992.

Bulman, R. A.; Griffin, R. J. Investigations into techniques for removing intracellular plutonium-III. Naturwissenschaften 67:483–484; 1981a.

Bulman, R. A.; Griffin, R. J. Investigations into techniques for removing intracellular plutonium-II. Complexing agents bound to macromolecules. Health Phys. 40:228–231; 1981b.

Bulman, R. A.; Sato, H.; Takahashi, S.; Kubota, Y. ^{59}Fe release from alveolar macrophages by macromolecular forms of chelating agents. J. Radiol. Protect. 13:127–133; 1993.

Crichton, R. R.; Roman, F.; Roland, F. Ferritin iron mobilization by chelating agents. FEBS Letters 110:271–274; 1987.

International Commision on Radiological Protection. The metabolism of compounds of plutonium and other actinides. New York: ICRP Publication 19; 1972.

Kreyling, W. G.; Godleski, J. J.; Kariya, S. T.; Rose, R. M.; Brain, J. D. *In vivo* dissolution of uniform cobalt oxide particles by human and canine alveolar macrophages. Am. J. Respir. Cell Mol. Biol. 2:413–422; 1990.

Lundborg, M.; Lind, B.; Camner, P. Ability of rabbit alveolar macrophage to dissolve metal. Exp. Lung Res. 7:11–22; 1984.

Lundborg, M.; Elkund, A.; Lind, B.; Camner, P. Dissolution of metals by human and rabbit alveolar macrophages. Brit. J. Ind. Med. 42:642–645; 1985.

Markley, J. F. Removal of polymeric plutonium from mice by combined therapy with the calcium chelate and pentaethyl ester of DTPA. Int. J. Radiat. Biol. 7:405–407; 1963.

Nieuwenhuizen, M. S.; Kieboom, A. P. G.; van Bekkum, H. Preparation and calcium complexation properties of a series of oxidized polysaccharides: Structural and conformational properties. Starch 37:192–199; 1985.

Priest, N. D.; Haines, J. W. The release of plutonium from macrophages in rats: The effects of changes in iron status. Health Phys. 42:415–423; 1982.

Robinson, A. V.; Schneider, R. P. Solubilization of $^{241}AmO_2$ in alveolar macrophage cultures. In: Pacific Northwest Laboratory Annual Report. PNL-3300 PT1, 1980: 210–211.

Rosenthal, M. W.; Brown, H.; Chladek, D. L.; Moretti, E. S.; Russell, J. J.; Lindenbaum, A. Removal of plutonium from mouse liver by glucan and DTPA. J. Radiat. Res. 53:102–114; 1973.

Sato, H.; Kubota, Y.; Takahashi, S.; Matsuoka, O. ^{59}Fe-release from alveolar macrophages ingested ^{59}Fe-iron dextran—Enhancement by combination of Ca-DTPA and macrophages activating substances. J. Radiat. Res. 27:105–111; 1986.

Silverstein, S. G.; Steinman, R. M.; Cohn, Z. A. Endocytosis. Ann. Rev. Biochem. 46:669–722; 1977.

Smith, H.; Stradling, G. N.; Loveless, B. W.; Ham, G. J. The *in vivo* solubility of plutonium-239 dioxide in the rat lung. Health Phys. 33:539–551; 1977.

Stather, J. W.; Smith, H.; James, A. C.; Rodwell. The experimental use of aerosol and liposomal forms of DTPA as a treatment for plutonium contamination. In: Diagnosis and treatment of incorporated radionuclides, proceedings of a seminar. Vienna: IAEA; 1976: 387–400.

Stevens, W.; Bruenger, F. W.; Stover, B. J. *In vivo* studies on the interactions of PuIV with blood constituents. J. Radiat. Res. 33:490–500; 1968.

Stover, B. J.; Bruenger, F. W.; Stevens W. The reaction of PuIV with the iron transport system in human blood serum. J. Radiat. Res. 33:381–395; 1968.

Takahashi, S.; Patrick, G. Pattern of lymphatic drainage to individual thoracic and cervical lymph nodes in the rat. Lab. Animals 21:31–34; 1987.

Valberg, P. A.; Chen, B.-H.; Brain, J. D. Endocytosis of colloidal gold by pulmonary macrophages. Exp. Cell Res. 141:1–14; 1982.

Yamada, M.; Takahashi, S.; Sato, H.; Kondo, T.; Kikuchi, T.; Furuya, K.; Tanaka, I. Solubility of nickel oxide particles in various solutions and rat alveolar macrophages. Biol. Trace Element Res. 36:89–98; 1993.

■ ■

INT. J. RADIAT. BIOL 1997, VOL. 72, NO. 1, 71–78

Effect of a maternal injection of ^{239}Pu on the number of CFU-S in the foetal liver of the C3H and BDF1 mouse

Y. KUBOTA,* S. TAKAHASHI and H. SATO

(Received 1 October 1996; accepted 7 March 1997)

Abstract. We investigated the effect of ^{239}Pu administered on day 4 of gestation on the number of CFU-S (spleen-colony forming units) in the foetal liver on day 17 of gestation in the C3H and BDF1 mouse. CFU-S numbers in the foetal liver were decreased significantly by ^{239}Pu at doses >30 kBq/kg body weight in the BDF1 mouse, but were not changed by up to 900 kBq/kg in the C3H strain. Quantitative autoradiography on days 6, 8 and 10 of gestation and liquid scintillation counting on days 13 and 17 of gestation revealed no significant differences in the distribution and concentration of ^{239}Pu between the foetoplacental units of these two strains. These findings suggest a strain difference in the effect of ^{239}Pu α-irradiation on the development of the foetal haematopoietic systems in the mouse.

1. Introduction

The embryo and foetus are considered to be more sensitive than the adult to ionizing radiation with regard to many biological aspects, including cancer induction (Brent *et al.* 1987). This conclusion is based on data from man and other animals exposed to external radiation (UNSCEAR 1986, Brent *et al.* 1987, Kato *et al.* 1989). In comparison with the estimation of external radiation doses, the assessment of embryonic or foetal doses from maternal intake of radionuclides is more complex, requiring information both on the uptake and distribution of radionuclides in the rapidly growing conceptus (Morgan *et al.* 1991).

Investigations into links between childhood leukaemias and radionuclide exposure in the vicinity of nuclear sites in the UK have focused attention on the need for foetal dosimetric models and risk estimation of embryo/foetus contaminated with radionuclides such as isotopes of plutonium and americium (Stather *et al.* 1988, Morgan *et al.* 1992). Thereafter, extensive studies have been performed to elucidate in detail the foetoplacental transfer and distribution of plutonium and americium and their effects, particularly on foetal haematopoietic tissues (van den Heuvel 1990, Morgan *et al.* 1991, Lord *et al.* 1991, 1992, Mason *et al.* 1991, 1992, Kubota *et al.* 1993). Some of these studies showed that maternal contamination with plutonium or americium at the early or mid-term of gestation resulted in haematopoietic damage to the foetal liver or bone marrow of offspring (van den Heuvel 1990, Lord *et al.* 1991, 1992, Mason *et al.* 1992). As a preliminary study, we examined the effect of ^{239}Pu administered to the pregnant C3H mouse at the early stages of gestation on foetal liver haematopoiesis, but we could not identify any effects at doses of up to 900 kBq/kg body weight. This was inconsistent with the findings of a study using the BDF1 mouse (Lord *et al.* 1992). We therefore compared the effects of ^{239}Pu on the foetal liver haematopoiesis between the C3H and BDF1 mouse. In the present paper, we report that plutonium administered at an early gestational stage decreased the number of CFU-S (colony forming units in the spleen) in the foetal liver of the BDF1, but not the C3H mouse, and that this strain difference was not attributed to the foetoplacental transfer and distribution of plutonium.

2. Materials and methods

2.1. *Animals*

All animal treatments were performed under the institutional regulations on the handling of experimental animals. Mice purchased from SLC Co. Ltd (Shizuoka, Japan) were housed in a controlled environment (22 ± 1°C, 14 h light), with access to food and water *ad libitum*. Nulparous female C3H/HeN and C57Black/6 mice, 12–18 weeks old, were caged nightly with C3H/HeN and DBA2 male mice respectively. Mating was confirmed the following morning by the presence of a vaginal plug and the day was defined as day 0 of gestation.

2.2. *Plutonium solution*

^{239}Pu-citrate was prepared from plutonium nitrate as described by Lindenbaum *et al.* (1968), with slight modification. In brief, the ^{239}Pu-citrate solution was prepared by adding a stock solution of ^{239}Pu-nitrate (52.5 MBq/ml 5N HNO_3) to trisodium citrate to a final molecular ratio of Pu to citrate of 1 : 100. This

*Author for correspondence.
The 4th Research Group, National Institute of Radiological Sciences, Anagawa 4-9-1, Inage-ku, Chiba-shi, Chiba, Japan.

solution was adjusted to pH 4 with 1N NaOH, then diluted with saline to the desired concentrations for injection and filtered through a 0·22μm Millipore filter. This procedure was carried out on the day of injection to avoid chemical change with time after preparation. On day 4 of gestation, groups of mice were anesthetized with pentobarbital (40 mg/kg body weight), then injected with ^{239}Pu-citrate intraperitoneally (i.p.) at doses of 30–900 kBq/kg body weight, or intravenously (i.v.) at 300 kBq/kg.

2.3. *Autoradiography*

Quantitative autoradiography was performed in tissue sections of the conceptuses on days 6, 8 and 10 of gestation according to the described procedures (Takahashi *et al.* 1994). In brief, pregnant animals injected with plutonium intraperitoneally at 300 kBq/kg body weight on day 4 of gestation were killed by cervical dislocation, after which their uteri were removed and washed with saline. The whole uterus was frozen on a plastic plate floated on liquid nitrogen after embedding in commercial medium (Lipshaw Manufacturing Corp., Detroit, MI, USA). The frozen uterus was cut into serial sections 20μm thick by a microtome in a cryostat maintained at -10 to -15°C, adhered to cover slips or adhesive tapes, placed on a hotplate at 50°C and allowed to dry completely. The cover slips and adhesive tapes with thin sections were then covered by a thin plastic film (Lumilar Membrane, Nakagawa Co. Ltd, Tokyo, Japan) and placed in contact with an imaging plate (Type BASIII, Fuji Photo Film Co. Ltd, Tokyo, Japan) for 5 days. The radioactive images recorded on the imaging plate were read by a laser beam scanner and analysed by an attached computer (BAS3000, Fuji Photo Film Co. Ltd, Tokyo, Japan). Analysis settings were as follows; pixel, 50 × 50 μm; sensitivity, 10 000; latitude, 4. In this image-analysis system, the radioactivity in the tissue sections was determined as the intensity of photostimulated luminescence (PSL). The cover slips after the contact with an imaging plate were stained with conventional haematoxylin and eosin for microscopic observation.

2.4. *Radiochemical analysis*

On days 13 and 17 of gestation, the animals were killed by cervical dislocation, after which their uteri were removed and washed with saline. The uterine wall was excized, and the conceptuses were placed in small dishes. Each conceptus was divided into three samples under a dissection microscope, care being taken to avoid cross contamination. The samples assayed consisted of the foetus, the yolk sac that included the visceral yolk sac and amnion, and the chorioallantoic placenta that included the parietal yolk sac, Reichert's membrane and part of the decidua. Plutonium activities in three conceptuses per litter were determined, at least two litters being used for each gestational age. Samples were dissolved in 0·5–1 ml tissue solubilizer (Protozol, New England Nuclear/Dupont, Wilmington, DE, USA) at 50°C for 12–24 h, then the solution was neutralized with 1N HCl. The radioactivity in a scintillation cocktail (Aquasol II, New England Nuclear/Dupont, Wilmington, DE, USA) was measured in a liquid scintillation counter (LKB/Wallac, Rack Beta 1219, Turku, Finland).

2.5. *CFU-S assay*

On day 17 of gestation, male foetal livers were carefully removed from the abdomen of the foetus and rinsed with ice-cold Hank's balanced salt solution (HBSS) in small dishes. Three foetal livers from each dam were collected and then gently dissociated in a sterile glass homogenizer. The homogenate was transferred to a sterile plastic bottle using a syringe with 26-gauge needle. Each foetal liver cell suspension was diluted with HBSS to give countable numbers (10–20) of colonies on the spleen of recipient mice and injected intravenously into a group of at least 15 syngeneic male recipient mice irradiated with 8 Gy γ-irradiation from a ^{137}Cs source at a dose-rate of 12 Gy/min. Twelve days later the recipient mice were killed, their spleens were excized and fixed for counting the colonies. The CFU-S number in a foetal liver was calculated from the data of recipient mice injected with the foetal liver cell suspension from one dam, and then the values were used to calculate the mean $\pm$ SD in each experimental group and to perform Student's *t*-test.

3. Results and discussion

Table 1 shows the effect of maternal contamination with ^{239}Pu on the number of CFU-S in the foetal liver on day 17 of gestation. In C3H mice, ^{239}Pu at doses up to 900 kBq/kg body weight did not affect the CFU-S number. In contrast, even at 30 kBq/kg, the number of CFU-S in the foetal liver of BDF1 mice was significantly decreased compared with non-contaminated controls. In the groups with 300 kBq/kg body weight, plutonium was administered intravenously or intraperitoneally, but there were no differences between the injection routes. Lord *et al.* (1992) reported that after contamination with ^{239}Pu at 30 kBq/kg on day 4 of gestation, the foetal liver of BDF1 mice developed only 50% of its

Table 1. Effect of ^{239}Pu injected on day 4 of gestation on the number of CFU-S in the foetal liver on day 17 of gestation[a].

Dose[b] (kBq/kg)	Injection route	Mouse strain	
		C3H	BDF1
0	–	1877 ± 291 (8)	2389 ± 109 (8)
30	i.p.	1801 ± 204 (4)	1636 ± 276[c] (4)
300	i.v.	2035 ± 568 (3)	1192 ± 492[c] (3)
300	i.p.	1951 ± 342 (7)	1255 ± 210[c] (7)
900	i.p.	1947 ± 287 (3)	1304 ± 79[c] (3)

[a]Values are mean ± SD of CFU-S per foetal liver. Values in parentheses are number of dam.

[b]Plutonium was maternally injected on day 4 of gestation (kBq/kg body weight).

[c]Significant difference between control and plutonium injected group determined with Student's *t*-test (significance level $p<0.05$).

complement of CFU-S. The present findings were consistent with those published data. However, there have been no similar investigations using different mouse strains. The present study showed that the C3H mouse was resistant with respect to foetal haematopoietic damage (deficient CFU-S in foetal liver) induced by maternal contamination with ^{239}Pu at an early gestational stage. There are two possible explanations for this strain difference. One is a difference in the foetoplacental transfer and distribution of ^{239}Pu, with smaller amounts of ^{239}Pu being transferred to the foetoplacental unit, particularly the foetal haematopoietic tissues such as the yolk sac and the foetal liver in C3H mice. The other is that the susceptibility of the foetal haematopoietic tissues to α-irradiation is different between the two strains of mice. To examine these explanations, we investigated the retention of ^{239}Pu in foetoplacental units at different stages of gestation. On days 6–10 of gestation, it is technically difficult to dissect a foetoplacental unit into its components to quantify the amount of radioactivity in each by liquid scintillation counting. Autoradiography may be only a way to study the retention of radioactivity in such small tissues. Imaging plates and laser beam scanning with computerized imaging analyser enables accurate quantitative autoradiography due to digital data processing, and shortens the exposure time due to high sensitivity. Therefore, we used this system to analyse the retention of ^{239}Pu in the foetoplacental unit on days 6, 8 and 10 of gestation. Plates A–C of Figure 1 show photographs of H&E-stained thin sections and their autoradiograms from either strain of mice on day 6, 8, 10 of gestation respectively. The histological observations of the conceptus and the plutonium distribution in it were essentially the same between BDF1 and C3H mice at the gestational stages examined.

On day 6 of gestation, a large part of the internal space of the uteri was occupied by maternal decidua, and the embryo surrounded by trophoblastic cells was located near the center of the decidua (Figure 1, A). The autoradiogram shows most ^{239}Pu activity in the outermost part of uteri, which was identified as the uterine perimetrium by a comparison with the histological sections. The ^{239}Pu activity was also relatively high in the embryo and the trophoblast. In contrast, the maternal decidua contained relatively low concentrations of ^{239}Pu. Morgan *et al.* (1991) investigated the foetoplacental transfer of ^{238}Pu in HMT rat and guinea-pig by CR-39 and photographic emulsion autoradiography. In their report, after contaminating the rats with ^{238}Pu on day 6·5 of gestation, the concentration of activity in a day 9·5 egg cylinder appeared to be higher than that in the surrounding maternal decidua, and ^{238}Pu was deposited not only in the cells forming the yolk sac but also in the trophoblastic and embryonic tissues of the egg cylinder. Although it is difficult to compare their findings directly with ours because of the differences in the animal species, gestational stage, and isotopic state of plutonium, the tendency for a relatively high concentration of plutonium to locate in the egg cylinder was consistent with the findings in the present study. ^{239}Pu was also concentrated in the uterine perimetrium. This phenomenon may be attributable to the injection route since ^{239}Pu was administered intraperitoneally. Some plutonium injected into the peritoneal cavity transfers to the lymphatic tissues via the perimetrium. On day 8, the foetus, the yolk sac, the trophoblastic giant cells, and the ectoplacental cone near which the chorioallantoic placenta was formed was discernable. The retention of ^{239}Pu was highest in the uterine perimetrium, being similar to the autoradiogram on day 6 of gestation, and the retention was also quite high in the region of the yolk sac and the trophoblastic giant cells (Figure 1, B). On day 10 of gestation, while the foetus, the chorioallantoic placenta and the allantois were rapidly developed, the retention of ^{239}Pu was similar to that on day 8 of gestation with high levels in the uterine perimetrium, as well as the region of the yolk sac and the trophoblastic giant cells (Figure 1, C). A high concentration of ^{239}Pu was never found in the foetus, decidua, chorioallantoic placenta, amnion and the amnionic cavity throughout the gestational stages examined.

Table 2 shows the relative concentrations of ^{239}Pu in the foetoplacental unit of C3H and BDF1 mice evaluated by quantitative autoradiography using a BAS3000. Values are the intensity of photostimulated luminescence (PSL). Although PSL does not directly express radioactivity, it has been demonstrated that

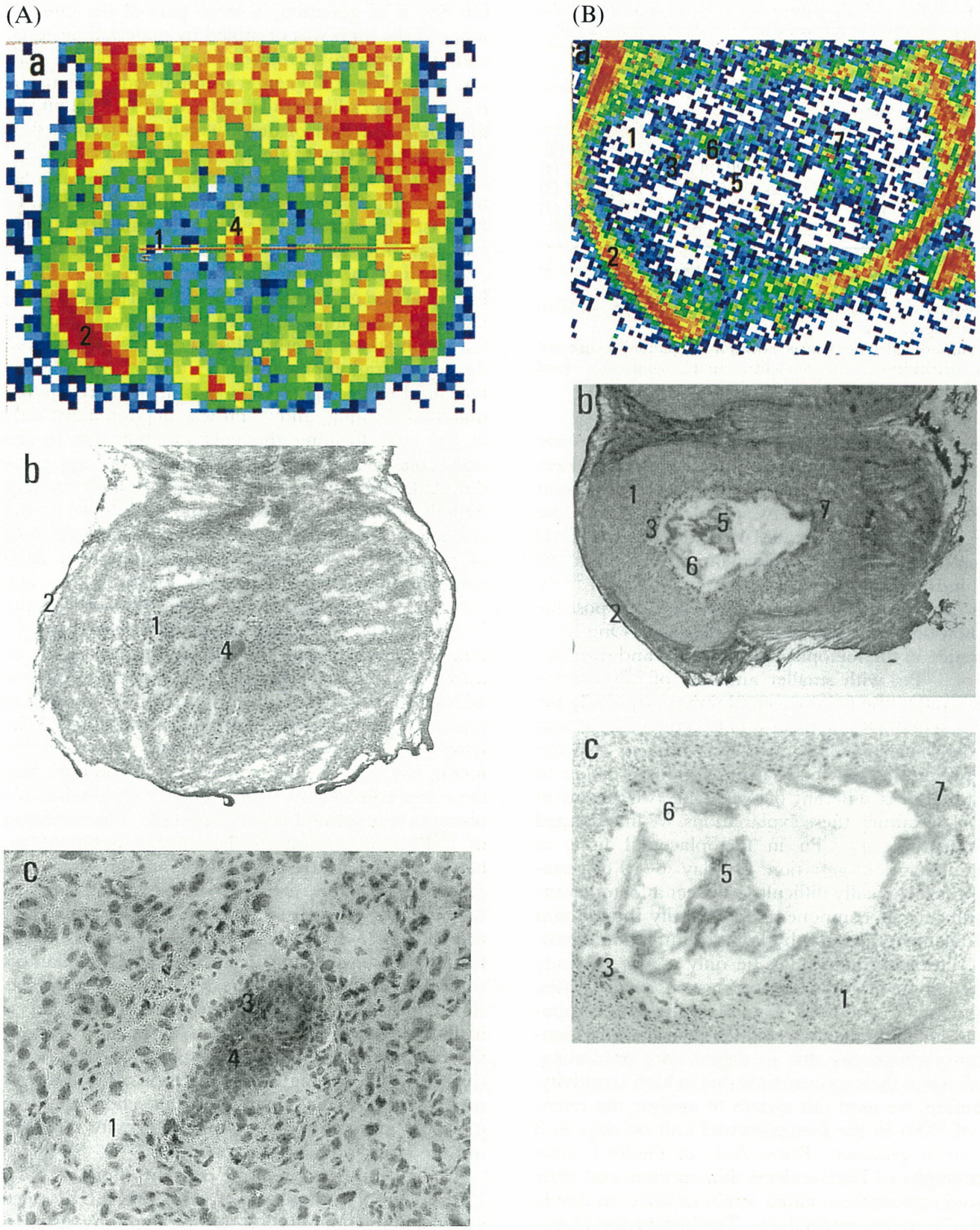

Figure 1. Histological sections and their autoradiographs of mouse uterus on days 6, 8 and 10 of gestation after the intraperitoneal injection of plutonium at a dose of 300 kBq/kg body weight on day 4 of gestation. (A) B6 mouse uterus on day 6 of gestation; (a) and (b) same magnification (× 32); (c) high magnification of the region of trophoblast and embryo. Similar observations were also obtained in the C3H mouse. (B) C3H mouse uterus on day 8 of gestation; (a) and (b) same magnification (× 16); (c) high magnification of the region of the foetus, yolk sac and trophoblastic giant cells. Similar observations were also obtained in the B6 mouse. (C) C3H mouse

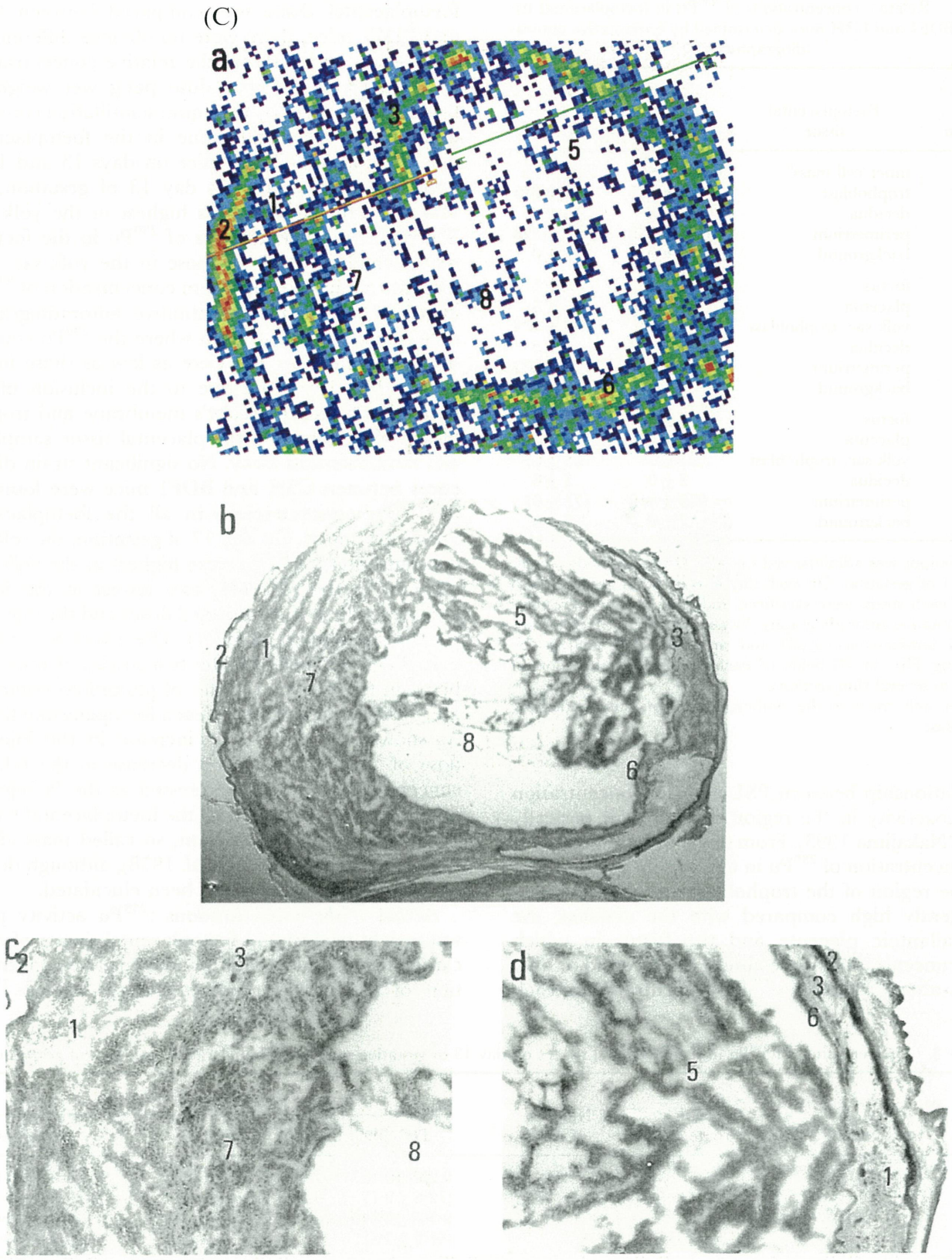

uterus on day 10 of gestation; (a) and (b) same magnification (× 16), (c) and (d) high magnification of the region of foetus, yolk sac and trophoblastic giant cells and the region of allantois, placenta and decidua respectively. Similar observations were also obtained in the B6 mouse. 1, decidua; 2, uterine perimetrium; 3, trophoblast or trophoblastic giant cells; 4, embryo; 5, foetus; 6, yolk sac; 7, immature placenta or placenta; 8, allantois.

Table 2. Relative concentrations of ^{239}Pu in foetoplacental tissues of BDF1 and C3H mice determined by quantitative autoradiography[a].

Day of gestation	Foetoplacental tissue	Mouse strain BDF1	Mouse strain C3H
6	inner cell mass[b]	194 ± 90	182 ± 75
	trophoblast	415 ± 135	471 ± 235
	decidua	10 ± 3	15 ± 3
	perimetrium	1109 ± 698	2163 ± 928
	background	2 ± 0	2 ± 0
8	foetus	3 ± 1	3 ± 1
	placenta	5 ± 1	8 ± 3
	yolk sac, trophoblast	140 ± 34	196 ± 103
	decidua	4 ± 1	5 ± 3
	perimetrium	959 ± 583	1278 ± 509
	background	2 ± 0	2 ± 0
10	foetus	3 ± 0	3 ± 0
	placenta	3 ± 1	3 ± 0
	yolk sac, trophoblast	196 ± 50	138 ± 65
	decidua	3 ± 0	2 ± 0
	perimetrium	303 ± 119	175 ± 87
	background	2 ± 0	2 ± 0

[a]Plutonium was administered i.p. at 300 kBq/kg body weight on day 4 of gestation. On each day 6, 8 or 10 of gestation two mice of each strain were sacrificed and their uterine were used for quantitative autoradiography. Values are mean PSL (photostimulated luminescence) ± SD and are based on analysis by measuring PSL in 20 fields of each foetoplacental region of interest in several thin sections.

[b]Inner cell mass is the embryonic region surrounded by trophoblast.

the relationship between PSL and the concentration of radioactivity in the region of interest is perfectly linear (Nakajima 1993). From day 6 to 10 of gestation, the concentration of ^{239}Pu in the uterine perimetrium and the region of the trophoblast and yolk sac, was consistently high compared with the decidua, the chorioallantoic placenta and the foetus in which ^{239}Pu concentrations were almost background or only slightly above. When the ^{239}Pu concentration in each foetoplacental tissue was compared between C3H and BDF1 mice, there were no obvious differences.

Tables 3 and 4 shows the relative concentrations of ^{239}Pu (% of injected dose per g wet weight of tissue), determined by the liquid scintillation counting of each foetoplacental tissue in the foetoplacental unit of C3H and BDF1 mice on days 13 and 17 of gestation respectively. On day 13 of gestation, the concentration of ^{239}Pu was highest in the yolk sac. The relative concentrations of ^{239}Pu in the foetuses were very low; $<1\%$ of those in the yolk sac. The placenta contained a medium concentration of ^{239}Pu, inconsistent with the quantitative autoradiographic data on day 10 of gestation where the ^{239}Pu concentrations in the placenta were as low as those in the foetus. This might be due to the inclusion of the parietal yolk sac, Reichert's membrane and trophoblastic giant cells into the placental tissue sample in this radiochemical assay. No significant strain differences between C3H and BDF1 mice were found in the ^{239}Pu concentrations in all the foetoplacental tissues examined. On day 17 of gestation, the relative concentrations of ^{239}Pu were highest in the yolk sac, medium in the placenta, and lowest in the foetal liver, regardless of the injected doses and the injection route of plutonium (Table 4). There was no remarkable difference between the two strains of mice and between the injection routes of plutonium regarding the ^{239}Pu concentrations in each foetoplacental tissue. As shown in Table 4, the increase in the injected dose of ^{239}Pu resulted in a decrease in the relative concentration of ^{239}Pu, expressed as the % injected dose per g wet weight, in all the foetoplacental tissues examined. This phenomenon, so called mass effect, has been reported (Weiss *et al.* 1978), although details of the mechanism have not been elucidated.

Actual ^{239}Pu concentrations (^{239}Pu activity per g wet weight of tissue) in foetoplacental tissues of mice can be calculated to multiply the relative concentration of ^{239}Pu by the injected dose. Actual ^{239}Pu

Table 3. Concentration of ^{239}Pu in foetoplacental tissues on day 13 of gestation after the administration on day 4 of gestation[a].

Dose[b]	Mouse strain	Injection route	Number of dam	Foetoplacental tissues: Placenta	Yolk sac	Foetus
300	BDF1	i.p.	4	0·263 ±0·127 (72·6 ± 9·1)	1·793 ±0·025 (21·4 ± 2·4)	0·012 ± 0·003 (119·3 ± 6·5)
300	C3H	i.p.	4	0·304 ±0·040 (64·8 ± 7·3)	1·456 ±0·391 (25·1 ± 4·5)	0·010 ± 0·001 (109·9 ± 9·5)

[a]Values are mean ± SD of the relative concentrations of ^{239}Pu, expressed as percentages of the injected dose per g wet weight of the tissue and are based on analysis of pooled foetal tissues from each dam. Values in parentheses are weights(mg) of the tissues and denote the mean ± SD.

[b]Plutonium was administered on day 4 of gestation (kBq/kg body weight).

Table 4. Concentration of ^{239}Pu in foetoplacental tissues on day 17 of gestation after the administration on day 4 of gestation[a].

Dose[b]	Mouse strain	Injection route	Number of dam	Foetoplacental tissues		
				Placenta	Yolk sac	Foetal liver
30	BDF1	i.p.	3	0·707 ± 0·290 (94·2 ± 12·6)	3·920 ± 0·482 (38·5 ± 4·4)	0·137 ± 0·005 (63·5 ± 11·0)
30	C3H	i.p.	3	1·020 ± 0·428 (90·4 ± 10·4)	3·715 ± 1·385 (42·5 ± 7·1)	0·110 ± 0·046 (57·3 ± 4·0)
300	BDF1	i.v.	3	0·614 ± 0·236 (85·7 ± 6·3)	3·225 ± 1·115 (35·8 ± 6·8)	0·086 ± 0·039 (57·9 ± 9·5)
300	BDF1	i.p.	3	0·588 ± 0·204 (90·7 ± 9·5)	2·566 ± 0·741 (33·9 ± 8·2)	0·068 ± 0·018 (61·7 ± 10·7)
300	C3H	i.v.	3	0·644 ± 0·234 (89·9 ± 10·5)	2·212 ± 0·336 (39·6 ± 7·1)	0·065 ± 0·031 (58·9 ± 7·7)
300	C3H	i.p.	3	0·629 ± 0·135 (88·2 ± 8·7)	2·454 ± 0·596 (36·5 ± 10·1)	0·061 ± 0·022 (55·4 ± 6·4)
900	BDF1	i.p.	3	0·332 ± 0·101 (92·8 ± 13·7)	1·155 ± 0·425 (36·9 ± 8·5)	0·032 ± 0·014 (59·7 ± 10·6)
900	C3H	i.p.	3	0·362 ± 0·069 (97·1 ± 31·7)	1·395 ± 0·331 (44·2 ± 9·1)	0·037 ± 0·006 (57·6 ± 9·5)

[a]Values are mean ± SD of the relative concentrations of ^{239}Pu, expressed as percentages of the injected dose per g wet weight of the tissue and are based on analysis of pooled foetal tissues from each dam. Values in parentheses are weights (mg) of the tissues and denote the mean ± SD.

[b]Plutonium was administered on day 4 of gestation (kBq/kg body weight).

concentrations in foetoplacental tissues of C3H mice injected at 900 kBq/kg were much higher than those in BDF1 mice injected at 30 kBq/kg. Even under these conditions, the number of CFU-S in the foetal liver of C3H mice was not affected by an injection of ^{239}Pu at 900 kBq/kg, whereas 30 kBq/kg significantly decreased the number in the BDF1 mouse foetal liver (Table 1).

These findings indicates that the transfer, distribution and retention of ^{239}Pu in conceptuses is similar between C3H and BDF1 mice throughout the gestational periods after maternal contamination with ^{239}Pu on day 4 of gestation. This suggests that there may be a strain difference associated with the susceptibility of the mouse foetal haematopoietic tissues to α-irradiation with ^{239}Pu. Lord *et al.* (1992) reported that after BDF1 mice were injected with ^{239}Pu on day 4 of gestation, the number of CFU-S in the foetal liver and the bone marrow of offspring decreased significantly. They also showed that this decrease in CFU-S resulting from embryonic phase contamination with ^{239}Pu was attributable to depletion of the haematopoietic stem cell population while the haematopoietic microenvironment developed normally. Considering their data and the results of the present study, the difference in the radiosensitivity of haematopoietic stem cells may be one probable mechanism involved in the strain difference in the effect of ^{239}Pu maternally injected on the CFU-S frequency in the foetal liver. However, the other more complicated issues involving the different probability of α-particle hit to target cells between mouse strains due to possible differences in the development and location of foetal haematopoietic stem cells or in the microdosimetric distribution of plutonium activities in the conceptus can not yet be excluded.

References

Brent, R. L., Beckman, D. A. and Jensh, R. P., 1987, Relative radiosensitivity of fetal tissue. *Advances in Radiation Biology*, **12,** 239.

Kato, H., Yoshimoto, Y. and Schull, W. J., 1989, Risk of cancer among children exposed to atomic bomb radiation *in utero*. In *Perinatal and Multigeneration Carcinogenesis*, edited by N. P. Napalkov, J. M. Rice, L. Tomati and H. Yamasaki (Oxford: IARC), pp. 365–374.

Kubota, Y., Sato, H., Koshimoto, C. and Takahashi, S., 1993, Transfer of ^{239}Pu to mouse fetoplacental tissues. *Journal of Radiation Research*, **34,** 157–163.

Lindenbaum, A., Lund, C., Smoler, M. and Rosenthal, M. W., 1968, Preparation, characterization and distribution in mouse tissues of graded polymeric and monomeric plutonium. In *Diagnosis and Treatment of Deposited Radionuclides*, edited by H.A. Kornberg *et al.* (Amsterdam: Excerpta Medica), pp. 56–64.

Lord, B. I., Mason, T. M. and Humphreys, E. R., 1992, Age-dependent uptake and retention of ^{239}Pu: its relationship to haemopoietic damage. *Radiation Protection Dosimetry*, **41,** 163–167.

Lord, B. I., Molineux, G., Humphreys, E. R. and Stones, V. A., 1991, Long-term effects of plutonium-239 and radium-224 on the distribution and performance of pluripotent haemopoietic progenitor cells and their regulatory

microenvironment. *International Journal of Radiation Biology*, **59,** 211–227.

MASON, T. M., HUMPHREYS, E. R. and LORD, B. I., 1991, Alpha-particle irradiation of haemopoietic tissue in pre- and postnatal mice. 1. Distribution of plutonium-239 after mid-term contamination. *International Journal of Radiation Biology*, **59,** 467–478.

MASON, T. M., LORD, B. I., MOLINEUX, G. and HUMPHREYS, E. R., 1992, Alpha-irradiation of haemopoietic tissue in pre- and postnatal mice. 2. Effects of mid-term contamination with ^{239}Pu *in utero*. *International Journal of Radiation Biology*, **61,** 393–403.

MORGAN, A., HAINES, J. W. and HARRISON, J. D., 1991, The incorporation of plutonium by the embryo and fetus of rats and guinea-pigs. *International Journal of Radiation Biology*, **59,** 1395–1413.

MORGAN, A., HARRISON, J. D. and STATHER, J. W., 1992, Estimates of embryonic and fetal doses from ^{239}Pu. *Health Physics*, **63,** 552–559.

NAKAJIMA, E., 1993, Radioluminography, a new method for quantitative autoradiography in drug metabolism studies. *Radioisotopes*, **42,** 228–236.

STATHER, J. W., CLARKE, R. H. and DUNCAN, K. P., 1988, *The Risk of Childhood Leukemia Near Nuclear Establishments*, (London: HMSO), NRPB-R215.

TAKAHASHI, S., KUBOTA, Y., KOSHIMOTO, C., SATO, H. and HATASHITA, S., 1994, Distribution of carbon-14 and associated radiation dose in rat fetal brain and liver after maternal injection of [^{14}C] thymidine. *Radiation Research*, **140,** 10–16.

UNSCEAR, 1986, *Genetic and Somatic Effects of Ionising Radiation. Report to the General Assembly, with Annexes* (New York: United Nations), pp. 306–419.

VAN DEN HEUVEL, R. L., 1990, Bone marrow from Balb/c mice radiocontaminated with ^{241}Am *in utero* shows a deficient *in vitro* haemopoiesis. *International Journal of Radiation Biology*, **57,** 103–115.

WEISS, J. F. and WALBURG, H. E., 1978, Influence of mass of administered plutonium on its cross-placental transfer in mice. *Health Physics*, **35,** 773–777.

J. RADIAT. RES., 38, 77–86 (1997)

High Frequency of Leukemic Lymphomas with Osteosarcomas but No Myeloid Leukemias in C3H Mice after ^{239}Pu Citrate Injection

YOICHI OGHISO, YUTAKA YAMADA and HARUZO IIDA

Division of Radiotoxicology and Protection, National Institute of Radiological Sciences
9–1, 4-chome, Anagawa, Inage-ku, Chiba 263, Japan

(Received, August 8, 1996)
(Revision received, February 24, 1997)
(Accepted, March 3, 1997)

Leukemia/Osteosarcoma/C3H mice/^{239}Pu citrate

Female C3H strain mice, which do not spontaneously exhibit frequent bone tumors and myeloid leukemias, were injected intraperitoneally with various doses of 10 to 12000 Bq/animal of monomeric ^{239}Pu citrate to clarify lifetime carcinogenesis caused by alpha-particles distributed mainly in the skeleton. Survival time was reduced significantly at mean skeletal doses of more than 2.93 Gy and was accompanied by marked life-shortening as compared to the controls due to an earlier increase in neoplastic or non-neoplastic death. Bone tumors, almost all of which were osteosarcomas, were not found in the controls, whereas their incidence increased sharply to a maximum of 96% at 6.92 Gy, then dropped at higher doses (20% at 42.4 Gy). Although lymphoid tumors were present in 20% of the control animals, their incidence dropped to zero at 6.92 Gy, then increased at higher doses (36% at 25.5 Gy). Non-thymic, mostly pre-B cell type, leukemic lymphomas mainly occurred at early time after ^{239}Pu-injection; whereas, in the controls thymic, lymphocytic or histiocytic lymphomas occurred only at a later time. Of the other soft tissue tumors, neither myeloid leukemias nor myelogenous neoplasms were found in the controls or the ^{239}Pu-injected animals. Tumors affecting the lungs, liver, ovaries, and skin were much fewer or not found at mean doses of more than 2.93 Gy. These results indicate dose-dependent, differential tumor induction resulting from bone and lymphoid tumor competition after an injection of plutonium.

INTRODUCTION

Bone-seeking radionuclides enter the body through circulating blood and are translocated to the skeleton, in which their microdistribution sites are the endosteal bone surfaces or bone minerals, depending on the chemical and metabolic properties of the nuclides. Although the local irradiation of these bone-seekers is retained for a long time and finally induces osteogenic sarcomas[1–4], there is little evidence that hematopoietic neoplasms are efficiently induced, even though bone marrow stem cells also may be exposed to radioactivity deposited along the trabecular bone surfaces. In fact, much lower frequencies of both myeloid and lymphoid tumors have been reported in experimental animals after injections of alpha- or beta-emitting bone-seekers

Correspondence: Dr. Yoichi Oghiso
Division of Radiotoxicology & Protection
National Institute of Radiological Sciences
9–1, 4-chome, Anagawa, Inage-ku, Chiba 263, Japan
(TEL: 043–251–2111 Ext 403, FAX: 043–256–9882)

as compared to the frequencies induced by the external irradiation of low linear energy transfer (LET) radiations[5–7]. The exception is the experimental results reported for CBA/H strain mice, in which relatively high injected doses of ^{239}Pu induced lymphomas[8], whereas the repeated injection of much lower doses of ^{239}Pu or ^{224}Ra[9,10] induced myeloid leukemias at a slightly higher, but not significant, frequency as compared to the controls and groups injected once with low doses. The reasons for such low efficiencies and the difficulty in inducing bone marrow-derived hematopoietic tumors by alpha-emitting bone-seekers have yet to be fully elucidated.

Previously, we reported that relatively high doses of injected ^{239}Pu induced lymphatic leukemias more efficiently than osteosarcomas in female C3H strain mice, whereas no myelogenous tumors were found in any of the controls or experimental groups injected with 500–10000 Bq per animal at a final mean skeletal dose of 3.1 Gy or more[11]. We here report new findings obtained by the addition of control and ^{239}Pu-injected animals to the previous groups that indicate differential induction of bone and lymphoid tumors due to competition, as well as high frequencies of non-thymic leukemic lymphomas and that there is no significant evidence of the appearance of myeloid leukemias even at low injected doses (10–100Bq/animal) or mean skeletal doses of less than 0.693 Gy.

MATERIALS AND METHODS

Experimental Animals and Cares

Six- to eight-week-old specific pathogen (*Salmonella spp., Mycoplasma spp.,* and *Tyzzer's organism*)-free (SPF) female C3H strain mice that were purchased from our animal breeding facility were fed on a commercial diet with water *ad libitum* and kept under barrier-filtered air before and after the experiments. The animal rooms were maintained on a 12 hr-daylight cycle at an air temperature of 23±1.0°C and a humidity of 55±5.0%. Animal care consisted of a change to clean cages weekly and daily checks of the animals' conditions.

Preparation and Injection of ^{239}Pu Citrate

As described elsewhere[11], a portion of a stock solution of ^{239}Pu nitrate (10 mM) was added to trisodium citrate solution (100mM) to obtain a molecular ratio of 1:50. This mixture was titrated to a final pH of 6.8–7.2 by the careful addition of droplets of 1N NaOH solution. Just before administration, part of the ^{239}Pu citrate solution was diluted with physiological saline and passed through both a 0.2 and 0.025 μm-pore milliporefilter to obtain monomeric ^{239}Pu citrate solution whose activity was counted as about 10^3–10^5 Bq/ml in a liquid scintillation spectrometer.

Six groups of 12- to 14-week-old mice weighing 25–28 g were injected intraperitoneally (ip) with different amounts of radioactivity in 0.1 ml of ^{239}Pu citrate solution. The injected activity per animal and the total numbers of animals, including those in the previous report[11], are 10–11 Bq/animal (total 50 animals), 110–111 Bq/animal (total 50 animals), 580–727 Bq/animal (total 40 animals, including 31 previous animals), 1120–1540 Bq/animal (total 45 animals, including 30 previous animals), 5160–6050 Bq/animal (total 40 animals, including 27 previous animals), and 10600–11600 Bq/animal (total 35 animals, including 29 previous animals). As the vehicle controls, a group of age-matched mice (total 100 animals, including 60 previous controls) was injected ip with 0.1 ml of saline. During their lifetimes, these animals were housed ten per

polycarbonate cage and kept in a closed-hood rack placed in the animal rooms.

Dose Calculation

Skeletal retention curves obtained by measuring the ^{239}Pu concentration in each group of animals that received a dose of 10 to 12000 Bq/animal, had almost similar components for half time and the initial skeletal fraction. The average cumulative skeletal (both surface and volume) dose (Gy) per animal until death was calculated using the previously reported equation[11];

$$D(T) = 3.8 \times 10^{-5} A \int_0^T R(t)dt$$

where T is the survival time (day), A the injected dose (Bq), and R (t) the retention function.

In the following description, dose refers to the mean of the average cumulative skeletal dose in each group, unless otherwise stated.

Pathological Examinations

All the control and ^{239}Pu-injected mice in the groups listed in Table 1 were available for pathological examinations after death. At autopsy, gross lesions were carefully examined, in particular as to the times of onset and distribution of tumors, after which the main organs and bones (including tumors) were fixed in 10% phosphate-buffered formalin. The bones and bone tumors were decalcified after fixation with a mixture of 10% formic acid and 10% neutral formalin. All the tissue samples were cut into small pieces, processed with graded ethanol and xylen in an automatic tissue processor, then embedded in paraffin. Sections 5 to 6 μm thick were prepared and stained with hematoxylin and eosin (HE) for the light microscope examinations, unless otherwise stated.

Statistics

Mean survival time is the arithmetical mean of the survival periods for a given dose group after a saline or ^{239}Pu injection. The 50% survival time is the period that half the animals survived, as estimated from the survival curve for each dose group. In practice, both the survival times and the competing risk of neoplastic or non-neoplastic death were calculated and analyzed by the Kaplan-Meier method using the Log-rank and Peto-Peto-Wilcoxon tests and commercially available computor software (Stat View®). Tumor frequency and the number of tumor-bearing animals in each group were estimated by the direct procedure for age-adjusted incidence[12], then compared for significant differences between the control and ^{239}Pu-injected animal groups using the Student's t-test.

RESULTS

Life-shortening and Early Death after ^{239}Pu-injection

As shown in Table 1, the mice were divided into one saline-injected (control) group and eight ^{239}Pu-injected groups on the basis of mean skeletal doses of 0 to 42.4 Gy, of which values correlated well with the mean injected doses of 0 to 11460 Bq. The mean and 50% survival times after the injection of ^{239}Pu were significantly reduced in the dose range from 2.93 to 42.4 Gy ($p < 0.001$), but were not significantly different from those of the control at doses of less than 0.693 Gy (Table 1). The cause of death was either neoplastic

Table 1. Dose and survival period after ^{239}Pu injection

No. of Animals	Injected Dose (Bq)[a]	Skeletal Dose (Gy)[b]	Mean Survival Time (Days)[c]	50% Survival Time (Days)[c]
100	0	0	770 ± 8.4	774 ± 8.7
50	10.7 ± 0.5	0.067 ± 0.01	728 ± 20	773 ± 31
50	110 ± 0.5	0.693 ± 0.115	730 ± 21	776 ± 14
30	632 ± 67	2.93 ± 0.48	499 ± 24*	508 ± 34*
30	1129 ± 332	4.66 ± 0.68	452 ± 22*	416 ± 62*
25	1456 ± 168	6.92 ± 0.67	479 ± 13*	452 ± 44*
25	5414 ± 329	17.3 ± 2.6	309 ± 10*	311 ± 12*
25	7870 ± 223	25.5 ± 3.7	325 ± 16*	338 ± 70*
25	11460 ± 280	42.4 ± 2.8	390 ± 8.5*	383 ± 4.2*

[a]Mean ± SD of the injected activity per animal in each group.
[b]Mean ± SD of the calculated dose per animal in each group.
[c]Mean ± SE of the survival period after injection estimated by the Kaplan-Meier method (see text).
Asterisks indicate a significant difference as compared to the controls ($p < 0.001$).

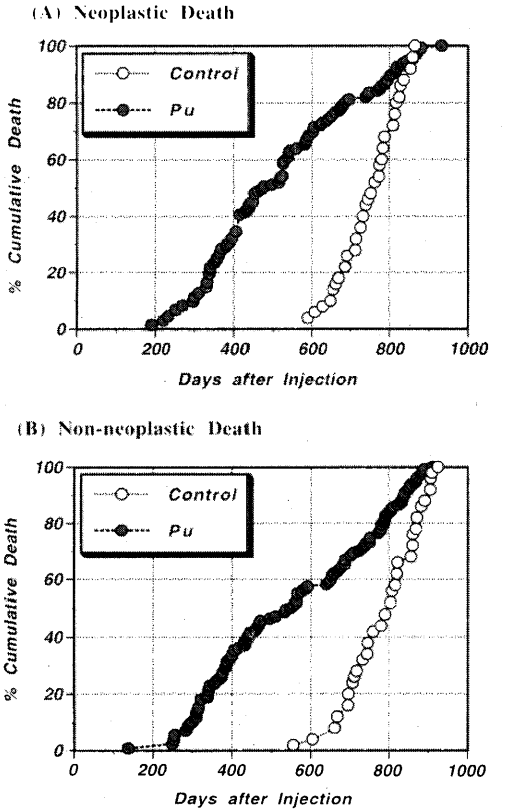

Fig. 1. Cumulative incidences of neoplastic (A) and non-neoplastic (B) death in all the groups of animals after the injection of ^{239}Pu citrate (Pu) or saline(control).

death due to fatal tumors or non-neoplastic death accompanied mainly by hematopoietic dysplasia, circulatory dysfunction, hepatosis, and nephritis. As compared to the controls, the neoplastic and non-neoplastic deaths of all the ^{239}Pu-injected animals appeared to occur much earlier, respectively on days 190 and 137, after ^{239}Pu-injection (Fig. 1).

Dose and Tumor Responses after ^{239}Pu-injection

The numbers of tumor bearing animals in the control and ^{239}Pu-injected groups are given in Table 2. Age-adjusted incidences for all the tumor bearing animals were significantly ($p < 0.001$) high only at the mean skeletal dose of 6.92 Gy as compared to the controls. Whereas the age-adjusted incidences for the fatal tumor bearers were significantly ($p < 0.01$) high at doses of 6.92 to 25.5 Gy, those for the incidental, non-fatal tumor bearers were significantly ($p < 0.01$) low at doses of more than 0.067 Gy. The other age-adjusted incidences for all the tumor bearers and fatal tumor bearers at doses of 0.067, 0.693, 2.93, 4.66 or 42.2 Gy were significantly ($p < 0.01$) low. Fatal tumors are mostly bone and lymphoid ones, and occasionally hepatocellular or chollangiocellular carcinomas; whereas, the incidental, non-fatal tumors are other soft tissue tumors: pulmonary adenomas or adenocarcinomas, ovary cystadenocarcinomas or granulosa cell tumors, uterus cystadenomas, and miscellaneous tumors such as dermal fibrosarcomas or histiocytomas and stomach adenocarcinomas. Of the fatal tumors, no bone tumors were found in the controls, and almost all the bone tumors in the ^{239}Pu-injected mice were osteosarcomas. The age-adjusted incidences for bone tumors were 14% at the mean skeletal dose of 0.693 Gy, increased to 43% at 4.66 Gy, and reaching a maximum of 96% at 6.92 Gy, then dropped to 48% at 17.3 Gy and reached a minimum of 20% at 42.2 Gy (Fig. 2). In contrast, the age-adjusted incidences for lymphoid tumors were 20% in the control, decreased to 10% or less at doses of 0.067 to 2.93 Gy, and reached 0% at doses of 4.66 to 6.92 Gy, but increased to 24% at 17.3 Gy, and reached a maximum of 36% at 25.5 Gy (Fig. 2). Age-adjusted incidences for soft tissue tumors other than bone and lymphoid tumors were not significantly different at doses of 0.067 to 0.693 Gy as compared to the incidence for the controls, but they showed a marked decrease to 13% or less at doses of 2.93 to 6.92 Gy, reached 0% at doses of 17.3 Gy or more (Fig. 2). Neither myeloid leukemias nor myelogenous neoplasms

Table 2. Numbers of tumor bearing animals after ^{239}Pu injection

Mean Skeletal Dose (Gy)	No. of Animals	No. of Tumor-Bearers[a]		
		All	Fatal Tumors	Incidental Tumors
0	100	78 (78.0 ± 2.1)	50 (50.0 ± 3.6)	60 (60.0 ± 2.5)
0.067	50	34 (68.0 ± 3.3)	20 (40.0 ± 4.5)*	19 (38.0 ± 3.5)*
0.693	50	38 (76.0 ± 3.3)	18 (36.0 ± 4.3)*	26 (52.0 ± 3.6)*
2.93	30	15 (50.0 ± 4.6)*	12 (40.0 ± 5.5)*	6 (20.0 ± 3.6)*
4.66	30	16 (53.0 ± 4.6)*	15 (50.0 ± 6.5)	2 (6.7 ± 2.3)**
6.92	25	25 (100)**	25 (100)**	1 (4.0 ± 1.9)**
17.3	25	18 (72.0 ± 4.5)	18 (72.0 ± 8.5)*	0 (0)**
25.5	25	17 (68.0 ± 4.6)	17 (68.0 ± 8.0)*	0 (0)**
42.2	25	8 (32.0 ± 4.6)*	8 (32.0 ± 5.5)*	0 (0)**

[a] The numbers of all, fatal, and incidental tumor bearing animals in each group with the age-adjusted incidence (% ± SE) in parentheses (see text).

Asterisks indicate a significant difference as compared to the controls (*$p < 0.01$ or **$p < 0.001$).

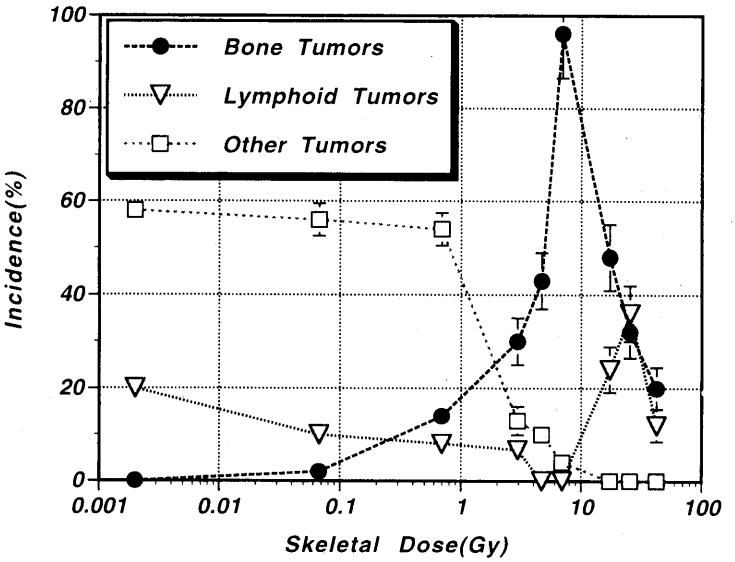

Fig. 2. Age-adjusted incidences (% ± SE) of bone, lymphoid, and other tumors as a function of the mean skeletal dose (Gy) after the injection of ^{239}Pu citrate.

were found in the controls or in any of the groups of ^{239}Pu-injected animals.

Differential Induction of Lymphoid Tumors after ^{239}Pu-injection

Lymphoid tumors in the ^{239}Pu-injected animals appeared to occur during early period between days 150–550, rather than during the later period between days 600–850 after injection, whereas those in the controls occurred only in the latter period (Fig 3). The lymphoid tumors in the control and ^{239}Pu-injected animals were classified into four types based on histopathological criteria: thymic lymphomas which mostly involved the thymus, some lymph nodes and the spleen; lymphocytic lymphomas which involved almost all the lymphoid organs, except the thymus, and occasionally the spleen and liver; leukemic lymphomas, in which leukemic lymphoblasts appeared in the peripheral blood and infiltrated the spleen, liver, and many of the lymphoid organs; and histiocytic lymphomas in which the neoplastic growth of histiocytes or reticular cells locally involved some superficial or intraperitoneal lymph nodes. The differential diagnosis of lymphocytic or leukemic lymphomas is based on the appearance of the lymphoblasts in the peripheral blood, subcutaneous malignant histiocytomas being excluded from the histiocytic lymphoma category. In addition, the available tissue specimens were stained immunohistochemically with monoclonal antibodies against mouse T-cells (Thy-1.2) and mouse pre-B cells (Ly 5;B220). These results show that all the thymic lymphomas examined were the T-cell type, whereas all the lymphocytic lymphomas were the pre-B cell type. Approximately 30% of the leukemic lymphomas were the T-cell type, and the remainder (70%) the pre-B cell type. Histiocytic lymphomas, however, were negative for both surface markers. Of the histologic phenotypes shown in Table 3, thymic lymphomas were found only in the controls and ^{239}Pu-injected animals at the mean skeletal dose of 0.067 Gy, but not at any dose of more than 0.693 Gy. Leukemic lymphomas

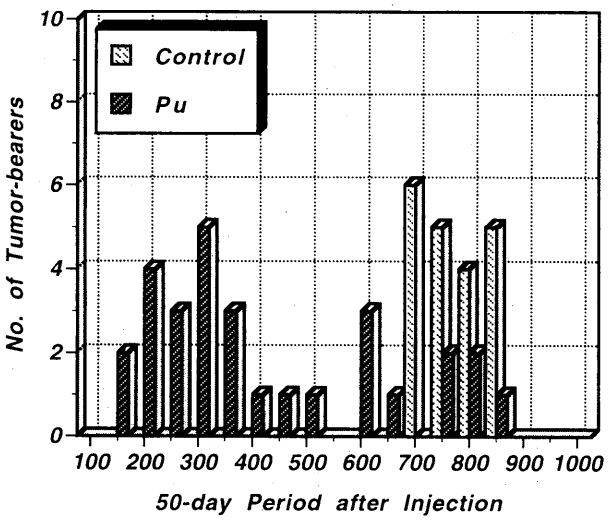

Fig. 3. Onset of lymphoid tumors in mice, shown by the numbers of affected animals in all groups during the 50-day period after the injection of ^{239}Pu citrate (Pu) or saline (control).

Table 3. Histological types of lymphoid tumors after ^{239}Pu injection

Mean Skeletal Dose (Gy)	No. of Animals	No. of Tumor Types[a]				
		All	Thymic	Lymphocytic	Leukemic	Histiocytic
0	100	20	5	8	0	7
0.067	50	5	1	4	0	0
0.693	50	4	0	4	0	0
2.93	30	2	0	2	0	0
4.66	30	0	0	0	0	0
6.92	30	0	0	0	0	0
17.3	25	6	0	1	5	0
25.5	25	9	0	1	8	0
42.4	25	3	0	1	2	0

[a] The numbers of all the types and individual histological types of lymphoid tumors found in each group, as differentially diagnosed on the criteria given in the text.

predominated in the ^{239}Pu-injected animals only at doses of 17.3 Gy or more. Lymphocytic or histiocytic lymphomas were present in the controls, but these were much fewer, or not found, in the ^{239}Pu-injected animals at doses of 4.66 Gy or more.

DISCUSSION

Our findings on the survival period of mice after ^{239}Pu-injection clearly indicate significant life-shortening, as compared to the controls, at the mean skeletal dose of 2.93 Gy or more but not at doses of less

than 0.693 Gy, indicative of a dose-dependent survival decrease with a threshold at low doses, as reported elsewhere[3,13]. Life-shortening also was due to neoplastic or non-neoplastic death which appeared to occur earlier in the ^{239}Pu-injected mice than the controls. Hematopoietic dysplasia, frequently observed among the non-neoplastic deaths, is related to the acute effects of alpha-particle irradiation on bone marrow stem cells; whereas, such disorders as circulatory dysfunction, hepatosis, and nephritis are considered cachectic symptoms that are directly or indirectly induced by irradiation.

No reasons are known for the significantly low incidences for the fatal and incidental tumor bearers at a mean skeletal dose of 0.693 Gy or less, even though there were no significant differences in incidences for all the tumor bearers, in comparison to the controls. The incidences for fatal tumor bearers, however, were significantly high, whereas those for incidental, non-fatal tumor bearers were significantly low, at doses of 6.92 to 25.5 Gy, indicative of competition between both types of tumor bearers in this dose range. The significantly low incidences for both fatal and incidental tumor bearers as well as for all the tumor bearers at doses of 2.93, 4.66, or 42.2 Gy may be due to the early occurrence of non-neoplastic death. A comparison of the incidences for tumor types shows that almost all the tumors in the controls and in ^{239}Pu-injected animals that received mean skeletal doses of less than 0.693 Gy were lymphoid or the other soft tissue tumors; whereas, most tumors were bone or lymphoid ones, and there was a much lower incidence of other soft tissue tumors at doses of more than 2.93 Gy. The incidence of bone tumors, mostly osteosarcomas, increased sharply in the dose range of 2.93 to 6.92 Gy, but decreased at doses of more than 17.3 Gy. In contrast, the incidence of lymphoid tumors was much lower, or zero, in the dose range of 2.93 to 6.92 Gy, but it increased in the dose range of 17.3 to 25.5 Gy. The differential tumor spectrum found in the low and high dose ranges, may be the result of competition between the bone and lymphoid tumors, as has been documented in CBA/H strain mice[8].

Although the maximum incidence (36%) of lymphoid tumors after ^{239}Pu-injection was significantly, but only slightly higher than the value (20%) for the controls, marked differences were noted both for the time of onset and histologic phenotype. Lymphoid tumors in the ^{239}Pu-injected mice showed two-phases of occurrence at an early and late time after the injection, whereas those in the controls occurred only at a late time. This suggests that at least some of the lymphoid tumors are the chronic type commonly seen in C3H strain mice, but the rest are classified mainly as the acute type induced only by ^{239}Pu-injection. Murine lymphoid tumors also are induced more effectively and acutely in other strains of mice by low or high LET radiation[14–17], but their frequencies and histologic phenotypes differ widely. The acute lymphoid tumors induced by X- and γ-radiation or by fast neutron exposure are mainly thymic lymphomas or malignant lymphocytic lymphomas if fractionated low dose rates are given. Most of the acute lymphomas in our C3H strain mice that appeared after ^{239}Pu-injection were non-thymic and leukemic lymphomas, whereas most of the chronic lymphoid tumors in the control mice were thymic, lymphocytic, or histiocytic ones with no expression of leukemia. The only difference from the control mice in terms of the histologic phenotypes of the lymphoid tumors induced by ^{239}Pu-injection appears to be the high frequency of non-thymic and leukemic lymphomas. Interestingly, results of immunohistochemical analyses showed that about 70% of these leukemic lymphomas had a surface marker specific for pre-B cells derived from the bone marrow, suggesting that pre-B cell type leukemic lymphomas are induced preferentially after ^{239}Pu-injection. In addition, the lymphocytic lymphomas in the controls and some of the ^{239}Pu-injected animals were all positive for pre-B cell surface markers. Although the reason for higher frequency of pre-B cell type lymphomas as compared to T-cell type thymic lymphomas is not clear, strain difference is plausible because another strain, C57Bl, is

more susceptible to spontaneous or radiation-induced thymic (T-cell type) lymphomas as compared to the other mouse strains[15–17].

Finally, neither myeloid leukemias nor myelogenous neoplasms were present in the controls or any of the dose groups of the ^{239}Pu-injected mice. There is little evidence of a significant yield of myeloid leukemias induced by ^{239}Pu or other alpha particle-emitting radionuclides, except the results of experiments using CBA/H strain mice injected with low doses of ^{239}Pu or ^{224}Ra[9,10], and rats injected with ^{239}Pu or ^{241}Am[5,18], both of which resulted in a slight but not significantly high incidence of myeloid leukemias even when the doses were fractionated. External irradiation by low and high LET radiations, however, effectively induces myeloid leukemias in some strains of mice, including C3H[15,19]. Taken together, the findings show that myeloid leukemias are unlikely to be induced in experimental animals by alpha-particles, whether at a single low dose-injection or multiple low doses. Factors modulating the induction of myeloid leukemias include not only the quality factor and the dose rate of radiation but the animal species or strain differences in susceptibility, as well as the cellular and molecular mechanisms of myeloid leukemogenesis.

In conclusion, we have presented an experimental model of life-span carcinogenesis characterized by differential tumor induction in ^{239}Pu-injected C3H strain mice. Osteosarcomas and lymphoid tumors (mostly non-thymic, pre-B cell type leukemic lymphomas) were competitively induced in a dose-dependent manner, whereas myeloid leukemias were not found even at much lower dose ranges. Further investigation is needed to verify what mechanisms underly the low frequencies of hematopoietic neoplasms induced by alpha-particle irradiation of bone marrow stem cells.

ACKNOWLEGEMENTS

This work was supported by a grant from the Research Fund for Project Research on the Detriment and Modifying Factors of Radiation Exposures of the Japan Science and Technology Agency. We are greatful to the staffs of Animal Care, Co. and Tokyo Nuclear Services, Co., for their respective help with animal care and radiation protection.

REFERENCES

1. Bleaney, B. (1969) Plutonium deposition on bone surfaces and in bone marrow following intravenous and intramuscular injections. In "Delayed Effects of Bone-Seeking Radionuclides", Eds. C. W. Mays, W. S. S. Jee, R. D. Lloyd, B. J. Stover, J. H. Dougherty and G. N. Taylor, pp. 125–135, The University of Utah Press, Salt Lake City, Utah.
2. Mays, C. W., Dougherty, T. F., Taylor, G. N., Lloyd, R. D., Stover, B. J., Jee, W. S. S., Christensen, J. H., Dougherty, J. H. and Atherton, D. R. (1969) Radiation-induced bone cancer in beagles. In "Delayed Effects of Bone-Seeking Radionuclides", Eds. C. W. Mays, W. S. S. Jee, R. D. Lloyd, B. J. Stover, J. H. Dougherty and G. N. Taylor, pp. 387–408, The University of Utah Press, Salt Lake City, Utah.
3. Taylor, G. N., Mays, C. W., Lloyd, R. D., Gradner, P. A., Talbot, L. R., McFarland, S. S., Pollard, T. A., Atherton, D. R., van Moorhem, D., Brammer, D., Brammer, T. W., Ayoroa, G. and Taysum, D. H. (1983) Comparative toxicity of ^{226}Ra, ^{239}Pu, ^{241}Am, ^{249}Cf and ^{252}Cf in C57BL/Do black and albino mice. Radiat. Res. **95**: 584–601.
4. Mays, C. W., Taylor, G. N. and Lloyd, R. D. (1986) Toxicity ratios: their use and abuse in predicting the risk from induced cancer. In "Life-Span Radiation Effects Studies in Animals: What Can They Tell Us?", Eds. R. C. Thompson

and J. A. Mahaffey, pp. 299–310, US DOE CONF-830951.
5. Taylor, D. M. (1986) The comparative carcinogenesis of ^{239}Pu, ^{241}Am and ^{244}Cm in the rat. In "Life-Span Radiation Effects Studies in Animals: What Can They Tell Us?", Eds. R. C. Thompson and J. A. Mahaffey, pp. 404–412, US DOE CONF-830951.
6. McClellan, R. O. and Jones, R. K. (1969) ^{90}Sr-induced neoplasia: a selective review. In "Delayed Effects of Bone-Seeking Radionuclides", Eds. C. W. Mays, W. S. S. Jee, R. D. Lloyd, B. J. Stover, J. H. Dougherty and G. N. Taylor, pp. 293–322, The University of Utah Press, Salt Lake City, Utah.
7. Mole, R. H., Papworth, D. G. and Corp, M. J. (1983) The dose-response for X-ray induction of myeloid leukemia in male CBA/H mice. Brit. J. Cancer **47**: 285–291.
8. Loutit, J. F. and Carr, T. E. F. (1978) Lymphoid tumors and leukemia induced in mice by bone-seeking radionuclides. Int. J. Radiat. Biol. **33**: 245–263.
9. Humphreys, E. R., Loutit, J. F. and Stones,V. A. (1987) The induction by ^{239}Pu of myeloid leukemia and osteosarcoma in female CBA mice. Int. J. Radiat. Biol. **51**: 331–339.
10. Humphreys, E. R., Issacs, K. R., Raine, T. A., Saunders, J., Stones, V. A. and Wood, D. L. (1993) Myeloid leukemia and osteosarcoma in CBA/H mice given ^{224}Ra. Int. J. Radiat. Biol. **64**: 231–235.
11. Oghiso,Y., Yamada,Y. and Ilda,H.(1994) Differential induction of bone and hematopoietic tumors in C3H mice after the injection of ^{239}Pu citrate. J.Radiat.Res. **35**: 236–247.
12. Ullrich, R. L. and Storer, J. B. (1979) Influence of γ irradiation on the development of neoplastic disease in mice. I. Reticluar tissue tumors. Radiat. Res. **80**: 303–316.
13. Finkel, M. P. and Biskis, B. O. (1962) Toxicity of plutonium in mice. Health Phys. **8**: 565–579.
14. Sasaki, S. and Kasuga, T.(1981) Life-shortening and carcinogenesis in mice irradiated neonatally with X rays. Radiat. Res. **88**: 313–325.
15. Maisin, J. R., Wambersie, A., Gerber, G. B., Mattelin. G., Lambiet-Collier, M., DeCoster, B. and Gueulette, J. (1988) Life-shortening and disease incidence in C57Bl mice after single and fractionated γ and high-energy neutron exposure. Radiat. Res. **113**: 300–317.
16. Janowski, M., Cox, R. and Strauss, P. G. (1990) The molecular biology of radiation-induced carcinogenesis: thymic lymphoma, myeloid leukemia and osteosarcoma. Int. J. Radiat. Biol. **57**: 677–691.
17. Chen, Y., Kubo, E., Sado, T. and Muto, M. (1996) Cytogenetic analysis of thymocytes during early stages after irradiation in mice with different susceptibilities to radiation-induced lymphomagenesis. J. Radiat. Res. **37**: 267–276.
18. Benstead, J. P. M., Chir, B., Taylor, D. M. and Sowby, F. D. (1965) The carcinogenic effects of americium-241 and plutonium-239 in the rat. Brit. J. Radiol. **38**: 920–925.
19. Seki, M., Yoshida, K., Nishimura, M. and Nemoto, K. (1991) Radiation-induced myeloid leukemia in C3H/He mice and the effect of predonisolone acetate on leukemogenesis. Radiat. Res. **127**: 146–149.

J. RADIAT. RES., 39, 61–72 (1998)

Differential Dose Responses of Pulmonary Tumor Types in the Rat after Inhalation of Plutonium Dioxide Aerosols

YOICHI OGHISO*, YUTAKA YAMADA, HARUZO IIDA and JIRO INABA

Division of Radiotoxicology and Protection, National Institute of Radiological Sciences, 9–1, 4-chome, Anagawa, Inage-ku, Chiba 263, Japan

(Received, September 26, 1997)
(Revision received, February 2, 1998)
(Accepted, February 6, 1998)

Rats/$^{239}PuO_2$/Alpha dose/Lung tumors/Phenotypes

Dose responses were compared among primary lung tumors and their histological types induced by a single inhalation exposure of female Wistar strain rats to submicron-size and polydispersed aerosols of plutonium dioxide ($^{239}PuO_2$). While the primary lung tumors were found only in 2.3% of the unexposed control animals, the frequency of all the primary lung tumors in the exposed animals was 44% at the mean lung dose of 0.71 Gy, and increased sharply at the doses of 1.5 Gy or more, reaching the maximum of 97% at 5.4 Gy, and the dose responses around at 1.0 Gy were different between benign and malignant lung tumors. Almost all the pulmonary tumors in the exposed animals were classified into epithelial types such as adenomas, adenocarcinomas, adenosquamous carcinomas, and squamous cell carcinomas. The dose responses were different between these tumor types as shown by the peak incidence of adenomas at 0.71 Gy, adenocarcinomas at 2.9 Gy, adenosquamous and squamous cell carcinomas at 5.4–8.5 Gy, respectively. As the magnitudes of neoplastic lesions in pulmonary carcinomas were expressed by histological scores, metaplasias and adenomatous lesions most frequently appeared at doses of 1.5 Gy, while the appearance and increase of carcinomatous lesions differed in the dose ranges as shown by the peak incidence of adenocarcinomatous lesions at 2.9 Gy, and adenosquamous or squamous lesions at 5.4–6.6 Gy. These results indicate a differential dose response of pulmonary carcinogenesis in which metaplasias and benign adenomas were induced at lower doses (< 1.0 Gy), whereas malignant carcinomas were induced at relatively higher doses (> 1.5 Gy). Together with the increase of carcinomatous lesions at higher doses, the intranuclear p53 protein accumulation was detectable, but only in a few percentages of malignant carcinomas.

* Correspondence: Dr. Yoichi Oghiso
Division of Radiotoxicology and Protection
National Institute of Radiological Sciences
9–1, 4-chome, Anagawa, Inage-ku, Chiba 263–8555, Japan
Phone: 043–251–2111 Ext 403, FAX: 043–256–9882

INTRODUCTION

The human dosimetric model for radiation protection against inhalation exposures to air-borne radioactive aerosols has been described as limits for intakes of radionuclides by workers, in ICRP 30[1], which has recently been revised in ICRP 66[2] as a new human respiratory tract model with anatomical, morphological, and physiological parameters to permit the calculation of the deposition and dose for inhaled particles in different human subjects. The biological effects of inhaled radionuclides on the target organs at risk following the inhalation exposures have been summarized in ICRP 31[3], and the linear dose response with no threshold in low dose levels' exposures to various sources of ionizing radiation has been proposed for the potentially carcinogenic effects of some inhaled radionuclides[4]. While it remains unknown whether the inhalation exposures to the air-borne plutonium, both ^{238}Pu and ^{239}Pu, might result in the increased lung cancer risks in humans, the epidemiological investigations on occupational exposures of nuclear workers to plutonium and other radiation sources, however, implies no significant evidence for the increase of lung cancer mortality as compared to that of the age-matched populations[5,6]. Only the animal studies can therefore provide an experimental evidence for the risk estimation of inhaled plutonium. The estimated lifetime pulmonary cancer risks of inhaled plutonium aerosols with chemically different forms in beagle dogs[7–9] are derived from an approximation of the quadratic dose response curves rather than a pure linear one with no threshold, while the experiments using both Wistar and Fischer 344 strain rats[10–12] after inhalation exposures to high-fired plutonium dioxide aerosols, however, have indicated a "practical" threshold at low doses around 1 Gy for the dose response of malignant lung carcinomas as compared to much lower frequencies of spontaneous lung tumors. Although the reasons and underlying mechanisms for such a threshold-like dose response of pulmonary malignancies remain unclear, the distribution of aerosol particles in the respiratory tract and alpha doses or dose rates to the lining epithelium might result in differential dose responses of neoplastic lesions. The relationships between dose and tumor malignancies by inhalation of alpha particles-emitted radionuclides are not, however, fully elucidated.

We previously reported a high incidence of malignant lung carcinomas at the lung doses of 4–12 Gy from the life-span animal study on pulmonary carcinogenesis in female Wistar strain rats exposed to submicron-size and polydispersed $^{239}PuO_2$ aerosols[13]. The present paper summarizes the current results on differential dose responses of pulmonary carcinomas found at the doses of 0.71–10 Gy, in a special reference to the malignancies and histopathological phenotypes of tumors, as well as the frequency of the intranuclear p53 protein accumulation as an indicator for malignant phenotypes resulted from the mutation of the tumor-suppressor gene[14].

MATERIALS AND METHODS

Experimental animals, inhalation exposures and care

Because of slower increase of the body weight and easier handling than the males, and no

significant differences in the lung tumor induction noted between both sexes[11,12], we used 8-week-old female Wistar strain (W/M) rats, which were purchased from our animal breeding facility, fed on a commercial diet with water *ad libitum*, and kept under a barrier-filtered air before and after the experiments. Following the previous training, 20 healthy rats (80- to 100-day-old) were placed each into a plastic hand-made holder for nose-only exposures and exposed once for a maximum of 60 min to high-fired $^{239}PuO_2$ aerosols in a multiport inhalation chamber device as described below. All the age-matched, exposed and unexposed control animals were housed five per a polycarbonate cage and kept in a closed hood rack placed in the animal rooms during their lifetimes until the death. The animal rooms were maintained on a 12 hr-daylight cycle with an air temperature of 23 ± 1.0°C and a humidity of 55 ± 5.0%. Animal care consisted of weekly change of clean cages and daily checking of the animals' conditions for survival and immediate pathological examinations of dead animals.

Generation and assessment of aerosols

As previously described[13], the plutonium hydroxide solution chemically converted from the nitrate solution was nebulized in a compressed air-driven nebulizer, passed through a tube heated at 300°C to dry the droplets in air, and then conducted into a high temperature furnace heated at 1150°C. An air flow containing high-fired $^{239}PuO_2$ aerosol particles was introduced through a negative pressure by an exhaust air-pump into a multiport inhalation chamber device. Aerosol samples were collected simultaneously on a 10-stage cascade impactor plate to determine the particle size distribution. The activity median aerodynamic diameter (AMAD) was ranged from 0.3 to 0.5 μm with a geometric standard deviation of 1.8–2.1 in all the experiments, indicating the generation of submicron-size and polydispersed aerosol particles.

Determination and calculation of lung doses

The initial lung deposition (ILD) was determined individually in the exposed rats by the whole body counting of the low energy LX-ray of 17 keV emitted from ^{239}Pu deposited in the lung, and the cumulative alpha dose absorbed in the entire lung tissue was calculated at the time of death, based on the time-integral of the ILD, retention function, and lung weights as previously described[13]. In the following description, the dose refers to the mean of cumulative lung dose in each group, unless otherwise mentioned.

Pathological examinations

The postmortem pathological examinations were available on total 440 (130 control and 310 exposed) rats after the lifetimes. At autopsy, the gross lesions were carefully examined, in particular as to the distribution of neoplastic foci in each lobe of the lung, trachea, bronchi, and tracheobronchial lymph nodes. These tissue samples and the other main organs were fixed in 10% phosphate-buffered formalin, cut into small pieces, processed with graded ethanol and xylen in an automatic tissue processor, and then were embedded in paraffin. Sections, 5 to 6 μm-thick, were prepared and stained with hematoxylin and eosin (HE) for the light microscopic examinations unless otherwise mentioned.

Differential diagnosis of the primary lung tumors from metastatic ones and between the

histological types was based on the WHO criteria[15]. All the primary lung tumors except for 2 non-epithelial types (fibrosarcomas or hemangiosarcomas) were classified into epithelial types such as ductal or papillary adenomas, ductal, papillary, or solid adenocarcinomas, solid and non-keratinized adenosquamous carcinomas, and keratinized and epidermoid squamous cell carcinomas, as previously described[13]. The magnitudes of metaplastic or neoplastic lesions in each histological specimen from these epithelial types of tumors, were further evaluated under a light microscopic field by the following histological score criteria; 0 point as negatively observed, 0.5 point as slightly observed in 1–2 areas, 1.0 point as mildly observed in 3–4 areas, and 2.0 point as severely observed in 5 areas or more. The sum of those scores given for each neoplastic lesion was compared between the groups of animals received various doses.

The immunohistochemical staining of the intranuclear p53 protein was applied on all the histological specimen from epithelial types of tumors by a modified method as described[14]. Briefly, deparaffinized sections on the silanized slide immersed into an antigen retrieval solution (DAKO Corp., Carpinteria, CA) were heated to 90–95°C for 30 min in a microwave oven to unmask antigens, and rinsed with phosphate-buffered saline (PBS). After the blocking of endogenous peroxidase activity with 0.3% H_2O_2 in methanol and of non-specific antibody binding with normal goat serum, either polyclonal rabbit serum (CM1) or monoclonal mouse IgG (DO-7), specific to both mutant and wild type human p53 protein, from Medac Inc., Germany, was applied at optimal concentration of 1/100–1/250 on pretreated sections. After the incubation at 4°C overnight, the sections were washed with PBS, then the biotinylated secondary antibody, anti-rabbit or anti-mouse IgG, and abidin-biotin-peroxidase complex (ABC) were reacted respectively with sections by using a commercial kit (Vectastain® ABC kit; Vector Laboratories, Inc., Burlingame, CA), and finally the peroxidase activity was visualized by using 3, 3'-diaminobenzidine (DAB) as a substrate. The positivity for the intranuclear accumulation of p53 protein detected under a light microscopic field was evaluated by the following criteria; (–) as negatively detectable in all nuclei, (±) slightly detectable in 10% or less, (+) as mildly positive in 20–40%, and (++) as severely positive in 50% or more of all nuclei of tumor cells, respectively.

Statistics

The survival period and lung tumor incidences were compared for significant differences between the control and exposed groups of animals by Student's *t*-test.

RESULTS

Lung dose, survival, and primary lung tumors after inhalation exposures

As shown in Table 1, total 310 exposed rats were divided into 7 groups based on the mean values of initial lung deposition and cumulative lung dose ranging from 0.71 to 8.5 Gy. As compared to the group of unexposed control animals, the mean survival period of the lowest dose (0.71 Gy) group significantly ($p < 0.01$) increased, while those of the groups received doses more than 1.5 Gy were significantly ($p < 0.01$ or 0.001) reduced, and dropped to almost 60% of the control value at 8.5 Gy. The crude incidence of the primary lung tumors was 44% at 0.71 Gy (p

Table 1. Dose, survival, and primary lung tumors after inhalation of $^{239}PuO_2$ aerosol

Experimental Group	No. of Animals	Initial Lung Deposition (Bq)[a]	Lung Dose (Gy)[b]	Survival Period (Day)[c]	Primary Lung Tumors[d]
Control	130	0	0	790 ± 144	3 (2.3)
Pu 1	43	97 ± 27	0.71 ± 0.19	871 ± 105*	19 (44.2)**
Pu 2	75	225 ± 48	1.52 ± 0.28	712 ± 162*	45 (60.0)**
Pu 3	60	461 ± 118	2.88 ± 0.51	631 ± 158**	46 (76.7)**
Pu 4	40	787 ± 79	4.67 ± 0.24	675 ± 98**	37 (92.5)**
Pu 5	31	948 ± 76	5.43 ± 0.29	622 ± 105**	30 (96.7)**
Pu 6	31	1147 ± 114	6.61 ± 0.28	550 ± 82**	29 (93.5)**
Pu 7	30	1672 ± 261	8.52 ± 0.67	458 ± 95**	27 (90.0)**

[a] Mean ± SD of the initially deposited activity per animal in each group.
[b] Mean ± SD of the cumulative lung dose per animal in each group.
[c] Mean ± SD of the survival period per animal in each group after the time of inhalation exposures.
[d] The numbers (% crude incidences) of animals with primary lung tumors in each group.
Asterisks indicate a significant difference as compared to the controls (* $p<0.01$ or ** $p<0.001$).

< 0.001), increased sharply at the doses of 1.5–4.7 Gy, and reached the maximum of about 97% at 5.4 Gy ($p < 0.001$) as compared to the control group which had only 3 primary tumor-bearing animals (2.3%) among 130 animals. Among these tumors, benign ones showing a localized growth of adenomatous foci were most frequently observed at the doses less than 1 Gy and decreased at higher doses over 1.5 Gy, whereas, malignant ones showing a widely spread and disseminated growth of carcinomatous or sarcomatous foci were much less at the doses less than 1 Gy, but sharply increased up to 35–80% at the doses of 1.5–4.7 Gy, and reached the maximum of 90% at 6.6 Gy as shown in Fig. 1.

The histological types of these primary lung tumors observed in the control and each of the dose groups were summarized in Table 2. While the control had only 2 adenomas (1.5 %), the crude incidence of benign adenomas was the highest (35%) at 0.71 Gy, but decreased at the doses of 1.5 Gy or more, then reaching the bottom at 8.5 Gy. The malignant carcinomas including adenocarcinomas, adenosquamous carcinomas, and squamous cell carcinomas, were much less in the control (0.8%; squamous cell carcinoma) and in the lowest dose group (9.3%; adenocarcinomas), but their crude incidences were increased sharply at higher doses of 1.5 Gy or more. The appearance and the increase of each carcinoma type were, however, differed in the dose ranges; adenocarcinomas were appeared at 0.71 Gy, increased and reached the peak of 43% at 2.9 Gy, adenosquamous carcinomas were appeared at 1.5 Gy, increased and reached the peak of 50% at 8.5 Gy, squamous cell carcinomas were appeared at 2.9 Gy, increased and reached the peak of 13% at 5.4 Gy, respectively. Other tumor types such as fibrosarcomas and hemangiosarcomas were found only in 2 animals (3.2%) at higher doses of 6.6 Gy or more.

Dose-related appearance and increase of neoplastic lesions in pulmonary carcinomas

Almost all the primary lung tumors were epithelial types, and their histological types were expressed as benign or malignant phenotypes in a dose-dependent manner as above described. Actually, not only metaplasia of the alveolar lining epithelium but also variable stages of neo-

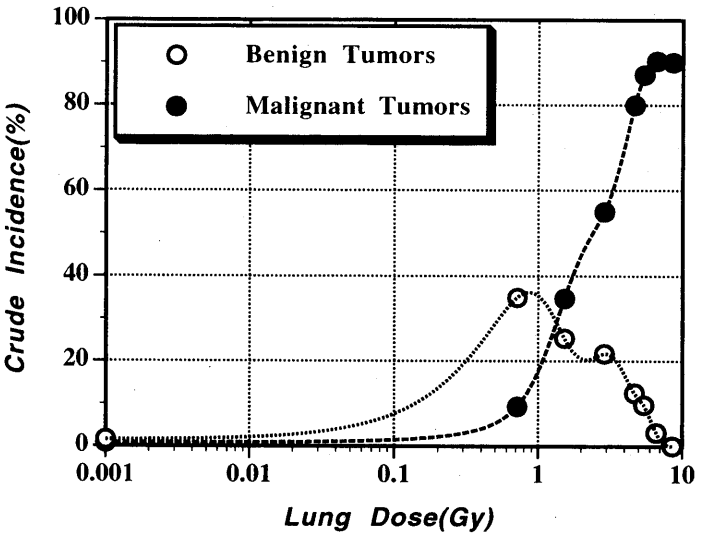

Fig. 1. The relations of the benign and malignant lung tumors to the lung doses in rats after inhalation exposures to $^{239}PuO_2$ aerosols. The crude incidences (%) of benign and malignant tumor-bearing animals as illustrated in the legend are plotted against the mean lung dose (Gy).

Table 2. Dose and histological types of primary lung tumors after inhalation of $^{239}PuO_2$ aerosol

Mean Dose(Gy)	No. of Animals	No. of Lung Tumors[a]				
		Adenoma	Adenocarcinoma	Adenosquamous carcinoma	Squamous cell carcinoma	Others[b]
0	130	2 (1.5)	0 (0)	0(0)	1 (0.8)	0 (0)
0.71	43	15 (34.9)	4 (9.3)	0(0)	0 (0)	0 (0)
1.52	75	19 (25.3)	22 (29.3)	4(5.3)	0 (0)	0 (0)
2.88	60	13 (21.7)	26 (43.3)	5(8.3)	2 (3.3)	0 (0)
4.67	40	5 (12.5)	14 (35.0)	13(32.5)	5 (12.5)	0 (0)
5.43	31	3 (9.7)	11 (35.5)	12(38.7)	4 (12.9)	0 (0)
6.61	31	1 (3.2)	10 (32.2)	14(45.1)	3 (9.7)	1 (3.2)
8.52	30	0 (0)	10 (33.3)	15(50.0)	1 (3.3)	1 (3.3)

[a] The numbers(% crude incidences) of animals with histological types of primary lung tumors in each dose group.

[b] Other types of tumors include fibrosarcomas and hemangiosarcomas.

plastic lesions were, however, observed in the same tissue specimen from an exposed rat under a light microscopic field. Further detailed analyses on the magnitudes of such metaplastic and neoplastic lesions in pulmonary carcinomas were performed by evaluating their histological scores in relation to the mean lung doses. As shown in Fig. 2, the sum of histological scores for both metaplasias and adenomatous lesions were the highest at 1.5 Gy and decreased at the doses of 2.9 Gy or more, whereas the scores for adenocarcinomatous lesions sharply increased at the doses of

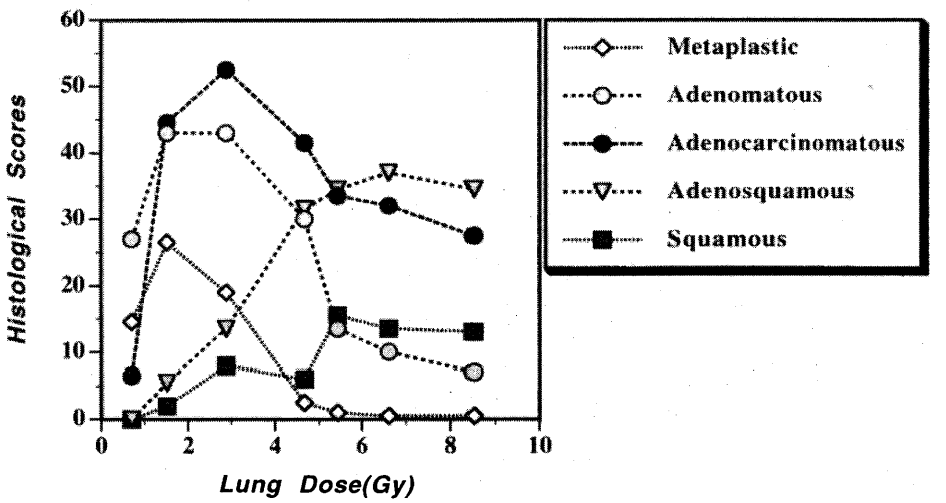

Fig. 2. The relations of the neoplastic lesions in pulmonary carcinomas to the lung doses in rats after inhalation exposures to $^{239}PuO_2$ aerosols. The histological scores for each of the neoplastic lesions as illustrated in the legend are plotted against the mean lung dose (Gy).

Table 3. Frequency of p53 protein expression in pulmonary carcinomas after inhalation of $^{239}PuO_2$ aerosol

Histological Types of Pulmonary Carcinomas	No. Examined	No. of p53-Positive Carcinomas[a]			
		Negative (–)	Slight (±)	Mild (+)	Severe (++)
Adenoma	56	56	0	0	0
Adenocarcinoma	97	85	11	1	0
Adenosquamous carcinoma	63	38	23	2	0
Squamous cell carcinoma	15	7	4	3	1
All types	231	186	38	6	1

[a] The numbers of pulmonary carcinomas showing intranuclear p53 protein with the variablr grades detected by immunohistochemistry (see text).

1.5 Gy or more, reached the peak at 2.9 Gy, and decreased at the doses of 4.6 Gy or more. The scores for both adenosquamous and squamous lesions increased at the doses of 2.9–4.6 Gy, and reached the peak at 5.4–6.6 Gy, sustaining the plateaux at 8.5 Gy. Such dose-dependent appearance and increase of variable neoplastic lesions were almost correlated with the dose responses of histological types of lung tumors as shown in Table 2.

p53 expression in pulmonary carcinomas

The frequency of the intranuclear p53 protein accumulation detectable in each of the histological types of pulmonary carcinomas is shown in Table 3. All adenomas showed negative staining, and three types of carcinomas were mostly negative or slighly positive. The mildly or severely positive staining was found only in 7 carcinoma types among 231 tumors; 1 of 97 adenocarcinomas, 2 of 63 adenosquamous carcinomas, and 4 of 15 squamous cell carcinomas,

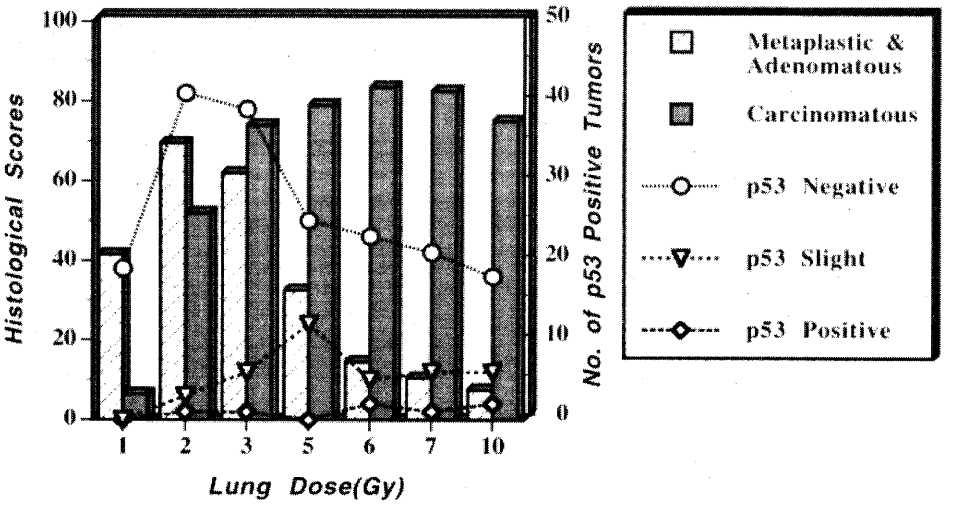

Fig. 3. The relations of the neoplastic lesions and p53-positive carcinomas to the lung doses in rats after inhalation exposures to $^{239}PuO_2$ aerosols. The histological scores for either metaplastic and adenomatous lesions or carcinomatous lesions, together with the number of either p53-negative, slightly positive, or mildly and severely positive tumors as illustrated in the legend, are plotted against the upper limit of mean lung dose (Gy).

respectively. Although the frequency of p53-positive pulmonary carcinomas was therefore very low, both slightly and mildly or severely positive carcinomas were increased together with the increase of carcinomatous lesions at the doses of 2 Gy or more, whereas the number of p53-negative tumors were reduced at higher doses as the decrease of metaplastic and adenomatous lesions (Fig. 3).

DISCUSSION

The present study showed a correlation between the survival reduction and increase of the primary lung tumors, especially malignant ones, in the $^{239}PuO_2$-exposed animals received the mean lung doses of 1.5 Gy or more. The mean survival period of the lowest dose (0.71 Gy) group of rats, however, significantly increased as compared to the controls, despite a significant increase of tumors which were, however, mostly benign adenomas found at later period after the inhalation exposures, suggesting that benign tumors are not the direct cause of death. These findings indicate a threshold-like dose range around at 1 Gy where the induction of benign or malignant lung tumors together with the survival reduction could differentially occur after inhalation exposures to $^{239}PuO_2$ aerosols. Although similar findings have been described elsewhere[10,11], the reasons and the background for a threshold-like response remain to be elucidated.

Among all the histological types of primary lung tumors found in the exposed animals, both adenomas and adenocarcinomas were the most frequent at the rate of about 66%, whereas either adenosquamous carcinomas or squamous cell carcinomas were respectively about 27% or 6.4%,

and non-epithelial sarcomas were only 0.8%. Such proportions of the tumor types are much differed from those described elsewhere[10–12] in which adenomas and adenosquamous carcinomas were 10% or less, while squamous cell carcinomas were 30–50% among all the tumor types. Since variable aerosol sizes have been used in those studies, one of plausible reasons for the differences in the histological phenotypes might be attributed to the distribution of inhaled aerosol particles with different sizes which could affect the deposition sites in the upper or lower respiratory tract, resulting in different carcinogenic responses of the target lining epithelium variably sensitive to alpha particles[2,3]. The dose responses were also differed among the histological types; the peak incidence of adenomas was found at the doses less than 1 Gy, whereas that of adenocarcinomas was at 2.9 Gy, adenosquamous carcinomas at 8.5 Gy, and squamous cell carcinomas at 5.4 Gy, respectively. These findings indicate a dose-dependent appearance and increase of the phenotypic expression of pulmonary carcinomas; higher doses could be required for the development of adenosquamous or squamous cell carcinomas, while adenomas or adenocarcinomas are inducible by relatively lower doses. Although the other investigations also implicated that squamous carcinomas more frequently increased in higher dose ranges than did adenocarcinomas as a result of the non-uniform dose distribution associated with plutonium particle aggregation either inside or outside of pulmonary regions[16,17], the susceptibility of the respiratory epithelium to carcinogenesis might be related to alpha doses and dose rates.

The evaluation on the magnitudes of neoplastic lesions by histological scores also indicated that both initial metaplasias and adenomatous lesions most frequently appeared at 1.5 Gy, while carcinomatous lesions increased in a dose-dependent manner as shown by the peak of adenocarcinomatous lesions at 2.9 Gy, and adenosquamous or squamous lesions at 5.4-6.6 Gy. Such a dose-dependent appearance of neoplastic lesions with variable stages suggests a successively phenotypic expression of the respiratory epithelium from an initially hyperplastic metaplasia to adenomatous, and then adenocarcinomatous or squamous metaplasias, reflecting a differential induction of variable histological types of pulmonary carcinomas as above described. The time course-dependent processes of neoplastic lesions are shown in both rats[18] and mice[19] sequentially sacrificed following the inhalation exposures to $^{239}PuO_2$; the respiratory epithelium consisted of either Type II alveolar cells or Clara cells, initially expressed hypertrophy or hyperplasia with the increased DNA synthesis from 30 to 90 days, and then metaplastic but pre-neoplastic changes in the middle stages around 180 days, followed by the onset of carcinomatous metaplasias in the later periods from 300 to 450 days, respectively after the exposures. It remains, however, to be elucidated whether such relatively early pathogenetic events in the pulmonary regions could be directly relevant to the long-term processes of the life-span carcinogenesis.

Dose-dependent and differential induction of pulmonary carcinomas with variable histological phenotypes as above described should be based on the cellular and molecular background such as an activation of protooncogenes and inactivation of tumor suppressor genes resulted from the mutations, leading to sequential appearance and expansion of pre-neoplastic cells[4], although there have scarcely been any of evidence on radiation-induced pulmonary carcinogenesis in experimental animals. For example, activation of K-ras oncogene as a result of the mutations could be related to an early pathogenetic event in human lung adenocarcinomas[20], while the mutations of a tumor suppressor gene, p53, are frequently detectable in human lung cancers from

radon-exposed uranium miners with variable histopathological phenotypes[21–24]. At least either or both of these genes are therefore considered as important candidates for mutations relevant to pulmonary carcinogenesis in humans. In contrast, experimental investigations on pulmonary carcinomas from the rats exposed to $^{239}PuO_2$ aerosols have shown that p53 mutations and intranuclear accumulation of mutant proteins were much less frequently detectable in carcinomatous lesions[14], whereas either K-ras activation or expression of growth factors were relatively well demonstrated[25,26]. Our results on the p53 protein expression of pulmonary carcinomas showed that all the benign adenomas were negative, and most of the malignant carcinomas were negative or slightly positive, except that only a few percentages of mildly or severely positive carcinomas appeared at relatively higher doses together with the increase of carcinomatous lesions. Further detailed analyses should be required for the frequency of mutations and molecular sequences of the p53 gene locus extracted from these pulmonary carcinomas, to determine whether the frequency of p53 gene mutations may play a major role in the rat pulmonary tumors induced by $^{239}PuO_2$-exposures. Genetic alterations of p53, erbB2 and K-ras were recently reported to be rare in the canine pulmonary tumors induced by inhalation of $^{239}PuO_2$ aerosols[27]. In addition, no alterations of K-ras and p53 genes are detected in X-ray-induced pulmonary tumors of the rat[28], whereas high frequencies of the p53 mutations and intranuclear protein accumulation are observed in the skin and bone tumors of mice after repeated beta particle-irradiation[29]. These findings indicate the interspecies differences but also differences of radiation quality in genetic alterations related to radiation carcinogenesis, and further implicate the possibility that the molecular pathogenesis of radiation-induced pulmonary carcinomas in the rat might be differed from that of bone and lymphoid tumors induced in the mice by ^{239}Pu-injection[30], or other radiation exposures.

In conclusion, the present results indicate a differential dose response between lung tumor types and neoplastic lesions induced by inhalation exposures of female Wistar rats to $^{239}PuO_2$ aerosols, while the pathogenetic processes and the molecular events including oncogenic mutations still remain unclear.

AKNOWLEDGEMENTS

This work was supported by a grant from the Research Fund for Project Research on Detriment and Modifying Factors of Radiation Exposures from Japan Science and Technology Agency. We are grateful to the staffs of Animal Care, Co. and Tokyo Nuclear Services, Co., for their help respectively with animal care and radiation control.

REFERENCES

1. ICRP (1979) ICRP Publication 30 Part 1 on Limits for Intakes of Radionuclides by Workers. Annals of the International Commission on Radiological Protection, 2(3/4), Pergamon Press, Oxford.
2. ICRP (1994) ICRP Publication 66 on Human Respiratory Tract Model for Radiological Protection. Annals of the International Commission on Radiological Protection, 24(1–3), Pergamon Press, Oxford.
3. ICRP (1980) ICRP Publication 31 on Biological Effects of Inhaled Radionuclides. Annals of the International

Commission on Radiological Protection, 4(1/2), Pergamon Press, Oxford.
4. BEIR V (1990) Health Effects of Exposure to Low Levels of Ionizing Radiation. National Research Council Committee on the Biological Effects of Ionizing Radiations, Board on Radiation Effects Research Commission on Life Sciences, National Academy of Sciences, National Academy Press, Washington, D. C.
5. Tietjen,G. L. (1987) Plutonium and lung cancer. Health Phys. **52**: 625–628.
6. Gilbert, E. S., Fry, S. A., Wiggs, L. D., Voelz, G. L., Cragle, D. L. and Petersen, G. R. (1989) Analyses of combined mortality data on workers at the Hanford site, Oak Ridge National Laboratory and Rocky Flats Nuclear Waeapons Plant. Radiat. Res. **120**: 19–35.
7. Fischer, D. R., Cannon, W. C., Hadley, R. T. and Park, J. F. (1986) Preliminary evaluation of lung doses for dogs exposed to $^{239}PuO_2$. In: Life-Span Radiation Effects Studies in Animals: What Can They Tell Us? Eds. R. C. Thompson & J. A. Mahaffey, US DOE CONF-830951, pp. 683–696.
8. Dagle, G. E., Parks, J. F., Gilbert, E. S. and Weller,R. E. (1989) Risk estimates for lung tumors from inhaled $^{239}PuO_2$, $^{238}PuO_2$, and $^{239}Pu(NO_3)_4$ in beagle dogs. Radiat.Protect. Dosimetry **26**: 173–176.
9. ICRP (1986) ICRP Publication 48 on the Metabolism of Plutonium and Related Elements. Annals of the International Commision on Radiological Protection, 2/3, Pergamon Press, Oxford.
10. Sanders, C. L., Lauhala, K. E. and McDonald, K. E. (1993) Lifespan studies in rats exposed to $^{239}PuO_2$ aerosol. III. Survival and lung tumours. Int. J. Radiat. Biol. **64**: 417–430.
11. Lundgren, D. L., Haley, P. J., Hahn, F. F., Diel, J. H., Griffith, W. C. and Scott, B. R. (1995) Pulmonary carcinogenicity of repeated inhalation exposure of rats to aerosols of $^{239}PuO_2$. Radiat. Res. **142**: 39–53.
12. Sanders,C. L. and Lundgren, D. L. (1995) Pulmonary carcinogenesis in the F344 and Wistar rat after inhalation of plutonium dioxide. Radiat. Res. **144**: 206–214.
13. Oghiso, Y., Yamada, Y., Ishigure, N., Fukuda, S., Iida, H., Yamada, Y., Sato, H., Koizumi, A. and Inaba, J. (1994) High incidence of malignant lung carcinomas in rats after inhalation of $^{239}PuO_2$ aerosol. J. Radiat. Res. **35**: 222–235.
14. Kelly, G., Stegelmeier, B. L. and Hahn, F. F. (1995) p53 alterations in plutonium-induced F344 rat lung tumors. Radiat. Res. **142**: 263–269.
15. WHO (1992) International Classification of Rodent Tumors, Part 1 The Rat, 1. Respiratory System. Ed. in-chief, U. Mohr, IARC Scientific Publications 122, Lyons.
16. Sanders, C. L., McDonald, K. E. and Lauhala, K. E. (1988) Promotion of pulmonary carcinogenesis by plutonium particle aggregation following inhalation of $^{239}PuO_2$. Radiat. Res. **116**: 393–405.
17. Sanders, C. L., McDonald, K. E. and Mahaffey, J. A. (1988) Lung tumor response to inhalated Pu and its implications for radiation protection. Health Phys. **55**: 455–462.
18. Herbert, R. A., Gillett, N. A., Rebar, A. H., Lundgren, D. L., Hoover, M. D., Chang, L. Y., Carlton, W. W. and Hahn, F. F. (1993) Sequential analysis of the pathogenesis of plutonium-induced pulmonary neoplasms in the rat: morphology, morphometry and cytokinetics. Radiat. Res. **124**: 29–42.
19. Taya, A., Black, A., Baker, S. T. and Humphreys, J. A. H. (1993) Proliferation of mouse lung epithelial cells after inhalation exposure to $^{239}PuO_2$. Radiat. Res. **136**: 366–372.
20. Rodenhuis, S., van de Wetering, M. L., Moot, W. J., Evers, S. G., van Zandwijk, N. and Bos, J. L. (1987) Mutational activation of the K-ras oncogene. A possible pathogenetic factor in adenocarcinoma of the lung. New Engl. J. Med. **317**: 929–935.
21. Vogelstein, B. and Kinzler, K. W. (1992) p53 function and dysfunction. Cell **70**: 523–526.
22. Harris, C. C. (1993) p53: At the crossroads of molecular carcinogenesis and risk assessment. Science **262**: 1980–1981.
23. Vähäkangas, K. H., Samet, J. M., Metcalf, R. A., Welsh, J. A., Bennett, W. P., Lane, D. P. and Harris, C. C. (1992) Mutation of p53 and ras genes in radon-associated lung cancer from uranium miners. Lancet **339**: 576–580.
24. Taylor, J. A., Watson, M. A., Devereux, T. R., Michels, R. Y., Saccomanno, G. and Anderson, M. (1994) p53 mutation hotspot in radon-associated lung cancer. Lancet **343**: 86–87.
25. Stegelmeier,B.L., Gillett,N.A., Rebar,A.H., and Kelly,G.(1991) The molecular progression of plutonium-239-induced rat lung carcinogenesis: Ki-ras expression and activation. Mol.Carcinogen. 4: 43–51.
26. Stegelmeier, B. L., Gillett, N. A., Hahn, F. F., Rebar, A. H., and Kelly, G. (1994) Expression of transforming

growth factor alpha and epidermal growth factor receptor in ^{239}Pu-induced rat lung neoplasms. Radiat. Res. **140**: 191–198.

27. Tierney, L. A., Hahn, F. F. and Lechner, J. F. (1996) p53, erbB-2 and K-ras gene alterations are rare in spontaneous and plutonium-induced canine lung neoplasia. Radiat. Res. **145**: 181–187.
28. Belinsky, S. A., Middleton, S. K., Picksley, S. M., Hahn, F. F. and Nikula, K. J. (1996) Analysis of the K-ras and p53 pathways in X-ray-induced lung tumors in the rat. Radiat. Res. **145**: 449–456.
29. Ootsuyama, A. (1996) Skin and bone tumors induced by repeated beta-irradiation of mice: threshold effects and p53 mutations. J. Radiat.Res. **37**: 151–159.
30. Oghiso, Y., Yamada, Y. and Iida, H. (1997) High frequency of leukemic lymphomas with osteosarcomas but no myeloid leukemias in C3H mice after ^{239}Pu citrate injection. J. Radiat. Res. **38**: 77–86.

RADIATION RESEARCH 152, S27–S30 (1999)
0033-7587/99 $5.00

Carcinogenesis in Mice after Injection of Soluble Plutonium Citrate

Yoichi Oghiso and Yutaka Yamada

Division of Radiotoxicology and Protection, National Institute of Radiological Sciences, 9-1, 4-chome, Anagawa, Inage-ku, Chiba 263-8555, Japan

Oghiso, Y. and Yamada, Y. Carcinogenesis in Mice after Injection of Soluble Plutonium Citrate. *Radiat. Res.* 152, S27–S30 (1999).

The carcinogenicity of injected soluble plutonium (^{239}Pu) citrate was investigated in life-span animal experiments using mice of three strains, C3H, C57BL/6 and their hybrid BC3F$_1$, that have different spectra of spontaneous and radiation-induced tumors. Bone tumors, mostly osteosarcomas, were induced at skeletal doses of 0.6 to 0.7 Gy, and the incidence increased markedly at doses of 2 to 4 Gy in all strains, while lymphoid tumors appeared to decrease at higher doses; the incidences of bone tumors remained higher at higher doses, suggesting a differential and competitive dose response between bone and lymphoid tumors. Among the histological phenotypes of lymphoid tumors, nonthymic, pre-B-cell type leukemic lymphomas were induced preferentially and early, while thymic lymphomas and myeloid leukemias were rarely or never observed in any of the strains after injection of ^{239}Pu. These findings indicate a specificity of ^{239}Pu-induced carcinogenesis in mice that is different from that of external low-LET irradiations. © 1999 by Radiation Research Society

INTRODUCTION

The experimental carcinogenesis induced by incorporated α-particle emitters is dependent on both their chemical forms and routes of entry. Specific or nonspecific tumor appearance can be modulated by metabolic behavior, distribution and deposition sites, and doses and dose rates in target organs. Numerous investigations indicate that almost all the soluble forms of bone seekers most frequently induce bone sarcomas after injection, whereas insoluble particulate thorium compounds (e.g. Thorotrast) tend to induce liver and spleen hemangiosarcomas as a result of preferential distribution into the reticuloendothelial tissues (*1*). However, there is little or no evidence of induction of hematopoietic or lymphoid tumors despite the fact that hematopoietic or lymphoid stem cells may be irradiated by α particles emitted from the deposition sites. In fact, the frequencies of myeloid leukemias and lymphomas induced by internal exposures to α-particle emitters are much lower, as shown by those found in CBA/H mice injected with ^{239}Pu or ^{224}Ra (*2–4*), than those induced by external low-LET or neutron irradiations (*5–7*). We showed previously that leukemic lymphomas were frequently induced at higher doses while no myeloid leukemias were observed in female C3H mice after injection of ^{239}Pu citrate (*8*). While it has not been determined whether such differences in myeloid or lymphoid carcinogenesis could be due to physical factors including radiation quality, dose and dose rate, the difference in susceptibility between the animal species and strains used may also be a factor that modulates carcinogenic responses. We show here the induction frequencies and characteristics of hematopoietic or lymphoid tumors after injection of soluble ^{239}Pu citrate into mice of several strains that are commonly used for studies of spontaneous and radiation-induced carcinogenesis.

MATERIALS AND METHODS

Preparation and Injection of ^{239}Pu Citrate Solution

As described previously (*8*), a mixture of 10 m*M* ^{239}Pu nitrate and 100 m*M* trisodium citrate at a molecular ratio of 1:50 was titrated to pH 6.8–7.2 by addition of 1 *N* NaOH, diluted with physiological saline, and passed through both a 0.2- and a 0.025-μm-pore millipore filter to obtain a monomeric ^{239}Pu solution with radioactivity of 10^3–10^5 Bq/ml. All experiments were performed with the approval of the institution's animal use committee. A total of 12 groups each containing 30 to 60 12- to 14-week-old female mice of three strains were injected intraperitoneally with amounts of radioactivity ranging from 100 to 1000 Bq per animal or with saline as the control. The strains used were C3H, which is characterized by a higher incidence of spontaneous hepatocellular carcinomas but fewer lymphoid tumors, C57BL/6, which has a higher incidence of spontaneous thymic lymphomas, and their F$_1$ hybrid strain, BC3F$_1$. All of these strains have much lower or no spontaneous occurrences of bone tumors and myeloid leukemias.

Pathological Examinations and Dose Responses

All the animals were kept in a closed-hood rack with barrier-filtered air during their lifetime. Almost all the animals injected with ^{239}Pu as well as 30 to 45 control animals had died by the end of February 1999. Postmortem pathological examinations were combined with histopathological diagnosis of tumors using hematoxylin and eosin (H&E)-stained tissue sections and immunohistochemical differential diagnosis of lymphoid tumors using Thy-1.2 and B220 monoclonal antibodies under light microscopy. The cumulative skeletal dose (Gy) was calculated for each animal until death and was averaged as the mean skeletal dose for each group of animals as described previously (*8*). The dose responses of all the observed tumors were analyzed based on the mean skeletal dose unless stated otherwise.

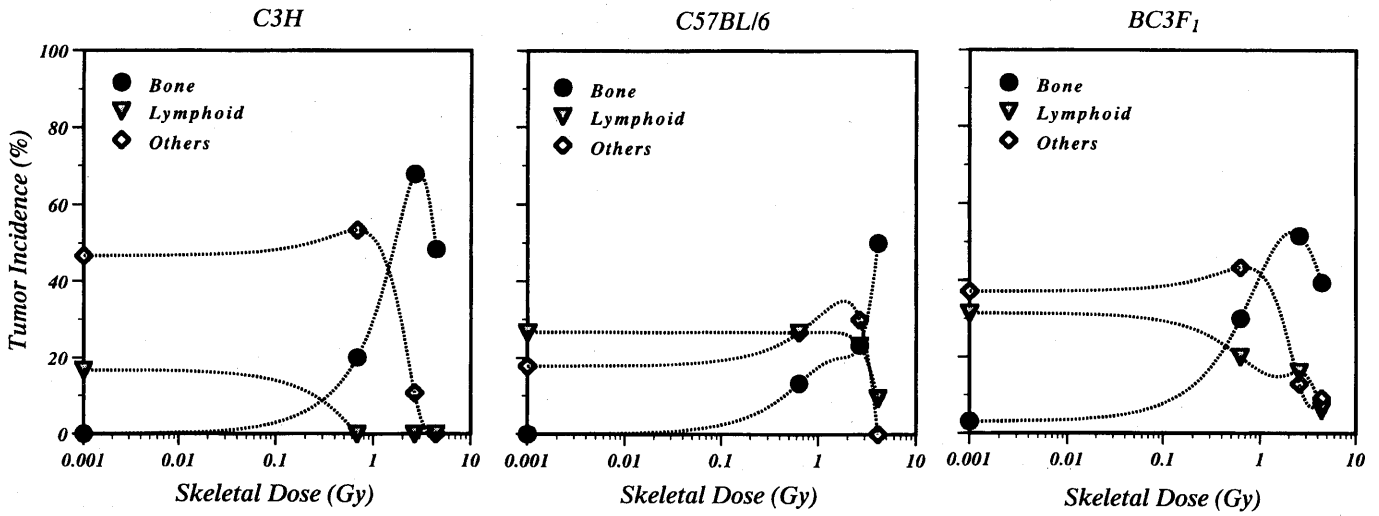

FIG. 1. Dose responses of bone, lymphoid and other tumors observed in three different strains of mice after injection of ^{239}Pu citrate.

RESULTS AND DISCUSSION

Differential and Competitive Dose Responses of Bone and Lymphoid Tumors

In the previous study (*8*), a dose-dependent and differential tumor induction was noted in C3H mice. Bone tumors, mostly osteosarcomas, increased sharply at a skeletal dose of 0.6 to 0.8 Gy up to a maximum of 96% at doses of 6 to 8 Gy, while lymphoid tumors increased significantly at doses of 10 to 30 Gy. Tumors occurred less frequently or not at all in the lung, liver, ovaries and skin at doses higher than 3.0 Gy. Neither myeloid leukemias nor any myelogenous neoplasms were found in the controls or the animals injected with ^{239}Pu. These findings indicate that there are differential and competitive dose responses between bone and lymphoid tumors but the induction of myeloid leukemias is unlikely in C3H mice after injection of ^{239}Pu citrate.

In this study, almost similar dose responses of both bone and lymphoid tumors were observed in the three strains after injection of ^{239}Pu, while the frequencies and the dose ranges were varied. As shown in Fig. 1, bone tumors increased up to a maximum of 70% from 1.0 to 3.0 Gy, and there was also a decrease to zero lymphoid tumors in C3H mice. In both C57BL/6 and BC3F$_1$ mice, the incidence of bone tumors increased sharply and significantly beyond 0.6 Gy up to a maximum of 50–60% at doses of 3.0 to 4.0 Gy, while lymphoid tumors were still observed frequently at doses from 2.0 to 3.0 Gy, but were reduced at 4.0 Gy or higher. Among the other tumors whose frequencies decreased above a dose of 1.0 Gy in all strains, myeloid leukemias were rarely observed in both C57BL and BC3F$_1$ mice, and none were observed in C3H mice (data not shown). These findings indicate the differential and competitive dose responses between bone and lymphoid tumors commonly induced in different strains of mice after injection of ^{239}Pu, suggesting that the main causes of death changed with increasing dose, although it is not clear whether bone and lymphoid tumors influenced the survival of mice after injection of ^{239}Pu citrate. Detailed mathematical analyses will be required to determine the competing causes of death. Further, these results indicate that myeloid leukemias or the other myelogenous tumors are induced much less frequently even though the susceptibility of bone marrow stem cells to radiation-induced hematopoietic abnormalities may be different among mouse strains (*9*).

Early Onset and Phenotypes of Lymphoid Tumors Specific to Animals Injected with ^{239}Pu

Because the onset periods and histological phenotypes of the lymphoid tumors were previously noted to be quite different between the control and ^{239}Pu-injected C3H mice (*8*), we tried further differential diagnosis and typing of those lymphoid tumors by immunohistochemistry using T- and B-cell markers. As shown in Table 1, all the lymphoid tumors of the controls were observed relatively late, at 650–900 days after the injection. Their histological phenotypes were Thy 1.2-positive thymic or T-cell lymphomas, B220-positive B-cell lymphomas, and histiocytic lymphomas being negative for both markers. In contrast, most of the lymphoid tumors from animals injected with ^{239}Pu appeared during the early period of 150–500 days, with some being observed during the late period of 600–900 days after the injection. Among the histological phenotypes of these lymphoid tumors, there were fewer thymic or T-cell lymphomas than in the controls, but B220-positive B-cell leukemic lymphomas were increased during the early period. These findings indicate the early onset with higher frequencies of nonthymic, B-cell leukemic lymphomas in C3H mice injected with ^{239}Pu. To characterize whether such preferential induction of B-cell leukemias could be due to strain

TABLE 1
Onset and Histological Phenotypes of Lymphoid Tumors in C3H Mice

Experimental group	No. of lymphoid tumors	Observation period (days)[a]	Phenotypes of lymphoid tumors[b]			
			T-cell lymphoma	B-cell lymphoma	B-cell leukemic lymphoma	Histiocytic lymphoma
Control	20	650–900	5	8	0	7
^{239}Pu-injected	20	150–500	1	6	13	0
	9	600–900	2	7	0	0

[a] The period between the first and last times that lymphoid tumors were observed in dead animals after the injection of saline (control) or ^{239}Pu citrate.

[b] The typing of thymic or T-cell lymphomas, B-cell lymphomas, B-cell leukemic lymphomas and histiocytic lymphomas as differentially diagnosed by immunohistochemistry using Thy 1.2 and B220 monoclonal antibodies.

differences, the histological phenotypes of the lymphoid tumors were compared in the three strains after injection of ^{239}Pu. Because no lymphoid tumors were observed in the C3H mice injected with ^{239}Pu in the present study, the data from the previous study shown in Table 1 were compared to those for the other two strains. As shown in Fig. 2, the proportion of thymic lymphomas was smaller, and B-cell leukemic lymphomas increased more in all the ^{239}Pu-injected mice than in their controls. However, the proportions of B-cell lymphomas were variable in both the controls and the ^{239}Pu-injected animals. These findings indicate that only the B-cell leukemic lymphomas are commonly induced by ^{239}Pu injection, suggesting the possibility that α-particle radiation induces hematopoietic derangements of putatively rescued bone marrow stem cells, leading to the development of pre-B-cell leukemia rather than myeloid leukemias or thymic lymphomas, which are frequently induced in mice by external low-LET irradiations (*10*).

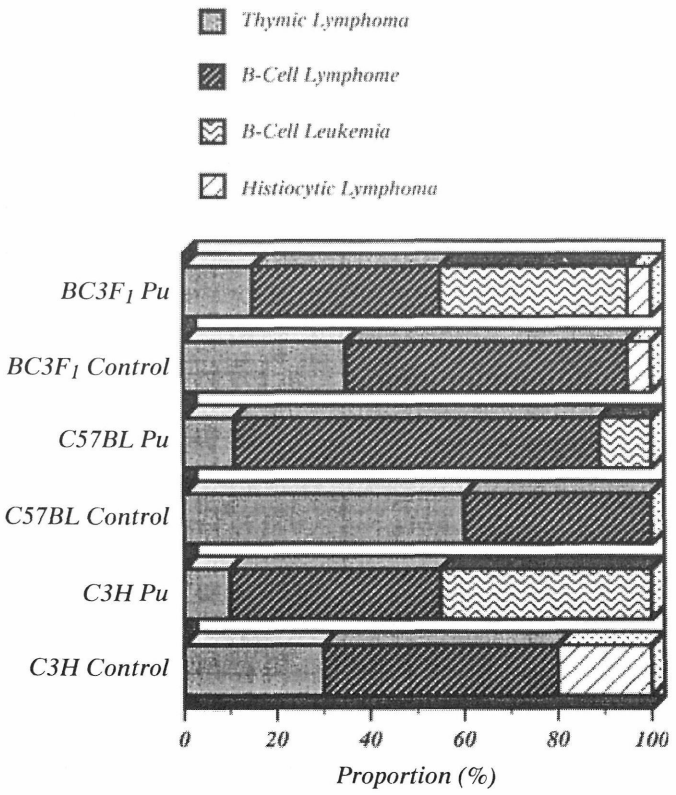

FIG. 2. The proportion of phenotypes of lymphoid tumors observed in three different strains of mice after injection of ^{239}Pu citrate. The data for C3H mice injected with ^{239}Pu are from the previous study as shown in Table 1.

CONCLUSIONS

The results presented here show the differential and competitive dose responses between bone and lymphoid tumors in three different strains of mice after the injection of soluble ^{239}Pu citrate. Bone tumors, mostly osteosarcomas, are significantly induced at a skeletal dose of 0.6 to 0.7 Gy in all the strains examined, while nonthymic, pre-B-cell leukemic lymphomas are preferentially induced in the early period after ^{239}Pu injection. Myeloid leukemias and the other myelogenous neoplasms are rarely observed or are not observed in any of the strains of mice. These findings suggest that α-particle radiation induces a different spectrum of tumors than external low-LET radiation.

ACKNOWLEDGMENTS

The authors are grateful to H. Iida and K. Fukutsu for their technical assistance, and acknowledge all the helpful support of the animal care and radiation control staffs of Animal Care Co. and Tokyo Nuclear Services Co.

REFERENCES

1. C. W. Mays, W. S. S. Jee, R. D. Lloyd, B. J. Stover, J. H. Dougherty and G. N. Taylor, *Delayed Effects of Bone-Seeking Radionuclides.* The University of Utah Press, Salt Lake City, 1969.
2. J. F. Loutit and T. E. F. Carr, Lymphoid tumors and leukemia induced in mice by bone-seeking radionuclides. *Int. J. Radiat. Biol.* **33**, 245–263 (1978).
3. E. R. Humphreys, J. F. Loutit and V. A. Stones, The induction by ^{239}Pu of myeloid leukemia and osteosarcoma in female CBA mice. *Int. J. Radiat. Biol.* **51**, 331–339 (1987).
4. E. R. Humphreys, K. R. Issacs, T. A. Raine, J. Saunders, V. A. Stones and D. L. Wood, Myeloid leukemia and osteosarcoma in CBA/H mice given ^{224}Ra. *Int. J. Radiat. Biol.* **64**, 231–235 (1993).
5. R. H. Mole, D. G. Papworth and M. J. Corp, The dose-response for X-ray induction of myeloid leukemia in male CBA/H mice. *Br. J. Cancer* **47**, 285–291 (1983).

6. S. Sasaki and T. Kasuga, Life-shortening and carcinogenesis in mice irradiated neonatally with X rays. *Radiat. Res.* **88**, 313–325 (1981).
7. J. R. Maisin, A. Wambersie, G. B. Gerber, G. Mattelin, M. Lambiet-Collier, B. DeCoster and J. Gueulette, Life-shortening and disease incidence in C57Bl mice after single and fractionated γ and high-energy neutron exposure. *Radiat. Res.* **113**, 300–317 (1988).
8. Y. Oghiso, Y. Yamada and H. Iida, High frequency of leukemic lymphomas with osteosarcomas but no myeloid leukemias in C3H mice after ^{239}Pu citrate injection. *J. Radiat. Res.* **38**, 77–86 (1997).
9. M. Janowski, R. Cox and P. G. Strauss, The molecular biology of radiation-induced carcinogenesis: Thymic lymphoma, myeloid leukemia and osteosarcoma. *Int. J. Radiat. Biol.* **57**, 677–691 (1990).
10. B. I. Lord, G. Molineux, E. R. Humphreys and V. A. Stones, Long-term effects of plutonium-239 and radium-224 on the distribution and performance of pluripotent hemopoietic progenitor cells and their regulatory microenvironment. *Int. J. Radiat. Biol.* **59**, 211–227 (1991).

J. RADIAT. RES., 40, 197–204 (1999)

Retention, Excretion and Translocation of ^{239}Pu in Rats Following Inhalation of $^{239}PuO_2$ Calcined at 1150 and 400°C

HIROSHI SATO[1]*, YUJI YAMADA[2], NOBUHITO ISHIGURE[2], TAKASHI NAKANO[2], HIROKO ENOMOTO[2], SENTARO TAKAHASHI[1], YOSHIHISA KUBOTA[1] and JIRO INABA[3]

[1]The 4th Research Group, [2]Division of Radiotoxicology and Protection, [3]Deputy Director-General, National Institute of Radiological Sciences, 4–9–1 Anagawa, Inage-ku, Chiba 263–8555, Japan

(Received, January 18, 1999)
(Revision received, May 14, 1999)
(Accepted, May 17, 1999)

$^{239}PuO_2$/Calcination temperature/Inhalation/Lung retention/Translocation

Wistar rats inhaled $^{239}PuO_2$ particles prepared by the calcination of ^{239}Pu hydroxide at 1150 and 400°C. Lung retention, fecal and urinary excretion, and translocation of ^{239}Pu were compared between the two calcination temperatures. The clearance of ^{239}Pu from the lungs was significantly faster in the rats exposed to $^{239}PuO_2$ calcined at 400°C (low-temperature group) than those exposed to $^{239}PuO_2$ calcined at 1150°C (high-temperature group). Both the fecal excretion of ^{239}Pu and the ratio of fecal excretion to urinary excretion was greater in the low-temperature group than in high-temperature group. The amounts of ^{239}Pu translocated from the lungs to the other organs were very small. Even in the liver, which accumulated the largest amount of ^{239}Pu except for the lungs, only 0.13–0.20% of the initial lung burden was retained 1 year after inhalation. The amount of ^{239}Pu deposited in the liver was greater in the high-temperature group than in the low-temperature group both at 1 month and 1 year after the inhalation. These findings clearly suggest that the lung retention of ^{239}Pu in rats is significantly affected by the calcination temperature of $^{239}PuO_2$.

INTRODUCTION

The potential risk of an accidental exposure of workers to plutonium (Pu) has increased in Japan because of a government policy to promote the nuclear-fuel-cycle where Pu is used as a fuel for fast reactors. Our institute launched a research project on the inhalation toxicology of

*Corresponding author: Phone; 043–206–3159, FAX; 043–251–4853, e-mail; hi_sato@nirs.go.jp

^{239}Pu, and a few reports have already been published by some of the authors. Ishigure et al have determined the lung retention of ^{239}Pu by whole body counting in rats inhaling $^{239}PuO_2$ aerosols[1,2]. Oghiso et al have demonstrated the induction of lung tumors in the same experimental animals[3,4].

The primary purpose of the present study is to supply some supplementary ^{239}Pu metabolic data to the above studies. We describe here lung retention, redistribution to other organs, and fecal and urinary excretion of ^{239}Pu in rats which were administered $^{239}PuO_2$ by inhalation under the same experimental conditions used in the above studies.

An additional purpose of the present study is to determine whether the metabolic parameters of ^{239}Pu following inhalation of $^{239}PuO_2$ aerosol are affected by the calcination temperature of the aerosol. Occupational exposure to Pu may occur during the fabrication of fuels, especially for fast reactors, and during the reprocessing of irradiated fuel. Since the release of Pu into the working place has accidentally occurred by fire or explosion, the chemical form of Pu released is mainly PuO_2 fired at different temperatures depending on the type of accident. It is assumed that the fired temperature may affect the solubility, chemical composition, and specific surface area of PuO_2 particles[5–7]. There is a discrepancy in the effects of calcination temperature on lung retention and translocation of ^{239}Pu after the inhalation of $^{239}PuO_2$. Mewhinney et al demonstrated that the solubility of inhaled $^{239}PuO_2$ in the lungs of beagle dogs depended upon the calcination temperature during its preparation[5]. In contrast, Morgan et al observed that the lung retention of $^{239}PuO_2$ in the mouse lung after inhalation was unaffected by calcination temperature in the range between 550–1250°C[6,7]. In the present study, therefore, we compared the lung retention, fecal and urinary excretion, and translocation of ^{239}Pu in the rats after inhalation of $^{239}PuO_2$ which was calcined at 400°C (low temperature) and 1150°C (high temperature).

MATERIALS AND METHODS

Preparation of $^{239}PuO_2$

The details of the experimental procedure for the preparation and inhalation of $^{239}PuO_2$ have been reported elswhere[2,8]. In brief, a colloidal suspension of $^{239}Pu(OH)_4$ prepared from a stock solution of $^{239}Pu(NO_3)_4$ by neutralization with NH_4OH was nebulized, dried at 300°C, and calcined by passing through a furnace maintained at 400 or 1150°C to change the chemical form from hydroxide to dioxide. The activity median aerodynamic diameters (AMADs) of the resultant $^{239}PuO_2$ aerosols were 0.29 and 0.38 μm with the geometric standard deviations (σ_g) of 2.1 and 1.7 for the aerosols prepared at 400 and 1150°C, respectively.

Inhalation of $^{239}PuO_2$

Animals used were female Wistar rats, 10-weeks-old and weighing 180–220 g at the time of $^{239}PuO_2$ inhalation. They were purchased from a domestic breeder (SLC, Shizuoka, Japan) at 4–5-weeks-old, housed in a controlled environment, and given pelleted diet and water *ad libitum*. At the administration, they were individually restrained in small plastic boxes and exposed to the $^{239}PuO_2$ aerosols for about 60 min by "nose only" inhalation using a special exposure system, as

described previously[1,2,8]. Twenty animals were administered simultaneously, five of which were then individually housed in metabolic cages. From these five rats, feces and urine were collected at scheduled times after exposure. The lung depositions of ^{239}Pu in all rats were determined periodically after inhalation exposure by the *in vivo* counting method using a whole-body counting system[1].

The initial alveolar deposition (IAD) defined the lung retention of Pu on the 2nd day after inhalation, according to the previous literature[2–4]. The average IADs of rats exposed to high- and low-temperature $^{239}PuO_2$ were 1.4 and 2.0 kBq, respectively.

Measurement of radioactivity

The rats were killed by cutting the abdominal aorta under anesthesia at 1 month and 1 year after $^{239}PuO_2$ administration. The lung, kidney, spleen and right femur were dissected. The tissue samples were acid-digested with conc. HNO_3, evaporated to dryness at 500°C for 24 hr, and dissolved with 7M HNO_3 containing a small amount of hydrogen fluoride. The feces were homogenized at first, and a known amount of the homogenate was treated by the same procedure as used for the tissues samples. The ^{239}Pu activities in these samples were measured by a liquid scintillation counter (LS 1214, LKB, Japan). The urine was filtered with a 0.22 μm Millipore Filter and measured directly by a liquid scintillation counter.

RESULTS

Figure 1 shows the retention of ^{239}Pu in the lungs after exposure to high- and low- temperature $^{239}PuO_2$. The retentions of ^{239}Pu were 79 ± 6.8 and 17 ± 2.9% IAD (mean ± s.d.) in the rats exposed to high-temperature $^{239}PuO_2$ 1 month and 1 year after exposure, respectively. In the rats exposed to low-temperature $^{239}PuO_2$, the ^{239}Pu retentions were 58 ± 4.0 and 8.9 ± 1.8% IAD 1 month and 1 year after exposure, respectively. The clearance of ^{239}Pu from the lungs was faster in the low-temperature than in the high-temperature group. Statistically significant differences between both groups were observed at 1 week, 1 month, and 1 year after exposure.

The fecal and urinary excretions of ^{239}Pu, expressed as % IAD per day, in the rats exposed to $^{239}PuO_2$ fired at different temperatures are shown in Fig. 2. In both groups, the fecal excretion of ^{239}Pu was larger soon after exposure and decreased gradually thereafter. On the other hand, the urinary excretions were relatively constant throughout the experimental period. The total amount of ^{239}Pu excreted is shown in Table 1. In the high-temperature group, 20 ± 1.5 and 52 ± 2.2% IAD were excreted into the feces 1 month and 1 year after exposure, respectively. In the low-temperature group, they were 32 ± 2.6 and 68 ± 1.4% IAD, respectively, which were significantly higher than those in the high-temperature group at a given period. Total excretions into the urine were 31 ± 5.9 and 23 ± 2.6% IAD in the high- and low-temperature groups, respectively, 1 year after exposure.

Table 2 shows the redistributions of ^{239}Pu to the major organs other than the lungs 1 month and 1 year after exposure. The amounts of ^{239}Pu redistributed from the lungs to the other organs were very small. Even in the liver, which showed the highest ^{239}Pu accumulation in organs other

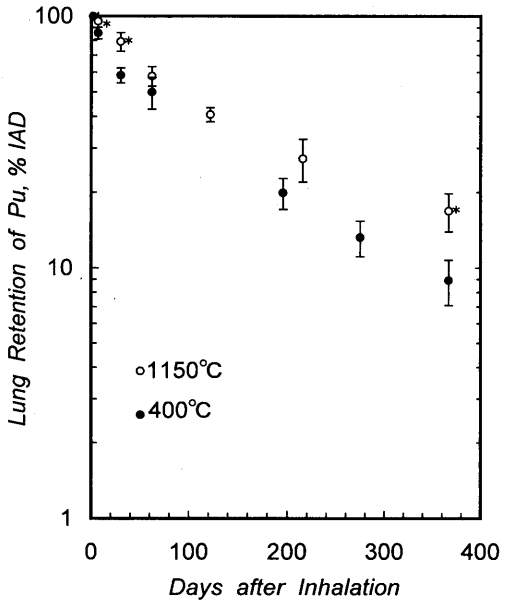

Fig. 1. Lung retention of Pu following the inhalation of PuO_2 calcined at different temperatures. The vertical bar denotes the standard deviation, and an asterisk indicates a significant difference between two groups ($P < 0.05$).

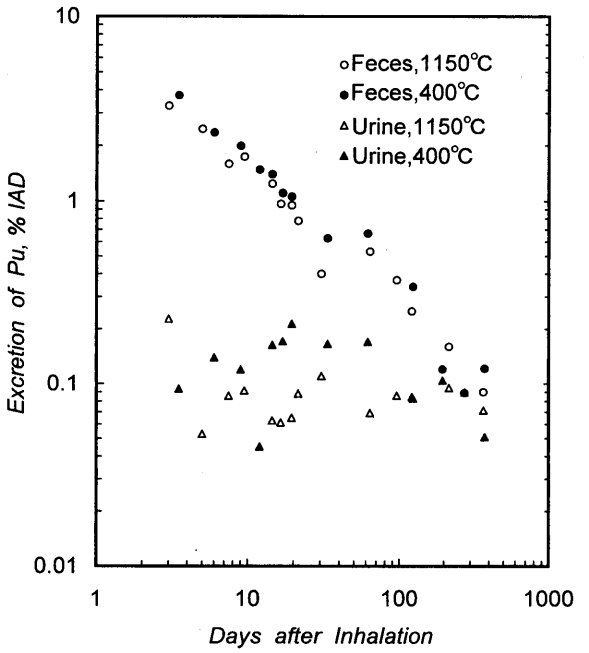

Fig. 2. Daily fecal and urinary excretion of Pu following inhalation of PuO_2 calcined at different temperatures. Each point is the mean of five rats.

Table 1. Cumulative excretions of Pu in rats inhaling PuO_2 calcined at 1150 and 400°C

organ/ excreta	1150°C		400°C	
	1 month[a]	1 year	1 month	1 year
Lung	79.2 ± 6.8[b]	16.8 ± 2.9	58.3 ± 4.0	8.9 ± 1.8
Feces	19.7 ± 1.5	52.3 ± 2.2	31.5 ± 2.6[c]	68.4 ± 1.4[c]
Urine	3.15 ± 0.23	30.8 ± 5.9	3.82 ± 0.73	22.7 ± 2.6[d]
Total	102.3 ± 7.1	99.7 ± 1.3	93.6 ± 2.7	100.0 ± 1.6

[a] 1 month and 1 year show time after inhalation of PuO_2.
[b] The values are mean ± SD of 4 rats, and expressed as %IAD.
[c] denotes significant difference from 1150°C at $P < 0.005$.
[d] $P < 0.05$.

Table 2. Translocation of Pu in rats inhaling PuO_2 calcined at 1150 and 400°C

Calcination Temp.(°C)	Time after inhalation	Liver	Kidney	Spleen	Femur
1150	1 month	0.046 ± 0.021[a]	0.0069 ± 0.0010	0.0049 ± 0.0030	0.0015 ± 0.0022
	1 year	0.13 ± 0.02[b]	0.0084 ± 0.0017	0.0091 ± 0.0035	0.0098 ± 0.0044[b]
400	1 month	0.088 ± 0.043	0.0032 ± 0.0012[c]	0.0023 ± 0.0011	0.0004 ± 0.0004
	1 year	0.20 ± 0.12	0.0045 ± 0.0012[c]	0.0192 ± 0.0105[b,d]	0.0028 ± 0.0024[c]

[a] The values are mean ± SD of 4 rats, and expressed as % IAD.
[b] denotes significant difference from 1 month at $P < 0.005$.
[c] denotes significant difference from 1150°C at 1 month and 1 year at $P < 0.005$, respectively.
[d] $P < 0.05$.

than the lungs, the retentions of ^{239}Pu (% IAD per organ) were 0.13 ± 0.02 and 0.20 ± 0.12% at 1 year in the high- and low-temperature groups, respectively.

A significant accumulation of ^{239}Pu, i.e., a significant increase in the concentrations of ^{239}Pu between 1 month and 1 year, was observed in the liver and femur of the high-temperature group, and in the spleen of the low-temperature group. The effect of calcination temperature on the amount of ^{239}Pu was significant in the kidney at 1 month after inhalation, and in the kidney and femur at 1 year.

DISCUSSION

In the metabolic parameters determined here, lung retention has already been investigated in previous studies in our series[2]. Two other metabolic parameters, i.e., fecal and urinary excretion, and redistribution to the other organs, were determined in the present study, since these parameters are important and essential for estimating the radiation doses and for evaluating the biological effect of inhaled $^{239}PuO_2$. The lung retention of ^{239}Pu (Fig. 1) was in good agreement with our previous data[2]. The lung retention of inhaled ^{239}Pu in rats has also been reported by

many other authors[9–13], where the clearance was somewhat quicker than that observed in this as well as in our previous study[1,2]. A possible reason for this slow clearance observed in our series of experiments has been discussed elsewhere in detail[2]. The excretion patterns of ^{239}Pu into feces and urine observed in the present study are in good agreement with those previously reported by other autors[5,9]. In the early period after inhalation, the amount of ^{239}Pu excreted into the feces was much higher than that into the urine (Fig. 2), suggesting that the clearance of ^{239}Pu from lungs to gastro-intestinal tract via upper airways was still dominant in this period. In contrast, the ^{239}Pu excretion into urine was relatively constant regardless of the time after inhalation. As has been well demonstrated in various types of particles[10], the fraction excreted into urine is considered to be cleared from the lungs after dissolution. Therefore, the present result may indicate that the dissolution of $^{239}PuO_2$ particles occurred at a relatively constant rate in the lungs.

Regarding the effect of firing temperature on the clearance of ^{239}Pu, two experiments have been carried out by Morgan et al[6,7] and Mewhinney et al[5], as described in our Introduction. Experimental conditions were different between these studies in respect to animal species, IAD and the preparation procedure of Pu oxide. Using beagle dogs, Mewhinney et al demonstrated that the solubility of inhaled $^{239}PuO_2$ in the lungs depended upon the temperature at which it was fired during its preparation[5]. They used polydispersed aerosols of ^{239}Pu nebulized from a solution of ^{239}Pu chloride fired at 325 to 1150°C. AMAD of both types of aerosols was 1.9 μm with σ_g of 1.2, and IADs ranged from 21 to 72 kBq per dog. On the other hand, Morgan et al showed that the lung retention of ^{239}Pu in mice after $^{239}PuO_2$ inhalation was not significantly affected by calcination temperatures in the range from 550 to 1250°C[6,7]. In their study, $^{239}PuO_2$ was prepared by firing the oxalates at 550°C, and the resulting materials were recalcined at temperatures of 750, 1000, and 1250°C. AMAD of the aerosols ranged from 1.4 to 1.6 μm with σ_g of 1.3, and IADs ranged from 0.1 to 0.23 kBq per mouse. Although the preparation procedures were different, the physicochemical characteristics of $^{239}PuO_2$ as well as IADs seemed to be similar in both studies. The only apparently different factor between their studies was the difference in animal species. Since the movement and dissolution of radioactive particles in the lungs differed greatly between the animal species[14], that one factor may be responsible, at least in part, for the different effects of calcination temperature on the lung retention of $^{239}PuO_2$ between mice and dogs. In the present study, the calcination temperatures and IADs (per gram tissues) were similar to those reported by Mewhinney et al[5] and Morgan et al[6,7]. However, the size (AMAD) of $^{239}PuO_2$ particles used here was much smaller, i.e., 0.29–0.38 μm in the present study vs. 1.4–1.9 μm in the previous ones. Therefore, it is difficult to compare the metabolic parameters in detail between the present experiment and their experiments. However, it is noteworthy that the lung retention of ^{239}Pu was affected by calcination temperature in both rats and dogs, although further investigations are necessary to elucidate the mechanism involved and the reason why the temperature effect was only observed in those two species.

In addition to ^{239}Pu retention in the lungs, some other metabolic parameters were different between the low- and high-temperature groups. The cumulative fecal excretion for 1 year after exposure in the high-temperature group was 52% IAD, and the cumulative urinary excretion was 31% (Table 1). The ratio of fecal to urinary excretion was 1.7. In the low-temperature group, the cumulative fecal and urinary excretion was 68 and 23% IAD, respectively, and the ratio of fecal

to urinary excretion was 3.1. The accumulation of ^{239}Pu in some organs was also influenced by the calcination temperature. The amounts of ^{239}Pu in the liver and spleen seemed to be higher in the low- than in the high-temperature group at 1 year after exposure (Table 2). In turn, the amounts in the kidney and femur were lower in the low-temperature group at 1 month and 1 year. As a result, the ratio of ^{239}Pu amount in the liver to that in the femur or kidney was consistently higher in the low-temperature group at 1 month and 1 year after administration. These two findings, i.e., the higher fecal/urinary excretion ratio and the higher liver/femur accumulation ratio in the low-temperature group, are clearly consistent with each other in terms of the general concept of ^{239}Pu metabolism. The higher fecal/urinary excretion ratio in the low-temperature group suggests that some ^{239}Pu derived from $^{239}PuO_2$ calcined at 400°C was distributed from lungs to circulating blood or lymph systems in a colloidal or particulate form. In other words, the amount of plutonium which will be bound to transferrin and removed to urine was relatively smaller in the low-temperature group. The higher liver/femur accumulation ratio in the low-temperature group also indicated that a colloidal or particulate form of ^{239}Pu, which tended to be trapped by reticuloendothelial tissues, might be abundant in the circulating blood of the rats in the low-temperature group.

As for risk estimation, the present data also indicate that the lungs are the major target organs for inhaled ^{239}Pu under the experimental conditions used here. The retention of ^{239}Pu in the other organs was very small compared to that in the lungs, regardless of the firing temperature. This supports the findings by Oghiso et al[4], which showed that tumor incidence increased in the lungs, but not in other organs of rats inhaling PuO_2 under the same experimental conditions used here. In conclusion, we presented here the metabolic data of ^{239}Pu in rats inhaling $^{239}PuO_2$ particles. These metabolic data, including lung retention, fecal and urinary excretion, and translocation to other organs, seemed to be affected by the calcination temperature of the $^{239}PuO_2$ particles. Clearance from the lungs and redistribution to other organs was faster in the rats inhaling $^{239}PuO_2$ calcined at a lower temperature.

REFERENCES

1. Ishigure, N., Nakano, T., Enomoto, H., Fukuda, S., Iida, H., Oghiso, Y., Yamada, Y. and Inaba, J. (1992) Assessment of initial alveolar deposition on rats exposed to plutonium aerosols using a whole body counter. Hoken Butsuri **27**: 135–142.
2. Ishigure, N., Nakano, T., Enomoto, H., Fukuda, S., Iida, H., Oghiso, Y., Sato, H., Takahashi, S., Yamada, Y., Koizumi, A., Yamada, Y., Miyamoto, K. and Inaba, J. (1994) Lung retention of Pu following inhalation of PuO_2 in rats measured using whole body counter. J. Radiat. Res. **35**: 16–25.
3. Oghiso, Y., Yamada, Y., Ishigure, N., Fukuda, S., Iida, H., Yamada, Y., Sato, H., Koizumi, A. and Inaba, J. (1994) High incidence of malignant lung carcinomas in rats after inhalation of $^{239}PuO_2$ aerosol. J. Radiat. Res. **35**: 222–235.
4. Oghiso, Y., Yamada, Y., Iida, H. and Inaba, J. (1998) Differential dose response of pulmonary tumor types in the rat after inhalation of plutonium dioxide aerosols. J. Radiat. Res. **39**: 61–72.
5. Mewhinney, J. A., Muggenburg, B. A., McClellan, R. O. and Miglio, J. J. (1976) The effect of varying physical and chemical characteristics of inhaled plutonium aerosols of metabolism and excretion. In: "Proc. An International Seminar on Diagnosis and Treatment of Incorporated Radionuclides", Vienna, IAEA-SR-6/29, pp. 87–97.

6. Morgan, A., Black, A., Knight, D. and Moores, S. R. (1988) The effect of firing temperature on the lung retention and translocation of Pu following the inhalation of $^{238}PuO_2$ and $^{239}PuO_2$ by CBA/H mice. Health Phys. **54**: 301–310.
7. Morgan, A. and Black, A. (1989) Lung retention and translocation of Pu in mice following inhalation of $^{238}PuO_2$, and $^{239}PuO_2$ fired at 550–1250°C and of (U, Pu) O_2 fired at 1400 and 1600°C. Radiat. Protect. Dosimet. **26**: 297–301.
8. Yamada, Y., Koizumi, A., Miyamoto, K., Sato, H., Ishigure, N., Nakano, T., Enomoto, H. and Inaba, J. (1992) Characteristics of plutonium oxide aerosol particles generated by nebulization. Hoken Butsuri **27**: 197–204. (in Japanese).
9. Sanders, C. L., McDonald, K. E. and Mahaffey, J. A. (1988) Lung tumor response to inhaled Pu and its implications for radiation protection. Health Phys. **55**: 455–462.
10. Sanders, C. L., Lauhala, K. E., McDonald, K. E. and Sanders, G. A. (1993) Lifespan studies in rats exposed to $^{239}PuO_2$ aerosol. Health Phys. **64**: 509–521.
11. Wu, D. C., Ye, C. Q., Gong, Y. F., Yan, X. S. and Xie, G. L. (1989) The study of the harmful effects of rat lung induced by inhaled $^{239}PuO_2$. Chinese J. Radiol. Med. and Prot. **9**: 305–312. (in Chinese).
12. Stradling, G. N., Stather, J. W., Gray, S. A., Moody, J. C., Baily, M. R., Hodgson, A. and Collier, C. (1987) Studies on the metabolic behavior of industrial actinide-bearing aerosols after deposition in the rat lung: an experimental basis for interpreting chest monitoring data and assessing limits on intake for workers. Human Toxicol. **6**: 365–375.
13. James, A. C., Stather, J. W., Strong, J. C., Hostford, J. E., Rodwell, P., Hodgson, A. and Kay, P. (1978) Lung clearance and translocation in rats and hamsters of inhaled dust containing mixed actinide oxides from a fuel fabrication plant. National Radiological Protection Board Annual Research and Development Report, 1977, NRPB/R & D2, pp. 57–64.
14. Bailey, M. R., Kreyling, W. G., Andre, S., Batchelor, A., Collier, C. G., Drosselmeyer, E., Ferron, G. A., Foster, P., Haider, B., Hodgson, A., Masse, R., Metivier, H., Morgan, A., Muller, H. -L., Patrick, G., Pearman, I., Pickering, S., Ramsden, D., Stirling, C. and Talbot, R. J. (1989) An interspecies comparison of the lung clearance of inhaled monodisperse cobalt oxide particles—Part I: Objectives and summary of results. J. Aerosol Sci. **20**: 169–188.

0163–4984/99/6902–0161 $13.50

Physicochemical Characteristics and Toxicity of Nickel Oxide Particles Calcined at Different Temperatures

SENTARO TAKAHASHI,*[,1] MASAHIRO OISHI,[2] ERIKO TAKEDA,[2] YOSHIHISA KUBOTA,[1] TADASHI KIKUCHI,[2] AND KEIICHI FURUYA[2]

[1]The 4th Research Group, National Institute of Radiological Sciences, Inageku, Chiba, Japan; and [2]Department of Applied Chemistry, Faculty of Science, Science University of Tokyo, Shinjuku, Tokyo, Japan.

Received August 3, 1998; Accepted October 13, 1998

ABSTRACT

The physicochemical characteristics and cytotoxicity of two types of commercial nickel oxide particles (black and green nickel oxide) and five types of nickel oxide particles prepared by calcination of the black nickel oxide at 600–1000°C were studied. Thermal analysis with mass spectroscopy showed that the black nickel oxide particles contained approximately 1.4% impurity, which seemed to be basic nickel carbonate. The calcination treatment at 600°C increased the nickel content and decreased the oxygen content, but these remained constant in the particles treated at higher temperatures (700–1000°C) and in the green nickel oxide particles. The water solubility of black nickel oxide particles was markedly greater than that of the other particles, especially in the first 24 h after mixing with water. The solubility of the calcined particles decreased with increasing calcination temperature. The cytotoxicity of these particles was evaluated by the viability of rat alveolar macrophages and by the inhibition of cell proliferation in Chinese hamster ovary cells. The black nickel oxide was the most cytotoxic of the particles examined, and this may be attributable, at least in

*Author to whom all correspondence and reprint requests should be addressed.

part, to a rapid dissolution of nickel from the contained impurity. The toxicity of the calcined particles decreased with increasing calcination temperature. These results indicate that water solubility, which depends on calcination temperature, modulates the acute cytotoxicity of nickel oxide particles.

Index Entries: Nickel oxide; physicochemical characteristic; calcination temperature; cytotoxicity.

INTRODUCTION

Nickel is a useful metal, particularly in various alloys, in batteries, and in nickel plating. Nickel compounds are used especially as catalysts and pigments. Although nickel is an essential element for animal nutrition and not a highly toxic metal, overexposure to nickel or nickel compounds presents a variety of health hazards *(1–4)*. The most important health problems because of exposure to nickel and nickel compounds are allergic dermatitis and increased incidence of cancers encountered among workers after long-term overexposure to nickel. Nickel refinery workers, especially those employed in the early part of this century, have shown a higher incidence of nasal and lung cancer *(5)*. In this respect, the most hazardous nickel compounds are considered to be nickel sulfide and nickel oxide, and inhalation is a primary route of human exposure *(1–5)*.

Nickel oxide particles (NiO) are poorly soluble, and toxicity is relatively lower than other nickel compounds when compared by acute or subchronic effects. In mice and rats administered different types of nickel compound by inhalation, a toxicity ranking was reported to be $NiSO_4$ > Ni_3S_2 > NiO, based on the toxicities of the compounds at equivalent mg Ni/m^3 exposure concentration *(6–8)*. Haley et al. found that the immunotoxicity of NiO was lower than that of $NiSO_4$ or Ni_3S_2 *(9)*. A similar tendency was also observed in in vitro cytotoxicity testing of nickel compounds *(10,11)*. The bioassays for the cytotoxicity and carcinogenicity of nickel oxide in animals or cultured cells have yielded highly variable results, suggesting that differences in physicochemical characteristics of various samples of NiO may account for variations in the results *(12–18)*. The physicochemical characteristics of nickel oxide are not constant because of its nonstoichiometric chemical properties. We have demonstrated that commercial nickel oxide particles varied in physicochemical characteristics such as particle size and solubility and in movement and dissolution in mouse respiratory tracts *(19,20)*. Sunderman et al. prepared a series of nickel oxide particles under controlled metallurgical conditions and found that some physicochemical parameters depended on the calcination temperature *(14,15)*. Those studies indicated that even

though they were in the same category of "nickel oxide," their physicochemical characteristics were significantly different. Regarding the toxicity of nickel oxide, two types of commercial nickel oxide particles produced by the same manufacturer were different with respect to cytotoxicity in cultured rat alveolar macrophages, morphological cell transformation, and renal histopathologic responses *(14,18)*. The exact reasons for this differing toxicity are not apparent, although it has been suggested that the presence of a high surface area and demonstrable Ni(III) were two physicochemical characteristics associated with the greatest biological effects *(14)*.

In the present study, we focused on these two types of nickel oxide particle: black nickel oxide and green nickel oxide [referred to as NiO(B) and NiO(G), respectively, in the following text]. These are commercial products prepared by the calcination of nickel carbonate in a rotary furnace operating at <650°C for NiO(B) and 1350°C for NiO(G). At first, the detailed physicochemical characteristics of these particles were investigated. Second, intermediate particles between NiO(B) and NiO(G) were prepared by recalcining of NiO(B) at different temperatures, and the physicochemical characteristics and cytotoxicity of these particles were examined to elucidate the major factors relating to the cytotoxic effects of nickel oxide.

MATERIALS AND METHODS

Preparation of Test Particles

Two types of nickel oxide particles, NiO(B) and NiO(G), both produced by the same manufacturer (INCO, Ltd., Toronto, Canada) were obtained from a domestic distributor. These particles were identical to those used in our previous studies *(19–21)*. To prepare the particles with intermediate chemical properties between NiO(B) and NiO(G), 2 g of NiO(B) were placed in dishes and calcined in a heated oven at either 600°C, 700°C, 800°C, 900°C, or 1000°C for 1 h under atmospheric conditions. After cooling to room temperature, these nickel oxide particles were stored in sealed glass vials. Abbreviations such as NiO(600) and NiO(700) are used to refer these five types of calcined nickel oxide particle in the following text.

Determination of Physicochemical Characteristics of Test Particles

The contents of nickel in the test particles were determined by atomic absorption spectrometry (AAS, Z-8000, Hitachi Co. Ltd., Tokyo, Japan) after dissolving a known amount of particles with $HF–HNO_3–HClO_4$ in Teflon beakers. The oxygen content was measured

using an inert-gas fusion analyzer (EMGA650, Horiba Co. Ltd., Kyoto, Japan) with nickel capsules. The crystalline structure and phase were examined by X-ray diffractometry (XRD, Model MXP3, MAC Science Co. Ltd., Kanagawa, Japan), at 30 kV of acceleration voltage, 15 mA of lamp current, and 4°/min of scanning speed. Particle sizes were determined by scanning electron microscopy (SEM, Model S-5000, Hitachi). To obtain information about the content of water and other impurities, thermal decomposition analysis was carried out with a thermal analysis mass spectrometer (TA-MS), which consisted of a thermoanalyzer (Model TGD 700RH, Ulvac Technologies, Inc., Methuen, USA) and a quadruple mass spectrometer (Model TE-600, Anelva Co. Ltd., Tokyo, Japan). The rate of temperature increase was set at 10°C/min from ambient temperature to 600°C under helium atmosphere.

Solubility of NiO Particles

In a 300-mL container, 50 mg of sample particles was mixed with 100 mL of pure water made using the Millipore Milli-XQ instrument (Millipore Ltd., Bedford, MA, USA). The particle suspension solutions were stirred for 24, 48, and 72 h under the closed conditions by sealing the container with a sheet of plastic film. The sample solutions were filtered with a 0.22-μm membrane filter to separate the residual particles. The concentration of nickel in the filtrates was determined by AAS after diluting to a suitable concentration with 1*N* HNO_3.

Cytotoxicity

The cytotoxicity of the sample particles was determined in rat alveolar macrophages and Chinese hamster ovary (CHO) cells cultured in vitro. Female Sprague–Dawley rats, aged 12–16 wk, were used as donors of alveolar macrophages. The animals were sacrificed under halothane anesthesia, and broncho-alveolar lavage cells were collected by washing the lungs with phosphate-buffered saline. The lavage cells were separated by centrifuge at 400*g* for 5 min, washed once, and resuspended in Eagle's minimum essential medium (E-MEM, Gibco-Oriental, Tokyo, Japan) supplemented with 10% fetal calf serum. The cells ([3.0–4.0] × 10^5 cells in 2 mL medium) were incubated in a 35-mm culture dish at 37°C under 5% CO_2 and 95% air. After 2 h, the culture supernatant and nonadherent cells were discarded. The adherent cells, consisting of more than 94% macrophages, were cultured again in media containing the nickel oxide particles at concentrations of 400 and 800 μg/mL. After incubation for 18, 42, or 72 h, the culture medium was recovered, and the culture dish was rinsed with phosphate-buffered solution to remove nonadherent macrophages and free particles. The recovered media and rinsed solutions were centrifuged to collect the nonadherent macrophages. The cell viability of the nonadherent cells recovered and the

adherent cells on the dish were determined by a dye exclusion test with Trypan Blue. CHO-K1 cells, purchased from the Cell Bank of Science and Chemical Institute (Riken, Saitama, Japan) were maintained in Ham F-12 medium (Gibco-Oriental, Tokyo, Japan) supplemented with 10% fetal calf serum. The cells were seeded into a 96-well microplate in 100 µL of complete medium at a concentration of 0.2×10^3 cells/well. After 24 h, 50 µL of supernatant was discarded, and 50 µL of particle suspension medium, which contained the nickel oxide particles at known concentrations, was added to each well. In the control wells, 50 µL of the fresh medium was added. After a further 24-h incubation, the supernatants in each well were removed and the NiO particles were washed out with medium. The cells were fixed with 10% formaldehyde for 30 min, stained with Giemsa/methanol (50% v/v), and counted under a light microscope. Cytotoxicity tests were carried out in triplicate or duplicate in at least three independent experiments. Statistical differences were analyzed using the Student's *t*-test (n = 6–9).

RESULTS

The physicochemical characteristics of the sample particles are summarized in Table 1. The contents of nickel, determined by AAS, were 74.3 ± 1.4% in NiO(B) to 80.8 ± 2.5% in NiO(G). The oxygen content in NiO(B) was 23.2 ± 0.3% and decreased with increasing calcination temperature to 20.5 ± 0.3% in NiO(G). As expected, the contents of nickel and oxygen in the NiO calcined at 600°C were intermediate values between NiO(B) and NiO(G), but those in the nickel oxides prepared at 700–1000°C were not significantly different from each other and yielded similar levels to those in NiO(G).

The X-ray diffraction (XRD) patterns of the sample particles are shown in Fig. 1, and the relative heights of XRD peaks in each sample are also presented in Table 1. The XRD patterns clearly showed that the nickel oxide, "bunsenite," was the major crystalline phase of all the sample particles. The characteristic XRD peaks of bunsenite at 1.48, 2.09, and 2.41 Å were observed. The peaks became sharper and higher with the increased calcination temperature, suggesting better crystalline-phase formation of NiO(G) and those particles calcined at higher temperatures. Scanning electron microscopy showed that count median particle diameters were 4.2 and 4.5 µm in NiO(B) and NiO(G), respectively, and that some of them were aggregates of smaller particles with diameters of less than 1 µm. The size of all the other particles, NiO(600) to NiO(1000), were in the range between 4.1 and 4.5 µm.

Figure 2 shows the thermogravimetrical curves of NiO(B) and NiO(G) in the thermal decomposition analysis. Approximately 1.4% weight loss was observed in NiO(B) in the course of the temperature

Table 1
Major Physicochemical Characteristics of Nickel Oxide Particles

	NiO(B)*	NiO(600)	NiO(700)	NiO(800)	NiO(900)	NiO(1000)	NiO(G)
Nickel content**	74.3±1.4	77.4±0.1	79.8±0.5	78.9±0.7	79.2±1.1	79.9±1.1	80.8±2.5
Oxygen content**	23.2±0.3	22.0±0.1	20.7±0.2	20.7±0.2	20.6±0.1	20.7±0.3	20.5±0.5
Color	Black	Grey-black	Grey	Grey	Dark-green	Dark-green	Green
Relative height of XRD peaks (%)***	12	44	56	58	80	101	100

*NiO(B) and Ni(G) denote the INCO black and green nickel oxide particles. NiO(600)–NiO(1000) are nickel oxide particles prepared by heating the NiO(B) at a temperature in parentheses.

**Nickel and oxygen contents are expressed as wt%, and mean ± S.E. of three measurements.

***Relative height of XRD peaks to that observed in NiO(G).

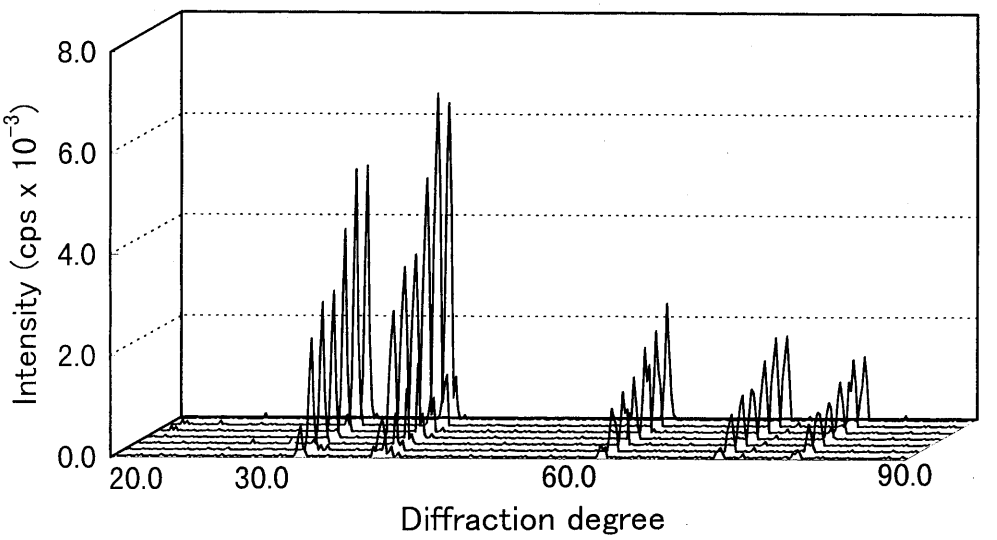

Fig. 1. The X-ray diffractometric pattern of the sample particles. The line of the frontmost side indicates the XRD pattern of NiO(B). The second to sixth lines are those of NiO(600) to NiO(1000), and the rear line is that of NiO(G). The characteristic XRD peaks of bunsenite were observed, and the peaks became higher and sharper with increasing calcination temperature.

increasing from room temperature to 600°C. In contrast, such a weight loss was not observed in NiO(G) or the other test particles of NiO(600) to NiO(1000). To investigate the reason for this weight loss, TA-MS analyses were performed. The mass fragmentgrams of NiO(B) and NiO(G) are shown in Fig. 3. As expected, MS detected very little amount of thermal-decomposed matter in NiO(G). On the other hand, NiO(B) decomposed at about 90°C evolving H_2O, and at around 225°C evolving H_2O and CO_2. These were assumed to be thermal decomposition products of basic

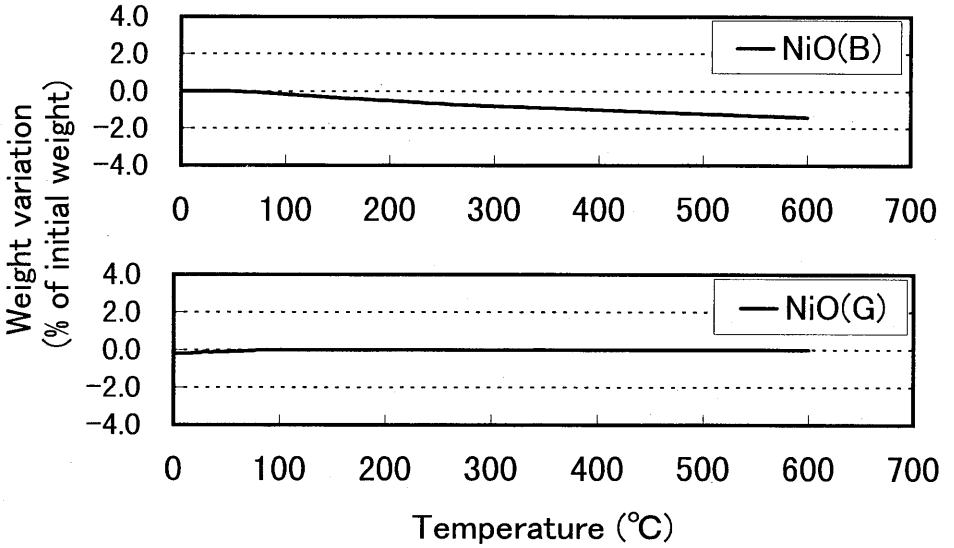

Fig. 2. Thermogravimetrical curves of NiO(B) and NiO(G) in the thermal decomposition analysis. Approximately 1.4% of weight loss was observed in NiO(B) during the course of temperature increase from room temperature to 600°C.

nickel carbonate ($NiCO_3 \cdot nNi(OH)_2 \cdot mH_2O$) from the mass spectrum pattern and the results of the reference material. The mass fragmentgrams of the calcined particles, NiO(600) to NiO(1000), were essentially the same as that of NiO(G).

The solubility of NiO particles into distilled water is shown in Fig. 4. The solubility of NiO(B) was markedly larger than those of the other samples. The solubility of NiO(600)–NiO(1000) was lower than that of NiO(B), and tended to decrease with the increasing calcination temperature. The solubility of NiO(G) was significantly lower than the other particles at all the time-points examined. In all the particles, except for NiO(G), dissolution occurred mainly during the first 24 h after mixing with water. The blank solubility (i.e., the solubility at 0 min) was less than 0.1 μg/mL for all the samples.

Figure 5 shows the viability of rat alveolar macrophages exposed to each of the nickel oxide particles at concentrations of 800 μg/mL for 18, 42, and 72 h. There was no significant decrease in the cell viability in any of the test groups at 24 h after exposure. At 48 h after exposure, a significant decrease in the cell viability was observed in the macrophages exposed to NiO(B). At 72 h, the cell viability was decreased to 15%, 65%, and 80% for NiO(B), NiO(600), and NiO(800), respectively. In the macrophages exposed to the other NiO particles, the viability tended to decrease but was not significantly different from the control culture. When the exposure dose was decreased to 400

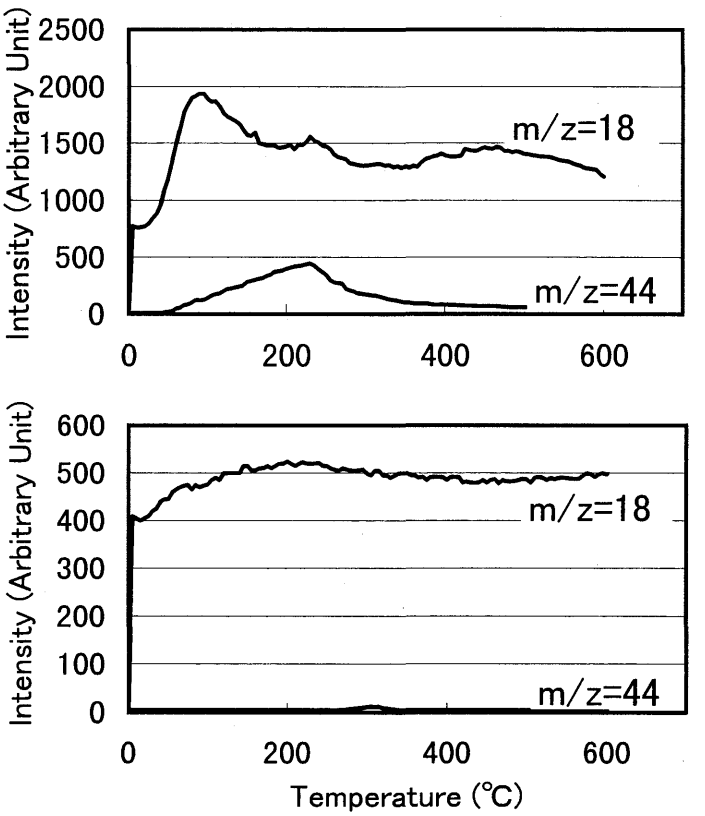

Fig. 3. Mass fragmentgrams of NiO(B) (upper) and NiO(G) (lower). NiO(B) decomposed at about 90°C evolving H_2O and around 225°C evolving H_2O and CO_2, whereas very little thermal-decomposed matter was detected in NiO(G). Note that the scales of the vertical axes are different for the upper and lower parts.

μg/mL, a significant decrease in cell viability was observed only for NiO(B) at 72 h (data not shown). In CHO cells, the cell proliferation was used as an index of particle toxicity (Fig. 6). The cell number increased to (1.2–1.5) × 10^3 in the control group at the end of culture. All the particles examined here significantly suppressed the cell proliferation at doses of 50 μg/mL or more. Because the cell number at the start of exposure was assumed to be approximately (3–4) × 10^2 cells/well, the average cell number of 328 cells/well in the group exposed to 100 μg/mL NiO(B) indicated that the cell proliferation was completely impaired at this dose. On increasing the dose to 200 μg/mL, the cell numbers at the end of culture became smaller than

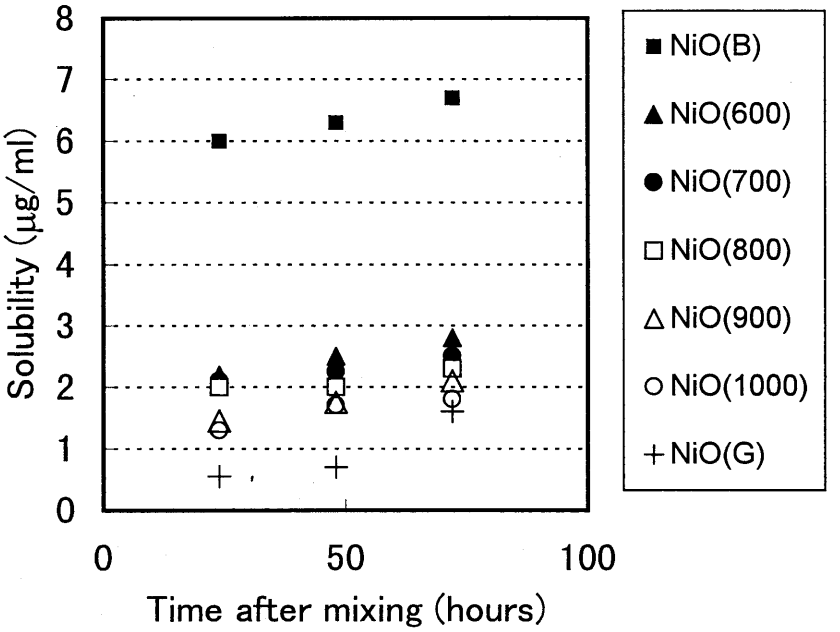

Fig. 4. Solubility of NiO particles into distilled water. The solubility of NiO(B) was markedly larger than that of other samples. The solubilities of NiO(600)–NiO(1000) were lower than that of NiO(B) and decreased with increasing calcination temperature. Data are the mean values of two independent experiments.

those at the start of exposure in all the treated groups, except for NiO(1000) and NiO(G) groups. This suggests that in this dose level, the detachment of cells from the culture dish had occurred through the death or the impairment of adherent capacity of the cells. For all three doses examined, there was an apparent tendency for the suppressive effect of NiO on CHO cell proliferation to become profound with decreased calcination temperature.

DISCUSSION

The loss of the weight in thermal analyses indicated that the black nickel oxide, NiO(B), used here might contain small amount of impurities. Although the exact chemical composition was not apparent, the impurities were assumed to be a kind of basic nickel carbonate ($NiCO_3 \cdot nNi(OH)_2 \cdot mH_2O$) from the mass analysis of thermal decomposition

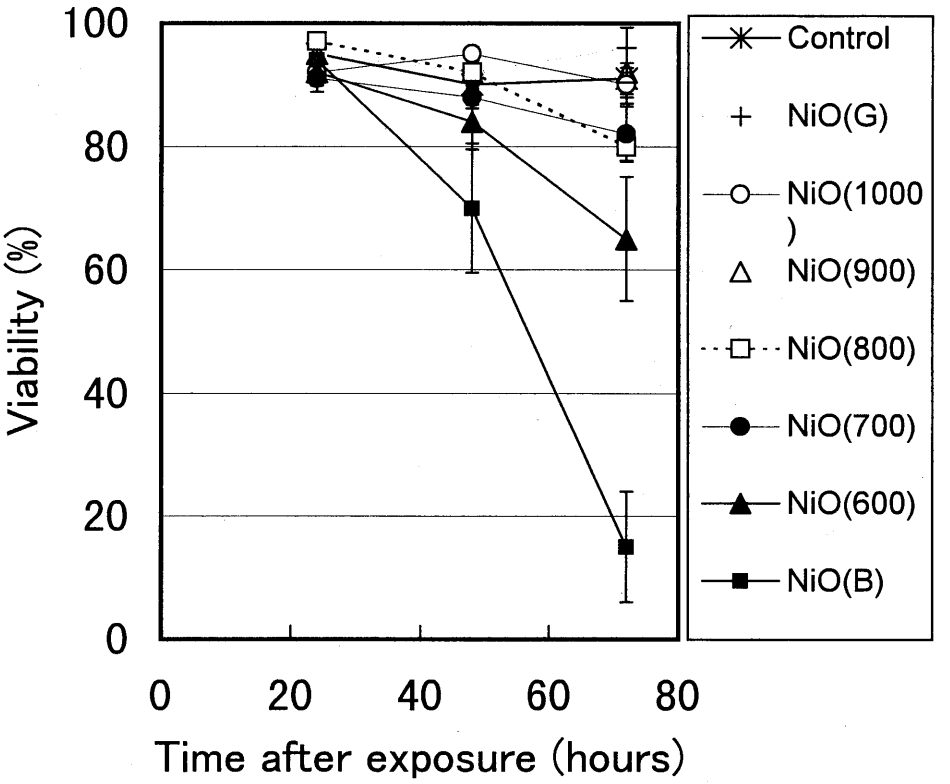

Fig. 5. Viability of rat alveolar macrophages exposed to nickel oxide particles at concentrations of 800 μg/mL for 18, 42, and 72 h. Viability was determined by trypan blue dye exclusion test. Each point and vertical bar denotes mean ± S.E. of six to nine cultures of at least three experiments.

products (Fig. 3). The cause of the impurities is not known at present. Because the NiO(B) is made from nickel carbonate particles, some of them might remain unchanged after thermal treatment. Another possibility is the denaturing reaction of nickel oxide with water and carbon oxide during the storage. This impurity could be successfully expelled by heating the particles to 600°C or higher for 1 h. The resultant five types of particle, NiO(600)–NiO(1000), seemed to be pure nickel oxides from TA-MS analyses.

In NiO(600), the nickel and oxygen content were 77.4% and 22.0%, respectively, as shown in Table 1. Because the theoretical contents of nickel and oxygen in stoichiometric nickel oxide (NiO) are 78.6% and 21.4%, respectively, NiO(600) was a so-called oxygen-rich compound. Heating to 700°C increased the nickel content to 79.8% and decreased the oxygen contents to 20.4%, but heating to temperatures higher than 700°C did not change the composition. The nickel to oxygen ratios were nearly constant in NiO(700)–NiO(1000) and NiO(G) and were larger than the theoretical value. The heating also affected the crystalline phase

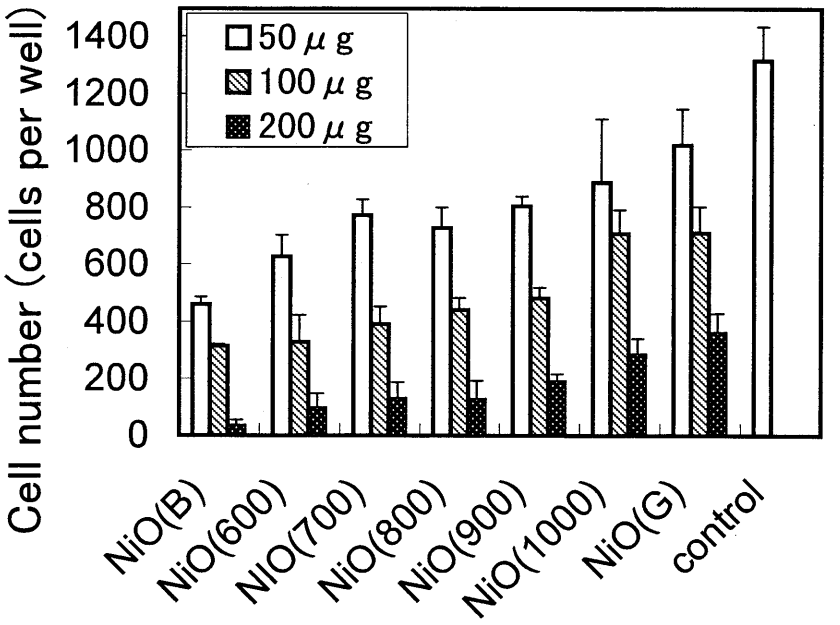

Fig. 6. The effect of nickel oxide particles on the proliferation of Chinese hamster ovary cells. Cell were exposed to 50, 100, and 200 mg/mL of each nickel oxide for 24 h. Each column and vertical bar denotes mean ± S.E. of four to six cultures in two independent experiments.

of the particles. The height of XRD peaks of bunsenite became sharper with increased calcination temperature. These findings are consistent with the previous report by Sunderman et al. *(14)*. Furthermore, we confirmed by inert-gas fusion analysis that the oxygen content decreased with heating to 700°C but was not changed further at higher temperatures.

As shown in Fig. 4, the solubility of NiO(B) was markedly higher than that of the other particles examined, and a portion of NiO(B) dissolved very rapidly in a short time after mixing with water. This finding is consistent with and extends our previous finding *(19)*; the solubility of NiO(B) particles was higher than five other types of commercial nickel oxide particle in several types of solution. We also found that the solubility of NiO(B) is markedly decreased by the calcination and that calcination expels the impurities, which may consist of a kind of nickel carbonate. Because the basic nickel carbonates are generally soluble, the higher solubility of NiO(B) may be, at least in part, attributed to these impurities. The solubility of nickel oxide particles also decreased with increasing calcination temperature (Fig. 4). This may be explained by the fact that the effective surface area of the particles became larger at higher calcination temperature *(14)*.

The cytotoxicity of NiO(B) toward rat alveolar macrophages and CHO cells was higher than that of the other particles examined (Figs. 5 and 6).

We have already demonstrated that NiO(B) is more toxic for cultured rat alveolar macrophages than NiO(G) *(21)*. Relatively more severe pathological effects of NiO(B) were also noticed in rat following intrarenal and intramuscle injection of test particles *(14,15)*. The reasons why NiO(B) was more toxic than the other nickel oxide particles are not readily apparent from the present study. Sunderman et al. suggested that the presence of a larger surface area and demonstrable Ni(III) were responsible for this *(14,15)*. Another possible reason may be that NiO(B) contained small but significant amounts of impurities assumed to be nickel carbonate. Nickel carbonate is very soluble into water, and many previous reports have indicated that higher solubility of nickel compounds results in higher toxicity *(6–8,16)*.

There are contrasting reports about the effects of calcination temperature on the cytotoxicity of nickel oxide. Sunderman et al. *(14,15)* reported that the toxicity of nickel oxide toward Syrian hamster embryo cells increased with calcination temperature. In contrast, Benson et al. *(10,11)* did not find significant differences in the toxicity of nickel oxide calcined at different temperatures. They exposed alveolar macrophages to test particles for 20 h, examined the toxicity by the Trypan Blue dye exclusion test, and found no temperature-related variation in cytotoxicity. In the present study, we also used rat alveolar macrophages, and the toxicity was evaluated by the same method. We found no differences in cytotoxicity among the particles at 24 h after exposure. At 72 h after exposure, however, the nickel oxide particles calcined at lower temperatures such as NiO(B) and NiO(600) were significantly more cytotoxic than those calcined at higher temperature. The alveolar macrophages were completely differentiated and nonproliferative. These cells did not perform further cell division in the culture conditions used here. Therefore, the observed cell death is so-called interphase cell death, and this type of cell death may be a less sensitive index to toxicants. To detect the difference in cytotoxicity with greater sensitivity, we used the proliferation of CHO cells as a toxicological index. As shown in Fig. 6, the proliferation of cells was markedly inhibited by the nickel oxide particles, and the order of the inhibitory effects depended on the calcination temperatures.

In conclusion, NiO(B) particles were more cytotoxic than NiO(G) or those calcined at 600–1000°C. Impurities in Ni(B), which were assumed to be basic nickel carbonate, may be one of the causes for this higher toxicity of NiO(B). The calcination temperature modified not only the physicochemical characteristics of nickel oxide particles but also their cytotoxicity. However, the difference in toxicity with calcination temperature was not so large, as the difference was only detectable in prolonged culture of alveolar macrophages or sensitive cell proliferation assay. The water solubility, which decreased with increasing calcination temperature, may be a cause of the different cytotoxicities of nickel oxide particles calcined at different temperatures.

ACKNOWLEDGMENTS

We thank Dr. Isamu Tanaka for providing sample particles and valuable advise. This work was supported by a Grant in Aid for Science Research on Priority Areas from the Ministry of Education, Science and Culture of Japan (5278113).

REFERENCES

1. F. W. Sunderman, Jr., A review of the metabolism and toxicology of nickel, *Ann. Clin. Lab. Sci.* **7,** 377–398 (1977).
2. V. Bencko, Nickel: a review of its occupational and environmental toxicology, *J. Hyg. Epidemiol. Microbiol. Immunol.* **27,** 237–247 (1983).
3. P. Grandjean, Human exposure to nickel, *IARC Sci. Publ.* **53,** 469–485 (1984).
4. H. Savolainen, Biochemical and clinical aspects of nickel toxicity, *Rev. Environ. Health* **11,** 167–173 (1996).
5. IARC, Nickel in the human environment, *IARC Sci. Publ.* **53,** 123–127 (1984).
6. J. K. Dunnick, J. M. Benson, C. H. Hobbs, F. E. Hahn, Y. S. Cheng, and A. F. Eidson, Comparative toxicity of nickel oxide, nickel sulfate hexahydrate, and nickel subsulfide after 12 days of inhalation exposure to F344/N rats and B6C3F mice, *Toxicology* **50,** 145–156 (1988).
7. J. K. Dunnick, M. R. Elwell, J. M. Benson, C. H. Hobbs, F. F. Hahn, P. J. Haly, et al., Lung toxicity after 13 week inhalation exposure to nickel oxide, nickel subsulfide, or nickel sulfate hexahydrate in F344/N rats and B6C3F1 mice, *Fundam. Appl. Toxicol.* **12,** 584–594 (1989).
8. J. M. Benson, D. G. Burt, Y. S. Cheng, F. F. Hahn, P. J. Haley, R. F. Henderson, et al., Biochemical responses of rat and mouse lung to inhaled nickel compounds, *Toxicology* **57,** 255–266 (1989).
9. P. J. Haley, G. M. Shopp, J. M. Benson, Y. S. Cheng, D. E. Bice, M. I. Luster, et al., The immunotoxicity of three nickel compounds following 13 week inhalation exposure in the mouse, *Fundam. Appl. Toxicol.* **15,** 476–487 (1990).
10. J. M. Benson, R. F. Henderson, and R. O. McClellan, Comparative cytotoxicity of four nickel compounds to canine and rodent alveolar macrophages in vitro, *J. Toxicol. Environ. Health* **19,** 105–110 (1986).
11. J. M. Benson, R. F. Henderson, and J. A. Pickerell, Comparative in vitro cytotoxicity of nickel oxide and nickel-copper oxides to rat, mouse and dog pulmonary alveolar macrophages, *J. Toxicol. Environ. Health* **24,** 373–383 (1988).
12. A. P. Wehner, R. H. Busch, R. J. Olson, and D. K. Craig, Chronic inhalation of nickel oxide and cigarette smoke by hamsters, *Am. Ind. Hyg. Assoc. J.* **36,** 801–810 (1975).
13. F. W. Sunderman, Jr., Carcinogenicity of nickel compounds in animals, in *Nickel in the Human Environment,* F. W. Sunderman, Jr., ed., Oxford University Press, Oxford, pp. 127–142 (1984).
14. F. W. Sunderman, Jr., S. M. Hopfer, J. A. Knight, K. S. McCully, A. G. Cecutti, P. G. Thornhill, et al., Physicochemical characteristics and biological effects of nickel oxides, *Carcinogenesis* **8,** 305–313 (1987).
15. F. W. Sunderman, Jr., S. M. Hopfer, M. C. Plounmann, and J. A. Knight, Carcinogenesis bioassays of nickel oxide and nickel copper oxides by intramuscular administration to Fisher-344 rats, *Res. Commun. Chem. Pathol. Pharmacol.* **70,** 103–113 (1990).
16. A. Horie, J. Haratake, I. Tanaka, Y. Kodama, and K. Tsuchiya, Electron microscopical findings with special reference to cancer in rats caused by inhalation of nickel oxide, *Biol. Trace Element Res.* **7,** 223–239 (1985).
17. J. Haratake, A. Horie, Y. Kodama, and I. Tanaka, Histopathological examination of rats treated by inhalations of various types of nickel compounds, *Inhalat. Toxicol.* **4,** 67–79 (1992).

18. S. Takahashi, M. Yamada, T. Kondo, H. Sato, K. Furuya, and I. Tanaka, Cytotoxicity of nickel oxide particles in rat alveolar macrophages cultured in vitro, *J. Toxicol. Sci.* **17,** 243–251 (1992).
19. M. Yamada, S. Takahashi, H. Sato, T. Kondo, T. Kikuchi, K. Furuya, et al., Solubility of nickel oxide particles in various solutions and rat alveolar macrophages, *Biol. Trace Element Res.* **36,** 89–98 (1993).
20. M. Ooishi, S. Takahashi, T. Kikuchi, and K. Furuya, Solubility of two types of nickel oxide particles in mouse respiratory tract and in five kinds of solvents, *Kankyo Kagaku (Environ. Sci. Jpn.)* **8,** 397–408 (1995) (in Japanese with English abstract).

RADIATION RESEARCH 152, S107–S109 (1999)
0033-7587/99 $5.00

Mutations in *Tp53* Gene Sequences from Lung Tumors in Rats That Inhaled Plutonium Dioxide

Yutaka Yamada and Yoichi Oghiso

Division of Radiotoxicology and Protection, National Institute of Radiological Sciences, Chiba 263-8555, Japan

Yamada, Y. and Oghiso, Y. Mutations in *Tp53* Gene Sequences from Lung Tumors in Rats That Inhaled Plutonium Dioxide. *Radiat. Res.* 152, S107–S109 (1999).

We investigated mutations of the *Tp53* tumor suppressor gene (formerly known as *p53*) in the lung tumors induced in rats after inhalation of plutonium dioxide ($^{239}PuO_2$) aerosols. Exons 5, 6, 7 and 8 of the *Tp53* gene were examined for mutations by single-strand conformation polymorphism (SSCP) analysis of polymerase chain reaction (PCR)-amplified fragments and direct sequencing analysis. Almost all the mutations were guanine (G) to adenine (A) transitions and were distributed in exons 5 and 6. The *Tp53* mutations occurred in lung tumors of various phenotypes and levels of immunohistochemical staining of Tp53 nuclear protein. These results indicate that the *Tp53* mutations are not associated with tumor phenotype and nuclear accumulation of Tp53 protein, and that the G to A transition could be a common point mutation in the lung tumors seen after the inhalation of plutonium dioxide. The point mutations in the *Tp53* gene seem to play a role in the development of lung tumors in rats after inhalation exposures to plutonium dioxide. © 1999 by Radiation Research Society

INTRODUCTION

Alpha-particle emitters are strong mutagens and carcinogens. Radon, radon progeny and transuranium elements including plutonium can induce lung cancers in experimental animals after exposure by inhalation. Recently, molecular techniques have been applied to elucidate the molecular mechanisms of carcinogenesis induced by α-particle emitters with special reference to tumor suppressor genes and oncogenes. It has been suggested that inactivation of the tumor suppressor gene *TP53* (formerly known as *p53*) is associated with the mechanism of carcinogenesis and that abnormalities of the *TP53* gene are frequently observed in malignant tumors in humans (*1*). The *TP53* gene is frequently mutated in lung cancers in uranium miners (*2*), indicating that the mutations of *TP53* could be associated with carcinogenesis induced by radon and radon progeny. It has been reported, however, that lung tumors induced in rats by inhalation of plutonium dioxide have a low incidence of *Tp53* mutation (*3*). Thus the role and nature of the *Tp53* mutation in the development of tumors induced by α-particle radiation remain unclear. We have performed life-span studies on the induction of lung tumors in rats after inhalation of plutonium dioxide and previously reported intranuclear accumulation of Tp53 protein with the increase in carcinomatous lesions in lung tumors (*4*). To ensure that the *Tp53* gene mutations were related to such protein accumulation and tumor phenotypes, we further investigated in this study the molecular characterization of *Tp53* gene sequences in DNA extracted from these lung tumors.

MATERIALS AND METHODS

Animals and Experimental Design

Female Wistar rats were used in this study. Eight-week-old rats were exposed by inhalation to high-fired $^{239}PuO_2$ aerosols in a nose-only exposure chamber. The activity median aerodynamic diameter (AMAD) ranged from 0.3 to 0.5 μm in all the experiments (*4*).

Pathological Examinations

A total of 310 exposed rats were subjected to postmortem pathological examinations. Lung tissues were fixed in phosphate-buffered formalin, embedded in paraffin, and stained with hematoxylin and eosin. Two hundred thirty-three of the animals were diagnosed with primary lung tumors, and immunohistochemical staining for the intranuclear Tp53 protein was done on preparations from these tumors. Polyclonal rabbit antiserum (CM1) and monoclonal mouse IgG antibody (DO-7), specific to both mutant and wild-type human TP53 protein, were purchased from Medac Inc. (Germany) and used for immunohistochemical staining (*4*).

DNA Isolation

Tumor tissues were dissected from unstained 15-μm-thick sections under a dissecting microscope and incubated overnight at 37°C in lysate buffer consisting of 10 m*M* Tris-HCl, pH 7.5, 5 m*M* EDTA, 0.5% sodium dodecyl sulfate, and 20 μg/ml Proteinase K. The DNAs were isolated using phenol-chloroform extraction and dissolved in TE buffer (10 m*M* Tris-HCl, pH 7.5, and 1 m*M* EDTA).

PCR-SSCP Analysis

Primers flanking exons 5, 6, 7, and 8 in the rat *Tp53* gene were synthesized according to Wang *et al.* (*5*). Intronic primers paired with exonic primers were used to exclude the detection of rat *Tp53* pseudo genes. The DNA template was mixed with 20 pmol of each primer pair in 20 μl of total reaction solution containing 10 m*M* Tris-HCl, pH 8.3, 50 m*M* KCl, 2.5 m*M* $MgCl_2$, 0.2 m*M* dNTPs and 0.4 U of Amplitaq Gold DNA polymerase (Perkin-Elmer Cetus). PCR amplification was car-

TABLE 1
Sequences of *Tp53* Mutations in Pulmonary Tumors after Inhalation of Plutonium Dioxide Aerosols

Case no.	Type of tumor	Staining[a]	SSCP[b]	Nucleotide and amino acid changes
R1-1-2	Adenoma	+	Exon 6	codon 199 **C**CG(Pro) to **T**CG(Ser)
C2-2-1	Squamous cell carcinoma	±	Exon 5	codon 154 C**G**T(Arg) to C**A**T(His)
D2-2-1	Adenosquamous carcinoma	±	Exon 5	codon 140 **C**CT(Pro) to **T**CT(Ser)
P1-2-3	Adenocarcinoma	±	Exon 5	codon 171 **G**TG(Val) to **A**TG(Met) and 10th base of intron 5 **G** to **A**
K1-3-5	Adenoma	−	Exon 5	13th base of intron 5 **C** to **T**
K2-2-5	Adenocarcinoma	−	Exon 6	codon 217 CC**G**(Pro) to CC**A**(Pro)
N2-2	Adenosquamous carcinoma	−	Exon 6	codon 216 **G**TA(Val) to **A**TA(Ile)
P1-3-4	Adenocarcinoma	−	Exon 6	codon 195 **G**TG(Val) to **A**TG(Met) and codon 219 GA**G**(Glu) to GA**A**(Glu)
P1-4-3	Adenocarcinoma	−	Exon 6	codon 219 **G**AG(Glu) to **A**AG(Lys)
Q1-4-4	Adenoma	−	Exon 6	codon 206 **G**AC(Val) to **A**AC(Asn) and codon 219 GA**G**(Glu) to GA**A**(Glu)
R1-3-3	Adenocarcinoma	−	Exon 6	codon 201 **G**CT(Ala) to **A**CT(Thr) and codon 216 **G**TA(Val) to **A**TA(Ile)

[a] Immunohistochemical grades of intranuclear Tp53 proteins: −; negative ±; slightly positive, +; positive.
[b] PCR products from the exons were investigated and indicated abnormalities in the SSCP analysis.

ried out in an automated thermal cycler for 35–60 cycles that consisted of denaturation at 95°C for 1 min, annealing at 55 to 62°C for 1 min, and extension at 72°C for 1 min. The PCR products were electrophoresed in 2% agarose gels to check optimal amplifications. Each of these products was reamplified using forward primers labeled at the 5′-ends with [γ-^{32}P]ATP-labeled and unlabeled reverse primers. The labeled products were loaded onto Mutation Detection Enhancement gels (FMC Bio-Products), and the gels were subjected to autoradiography with X-ray film for detection of potential mutations.

Direct DNA Sequencing

The PCR products showing abnormalities in SSCP analysis were purified using glass powder and were then subjected to DNA sequence analysis using an Applied Biosystems Model 377 DNA Sequencing System.

RESULTS AND DISCUSSION

PCR amplifications were performed for 88 of the 231 cases diagnosed as primary lung tumors, and in 82 cases either all or some of the exons were effectively amplified. Aberrations indicating the candidates for certain mutations in the SSCP analysis were detected from 23 cases among 82 tumors: 3 of 10 adenomas, 9 of 24 adenocarcinomas, 7 of 35 adenosquamous carcinomas, and 4 of 13 squamous cell carcinomas. It has been shown that *TP53* mutations occur in 56% of human lung tumors and that the *TP53* pathway could be related to tumorigenesis in human lungs (*1*). In the present study, mutations of the *Tp53* gene detected by SSCP analysis were found in 28% (23 of 82 cases), a relatively higher frequency compared to other studies (*3*), suggesting that the mutations of *Tp53* may play a role in the development of lung tumors in rats after inhalation of plutonium dioxide. Although it remains unclear how irradiation with α particles from plutonium causes mutations in the *Tp53* gene, it has been reported that radiation-induced genomic instability occurs after exposure to either high- or low-linear energy transfer (LET) radiations (*6, 7*). The instability is the first cellular event in the multistep carcinogenesis induced by radiation, leading to mutations of genes at risk for cancer (*8*). While normal Tp53 protein suppresses cell proliferation and tumor growth to permit apoptosis in cells exposed to DNA-damaging agents including ionizing radiation (*9*), mutated Tp53 proteins lose those abilities, and this may result in the development of tumor cells.

Only 11 mutants were confirmed in 23 cases by direct sequencing; the mutations are summarized in Table 1. The table also shows that the mutations were detected in both benign and malignant tumor types despite the degree of immunohistochemical staining. Although two different mutations were coincidentally found in the same PCR product from four cases (P1-2-3, P1-3-4, Q1-4-4 and R1-3-3), it is unclear whether the cases include multiple clones or dual mutations in the same clone. Mutation in the intron (P1-2-3 and K1-3-5) may cause an alternative splicing of mRNA. All mutations detected in the present study were distributed from exon 5 (codons 140, 154 and 171) to exon 6 (codons 195, 199, 201, 206, 216, 217 and 219) and only the G to A transition was found in the mutations, except for three cases of cytosine (C) to thymine (T) transition (G to A on the opposite strand). In the remaining 12 cases, no mutation could be detected by direct sequencing analysis. Although the reasons for this are not clear, normal signals from wild-type DNA might overwhelm the effect of the mutation, or in fact no mutation may be present. Further analysis, such as subcloning of the PCR products, is required for confirmation of this possibility.

In conclusion, these results indicate that *Tp53* gene mutations could occur in lung tumors in rats induced by plutonium dioxide, despite the variable accumulation of Tp53 nuclear protein and the tumor phenotype, and that the G to A transition could be a common point mutation.

REFERENCES

1. M. Hollstein, D. Sidransky, B. Vogelstein and C. C. Harris, *p53* mutations in human cancers. *Science* **253**, 49–53 (1991).
2. K. H. Vähäkangas, J. M. Samet, R. A. Metcalf, J. A. Welsh, W. P. Bennett, D. P. Lane and C. C. Harris, Mutation of *p53* and *ras* genes in radon-associated lung cancer from uranium miners. *Lancet* **339**, 576–579 (1992).

3. G. Kelly, B. L. Stegelmeier and F. F. Hahn, *p53* alterations in plutonium-induced F344 rat lung tumors. *Radiat. Res.* **142**, 263–269 (1995).
4. Y. Oghiso, Y. Yamada, H. Iida and J. Inaba, Differential dose responses of pulmonary tumor types in the rat after inhalation of plutonium dioxide aerosols. *J. Radiat. Res.* **39**, 61–72 (1998).
5. D. Wang, L. You, J. Sneddon, S-J. Cheng, R. Jamasbi and G. D. Stoner, Frameshift mutation in codon 176 of the *p53* gene in rat esophageal epithelial cells transformed by benzo[a]pyrene dihydrodiol. *Mol. Carcinogen.* **14**, 84–93 (1995).
6. M. A. Kadhim, S. A. Lorimore, K. M. Townsend, D. T. Goodhead, V. J. Buckle and E. G. Wright, Radiation-induced genomic instability: Delayed cytogenetic aberrations and apoptosis in primary human bone marrow cells. *Int. J. Radiat. Biol.* **67**, 287–293 (1995).
7. J. B. Little, H. Nagasawa, T. Pfenning and H. Vetrovs, Radiation-induced genomic instability: Delayed mutagenic and cytogenetic effects of X rays and alpha particles. *Radiat. Res.* **148**, 299–307 (1997).
8. S. Selvanayagam, C. M. Davis, M. N. Cornforth and R. L. Ullrich, Latent expression of *p53* mutations and radiation-induced mammary cancer. *Cancer Res.* **55**, 3310–3317 (1995).
9. S. W. Lowe, E. M. Shmitt, S. W. Smith, B. A. Osborne and T. Jacks, *p53* is required for radiation-induced apoptosis in mouse thymocytes. *Nature* **362**, 847–848 (1993).

RADIATION RESEARCH 154, 253–260 (2000)
0033-7587/00 $5.00

Pathogenetic Process of Lung Tumors Induced by Inhalation Exposures of Rats to Plutonium Dioxide Aerosols

Y. Oghiso[1] and Y. Yamada

Division of Radiotoxicology and Protection, National Institute of Radiological Sciences, Chiba 263-8555, Japan

Oghiso, Y. and Yamada, Y. Pathogenetic Process of Lung Tumors Induced by Inhalation Exposures of Rats to Plutonium Dioxide Aerosols. *Radiat. Res.* 154, 253–260 (2000).

Sequential examinations were done on the pulmonary cytokinetics and pulmonary lesions in rats after inhalation exposure to $^{239}PuO_2$ aerosols to investigate the pathogenesis of lung tumors. Total cell yields of lavaged bronchoalveolar cells as well as the estimated numbers of pulmonary alveolar macrophages were significantly reduced from 1 to 3 months after exposure but recovered thereafter to the control levels. The proportions of multinucleated or micronucleated pulmonary alveolar macrophages increased significantly in lavaged cells from 1 month, and the increase was sustained up to 18 months after exposure. Both tumor necrosis factor and nitric oxide were shown to be differentially released from stimulated cultures of pulmonary alveolar macrophages during the period from 6 to 18 months after exposure. The labeling indices of alveolar and bronchiolar epithelial cells treated with 5-bromo-2′-deoxyuridine increased significantly in lungs from 3 months and were sustained up to 18 months after exposure. Histopathological examinations revealed that after the early inflammation, hyperplasia and metaplasia of the lining of the bronchioloalveolar epithelium were predominant from 3 to 6 months, while adenomatous or adenocarcinomatous lesions appeared and developed from 12 months after exposure. The appearance of primary lung tumors, almost all of which were adenomas and adenocarcinomas, was found in the dose range of 1 to 2 Gy from 12 months after exposures. These results indicate that the pathogenetic process initiated by early cellular damage and alterations associated with inflammation is followed by the proliferative and metaplastic lesions of pulmonary epithelium, leading to the appearance and development of pulmonary neoplasms from 1 year after the inhalation exposures in rats that received a minimum lung dose of more than 1 Gy. © 2000 by Radiation Research Society

INTRODUCTION

The cancer risks of inhaled plutonium compounds in nuclear facilities or in public environments can be derived only from animal studies because of the uncertainties in the epidemiological evidence for humans. Lung cancer risks evaluated from extensive life-span studies (*1, 2*) in beagle dogs have been determined after exposure to different isotopic and physicochemical forms of $^{238}PuO_2$, $^{239}PuO_2$ and $^{239}Pu(NO_3)_4$, and the results suggest that the differences in solubility, intrapulmonary deposition and retention, α-particle dose rate, and specific activity of inhaled aerosols affect pulmonary carcinogenesis. The highest level of pulmonary carcinogenicity of inhaled, insoluble $^{239}PuO_2$ aerosols has been shown in rats in several life-span studies including ours (*3–5*). Remarkable differences have been noted, however, when those data are compared, particularly in relationships between the dose and lung tumors; the lowest dose ranges for significant induction of lung tumors varied from 0.01 to 1 Gy, and those for the maximum incidences of tumors varied from 6 to 30 Gy. The histopathological phenotypes of lung tumors were differentially induced in rats that received lower and higher lung doses; adenomas and adenocarcinomas were observed more frequently in the relatively lower dose ranges, whereas adenosquamous and squamous cell carcinomas were predominant at higher doses. While such differences could result from pulmonary deposition, α-particle dose distribution, and dose rates due to the particle size distribution of inhaled aerosols (*6*), and from the susceptibility of target epithelial cells to carcinogenic responses, the exact dose ranges and latent periods for the induction and development of various lung tumor types remain unclear. In addition, the overall pathogenetic processes leading to pulmonary carcinogenesis after inhalation exposures to $^{239}PuO_2$ have not been fully elucidated even in some animal models that have shown early proliferation of pulmonary epithelial cells (*7*) or histogenesis from the early to middle stages (*8*).

In the present study, we focused on the cellular events and pathological consequences leading to the appearance and development of primary lung tumors in rats from the early to late period after inhalation of $^{239}PuO_2$ aerosols to investigate morphological changes including (1) nuclear aberrations of pulmonary alveolar macrophages (PAM) as primary target cells for phagocytosis and clearance of inhaled particles (*9–12*), (2) functional capacities of PAM to release inflammatory and cytocidal mediators or cytokines such as

[1] Author to whom correspondence should be addressed at Division of Radiotoxicology & Protection, National Institute of Radiological Sciences, 9-1, 4-chome, Anagawa, Inage-ku, Chiba 263-8555, Japan.

nitric oxide (NO) and tumor necrosis factor (TNF) in response to biological response modifiers (*13, 14*), (3) DNA synthesis in both alveolar and bronchiolar epithelial cells as the most important target cells for a carcinogenic response to α particles, (4) pulmonary lesions and histogenesis from the initial inflammatory process to middle preneoplastic and late neoplastic stages, and (5) the minimum dose and period required for induction of primary lung tumors. The results are discussed in relation to those obtained using different experimental models and systems with particular reference to the pathogenesis and mechanisms of α-particle-specific pulmonary carcinogenesis.

MATERIALS AND METHODS

Animals

A total of 150 8-week-old female Wistar strain rats were obtained from the breeding colony of the National Institute of Radiological Sciences and were housed 5 per polycarbonate cage and kept under barrier-filtered air conditions with a γ-ray-sterilized commercial diet (Funabashi Farm Co.) and water *ad libitum*. The animal rooms were maintained on a 12-h light:dark cycle at 23 ± 1.0°C with a humidity of 55 ± 5.0%. After inhalation exposures, all the exposed animals were kept under the same conditions as described above in a closed hood rack for radiation safety during their lifetimes until they were killed humanely or died. The animal care including weekly change of cages and daily check of the animals' condition and all the experimental treatments were performed with the approval of the institution's animal use committee.

Generation of Aerosols and Inhalation Exposures

As described previously (*5*), plutonium hydroxide solution prepared from a stock nitrate solution was nebulized in a compressed air-driven nebulizer, passed through a tube heated at 300°C to dry the droplets in the air, and then conducted into a high-temperature furnace heated at 1150°C. An air flow containing high-fired $^{239}PuO_2$ aerosols was introduced through a negative pressure by an exhaust air pump into a multiport inhalation chamber device. The aerosol size determined by a 10-stage cascade impactor during the exposures was an activity median aerodynamic diameter (AMAD) of 0.40 ± 0.005 μm and a geometric standard deviation (GSD) of 2.2 ± 0.1. Inhalation exposures were performed a total of five times. For each experiment, 20 rats (95 days old) were each placed into a plastic holder for a nose-only exposure and exposed once for 30 min to high-fired $^{239}PuO_2$ aerosols. Age-matched but unexposed rats were used for the controls.

Dosimetry

As described previously (*15*), the initial lung deposition (ILD) of each exposed animal was determined by whole-body counting of the low-energy L-shell X ray of 17 keV emitted from ^{239}Pu, and the cumulative α-particle dose absorbed in the whole lung at the time of death was calculated using the retention function obtained by a follow-up whole-body counting up to 500 days after inhalation exposure by calculations based on the time integral of the ILD and the retention function as described previously (*5*). The ILD of a total of 100 exposed animals varied from 168 to 558 Bq (mean ± SD: 351 ± 107 Bq). The average lung doses were estimated to be 2 to 3 Gy at 400 days after exposure. These levels were expected to result in approximately 60% lung tumor incidence during the period of 1 to 2 years after exposure, based on previous data on the dose responses and appearance of lung tumors (*5*).

Experimental Design

Groups of animals consisting of 10 or 20 exposed animals and 5 controls each were randomly killed humanely by chloroform anesthesia at 1, 3, 6, 12 and 18 months after exposure for cytological and histopathological examinations, and 9 exposed animals were killed at 24 months for histopathology, so that a total of 79 exposed and 25 control animals were killed for sequential examinations. The remaining 21 exposed rats died spontaneously 155 to 795 days after exposure and were examined only for the histopathology of lung tumors.

Assays for Cytokinetics of Lavaged Lung Cells and PAM

Bronchoalveolar lavage was performed three times with Ca^{++}- and Mg^{++}-free phosphate-buffered saline (PBS; pH 6.8–7.0) to obtain free lung cells from six exposed and three control animals at each time from 1 to 18 months after exposure as described previously (*16*). The total cell yields were enumerated using a Coulter counter (Coulter Electronics), and the proportions of cellular constituents and multinucleated or micronucleated PAM as indicators for nuclear aberrations as determined previously (*9–12*) were evaluated by counting a minimum of 2,000 cells in cytocentrifuged cell preparations stained with May Grünwald-Giemsa by light microscopy.

Assays for Tnf and NO Released from Cultures of PAM

The lavaged, free lung cells were washed twice and resuspended in RPMI 1640 medium (Flow Laboratories) supplemented with 10% fetal bovine serum (FBS; GIBCO), 100 U/ml penicillin, and 100 μg/ml streptomycin. Cells at a concentration of 2–2.5 × 10^5 cells/ml were placed into 24-well flat-bottom culture plates (Falcon 3047; Becton Dickinson Labware) in 1 ml of FBS-supplemented medium, incubated for 2 h to allow complete adherence of PAM, and then washed gently and resuspended in 1 ml of FBS-supplemented medium. The cultures containing 95% or more of viable and adherent PAM were then incubated in the absence or presence of 100 ng/ml of lipopolysaccharides (LPS, 055:B5; Difco Laboratories) and/or 100 U/ml of recombinant murine interferon gamma (Ifng; Genzyme Corp.) for either 6 or 24 h to harvest cell-free supernatants for assays of Tnf and NO activities by a modification of methods described elsewhere (*17, 18*). Briefly, for Tnf assays, serially diluted supernatants harvested from 6-h cultures were added to the cultures of Tnf-sensitive L-929 cells with 1 μg/ml of actinomycin D (Sigma) in 96-well flat-bottom microculture plates (Falcon 3072) and incubated for 18 h. After they were washed extensively with PBS, microculture plates were stained with 0.2% crystal violet solution, dried and redissolved in 0.5% sodium dodecyl sulfate (SDS), and the absorbance was analyzed using a microplate reader (MTP-32; Corona Electric Co.) at 550 nm with a reference wavelength of 690 nm to determine half-maximum cytotoxicity compared to that of recombinant Tnf (Asahi Chemical Industry Co.). For NO assays, the supernatants harvested from 24-h cultures were incubated for 10 min with an equal volume of Griess reagent (*18*) in 96-well flat bottom microculture plates (Falcon 3072), and the absorbance was analyzed using a microplate reader (MTP-32) at 550 nm with a reference wavelength of 690 nm to determine the concentration of nitrite (NO_2^-) by a standard curve of sodium nitrite solution.

Assays for Proliferation of Pulmonary Epithelial Cells

To detect cell proliferation of the lining of the pulmonary epithelium, immunohistochemistry of 5-bromo-2′-deoxyuridine (BrdU) incorporated into DNA as an analogue for [^{3}H]dThd was performed on histological sections of lungs by a modification of a method described elsewhere (*7*). Briefly, three exposed and two control animals at each time from 1 to 18 months after exposure were injected intraperitoneally with 0.5 ml per rat of 100 mg/ml BrdU (Sigma) and were killed humanely 3 h later. After perfusion with PBS and fixation of whole lung tissues in 70% ethanol, several tissue blocks from each lung lobe were processed by dehydration with graded ethanol and clearing with xylene and embedded in paraffin.

TABLE 1
Total Numbers and Proportions of Lung Cells from Rats after Exposure to $^{239}PuO_2$ Aerosols

Group of animals	Months after exposure	No. of rats examined	Estimated lung dose (Gy)	No. of cells recovered ($\times 10^{-6}$)[a]	Percentage of cells[b]		
					PAM	PMN	MN
Control	1–18	15	0	5.1 ± 1.9	95.7 ± 2.1	1.7 ± 0.8	2.3 ± 1.1
Exposed	1	6	0.30 ± 0.08	1.7 ± 0.8*	91.8 ± 1.5	5.2 ± 1.8*	3.0 ± 1.4
	3	6	1.14 ± 0.23	2.5 ± 1.2*	93.6 ± 1.8	3.1 ± 1.3**	2.9 ± 1.2
	6	6	1.37 ± 0.23	5.9 ± 1.3	95.9 ± 2.3	1.9 ± 1.2	2.1 ± 1.1
	12	6	1.53 ± 0.28	5.2 ± 1.1	91.2 ± 3.6	3.8 ± 1.7*	4.4 ± 1.8**
	18	6	2.25 ± 0.63	6.0 ± 1.2	93.2 ± 2.6	2.9 ± 1.6**	3.8 ± 1.7**

Note. All values represent mean ± SD of animals examined, and asterisks indicate significant differences compared to the controls in each category (*$P < 0.01$, **$P < 0.05$).

[a] Total cell yields obtained by bronchoalveolar lavage.

[b] The percentage of pulmonary alveolar macrophages (PAM), polymorphonuclear leukocytes (PMN), and mononuclear leukocytes (MN) in lavaged bronchoalveolar cells.

The 5-μm-thick deparaffinized sections were treated with 3% H_2O_2 in methanol for 30 min to block endogenous peroxidase activity and incubated for 30 min in 1 N HCl to denature DNA, followed by treatment with 0.1% trypsin (Sigma) for 10 min. After this treatment, immunohistochemical staining was carried out by blocking with normal horse serum, incubating with 1:500 dilution of anti-BrdU antibody (BU-33; Sigma) for 2 h, and coupling bound antibody to biotinylated anti-mouse IgG for 1 h and subsequently with avidin-biotin-peroxidase complex reagents (ABC; Vector Laboratories) for 30 min, followed by visualization with a substrate, 3,3′-diaminobenzidine (DAB; Sigma) plus nickel ions for 5 min and by counterstaining of the cytoplasm with eosin. For quantification of DNA synthesis in epithelial cells in the non-neoplastic areas, the numbers of BrdU-labeled alveolar or bronchiolar lining cells were counted in 20 randomly selected high-power (400×) fields for each section viewed by light microscopy. After they were stained with hematoxylin, the same microscopic fields were found to contain an average of 1000–2000 alveolar cells and 800–1200 bronchiolar cells, respectively. The labeling indices were expressed as the mean percentage of BrdU-labeled cells in the total cells counted in each lung section.

Histopathology of Pulmonary Lesions and Neoplasms

The lung tissues from all the animals that were killed or died after exposure, including the specimens used for bronchoalveolar lavage and immunohistochemistry, were fixed in 10% phosphate-buffered formalin, dehydrated with graded ethanol, cleared with xylene, and embedded in paraffin. The 5-μm-thick serial sections prepared from each lobe were stained with hematoxylin and eosin (H&E) and examined histopathologically for pulmonary inflammation or fibrosis and preneoplastic and neoplastic lesions using light microscopy. Using the diagnostic criteria described previously (*5*), primary lung tumors after inhalation exposures to $^{239}PuO_2$ aerosols were classified mainly into the following epithelial types: ductal or papillary adenomas, papillary or solid adenocarcinomas, solid and nonkeratinized adenosquamous carcinomas, keratinized and epidermoid squamous cell carcinomas, and nonepithelial types such as fibrosarcomas and hemangiosarcomas. The nonepithelial types occurred at a much lower frequency.

Statistics

The data on the cytokinetics of PAM and the activities of releasing NO and Tnf and proliferation of pulmonary epithelial cells in each period were expressed as the mean ± SD of those obtained from each group of control and exposed animals, and the significant differences between the control and the exposed groups were compared by the unpaired Student's *t* test.

RESULTS

Cytokinetics of Lavaged Lung Cells and PAM

Table 1 shows total cell numbers and proportions of free lung cell populations obtained by bronchoalveolar lavage from control and exposed animals at each time after exposure. The numbers of cells recovered, although not reflecting the absolute numbers of lung cells, were significantly reduced from 1 to 3 months after exposure but increased again up to the level of the controls. Since most constituents of the lavaged lung cell populations were PAM, and their proportions in exposed animals were similar to that in the controls, the estimated numbers of PAM recovered were reduced during the early periods after exposure. Among the remaining cell constituents, the proportions of polymorphonuclear leukocytes (PMN), mainly neutrophils, were smaller but increased significantly from 1 to 3 months after exposure, while those of mononuclear leukocytes, mainly lymphocytes, increased significantly, as did the PMN, during the late period from 12 to 18 months after exposure. These findings indicate that the cellular events involve a transient reduction of PAM and inflammatory exudation of peripheral blood leukocytes in the lung from the early to the late period after exposure to $^{239}PuO_2$.

The nuclear aberrations in the PAM that were recovered were also noted after exposure. As shown in Fig. 1, the proportions of both multinucleated (mostly with 2–3 nuclei) and micronucleated PAM were significantly elevated from 1 to 6 months and then declined but remained significantly higher for up to 18 months after exposures compared to the controls. The other prominent morphological changes in the PAM were the variable size of cytoplasm, ranging from approximately 0.5 to 2.5 times the diameter of normal cells, and the appearance of large and foamy PAM from the early to late period after exposure (data not shown). These findings indicate that cellular damage and alterations of PAM persisted in the lung after exposure to $^{239}PuO_2$.

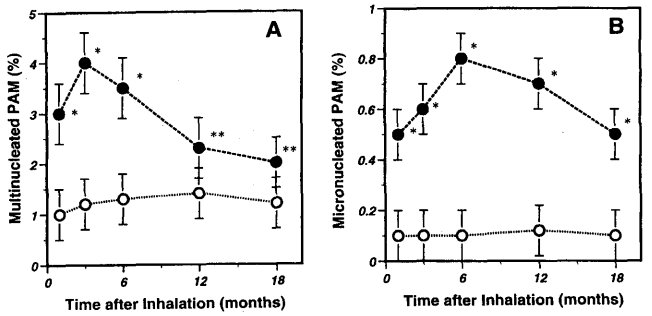

FIG. 1. Nuclear alterations of pulmonary alveolar macrophages (PAM) from rats after inhalation exposure to $^{239}PuO_2$ aerosols. Values with bars indicate mean ± SD of the proportions of multinucleated PAM (panel A) and micronucleated PAM (panel B) in lavaged bronchoalveolar cells from three control (open circles) and six exposed (closed circles) animals at each time. Asterisks indicate the significant differences in exposed animals compared to the controls at each time (*$P < 0.01$, **$P < 0.05$).

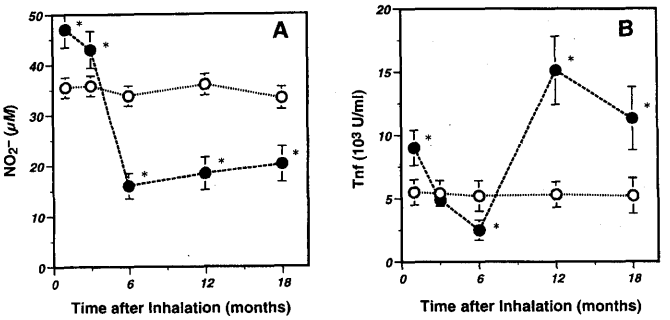

FIG. 2. Activities of nitric oxide (NO) and tumor necrosis factor (Tnf) released from both Ifng- and LPS-stimulated cultures of PAM in rats after inhalation exposure to $^{239}PuO_2$ aerosols. Values with bars indicate mean ± SD of NO (panel A) and Tnf (panel B) activities in the culture supernatants of PAM from three control (open circles) and six exposed (closed circles) animals at each time. Asterisks indicate the significant differences in exposed animals compared to the controls at each time (*$P < 0.01$).

Release of NO and Tnf from PAM

The functional capacity of rat PAM to release both macrophage-specific products, NO and Tnf, is dependent on stimulation in culture; the NO activity is induced by Ifng and is enhanced by the combination of Ifng and LPS, while Tnf activity is induced only by LPS and is enhanced by the combination of Ifng and LPS. The activities of NO and Tnf in the cultures of PAM in the absence or presence of Ifng were not significantly different in the control and exposed animals at each time after exposure to $^{239}PuO_2$ (data not shown). Based on these findings, we compared both activities in the cultures of PAM stimulated with the combination of Ifng and LPS in control and exposed animals as shown in Fig. 2. The NO activity was significantly higher from 1 to 3 months, but lower from 6 to 18 months after exposure compared to the levels in the controls (Fig. 2A), while the Tnf activity was significantly higher at 1 month, declined from 3 to 6 months, and was again significantly elevated from 12 to 18 months after exposure compared to the levels in the controls (Fig. 2B). These findings indicate that there are differences in the functional capacity of stimulated PAM to release either NO or Tnf during the middle to late period after exposure to $^{239}PuO_2$.

Proliferation Kinetics of Pulmonary Epithelium

The DNA synthesis of alveolar or bronchiolar epithelial cells was scarcely detectable by BrdU labeling in the lung tissue from the control rats killed at each time. The BrdU-labeling indices of both alveolar and bronchiolar cells, however, increased significantly in non-neoplastic areas of the lungs of exposed rats from 3 to 6 months; thereafter, the levels declined but remained elevated up to 18 months after exposure compared to the controls (Fig. 3). The percentages of BrdU-labeled alveolar cells were almost 1.5 times higher than those of bronchiolar cells. These findings indicate the relatively early and persistent proliferation of pulmonary epithelial cells in the lung after exposure to $^{239}PuO_2$.

Kinetics of Pulmonary Lesions and Appearance of Neoplastic Lesions

The lungs of all the control animals killed at each time showed few or no obvious histopathological lesions except for a slight to moderate hyperplasia of peribronchial lymphoid tissues. No primary lung tumors were observed in the control animals. The results of histopathological examinations of the lungs from exposed animals are summarized in Table 2. The inflammatory lesions, characterized mainly by infiltration of neutrophils and accumulation of foamy macrophages in the bronchiolar lumen and alveolar sacs, were prominently observed in most animals from 1 to 3 months, but decreased rapidly from 6 months after exposure. The fibrotic lesions involving particularly the subpleural alveolar walls or peribronchiolar connective tissues appeared prominently from 3 months and increased up to 18 months after exposure. Fibrotic areas were also frequently accompanied by infiltration of lymphocytes. Correlating with this fibrosis, hyperplastic and metaplastic lesions of

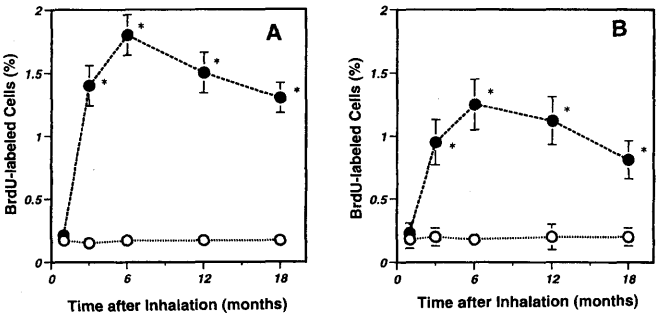

FIG. 3. DNA synthesis in pulmonary epithelial cells in the lungs from rats after exposure to $^{239}PuO_2$ aerosols. Values with bars indicate mean ± SD of the percentages of BrdU-labeled alveolar (panel A) and bronchiolar (panel B) epithelial cells in the lungs from three control (open circles) and six exposed (closed circles) animals at each time. Asterisks indicate the significant differences in exposed animals compared to the controls at each time (*$P < 0.01$).

TABLE 2
Appearance and Kinetics of Pulmonary Lesions and Neoplasms in Rats after Exposure to $^{239}PuO_2$ Aerosols

Months after exposure	Number of rats examined	Number of rats with pulmonary lesions (%)[a]					
		Inflammation	Fibrosis	Hyperplasia and metaplasia	Adenoma	Adenocarcinoma	Squamous carcinoma
1	10	8 (80)	0 (0)	0 (0)	0 (0)	0 (0)	0 (0)
3	10	5 (50)	2 (20)	3 (30)	0 (0)	0 (0)	0 (0)
6	20	3 (15)	8 (40)	12 (60)	0 (0)	0 (0)	0 (0)
12	20	2 (10)	18 (90)	18 (90)	12 (60)	3 (15)	0 (0)
18	10	1 (10)	9 (90)	9 (90)	9 (90)	9 (90)	0 (0)
24	9	1 (11)	6 (67)	8 (89)	8 (89)	9 (100)	1 (11)

[a] Number of rats with each pulmonary lesion/number of rats examined × 100 at each time after exposure.

the alveolar, bronchiolar and bronchial epithelium were observed and increased from 3 to 24 months after exposure. Neoplastic lesions were not found in the lungs of exposed animals until 12 months, when adenomatous and adenocarcinomatous lesions were first noted in alveolar and bronchiolar regions, and increased up to 24 months after exposure. Squamous or adenosquamous lesions were observed in only one rat killed 24 months after exposure. These findings indicate the sequential histokinetics of pulmonary lesions that are initiated by inflammatory and degenerative changes of bronchioloalveolar regions in the early stage, followed by regenerative, hyperplastic and metaplastic renewal of the lining epithelium associated with fibrosis in the middle to late stages, and eventually leading to the appearance and development of neoplasms in the late stages after exposure to $^{239}PuO_2$.

Relationship of Dose and Time to Induction of Lung Tumors

Primary lung tumors were found in 47 exposed animals, while only metaplasias were found in 25 exposed animals, among the 100 animals that were killed or died after exposure. The numbers of histological types among 47 tumors were 18 adenomas, 26 adenocarcinomas, and 3 adenosquamous or squamous cell carcinomas. Nonepithelial tumors such as fibrosarcomas and hemangiosarcomas were not observed. The relationships of estimated lung doses and observation periods to the occurrence of primary lung tumors are shown in Fig. 4. The numbers of animals bearing adenomas appeared after doses less than 1.0 Gy and increased from 1.0 to 2.0 Gy, while adenocarcinoma-bearing animals appeared after doses of 1.0 to 2.0 Gy and increased up to the maximum from 2.0 to 3.0 Gy (Fig. 4A). No primary lung tumors were found until 300 days after exposure. Adenomas and adenocarcinomas appeared at 300 to 400 days and increased thereafter up to 600 to 800 days after exposure (Fig. 4B). Squamous cell carcinomas, including adenosquamous carcinomas, were found only in the dose range of 3.0 to 4.0 Gy, and from 600 to 800 days after exposure. These findings indicate that primary lung tumors, mostly adenomas and adenocarcinomas, are induced at a minimum dose of 1.0 Gy from at least 1 year after exposure to $^{239}PuO_2$.

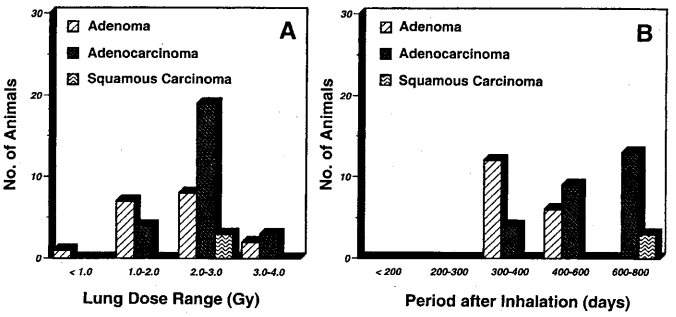

FIG. 4. Relationship between lung dose and time to the occurrence of primary lung tumors in rats after inhalation exposure to $^{239}PuO_2$ aerosols. The columns indicate the numbers of killed and dead animals bearing each type of tumors (adenomas, adenocarcinomas and squamous cell carcinomas) as a function of the estimated lung dose range (panel A) and the observation period (panel B) after exposure.

DISCUSSION

The present study was undertaken to investigate the cellular kinetics of pulmonary alveolar macrophages (PAM) and the lining epithelial cells and the histopathological consequences in the lungs from rats after inhalation exposure to submicrometer-size, polydispersed aerosols of high-fired $^{239}PuO_2$ with an initial lung deposition (ILD) of 351 ± 107 Bq. Primary lung tumors were induced in almost 50% of both the animals that were killed and dead animals that had received lung doses of more than 1.0 Gy during the period from 1 to 2 years after exposure. The experimental regimens are different from those of other studies of cytokinetics in mice exposed to 500 Bq of polydispersed 1.7-μm-size aerosols (*7*) and of sequential pathology in rats exposed to 3.7 kBq of polydispersed 1.2-μm-size aerosols (*8*) of $^{239}PuO_2$. However, similar trends in the cellular responses and pathological features were noted in our rat model compared to those results except for the periods observed.

With regard to the cytokinetics of PAM as an important target cell in terms of the initial phagocytosis and clearance of intrapulmonary deposited particles, a conspicuous and significant reduction of total cell yields of lavaged bron-

choalveolar cells as well as the estimated numbers of PAM recovered was noted in the early period from 1 to 3 months after exposure. Since the self-renewal of PAM themselves has been recognized in several mouse models to be independent of depleted hematopoietic precursors and circulating blood monocytes (*19, 20*), but to be affected by instilled fibrogenic dusts (*21*), the early reduction of PAM could result from a decrease in the absolute pool of PAM populations due to radiation-induced cell death or an inability to synthesize DNA as described in mice after exposure to $^{239}PuO_2$ (*22*). The increase in PAM populations up to the control levels in the middle to late period after exposure might have resulted from either the recovery of the self-renewal capacity of PAM or local exudation and proliferation of circulating blood monocytes as shown in mouse peritoneal macrophages as a result of inflammation (*23*). Such population renewal of PAM might affect their overall capacities to release macrophage-specific products after stimulation with Ifng and LPS. Both NO and Tnf released from the stimulated PAM increased in the early period after exposure, suggesting the activation of surviving PAM populations in the early inflammatory stage, while in contrast, a persistent depression of NO activity and a temporary depression followed by an increase in Tnf activity in the middle to late stages might reflect the functional diversity among PAM subpopulations as a result of their renewal. Since the significance of the production of NO and Tnf by macrophages has been focused on bactericidal or tumoricidal mechanisms in both *in vitro* and *in vivo* models (*24–28*), PAM, through either NO- or Tnf-dependent mechanisms, may act against progression of pulmonary carcinogenesis in the middle to late periods after exposure to $^{239}PuO_2$. In this regard, since there is no direct evidence of a relationship between tumor growth and tumoricidal activities, the activities of both NO and Tnf could be relevant to PAM-associated inflammatory responses in either the early or late period after exposure to $^{239}PuO_2$. In addition to changes in populations and function, PAM from exposed animals showed nuclear aberrations and cytoplasmic alterations from the early to late period after exposure, suggesting persistent radiation-induced damage and alterations of PAM associated with their own cell division mechanisms after phagocytosis of inhaled radiotoxic particles, as described elsewhere (*10–12*). The appearance of such damaged or altered PAM would reflect inflammatory events but is not likely to be related directly to pulmonary carcinogenesis.

Concerning the proliferative kinetics of pulmonary lining epithelial cells as the most susceptible target cells for carcinogenesis, both alveolar and bronchiolar epithelial cells showed significant DNA synthesis from the relatively early to late period after exposure. Interestingly, the level of DNA synthesis of alveolar cells was almost 1.5-fold higher than that of bronchiolar cells. Concomitantly, the hyperplasia and metaplasia were histopathologically localized in the bronchioloalveolar epithelium of the lungs from the exposed animals. These results, taken together, indicate the significance of type II pneumocytes as one of the most susceptible target cells at risk for pulmonary carcinogenesis as described (*7, 8*) and suggest that proliferation of pulmonary epithelial cells after initial damage could be related to preneoplastic sequela after inhalation exposure to $^{239}PuO_2$.

Histopathology of the lungs from exposed animals also revealed time-dependent sequences of pulmonary lesions related to pulmonary cytokinetics as mentioned above, and a latent period for the appearance and development of neoplasms. In the early period from 1 to 3 months, inflammatory lesions characterized by exudation of neutrophils and accumulation of foamy PAM in subpleural or bronchioloalveolar regions were predominant. After the reduction of pulmonary inflammation, pulmonary fibrosis with lymphocytic infiltration was prominent, and hyperplasia and metaplasia of bronchioloalveolar lining epithelium were apparent concomitantly from 3 months after exposure. Such histological kinetics of pulmonary lesions leading to preneoplastic growth of epithelial cells is similar to the cell kinetics of PAM and pulmonary epithelial cells, and both pulmonary fibrosis and epithelial hyperplasia and metaplasia should be important processes for the initiation of plutonium-induced pulmonary carcinogenesis, as suggested by previous studies (*8, 29, 30*). After the cessation of inflammation and successive initiation of preneoplastic lesions, neoplastic lesions with mostly adenomatous and adenocarcinomatous features appeared from 12 months and developed up to 24 months. These results are similar to those of others (*8*), except that few adenosquamous or squamous lesions were found in our experiments. It should be noted that the latent period for the onset of pulmonary neoplasms would be estimated to be approximately 1 year after exposure, the period during which target bronchioloalveolar epithelial cells would be regenerated from radiation-induced injury to be successively mutated and finally transformed into specified phenotypes of adenomas and adenocarcinomas. The molecular mechanisms underlying the processes of pulmonary carcinogenesis, however, have not been fully elucidated despite some evidence of the relevance of mutation frequencies of the *Kras* proto-oncogene (*31*) but not of the *Tp53* tumor suppressor gene (*32*) to carcinogenesis.

Finally, concerning the estimated lung doses and the time required for the induction of primary lung tumors, the evaluation of 47 tumors from 100 exposed animals revealed that adenomas were found after doses of more than 1.0 Gy, adenocarcinomas being predominant at doses more than 2.0 Gy, and that both types of tumors were found from 300 days after exposure. While a malignant differentiation of adenomas into adenocarcinomas is plausible, adenosquamous or squamous cell carcinomas were rarely found at 3.0 Gy or more and from 600 days after exposure. It is therefore suggested that pulmonary adenomas and adenocarcinomas can be induced in rats at a minimum dose of 1.0 Gy from at least 1 year after exposure. Comparing these values

with those of other studies of rats exposed to $^{239}PuO_2$, there may be a threshold dose of 1.0 Gy for induction of malignant tumors as suggested by the life-span study (*3*), and also a latent period of 308 days for the initial observation of pulmonary carcinomas as indicated by the sequential study (*8*).

In conclusion, the present study of the cytokinetics of pulmonary cells and the histogenesis of pulmonary lesions in female Wistar rats after inhalation exposures to $^{239}PuO_2$ aerosols indicates a sequential pathogenetic process leading to pulmonary carcinogenesis as follows: (a) initial damage and alterations of the PAM population including their functional capacity to release NO and Tnf, (b) successive proliferation of the pulmonary lining epithelial cells correlated with hyperplasia and metaplasia in the bronchioloalveolar regions, (c) progressive appearance and development of neoplastic lesions, and (d) final induction of primary adenomas and adenocarcinomas at doses of more than 1.0 Gy and approximately 1 year after exposure.

ACKNOWLEDGMENTS

This research was supported by a research grant from Japan Science and Technology Agency. The authors are grateful to all the laboratory staff for their technical assistance with the inhalation experiments and dosimetry, and to the technical staff of Animal Care Co. for their support of animal care.

Received: December 15, 1999; accepted: May 5, 2000

REFERENCES

1. W. J. Bair, J. F. Park, G. E. Dagle and A. C. James, Overview of biological consequences of exposure to plutonium and higher actinides. *Radiat. Prot. Dosim.* **26**, 125–135 (1989).
2. G. E. Dagle, J. F. Parks, E. S. Gilbert and R. E. Weller, Risk estimates for lung tumors from inhaled $^{239}PuO_2$, $^{238}PuO_2$, and $^{239}Pu(NO_3)_4$ in beagle dogs. *Radiat. Prot. Dosim.* **26**, 173–176 (1989).
3. C. L. Sanders, K. E. Lauhala and K. E. McDonald, Lifespan studies in rats exposed to $^{239}PuO_2$ aerosol. III. Survival and lung tumors. *Int. J. Radiat. Biol.* **64**, 417–430 (1993).
4. D. L. Lundgren, P. J. Haley, F. F. Hahn, J. H. Diel, W. C. Griffith and B. R. Scott, Pulmonary carcinogenicity of repeated inhalation exposure of rats to aerosols of $^{239}PuO_2$. *Radiat. Res.* **142**, 39–53 (1995).
5. Y. Oghiso, Y. Yamada, H. Iida and J. Inaba, Differential dose responses of pulmonary tumor types in the rat after inhalation of plutonium dioxide aerosols. *J. Radiat. Res.* **39**, 61–72 (1998).
6. ICRP, *Human Respiratory Tract Model for Radiological Protection.* Publication 66, *Annals of the ICRP*, Vol. 24, No. 1–3, Pergamon Press, Oxford, 1994.
7. A. Taya, A. Black, S. T. Baker and J. A. H. Humphreys, Proliferation of mouse lung epithelial cells after inhalation exposure to $^{239}PuO_2$. *Radiat. Res.* **136**, 366–372 (1993).
8. R. A. Herbert, N. A. Gillett, A. H. Rebar, D. L. Lundgren, M. D. Hoover, I. Y. Chang, W. W. Carlton and F. F. Hahn, Sequential analysis of the pathogenesis of plutonium-induced pulmonary neoplasms in the rat: Morphology, morphometry, and cytokinetics. *Radiat. Res.* **134**, 29–42 (1993).
9. S. R. Moores, R. J. Talbot, N. Evans and B. E. Lambert, Macrophage depletion of mouse lung following inhalation of $^{239}PuO_2$. *Radiat. Res.* **105**, 387–404 (1986).
10. R. J. Talbot, L. Nicholls, A. Morgan and S. R. Moores, Effect of inhaled α-emitting nuclides on mouse alveolar macrophages. *Radiat. Res.* **119**, 271–285 (1989).
11. A. Morgan, S. R. Moores, H. Morris, L. G. Nicholls and R. J. Talbot, Induction of nuclear aberrations in mouse alveolar macrophages following exposure to $^{239}PuO_2$. A dose–response study. *J. Radiol. Prot.* **9**, 129–135 (1989).
12. A. Morgan and J. Talbot, Effects of inhaled alpha-emitting actinides on mouse alveolar macrophages. *Environ. Health Perspect.* **97**, 177–184 (1992).
13. C. F. Nathan, Secretary products of macrophages. *J. Clin. Invest.* **79**, 319–326 (1987).
14. D. C. Morrison and J. L. Ryan, Bacterial endotoxins and host immune responses. *Adv. Immunol.* **28**, 293–450 (1979).
15. N. Ishigure, T. Nakano, H. Enomoto, S. Fukuda, H. Iida, Y. Oghiso, H. Sato, S. Takahashi, Y. Yamada and J. Inaba, Lung retention of Pu following inhalation of PuO_2 in rats measured using a whole body counter. *J. Radiat. Res.* **35**, 16–25 (1994).
16. E. Kagan, Y. Oghiso and D. P. Hartmann, The effects of chrysotile asbestos on the lower respiratory tract: analysis of bronchoalveolar lavage constituents. *Environ. Res.* **32**, 382–397 (1983).
17. M. R. Ruff and G. E. Gifford, Tumor necrosis factor. In *Lymphokines*, Vol. 2 (E. Pick, Ed.), pp. 235–272. Academic Press, New York, 1981.
18. A. H. Ding, C. F. Nathan and D. J. Stuehr, Release of reactive nitrogen intermediates and reactive oxygen intermediates from mouse peritoneal macrophages. Comparison of activating cytokines and evidence for independent production. *J. Immunol.* **141**, 2407–2412 (1988).
19. Y. Oghiso and Y. Yamada, Heterogeneity of the radiosensitivity and origins of tissue macrophage colony-forming cells. *J. Radiat. Res.* **33**, 334–341 (1992).
20. Y. Oghiso, Y. Yamada, Y. Shibata and T. Yoshida, Maintenance of radioresistant alveolar colony-forming cells in mice bearing pulmonary foreign-body inflammation after ^{89}Sr-injection. *Reg. Immunol.* **3**, 318–322 (1990–91).
21. Y. Oghiso, Y. Yamada and Y. Shibata, Effects of instilled fibrogenic particles on the clonal growth of murine pulmonary alveolar macrophages. *Environ. Health Perspect.* **97**, 159–161 (1992).
22. J. P. Kellington, K. Gibson, T. M. Buckle, R. J. Talbot and S. B. Hornby, Alveolar macrophage kinetics after inhalation of $^{239}PuO_2$ by CBA/Ca mice: Changes in synthesis of DNA. *Environ. Health Perspect.* **97**, 69–75 (1992).
23. Y. Oghiso, Y. Yamada and Y. Shibata, Exudation of proliferative macrophages in local inflammation in the peritoneum. *J. Leukoc. Biol.* **52**, 421–424 (1992).
24. L. S. Soderberg, L. W. Chang and J. B. Barnett, Enhanced TNF-α and inducible nitric oxide production by alveolar macrophages after exposure to a nitrite inhalant. *J. Leukoc. Biol.* **60**, 459–464 (1996).
25. R. Keller, S. Bassetti, R. Keist, A. Mulsch and S. Klauser, Induction of nitric oxide synthase is a necessary precondition for expression of tumor necrosis factor-independent tumoricidal activity by activated macrophages. *Biochem. Biophys. Res. Commun.* **184**, 1364–1371 (1992).
26. J. Klostergaard, M. E. Leroux and M. C. Hung, Cellular models of macrophage tumoricidal effector mechanisms *in vitro*. Characterization of cytolytic responses to tumor necrosis factor and nitric oxide pathways *in vitro*. *J. Immunol.* **147**, 2802–2808 (1991).
27. S. J. Skerrett and T. R. Martin, Roles for tumor necrosis factor α and nitric oxide in resistance of rat alveolar macrophages to Legionella pneumophilia. *Infect. Immun.* **64**, 3236–3243 (1996).
28. K. J. Pendino, J. D. Laskin, R. L. Shuler, C. J. Punjabi and D. L. Laskin, Enhanced production of nitric oxide by rat alveolar macrophages after inhalation of a pulmonary irritant is associated with increased expression of nitric oxide synthase. *J. Immunol.* **151**, 7196–7205 (1993).
29. C. L. Sanders, K. E. McDonald and J. A. Mahaffey, Lung tumor

response to inhaled Pu and its implications for radiation protection. *Health Phys.* **55**, 455–462 (1988).

30. C. L. Sanders, K. E. McDonald and K. E. Lauhala, Promotion of pulmonary carcinogenesis by plutonium particle aggregation following inhalation of $^{239}PuO_2$. *Radiat. Res.* **116**, 393–405 (1988).

31. B. L. Stegelmeier, N. A. Gillett, A. H. Rebar and G. Kelly, The molecular progression of plutonium-239-induced rat lung carcinogenesis: Ki-ras expression and activation. *Mol. Carcinogen.* **4**, 43–51 (1991).

32. G. Kelly, B. L. Stegelmeier and F. F. Hahn, p53 alterations in plutonium-induced F344 rat lung tumors. *Radiat. Res.* **142**, 263–269 (1994).

RADIATION RESEARCH 154, 447–454 (2000)
0033-7587/01 $5.00

Strain Differences in Carcinogenic and Hematopoietic Responses of Mice after Injection of Plutonium Citrate

Y. Oghiso[1] and Y. Yamada

Division of Radiotoxicology and Protection, National Institute of Radiological Sciences, Chiba 263-8555, Japan

Oghiso, Y. and Yamada, Y. Strain Differences in Carcinogenic and Hematopoietic Responses of Mice after Injection of Plutonium Citrate. *Radiat. Res.* 154, 447–454 (2000).

The carcinogenicity of injected ^{239}Pu citrate was compared in female mice of the C3H, C57BL/6 and BC3F$_1$ hybrid strains with different spectra of spontaneous or radiation-induced tumors. A significant reduction in survival due to early death caused particularly by the induction of osteosarcomas was noted in each strain after injection of 500 Bq or more. The dose response of osteosarcomas appeared to have a similar pattern in each strain except for the differences in the skeletal dose ranges for the maximum induction. While the incidence of lymphoid tumors decreased as that of osteosarcomas increased sharply to the maximum at higher doses, their histological phenotypes were predominantly non-thymic, pre-B-cell leukemic lymphomas compared to the controls in each strain. Myeloid leukemias were not highly induced in any of the control and ^{239}Pu-injected mice, and solid tumors involving the other organs were reduced in each strain after injection of 500 Bq or more. To follow up the hematological kinetics related to α-particle irradiation of bone marrow stem cells, sequential examinations were done in mice of each strain within 1 year after injection of 5000 Bq. The numbers of peripheral white blood cells and bone marrow cells were consistently reduced in each strain from 90 days on, while spleen cells increased from 180 days on. Granulocyte-macrophage and macrophage colony-forming cells were also consistently reduced in the bone marrow, with a compensatory increase in the spleen from 90 days on. These findings indicate that the carcinogenic and hematopoietic responses were specific to α-particle irradiation and were independent of mouse strain after injection with ^{239}Pu citrate. © 2000 by Radiation Research Society

INTRODUCTION

The carcinogenicity of injected ^{239}Pu and the other α-particle-emitting bone-seekers was demonstrated in early studies in animals (*1–4*) to be greater for osteogenic sarcomas but much less for hematopoietic malignancies despite the experimental evidence that α-particle irradiation of bone marrow was closely related to the long-term deposition of ^{239}Pu on endosteal bone surfaces (*5*). Other studies using mice, however, have shown that either myeloid leukemias or lymphoid tumors could be induced more efficiently than osteosarcomas by multiple injections of ^{224}Ra or ^{239}Pu for protracted α-particle doses (*7–9*). Our previous study (*10*) also showed a relatively higher frequency of leukemic lymphomas than osteosarcomas at higher doses but no myeloid leukemias in C3H female mice after injection of ^{239}Pu citrate. All of these studies raise the possibility that hematopoietic and lymphoid tumors could be derived from bone marrow progenitor cells by α-particle irradiation, although the underlying mechanisms remain unclear. In addition to such physical factors as the α-particle dose and dose rate, the susceptibility of target progenitor cells, based on the genetic background of animal species or strains, to hematopoietic derangements might also be a plausible explanation of the different responses. However, it has not been determined whether hematopoietic responses leading to malignancies after injection of ^{239}Pu could be specifically induced by α-particle irradiation of bone marrow cells, or could be modulated by the strain differences in the mice.

As a follow-up to our preliminary study (*11*), we report here more detailed results on the carcinogenic and hematopoietic responses compared in mice of the C3H, C57BL/6 and BC3F$_1$ hybrid strains after injection of ^{239}Pu. These three strains have much lower or no spontaneous occurrence of bone tumors and myeloid leukemias, while the C3H strain is characterized by a higher frequency of spontaneous hepatocellular carcinomas, and the C57BL/6 strain has a higher frequency of spontaneous or radiation-induced thymic lymphomas. The results indicate the specificity of injected ^{239}Pu citrate, independent of mouse strain, in the induction of osteosarcomas and non-thymic, pre-B-cell leukemic lymphomas but a much lower frequency of myeloid leukemias, and in the initial to mid-term kinetics of hematopoietic progenitor cells. The mechanisms of α-particle-induced leukemogenesis and/or lymphomagenesis compared to those of external radiation exposures are also discussed.

MATERIALS AND METHODS

Experimental Animals

Eight- to 10-week-old specific-pathogen-free female mice of three strains, C3H, C57BL/6 and their hybrid BC3F$_1$, were obtained from our

[1] Author to whom correspondence should be addressed at Division of Radiotoxicology and Protection, National Institute of Radiological Sciences, 9-1, 4-chome, Anagawa, Inage-ku, Chiba 263-8555, Japan.

animal breeding facility. All the animals were housed 10 per polycarbonate cage, given a commercial diet with water *ad libitum*, and kept under barrier-filtered air before and after all the experiments, which were performed with the approval of the institution's animal use committee. The animal rooms were maintained on a 12-h light:dark cycle at an air temperature of 23 ± 1.0°C and a humidity of 55 ± 5.0%. Animal care consisted of weekly exchange of clean cages and daily checks of the condition of the animals.

Experimental Design

A mixture of 10 m*M* ^{239}Pu nitrate and 100 m*M* trisodium citrate at a molecular ratio of 1:50 was titrated to pH 6.8–7.2 by addition of 1 N NaOH, diluted with physiological saline, and passed through both 0.2- and 0.025-μm-pore Millipore filters to obtain a monomeric ^{239}Pu citrate solution with a radioactivity of 10^3–10^5 Bq/ml. For life-span studies of carcinogenesis, a total of 15 groups each containing 30 to 60 on 12–14-week-old mice of each strain were injected intraperitoneally with amounts of radioactivity ranging from 100 to 5000 Bq per animal or with saline as the control and were kept in a closed-hood rack during their lifetime. For sequential studies of hematopoietic responses, 20 experimental mice as well as 10 control mice of each strain were injected i.p. with the highest amount used, 5000 Bq per animal, to induce hematopoietic damage or with saline as the carrier control, and four injected and two control animals were killed humanely and examined at 30, 90, 180, 240 and 340 days after injection. The cumulative skeletal dose until death was estimated for each animal and was averaged as the mean skeletal dose for each group of animals as described previously (*10*).

Histopathology and Immunohistochemistry

All the control and ^{239}Pu-injected animals, irrespective of postmortem changes, were autopsied to examine gross lesions of main organs and skeletal bones, all of which were fixed in 10% phosphate-buffered formalin. Bones and bone tumors were then decalcified with a mixture of 10% formic acid and 10% neutral formalin. All the tissue specimens were cut into small pieces, processed with graded ethanol and xylene in an automatic tissue processor, and embedded in paraffin. Five- to 6-μm-thick sections were prepared and stained with hematoxylin and eosin (H&E) for histopathological examinations using a light microscope. As diagnostic criteria for myeloid leukemia, the gross appearance of grayish hepatomegaly and splenomegaly was seen most frequently in combination with the histopathological appearance of ovoid or polymorphic cells with rod- or ring-shaped nuclei infiltrated in the liver sinusoids, splenic red pulp and bone marrow sinusoids. For differential diagnosis of lymphoid tumors by light microscopy, immunohistochemistry was applied on deparaffinized sections unmasked by heating to 90°C in target antigen-retrieval solution (S1699; DAKO Corp.). The monoclonal antibodies, Thy 1 (CD90; Pharmingen) and B220 (CD45R; Pharmingen) were used for the detection of surface markers of T cells and B cells, respectively, as combined with biotinylated anti-rat IgG and avidin-biotin-peroxidase complex reagents (ABC; Vector Laboratories) followed by visualization with 3,3′-diaminobenzidine (DAB; Sigma). The criteria for the histological phenotypes of lymphoid tumors are as follows: (1) Thy 1-positive thymic or T-cell lymphomas involved mainly the thymus and local lymph nodes; (2) B220-positive B-cell lymphomas involved almost all the systemic lymph nodes; (3) either Thy 1- or B220-positive leukemias involved the liver, spleen and systemic lymph nodes; and (4) histiocytic lymphomas, which are distinct from other lymphomas in their morphological appearance with spindle-shaped cytoplasm and ovoid nuclei, being negative for both markers and involved particularly the spleen or local lymph nodes.

Hematology

After the mice were killed under anesthesia with ether at selected times, peripheral blood was collected through the posterior vein for hemocytometric examinations including total and differential counts of white blood cells (WBC) as described elsewhere (*12*). The thymus was carefully removed from the chest, weighed and teased through a screen mesh for cell preparations. Both spleen cells and femoral bone marrow cells were prepared and suspended in RPMI 1640 medium (Flow Laboratories) supplemented with 10% fetal bovine serum (Gibco), 100 U/ml penicillin, and 100 μg/ml streptomycin. The nucleated cells in these cell preparations were enumerated with a Coulter counter (Model ZM; Coulter Electronics). For the factor-dependent colony-forming cell (CFC) assays as described elsewhere (*13*), 2×10^4 bone marrow cells or 4×10^4 spleen cells were plated into 0.3% agarose (Sea Plaque; FMC Bioproducts) medium containing either 500 U/ml murine recombinant granulocyte-macrophage colony-stimulating factor (rGM-CSF, now known as Csf2; Genzyme Corp.) or 500 U/ml highly purified murine macrophage colony-stimulating factor (mM-CSF, now known as Csf1; a gift from Dr. R. K. Shadduck) in triplicate 35-mm dishes (Falcon 3001; Becton Dickinson Labware), and were incubated for 7 days at 37°C in a humidified atmosphere of 5% CO_2 in air. After fixation and staining with Giemsa, the numbers of colonies (>50 cells) were scored using a dissecting microscope and were adjusted to the numbers of GM- or M-CFC per femoral bone marrow or spleen.

Statistics

Survival and competing risks of neoplastic or non-neoplastic death after ^{239}Pu injection were analyzed by the Kaplan-Meier method using the log-rank and Peto-Wilcoxon tests as described previously (*10*). The data on survival in the life-span studies and hematological kinetics in sequential studies were expressed as the mean ± SD of those obtained from each group, and the significant differences between the control and injected groups of mice were compared by the unpaired Student's *t* test.

RESULTS

Reduction of Survival and Induction of Tumor after Injection of ^{239}Pu

As shown in Table 1, the mean survival periods were significantly ($P < 0.01$) reduced in each strain after injection of 500 Bq or more of ^{239}Pu, while those of the mice injected with 100 Bq were slightly longer but not significantly different from the controls. As assessed by the competing risks with non-neoplastic death, the cumulative incidence of neoplastic death of all the groups of ^{239}Pu-injected mice appeared to increase at times before 200 days after injection compared to the controls in each strain (Fig. 1). Among the tumors related to neoplastic death, bone tumors, mostly diagnosed as osteosarcomas, were induced most frequently and appeared early from 300 days after injection; lymphoid tumors, although less frequent than bone tumors, also appeared early or concomitantly with bone tumors from 200–400 days after injection in all strains (Fig. 2). No animals bearing both bone and lymphoid tumors were found, and the appearance periods of the other tumors were late after injection, i.e. similar to the controls (data not shown). These findings indicate the reduction of survival due to early neoplastic death particularly caused by the high frequency of induction of bone tumors after ^{239}Pu injection.

The dose responses of tumors induced in each strain were compared with the respect to incidences and estimated skeletal doses for the groups of animals injected with different

TABLE 1
Survival Periods and Tumors Induced in the Three Strains of Mice after Injection of ^{239}Pu Citrate

Mouse strain	Injected dose (Bq)	No. of animals	Survival period (days)[a]	Skeletal dose (Gy)[b]	No. of tumor-bearing animals (%)[c]			
					Bone	Lymphoid	Myeloid	Others
C3H	0	60	763 ± 137	0	0 (0)	11 (18.3)	0 (0)	24 (40.0)
	100	30	808 ± 82	0.68 ± 0.04	7 (23.3)	0 (0)	0 (0)	17 (56.7)
	500	30	592 ± 107*	2.71 ± 0.36	19 (63.3)	0 (0)	0 (0)	3 (10.0)
	1000	30	452 ± 73*	4.42 ± 0.58	14 (46.7)	0 (0)	0 (0)	0 (0)
	5000	30	315 ± 48*	16.3 ± 2.1	12 (40.0)	6 (20.0)	0 (0)	0 (0)
C57BL/6	0	60	672 ± 183	0	0 (0)	18 (30.0)	2 (3.3)	6 (10.0)
	100	30	727 ± 102	0.63 ± 0.06	4 (13.3)	8 (26.7)	0 (0)	7 (23.3)
	500	30	580 ± 119*	2.66 ± 0.43	7 (23.3)	8 (26.7)	2 (6.7)	2 (6.7)
	1000	30	412 ± 85*	4.08 ± 0.69	16 (53.3)	3 (10.0)	0 (0)	0 (0)
	5000	30	361 ± 48*	18.3 ± 2.0	20 (66.7)	0 (0)	0 (0)	0 (0)
$BC3F_1$	0	60	742 ± 161	0	1 (1.7)	19 (31.7)	5 (8.3)	19 (31.7)
	100	30	730 ± 109	0.63 ± 0.06	9 (30.0)	7 (23.3)	1 (3.3)	13 (43.3)
	500	30	567 ± 116*	2.62 ± 0.37	17 (56.7)	5 (16.7)	0 (0)	4 (13.3)
	1000	30	449 ± 65*	4.38 ± 0.51	13 (43.3)	2 (6.7)	1 (3.3)	2 (6.7)
	5000	30	326 ± 40*	16.8 ± 1.8	10 (33.3)	0 (0)	0 (0)	1 (3.3)

[a] Mean ± SD of the survival periods after injection of saline (controls) or ^{239}Pu in each group. Asterisk indicates a significant difference compared to the controls ($P < 0.01$).

[b] Mean ± SD of the calculated skeletal doses of dead animals after injection of ^{239}Pu in each group.

[c] The numbers and percentage in parentheses of animals bearing bone, lymphoid, myeloid and the other solid tumors among animals in each group.

amounts of ^{239}Pu citrate as shown in Table 1. The incidence of bone tumors, which were observed less frequently or not at all in the controls, increased sharply from a skeletal dose of 0.6–0.7 Gy in all the strains and reached a maximum at 2.0–3.0 Gy in C3H and $BC3F_1$ mice and at 18 Gy in C57BL/6 mice. In contrast, lymphoid tumors, which occurred with relatively higher incidences in the controls, were reduced significantly at skeletal doses above 0.6 Gy, the ranges in which bone tumors increased to the maximum, only except in C3H mice, which again showed an increase in the incidence of lymphoid tumors to almost the control level at skeletal doses higher than 16 Gy. Myeloid leukemias were not found in either control or ^{239}Pu-injected C3H mice, whereas they were observed in C57BL/6 and $BC3F_1$ mice after ^{239}Pu injection but not at significantly different levels from the controls. Other tumors were present in the controls of each strain of mice, including pulmonary adenomas, hepatocellular carcinomas, ovarian carcinomas or granulosa cell tumors, subcutaneous fibrosarcomas or mammary carcinomas, and miscellaneous solid tumors. The incidences of the other tumors were significantly reduced in mice that received skeletal doses higher than 2.0 Gy, which induced bone tumors more frequently. These findings indicate the differential dose responses of the tumor types that appeared early and later after ^{239}Pu injection, thus apparently reducing the incidence of the late-appearing tumors.

Characteristics of Lymphoid Tumor Phenotypes Induced by ^{239}Pu Injection

Although the incidences of lymphoid tumors were lower at higher doses in mice of each strain that were injected with ^{239}Pu citrate compared to the controls, their histological phenotypes were differentially characterized by combinations of histological features with immunohistochemistry for both T- and B-cell surface markers as shown in Table 2. Among lymphoid tumors observed in all the ^{239}Pu-injected mice, the proportion of thymic (T-cell) lymphomas was lower, whereas those of B-cell lymphomas and particularly B-cell leukemias were much higher, compared to those in the controls in each strain. No T-cell leukemias were found, and histiocytic lymphomas were rarely observed in either control or ^{239}Pu-injected mice of the three strains. While the appearance of thymic lymphomas was mostly late in each strain, B-cell lymphomas and leukemias tended to occur early after ^{239}Pu injection (data not shown). Since the B220 used as the B-cell surface marker is recognized to be expressed widely in immature to mature B cells, these findings indicate a predominant and relatively early induction of pre-B-cell-type leukemic lymphomas rather than thymic lymphomas after ^{239}Pu injection.

Hematological Kinetics after ^{239}Pu Injection

Since myeloid leukemias were observed rarely or not at all and pre-B-cell leukemias were induced more frequently after ^{239}Pu injection, it is conceivable that any derangements of bone marrow-derived progenitor cells could be related to the lineage and frequency of hemato-lymphoid malignancies. The initial and mid-term hematological kinetics were compared among the three strains injected with 5000 Bq of ^{239}Pu citrate, an amount that would not be expected to induce more lymphoid or myeloid tumors but would be expected to induce maximum changes in the cellularity and hematopoietic responses of the bone marrow, spleen and circulating peripheral blood leukocytes in mice that received estimated skeletal doses of 2.0 to 17 Gy. As shown

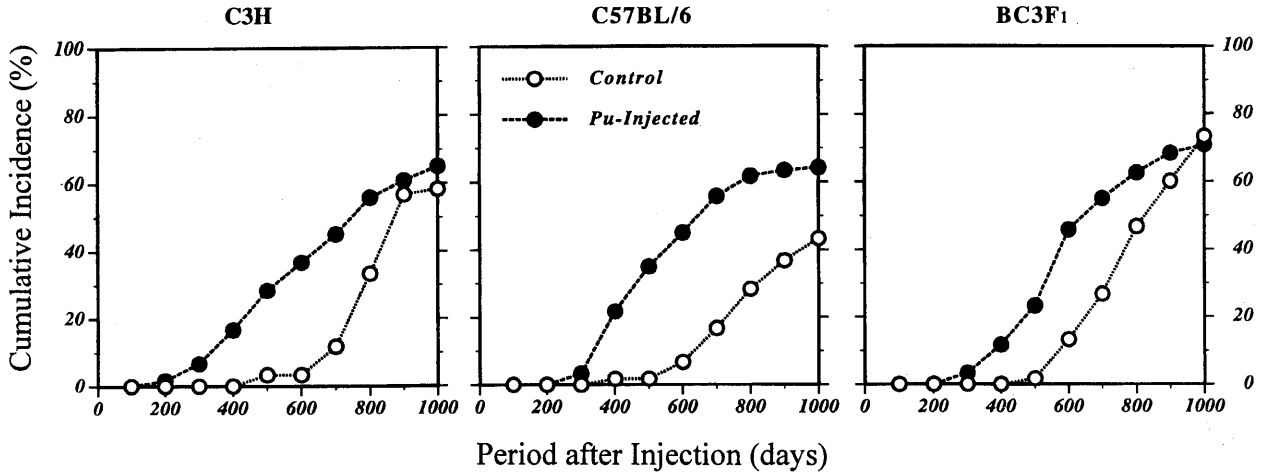

FIG. 1. Cumulative incidence of neoplastic death in C3H, C57BL/6 and $BC3F_1$ mice after injection of ^{239}Pu citrate. Values indicate the percentage cumulative incidence of animals that died with fatal tumors in the controls (open circles) and ^{239}Pu-injected mice (closed circles) for each time.

in Fig. 3, the numbers of peripheral WBC and bone marrow cells were persistently and significantly ($P < 0.05$) reduced to 30–60% of the control levels determined on day 0 as the combined value from 30 through 340 days after ^{239}Pu injection in each strain. The numbers of spleen cells were lower than those in the controls during the period from 30 to 90 days, but they increased up to approximately 120–150% of the control levels from 180 days after ^{239}Pu injection in each strain. The differential counts of WBC showed only a slight increase (approximately in the proportion of 4.0–8.0%) of immature granulocytes and meta- or pro-myelocytes during the entire period after ^{239}Pu injection. The capacity of hematopoietic progenitor cells to differentiate into granulocytic or monocytic lineage cells was examined by GM- or M-CSF-dependent colony-forming cell (CFC) assays. As shown in Fig. 4, bone marrow GM-CFC were persistently and significantly ($P < 0.05$) reduced to 20–46% of the control levels plotted on day 0 as the combined value from 30 through 340 days after ^{239}Pu injection in each strain, while in contrast, splenic GM-CFC increased early and significantly ($P < 0.05$) to approximately 3–50 times the control levels from 90 days after ^{239}Pu injection. Such reverse kinetics of both bone marrow and splenic M-CFC was also observed in each strain after ^{239}Pu injection (data not shown).

Taken together, these findings indicate the persistent reduction of bone marrow hematopoiesis and peripheral blood cellularities with a slight shift in the leukocyte proportions to immature types, and a compensatory increase of spleen cell constituents due to extramedullary hematopoiesis after ^{239}Pu injection. Nevertheless, myeloid leukemias or the other myeloproliferative disorders were not ob-

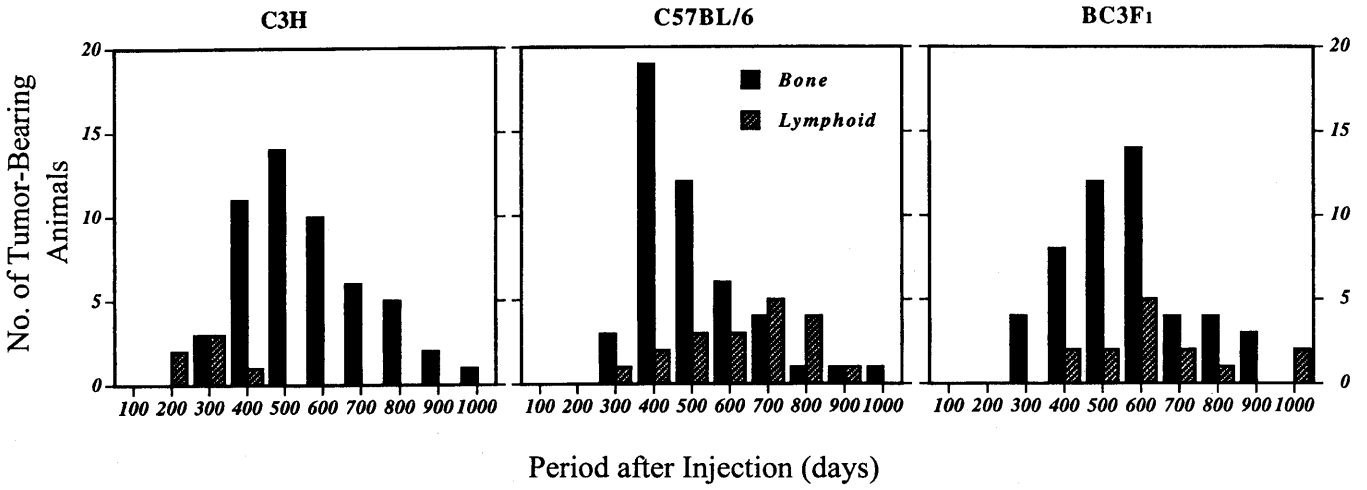

FIG. 2. Appearance times of bone and lymphoid tumors in C3H, C57BL/6 and $BC3F_1$ strains of mice after injection of ^{239}Pu citrate. Values indicate numbers of animals bearing either bone tumors (black columns) or lymphoid tumors (hatched columns) in all the groups of ^{239}Pu-injected mice for each time.

TABLE 2
Histological Phenotypes of Lymphoid Tumors in the Three Strains of Mice after Injection of ^{239}Pu Citrate

Mouse strain	Group	No. of tumors[a]	No. of tumor phenotypes (%)[b]			
			Thymic lymphoma	B-cell lymphoma	B-cell leukemia	Histiocytic lymphoma
C3H	Control	11	5 (45.5)	5 (45.4)	0 (0)	1 (9.1)
	Pu-injected	6	1 (16.7)	3 (50.0)	2 (33.3)	0 (0)
C57BL/6	Control	18	8 (44.4)	7 (38.9)	0 (0)	3 (16.7)
	Pu-injected	19	3 (15.8)	13 (68.4)	3 (15.8)	0 (0)
$BC3F_1$	Control	19	8 (42.1)	10 (52.6)	0 (0)	1 (5.2)
	Pu-injected	14	2 (14.3)	6 (42.8)	5 (35.7)	1 (7.1)

[a] Total numbers of lymphoid tumors found in the controls (60 mice) and all the ^{239}Pu-injected animals (120 mice) of each strain.
[b] The numbers and percentage proportions in parentheses of lymphoid tumor phenotypes among total numbers of lymphoid tumors found in each group. The diagnostic criteria as combined with immunohistochemistry using Thy 1 and B220 monoclonal antibodies are given in the text.

served in any strains during 1 year after ^{239}Pu injection. As well, no lymphoid tumors were found, while flow cytometric analysis showed that the proportions of Thy 1- or B220-positive lymphocytes were not significantly different in bone marrow cell preparations but were reduced in spleen cell preparations particularly from 180 days after ^{239}Pu injection (data not shown). There were no significant differences in the weight, cell numbers, and Thy 1-positive cell distribution of the thymus between the control and ^{239}Pu-injected mice of each strain at each time (data not shown).

DISCUSSION

The present study, which was undertaken to investigate the strain differences in carcinogenic and hematopoietic responses after injection of ^{239}Pu citrate, indicated that overall the biological effects were specific to internal α-particle

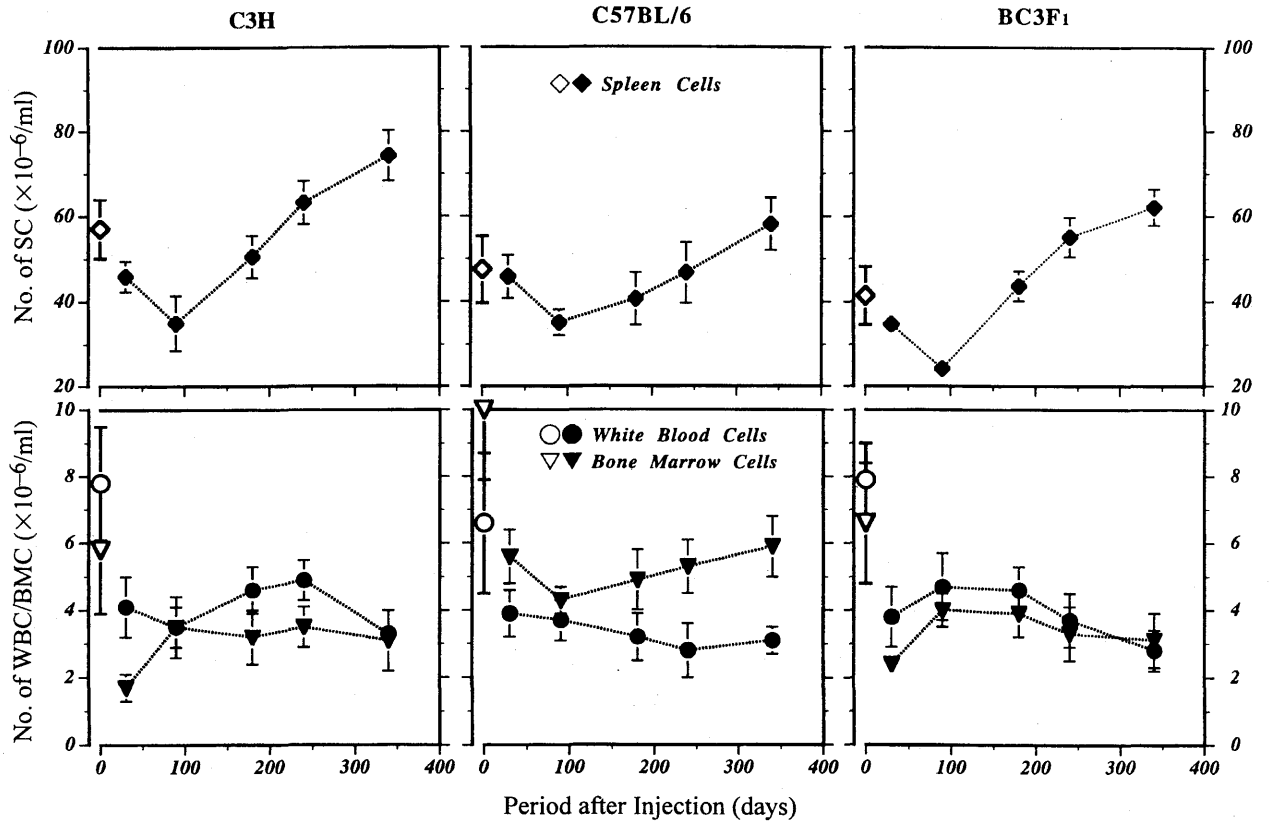

FIG. 3. Kinetics of blood leukocytes and hematopoietic tissue cells in C3H, C57BL/6 and $BC3F_1$ mice after injection of ^{239}Pu citrate. Values with bars indicate mean ± SD of the numbers of peripheral white blood cells (WBC; circles), femoral bone marrow cells (BMC; triangles), and spleen cells (spleen cells; diamonds) in the controls (open symbols) plotted for day 0 as the combined value for 30–340 days after injection and ^{239}Pu-injected animals (closed symbols) for each time.

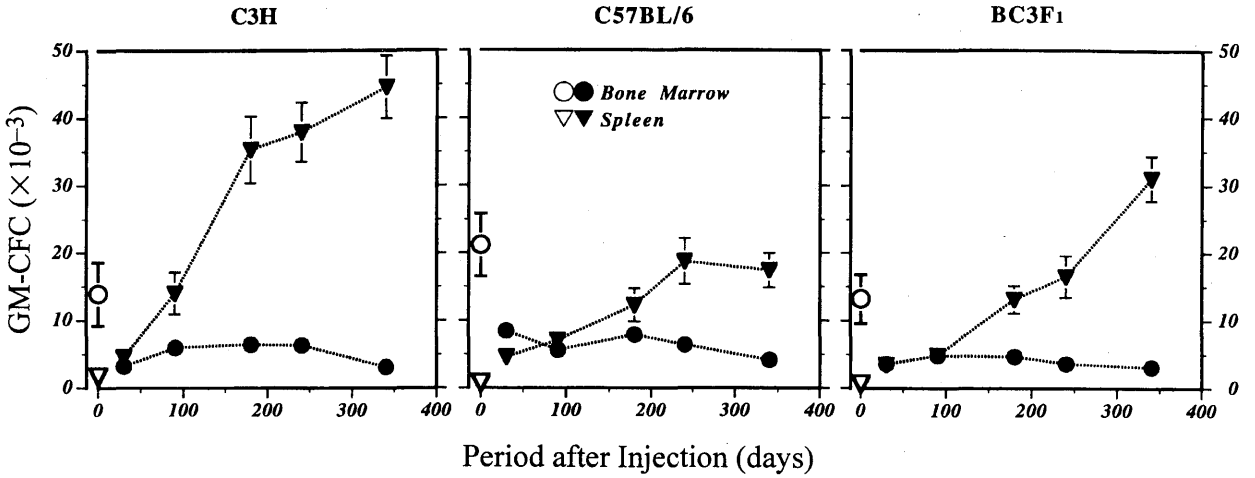

FIG. 4. Kinetics of granulocyte-macrophage colony-forming cells (GM-CFC) in C3H, C57BL/6 and $BC3F_1$ mice after injection of ^{239}Pu citrate. Values with bars indicate mean ± SD of the numbers of GM-CFC per femoral bone marrow (circles) or spleen (triangles) in the controls (open symbols) plotted for day 0 as the combined value for 30–340 days after injection and ^{239}Pu-injected animals (closed symbols) for each time.

irradiation but were different from those seen after exposure to external low-linear energy transfer (LET) radiation. Significant reduction of survival was commonly noted among the three strains after injection of 500 Bq or more and was due to early neoplastic death caused in particular by the early appearance of and increase in bone tumors, mostly osteosarcomas, in all the mice that received average cumulative skeletal doses of 2.0 Gy or more as estimated. No significant differences in survival periods compared to the controls, noted in all mice of all strains injected with 100 Bq, are considered to result from the late occurrence of either non-neoplastic or neoplastic death mostly due to the late appearance of the other solid tumors, as noted similarly in the controls. The dose responses of bone tumors appeared to show similar patterns in all the strains, except for the differences in skeletal dose ranges for the maximum induction: from 2.0 to 3.0 Gy in both C3H and $BC3F_1$ mice, but a higher dose of 18 Gy in C57BL/6 mice. The dose responses of the lymphoid tumors, in contrast, were the opposite of those of bone tumors, decreasing at skeletal doses of 0.6 Gy or more in all the strains, and their incidences increased again at doses of 16 Gy in C3H mice. This second increase might be due to the earlier appearance of lymphoid tumors compared to bone tumors, as shown in Fig. 2. These findings may suggest a competition between bone and lymphoid tumors that appeared early or concomitantly and may also implicate the differences in the susceptibility of the respective target progenitor cells to bone or lymphoid malignancies among the mouse strains. Direct evidence could not be derived from the present results regarding the significant induction of myeloid leukemias in each strain after ^{239}Pu injection. No myeloid leukemias were found in our C3H mice, which have a similar genetic background to CBA/H mice and in which a lower but significant incidence of myeloid leukemias was found in previous studies (*7, 8*). Such a discrepancy is not likely to be due merely to the small size of experimental groups in the present study compared to others (*9*), but rather may result from differences in either the susceptibilities of these mouse colonies to carcinogenic responses or the diagnostic criteria used for myeloid leukemia. The other solid tumors were somewhat reduced in all the strains after injection of 500 Bq or more, suggesting a competitive reduction of these spontaneous tumors with early induction of bone and/or lymphoid tumors, as has been shown previously (*10*).

Taken together, these findings indicate that only osteosarcomas are induced specifically but independently of mouse strain, while lymphoid, myeloid and the other solid tumors may not be specific for ^{239}Pu injection. Such tumor spectra are quite different from those for external low- and high-LET radiations in various strains of mice. Despite the various dose rates and doses used, thymic lymphomas and myeloid leukemias are significantly induced by X or γ radiation (*14–16*), and solid tumors other than bone tumors are frequently found after single or fractionated exposures to neutrons (*17–19*). Thymic lymphomas, which are more frequently induced in C57BL mice and substrain B10 than in C3H mice after fractionated X irradiation (*20*), were observed less frequently, but pre-B-cell type leukemic lymphomas were found commonly and predominantly in ^{239}Pu-injected C3H, C57BL/6 and $BC3F_1$ mice compared to their controls. These findings may provide some plausible explanations of the different mechanisms for radiation-induced leukemogenesis and lymphomagenesis after external radiation and internal α-particle exposures. The low-LET radiations could induce thymic lymphomas and/or myeloid leukemias indirectly through interactions between bone marrow-derived progenitors and marrow or thymic stromal cells, as described elsewhere (*16, 21–22*), whereas α particles would more likely cause lethal damage of putatively potential bone marrow stem cells rather than sublethal damage, as suggested by the much lower yields of myeloid

leukemias induced by ^{239}Pu (*23*). Otherwise, insufficient but sublethal α-particle doses could induce hematopoietic derangements of rescued bone marrow progenitor cells, leading to the development of pre-B-cell leukemia rather than thymic or T-cell lymphomas through microenvironmental modulation, directed into B-cell lineage differentiation after injection of ^{239}Pu. In this regard, not only modifiers of radiosensitivity or latency as described elsewhere (*24*) but also factors that influence the genome such as targeting of the *Trp53* tumor suppressor gene (*25*) and specificity of loss of heterozygosity (*26*) should be taken into account for radiation leukemogenesis.

The sequential examinations of the initial to mid-term hematopoietic kinetics after injection of a relatively higher dose of ^{239}Pu revealed in all strains the persistent reduction of bone marrow cellularity and hematopoietic progenitor cells (CFC) committed to both granulocyte and monocyte/macrophage lineages, with a compensatory increase in the spleen. Peripheral white blood cells were consistently reduced with a slight shift in the leukocyte proportions to immature types, and the proportions of T and B lymphocytes were not altered in the bone marrow but were somewhat reduced in the spleen. No specific effects were observed on the cellularity and lymphocyte population of the thymus after ^{239}Pu injection. Almost all of the hemocytological changes described above, although they do not necessarily mirror each other, are thought to result from bone marrow hypoplastic and splenic extramedullary hematopoiesis. No myeloid or lymphoid tumors were observed, however, in any of the mice examined during 1 year after ^{239}Pu injection. Other studies have shown that the numbers and self-renewal capacity of pluripotent hematopoietic stem cells (CFU-S) were reduced relatively early (*23, 27*) and chromosomal aberrations of bone marrow cells appeared early (*28*) in mice after injection of leukemogenic or relatively lower amounts of ^{239}Pu. Taken together, these findings provide evidence of acute to subchronic hematopoietic responses induced directly or indirectly by α-particle irradiations of bone marrow hematopoietic stem cells that are not related directly to any hematopoietic derangements leading to malignancies. As a plausible reason for this, hematopoietic progenitors in the bone marrow, which could be capable of causing leukemia, may be sterilized or inactivated by the α-particle irradiation (*7, 23*) to a much lesser extent for their renewal proliferation and differentiation or transformation into pre-leukemic or pre-lymphoma cells, although further experimental evidence, particularly data on stem cell kinetics and molecular susceptibility to leukemogenesis, would be needed to confirm such hypothetical mechanisms.

In conclusion, the present study compared both carcinogenic and hematopoietic responses after injection of ^{239}Pu citrate in female mice of three strains with different backgrounds for spontaneous and radiation carcinogenesis. The results can be summarized as follows: (1) a significant reduction of survival due to early neoplastic death, particularly caused by early induction of osteosarcomas formed at the highest frequency; (2) a similar pattern of dose responses for osteosarcomas even when the dose ranges for the maximum level of induction are different; (3) induction predominantly of pre-B-cell leukemic lymphomas but with fewer thymic lymphomas; (4) no evidence of a significantly higher induction of myeloid leukemias; and (5) a persistent reduction of bone marrow progenitor cells and a compensatory increase of splenic hematopoietic progenitor cells. These findings were common in the three mouse strains, suggesting no obvious strain differences in both carcinogenic spectra and hematopoietic responses that are specific to α-particle irradiation but are different from external radiation exposures.

ACKNOWLEDGMENTS

This work was partly supported by a grant for the Research on Analysis of Radiation Risk and Safety from Japan Science and Technology Agency. The authors are grateful to H. Iida and K. Fukutsu for their technical assistance in all the experimental procedures, and acknowledge all the staff of Animal Care Co. for their helpful support of animal care.

Received: February 22, 2000; accepted: June 23, 2000

REFERENCES

1. M. P. Finkel and B. O. Biskis, Toxicity of plutonium in mice. *Health Phys.* **8**, 565–579 (1962).
2. J. P. M. Bensted, B. Chir, D. M. Taylor and F. D. Sowby, The carcinogenic effects of americium 241 and plutonium 239 in the rat. *Br. J. Radiol.* **38**, 920–925 (1965).
3. G. N. Taylor, C. W. Mays, R. D. Lloyd, P. A. Gardner, L. R. Talbot, S. S. McFarland, T. A. Pollard, D. R. Atherton, D. Van Moorhem and D. H. Taysum, Comparative toxicity of ^{226}Ra, ^{239}Pu, ^{241}Am, ^{249}Cf, and ^{252}Cf in C57BL/Do black and albino mice. *Radiat. Res.* **95**, 584–601 (1983).
4. D. M. Taylor, The comparative carcinogenesis of ^{239}Pu, ^{241}Am and ^{244}Cm in the rat. In *Life-Span Radiation Effects Studies in Animals: What Can They Tell Us?* (R. C. Thompson and J. A. Mahaffey, Eds.), pp. 404–412. CONF-830951, U.S. Department of Energy, Washington, DC, 1986.
5. B. Bleaney, Plutonium deposition on bone surfaces and in bone marrow following intravenous and intramuscular injections. In *Delayed Effects of Bone-Seeking Radionuclides* (C. W. Mays, W. S. S. Jee, R. D. Lloyd, B. J. Stover, J. H. Dougherty and G. N. Taylor, Eds.), pp. 125–135. The University of Utah Press, Salt Lake City, 1969.
6. J. F. Loutit and T. E. F. Carr, Lymphoid tumors and leukaemia induced in mice by bone-seeking radionuclides. *Int. J. Radiat. Biol.* **33**, 245–263 (1978).
7. E. R. Humphreys, J. F. Loutit and V. A. Stones, The induction by ^{239}Pu of myeloid leukaemia and osteosarcoma in female CBA mice. *Int. J. Radiat. Biol.* **51**, 331–339 (1987).
8. E. R. Humphreys, K. R. Isaacs, T. A. Raine, J. Saunders, V. A. Stones and D. L. Wood, Myeloid leukemia and osteosarcoma in CBA/H mice given ^{224}Ra. *Int. J. Radiat. Biol.* **64**, 231–235 (1993).
9. W. A. Müller, A. Luz, A. B. Murray and U. Linzner, Induction of lymphoma and osteosarcoma in mice by single and protracted low α doses. *Health Phys.* **59**, 305–310 (1990).
10. Y. Oghiso, Y. Yamada and H. Iida, High frequency of leukemic lymphomas with osteosarcomas but no myeloid leukemias in C3H mice after ^{239}Pu citrate injection. *J. Radiat. Res.* **38**, 77–86 (1997).
11. Y. Oghiso and Y. Yamada, Carcinogenesis in mice after injection of soluble plutonium citrate. *Radiat. Res.* **152** (Suppl.), S27–S30 (1999).

12. Y. Oghiso, Y. Kubota, S. Takahashi and H. Sato, Effect of ^{89}Sr-induced monocytopenia on splenic and pulmonary alveolar macrophage populations in a normal steady state. *J. Radiat. Res.* **29**, 189–202 (1988).

13. Y. Oghiso, Y. Yamada, K. Ando, H. Ishihara and Y. Shibata, Differential induction of prostaglandin E_2-dependent and -independent immune suppressor cells by tumor-derived GM-CSF and M-CSF. *J. Leukoc. Biol.* **53**, 86–92 (1993).

14. S. Sasaki and T. Kasuga, Life-shortening and carcinogenesis in mice irradiated neonatally with X rays. *Radiat. Res.* **88**, 313–325 (1981).

15. M. Seki, K. Yoshida, M. Nishimura and K. Nemoto, Radiation-induced myeloid leukemia in C3H/He mice and the effect of prednisolone acetate on leukemogenesis. *Radiat. Res.* **127**, 146–149 (1991).

16. R. H. Mole, D. G. Papworth and M. J. Corp, The dose-response for X-ray induction of myeloid leukaemia in male CBA/H mice. *Br. J. Cancer* **47**, 285–291 (1983).

17. J. R. Maisin, A. Wambersie, G. B. Gerber, G. Mattelin, M. Lambiet-Collier, B. De Coster and J. Gueulette, Life-shortening and disease incidence in C57Bl mice after single and fractionated γ and high-energy neutron exposure. *Radiat. Res.* **113**, 300–317 (1988).

18. V. Covelli, M. Coppola, V. Di Majo, S. Rebessi and B. Bassani, Tumor induction and life shortening in $BC3F_1$ female mice at low doses of fast neutrons and X rays. *Radiat. Res.* **113**, 362–374 (1988).

19. V. Di Majo, M. Coppola, S. Rebessi, A. Saran, S. Pazzaglia, L. Pariset and V. Covelli, Neutron-induced tumors in $BC3F_1$ mice: Effects of dose fractionation. *Radiat. Res.* **138**, 252–259 (1994).

20. H. Kamisaku, S. Aizawa, M. Kitagawa, Y. Ikarashi and T. Sado, Limiting dilution analysis of T-cell progenitors in the bone marrow of thymic lymphoma-susceptible B10 and -resistant C3H mice after fractionated whole-body X-irradiation. *Int. J. Radiat. Biol.* **72**, 191–199 (1997).

21. M. Janowski, R. Cox and P. G. Strauss, The molecular biology of radiation-induced carcinogenesis: thymic lymphoma, myeloid leukaemia and osteosarcoma. *Int. J. Radiat. Biol.* **57**, 677–691 (1990).

22. E. Naparstek, T. J. FitzGerald, M. A. Sakakeeny, V. Klassen, J. H. Pierce, B. A. Woda, J. Falco, S. Fitzgerald, P. Nizin and J. S. Greenberger, Induction of malignant transformation of cocultivated hematopoietic stem cells by X-irradiation of murine bone marrow stromal cells *in vitro*. *Cancer Res.* **46**, 4677–4684 (1986).

23. B. I. Lord, G. Molineux, E. R. Humphreys and V. A. Stones, Long-term effects of plutonium-239 and radium-224 on the distribution and performance of pluripotent haemopoietic progenitor cells and their regulatory microenvironment. *Int. J. Radiat. Biol.* **59**, 211–227 (1991).

24. R. E. J. Mitchel, J. S. Jackson, R. A. McCann and D. R. Boreham, The adaptive response modifies latency for radiation-induced myeloid leukemia in CBA/H mice. *Radiat. Res.* **152**, 273–279 (1999).

25. C. J. Kemp, T. Wheldon and A. Balmain, P53-deficient mice are extremely susceptible to radiation-induced tumorigenesis. *Nat. Genet.* **8**, 66–69 (1994).

26. H. J. Cleary, E. Wright and M. Plumb, Specificity of loss of heterozygosity in radiation-induced mouse myeloid and lymphoid leukaemias. *Int. J. Radiat. Biol.* **75**, 1223–1230 (1999).

27. R. Schofield, B. I. Lord, E. R. Humphreys and V. A. Stones, Effects of plutonium-239 on haemopoiesis. I. Quantitative and qualitative changes in CFU-S in different regions of the mouse femur and vertebrae. *Int. J. Radiat. Biol.* **49**, 1021–1029 (1986).

28. V. Svoboda, A. Sedlak, H. Kypenova and D. Bubenikova, Long-term effects of low level ^{239}Pu contamination on murine bone-marrow stem cells and their progeny. *Int. J. Radiat. Biol.* **52**, 517–526 (1987).

EFFECTS OF GADOLINIUM ON THE RETENTION AND TRANSLOCATION OF ^{239}Pu-HYDROXIDE

H. Sato, S. Takahashi, and Y. Kubota*

Abstract—**The effect of gadolinium on the lung retention, excretion, and translocation of plutonium was studied in rats instilled intratracheally with plutonium hydroxide with and without gadolinium. Three types of plutonium hydroxide were prepared: pure ^{239}Pu-hydroxide colloid, that containing a high concentration of gadolinium, and that containing a low concentration of gadolinium. The lung retention of ^{239}Pu was higher and the fecal excretion was lower in the rats administered ^{239}Pu-hydroxide containing a high concentration of gadolinium than those administered pure ^{239}Pu-hydroxide colloid. The translocation of ^{239}Pu from lung to other organs including the liver, spleen, femur, and kidney was not affected by gadolinium. The cytological examination of bronchoalveolar lavage cells showed that the administration of ^{239}Pu-hydroxide containing a high concentration of gadolinium induced the inflammatory reactions in the lung. The delayed alveolar clearance of plutonium in the rats administered ^{239}Pu-hydroxide colloid containing a high concentration of gadolinium may be attributable to the change in physicochemical characteristics of colloid and the inflammation induced in the lung by gadolinium.**

Health Phys. 80(2):164–169; 2001

Key words: plutonium; rat; lungs, rodent; biokinetics

INTRODUCTION

Gadolinium (Gd), one of the rare earth elements, is used as a material in semiconductor and magnetic substances in industry, and as a contrast agent for magnetic resonance imaging in clinical medicine (Hirano and Suzuki 1996; Weinmann et al. 1984; Runge and Parker 1997). Gadolinium is also used as a neutron absorber in the nuclear industry. In a newly developed facility for reprocessing of nuclear fuel in Japan, gadolinium nitrate is added to the nitric acid solution as a neutron absorber during the fuel-dissolution process. There is concern, therefore, that workers could be simultaneously exposed to gadolinium and radioactive nuclides in an accident. Gadolinium is a toxic element, especially for reticuloendothelial cells such as alveolar macrophages (O'Neill et al. 1994; Yoneda et al. 1995; Suzuki et al. 1996; Ruttinger et al. 1996), and thus may affect the metabolism of radionuclides in the human body. However, little is known about the effects of gadolinium on the retention and metabolism of radionuclides in the human body.

Inhalation may be a possible route for the accidental contamination by gadolinium and radionuclides. In such a case, plutonium would be one of the important radionuclides. In the present study, therefore, an animal experiment was carried out to elucidate whether or not the co-existence of gadolinium may affect the retention and translocation of plutonium in the lung. Plutonium hydroxide with and without gadolinium was instilled into the rat lung, and the lung retention and translocation of plutonium were compared.

MATERIALS AND METHODS

$^{239}PuO_2$ was obtained from the Japan Atomic Energy Research Institute† and converted to ^{239}Pu nitrate by a procedure described elsewhere (Black and Drummond 1965). Then gadolinium nitrate, $Gd(NO_3)_3$, was added to the plutonium nitrate solution, and the pH of the solution was adjusted to 7.2 with 0.1 M sodium hydroxide under vigorous agitation. By this neutralization, a colloidal form of plutonium hydroxide containing gadolinium was formed. The resultant hydroxide colloids were stabilized with 0.2% gelatin and made isotonic with 0.25 M glucose. Two types of ^{239}Pu-hydroxide colloid containing gadolinium were prepared. One was ^{239}Pu-hydroxide containing a high level of gadolinium (0.9 mg Gd mL^{-1} in the final solution, referred to as Pu-Gd-H in the following), and another containing a low level of gadolinium (0.22 mg Gd mL^{-1}, referred to as Pu-Gd-L). ^{239}Pu-hydroxide colloid was also prepared by the same procedures described above without addition of gadolinium. The radioactive concentration of ^{239}Pu in the final colloidal solutions was 15 kBq mL^{-1} in all three solutions. The reagents used for these procedures were analytical grade (Wako Pure Chemical Industries‡).

* The 4th Research Group, National Institute of Radiological Sciences, 9-1, Anagawa 4-chome, Inage-ku, Chiba-shi, Chiba 263-8555, Japan.

For correspondence or reprints contact H. Sato at the above address, or email at hi_sato@nirs.go.jp.

(*Manuscript received* 23 *November* 1999; *revised manuscript received* 18 *May* 2000, *accepted* 22 *September* 2000)

0017-9078/01/0

† Japan Atomic Energy Research Institute, 2-4, Shirane, Shirakata, Tokai-mura, Ibaraki 319-1195, Japan.

‡ Wako Pure Chemical Industries, Ltd., 5-13, Honcho 4-chome, Nihonbashi, Chuo-ku, Tokyo 103-0023, Japan.

Nine-week-old male Sprague-Dawley rats, weighing about 300 g, were obtained from a domestic breeder.[§] All animals were kept in an air-conditioned room (22±2°C), and given a commercial rat chow[‖] and drinking water *ad libitum*. The animals were divided into three groups consisting of fourteen rats each, and the colloidal solution of Pu and Gd was administered into lung with intratracheal instillation. The detail of the procedure has been described elsewhere (Sato et al. 1994). In brief, the animals were anesthetized with pentobarbital, and 0.3 mL of ^{239}Pu-hydroxide, Pu-Gd-H, or Pu-Gd-L was administered with a single and rapid instillation via an intratracheal cannula. It has been previously found that this dose of Pu-hydroxide colloidal solutions induces no significant inflammatory reactions in the lung (Sato et al. 1994; Takahashi and Sato 1991).

Four weeks after instillation, three rats of each group were sacrificed to determine the lung retention and translocation of ^{239}Pu. The lung, liver, kidney, spleen, and right femur were dissected. Feces and urine were collected 4 d, 1 wk, 2 wk, 3 wk, and 4 wk after instillation. The activity of ^{239}Pu was measured by liquid scintillation counting as described by Keough and Powers (1970). In brief, the tissue samples and feces were ashed at 550°C for 12 h, and the residues were dissolved in 0.2 mL of 7 M nitric acid containing a small amount of concentrated hydrogen fluoride. Then 3.6 mL of scintillation cocktail was added to the sample solution, and the activity was measured using a liquid scintillation counter.[¶] The activity of ^{239}Pu in urine was measured directly with a liquid scintillation counter after filtering through a 0.22 μm membrane filter.[#] The lung retention, excretion, and translocation of ^{239}Pu were represented as a percent of the initial alveolar deposition. The initial alveolar deposition (IAD) was defined as the whole body retention of ^{239}Pu on the third day after administration (i.e., the administered ^{239}Pu minus that excreted up to the third day). This value did not exactly represent the actual retention of ^{239}Pu in the lung, since the activity of ^{239}Pu in organs other than the lung is also included. However, this value could be used for IAD, since the activity of ^{239}Pu in organs other than the lung is assumed to be negligible (Ishigure et al. 1994; Oghiso et al. 1994).

To monitor the occurrence of inflammation in the lung, the remaining animals were serially killed, and bronchoalveolar lavage cells were collected by lung lavage with sterilized Dulbecco's phosphate-buffered saline. The total number of cells collected was determined with a hematocytometer, and differential cell counts were performed on smeared cells after Giemsa staining.

Means of the groups were compared by single-tailed *t*-tests to determine the level of significance. An observed difference was considered statistically significant if $p < 0.05$.

[§] Japan SLC Inc., 3371-8, Koto, Hamamatsu-shi, Shizuoka 431-1103, Japan.

[‖] MB-1, Funabashi Farms, 2-465, Kamiyama, Funabashi-shi, Chiba 273-0046, Japan.

[¶] LS 1214, Wallac Oy, P.O. Box 10, SF-20101, Turku, Finland.

[#] Japan Millipore Ltd., 3-12, Kitashinagawa 1-chome, Shinagawa-ku, Tokyo 140-0001, Japan.

RESULTS

As shown in Table 1, the ratios of IAD to instilled activity were 0.30±0.15, 0.38±0.13, and 0.41±0.19 in the rats administered ^{239}Pu-hydroxide, Pu-Gd-L, and Pu-Gd-H, respectively. There was no statistically significant difference among the 3 groups.

Whole-body retention and total excretion of ^{239}Pu are shown in Fig. 1. The retention of ^{239}Pu in the lungs and the fecal and urinary excretions are shown in Fig. 2. In the rats administered ^{239}Pu-hydroxide, the lung retention of ^{239}Pu was 25.8±2.5% IAD 4 wk after administration. In contrast, the lung retention of ^{239}Pu in the rats administered Pu-Gd-H was 43.2±4.4% IAD. The difference between the groups was statistically significant ($p < 0.05$). The lung retention of ^{239}Pu in the Pu-Gd-L group was similar to that in the ^{239}Pu-hydroxide group. The fecal excretions of ^{239}Pu decreased with the increase in gadolinium contents: 51.9±5.9, 40.9±6.4, and 28.2±0.6% IAD in the ^{239}Pu-hydroxide, Pu-Gd-L, and Pu-Gd-H groups, respectively. The urinary excretion of ^{239}Pu in the Pu-Gd-L group was significantly higher than in the other groups ($p < 0.005$). Figs. 3 and 4 show the daily and cumulative excretion of ^{239}Pu in feces and urine. The daily fecal excretion was significantly lower in the Pu-Gd-H group than the ^{239}Pu-hydroxide group throughout the experimental period (4 d to 4 wk after the administration, $p < 0.05$). In the Pu-Gd-L group, the daily fecal excretion was significantly lower than the ^{239}Pu-hydroxide group only 3 wk after administration ($p < 0.01$). Cumulative fecal excretion was similar to that in the ^{239}Pu-hydroxide group. As shown in Fig. 4, the daily urinary excretion was significantly higher in the Pu-Gd-L group than the ^{239}Pu-hydroxide group 4 d, 1 wk, 2 wk, and 4 wk after administration ($p < 0.05$). Interestingly, there was no significant difference between Pu-hydroxide and Pu-Gd-H groups for the daily and cumulative excretion in urine.

Fig. 5 shows the translocations of ^{239}Pu to the major organs, expressed as % IAD per organ. The amounts of ^{239}Pu in the liver of rats administered ^{239}Pu-hydroxide, Pu-Gd-L, and Pu-Gd-H were 3.16±0.29, 3.38±1.14, and 2.89±0.42%, respectively. The amounts of ^{239}Pu translocated from lung to kidney, spleen, and femur were less than 1% in all groups. In all the organs examined, no

Table 1. Instilled activity and initial alveolar deposition (IAD) of ^{239}Pu and the ratio of IAD to instilled activity in 3 groups.[a]

	Instilled activity[b]	IAD[b]	IAD/Instilled
Pu-hydroxide	4289 ± 306	1242 ± 572	0.30 ± 0.15
Pu-Gd-L	1757 ± 357	647 ± 219	0.38 ± 0.13
Pu-Gd-H	2961 ± 457	1163 ± 439	0.41 ± 0.19

[a] All values are expressed as mean ± SD ($N = 3$).
[b] The values are expressed as Bq.

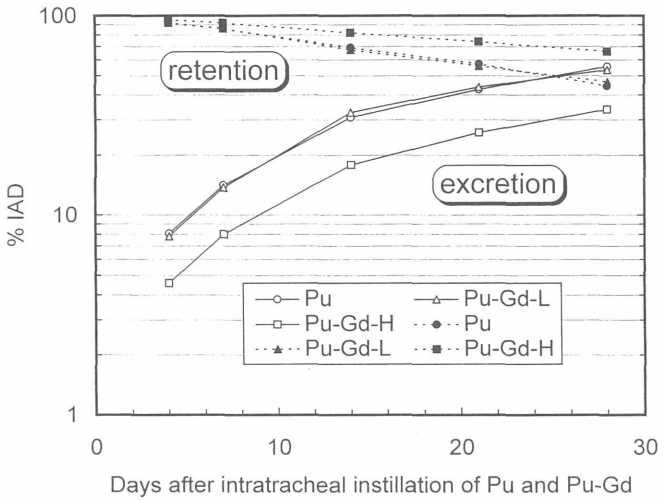

Fig. 1. Whole body retention and cumulative excretion of ^{239}Pu in rats following intratracheal instillation of ^{239}Pu-hydroxide, Pu-Gd-L, and Pu-Gd-H. Each point is the mean of three rats.

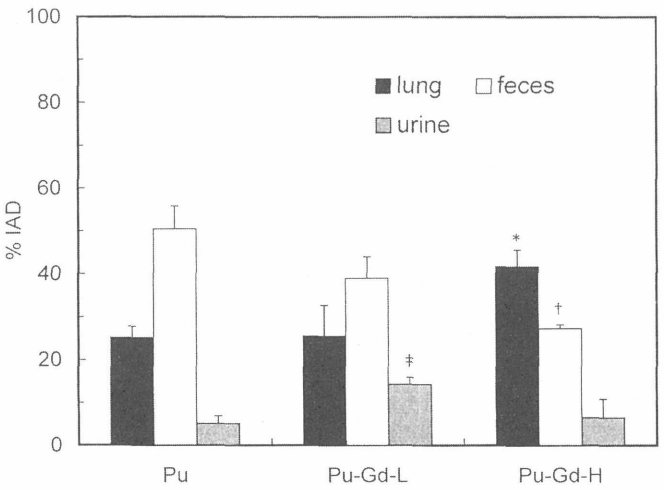

Fig. 2. Lung retention and cumulative excretion of ^{239}Pu in feces and urine 4 wk after intratracheal instillation of ^{239}Pu-hydroxide, Pu-Gd-L, and Pu-Gd-H. Vertical bar shows SD of three rats. * denotes significant difference from ^{239}Pu-hydroxide group at $p < 0.05$.; † $p < 0.01$; ‡ $p < 0.005$.

statistically significant differences in the ^{239}Pu translocation were observed between these groups.

Fig. 6 shows time-course changes in the numbers of alveolar macrophages and neutrophils in bronchoalveolar lavage cells of the rats administered Pu-Gd-H. Neutrophils appeared 1 d after administration, increased with time, and reached a maximum level 4 d after the instillation. The number of alveolar macrophages decreased during the first 2 d and then recovered to the control value. In the rats administered Pu-Gd-L, the number of neutrophils was low, but did not significantly increase during the first 2 d (data are not shown). Neutorophil number did not change in the rats administered ^{239}Pu-hydroxide. No changes in the number of

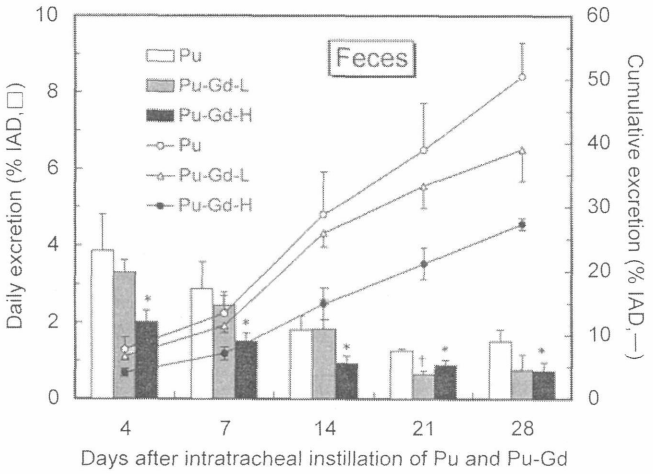

Fig. 3. Daily and cumulative excretion of ^{239}Pu in feces following intratracheal instillation of ^{239}Pu-hydroxide, Pu-Gd-L, and Pu-Gd-H. Vertical bar shows SD of three rats. * denotes significant difference from ^{239}Pu-hydroxide group at $p < 0.05$; † $p < 0.01$.

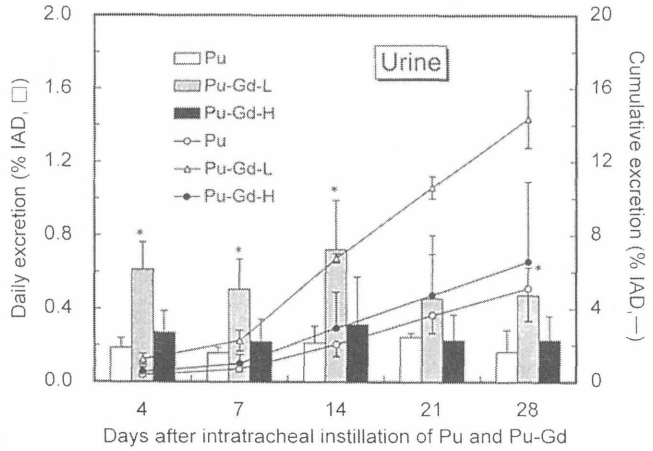

Fig. 4. Daily and cumulative excretion of ^{239}Pu in urine following intratracheal instillation of ^{239}Pu-hydroxide, Pu-Gd-L, and Pu-Gd-H. Vertical bar shows SD of three rats. * denotes significant difference from ^{239}Pu-hydroxide group at $p < 0.05$.

macrophages were observed in the rats administered Pu-Gd-L and ^{239}Pu-hydroxide.

DISCUSSION

In the respiratory tract model, the clearance of ^{239}Pu from the lung following acute intake of ^{239}Pu-hydroxide is about 50% a month after intake. The daily excretion of plutonium into feces reaches a maximum 2 d after intake and then declines. The level of daily fecal excretion declines slowly from about 10 d after intake. The daily excretion of plutonium into urine reaches a maximum 1 d after intake and then declines continuously (ICRP 1988). In this study, the clearance of plutonium from the lung of rats was faster than the ICRP model and 75% IAD was cleared 4 wk after administration. The daily excretion of

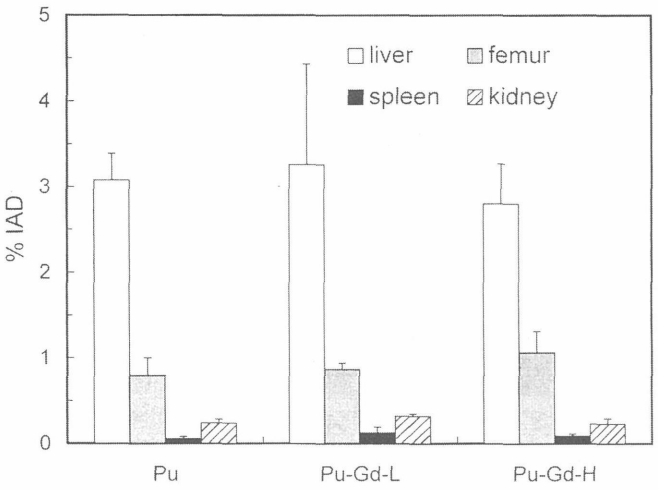

Fig. 5. Translocation of ^{239}Pu from lung to other organs following intratracheal instillation of ^{239}Pu-hydroxide, Pu-Gd-L, and Pu-Gd-H. Vertical bar shows SD of three rats.

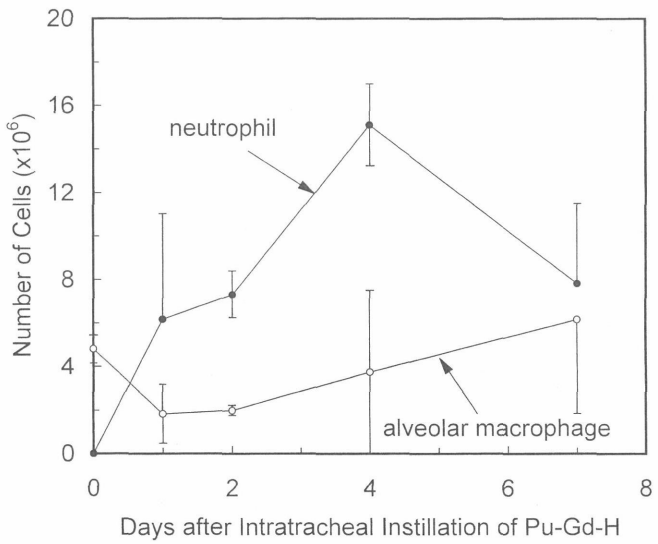

Fig. 6. Time-course changes in the number of alveolar macrophages and neutrophils in the bronchoalveolar lavage cells following intratracheal instillation of Pu-Gd-H. Data represent mean±SD of three rats. The data at day 0 represent the number of cells in non-treated rats.

plutonium in feces from 2 to 4 wk after administration was a constant to very little in variation. This excretion pattern is very similar to the ICRP model. The differences in the daily excretion of plutonium into urine was small; that is, the level of daily excretion was similar throughout the experimental period.

The alveolar clearance of inhaled particles depends on many factors, including the physicochemical characteristics of particles such as size and solubility, as well as the physiological and pathological conditions of the animals (ICRP 1994). The present study demonstrated that the clearance of ^{239}Pu from the lung was slower in the rats instilled with ^{239}Pu-hydroxide containing a high level of gadolinium (Pu-Gd-H) than those instilled with pure ^{239}Pu-hydroxide. It is well known that plutonium nitrate forms hydroxide colloids at near neutral pH, and the physicochemical properties of the resultant colloid particles are affected by reaction conditions including pH, concentration of plutonium, co-existing substances and ionic strength of the solution (Ockenden and Welch 1956; Lindenbaum and Westfall 1965). Therefore, it is likely that the physicochemical properties were different between the Pu-Gd-H and pure ^{239}Pu-hydroxide and that this difference was responsible for the different clearance rate of plutonium from the lung.

Another possible cause of the slower clearance of ^{239}Pu in the rats administered Pu-Gd-H colloids may be the gadolinium-induced inflammation in the lung. There are a few reports indicating that gadolinium is toxic for respiratory cells, especially for alveolar macrophages, and induces acute inflammatory pneumonia (Yoneda et al. 1995; Mizgerd et al. 1996). The number of alveolar macrophages decreased during the first 2 d after the instillation, and then gradually increased in the Pu-Gd-H group (Fig. 6). This pattern of change in the number of alveolar macrophages was a similar finding observed in the pulmonary inflammation after gadolinium administration (Yoneda et al. 1995). The increase in the number of neutrophils in bronchoalveolar lavage apparently indicated that an acute lung inflammation was induced in the Pu-Gd-H group in the present study.

A number of studies have demonstrated that inflammatory reactions in the lung retarded the alveolar clearance of inhaled particles (Sanders et al. 1975; Kubota et al. 1988; Slauson et al. 1989; Benson et al. 1995). For example, Sanders et al. (1975) have reported that the clearance of plutonium from the lungs of rats was decreased to 60% of the normal rate in animals with acute pneumonia induced by beryllium oxides. The authors have also shown that delayed type-hypersensitive pneumonia impaired the alveolar clearance mechanisms of inhaled ^{198}Au-colloid particles in rats (Kubota et al. 1988). Initial pulmonary deposition of ^{198}Au-colloid was decreased in DTH rats, but in this study IAD/instilled ratio was not different among the 3 groups; that is, the initial deposition of Pu-hydroxide was not affected by Gd. The clearance of particles is impaired not only in acute but also chronic inflammation. It has been reported that clearance of particles from the lung is delayed in chronic airway disease, chronic bronchitis or pulmonary fibrosis (Camner et al. 1973; Bohning et al. 1982).

In the human respiratory tract model, the clearance rate of particles from bronchial and bronchiolar regions of the lungs in asthma, chronic bronchitis, and *mycoplasma pneumonia* are assumed 70, 50, and 30% of normal, respectively (ICRP 1994). Therefore, it appears that inflammatory reactions induced in the lung by gadolinium may be, at least in part, responsible for the delayed clearance of ^{239}Pu from the lung. Neither the lung retention of ^{239}Pu nor the population of bronchoalveolar lavage cells changed significantly in the rats

administered ^{239}Pu-hydroxide containing a low level of gadolinium (Pu-Gd-L group). This may indirectly indicate the relationship between the inflammation and delayed alveolar clearance of plutonium by gadolinium.

The urinary excretion of ^{239}Pu only increased in this Pu-Gd-L group. This may suggest the occurrence of some metabolic disturbance in the respiratory tract, but the detailed mechanisms of such a phenomenon are unclear.

The doses of gadolinium used here were 0.9 and 0.22 mg kg^{-1} body weight for Pu-Gd-H and Pu-Gd-L groups, respectively. These doses are deemed to be relevant to those exposed in a practical setting under the following conditions. The solution in nuclear fuel reprocessing in the Japanese facility contains 0.7% of gadolinium, and it is supposed that this solution is released as aerosol into the environment, it would contain 5 g water m^{-3} air, which corresponds to a dense fog (Green and Lane 1964). If the reference man breathing under a working physiological condition is exposed to the gadolinium aerosol, he will inhale 0.9 and 0.22 mg kg^{-1} body weight in 40 min and 10 min, respectively. This indicates that in the case of accidental exposure, there is a possibility that workers may be exposed to levels of gadolinium used in this study.

CONCLUSION

The present study demonstrates that the coexistence of gadolinium may influence the alveolar clearance of plutonium administered as a hydroxide colloid, although the exact mechanisms remain unclear. This indicates that when plutonium is inhaled accidentally with gadolinium and the inhaled amount of gadolinium is so high that an inflammatory reaction is induced and the physicochemical properties of plutonium hydroxide is changed, the lung retention of plutonium and thus the radiation dose in lung may become larger than in ordinary cases.

REFERENCES

Benson, J. M.; Chang, I-Y.; Cheng, Y. S.; Hahn, F. F.; Kennedy, C. H.; Barr, E. B.; Maples, K. R.; Snipes, M. B. Particle clearance and histopathology in lungs of F344/N rats and B6C3F$_1$ mice inhaling nickel oxide or nickel sulfate. Fundam. Appl. Toxicol. 28:232–244; 1995.

Black, R. M.; Drummond, J. L. A comparison of procedures for dissolving ignited plutonium oxides for analysis. Warrington, U.K.: The Reactor Group; TRG report 1072(D):1–9; 1965.

Bohning, D. E.; Atkins, H. L.; Cohn, S. H. Long-term particle clearance in man: Normal and impaired. Ann. Occup. Hyg. 26:259–271; 1982.

Camner, P.; Mossberg, B.; Philipson, K. Tracheobronchial clearance and chronic obstructive lung disease. Scand. J. Respir. Dis. 54:272–281; 1973.

Green, H. L.; Lane, W. R. Aerosol in nature. In: Particulate clouds: Dusts, smokes and mists, 2nd Ed. London: E & F. N. Spon Ltd.; 1964: 410–439.

Hirano, S.; Suzuki, K. T. Exposure, metabolism, and toxicity of rare earth and related compounds. Environ. Health Perspect. 104:85–95; 1996.

International Commission on Radiological Protection. Monitoring data for individual radionuclides: Plutonium. In: Individual monitoring for intakes of radionuclides by workers: Design and interpretation. Oxford: Pergamon Press; ICRP Publication 54, Appendix; Ann. ICRP 19(1–3); 1988: 237–273.

International Commission on Radiological Protection. Clearance of particles from the respiratory tract. In: Human respiratory tract model for radiological protection. Oxford: Pergamon Press; ICRP Publication 66, Annex E; Ann. ICRP 24(1–3); 1994: 301–413.

Ishigure, N.; Nakano, T.; Enomoto, H.; Fukuda, S.; Iida, H.; Oghiso, Y.; Sato, H.; Takahashi, S.; Yamada, Y.; Koizumi, A.; Yamada, Y.; Miyamoto, K.; Inaba, J. Lung retention of Pu following inhalation of PuO_2 in rats measured using whole body counter. J. Radiat. Res. 35:16–25; 1994.

Keough, R. F.; Powers, G. J. Determination of plutonium in biological materials by extraction and liquid scintillation counting. Anal. Chem. 42:419–421; 1970.

Kubota, Y.; Takahashi, S.; Sato, H.; Yamada, Y.; Matsuoka, O. Pulmonary deposition and clearance of inhaled or instilled ^{198}Au-colloid in the rat after the induction of pulmonary delayed type sensitivity reactions. Hoken Butsuri 23:295–302; 1988.

Lindenbaum, A.; Westfall, W. Colloidal properties of plutonium in dilute aqueous solution. Int. J. Appl. Rad. Isotopes 16:545–553; 1965.

Mizgerd, J. P.; Molina, R. M.; Stearns, R. C.; Brain, J. D.; Warner, A. E. Gadolinium induces macrophage apoptosis. J. Leukoc. Biol. 59:189–195; 1996.

Ockenden, D. W.; Welch, G. A. The preparation and properties of some plutonium compounds. Part V. Colloidal quadrivalent plutonium. J. Chem. Soc. 3358–3363; 1956.

Oghiso, Y.; Yamada, Y.; Ishigure, N.; Fukuda, S.; Iida, H.; Yamada, Y.; Sato, H.; Koizumi, A.; Inaba, J. High incidence of malignant lung carcinomas in rats after inhalation of $^{239}PuO_2$ aerosol. J. Radiat. Res. 35:222–235; 1994.

O'Neill, P. J.; Ayala, A.; Wang, P.; Ba, Z. F.; Morrison, M. H.; Schultze, A. E.; Reich, S.; Chaudry, I. H. Role of Kupffer cells in interleukin-6 release following trauma-hemorrhage and resuscitation. Shock 1:43–47; 1994.

Runge, V. M.; Parker, J. R. Worldwide clinical safety assessment of gadoteridol injection: an update. Eur. J. Radiol. 7:243–245; 1997.

Ruttinger, D.; Vollmar, B.; Wanner, G. A.; Messmer, K. *In vivo* assessment of hepatic alterations following gadolinium chloride-induced Kupffer cell blockade. J. Hepatol. 25:960–967; 1996.

Sanders, C. W.; Cannon, W. C.; Powers, G. J.; Adee, R. R.; Meier, D. M. Toxicology of high-fired beryllium oxide inhaled by rodents I. Metabolism and early effects. Arch. Environ. Health 30:546–551; 1975.

Sato, H.; Bulman, R. A.; Takahashi, S.; Kubota, Y. Effects of macromolecular chelating agents on the release of ^{239}Pu and ^{59}Fe from rat alveolar macrophages after phagocytic uptake of ^{239}Pu-^{59}Fe-iron hydroxide colloid. Health Phys. 66:545–549; 1994.

Slauson, D. O.; Lay, J. C.; Castleman, W. L.; Neilsen, N. R. Acute inflammatory lung injury retards pulmonary particle clearance. Inflammation 13:185–199; 1989.

Suzuki, S.; Nakamura, S.; Serizawa, A.; Sakaguchi, T.; Konno, H.; Muro, H.; Kosugi, I.; Baba, S. Role of Kupffer cells and

the spleen in modulation of endotoxin-induced liver injury after partial hepatectomy. Hepatology 24:219–225; 1996.

Takahashi, S.; Sato, H. New method to estimate the solubility of radioactive particles in the respiratory tract: Comparison of solubility between ^{59}Fe- ^{239}Pu-hydroxide colloid particles. Hoken Butsuri 26:351–353; 1991.

Weinmann, H. J.; Brasch, R. C.; Press, W. R.; Wesbey, G. E. Characterization of gadolinium-DTPA complex: a potential NMR contrast agent. Am. J. Roentgenol. 142:619–624; 1984.

Yoneda, S.; Yoneda, N.; Emi, Y.; Fujita, M.; Ohmichi, S.; Hirano, S.; Suzuki, K. T. Effects of gadolinium chloride on the rat lung following intratracheal instillation. Fundam. Appl. Toxicol. 28:65–70; 1995.

■ ■

J. RADIAT. RES., 43, 301–311 (2002)

Immunohistochemical Study on Cellular Origins of Rat Lung Tumors Induced by Inhalation Exposures to Plutonium Dioxide Aerosols as Compared to Those by X-ray Irradiation

YOICHI OGHISO[1]* and YUTAKA YAMADA[1]

Immunohistochemistry / Rat / Lung tumors / Plutonium-exposure / X-irradiation

Immunohistochemical examinations were performed on rat pulmonary tumors induced by inhalation exposures to $^{239}PuO_2$ aerosols, or by X-ray-irradiation to identify and compare cellular origins or, in turn, target cells at risk for radiation carcinogenesis. Both plutonium-induced and X-ray-induced pulmonary tumors appeared to occur from the lower respiratory tract epithelium through bronchioles into alveoli, and were histopathologically diagnosed as adenoma, adenocarcinoma, adenosquamous carcinoma, and squamous cell carcinoma. Immunohistochemical staining of neoplastic lesions using rabbit polyclonal antibodies to rat surfactant apoprotein A specific for alveolar type II pneumocytes, and Clara cell antigen specific for nonciliated bronchiolar Clara cells, showed that most of the adenomatous and adenocarcinomatous lesions from plutonium-exposed or X-irradiated rats were positive for either or both antigens, while, in contrast, adenosquamous and squamous lesions were mostly negative for both antigens. Even though there were some differences in the proportions and distributions of immunoreactive cells between plutonium- and X-ray-induced tumors and among neoplastic lesions, the results indicate that radiation-induced pulmonary adenomas and adenocarcinomas mostly originate from either alveolar type II pneumocytes or bronchiolar Clara cells, while adenosquamous and squamous carcinomas may be derived from the other epithelial cell components, or might have lost specific antigenicity during their transforming differentiation.

INTRODUCTION

In risk assessments of radiation carcinogenesis, it is essentially important to identify the cellular origins of radiation-induced tumors for determining target cells at risk, and for more accurate dose estimation to induce neoplastic changes in the most sensitive cells.

*Corresponding author: Phone: + 81 43 206 3100
FAX: +81 43 284 1389
e-mail: y_oghiso@nirs.go.jp
[1] Internal Radiation Effects Research Group, Research Center for Radiation Safety, National Institute of Radiological Sciences, 9–1, 4-chome, Anagawa, Inage-ku, Chiba 263–8555, Japan

In our previous studies on pulmonary carcinogenesis in rats following inhalation exposures to an alpha-emitting radionuclide, $^{239}PuO_2$ aerosols, most predominantly induced primary lung tumors were epithelial types derived from the lower respiratory tract epithelium through bronchioles into alveoli, such as adenomas and adenocarcinomas, or, to a lesser degree, adenosquamous and squamous cell carcinomas[1)]. Initial pulmonary damage of the bronchioloalveolar lining epithelium resulted in hyperplastic and metaplastic lesions that finally transformed to adenomas and adenocarcinomas in 6–12 months after inhalation exposures[2)]. Such findings implicate that the majority

of lung tumors from the lower respiratory tract epithelium originate from nonciliated bronchiolar Clara cells and/or alveolar type II pneumocytes as described to be radiosensitive precursor cells at risk for lung tumors[3,4]. It is, however, still uncertain or controversial what types of cells are the origins of experimentally induced pulmonary epithelial tumors, and whether there are any differences in the cellular origins of tumors among radiation sources and chemical carcinogens for the initiation and/or promotion of tumors. Concerning the cellular origins of plutonium-induced rat lung tumors, Clara cells appear to be possible target cells for histogenesis of bronchogenic or bronchioloalveolar carcinomas by light and electron microscopic studies[5,6], whereas immunohistochemistry combined with electron microscopy of both preneoplastic and neoplastic lesions implied more clearly the major origin of lung tumors from type II pneumocytes[7]. Although such differences in demonstration and estimation of cellular origins are resulted from the methodological approach, they could also be based on the pulmonary deposition of inhaled aerosols, and the dose distribution throughout the respiratory system, which is dependent on the aerosol particle size and physicochemical states of inhaled plutonium[1,3,4]. Thus, submicron-sized aerosols tend to deposit in the lower respiratory tract regions, *i.e.* bronchial-bronchiolar to alveolar epithelium, which should be most likely to be targetted by alpha particles, while a more soluble form of inhaled aerosols could be distributed more uniformly in the whole lung lobes, so that target cells should be more widely distributed from bronchial to alveolar epithelium. In addition, the susceptibility of target cells for radiation carcinogenesis could affect phenotypic clonalities and differentiation of tumor cells, although this has not yet been clarified.

In the present study, we performed immunohistochemical examinations on primary lung tumors from $^{239}PuO_2$-exposed rats to detect either a type II cell- or a Clara cell-specific antigen, and compared the pattern of positive staining and the distribution of antigens with those of X-ray-induced primary lung tumors. The results are discussed on the cellular origins of radiation-induced lung tumors, as compared to the previous data including human and experimentally induced lung tumors.

MATERIALS AND METHODS

Animals

Female Wistar (W/M) strain rats, purchased from a breeding colony of the National Institute of Radiological Sciences, were used for either inhalation exposures to plutonium dioxide aerosols or X-ray-irradiations at the age of 100 to 120 days after birth. Before and after the experiments, animals were housed 5 per polycarbonate cage and kept under a barrier-filtered air condition with a commercial diet (Funabashi Farm Co.) and water *ad libitum*. The animal rooms were maintained on a 12-hr light:dark cycle at 23±1.0°C with a humidity of 55±5.0%. The animal care included a weekly change of cages and a daily check of the animals' conditions during their lifetimes. All the experimental treatments were performed with the approval of the institution's animal use committee.

Experimental Treatments

For inhalation exposures to plutonium(Pu) aerosols, nose-only inhalation exposures to submicron-sized and polydispersed aerosols (AMAD of 0.40±0.005 μm with GSD of 2.2±0.1 μm) of high-fired $^{239}PuO_2$ were performed to achieve an initial lung deposition of 30 to 3000 Bq and a mean absorbed lung dose of 0.5 to 12 Gy, as previously described[1,2]. The mean survival time (day) ± SD and the mean lung dose (Gy) ± SD of Pu-exposed rats selected for immunohistochemical examinations on lung tumor specimens were 728±159 and 3.38±2.23 (n=135), respectively. For X-ray-irradiations, either whole-body, fractionated irradiations with a dose rate of 0.1 Gy/min or local (thoracic), single irradiations with a dose rate of 0.6 Gy/min were performed under the condition of 200 keV and 10–20 mA, with a filter of 0.5 Cu and 0.5 Al and with FSD of 75–100 cm using Pantak HF 320S (Shimadzu) to achieve an accumulated dose of 0.5 to 10 Gy (unpublished). The mean survival time (day) ±

Table 1. List of the numbers and histopathological types of lung tumors examined.

Lung tumor types	Pu-exposed	X-irradiated*
Adenoma (AD)	14	17 (3+14)
Adenocarcinoma (AC)	65	18 (9+ 9)
Adenosquamous carcinoma (ASC)	37	1 (1+ 0)
Squamous cell carcinoma (SCC)	19	5 (0+ 5)
Total	135	41 (13+28)

* No. of cases from whole body irradiations(left) and local (thoracic) irradiations(right), respectively in parenthesis

SD and the mean lung dose(Gy) ± SD of both whole-body and local X-irradiated rats selected for immunohistochemical examinations on lung tumor specimens were 718±131 and 5.60±3.07 (n=41), respectively.

Histopathological Examinations

All of the dead or moribund and sacrificed animals were autopsied, and the main organs, including the lungs, were fixed in 10% phosphate-buffered formalin, dehydrated, and embedded in paraffin. Then, 5-μm-thick serial sections were prepared from each lobe, and one of them was stained with hematoxylin and eosin (HE) to be examined under a light microscope for histopathological diagnoses of primary lung tumors, as previously described[1,2]. Almost all histopathological types of lung tumors from both Pu-exposed and X-irradiated rats were epithelial types, being classified into adenoma (AD), adenocarcinoma (AC), adenosquamous carcinoma (ASC) and squamous cell carcinoma (SCC). In the present study, only lung tumor specimens with little postmortem changes were selected from Pu-exposed and X-irradiated rats for immunohistochemical staining; each of the numbers and diagnoses of histopathological types are as given in Table 1.

Immunohistochemistry

Immunohistochemical staining of lung tumors selected from both Pu-exposed and X-irradiated rats was performed using an avidin-biotin-immunoperoxidase complex (ABC) method (Vectastain ABC kit, Vector Laboratories, Burlingame, CA) with rabbit polyclonal antibodies to either surfactant apoprotein A(SP-A) specific for rat type II pneumocytes[8] and rat Clara cell 10-kd protein (CC-10) specific for nonciliated terminal bronchiolar Clara cells[9], both of which were courteously given by Dr. Gurmukh Singh, University of Pittsburgh, PA. Briefly, unstained 5-μm-thick paraffin sections were deparaffinized with xylen and graded ethanol, rehydrated, and pretreated with 0.3% hydrogen peroxide in methanol at room temperature for 30 min to inactivate the endogenous peroxidase activity. After washing with 0.05% Tris (pH 7.6)-buffered saline (TBS), sections were incubated with normal goat serum at room temperature for 1 hr to block any nonspecific Fc-binding of a secondary antibody, and then incubated with each of the primary antibodies (SP-A diluted 1:200 and CC-10 diluted 1:400) at 4°C for overnight. After washing with TBS, sections were reacted with biotinylated secondary goat anti-rabbit IgG antibody at room temperature for 1 hr, and then coupled with ABC at room temperature for 30 min. After washing with TBS, sections were treated with the substrate, 3,3'-diaminobenzidine tetrachloride (DAB), to visualize the immunoreactivity, and counterstained with hematoxylin. As negative controls, other sections were only incubated with normal rabbit serum instead of primary antibodies under conditions similar to those described above. As positive controls, normal alveolar epithelium and the terminal bronchiole surrounding neoplastic lesions of the stained sections were examined respectively for the staining reactivity of type II pneumocytes and Clara cells. Actually, almost all normal alveolar type II and bron-

chiolar Clara cells, respectively, showed strongly diffuse or granular staining patterns within their cytoplasms, while most neoplastic lesions were variably stained, with slight to moderate intensity, with weakly and partly positive patterns, and at almost negligible levels. Thus, to evaluate immunostaining with SP-A and CC-10, each neoplastic lesion was observed with a light microscope to detect and assess the immunoreactivity based on the following criteria: (–) as negative staining in 90% or more, and (+) as positive staining in 20% or more of at least 2,000 neoplastic cells randomly counted in 20 high-power (×400) fields. All the neoplastic lesions were finally classified into SP-A or CC-10 single positive ($SP\text{-}A^{+}/CC\text{-}10^{-}$ or $SP\text{-}A^{-}/CC\text{-}10^{+}$), double positive ($SP\text{-}A^{+}/CC\text{-}10^{+}$) or double negative ($SP\text{-}A^{-}/CC\text{-}10^{-}$).

RESULTS

Morphological and Immunohistochemical Appearances of Neoplastic Lesions

As described above, all the neoplastic lesions examined on the selected lung tumor specimens from both Pu-exposed and X-irradiated rats were classified into four histological types: adenoma (AD), adenocarcinoma (AC), adenosquamous carcinoma (ASC) and squamous cell carcinoma (SCC). The morphological appearance of each neoplastic lesion was similar in both Pu-exposed and X-irradiated rats; however, the number and size of lesions distributed in the lung were smaller in X-irradiated rats than in Pu-exposed rats, and were larger under local (thoracic) X-irradiations than under whole-body X-irradiations (data not shown). Ductal and papillary forms of AD lesions were most predominantly located in peripheral, and subpleural, or peribronchiolar regions. AC lesions were mostly ductal and papillary, but partly solid and compact, and were distributed more extensively from peripheral and subpleural regions into deep bronchial-bronchiolar and alveolar regions than AD lesions. ASC lesions, showing solid and compact features, were more frequently distributed in peribronchial or peribronchiolar regions adjacent to AC lesions, whereas SCC lesions, with larger nodules with amounts of keratin and necrotic cellular debris in the center, appeared to extend widely from the bronchial-bronchiolar regions into the peribronchial and alveolar regions. In many lung tumors from Pu-exposed rats, there were mixed neoplastic foci, or sometimes transitional areas, between AD and AC, AC and ASC, or ASC and SCC lesions in one tumor specimen. The immunohistochemical staining was variable among histological types of neoplastic lesions in lung tumors from both Pu-exposed and X-irradiated rats. Although an overall comparison of immunohistochemical staining could not be done between whole-body and local (thoracic) X-irradiations because of fewer numbers of lung tumor types examined, different staining patterns were not observed in AD and AC lesions between two irradiation patterns. Both AD and AC lesions with papillary or ductal forms were weakly to mildly positive for diffuse or granular cytoplasmic staining with either SP-A or CC-10 (Figs. 1B, 1D, 2B, & 2D), and solid forms of AC lesions were weakly and diffusely stained with SP-A. On some occasions of papillary AD and AC lesions, double positive, but weak and diffuse, staining with both SP-A and CC-10 was observed in the same neoplastic lesions (Figs. 1F & 1G). However, most ASC and SCC lesions in the lung tumors from Pu-exposed and X-irradiated rats were negatively stained with SP-A and CC-10, as compared to the intensities of positive staining of AD and AC lesions, and normal alveolar and bronchiolar epithelial cells detectable in the same histological specimens (data not shown). Only some of ASC lesions from Pu-exposed rats showed weak and diffuse immunostaining with SP-A or CC-10 (data not shown).

Patterns and Distribution of SP-A and CC-10 Immunostaining in Neoplastic Lesions

All the neoplastic lesions examined were classified into four patterns of immunostaining as single or double positive, and double negative for SP-A and CC-10. The distribution of each immunostaining pattern was expressed as the percentage in the total numbers of neoplastic lesions per each histological type in lung tumors from both Pu-exposed and X-irradiated

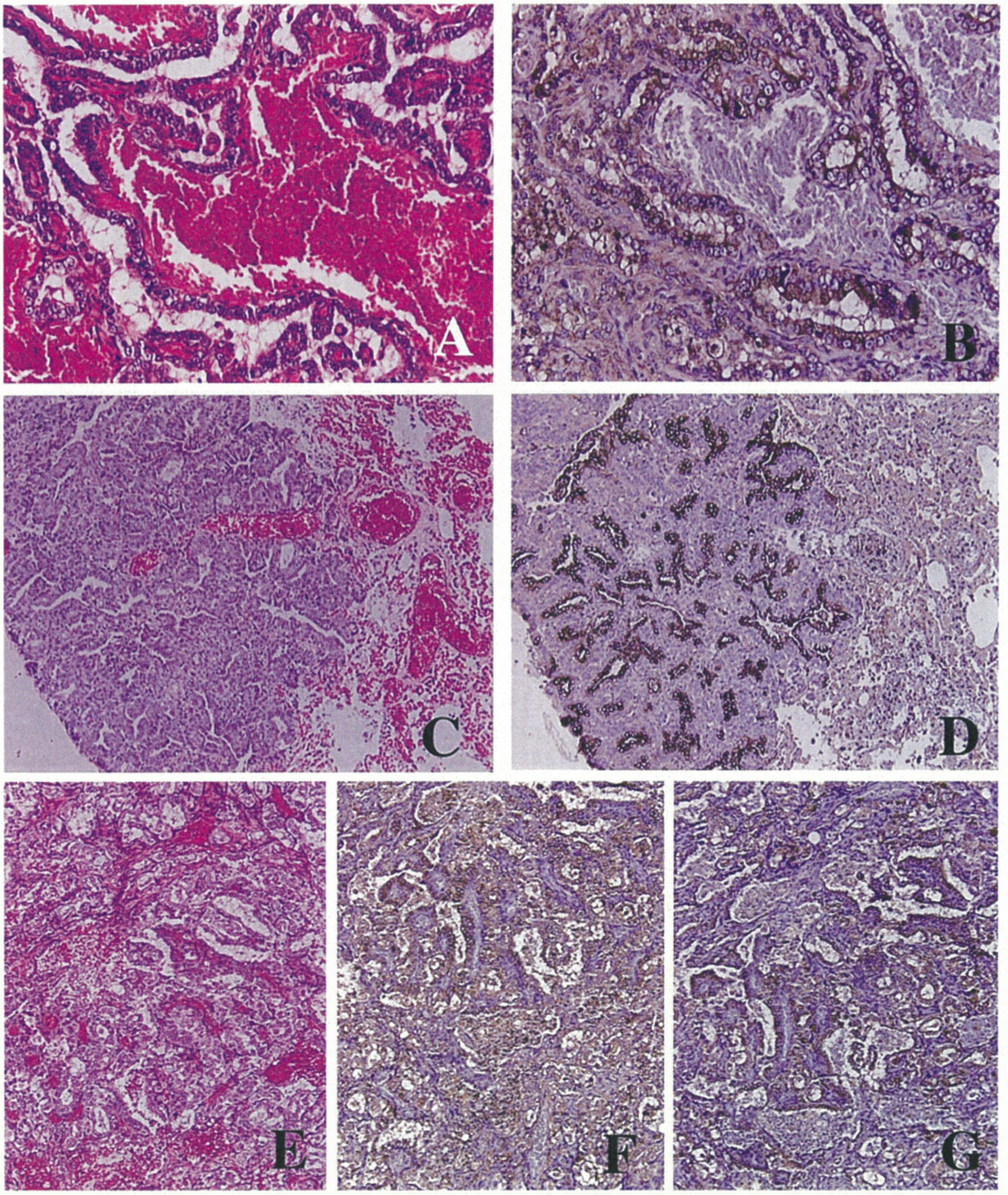

Fig. 1. Light microscopy of $^{239}PuO_2$-induced rat lung tumors. Papillary adenoma stained with HE (A), and its positive immunostaining with SP-A antibody (B). Ductal adenocarcinoma stained with HE (C) and its positive immunostaining with CC-10 antibody (D). Papillary adenoma stained with HE (E), and its positive immunostaining with SP-A antibody (F) and CC-10 antibody (G).

rats (Table 2). In the lung tumors from Pu-exposed rats, 56% (59 out of 105 neoplastic lesions examined) of the AD lesions showed double positive staining with both SP-A and CC-10, while either 19% (20 out of 105) or 23% (24 out of 105) of AD lesions was SP-A or CC-10 single positive, respectively. A similar trend, but slightly different distribution of immunostaining patterns, was noted for AC lesions of lung tumors from Pu-exposed rats; almost half, 46% (54 out of 118), of the AC lesions were SP-A single positive and 36% (43 out of 118) were SP-A and CC-10 double positive, while only 10% (12 out of 118) were

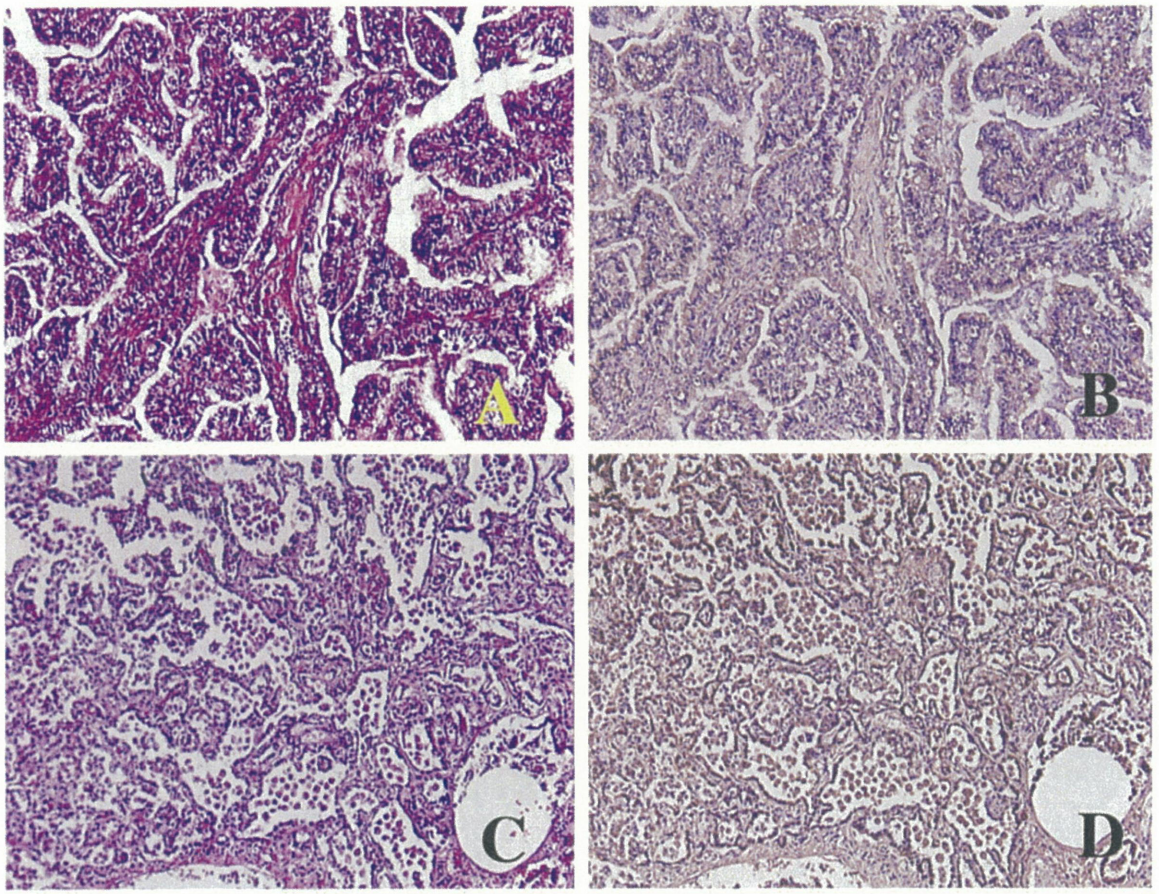

Fig. 2. Light microscopy of X-ray-induced rat lung tumors. Papillary adenocarcinoma stained with HE (A), and its positive immunostaining with SP-A antibody (B). Ductal and papillary adenoma stained with HE (C) and its positive immunostaining with CC-10 antibody (D).

CC-10 single positive. On the other hand, most of the ASC (77%) and SCC (96%) lesions were SP-A and CC-10 double negative, except that 15% (9 out of 58) of the ASC lesions were SP-A single positive, and only 5% (3 out of 58) of ASC lesions were CC-10 single positive. Only 3.8% (2 out of 52) of the SCC lesions were SP-A single positive. In the lung tumors from X-irradiated rats, almost a third to a half, 37% (19 out of 51) and 43% (22 out of 51) of the AD lesions were CC-10 single positive or SP-A and CC-10 double positive, respectively, while 63% (22 out of 35) of AC lesions were SP-A and CC-10 double positive (Table 2). The remaining 10 to 14% each of the AD and AC lesions showed either single positive or double negative staining with SP-A and CC-10. All of the ASC and SCC lesions, in contrast, showed double negative staining with SP-A and CC-10, although the total numbers of ASC and SCC lesions examined were fewer than those of the AD and AC lesions. Such differences in the distribution of the immunostaining patterns among histological types of neoplastic lesions and between lung tumors from Pu-exposed and X-irradiated rats were more clearly shown by expressing as either SP-A or CC-10 positive lesions (Fig. 3). Thus, in lung tumors from Pu-exposed rats, almost 75% to 80% of the AD lesions were either SP-A or CC-10 positive, and 82% of the AC lesions were SP-A positive, while 47% of the AC lesions were CC-10 positive (Fig. 3A). In lung tumors from X-irradiated rats, 53% to 80% of the AD lesions showed SP-A or CC-10 positive staining, respectively, while almost two-thirds, 74% of the AC lesions were positive with SP-A or CC-10 (Fig. 3B). Taking into account for the differences in both findings, the AD lesions from X-irradiated rats appeared to be CC-10 positive, while the AC lesions from Pu-exposed rats preferentially showed SP-A pos-

Table 2. Immunostaining of pulmonary neoplastic lesions from $^{239}PuO_2$-exposed and X-irradiated rats.

$^{239}PuO_2$-exposed rats					
Neoplastic lesions examined		SP-A/CC-10 immunostaining (%)[a]			
Histological types	No.	+/–	+/+	–/+	–/–
Adenoma	105	20 (19.0)	59 (56.2)	24 (22.9)	2 (1.9)
Adenocarcinoma	118	54 (45.8)	43 (36.4)	12 (10.2)	9 (7.6)
Adenosquamous carcinoma	58	9 (15.5)	1 (1.7)	3 (5.2)	45 (77.6)
Squamous cell carcinoma	52	2 (3.8)	0 (0)	0 (0)	50 (96.2)
X-irradiated rats					
Neoplastic lesions examined		SP-A/CC-10 immunostaining (%)[a]			
Histological types	No.	+/–	+/+	–/+	–/–
Adenoma	51	5 (9.8)	22 (43.1)	19 (37.3)	5 (9.8)
Adenocarcinoma	35	4 (11.4)	22 (62.9)	4 (11.4)	5 (14.3)
Adenosquamous carcinoma	5	0 (0)	0 (0)	0 (0)	5 (100)
Squamous cell carcinoma	5	0 (0)	0 (0)	0 (0)	5 (100)

[a] No. of lesions with SP-A single positive (+/–), CC-10 single positive (–/+), SP-A and CC-10 double positive (+/+) or double negative (–/–) staining, and percentage in total numbers of each neoplastic lesion examined in parenthesis.

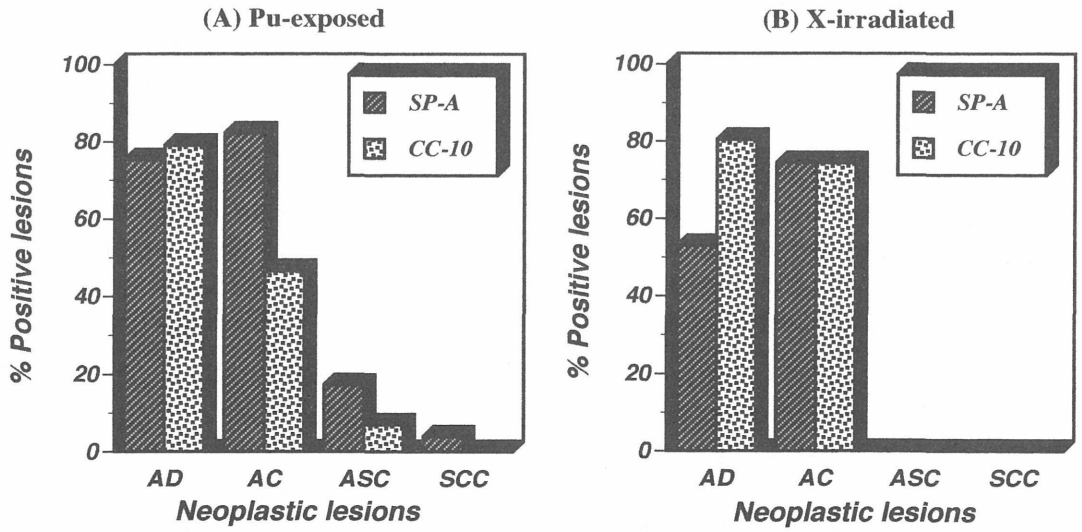

Fig. 3. Distribution of SP-A positive and CC-10 positive neoplastic lesions in rat lung tumors induced by inhalation exposures to $^{239}PuO_2$ (A) and by X-ray-irradiation (B). The columns indicate the percentage of neoplastic lesions positively stained with either SP-A or CC-10 antibody in the number of each neoplastic lesion showing adenoma (AD), adenocarcinoma (AC), adenosquamous carcinoma (ASC), and squamous cell carcinoma (SCC).

itive staining. Contrary to this, the AD lesions from Pu-exposed rats and the AC lesions from X-irradiated rats almost equally showed highly positive staining with both SP-A and CC-10. Except for SP-A positive staining (17%) of ASC lesions in lung tumors from Pu-exposed rats, most or all of the ASC and SCC lesions from both Pu-exposed and X-irradiated rats showed negative staining with both SP-A and CC-10

(Fig. 3A&B). These results indicate that the AD and AC lesions were mostly SP-A and/or CC-10 positive in radiation-induced rat lung tumors, although some differences in the distribution of immunostaining patterns were present between lung tumors from Pu-exposed and X-irradiated rats. ASC and SCC lesions, however, showed nearly negative staining with SP-A or CC-10.

DISCUSSION

Our previous studies[1,2] have implicated that most pulmonary tumors induced in rats by inhalation exposures to submicron-sized and polydispersed $^{239}PuO_2$ aerosols were adenomas and adenocarcinomas, both of which were distributed in the lower pulmonary regions, and therefore thought to arise from the bronchioloalveolar lining epithelium, such as nonciliated bronchiolar Clara cells and/or alveolar type II pneumocytes. The present immunohistochemical analysis revealed that almost 80% of adenomas showed either type II cell or Clara cell origins, while the adenocarcinomas appeared to be derived from type II pneumocytes (Fig. 3A). These results differ from those of another study on plutonium-induced rat pulmonary tumors, which indicated a majority from type II pneumocytes with the exception of one adenosquamous carcinoma being positive and all the squamous cell carcinomas being negative for both a surfactant apoprotein and a Clara cell antigen[7]. Double positive staining with both type II and Clara cell antigens was also observed in our cases of adenomas and adenocarcinomas (56% and 36% respectively), suggesting that some parts of pulmonary tumors could concomitantly express both antigens in a certain differentiation state despite their origins either from type II or Clara cells. We supposed that most neoplastic cells became anaplastic toward immature embryonic stages; this, however, is not surprising because of evidence that embryonic murine type II pneumocytes and Clara cells are derived from the same stem cells[10]. Mason et al. [11] showed that only SP-C among a series of isotypic surfactant apoproteins was specific for type II cells in normal murine lungs, while the remaining SP-A, SP-B and SP-D apoproteins were expressed in both type II cells and CC-10 positive Clara cells. From these results, it may be indicated in the present study that SP-A single positive cells should be type II cells, while double positive cells and CC-10 single positive cells could be Clara cells under a differentiated, but also neoplastic state. Most of the adenosquamous and squamous cell carcinomas from Pu-exposed rats were negative for both antigens, except for only a small part (15%) of the adenosquamous carcinomas, which could be derived from type II cells. This suggests that the origins of pulmonary tumors characterized with squamous metaplasias should be cells other than type II and Clara cells, or that type II or Clara cell-specific antigens expressed during the onset of tumor cells may have disappeared under differentiation processes into other cell types[7]. The latter possibility is likely to occur during a transition in certain genetic and immunohistochemical components of human non-small cell pulmonary carcinomas among the adenocarcinomas, adenosquamous carcinomas and squamous cell carcinomas[12].

The present study also implied the cellular origins of X-ray-induced rat pulmonary tumors, although the total numbers examined were much fewer than those of Pu-induced tumors. As compared to Pu-induced pulmonary tumors, the only differences were in the proportions of SP-A and CC-10 positive lesions between adenomas and adenocarcinomas, as shown in Fig.3B. Almost 80% of the adenocarcinomas could originate from either type II or Clara cells, while the adenomas would be derived from Clara cells rather than type II cells. Such differences from those of Pu-induced tumors are not, however, significant because less than 14% of the adenomas or adenocarcinomas, and all of the adenosquamous and squamous cell carcinomas were double negative for both antigens. This suggests that most of the adenomas and adenocarcinomas from X-irradiated rats originate from either type II or Clara cells, and that adenosquamous and squamous cell carcinomas derive from other cell types, or have lost type II or Clara cell-specific antigenicity, as described above in Pu-induced tumors. Taken together

with those findings on the cellular origins of radiation-induced pulmonary tumors including ^{239}Pu[6,7] and other α-emitter, ^{210}Po[13], the cellular origins of bronchioloalveolar adenomas and adenocarcinomas from radiation-exposed animals are mostly type II pneumocytes and/or Clara cells. In this respect, both ICRP[3] and NCRP[4] have described these cells as being radiosensitive precursor cells at risk for radiation-induced lung tumors, but have not referred to the other cell types for the candidate origins of squamous cell carcinomas. In this regard, the upper respiratory tract epithelium could also be susceptible for radiation carcinogenesis based on the experimental evidence that rat tracheal epithelial cells showed a preneoplastic transformation *in vitro* by α- or γ-irradiations[14].

Numerous investigations of the cellular origins of chemically induced pulmonary tumors in small rodents have, however, resulted in controversy. Type II pneumocytes-derived lung tumors have been noted in N-nitrosomethylurea(NMU)-induced adenomas and carcinomas from F344 rats[15], N-nitrosodiethylamine (DEN)-induced adenomas and adenocarcinomas from B6C3F1 and A mice[16], or transplacentally N-nitrosoethylurea (ENU)-induced adenomas and carcinomas from C3H and Swiss mice[17], while a part of transplacentally ENU-induced bronchiolar papillary adenomas from Swiss mice[18], N-nitrosodiethylamine(NDEA)-induced bronchiolar carcinomas from syrian golden hamsters[19], and NMU- or ENU-induced bronchiolar squamous cell or adenosquamous carcinomas from Swiss mice[20] have been reported to originate from Clara cells. Such diversity concerning the cellular origins of chemically induced lung tumor models in animals may reflect the sensitivity of target epithelial cells, and their morphologic and biochemical plasticity after arising from multipotent stem cells, as have been referred to murine urethane-induced solid (type II cell) and papillary (Clara cell) adenomas[21,22]. It should be noted that there have also been descriptions on the type II cell-origins of human bronchioloalveolar carcinomas[23–25], while only a part of the bronchioloalveolar and squamous cell carcinomas appears to have phenotypic expression specific for Clara cells[26,27]. Since even human Clara cells as well as murine ones[11] could produce surfactant apoproteins, it may be plausible that some bronchioloalveolar carcinomas, even if they were originated from Clara cells, had lost the ability to produce Clara cell antigens, but, instead, increased the ability to produce surfactant apoproteins during their transformation[28]. Such phenotypic changes from Clara cells into type II cells, or the reverse could result in a variety of cellular origins of pulmonary tumors from experimental animals as well as humans.

In conclusion, except for the small differences in the proportions and distributions of type II or Clara cell antigens among neoplastic lesions from Pu-exposed and X-ray-irradiated rats, most of the radiation-induced pulmonary adenomas and adenocarcinomas originate from either alveolar type II pneumocytes or bronchiolar Clara cells, while the majority of adenosquamous and squamous cell carcinomas may be derived from the other epithelial cell components, or might have lost antigenicity specific for either type II or Clara cells during their transforming differentiation.

ACKNOWLEDGEMENTS

This research was partly supported by a research grant from Japan Ministry of Education, Culture, Science and Technology. The authors are grateful to all the laboratory staff for their technical assistance and support of animal care.

REFERENCES

1. Oghiso, Y., Yamada, Y., Iida, and Inaba, J. (1998) Differential dose responses of pulmonary tumor types in the rat after inhalation of plutonium dioxide aerosols. J. Radiat. Res. **39**: 61–72.
2. Oghiso, Y, and Yamada, Y. (2000) Pathogenetic process of lung tumors induced by inhalation exposures of rats to plutonium dioxide aerosols. Radiat. Res. **154**: 253–260.
3. ICRP (1994) Human Respiratory Tract Model for Radiological Protection, Publication 66, Annals of the ICRP **24** (**1–3**), Pergamon Press, Oxford.

4. NCRP (1997) Deposition, Retention and Dosimetry of Inhaled Radioactive Substances, Recommendations of the National Council on Radiation Protection and Measurements, NCRP Report **125**, NCRPM, Bethesda, MD.
5. Masse, R. (1980) Histogenesis of lung tumors induced in rats by inhalation of alpha emitters: an overview. In: Pulmonary Toxicology of Respirable Particles, CONF-791002, NTIS, US DOC, pp. 498–521, Springfiled, VA.
6. Sanders, C. L., McDonald, K. E., and Lauhala, K. E. (1988) Promotion of pulmonary carcinogenesis by plutonium particle aggregation following inhalation of $^{239}PuO_2$. Radiat. Res. **116**: 393–405.
7. Herbert, R. A., Stegelmeier, B. S., Gillet, N. A., Rebar, A. H., Carlton, W. W., Singh, G., and Hahn, F. F. (1994) Plutonium-induced proliferative lesions and pulmonary epithelial neoplasms in the rat: immunohistochemical and ultrastructural evience for their origin from type II pneumocytes. Vet. Pathol. **31**: 366–374.
8. Katyal, S. L., and Singh, G. (1979) An immunologic study of the apoproteins of rat lung surfactant. Lab. Invest. **40**: 562–567.
9. Singh, G., and Katyal, S. L. (1984) An immunologic study of the secretory products of rat Clara cells. J. Histochem. Cytochem. **32**: 49–54.
10. Ten Have-Opbroek, A. A. W., Dubbeldam, J. A., and Otto-Verberne, C. J. M. (1988) Ultrastructural features of type II alveolar epithelial cells in early embryonic mouse lung. Anat. Rec. **221**: 846–853.
11. Mason, R. J., Kalina, M., Nielsen, L. D., Malkinson, A. M., and Shannon, J. M. (2000) Surfactant protein C expression in urethane-induced murine pulmonary tumors. Am. J. Pathol. **156**: 175–182.
12. Kanazawa, H., Ebina, M., Ino-oka, N., Simizukawa, M., Takahashi, T., Fujimura, S., Imai, T., and Nukiwa, T. (2000) Transition from squamous cell carcinoma to adenocarcinoma in adenosquamous carcinoma of the lung. Am. J. Pathol. **156**: 1289–1298.
13. Kennedy, A. R., McGandy, R. B., and Little, J. B. (1977) Histochemical, light and electron microscopic study of polonium-210 induced peripheral tumors in hamster lungs: evidence implicating the Clara cell as the cell of origin. Eur. J. Cancer **13**: 1325–1340.
14. Poncy, J.-L., Kugel, C., Tourdes, F., and Bailly, I. (2002). *In vitro* radiation-induced effects on rat tracheal epithelial cells. II) Different preneoplastic cell transformation after α and γ irradiations. J. Radiat. Res. **43**: 35–42.
15. Ohshima, M., Ward, J. M., Singh, G., and Katyal, S. L. (1985) Immunocytochemical and morphological evidence for the origin of N-nitrosomethylurea-induced and naturally occurring primary lung tumors in F344/NCr rats. Cancer Res. **45**: 2785–2792.
16. Ward, J. M., Singh, G., Katyal, S. L., Anderson, L. M., and Kovatch, R. M. (1985) Immunocytochemical localization of the surfactant apoprotein and Clara cell antigen in chemically induced and naturally occurring pulmonary neoplasms of mice. Am. J. Pathol. **118**: 493–499.
17. Rehm, S., Ward, J. M., Ten Have-Opbroek, A. A. W., Anderson, L. M., Singh, G., Katyal, S. L., and Rice, J. M. (1988) Mouse papillary lung tumors transplacentally induced by N-nitrosoethylurea: evidence for alveolar type II cell origin by comparative light microscopic, ultrastructural, and immunohistochemical studies. Cancer Res. **48**: 148–160.
18. Kauffman, S. L., Alexander, L., and Sass, L. (1979) Histologic and ultrastructural features of the Clara cell adenoma of th mouse lung. Lab. Invest. **40**: 708–716.
19. Rehm, S., Takahashi, M., Ward, J. M., Singh, G., Katyal, S. L., and Henneman, J. R. (1989) Immunohistochemical demonstration of Clara cell antigen in lung tumors of bronchiolar origin induced by N-nitrosodiethylamine in syrian golden hamsters. Am. J. Pathol. **134**: 79–87.
20. Rehm, S., Lijinsky, W., Singh, G., and Katyal, S. L. (1991) Mouse bronchiolar cell carcinogenesis. Histologic characterization and expression of Clara cell antigen in lesions induced by N-nitrosobis-(2-chloroethyl)ureas. Am. J. Pathol. **139**: 413–422.
21. Malkinson, A. M. (1991) Mouse pulmonary carcinogenesis: a symposium to honor the memory of Dr. Michael B. Shimkin. Cancer Res. **51**: 450–453.
22. Forkert, A., Parkinson, P. G., Thaete, L. G., and Malkinson, A. M. (1992) Resistance of murine lung tumors to xenobiotic-induced cytotoxicity. Cancer Res. **52**: 6797–6803.
23. Jacques, J., and Currie, W. (1977) Bronchiolo-alveolar carcinoma: a Clara cell tumor? Cancer **40**: 2171–2180.
24. Singh, G., Katyal, S. L., and Torikata, C. (1981) Carcinoma of type II pneumocytes. Immunodiagnosis of a subtype of "bronchioloalveolar carcinomas" Am. J. Pathol. **102**: 195–208.
25. Dairaku, M., Sueishi, K., Tanaka, K., and Horie, A. (1983) Immunohistochemical analysis of surfactant apopotein in the bronchiolo-alveolar carcinoma. Virchows Archiv. Abt. A Pathol. Anat. **400**: 223–234.
26. Broers, J. L., Jensen, S. M., Travis, W. D., Pass, H., Whitsett, J. A., Singh, G., Katyal, S. L., Gazdar, A. F., Minna, J. D., and Linnoila, R. I. (1992) Expression of surfactant associated protein-A and Clara cell 10 kilodalton mRNA in neoplastic and non-neoplastic human lung tissue as detected by in situ hybridization. Lab. Invest. **66**: 337–346.
27. Kitamura, H., Kameda, Y., Ito, T., Hayashi, H., Nakamura, N., Nakatani, Y., Inayama, Y., and Kanisawa, M.

(1997) Cytodifferentiation of atypical adenomatous hyperplasia and bronchioloalveolar lung carcinoma: immunohistochemical and ultrastructural studies. Virchows Archiv. **431**: 415–424.

28. Nomori, H., Morinaga, S., Kobayashi, R., and Torikata, C. (1994) Protein 1 and Clara cell 10-kDa protein distribution in normal and neoplastic tissues with emphasis on the respiratory system. Virchows Archiv. **424**: 517–523.

Received on March 28, 2002
1st. Revision on May 9, 2002
Accepted on June 19, 2002

*J Toxicol Pathol 2003; **16**: 93–102*

Original

Pre-B-Cell Lymphomas in Mice Following Injection of ^{239}Pu Citrate: Comparison with MNU-Induced T-Lymphoblastic Lymphomas

Yoichi Oghiso[1] and Yutaka Yamada[1]

[1] Internal Radiation Effects Research Group, Research Center for Radiation Safety, National Institute of Radiological Sciences, 4–9–1 Anagawa, Inage-ku, Chiba 263–8555, Japan

Abstract: Lymphoid neoplasms occurring in three different (C3H/He, C57BL/6, and B6C3F$_1$) strains of female mice after injection of the bone-seeking and alpha-emitting radionuclide, ^{239}Pu citrate were compared by immunohistochemistry with those from the alkylating agent, N-methyl-N-nitrosourea (MNU)-injected mice. There was a variety of phenotypes from either T-cell to B-cell or histiocytic lineages in lymphoid neoplasms of the control, saline-injected mice. While strain differences were noted in the incidence and proportion, lymphoid neoplasms occurring early after ^{239}Pu-injection were, however, characterized by B220$^+$ phenotypes but negative for both T-cell-specific markers (Thy 1, CD3) and B-cell markers (CD5, CD19, CD79b) to be classified into pre-B-cell lymphomas derived from progenitor B-cells. In contrast, almost all the MNU-induced lymphomas were shown to be CD3$^+$ or rarely Thy 1$^+$ but B220$^-$ T-lymphoblastic lymphomas. These results indicate differences in immunophenotypic expression but also might reflect different carcinogenic processes between chemical- and radiation-induced murine lymphomas.
(J Toxicol Pathol 2003; **16**: 93–102)

Key words: murine lymphomas, immunohistochemistry, strain differences, alpha radiation, alkylating agent

Introduction

Murine lymphoid neoplasms have been well described in the NFS strain congenic for ecotropic murine leukemia virus[1–3] to be mostly classified into B-cell lymphomas matching well the histopathological and immunophenotypic classification of human non-Hodgkin's lymphoid neoplasms[4,5]. Although naturally occurring as well as chemical-induced lymphomas in a certain inbred or genetically engineered strain of aged mice have also been reported[6–8], their phenotypes varied from B-cell to T-cell lineages. It has long been recognized that external X- or γ-radiation and neutron exposures under certain exposure regimens induce more frequently thymic lymphomas as well as myeloid leukemias in some strains of mice[9,10]. Non-thymic but malignant systemic lymphomas have been occasionally found in mice as well as osteosarcomas following internal radiation exposures of skeletal bones by the injection of α- or β-emitting bone-seeking radionuclides[11,12], although their morphologic and immunohistochemical features have not been fully elucidated as compared to those of congenic strains as above described.

We have also encountered malignant lymphomas occurring early in three different (C3H/HeN, C57BL/6J and their hybrid B6C3F$_1$) strains of mice following injection of an α-emitting bone-seeker, ^{239}Pu citrate, and tentatively defined their phenotypes as precursor B-cell lymphomas with Thy 1$^-$ but B220$^+$ surface markers[13,14]. Further immunohistochemical characterization, using the other T- or B-lineage-specific surface markers, was performed in the present study by comparing the differences in the onset periods, frequencies, and phenotypes among lymphoid neoplasms from the control, ^{239}Pu-injected and methylnitrosourea (MNU)-injected mice. In addition, since phenotypic expression of lymphomyeloid neoplasms are closely related to their ontogenic and differentiation stages from bone marrow precursors, the differences in the carcinogenic processes were discussed including susceptibilty to T- or B-lineage neoplastic cells from bone marrow stem cells between radiation- and chemical-induced murine lymphomas.

Received: 10 February 2003, Accepted: 17 April 2003
Mailing address: Yoichi Oghiso, Internal Radiation Effects Research Group, Research Center for Radiation Safety, National Institute of Radiological Sciences, 4–9–1 Anagawa, Inage-ku, Chiba 263–8555, Japan
TEL: 81-43-206-3100 FAX: 81-43-284-1389
E-mail: y_oghiso@nirs.go.jp

Materials and Methods

Experimental animals

Specific-pathogens (*Salmonella spp.*, *Mycoplasma spp*, *HVJ*, and *MHV*)-free female mice of three strains, C3H/HeN (C3H), C57BL/6J (C57) and their hybrid B6C3F$_1$ (BC3), were purchased from the breeding facility (Japan SLC Co.), and all the animals were housed 10 per polycarbonate cage (22 cm-width × 38 cm-depth × 20 cm-hight), given a commercial diet (Funabashi Farm Co.) with water *ad libitum*, and kept under a barrier-filtered air condition before and after all the experiments. The animal rooms were maintained on a 12-hr light:dark cycle at an air temperature of 23 ± 1.0°C and in a humidity of 55 ± 5.0%. The animal care included a weekly change of cages and a daily check of the animals' condition during their lifetime. All the experimental treatments were performed with the approval of the institution's animal use committee.

Experimental design

For the control group, 60 mice of each strain at 100 to 120 days old were injected intraperitoneally (ip) with 0.1 ml of saline as the carrier control. For the groups of plutonium (Pu), each of 30 age-matched mice of each strain was also injected ip with a different radioactivity; 100, 500, 1000, 5000, or 10000 Bq of ^{239}Pu citrate (Pu) in saline solution (pH 6.8–7.2) prepared by the previously described method[13]. For the group of methylnitrosourea (MNU), 60 mice of each strain initially at 100 days old were injected ip 5 times weekly with 40 mg/kg body weight of N-methyl-N-nitrosourea (Sigma) prepared by the previously described method[15]. All of these groups were kept in a closed-hood rack during their lifetime.

Histopathology and immunohistochemistry

All the groups of animals of each strain were autopsied after death or killed under anesthesia with ether on the occasion of a moribund state to examine gross lesions of the main organs and skeletal bones. All the tissue specimens including tumors were fixed in the mixture of 10% phosphate-buffered formalin and 4% paraformaldehyde for 5 days, cut into small pieces, processed with graded ethanol and xylene in an automatic tissue processor, and embedded in paraffin to prepare 5- to 6-μm-thick serial sections on a silanized glass slide (DAKO). For histopathological examinations of lymphoid neoplasms, one of serial sections was routinely stained with hematoxylin and eosin (HE), and the other unstained sections were treated for immunohistochemical typing using specific marker antibodies as follows: monoclonal rat IgG antibodies to CD45R (B220, RA3–6B2; Pharmingen), CD90 (Thy 1, G7; Pharmingen), and CD5 (Ly 1, 53–7.3; Pharmingen) as well as polyclonal goat antibodies to CD3-ε (M-20; Santa Cruz), CD19 (R-20; Santa Cruz), and CD79b (V-18; Santa Cruz). Briefly, deparaffinized and rehydrated sections were pretreated with 0.3% hydrogen peroxide in methanol at room temperature for 20 min to inactivate

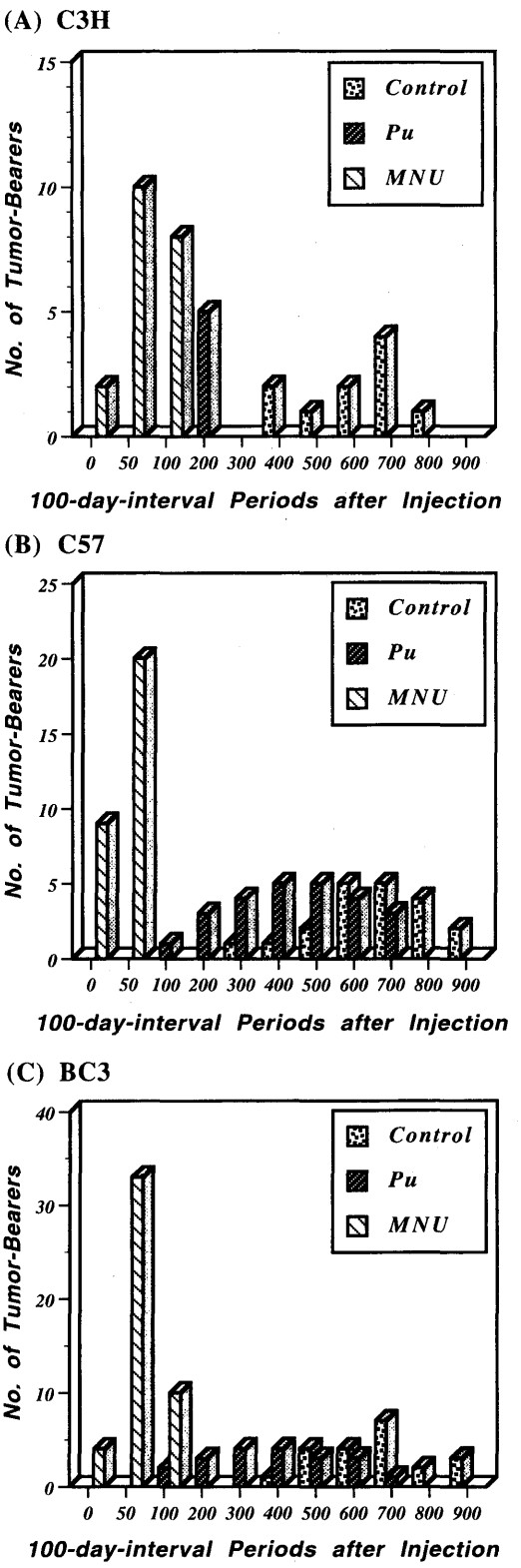

Fig. 1. Appearance periods of lymphoid neoplasms in C3H (A), C57 (B) and BC3 (C) strain mice after injection of saline (control), ^{239}Pu citrate (Pu), or methylnitrosourea (MNU). The columns indicate the number of tumor-bearing animals from all the control, Pu- or MNU-groups in every 100-day-interval periods after the injection.

Table 1. Tumor Frequencies in Three Strains of Mice Following Injection of Pu or MNU

Mouse strain	Group treatment	Total No. of animals	No. of tumor-bearers (% ± SE)[a]			
			Bone tumors	Lymphoid neoplasms	Myeloid leukemias	Other solid tumors
C3H	Control	60	0	10 (16.7 ± 4.8)	0	33 (55.0 ± 6.4)
	Pu	150	60 (40.0 ± 4.0)	5 (3.3 ± 1.4)	0	14 (9.3 ± 2.4)
	MNU	60	0	20 (33.3 ± 5.1)	0	11 (18.3 ± 5.0)
C57	Control	60	0	20 (33.3 ± 6.1)	2 (3.3 ± 2.3)	9 (15.0 ± 4.6)
	Pu	150	42 (28.0 ± 3.7)	25 (16.7 ± 3.0)	2 (1.3 ± 0.9)	6 (4.0 ± 1.6)
	MNU	60	0	29 (48.3 ± 6.4)	0	0
BC3	Control	60	0	21 (35.0 ± 6.1)	4 (6.7 ± 3.2)	28 (46.7 ± 6.4)
	Pu	150	58 (38.7 ± 4.0)	20 (13.3 ± 2.8)	1 (0.7 ± 0.7)	8 (5.3 ± 1.8)
	MNU	60	0	47 (78.3 ± 5.3)	0	2 (3.3 ± 2.3)

a: Percent incidence ± SE in parenthesis of tumor-bearing animals out of total number of animals in each group.

endogenous peroxidase activity. After washing with 0.05% Tris-buffered saline (TBS, pH 7.6), sections were immersed into an antigen retrieval solution (DAKO) and heated to 90–95°C for 25 min in a microwave oven to unmask cell surface antigens. Following washing with TBS, sections were incubated with normal rat or normal goat serum at room temperature for 1 hr to block any nonspecific Fc-binding of a secondary antibody, and then incubated with each of the primary antibodies (10 μg/ml for monoclonal antibodies and 1:100 dilution for polyclonal antibodies) at 4°C for overnight. After washing with TBS, sections were reacted with biotinylated secondary anti-rat or anti-goat IgG antibody (Vectastain Elite ABC kit; Vector Lab) at room temperature for 1 hr, and then coupled with avidin-biotin-immunoperoxidase complex (ABC) at room temperature for 30 min. After washing with TBS, sections were treated with the substrate, 3,3'-diaminobenzidine tetrachloride (DAB) to visualize immunoreactivity, and counterstained with hematoxylin. As negative controls, normal rat or goat serum was applied on the sections instead of primary antibodies, and then processed under similar conditions to those described above. On light microscopic examinations of these stainings, differential diagnosis and histological classification were performed according to those of morphologic or some immunohistochemical criteria for murine lymphoid neoplasms as described[16,17].

Statistics

All the cases of lymphoid neoplasms from the control, Pu and MNU groups were selected and analysed for survival periods and competing risks with the other tumors, particularly bone tumors, or non-neoplastic death by the Kaplan-Meier method using the log-rank and Peto-Wilcoxon tests as described previously[14].

As each of the solid tumors was considered to be independently induced following Pu- or MNU-injections, the standard errors (SE) for the incidence of lymphoid neoplasms as well as the other tumors in each group were calculated according to the following equation as described[18],

$$SE = \{p(1-p)/N\}^{1/2}$$

where p = proportion of animals with lymphoid neoplasms or the other tumors and N = total number of animals examined.

Results

Appearance periods and frequencies of lymphoid neoplasms

The periods for the appearance of lymphoid neoplasms at autopsy were differed among three strains of the control mice examined, but were mostly late over 400–500 days after injection of saline as shown in Fig. 1. As compared to the controls, the appearance periods of lymphoid neoplasms from Pu-injected C3H mice were only found within 200 days, while those from C57 and BC3 mice were relatively early within 200–400 days after the injection of 5000 Bq or more of Pu. In contrast, lymphoid neoplasms from three strains of MNU-injected mice appeared much earlier during the periods from 30 to 150 days after the injection.

The frequencies of solid tumors as well as myeloid leukemias found in the control, Pu-, and MNU-groups of three strains of mice are summarized in Table 1. While strain differences were noted, total incidences of lymphoid neoplasms as well as the other solid tumors from Pu-injected mice were reduced than those of the controls because of the competition with early and highly induced bone tumors as described previously[14]. The incidences of lymphoid neoplasms occurred much earlier in three strains of MNU-injected mice, however, increased predominantly up to approximately 1.5- to 2.0-fold of the control values, and therefore bone and the other solid tumors nor myeloid leukemias were scarcely found within 150 days after the injection of MNU. Although total incidences of lymphoid neoplasms in all the Pu-injected animals were lower than the control and MNU-injected animals, the dose responses apperared to be inversely proportional to the injected

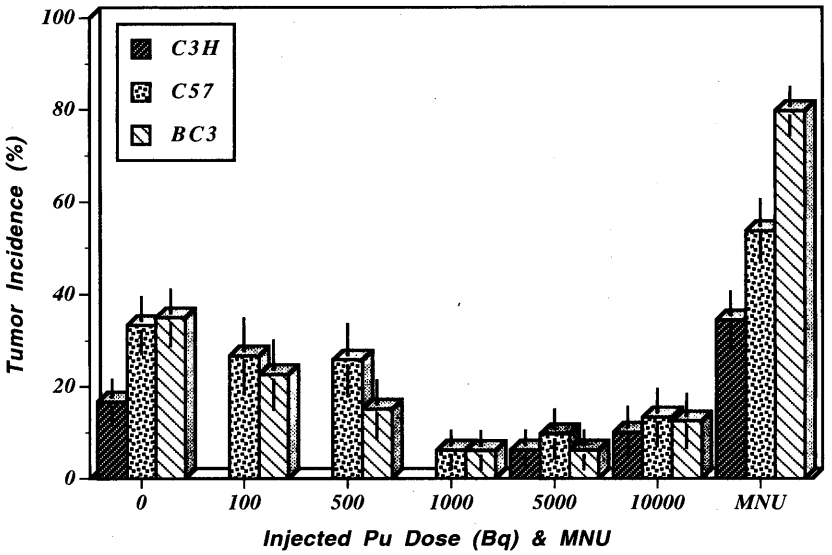

Fig. 2. Dose response for the incidence of lymphoid neoplasms in three (C3H, C57, and BC3) strains of mice after injection of saline (control), ^{239}Pu citrate (Pu) or methylnitrosourea (MNU). The columns with vertical bars indicate the percent incidence ± SE of neoplasms from each strain of mice as a function of injected Pu dose (Bq) and MNU.

radioactivity of Pu (Fig. 2). Thus, none or less lymphoid neoplasms were found in three strains of mice after injection of Pu radioactivity of 100–1000 Bq as compared to the controls, while their incidences again but slightly increased in the dose ranges more than 5000 Bq. In contrast, the dose responses for the incidences of bone tumors from the three strains of mice were proportional to the injected doses increasing from 100 to 1000 Bq, and then declined at the doses of more than 5000 Bq (data not shown).

Histological and immunohistochemical appearances of lymphoid neoplasms

Although strain differences were noted, variable types of lymphoid neoplasms were observed in the control, saline-injected mice. Many of them appeared grossly to be systemic lymphomas in which the whole-body lymph nodes were enlarged, accompanied mostly with hepatosplenomegaly and sometimes with thymic enlargement. Histologically, these neoplasms appeared to be composed of medium to large, round, ovoid or polygonal cells with relatively abundant and pale cytoplasm, and with chromatin-rich nuclei and prominent nucleoli. The growth pattern of neoplastic cells was almost diffuse or sometimes follicular, and distributed in the whole areas of the lymph nodes, thymus, and spleen, and in the sinusoidal and periportal areas of the liver, associated with perivascular or peribronchiolar infiltration in the kidney and lung. Immunohistochemistry of these lymphoma cells further revealed a variety of phenotypes such as Thy 1$^+$ or CD3$^+$ (Fig. 3A) T-cell lineage lymphomas, and B220$^+$ or CD5$^+$ (Fig. 3B) B-cell lineage lymphomas, whereas CD19$^+$ (Fig. 3C) or CD79b$^+$ B-cell lineage lymphomas were rarely or scarcely found in the control animals. Only a few of the lymphoid neoplasms from the control mice were grossly found to be localized either in local lymph nodes, in the spleen or occasionally in the liver. These neoplasms were characterized by diffuse or focal proliferation of spindle-shaped or polygonal cells with eosinophilic and brilliant cytoplasms, and frequently mixed with multinucleated giant cells (Fig. 3D). Since none of the above T- or B-cell lineage-specific markers were positive, these neoplasms were diagnosed as histiocytic lymphomas.

Such histopathological and immunohistochemical features of the lymphomas from the control animals as described above changed into more immature or progenitor phenotypes in Pu-injected mice. Grossly, almost all the neoplastic lesions were distributed in the whole-body lymph nodes, liver, and spleen, all of which appeared to be more pale and swollen than the controls. The histological appearances of such systemic lymphoma cells from Pu-injected animals were almost similar to the above described findings in the controls, but rather showing more extensive growth and leukemic infiltration of neoplastic cells in the liver (Fig. 4A) or more diffuse proliferation accompanied with typical starry sky effects by increased tingible-body macrophages in the lymphoid follicles (Fig. 4B). The most prominent and specific features were shown by immunohistochemical staining for these lymphomas; thus, only B220$^+$ progenitor B-cell (pre-B-cell) lymphomas were more predominantly observed in the liver (Fig. 4C) and spleen or lymph nodes (Fig. 4D) than Thy 1$^+$ or CD3$^+$ T-cell lineage lymphomas and CD5$^+$, or CD19$^+$ B-cell lineage lymphomas.

Contrary to pre-B-cell lymphomas from Pu-injected mice, the MNU-induced lymphoid neoplasms, were characterized by a specified spectrum of T-lymphoblastic lymphoma; grossly prominent thymic enlargement as well as

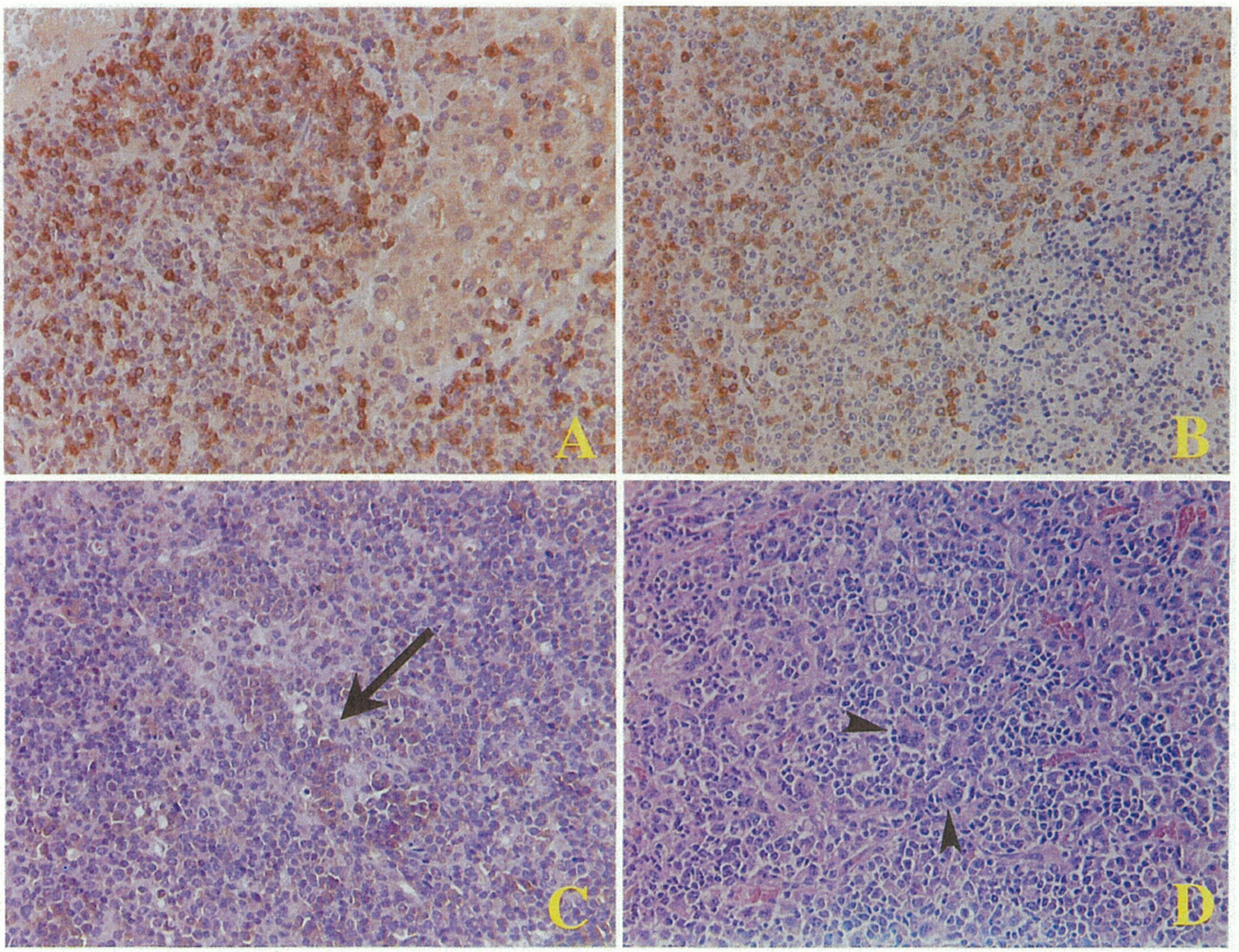

Fig. 3. Microscopic features and immunohistochemistry of lymphoid neoplasms in the control mice after injection of saline. (A) infiltration and proliferation of $CD3^-$ lymphoma cells in the liver from BC3 mouse on Day 981. ABC. ×200. (B) infiltration and proliferation of $CD5^+$ lymphoma cells inside the marginal zone of the splenic follicle from BC3 mouse on Day 597. ABC. ×200. (C) aggregation of weakly stained $CD19^+$ lymphoma cells around the high endothelial venule (arrow) in the mesenteric lymph node from C57 mouse on Day 644. ABC. ×200. (D) diffuse proliferation of spindle-shaped or polygonal cells mixed with multinucleated giant cells (arrowheads) in the mesenteric lymph node diagnosed as histiocytic lymphoma from C57 mouse on Day 652. HE. ×200.

enlargement of whole-body lymph nodes and spleen; histologically diffuse or follicular proliferation of medium to large, and cohesive lymphoblasts with mitoses and starry sky effects in the thymus (Fig. 5A) and other lymphoid organs. These lymphoma cells exclusively expressed $CD3^+$ but not always Thy 1^+ T-cell lineage-specific phenotypes (Figs. 5B, 5C, and 5D), while, instead, either $B220^+$, $CD5^+$, or $CD19^+$ B-cell lineage lymphomas were scarcely found.

Immunophenotypic distribution of lymphoid neoplasms

Based on the above findings, immunohistochemical typing of lymphoid neoplasms from the control, Pu, and MNU groups are summarized in Table 2. Despite strain differences in the positive proportion of each surface marker, lymphomas from the control groups were variably positive for T-cell lineage markers (Thy 1, CD3), and B-cell lineage markers (B220, CD5, CD19). While early occurring lymphomas from the Pu groups were rather positive for pre-B-cell marker, B220, or B-cell markers (CD5, CD19) than T-cell markers (Thy 1, CD3), almost all the MNU-induced lymphomas expressed T-cell-specific marker, CD3, but not B-cell lineage markers (CD19, CD79b). According to such immunophenotypic characterization and histological criteria as described[16,17], murine lymphomas are classified into the following phenotypes: $B220^-$ $CD3^+$ or rarely Thy 1^+ T-cell lineages including thymic or T-lymphoblastic lymphomas and T-lymphocytic lymphomas; $B220^+$ B-cell lineages including Thy 1^- $CD3^-$ pre-B-cell lymphoma and $CD5^+$ or $CD19^+$ B-cell lymphomas; histiocytic lymphomas negative for any T- and B-cell-specific markers. As this category was applied to all the cases of lymphoid neoplasms, phenotypic lineage distribution in each group was shown by the percent

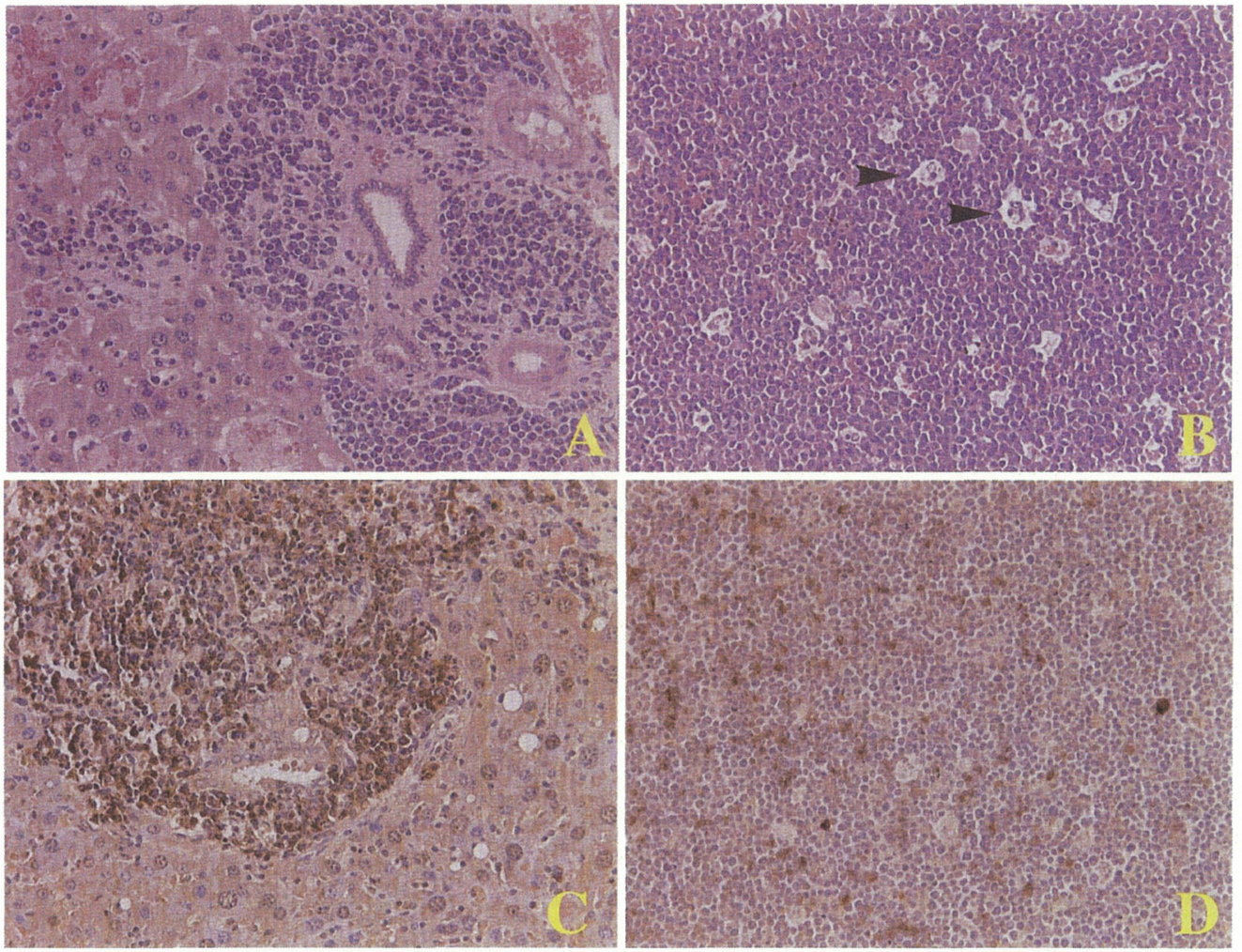

Fig. 4. Microscopic features and immunohistochemistry of lymphoid neoplasms after injection of 1000–10000 Bq of ^{239}Pu citrate. (A) periportal and sinusoidal infiltration of round or ovoid lymphoma cells in the liver from BC3 mouse on Day 291. HE. ×200. (B) diffuse proliferation of lymphoma cells accompanied with tingible-body macrophages (arrowheads) in the spleen from C57 mouse on Day 336. HE. ×200. (C) infiltration of B220$^+$ lymphoma cells in the liver from BC3 mouse on Day 397. ABC. ×200. (D) diffuse proliferation of B220$^+$ lymphoma cells in the superficial lymph node from C3H mouse on Day 290. ABC. ×200.

proportion of each lineage to all the neoplasms in Fig. 6. While almost 50–60% of neoplasms from the control groups were classified into T-cell lineage, the proportions of pre-B-cell lineage prominently increased in the Pu groups up to 80% in C3H, or 45% both in C57 and BC3 strains of mice. Total proportions of B-cell lineage neoplasms including B-cell lymphomas ranging 20–32% in the control groups increased up to 65–100% but the proportions of T-cell lineage, instead, decreased down to 30% or less in the Pu groups. On the contrary, the proportion of T-cell lineage neoplasms exclusively increased up to 80–90% in the MNU groups.

Discussion

Although internal radiation exposures by bone-seeking radionuclides occasionally induce lymphoid neoplasms as well as osteosarcomas in mice[11,12], the entity for pathological features and the differences from those by exposures to external radiations or chemical carcinogens have not been fully elucidated. The present study first characterized the histopathological features and immunophenotypes of murine lymphoid neoplasms occurring relatively early in three strains of mice having different spontaneous and radiation-induced tumor spectra after the injection of α-emitting, bone-seeking ^{239}Pu citrate. As compared to the saline-injected (control) and chemical carcinogen (MNU)-injected groups, frequencies of lymphoid neoplasms from Pu-injected mice were much lower despite a slight increase at higher doses of more than 5000 Bq, which were assumed to be a competing dose range with osteosarcomas occurring relatively early as described previously[13,14].

Morphologic and immunohistochemical typing of lymphoid neoplasms from Pu-injected mice revealed that

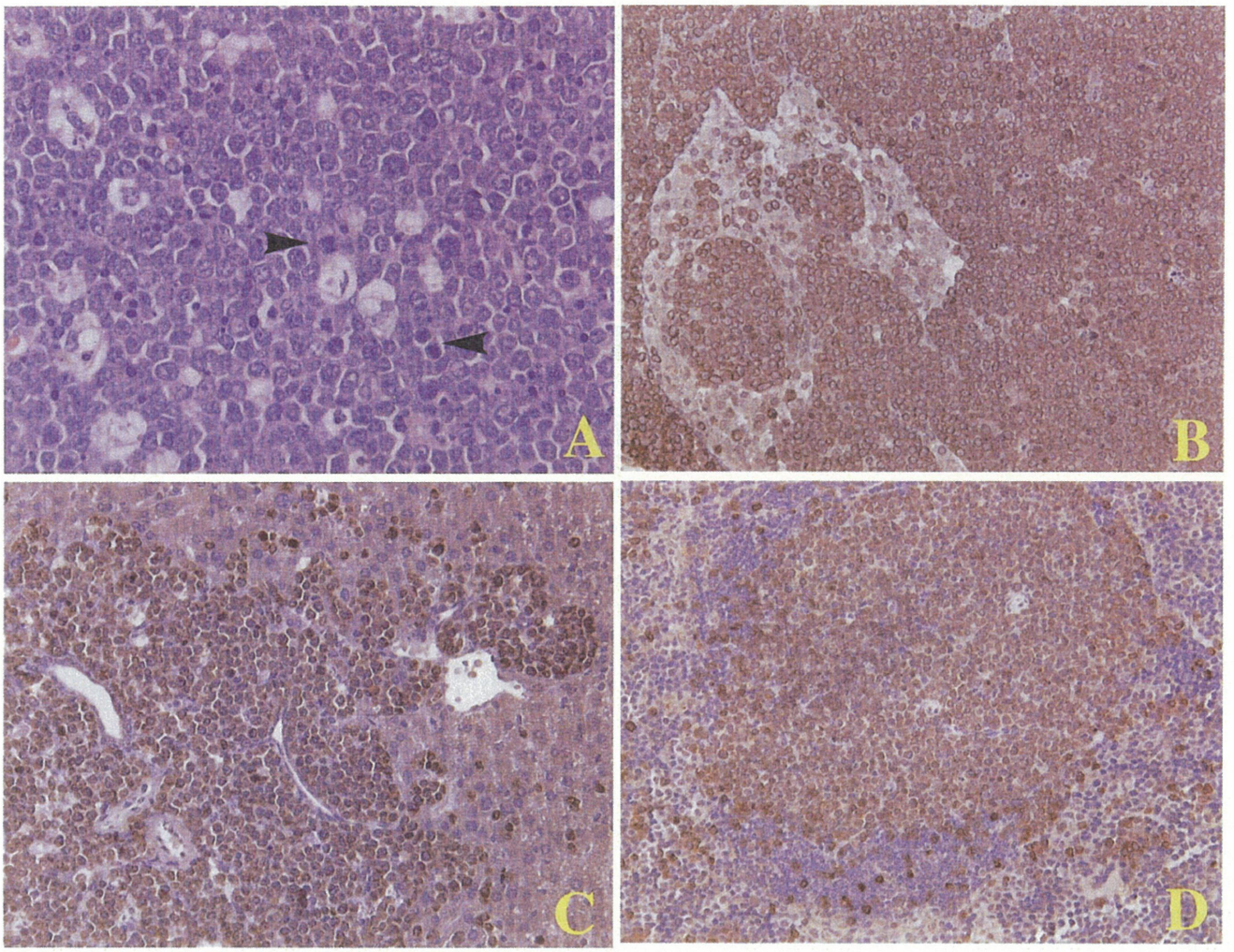

Fig. 5. Microscopic features and immunohistochemistry of thymic (T-lymphoblastic) lymphomas after injection of MNU. (A) proliferation of lymphoma cells with mitoses (arrowheads) and tingible-body macrophages in the thymus from BC3 mouse on Day 74. HE. ×400. (B) proliferation of $CD3^+$ lymphoma cells in the thymus from C57 mouse on Day 57. ABC. ×200. (C) infiltration and proliferation of $CD3^+$ lymphoma cells in the liver from C3H mouse on Day 67. ABC. ×200. (D) infiltration of $CD3^+$ lymphoma cells into periarterial lymphoid sheath of the splenic white pulp from BC3 mouse on Day 61. ABC. ×200.

Table 2. Immunohistochemical Typing of Murine Lymphoid Neoplasms (LN) Following Injection of Pu or MNU

Mouse strain	Group	Total No. of LN examined	Immunohistochemistry of LN[a]					
			Thy1	B220	CD5	CD3	CD19	CD79b
C3H	Control	10	1/10	2/10	1/10	6/10	1/10	0/10
	Pu	5	0/5	4/5	1/5	0/5	0/5	0/5
	MNU	20	5/20	4/20	4/20	18/20	0/20	0/20
C57	Control	20	4/20	4/20	2/20	10/20	1/20	0/20
	Pu	25	2/25	11/25	3/25	5/25	3/25	0/25
	MNU	29	6/29	2/29	3/29	25/29	0/29	0/29
BC3	Control	21	6/21	3/21	3/21	12/21	1/21	1/21
	Pu	20	4/20	9/20	1/20	7/20	2/20	0/20
	MNU	47	9/47	4/47	4/47	43/47	0/47	0/47

a: Number of LN with positive neoplastic cells for each surface marker per total number of LN examined in each group.

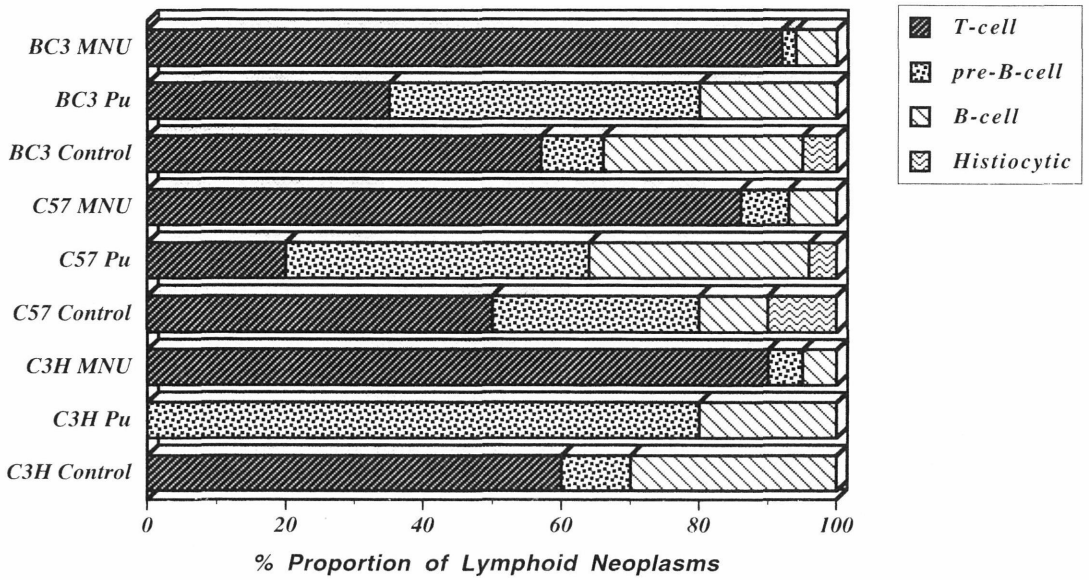

Fig. 6. Distribution of phenotypic lineages of lymphoid neoplasms in three (C3H, C57, and BC3) strains of mice after injection of saline (control), ^{239}Pu citrate (Pu), or methylnitrosourea (MNU). The columns indicate the percent proportion of T-cell, pre-B-cell, B-cell, or histiocytic lineage neoplasms among all the lymphoid neoplasms from each group.

systemic or leukemic lymphoma cells mostly have B220$^+$ but Thy 1$^-$ CD3$^-$ and CD5$^-$ CD19$^-$ CD79b$^-$ phenotypes specific to early B lymphomyeloid progenitor cells as described for X-ray-induced leukemias in *BCL*-2 transgenic mice[19]. As compared to the phenotypic distribution of lymphoid neoplasms from the control group, such progenitor B-cell lymphomas classified into pre-B-cell lymphomas were more predominant in Pu-groups despite the strain differences in the proportion varied from 45 to 80%, and total B-cell lineage neoplasms including CD5$^+$ or CD19$^+$ B-cell lymphomas increased up to 65–100%, while B220$^-$ CD3$^+$ or rarely Thy 1$^+$ T-cell lineage lymphomas, instead, decreased down to 30% or less. However, CD3$^+$ or Thy 1$^+$ T-cell lineage lymphomas, mostly thymic or T-lymphoblastic lymphomas, were exclusively 80–90% in MNU-groups, as expected.

Myeloid leukemias and thymic lymphomas were scarcely or not found in the three strains of Pu-injected mice in the present study. While external radiation exposures more frequently induce both of these lymphomyeloid neoplasms in some strains (C57BL/6, BALB/c, and CBA/H) of mice[10], even internal α-radiation exposures by bone-seeking radionuclides significantly induce myeloid leukemias and osteosarcomas in CBA/H strain mice[20–22]. Thus, strain differences in radiation-induced lymphomyeloid neoplasms, not only with the incidences, latency periods, and systemic or localized growth, but also phenotypes such as T- or B-cell lymphomas and myelogenous leukemias, reflect the genetic control of the susceptibility to radiation-induced lymphomyeloid neoplasms as described in either resistant, susceptible or recombinant congenic strains[23]. The susceptibility to external X- or γ-radiation-induced acute myeloid leukemias or thymic lymphomas in both CBA/H and C57BL/6 strains of mice currently appears to depend on the specific loss of heterozygosity over 7 chromosomes or genomic instability[24,25].

The cellular and molecular mechanisms for radiation-induced lymphomyeloid neoplasms were not fully elucidated, as compared to the chemical-induced neoplasms. For example, mutation frequency of a tumor suppressor gene, *p53* was lower both in γ-ray- and MNU-induced thymic lymphomas from C57BL/6J mice suggesting no major role of *p53* mutations on the lymphomagenesis[26], while codon 12 Ki-*ras* mutation is closely associated with early stage of MNU-induced thymic lymphomas but not detected in any stages of γ-ray-induced thymic lymphomas[27]. The K-*ras* mutations of X-ray-induced thymic lymphomas from B6C3F$_1$ mice are described to be closely associated with loss of heterozygosity on specific chromosomes[28], although its significance for lymphomagenesis remains unknown. So far, any evidence for genetic alterations specific to radiation-induced murine lymphomas was not verified, whereas cyclin D$_1$[29] was highly expressed by all pre-B and B-cell lymphomas, and *BCL-6* gene alterations[30] might be involved in diffuse large B cell lymphomas, both from NFS congenic strain for ecotropic murine leukemia virus, as similarly shown by human B-cell lymphomas. It is only a speculation that since pluripotent hemopoietic progenitor cells could be radiosensitive but also target cells for lymphomyeloid neoplasms after long-term and lower dose rate exposures to α-emitting bone-seekers[31,32], the susceptibility to either myeloid leukemias or B-cell or T-cell lineage lymphomas might be modulated by such alterations of the hemopoietic microenvironment through radiation

damage.

In conclusion, the present study first describes immunophenotypic characterization of lymphoid neoplasms from three different strains of mice after the internal radiation exposures to an α-emitting and bone-seeking radionuclide, ^{239}Pu citrate. The results indicate predominant occurrence of B220$^+$ pre-B-cell lymphomas, as compared to exclusive increase of CD3$^+$ T-lymphoblastic lymphomas induced by an alkylating agent, MNU. Such immunophenotypic difference might also reflect different carcinogenic processes between chemical- and radiation-induced murine lymphomas.

Acknowledgements: This work was partly supported by a research grant from the Japan Ministry of Education, Culture, Science and Technology. The authors are grateful to Mr. Isao Takahashi from Tokyo Nuclear Services, Co. for his excellent preparations of histological tissue sections, and to the staffs of Animal Care Co. for their helpful support of animal cares.

References

1. Fredrickson TN, Lennert K, Chattopadhyay SK, Morse III HC, and Hartley JW. Splenic marginal zone lymphomas of mice. Am J Pathol 1999; **154**: 805–812.
2. Hartley JW, Chattopadhyay SK, Lander MR, Taddesse-Heath L, Naghashfar Z, Morse III HC, and Fredrickson TN. Accelerated appearance of murine B cell lymphoma types in NFS/N mice congenic for ecotropic murine leukemia viruses. Lab Invest 2000; **80**: 159–169.
3. Pattengale PK. Tumors of the lymphaematopoietic system. In: Pathology of Tumors in Laboratory Animals. Vol. II Tumors of the mouse, 2nd ed., VS Turusov and U Mohr (eds), IARC Scientific Publications No.111, Lyon, 651–679, 1994.
4. Narris NL, Jaffe ES, Stein H, Banks PM, Chan JKC, Cleary ML, Delsol G, de Wolf-Peeters C, Falini B, Gatter KC, Grogan TM, Isaacson PG, Knowles DM, Mason DY, Muller-Hermelink H-K, Pileri SA, Piris MA, Ralfkiaer E, and Warnke RA. A revised European-American classification of lymphoid neoplasms: a proposal from the international lymphoma study group. Blood 1994; **84**: 1361–1392.
5. Jaffe ES, Harris NL, Diebold J, and Muller-Hermelink HK. World Health Organization classification of neoplastic diseases of the hematopoietic and lymphoid tissues. A progress report. Am J Clin Pathol 1999; **111**(suppl. 1): S8–S12.
6. Haines DC, Chattopadhyay S, and Ward JM. Pathology of aging B6; 129 mice. Toxicol Pathol 2001; **29**: 653–661.
7. Joshi VV and Frei JV. Gross and microscopic changes in the lymphoreticular system during genesis of malignant lymphoma induced by a single injection of methylnistrosourea in adult mice. J Natl Cancer Inst 1970; **44**: 379–394.
8. Frei JV and Lawley PD. Thymomas induced by simple alkylating agents in C57BL/Cbi mice: kinetics of the dose response. J Natl Cancer Inst 1980; **64**: 845–856.
9. Maison JR, Wambersie A, Gerber GB, Mattelin G, Lambiet-Collier M, De Coster B, and Gueulette J. Life-shortening and disease incidence in C57Bl mice after single and fractionated $\gamma$and high-energy neutron exposure. Radiat Res 1988; **113**: 300–317.
10. Janowski M, Cox R, and Strauss PG. The molecular biology of radiation-induced carcinogenesis: thymic lymphoma, myeloid leukemia and osteosarcoma. Int J Radiat Biol 1990; **57**: 677–691.
11. Loutit JF and Carr TEF. Lymphoid tumors and leukemia induced in mice by bone-seeking radionuclides. Int J Radiat Biol 1978; **33**: 245–263.
12. Müller WA, Luz A, Murray AB, and Linzner U. Induction of lymphoma and osteosarcoma in mice by single and protracted low α doses. Health Phys 1990; **59**: 305–310.
13. Oghiso Y, Yamada Y, and Iida H. High frequency of leukemic lymphomas with osteosarcomas but no myeloid leukemias in C3H mice after ^{239}Pu citrate injection. J Radiat Res 1997; **38**: 77–86.
14. Oghiso Y and Yamada Y. Strain differences in carcinogenic and hematopoietic responses of mice after injection of plutonium citrate. Radiat Res 2000; **154**: 447–454.
15. Newcomb EW, Steinberg JJ, and Pellicer A. *ras* oncogenes and phenotypic staging in N-methylnitrosourea- and γ-irradiation-induced thymic lymphomas in C57BL/6J mice. Cancer Res 1988; **48**: 5514–5521.
16. Pattengale PK and Taylor CR. Experimental models of lymphoproliferative disease. The mouse as a model for human non-Hodgkin's lymphomas and related leukemias. Am J Pathol 1983; **113**: 237–265.
17. Pattengale PK. Neoplastic lesions of the mouse lymphoid system. In: Pathology of Neoplasia and Preneoplasia in Rodents, P Bannasch and W Gössner (eds), EULEP Color Atlas, Stuttgart & New York: Chattauer, 168–176, 1994.
18. Coggle JE, Peel DM, and Tarling JD. Lung tumour induction in mice after uniform and non-uniform external thoracic X-irradiation. Int J Radiat Biol 1985; **48**: 95–106.
19. Gibbons DL, MacDonald D, McCarthy KP, Cleary HJ, Plumb M, Wright EG, and Greaves MF. An *Eμ-BCL-2* transgene facilitate leukaemogenesis by ionizing radiation. Oncogene 1999; **18**: 3870–3877.
20. Humphreys ER, Loutit JF, and Stones VA. The induction by ^{239}Pu of myeloid leukemia and osteosarcoma in female CBA mice. Int J Radiat Biol 1987; **51**: 331–339.
21. Humphreys ER, Isaacs KR, Raine TA, Saunders J, Stones VA, and Wood DL. Myeloid leukemia and osteosarcoma in CBA/H mice given ^{224}Ra. Int J Radiat Biol 1993; **64**: 231–235.
22. Ellender M, Harrison JD, Pottinger H, and Thomas JM. Induction of osteosarcoma and myeloid leukemia in CBA/H mice by the alpha-emitting nuclides, uranium-233, plutonium-239 and americium-241. Int J Radiat Biol 2001; **77**: 41–52.
23. Szymanska H, Sitarz M, Krysiak E, Piskorowska J, Czarnomska A, Skurzak H, Hart AAM, de Jong D, and Demant P. Genetics of susceptibility to radiation-induced lymphomas, leukemias and lung tumors studied in recombinant congenic strains. Int J Cancer 1999; **83**: 674–678.
24. Cleary HJ, Wright E, and Plumb M. Specificity of loss of heterozygosity in radiation-induced mouse myeloid and lymphoid leukaemias. Int J Radiat Biol 1999; **75**: 1223–1230.

25. Boulton E, Cleary H, Papworth D, and Plumb M. Susceptibility to radiation-induced leukaemia/lymphoma is genetically separable from sensitivity to radiation-induced genomic instability. Int J Radiat Biol 2001; **77**: 21–29.
26. Brathwaite O, Bayona W, and Newcomb EW. *p53* mutations in C57BL/6J murine thymic lymphomas induced by γ-irradiation and N-methylnitrosourea. Cancer Res 1992; **52**: 3791–3795.
27. Newcomb EW, Bayona W, and Pisharody S. N-methylnitrosourea-induced Ki-*ras* codon 12 mutations: early events in mouse thymic lymphomas. Mol Carcinogenesis 1995; **13**: 89–95.
28. Shimada Y, Nishimura M, Kakinuma S, Takeuchi T, Ogiu T, Suzuki G, Nakata Y, Sasanuma S, Mita K, and Sado T. Characteristic association between K-ras gene mutation with loss of heterozygosity in X-ray-induced thymic lymphomas of the B6C3F_1 mouse. Int J Radiat Biol 2001; **77**: 465–473.
29. Qi CF, Chattopadhyay SK, Lander M, Kim Y, Fredrickson TN, Hartley JW, and Morse III HC. Expression of cyclin D_1 in mouse B cell lymphomas of different histologic types and differentiation stages. Leukemia Res 1998; **22**: 395–404.
30. Qi CF, Hori M, Coleman AE, Torrey TA, Taddesse-Heath L, Ye BH, Chattopadhyay SK, Hartley JW, and Morse III HC. Genomic organisation and expression of *BCL 6* in murine B-cell lymphomas. Leukemia Res 2000; **24**: 719–732.
31. Lord BI, Molineux G, Humphreys ER, and Stones VA. Long-term effects of plutonium-239 and radium-224 on the distribution and performance of pluripotent haemopoietic progenitor cells and their regulatory microenvironment. Int J Radiat Biol 1991; **59**: 211–227.
32. Lord BI, Austin AL, Ellender M, Haines JW, and Harrison JD. Tumorigenic target cell regions in bone marrow studied by localized dosimetry of ^{239}Pu, ^{241}Am and ^{233}U in the mouse femur. Int J Radiat Biol 2001; **77**: 665–678.

J. RADIAT. RES., 44, 125–132 (2003) http://jrr.jstage.jst.go.jp

The Specific Induction of Osteosarcomas in Different Mouse Strains after Injections of ^{239}Pu Citrate

YOICHI OGHISO* and YUTAKA YAMADA

Carcinogenicity/Bone tumors/Soluble ^{239}Pu/Strain differences/Mouse.

Lifetime bone tumor induction by the injection of a bone-seeking alpha emitter, ^{239}Pu citrate, was compared among 630 female mice from three strains (C3H/He, C57BL/6 and B6C3F$_1$) showing different genetic backgrounds for carcinogenesis. Bone tumors, mostly osteosarcomas, appeared early during the period from 200 to 600 days after the injection, showing an almost similar dose responsiveness with a peak incidence of 50% to 63% at skeletal doses of 2–3 Gy, in all mouse strains. The primary sites of bone tumors from these strains were also predominantly distributed in 80% to 90% of the skeletal bones, which had well-developed trabecular bone surfaces and large vascular sinusoids. The frequency of lymphoid neoplasms was significantly lower than the control values, and some appeared earlier at the higher injected doses than those of the controls. Fewer or no myeloid leukemias were found in all the control and injected animals, and the incidences of other solid tumors decreased, reaching zero at doses where the maximum incidences of bone tumors were noted. These findings indicate that osteosarcoma is the only specific tumor commonly observed among different mouse strains following the injection of soluble plutonium compounds.

INTRODUCTION

It has been well recognized that bone-seeking and alpha-emitting radionuclides preferentially induce bone tumors in the human cohorts of radium (^{226}Ra) dial painters[1], radium (^{224}Ra)-injected ankylosing spondylitis patients[2], and recently in Mayak workers who have been exposed to plutonium (^{239,238}Pu) compounds[3]. However, limited information or statistical uncertainty from these epidemiological studies does not fully permit estimates of risk factors and toxicity for bone cancer induction by alpha emitters. Experimental studies on bone carcinogenesis by injection of plutonium and other alpha emitters have been fully described in mice[4,5], rats[6], and dogs[7,8], implying that the toxicity ratio of ^{239}Pu in comparison to ^{226}Ra for bone carcinogenesis is the highest (approximately 15 to 16) among bone-seeking alpha emitters, irrespective of animal species. Supposing that the toxicity ratios are common between animals and humans, the risk factor for bone cancers from plutonium is estimated to be 1,200 in humans vs. 12,000 in dogs per 10^6 rad as described[9]. Nevertheless, it has not been elucidated whether only bone tumors are specific to alpha-emitting bone-seekers translocated through blood into the skeletal bones, and whether such a tumor spectrum is common among animal species and strains with different genetic backgrounds for spontaneous and radiation carcinogenesis. Our previous studies showed a relatively higher frequency of lymphoid neoplasms in C3H/He mice at higher skeletal doses over 10 Gy after injections of soluble ^{239}Pu citrate[10], whereas both osteosarcomas and lymphomas were differentially induced by ^{239}Pu-injection in C3H/He, C57BL/6, and B6C3F$_1$ mice, which respectively show different tumor spectra before and after external radiation exposures[11].

In consideration of these findings, the present study was done to clarify the specific carcinogenicity of injected soluble ^{239}Pu citrate to induce osteosarcomas by comparing the differences in lifespan carcinogenesis among three strains of mice. The results are discussed in comparison to other alpha emitters or radiations and as focused on the sensitivity and related mechanisms for bone tumorigenesis.

*Corresponding author: Phone: +81 43 206 3100,
Fax: +81 43 284 1389,
E-mail: y_oghiso@nirs.go.jp
Internal Radiation Effects Research Group, Research Center for Radiation Safety, National Institute of Radiological Sciences, 9-1, 4-chome, Anagawa, Inage-ku, Chiba 263-8555, Japan.

MATERIALS AND METHODS

Experimental animals

Specific pathogen-free female mice of three strains, C3H/HeN (C3H), C57BL/6J (C57), and their hybrid B6C3F1 (BC3), were purchased from a breeding facility (Japan SLC Co.), and all the animals were housed 10 per polycarbonate cage, given a commercial diet (Funabashi Farm Co.) with water *ad libitum*, and kept under barrier-filtered air conditions before and after all the experiments. The animal rooms were maintained on a 12-h

light:dark cycle at an air temperature of 23 ± 1.0°C and in a humidity of 55 ± 5.0%. The animal care included a weekly change of cages and a daily check of conditions during the animals' lifetimes. All the experimental treatment were performed with the approval of the institution's animal use committee.

Experimental design

For the preparation of soluble plutonium as described previously[11], a mixture of 10 mM ^{239}Pu nitrate and 100 mM trisodium citrate at a molecular ratio of 1:50 was titrated to pH 6.8–7.2 by an addition of 1 N NaOH, diluted with physiological saline, and passed through 0.2- and 0.025-μm-pore Millipore filters to obtain a monomeric ^{239}Pu citrate solution with a radioactivity of 10^3–10^5 Bq/ml. For an injection of ^{239}Pu citrate solution, 18 groups each containing 30 to 60 animals of each strain at 100–120 days old were injected intraperitoneally with amounts of radioactivity ranging from 100 to 10,000 Bq per animal or with saline as the carrier control. They were kept in a closed-hood rack during their lifetimes. The cumulative skeletal dose until death was estimated for each animal and was averaged as the mean skeletal dose ± SD for each group of animals as described previously[10].

Histopathology

All control and ^{239}Pu-injected animals were autopsied after death or killed on the occasion of a moribund state to examine the gross lesions of the main organs and skeletal bones. All organs were fixed in 10% phosphate-buffered formalin, and skeletal bones and bone tumors were then decalcified with a mixture of 10% formic acid and 10% neutral formalin. All tissue specimens were cut into small pieces, processed with graded ethanol and xylene in an automatic tissue processor, and embedded in paraffin to prepare 5- to 6-μm-thick sections on glass slides, stained with hematoxylin and eosin (H&E) for histopathological examinations using a light microscope. Differential diagnosis of bone tumors was performed either according to morphologic criteria or by some histochemical stainings as described[12,13]. The other tumors, including hematopoietic and lymphoid neoplasms, were routinely diagnosed by morphologic criteria and immunohistochemical stainings as described previously[11].

Statistics

Survival periods with the competing risks of neoplastic or non-neoplastic death after the injection of ^{239}Pu citrate were analyzed by the Kaplan-Meier method by using the log-rank and Peto-Wilcoxon tests as described previously[10]. The standard errors (SE) for each tumor frequency in experimental groups were calculated according to the following formula, as described[14],

$$SE = \{p(1-p)/N\}^{1/2}$$

where p = the proportion of animals with tumors and N = the total number of animals examined.

The significant differences between the control and the ^{239}Pu-injected groups of mice were compared by the unpaired Student's t test.

RESULTS

Survival reduction and early appearance of bone tumors after ^{239}Pu-injection

As shown in Table 1, the survival periods after injections of 500 Bq or more of ^{239}Pu citrate were significantly reduced in each strain of mice examined, and those of the groups of C3H and C57 mice injected with the lowest dose of 100 Bq were slightly longer but not significantly different from the controls. Such survival reduction was due to either neoplastic death caused by fatal tumors or non-neoplastic death caused mainly by acute or subacute hematopoietic dysplasias. The incidences of bone tumors were significantly higher in all groups injected with 100 Bq or more of ^{239}Pu citrate than in those of the controls showing the minimum value, zero in each strain (Table 1). Lymphoid tumors, mainly systemic lymphomas, found in variable proportions of the control animals from each strain were, however, significantly reduced after ^{239}Pu-injection, but they were slightly increased again in the higher dose groups injected with 5,000 or 10,000 Bq, even though their frequencies were still lower than those of the controls. In contrast, fewer or no myeloid leukemias were observed in all groups from each strain, and the other solid tumors affecting the soft tissues were significantly reduced after injections of 100 Bq or more of ^{239}Pu citrate, and their frequencies reached zero over 1,000 Bq. These solid tumors included pulmonary adenomas, hepatocellular or chollangiocellular carcinomas, ovarian adenocarcinomas or granulosa cell tumors, dermal fibrosarcomas or histiocytomas, and mammary adenocarcinomas. Only a small number of bone tumors was found during the late period from 600 to 800 days after the injection of the lowest dose of 100 Bq, though all data on the dose and appearance time are not shown. As the number of tumor-bearers for each tumor from all the dose groups was plotted against every 100-day-interval after ^{239}Pu-injection as shown in Fig. 1, most bone tumors appeared early during the period from 200 to 600 days after the injection in each strain, while all the other solid tumors appeared late, from 600 days or more. The appearance time of lymphoid tumors was almost coincident with that of bone tumors during the period from 200 to 600 days, except for C3H mice, in which lymphoid tumors appeared much earlier within 200 days after the injection. It was noteworthy that both the bone and lymphoid tumors did not concomitantly occur in the same animals. These findings indicate that significant survival reduction is due to the early appearance of bone tumors and some lymphoid tumors induced at higher injected doses of more than 5,000 Bq, while lymphoid and the other solid tumors were competitively reduced by the early increase of bone tumors.

Table 1. Summary of survivals and tumor frequencies in three strains of mice after injections of ^{239}Pu citrate.

C3H						
Injected dose (Bq)	Total No. of animals	Survival period (day)[a]	No. of tumor-bearers (% ± SE)[b]			
			Bone	Lymphoid	Myeloid	Other solid
0	60	763 ± 136	0	10 (16.7 ± 4.8)	0	33 (55.0 ±6.4)
100	30	808 ± 81	4 (13.3 ± 6.2)**	0	0	11 (36.7 ±8.8)*
500	30	592 ± 105*	19 (63.3 ± 8.8)**	0	0	3 (10.0 ±5.5)**
1,000	30	454 ± 72*	14 (46.7 ± 9.1)**	0	0	0
5,000	32	314 ± 50**	15 (46.9 ± 8.8)**	2 (6.2 ± 4.2)*	0	0
10,000	30	309 ± 67**	8 (26.7 ± 8.1)**	3 (10.0 ± 5.5)	0	0
C57						
Injected dose (Bq)	Total No. of animals	Survival period (day)[a]	No. of tumor-bearers (% ± SE)[b]			
			Bone	Lymphoid	Myeloid	Other solid
0	60	675 ± 183	0	20 (33.3 ± 6.1)	2 (3.3 ± 2.3)	9 (15.0 ±4.6)
100	30	727 ± 100	3 (10.0 ± 5.5)**	8 (26.7 ± 8.1)	1 (3.3 ± 3.3)	5 (16.7 ±6.8)
500	31	580 ± 117*	7 (22.6 ± 7.5)**	8 (25.8 ± 7.8)	1 (3.2 ± 3.2)	1 (3.2 ±3.2)**
1,000	32	412 ± 84*	16 (50.0 ± 8.8)**	2 (6.2 ± 4.2)**	0	0
5,000	31	343 ± 87**	12 (38.7 ± 8.7)**	3 (9.7 ± 5.3)**	0	0
10,000	30	326 ± 68**	4 (13.3 ± 6.2)**	4 (13.3 ± 6.2)*	0	0
BC3						
Injected dose (Bq)	Total No. of animals	Survival period (day)[a]	No. of tumor-bearers (% ± SE)[b]			
			Bone	Lymphoid	Myeloid	Other solid
0	60	746 ± 162	0	21 (35.0 ± 6.1)	4 (6.7 ± 3.2)	28 (46.7 ±6.4)
100	31	730 ± 107	8 (25.8 ± 7.8)**	7 (22.6 ± 7.5)	1 (3.2 ± 3.2)	6 (19.3 ±7.1)**
500	33	567 ± 115*	17 (51.5 ± 8.7)**	5 (15.1 ± 6.2)*	0	2 (6.1 ±4.2)**
1,000	33	449 ± 64*	12 (36.4 ± 8.4)**	2 (6.1 ± 4.2)**	0	0
5,000	32	325 ± 118**	10 (31.2 ± 8.2)**	2 (6.2 ± 4.2)**	0	0
10,000	32	322 ± 95**	11 (34.4 ± 8.4)**	4 (12.5 ± 5.8)*	0	0

[a]Mean ± SD of the survival periods after injections of saline (controls) or ^{239}Pu citrate in each group. Asterisks indicate significant differences in comparison to the controls (*$p < 0.05$, **$p < 0.01$). [b]Percent incidence ± SE in parenthesis of tumor-bearing animals out of total number of animals in each group. Asterisks indicate significant differences in comparison to the controls (*$p < 0.01$, **$p < 0.001$).

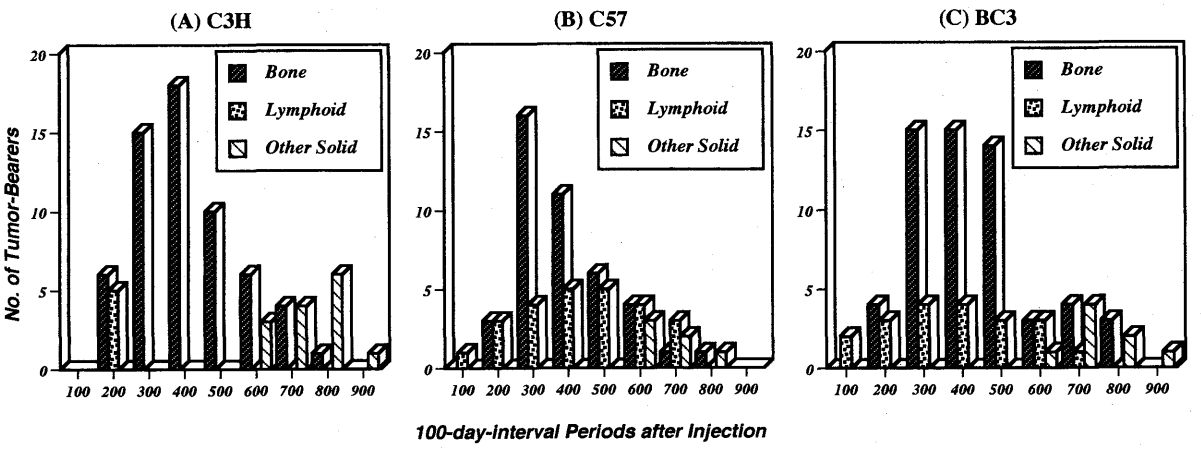

Fig. 1. The appearance time of bone, lymphoid, and other solid tumors from C3H (A), C57 (B), and BC3 (C) strain mice after injections of ^{239}Pu citrate. The columns indicate the number of tumor-bearers for each tumor from all the dose groups found in every 100-day-interval after ^{239}Pu-injection.

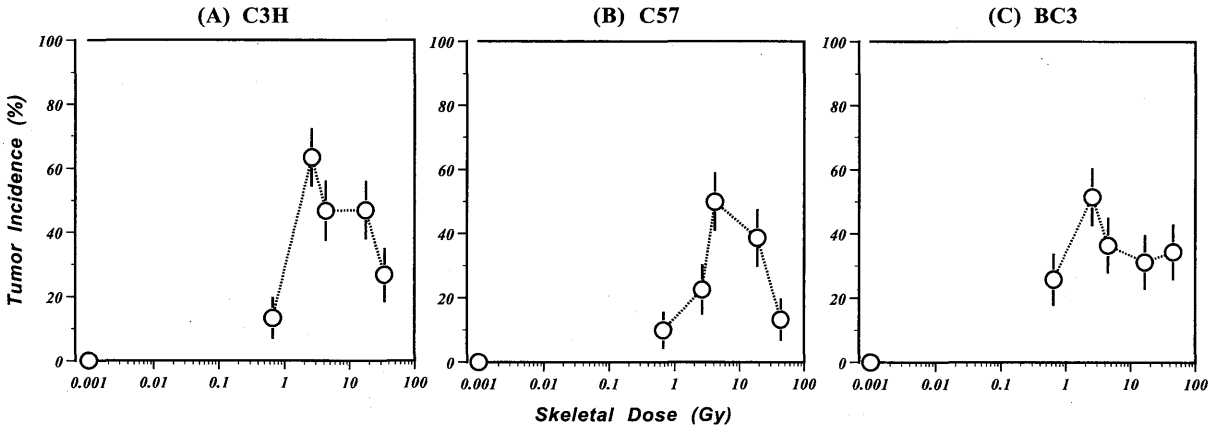

Fig. 2. The dose response for the incidence of bone tumors from C3H (A), C57 (B), and BC3 (C) strain mice after injections of ^{239}Pu citrate. The open circles with vertical bars indicate the percent incidence ± SE of bone tumors as a function of estimated mean skeletal doses (Gy).

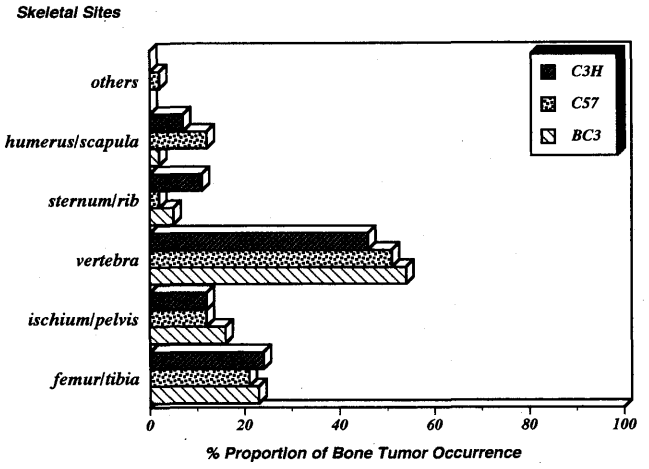

Fig. 3. The distribution of skeletal bone sites for the occurrence of bone tumors after injections of ^{239}Pu citrate. The columns indicate the proportion of bone tumors found in each skeletal bone site to all the bone tumors from each strain of mice.

Dose responses for the incidences of bone tumors after ^{239}Pu-injection

The dose response curves in Fig. 2 implicate that the significantly higher bone tumor induction was noted in all the strains of mice at the lowest skeletal doses of 0.6 to 0.7 Gy, in comparison to the control value, zero. Moreover, their incidences increased sharply from 1 Gy, reached a maximum of 50 to 63% at doses of 2 to 3 Gy, then dropped to the lower incidences of 16 to 31% at doses over 10 Gy. Such a bell-shaped pattern of dose responsiveness was almost similar among three strains of mice, though small differences were noted in the dose ranges and magnitudes for the maximum responses. The reduced incidences of bone tumors at higher skeletal doses resulted mainly from non-neoplastic death by acute or subacute hematopoietic dysplasias or partly from lymphoid neoplasms at the higher doses (data not shown), since none of the other solid tumors were found in animals that died as early as 200 days at higher dose ranges of more than 5,000 Bq or 10 Gy (Table 1 and Fig. 1).

Macroscopic and microscopic appearances of bone tumors after ^{239}Pu-injection

The primary bone tumors found macroscopically (larger than 5 mm in diameter) or microscopically (smaller than 2 mm in diameter) were distributed in almost the same skeletal bone sites of the three strains of mice (Fig. 3). Thus, bone tumors were distributed in the thoracic and lumbar vertebra with the highest proportions (46 to 54%) to all the bone tumors, the second higher proportions (20 to 24%) in the femur and tibia, and the smaller proportions (10 to 16%) in the ischium and pelvis, or humerus and scapula. No tumors were found in the other skeletal bone sites, such as the cranium and radius, except for submandibular bones from one C57 strain mouse. No clear differences in the skeletal distribution sites were seen among experimental groups with different injected or skeletal doses (data not shown). Although the macroscopic sizes of bone tumors varied from 5 mm to 30 mm in diameter, their occurrence was mostly single and unilateral in the skeletal bones, and gross appearances were mostly expressed as being white or yellowish-colored, variably calcified, and smooth- or rough-surfaced tumor masses.

Histopathological features of these bone tumors include fewer osteomas characterized by the relatively regular growth of spindle-shaped osteoblasts along with trabecular bone formation (Fig. 4A) and mostly osteogenic sarcomas with a variety of growth patterns and predominant cellular or stromal components. Many osteosarcomas were characterized by an irregular growth of large polygonal osteoblasts with osteoid and trabecular bone formations (Fig. 4B), whereas some osteosarcomas showed fibroblastic or histiocytic appearances accompanied with fibrous connective tissue stromas (Fig. 4C), or predominant cellular growth along endosteal bone surfaces and invasion into the bone marrows (Fig. 4D). A few cases of osteogenic sarcomas were rich in multinucleated giant cells or appeared to be giant cell osteogenic sarcomas with a predominant growth of osteo-

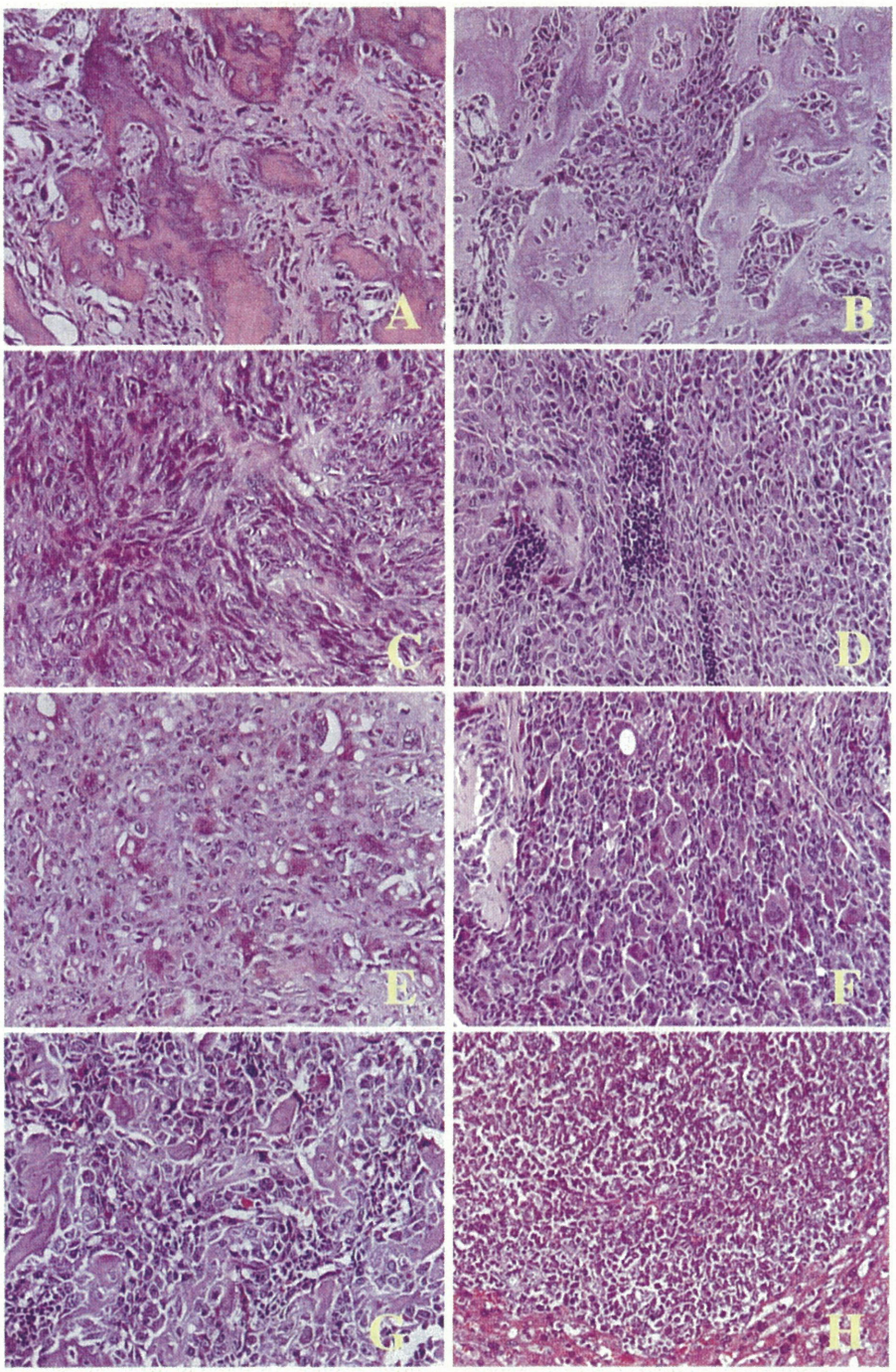

Fig. 4. The light microscopic features of bone tumors from mice after injections of ^{239}Pu citrate (H-E staining under a magnification of ×200). (A) Osteoma with spindle-shaped osteoblasts and trabecular bone formation (C3H, Day 407); (B) Osteosarcoma with polygonal osteoblasts as well as osteoid and trabecular bone formations (C57, Day 381); (C) Osteosarcoma with fibrous stromal components (C57, Day 363); (D) Osteosarcoma with cellular growth along endosteal bone surfaces and into bone marrows (BC3, Day 580); (E) Osteosarcoma with many multinucleated giant cells (C3H, Day 531); (F) Giant cell osteogenic sarcoma with abundant osteoclast-like giant cells (C57, Day 466); (G) Primary osteosarcoma with osteoid in the femur (C57, day 573); (H) Metastatic osteosarcoma without osteoid in the liver (the same animal as G)

clast-like giant cells (Fig. 4, E and F). Although they had no obvious relations to the injected doses or skeletal doses, metastatic osteogenic sarcomas were occasionally found in the lung, liver, kidney, spleen, or regional lymph nodes. Morphological features of these metastatic osteosarcomas were sometimes different from those of the primary site (Fig. 4, G and H).

DISCUSSION

The present results implicated that survival reduction as the administered doses increased was commonly observed in three mouse strains that have been found to show different carcinogenic responses before and after external exposures to ionizing radiations, and also that the cause of death was mostly the bone tumors increased significantly during the earlier periods, though a few were due to the early onsets of lymphoid neoplasms or non-neoplastic, hematopoietic dysplasias at higher dose ranges. Even though different isotopes, chemical forms, and entry routes were applied to experimental animals, alpha-emitting bone-seekers predominantly induced bone tumors, which were the most common causes of death, occurring early after either the inhalation exposures of beagle dogs to $^{238}PuO_2$ aerosols[15,16], injections of ^{224}Ra into the dog[17], or injections of ^{237}Np into rats[18]. The other solid tumors affecting the liver, ovary, lung, and skin or mammary glands, rather decreased much less in ^{239}Pu-injected mice than in the controls, and they appeared as late as the spontaneous occurrence in the control animals. This should be a result of the competition with the early occurrence of bone and a few lymphoid tumors, as described previously[11]. It also implies that most of the other solid tumors, if observed, were spontaneous but not significant causes of death, suggesting the differences in the dose distribution and target organs from low LET radiation exposures[19]. Lymphoid neoplasms, which are frequently observed in mice before or after low LET radiation exposures, were not, however, significantly induced; they slightly increased during the early periods after the injections of higher doses in which bone tumors were rather reduced. Although these findings are not consistent with those of mice after fractionated ^{224}Ra-injections[20], which induced early malignant lymphomas with an incidence of 13.5%, followed by the late occurrence of osteosarcomas with an incidence of 7%, the protracted exposures to low-dose alpha particles with lower dose rates should be important for the induction of lymphoid neoplasms. Whereas spontaneous murine bone tumors are only speculated to be closely associated with lymphomas, but not with the other solid tumors because of a common viral agent or competing risks in CF1 strain[21], it might be conceivable that lymphoid neoplasms after alpha radiations appear to be indirectly induced by some damaged but still rescued hemopoietic stem cells that migrated into peripheral lymphoid tissues. Myeloid leukemias, in contrast, were much less or scarcely observed in the control and ^{239}Pu-injected mice from three strains, even though lower but significant incidences of myeloid leukemias could be yielded in CBA/H mice after fractionated injections of lower doses of ^{239}Pu or ^{224}Ra[22,23]. Taken together, only the bone tumor is the major malignancy specific to ^{239}Pu-injection; the other solid tumors and lymphomyeloid neoplasms do not result directly from the internal exposures of the committed organs to alpha particles.

The bell-shaped dose response curves, characterized by significant increases at skeletal doses of more than 0.6 to 0.7 Gy, peak incidences at 2 to 3 Gy, and declines over 10 Gy, were commonly noted in three different mouse strains, though slight differences were present in the dose ranges and magnitudes for maximum responses. Moreover, the distribution pattern of macroscopic and microscopic bone tumors was almost similar in three strains of mice because approximately 70 to 80% of primary tumors were found in the vertebra, femur, and tibia, and the remaining 10 to 20% were distributed in the ischium, pelvis, humerus, and scapula. Interestingly, all of these skeletal bone sites have well-developed trabecular bone surfaces with a higher rate of trabecular bone formation, and large vascular sinusoids with discontinuous endothelial linings as described in the beagle dogs[24,25]. Thus, based on the findings that metabolic behavior and toxicity ratio of ^{239}Pu in the mouse skeletal bones are almost similar to those of the dog[5,7], it is noteworthy that such anatomical structures ensure initial contact with the endothelium along closed capillary beds, and then a higher deposition of plutonium on trabecular bone surfaces, resulted in a more effective irradiation of target osteoblasts for carcinogenic processes. Histological appearances of bone tumors, mostly osteosarcomas, were characterized commonly in all the strains of mice by an irregular growth of osteoblasts along or inside endosteal bone surfaces accompanied by trabecular bone formation. All of these findings, taken together, indicate again that osteosarcoma is only the neoplasm specifically and commonly induced by alpha particles emitted from plutonium deposited on the trabecular bone surfaces independent of animal species or strains. Concerning the strain differences, the genetic background of mouse strains may influence the latent periods and metastasis of osteosarcomas induced by ^{224}Ra, as described[26].

The radiosensitivity for bone cancer induction in dogs following an injection of ^{239}Pu or ^{226}Ra is closely related to the skeletal dose distribution, which depends on breed-specific bone mass and deposition of radioactivity[27], or on age-related bone metabolism[28], but not on body size[29]. In this respect, the susceptibility of three strains of age-matched mice to bone tumorigenesis, as expressed by the order of C3H $\approx$ BC3 > C57, might be due to strain-specific differences in bone mass and the skeletal distribution of ^{239}Pu. In comparison to ^{239}Pu and other alpha-emitting bone seekers, the other radiation sources, even beta-emitting bone seekers induce less effectively bone tumors. Only a single injection of 50 to 100 times higher doses of ^{90}Sr than those of alpha emitters resulted in osteosarcomas in mice with the highest incidence of approximately 60 to 70%, as well as with increased frequencies of hemopoietic and vascular neoplasms[30]. The inhalation exposures of dogs to soluble ^{144}Ce chloride induced liver, lung, and nasal mucosal neoplasms rather than primary bone tumors, despite the highly skeletal deposition[31]. It seems more difficult to induce osteosarcomas in mice by chemical carcinogens as described elsewhere[32], though spontaneous osteosarcomas with very low incidences were observed in a colony of C57BL mice, and transplants from some primary tumors were bone forming, suggesting the relations of viral agents[33]. Evi-

dence for the viral etiology of murine osteosarcomas was demonstrated first in CF1 mice by Finkel *et al.*[34], who have developed the experimental model for carcinogenesis to introduce pathogenetic mechanisms common to ^{90}Sr- and virus-induced osteosarcomas[35]. The murine osteosarcoma virus termed FBJ or FBR-MSV has been characterized to bear a transforming sequence of *fos* protooncogenes[36], and the recent study further revealed that deregulated c-*fos* or v-*fos* expression in bone cells induces tumorigenicity and the other factors related to metastasis[37]. The molecular basis for ^{239}Pu-induced bone tumorigenesis, however, remains to be fully elucidated, but would be responsible for the largest and specific carcinogenicity of plutonium compounds among bone seekers.

In conclusion, the injection of soluble ^{239}Pu citrate most effectively and specifically induces osteogenic sarcomas commonly in three strains of mice, irrespective of genetic background for carcinogenesis, with almost similar patterns of dose responsiveness, skeletal distribution sites, and histopathological features. Except for lymphoid neoplasms that appeared as early as bone tumors at the higher dose ranges after ^{239}Pu-injection, the other solid tumors and myeloid leukemias were rather reduced, or reduced much less than the controls, because of the competition with bone tumors, suggesting that neoplasms besides the bone tumors showed non-specific and spontaneous occurrence after the injection of soluble plutonium compounds.

ACKNOWLEDGEMENTS

This work was partly supported by a research grant from the Ministry of Education, Culture, Sports, Science and Technology of Japan. The authors are grateful to Mr. Isao Takahashi from Tokyo Nuclear Services, Co., for his excellent preparations of histological tissue sections, and to the personnel of Animal Care Co. for their helpful support of animal care.

REFERENCES

1. Wick, R. R. and Gössner, W. (1983) Follow-up study of late effects in ^{224}Ra treated ankylosing spondylitis patients. Health Phys. **44** Suppl: 187–195.
2. Rowland, R. E., Stehney, A. F. and Lucas, H. F. (1983) Dose-response relationships for radium-induced bone sarcomas. Health Phys. **44** Suppl: 15–31.
3. Koshurnikova, N.A., Gilbert, E. S., Sokolnikov, M., Khokhryakov, V. F., Miller, S., Preston, D. L., Romanov, S. A., Shilnikova, N. S., Suslova, K. G. and Vostrotin, V. V. (2000) Bone cancers in Mayak workers. Radiat. Res. **154**: 237–245.
4. Finkel, M. P. and Biskis, B. O. (1962) Toxicity of plutonium in mice. Health Phys. **8**: 565–579.
5. Taylor, G. N., Mays, C. W., Lloyd, R. D., Gardner, P. A., Talbot, L. R., McFarland, S. S., Pollard, T. A., Atherton, D. R., van Moorhem, D., Brammer, D., Brammer, T. W., Ayoroa, G. and Taysum, D. H. (1983) Comparative toxicity of ^{226}Ra, ^{239}Pu, ^{241}Am, ^{249}Cf, and ^{252}Cf in C57BL/Do black and albino mice. Radiat. Res. **95**: 584–601.
6. Taylor, D. M. (1986) The comparative carcinogenesis of ^{239}Pu, ^{241}Am and ^{244}Cm in the rat. In: Life-Span Radiation Effects Studies in Animals: What Can They Tell Us?, Eds. R. C. Thompson and J. A. Mahaffey, pp. 404–412, US DOE CONF-830951.
7. Mays, C. W., Taylor, G. N. and Lloyd, R. D. (1986) Toxicity ratios: their use and abuse in predicting the risk from induced cancer. In: Life-Span Radiation Effects Studies in Animals: What Can They Tell Us?, Eds. R. C. Thompson and J. A. Mahaffey, pp. 299–310, US DOE CONF-830951.
8. Mays, C. W., Lloyd, R. D., Taylor, G. N. and Wrenn, M. E. (1987) Cancer incidence and lifespan vs. alpha-particle dose in beagles. Health Phys. **52**: 617–624.
9. Muggenburg, B. A., Mewhinney, J. A., Griffith, W. C., Hahn, F. F., McClellan, R. O., Boecker, B. B. and Scott, B. R. (1983) Dose-response relationships for bone cancers from plutonium in dogs and people. Health Phys. **44**: 529–535.
10. Oghiso, Y., Yamada, Y. and Iida, H. (1997) High frequency of leukemic lymphomas with osteosarcomas but no myeloid leukemias in C3H mice after ^{239}Pu citrate injection. J. Radiat. Res. **38**: 77–86.
11. Oghiso, Y. and Yamada, Y. (2000) Strain differences in carcinogenic and hematopoietic responses of mice after injection of plutonium citrate. Radiat. Res. **154**: 447–454.
12. Stanton, M. F. (1979) Tumors of the bone. In: Pathology of Tumors in Laboratory Animals, vol. II, Tumors of the Mouse, Ed-in-Chief, V. S. Turusov, pp. 577–610, IARC Scientific Publications No. **23**, Lyon.
13. Luz, A. and Gössner, W. (1994) Neoplastic bone lesions in the mouse. In: Pathology of Neoplasia and Preneoplasia in Rodents, Eds. P. Bannasch and W. G–ssner, pp. 142–154, EULEP Color Atlas, Chattauer, Stuttgart & New York.
14. Coggle, J. E., Peel, D. M. and Tarling, J. D. (1985) Lung tumor induction in mice after uniform and non-uniform external thoracic X-irradiation. Int. J. Radiat. Biol. **48**: 95–106.
15. Park, J. F., Buschbom, R. L., Dagle, G. E., James, A. C., Watson, C. R. and Weller, R. E. (1997) Biological effects of inhaled $^{238}PuO_2$ in beagles. Radiat. Res. **148**: 365–381.
16. Muggenburg, B. A., Guilmette, R. A., Mewhinney, J. A., Gillett, N. A., Mauderly, J. L., Griffith, W. C., Diel, J. H., Scott, B. R., Hahn, F. F. and Boecker, B. B. (1996) Toxicity of inhaled plutonium dioxide in beagle dogs. Radiat. Res. **145**: 361–381.
17. Muggenburg, B. A., Hahn, F. F., Griffith Jr, W. C., Lloyd, R. D. and Boecker, B. B. (1996) The biological effects of radium-224 injected into dogs. Radiat. Res. **146**: 171–186.
18. Sontag, W., Wirth, R., Luz, A., Schäffer, E. and Volf, V. (1997) Dosimetry and pathology of ^{237}Np in female rats. Hum. Exp. Toxicol. **16**: 89–100.
19. Sasaki, S. and Fukuda, N. (2002) Dose-response relationship for lifetime excess mortality and temporal patterns of manifestation in mice irradiated neonatally with gamma rays. J. Radiat. Res. **43**: 313–323.
20. Müller, W. A., Luz, A., Murray, A. B. and Linzner, U. (1990) Induction of lymphoma and osteosarcoma in mice by single and protracted low a doses. Health Phy. **59**: 305–310.
21. Breslow, N. E., Day, N. E., Tomatis, L. and Turusov, V. S. (1974) Associations between tumor types in a large-scale carcinogenesis study of CF-1 mice. J. Natl. Cancer Inst. **52**: 233–

239.
22. Humphreys, E. R., Loutit, J. F. and Stones, V. A. (1987) The induction by ^{239}Pu of myeloid leukemia and osteosarcoma in female CBA mice. Int. J. Radiat. Biol. **51**: 331–339.
23. Humphreys, E. R., Issacs, K. R., Raine, T. A., Saunders, J., Stones, V. A. and Wood, D. L. (1993) Myeloid leukemia and osteosarcoma in CBA/H mice given ^{224}Ra. Int. J. Radiat. Biol. **64**: 231–235.
24. Wronski, T. J., Smith, J. M. and Jee, W. S. S. (1980) The microdistribution and retention of injected ^{239}Pu on trabecular bone surfaces of the beagle; implications for the induction of osteosarcoma. Radiat. Res. **83**: 74–89.
25. Smith, J. M., Miller, S. C. and Jee, W. S. S. (1984) The relationships between bone marrow type and microvasculature to the microdistribution and local dosimetry of plutonium in the adult skeleton. Radiat. Res. **99**: 324–335.
26. Luz, A., Müller, W. A., Linzner, U., Strauß, P. G., Schmidt, J., Müller, K., Atkinson, M. J., Murray, A. B., Gössner, W., Erfle, V. and Höfler, H. (1991). Bone tumor induction after incorporation of short-lived radionuclides. Radiat. Environ. Biophys. **30**: 225–227.
27. Taylor, G. N., Lloyd, R. D., Mays, C. W., Miller, S. C., Jee, W. S., Mori, S., Shabestari, L. and Li, X. J. (1997) Relationship of natural incidence and radiosensitivity for bone cancer in dogs. Health Phys. **73**: 679–683.
28. Lloyd, R. D., Taylor, G. N., Jee, W. S. and Miller, S. C. (1999) Relative radiosensitivity of bone tumor induction among beagles as a function of age at injection of ^{239}Pu or ^{226}Ra. Health Phys. **76**: 50–56.
29. Lloyd, R. D., Taylor, G. N. and Miller, S. C. (2000) Does body size contribute to sensitivity of bone tumor induction by radionuclide exposure? Health Phys. **79**, 199–202.
30. McClellan, R. O. and Jones, R. K. (1969) ^{90}Sr-induced neoplasia: a selective review. In: Delayed Effects of Bone-Seeking Radionuclides, Eds. C. W. Mays, W. S. S. Jee, R. D. Lloyd, B. J. Stover, J. H. Dougherty and G. N. Taylor, pp. 293–322, The University of Utah Press, Salt Lake City, Utah.
31. Hahn, F. F., Boecker, B. B., Griffith, W. C. and Muggenburg, B. A. (1997) Biological effects of inhaled $^{144}CeCl_3$ in beagle dogs. Radiat. Res. **147**: 92–108.
32. Frith, C. H., Johnson, B. P. and Highman, B. (1982) Osteosarcomas in BALB/c female mice. Lab. Animal Sci. **32**: 60–63.
33. Franks, L. M., Rowlatt, C. and Chesterman, F. C. (1973) Naturally occurring bone tumors in C57BL/lcrf mice. J. Natl. Cancer Inst. **50**: 431–438.
34. Finkel, M. P., Biskis, B. O. and Jinkins, P. B. (1966) Virus induction of osteosarcoma in mice. Science **151**: 698–701.
35. Finkel, M. P., Reilly Jr., C. A. and Biskis, B. O. (1976) Pathology of radiation and virus-induced bone tumors. In: Recent Results in Cancer Research, vol. **54**, Ed. E. Grundmann, pp. 92–103, Springer-Verlag, Berlin, Heidelberg New York.
36. Goralczyk, R., Closs, E.I., Rüther, U., Wagner, E.F., Strauss, P.G., Erfle, V. and Schmidt, J. (1990) Characterization of fos-induced osteogenic tumours and tumour-derived murine cell lines. Differentiation **44**: 122–131.
37. Rupp, B., Lorenz, U., Schmidt, J. and Wewrenskiold, A. K. (1998) Discordant effects of activator protein-1 transcription factor on gene regulation, invasion, and metastasis in spontaneous, radiation-induced, and fos-induced osteosarcomas. Mol. Carcinogen. **23**: 69–75.

Received on November 26, 2002
1st Revision on February 13, 2003
Accepted on March 19, 2003

J. RADIAT. RES., 44, 261–270 (2003) http://jrr.jstage.jst.go.jp

Comparisons of Pulmonary Carcinogenesis in Rats Following Inhalation Exposure to Plutonium Dioxide or X-ray Irradiation

YOICHI OGHISO* and YUTAKA YAMADA

Lung tumors/Rats/$^{239}PuO_2$/X-ray/Relative effectiveness.

Radiation-induced pulmonary carcinogenesis was compared in female Wistar rats following either inhalation exposure to alpha-emitting $^{239}PuO_2$ aerosols, whole-body or thoracic X-ray irradiation. Dose-dependent survival reduction was correlated with increased malignant lung tumors at doses over 0.45 Gy, reaching the maximum incidence of 90% at 6.6–8.5 Gy in ^{239}Pu-exposed rats. While the differential dose responses for each histopathological type of tumors were noted, almost 70–80% were carcinomas among all of the primary tumors from ^{239}Pu-exposed rats. As the dose response curves for lung carcinomas were compared, the slope of the fit linear equation and the calculated relative effectiveness for 50% incidence of lung carcinomas were approximately 11-times as high in ^{239}Pu-exposure as those of thoracic X-irradiation. The numbers of tumor lesions distributed in the lung per tumor-bearing animal were about 2-fold more in ^{239}Pu-exposed rats, while the proportions of their histopathological types were similar between ^{239}Pu-exposure and X-irradiation. These results indicate that the magnitudes of the relative effectiveness or risk for pulmonary carcinogenesis are greater in ^{239}Pu-exposure than X-irradiation, and that radiation-induced lung tumors appear to originate mostly from the same target epithelial cells.

INTRODUCTION

The risk of human lung tumors derived from internal, *i.e.* inhalation exposure to plutonium or actinide compounds produced by nuclear facilities remains to be fully elucidated, since ICRP Publication 31 in 1980 summarized animal data on their biological effects.[1] While there are uncertainties in approaches to the risk estimation on human lung cancers due to plutonium and/or external radiations in U.S. nuclear workers,[2,3] a series of epidemiological studies on Mayak nuclear workers recently suggested the significant and close association of inhaled plutonium compounds with lung cancer incidence and mortality.[4–6] Irrespective of such human data, animal studies on the lung cancer risk and related mechanisms are, however, essential to clarify variable factors for biokinetics, dosimetry, and biological effectiveness, as has been suggested by lifespan studies.[7]

Animal studies on comparative carcinogenicity after inhalation exposure of rats to insoluble ^{238,239}Pu, ^{244}Cm, and ^{241}Am dioxide aerosols[8–11] have led to comprehensive results on lifetime pulmonary carcinogenesis in rats after inhalation exposure to $^{239}PuO_2$ aerosols.[12–14] In addition, large-scale experiments using beagle dogs have demonstrated the differences in carcinogenicity due to the solubility[15] and in biokinetics due to the aerosol particle size[16] of plutonium compounds, respectively. Such factors as solubility, particle size or specific activity of aerosols could strongly influence the dose distribution and the dose rate responsible for lung tumor induction. However, the relative biological effectiveness or the quality factor required for a risk estimation based on the same dosimetric unit, *i.e.* dose equivalent for the same target cells and tissues, has not been determined.

We have long performed lifespan studies on pulmonary carcinogenesis in rats following inhalation exposure to submicron and polydispersed, high-fired $^{239}PuO_2$ aerosols, and showed differential dose responses of lung tumor types[17] and pathogenetic processes.[18] The present study was done to summarize the final data from ^{239}Pu-exposed rats and to compare the effectiveness for pulmonary carcinogenesis with that of low linear energy transfer (LET) X-ray irradiation in the same strain of animals. The differences in carcinogenicity and related mechanisms from the other alpha-emitting actinides or radiation sources are discussed.

MATERIALS AND METHODS

Animals

Because of easier handling for long-term animal care and the lower incidences of spontaneous lung tumors, female Wistar

*Corresponding author: Phone: +81-43-206-3100,
Fax: +81-43-284-1389,
E-mail: y_oghiso@nirs.go.jp
Internal Radiation Effects Research Group, Research Center for Radiation Safety, National Institute of Radiological Sciences, 9-1, 4-chome, Anagawa, Inage-ku, Chiba 263-8555, Japan.

(W/M) strain rats purchased from a breeding colony (Japan SLC Co.) were used for either inhalation exposure to plutonium dioxide aerosols or X-ray irradiation at the age of 100 to 120 days after birth, as previously described.[13,14,17] Before and after all of the experiments, animals were housed 5 per polycarbonate cage in a closed hood rack for groups of plutonium-exposed rats or 5 per stainless-steel cage in a cascade cage rack for the groups of X-irradiated rats, respectively, and kept under a barrier-filtered air condition with a commercial diet (Funabashi Farm Co.) and water *ad libitum*. All of the animal rooms were maintained on a 12-h light:dark cycle at a room temperature of 23 ± 1.0°C with a humidity of 55 ± 5.0%. The animal care included a weekly change of cages and a daily check of the animals' condition during their lifetimes. All of the experimental treatments were performed with the approval of the institution's animal use committee.

Inhalation exposure and dose calculation

As previously described,[17,18] a plutonium hydroxide solution prepared from a stock nitrate solution was nebulized in a compressed air-driven nebulizer, passed through a tube heated at 300°C to dry the droplets in the air, and then conducted into a high-temperature furnace heated at 1,150°C to make high-fired $^{239}PuO_2$ aerosols with an average of activity median aerodynamic diameter (AMAD) of 0.40 ± 0.005 μm and an average of geometric standard deviation (GSD) of 2.2 ± 0.1. The air flow containing such polydispersed and submicron aerosols was introduced through a negative pressure by an exhaust air pump into a multiport inhalation chamber device in which 20 animals per each experiment were placed into a plastic holder for a nose-only exposure once for the minimum of 5 min to the maximum of 60 min to $^{239}PuO_2$ aerosols. The initial lung deposition of each exposed animal was determined by whole-body counting of the low-energy (17 keV) LX-rays emitted from ^{239}Pu deposited in the lung 7 days after the exposure, as described previously,[17] ranged from the minimum of 7 Bq to the maximum of 2,200 Bq in the present study. The cumulative alpha-particle dose absorbed in the whole lung was calculated at the time of death by using the time integral of the initial lung deposition and the retention function obtained from the follow-up whole-body counting of another 20 exposed animals until 400 days after the exposure, ranged from the minimum of 0.05 Gy to the maximum of 10.5 Gy in the present study.

X-ray irradiation and dose measurement

We initially tried to achieve intermittent and fractionated whole-body X-irradiation (WBX) using X-rays of 200 kVp and 6.0 mA with 0.5 mm Cu and 0.5 mm Al filters and with FSD (field-source-distance) of 100 cm at a dose rate of 0.1 Gy/min using Pantak HF 320S (Shimadzu). Five animals per each irradiation were exposed repeatedly, 3-times a week, in a cylindrical Lucite holder with 6-separated chambers to fractionated X-rays by a split dose of 0.5 Gy to achieve a total accumulated dose of 0.5 to 10 Gy. For local, thoracic X-irradiation (ThX), 5 animals per each irradiation were anesthetized with intraperitoneal injection of sodium pentbarbital, and exposed once in a rectangular Lucite holder separated by 6 chambers, shielded with a 5 mm-thick lead sheet, except for the thorax, to a single dose of X-rays of 200 kVp and 20 mA with 0.5 mm Cu and 0.5 mm Al filters and with FSD of 75 cm at a dose rate of 0.6 Gy/min to achieve a total accumulated dose of 1.0 to 10 Gy. Dosimetry was carried out during all irradiation processes with a 0.6 ml C-110 ionization chamber in conjunction with a thermoluminescent dosemeter (model AE-1321M, Applied Engineering Inc.) put onto the central or thoracic position of an empty chamber of the Lucite holder used for both irradiation regimens. The average total accumulated dose measured by the above dosimetry was regarded as the absorbed dose in the whole lung of each experimental group.

Pathological examinations

Postmortem pathological examinations were performed on all the dead or moribund and sacrificed animals from all of the experimental groups, except for those which lost main organs by cannibalism or were severely autolysed. At autopsy, the gross lesions were carefully examined, particularly on the distribution of neoplastic lesions in each lobe of the lung, and other parts of the respiratory tracts. The whole lungs and the other main organs, except for the central nervous system, were fixed in 10% phosphate-buffered formalin, dissected into either at least a total 15 sagittal sections from the whole lung lobes as well as tumor mass, or a few small pieces from each of the other main organs, processed with graded ethanol and xylene in an automatic tissue processor. They were then embedded in paraffin. Five to 6 μm-thick sections were prepared from each paraffin-embedded tissue block, and stained routinely with hematoxylin and eosin (HE) for light microscopic examinations. Differential diagnoses of the primary lung tumors from metastatic tumors and between histopathological types of tumors were performed morphologically, according to those criteria described.[19,20] Almost all of the primary lung tumors, except for only a few percentage of non-epithelial types, such as fibrosarcomas and hemangiosarcomas, were classified into 4 epithelial types: benign adenomas and malignant carcinomas including adenocarcinomas, adenosquamous carcinomas and squamous cell carcinomas. The numbers of these epithelial types of lung tumor lesions distributed in the whole lung were estimated by enumerating those numbers observed in serial sections prepared from at least 15 sagittal tissue sections of the whole lung lobes from each tumor-bearing animal.

Statistics

The survival period after ^{239}Pu-exposure or X-irradiation was analysed for the competing risk of neoplastic or non-neoplastic death by Kaplan-Meier non-parametric analysis, and compared as well as primary lung tumor incidences for statistically significant differences between the control and ^{239}Pu-exposed or X-irradiated groups using Student's *t*-test. The standard errors for

the primary lung tumor incidences were calculated using the following formula[21]:

$$SE = [p(1-p)/n]^{1/2},$$

where p is the proportion of animals with lung tumors and n the total number of animals examined in each group.

A linear regression analysis based on the least-squares method was applied to the dose response curves of lung carcinomas from both ^{239}Pu-exposed and X-irradiated rats to introduce a fit linear equation with square correlation coefficients, as described.[22]

RESULTS

Dose and survival periods

As shown in Table 1, total 600 $^{239}PuO_2$-exposed rats were divided into 8 groups (Pu 1 to Pu 8) based on the mean values of the intial lung deposition and lung dose from 0.16 Gy to 8.52 Gy. As compared to the control group of total 206 unexposed animals, the mean survival periods of the groups (Pu 2–Pu 8) of rats that received mean lung doses of more than 0.45 Gy were significantly ($p < 0.01$ or 0.001) reduced, while that of the group (Pu 1) of rats that received the lowest dose of 0.16 Gy was not significantly different from the controls. Among the primary lung tumors observed, benign tumors, all the adenomas, showed incidences of 20–24% at lower to middle doses of 0.16–2.76 Gy, but then decreased down to the bottom at higher doses of 4.67–8.52 Gy. In contrast, the incidence of malignant tumors, including carcinomas and a few sarcomas, was not significantly different in the lowest dose group (Pu 1) that received 0.16 Gy from that

Table 1. Survival period and lung tumor induction following inhalation exposure to $^{239}PuO_2$ aerosols.

Group name	No. of animals	Initial lung deposition (Bq)[a]	Lung dose (Gy)[b]	Survival period (day)[c]	No. of primary lung tumor-bearers (% ± SE)[d]	
					Benign	Malignant
Control	206	0	0	817 ± 146	3 (1.5 ± 0.8)	1 (0.5 ± 0.5)
Pu 1	80	24 ± 8	0.16 ± 0.05	855 ± 124	16 (20.0 ± 4.5)**	1 (1.2 ± 1.2)
Pu 2	134	65 ± 30	0.45 ± 0.24	764 ± 165*	33 (24.6 ± 3.7)**	12 (8.9 ± 2.4)*
Pu 3	128	228 ± 48	1.59 ± 0.32	765 ± 155*	30 (23.4 ± 3.7)**	60 (46.9 ± 4.4)**
Pu 4	126	416 ± 98	2.76 ± 0.43	692 ± 148**	29 (23.0 ± 3.7)**	78 (61.9 ± 4.3)**
Pu 5	40	787 ± 79	4.67 ± 0.24	675 ± 98**	5 (12.5 ± 5.2)**	32 (80.0 ± 6.3)**
Pu 6	31	948 ± 76	5.43 ± 0.29	622 ± 105**	3 (9.7 ± 5.3)*	27 (87.1 ± 6.0)**
Pu 7	31	1,147 ± 114	6.61 ± 0.28	550 ± 82**	1 (3.2 ± 3.1)	28 (90.3 ± 5.3)**
Pu 8	30	1,672 ± 261	8.52 ± 0.67	458 ± 95**	0	27 (90.0 ± 5.5)**

[a]Mean ± SD of the initially deposited activity estimated per animal in each group. [b]Mean ± SD of the cumulative lung dose calculated per animal in each group. [c]Mean ± SD of the survival period per animal after the time of inhalation exposure in each group. [d]The numbers and percent incidence ± SE in parenthesis of tumor-bearing animals examined in each group. Benign tumors are adenomas, and malignant tumors include all the carcinomas and a few sarcomas. Asterisks indicate a significant difference compared to the controls (*$p < 0.01$, **$p < 0.001$).

Table 2. Survival period and lung tumor induction following whole-body or thoracic X-irradiation.

Group name	No. of animals	Dose (Gy)[a]	Survival period (day)[b]	No. of primary lung tumor-bearers(% ± SE)[c]	
				Benign	Malignant
Whole-body X-irradiation					
Control	99	0	812 ± 125	1 (1.0± 1.0)	0
A	46	0.5	780 ± 139	0	1 (2.2 ± 2.0)
B	47	1.0	800 ± 163	2 (4.2 ± 2.9)	1 (2.1 ± 2.1)
C	45	2.0	767 ± 156*	3 (6.7 ± 4.0)*	0
D	47	3.0	711 ± 140**	3 (6.4 ± 3.6)*	3 (6.4 ± 3.6)*
E	45	5.0	698 ± 131**	2 (4.4 ± 3.1)	3 (6.7 ± 3.7)*
F	45	10.0	584 ± 150**	3 (6.7 ± 3.7)*	4 (8.9 ± 4.2)*
Thoracic X-irradiation					
Control	47	0	828 ± 162	1 (2.1 ± 2.1)	0
G	70	1.0	803 ± 142	3 (4.3 ± 2.4)*	3 (4.3 ± 2.4)*
H	85	3.0	798 ± 128	7 (8.2 ± 3.0)*	8 (9.4 ± 3.1)*
I	84	5.0	687 ± 168**	11(13.1 ± 3.7)**	11 (13.1 ± 3.7)**
J	53	10.0	577 ± 145**	13(24.5 ± 5.9)**	8 (15.1 ± 4.9)**

[a]The average accumulated dose measured by a thermoluminescent dosimetry in each group. [b]Mean ± SD of the survival period per animal after the cessation of irradiation in each group. [c]The numbers and percent incidence ± SE in parenthesis of tumor-bearing animals examined in each group. Benign tumors are adenomas, and malignant tumors include all the carcinomas and a few sarcomas. Asterisks indicate a significant difference compared to the controls (*$p < 0.01$, **$p < 0.001$).

Table 3. Incidence of primary lung tumors following $^{239}PuO_2$-exposure or X-irradiation.

Group name	Mean dose (Gy)	No. of animals	No. of primary lung tumor-bearers (% ± SE)[a]				
			Adenoma	Adenocarcinoma	Adenosquamous carcinoma	Squamous cell carcinoma	Others
$^{239}PuO_2$-exposure							
Control	0	206	3 (1.5 ± 0.8)	0	0	1 (0.5 ± 0.5)	0
Pu 1	0.16	80	16 (20.0 ± 4.5)	1 (1.2 ± 1.2)	0	0	0
Pu 2	0.45	134	33 (24.6 ± 3.7)	11 (8.2 ± 2.4)	0	1 (0.7 ± 0.7)	0
Pu 3	1.59	128	30 (23.4 ± 3.7)	53 (41.4 ± 4.3)	4 (3.1 ± 1.5)	3 (2.3 ± 1.3)	0
Pu 4	2.76	126	29 (23.0 ± 3.7)	63 (50.0 ± 4.4)	9 (7.1 ± 2.3)	6 (4.7 ± 1.9)	0
Pu 5	4.67	40	5 (12.5 ± 5.2)	14 (35.0 ± 7.5)	13 (32.5 ± 7.4)	5 (12.5 ± 5.2)	0
Pu 6	5.43	31	3 (9.7 ± 5.3)	11 (35.5 ± 8.6)	12 (38.7 ± 8.7)	4 (12.9 ± 6.0)	0
Pu 7	6.61	31	1 (3.2 ± 3.1)	10 (32.2 ± 8.4)	14 (45.2 ± 8.9)	3 (9.7 ± 5.3)	1 (3.2 ± 3.1)
Pu 8	8.52	30	0	10 (33.3 ± 8.6)	15 (50.0 ± 9.1)	1 (3.3 ± 3.2)	1 (3.3 ± 3.2)
Whole-body X-irradiation							
Control	0	99	1 (1.0 ± 1.0)	0	0	0	0
A	0.5	46	0	1 (2.2 ± 2.0)	0	0	0
B	1.0	47	2 (4.2 ± 2.9)	1 (2.1 ± 2.1)	0	0	0
C	2.0	45	3 (6.7 ± 4.0)	0	0	0	0
D	3.0	47	3 (6.4 ± 3.6)	2 (4.2 ± 2.9)	1 (2.1 ± 2.1)	0	0
E	5.0	45	2 (4.4 ± 3.1)	2 (4.4 ± 3.1)	0	1 (2.2 ± 2.2)	0
F	10.0	45	3 (6.7 ± 3.7)	2 (4.4 ± 3.1)	0	1 (2.2 ± 2.2)	1 (2.2 ± 2.2)
Thoracic X-irradiation							
Control	0	47	1 (2.1 ± 2.1)	0	0	0	0
G	1.0	70	3 (4.3 ± 2.4)	2 (2.9 ± 2.0)	0	0	1 (1.4 ± 1.4)
H	3.0	85	7 (8.2 ± 3.0)	7 (8.2 ± 3.0)	0	1 (1.2 ± 1.2)	0
I	5.0	84	11 (13.1 ± 3.7)	7 (8.3 ± 3.0)	1 (1.2 ± 1.2)	3 (3.6 ± 2.0)	0
J	10.0	53	13 (24.5 ± 5.9)	7 (13.2 ± 4.6)	0	1 (1.9 ± 1.9)	0

[a]The numbers and percent incidence ± SE in parenthesis of tumor-bearing animals examined in each group. Others include fibrosarcomas or hemangiosarcomas.

of the controls, but significantly and drastically increased up to the maximum of about 90% at doses of 0.45–6.61 Gy, and then reached a plateau at 6.61–8.52 Gy. These findings indicate that significant survival reduction was well correlated with the increase of malignant lung tumors from $^{239}PuO_2$-exposed rats that received a mean lung dose of 0.45 Gy or more. Malignant tumors appeared relatively early from 350 days to the middle periods of 500 days after exposure (data not shown).

On the other hand, a total of 275 whole-body X-irradiated rats and a total of 292 thoracic X-irradiated rats were divided into 6 groups (A to F) and 4 groups (G to J), respectively. As compared to each control group, the mean survival periods were significantly ($p < 0.01$ or 0.001) reduced at 2.0 Gy or more in whole-body X-irradiated rats and at 5.0 Gy or more in thoracic X-irradiated rats, respectively (Table 2). Both benign and malignant lung tumors from whole-body X-irradiated rats were significanly observed, but with lower frequencies at doses of 2.0–10 Gy, whereas those from thoracic X-irradiated rats significantly increased at doses of 3.0–5.0 Gy, and reached the maximum of only 15–24% at the highest dose of 10 Gy. Thus, the incidences of primary lung tumors, particularly malignant ones, were much lower in both X-irradiated rats than those of $^{239}PuO_2$-exposed rats, indicating that significant survival reduction observed at higher doses of more than 3.0 or 5.0 Gy of X-irradiation was not correlated with the increase of malignant lung tumors, but was rather due to an early increase of the other solid tumors, such as mammary and ovary tumors (data not shown).

Dose and lung tumor incidences

Primary lung tumors from both $^{239}PuO_2$-exposed and X-irradiated rats were classified mostly into 4 epithelial types (adenomas, adenocarcinomas, adenosquamous carcinomas and squamous cell carcinomas) and only a few non-epithelial types (fibrosarcomas and hemangiosarcomas), as described in materials and methods. As shown in Table 3, the incidence of adenomas from $^{239}PuO_2$-exposed rats reached a plateau of 20–24% at lower to middle doses of 0.16–2.76 Gy, then declined down to the bottom at the higher doses of 4.67–8.52 Gy, while the remaining 70–80% of primary tumors were carcinomas, showing differential dose responses for each histopathological type: adenocarcinomas increased drastically up to a maximum of about 50% at middle doses of 1.59–2.76 Gy, then reduced slightly down to a plateau of 32–35% at higher doses of 4.67–8.52 Gy; adenosquamous carcinomas increased drastically at doses of 4.67 Gy or more, then reached a maximum of about 50% at the highest dose of 8.52 Gy; squamous cell carcinomas

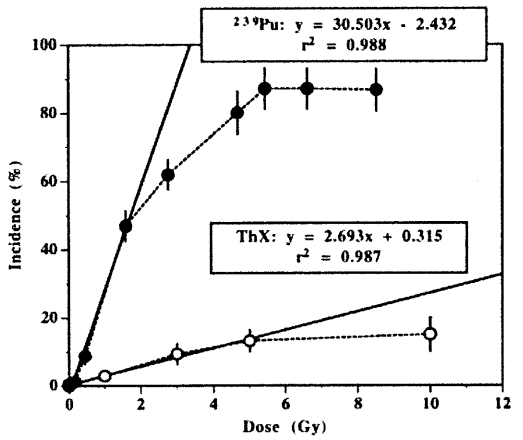

Fig. 1. Comparisons of dose response curves for rat lung carcinomas following $^{239}PuO_2$-exposure or thoracic X-irradiation. A linear correlation analysis was applied to both dose response curves of lung carcinomas for inhalation exposure to $^{239}PuO_2$ (^{239}Pu) or thoracic X-irradiation (ThX) to introduce a fit linear equation with a square correlation coefficient, as shown in the frame, respectively.

were, however, fewer than the other epithelial types of tumors to show only slight increase at higher doses of 4.67–6.61 Gy. In contrast, almost 80–90% of the primary lung tumors from both X-irradiated rats were adenomas and adenocarcinomas, whereas adenosquamous and squamous cell carcinomas were scarce (Table 3). The incidences of both adenomas and adenocarcinomas from whole-body X-irradiated rats were, however, much lower, while adenomas and adenocarcinomas from thoracic X-irradiated rats prominently increased up to incidences of 13–24% only at higher doses of 5.0–10 Gy to show a significant dose response, respectively. Thus, together with the above findings on ^{239}Pu-induced lung tumors, dose response curves for primary lung carcinomas are available for comparisons between $^{239}PuO_2$-exposed and thoracic X-irradiated rats.

Comparisons of fit linear dose response curves for lung carcinomas

Because almost all of the malignant lung tumors from $^{239}PuO_2$-exposed rats were carcinomas, and a significant dose response of lung carcinomas from thoracic X-irradiated rats was only available for comparisons, as described above, a linear regression analysis was done for both dose response curves of lung carcinomas from $^{239}PuO_2$-exposed and thoracic X-irradiated rats. As shown in Fig. 1, a linear correlation was only applied to the initial linear portion of the respective dose response curve at the lower to middle dose ranges, *i.e.* 0.16–1.59 Gy for $^{239}PuO_2$ (^{239}Pu), and 1.0–5.0 Gy for thoracic X (ThX) to introduce a well-fitted linear equation with a significant square correlation coefficient. Both fit linear equations showed high correlation coefficients, $r^2 = 0.988$ for ^{239}Pu and $r^2 = 0.987$ for ThX; the slope of the linear equation from ^{239}Pu appeared to be approximately 11-fold of that from ThX. The effective doses for 50% incidence of lung carcinomas were calculated from these linear equations shown in Fig. 1 to be 1.72 (Gy) for ^{239}Pu and 18.4 (Gy) for ThX. So far, the relative effectiveness for 50% incidence of ^{239}Pu-induced lung carcinomas to that of ThX-induced carcinomas is assumed to be approximately 10.7. Thus, both the slope and the relative effectiveness obtained from the fit linear dose response curves indicate almost 11-fold differences in the dose and effectiveness for pulmonary carcinogenesis between $^{239}PuO_2$-exposure and thoracic X-irradiation.

Histopathology of lung tumor lesions

Typical histopathological features of each lung tumor type from $^{239}PuO_2$-exposed rats are shown in Fig. 2. Most of the epithelial types of tumors were found either in the bronchiolo-alveolar or peripheral and subpleural alveolar regions, while only a few squamous cell carcinomas were distributed in the bronchial or bronchiolar regions. All of the adenomas were localized, and appeared to show ductal forms with columnar or cuboidal epithelium (Fig. 2A), or sometimes papillary structures surrounded by a monolayer of cuboidal epithelium with the connective tissue stroma, as shown in Fig. 2B. Adenocarcinomas were more extensively distributed in the alveolar sacs or bronchiolar lumens to make multiple foci, mostly showing papillary and intraductal growth of variable-sized and irregular-shaped epithelial cells (Fig. 2C), or occasionally solid appearances due to closely compact growth of large epithelial cells (Fig. 2D). Adenosquamous carcinomas were found, mostly in areas adjacent to the foci of such solid adenocarcinomas, to show pearl-like structures of concentrically growing epithelial cells with none, or lesser, keratinization, as shown in Fig. 2E, while squamous cell carcinomas appeared to show more irregular-shaped, pearl-like structures with amounts of keratin (Fig. 2F) and mostly contained necrotic cellular debris inside the carcinoma foci..

These histopathological appearances of $^{239}PuO_2$-induced lung tumor types were similar to those of X ray-induced tumor types, and the proportions of each histopathological type of lung tumor lesions distributed in the lungs from all the $^{239}PuO_2$-exposed tumor-bearers were also similar to those from both X-irradiated tumor-bearers (Fig. 3). Thus, almost 50% were adenomas, 30–40% adenocarcinomas, and 10–20% adenosquamous and squamous cell carcinomas, respectively. The numbers of lung tumor lesions were, however, different as compared among the $^{239}PuO_2$-exposed and X-irradiated tumor-bearers. As shown in Table 4, the average numbers of adenomatous lesions distributed in the lung per a tumor-bearing animal from $^{239}PuO_2$-exposed and both of X-irradiated groups were not different, despite some variety among doses, while the average numbers of carcinomatous lesions per $^{239}PuO_2$-exposed tumor-bearers, were approximately 2-fold more than those of both X-irradiated tumor-bearers, particularly at higher doses of more than 4–5 Gy. The microscopic sizes of these carcinomatous lesions also appeared to be larger in $^{239}PuO_2$-exposed rats than in X-irradiated rats (data not shown).

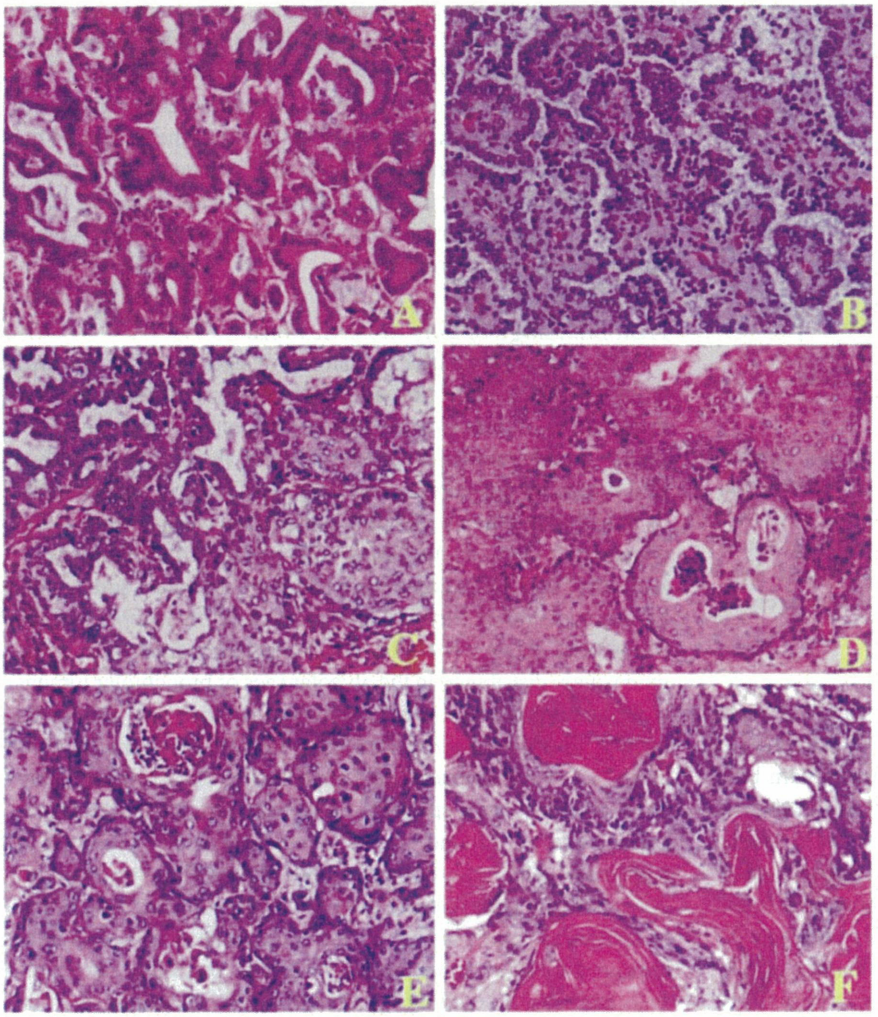

Fig. 2. Typical histopathological features of rat lung tumors following inhalation exposure to $^{239}PuO_2$ aerosols. (A) Columnar duct adenoma in the bronchiolo-alveolar region of the lung from a rat that received 0.19 Gy in 838 days after exposure. (B) Papillary adenoma in the alveolar region of the lung from a rat that received 0.16 Gy in 924 days after exposure. (C) Papillary and duct adenocarcinoma in the bronchiolo-alveolar region of the lung from a rat that received 2.10 Gy in 804 days after exposure. (D) Solid adenocarcinoma in the bronchiolo-alveolar region of the lung from a rat that received 4.15 Gy in 636 days after exposure. (E) Adenosquamous carcinoma in the bronchiolo-alveolar region of the lung from a rat that received 3.08 Gy in 779 days after exposure. (F) Squamous cell carcinoma in the bronchiolo-alveolar region of the lung from a rat that received 6.53 Gy in 580 days after exposure. All of the specimens were stained with HE under a ×200 high-power magnification.

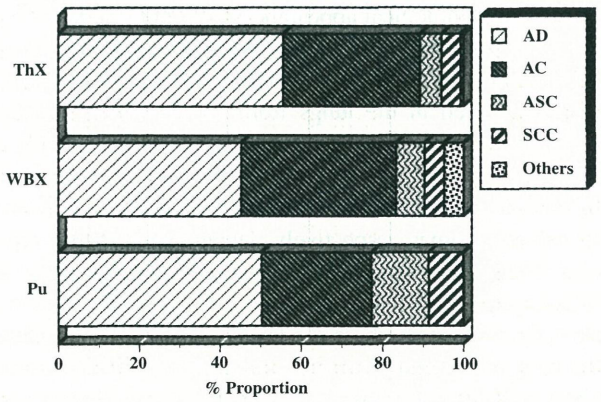

Fig. 3. Proportions of tumor lesions distributed in rat lungs following $^{239}PuO_2$-exposure or X-irradiation. The percent proportions of each lung tumor lesions, adenomas (AD), adenocarcinomas (AC), adenosquamous carcinomas (ASC), squamous cell carcinomas (SCC) and other types including fibrosarcomas or hemangiosarcomas, are shown among all of the tumor lesions found after inhalation exposure to $^{239}PuO_2$ (Pu), and whole-body X-irradiation (WBX) or thoracic X-irradiation (ThX), respectively.

DISCUSSION

In the present study, the dose-dependent survival reduction, due to the increased and relatively early occurring carcinomas after inhalation exposures of rats to $^{239}PuO_2$, was only apparent at more than 0.45 Gy, but not significantly observed at the lowest dose of 0.16 Gy. This clearly indicates the plausible threshold-like dose around 0.16 Gy for the survival reduction and induction of carcinomas, as has been described previously to be noted around 0.5–1.0 Gy.[12,13,17] The relevance of lung carcinomas with lower frequencies from both whole-body or thoracic X-irradiated rats to the significant survival reduction even at higher doses was, however, considered to be much less while, instead, malignant and occasionally metastatic solid tumors, such as ovary and mammary carcinomas, other than the primary lung tumors, might influence early neoplastic death, leading to survival reduction.

While the dose response for lung carcinomas, accounting for almost 70–80% of all primary lung tumors from $^{239}PuO_2$-exposed rats, was much different from those of both whole-body

Table 4. Numbers of adenoma and carcinoma lesions following $^{239}PuO_2$-exposure or X-irradiation.

Group name	Mean dose (Gy)	No. of lung tumor-bearers	No. of lung tumor lesions[a]		
			All	Adenoma	Carcinomas
$^{239}PuO_2$-exposure					
Control	0	4	7 (1.7)	5 (1.2)	2 (0.5)
Pu 1	0.16	17	25 (1.5)	18 (1.1)	7 (0.4)
Pu 2	0.45	45	101 (2.2)	83 (1.8)	18 (0.4)
Pu 3	1.59	90	270 (3.0)	167 (1.8)	103 (1.1)
Pu 4	2.76	107	340 (3.2)	195 (1.8)	145 (1.4)
Pu 5	4.67	37	107 (2.9)	38 (1.0)	69 (1.9)
Pu 6	5.43	30	100 (3.3)	26 (0.9)	74 (2.5)
Pu 7	6.61	29	92 (3.2)	21 (0.7)	69 (2.4)
Pu 8	8.52	27	89 (3.3)	15 (0.6)	72 (2.7)
Whole-body X-irradiation					
Control	0	1	1 (1.0)	1 (1.0)	0 (0)
A	0.5	1	2 (2.0)	1 (1.0)	1 (1.0)
B	1.0	3	5 (1.7)	3 (1.0)	2 (0.7)
C	2.0	3	6 (2.0)	4 (1.3)	2 (0.7)
D	3.0	6	8 (1.3)	4 (0.7)	4 (0.7)
E	5.0	5	10 (2.0)	4 (0.8)	6 (1.2)
F	10.0	7	11 (1.6)	3 (0.4)	7 (1.0)
Thoracic X-irradiation					
Control	0	1	1 (1.0)	1 (1.0)	0 (0)
G	1.0	6	7 (1.2)	4 (0.7)	2 (0.3)
H	3.0	15	33 (2.2)	15 (1.0)	18 (1.2)
I	5.0	22	59 (2.7)	32 (1.4)	27 (1.2)
J	10.0	21	70 (3.3)	43 (2.0)	27 (1.3)

[a]Total enumerated numbers of lung tumor lesions distributed in the whole lungs from lung tumor-bearers and the numbers in parenthesis indicate the average numbers of lesions per a lung tumor-bearer examined in each group.

and thoracic X-irradiated rats, only the dose response curve for lung carcinomas from thoracic X-irradiated rats was available for a comparison with that of carcinomas from $^{239}PuO_2$-exposed rats. Because the slope of the fit linear curve and the calculated relative effectiveness for 50% incidence of lung carcinomas were estimated to be about 11-times as high in ^{239}Pu-induced carcinomas as those of thoracic X-induced carcinomas, the differences in the relative effectiveness or risk for pulmonary carcinogenesis would be larger, as expected between ^{239}Pu and X-rays. The rat lung tumors induced by both whole-body and thoracic X-irradiation have also been documented to show a lower incidence of at most 6.6%, even at the highest accumulated thoracic dose of 38 Gy in Fischer 344 rats,[23] while the exposure to high-LET radiations, such as neutrons, and radon and progeny could induce more lung tumors in Sprague-Dawley rats with higher relative biological effectiveness of about 50 or more, as compared to low-LET γ-rays.[24] In addition, there have been some descriptions on the differences in dose responsiveness and lung tumor types induced in rats following either fission fragment irradiation or exposure to enriched uranium oxide,[25] fission neutron exposure, as compared to γ-ray irradiation,[26] β-ray irradiation by inhalation exposure to insoluble ^{144}Ce-infused alminosilicate aerosols,[27,28] or α-particle irradiation by inhalation exposure to uranium ore dust.[29] Because of variable irradiation regimens and the dose rates used in these studies, comparisons with the present results are not easy to introduce differences in the relative effectiveness or radiation quality in pulmonary carcinogenesis, but it appears that the incidence and types of rat lung tumors would be rather more dependent on the radiation quality than on the radiation doses distributed in the lung.

In addition to the 11-fold difference in the relative effectiveness for carcinogenesis, the numbers of carcinoma lesions distributed in the lung per tumor-bearing animal were 2-fold more in $^{239}PuO_2$-exposure than in both types of X-irradiation, implicating the differences, as well as the sizes of the foci, in the extent of severity of carcinoma lesions. Irrespectively, the proportions of each histopathological type of lung tumor lesions distributed in the lung were similar, as shown by the proportions of approximately 80–90% adenomas and adenocarcinomas, and 10–20% adenosquamous and squamous cell carcinomas, in both $^{239}PuO_2$-exposure and X-irradiation, suggesting that most of primary lung tumors, adenomas and adenocarcinomas, induced by α-particles from ^{239}Pu or by X-rays, despite the differences in the dose and effectiveness, originate from the same target epithelial cells, such as alveolar type II pneumocytes and/or bronchiolar Clara cells, as previously described,[30] and supported by the review of the ICRP Publication 66 (1994)[31] and the NCRP report (1997).[32]

Among α-emitting actinides, there seems to be a variety in the dose responsiveness of malignant lung tumors in rats following

inhalation exposure to $^{244}Cm_2O_3$[33], or $^{237}NpO_2$[34], as compared to ^{239}Pu compounds. Such differences as the relative effectiveness or risk for pulmonary carcinogenesis appeared to be due to a larger dose delivery resulting from the aggregation of inhaled $^{239}PuO_2$ aerosol particles in the pulmonary fibrotic scar tissues,[35–37] whereas the contradictory results and implications were obtained concerning pre-existing pulmonary fibrosis, which appeared to modify to a lesser extent the initial lung deposition of inhaled $^{239}PuO_2$ aerosols, dose delivery to the target epithelial cells, and the resultant pulmonary carcinogenesis in rats as compared between groups with similar alpha doses to the lung.[38] Otherwise, either homogenous dose distribution, such as exposure to radon and uranium ore dust, or specific activity of non-uniformly deposited aerosol particles, such as actinides, might influence more the risk for pulmonary carcinogenesis.[22]

As described previously in our paper,[17] the dose responsiveness as well as lung tumor types were different as compared among three experiments, including ours, performed in rats exposed to $^{239}PuO_2$ aerosols with different particle sizes.[12,14] In consideration of the descriptions of both ICRP and NCRP reports[31,32] that the deposition and dose distribution of inhaled aerosol particles in the respiratory tract depend on the aerosol size, submicron aerosols with AMAD of 0.4 μm (estimated geometric diameter of 0.1–0.2 μm) in our experiments may induce a more uniform alpha particle dose distribution to irradiate more efficiently target epithelial cells distributed in the bronchiolo-alveolar regions with lower dose rate as compared to the other two experiments using aerosols with AMAD of 1.0–1.5 μm (estimated geometric diameter of 1.0–2.0 μm), which probably cause particle aggregations in the fibrotic scar, as described elsewhere,[35–37] and a more non-uniform dose distribution with a higher dose rate, resulting in a shift of the peak incidence of lung carcinomas from the lower to higher dose ranges, and an increased proportion of squamous cell carcinomas in the bronchial to bronchiolar regions. Such speculation would be available for the present results that adenomas in the alveolar regions were still more frequently observed at lower doses below 1.59 Gy, and adenocarcinomas increased up to the maximum incidence of 50% at the middle dose of 2.76 Gy, while adenosquamous or squamous cell carcinomas increased at higher doses of more than 4.67 Gy, respectively. Such trends for differential dose responses of carcinoma types are consistent with those results that adenocarcinomas are more frequently induced by lower doses less than 1.4 Gy, while squamous carcinomas increased at higher doses of more than 8.0 Gy, implicating the dose rate effects due to non-uniform distribution of aggregated aerosol particles in the fibrotic scar, as described.[37] Concerning the dose-rate effects of a uniform alpha particle distribution on pulmonary carcinogenesis, there has, however, been an argument on the reverse dose-rate effects either in lower dose ranges below 25 WLM (working level month) or higher dose ranges over 1,000 WLM of inhalation exposure of rats to radon and progeny on the incidences of pulmonary cancers,[39–41] even though alpha particles from gaseous or ultrafine attached aerosol elements of radon and progeny could more uniformly irradiate target epithelial cells, irrespective of different dose rates.

In conclusion, we have shown the following results by lifetime animal experiments using 600 ^{239}Pu-exposed and almost 600 X-irradiated female Wistar rats: the magnitudes of the relative effectiveness or risk for pulmonary carcinogenesis were approximately 11-fold greater in ^{239}Pu-exposure than those of thoracic X-irradiation, and the numbers of lung tumor lesions distributed in the lung of tumor-bearing animals were about 2-fold different, while their proportions of each histopathological type were almost similar between ^{239}Pu-exposed and both X-irradiated rats, suggesting that lung tumors induced by alpha particles or X-irradiation appear to originate mostly from the same target epithelial cells.

ACKNOWLEDGEMENTS

This work was partly supported by a grant from Japan Ministry of Education, Culture, Science and Technology. The authors wish to express gratitudes to Dr. Yuji Yamada from the radon research group, NIRS for his aerosol assessments, Dr. Nobuhito Ishigure from the environmental radiation protection research group, NIRS for his lung dosimetry, and Dr. Paul Fritsch from the laboratoire de radiotoxicologie, DRR/DSV/CEA, France for his discussion and comments on the dose and lung tumor induction. We are also grateful to Mr. Isao Takahashi from Tokyo Nuclear Services, Co. for his effortive preparations of histological tissue sections, and the members of Animal Care Co. for their helpful support of animal care.

REFERENCES

1. ICRP (1980) Biological effects of inhaled radionuclides. ICRP Publication 31, Annals of the ICRP 4(1/2), Pergamon Press, Oxford.
2. Tietjen, G. L. (1987) Plutonium and lung cancer. Health Phys. **52**: 625–628.
3. Gilbert, E. S., Fry, S. A., Wiggs, L. D., Voelz, G. L., Cragle, D. L. and Petersen, G. R. (1989) Analyses of combined mortality data on workers at the Hanford site, Oak Ridge National Laborartory and Rocky Flats nuclear weapons plant. Radiat. Res. **120**: 19–35.
4. Tokarskaya, Z. B., Okladnikova, N. D., Belyaeva, Z. D. and Drozhko, E. G. (1995) The influence of radiation and nonradiation factors on the lung cancer incidence among the workers of the nuclear enterprize Mayak. Health Phys. **69**: 356–366.
5. Koshurnikova, N. A., Bolotnikova, M. G., Ilyin, L. A., Keirim-Markus, I. B., Menshikh, Z. S., Okatenko, P. V., Romanov, S. A., Tsvetkov, V. I. and Shilnikova, N. S. (1998) Lung cancer risk due to exposure to incorporated plutonium. Radiat. Res. **149**: 366–371.
6. Kreisheimer, M., Koshurnikova, N. A., Nekolla, E., Khokhryakov, V. F., Romanov, S. A., Sokolnikov, M. E., Shilnikova, N. S., Okatenko, P. V. and Kellerer, A. M. (2000) Lung cancer mortality among male nuclear workers of the Mayak facilities

in the former Soviet Union. Radiat. Res. **154**: 3–11.
7. Bair, W. J., Park, J. F., Dagle, G. E. and James, A. C. (1989) Overview of biological consequences of exposure to plutonium and higher actinides. Radiat. Protect. Dosimetry **26**: 125–135.
8. Sanders, C. L., Dagle, G. E., Cannon, W. C., Craig, D. K., Powers, G. J. and Meier, D. M. (1976) Inhalation carcinogenesis of high-fired $^{239}PuO_2$ in rats. Radiat. Res. **68**: 349–360.
9. Sanders, C. L., Dagle, G. E., Cannon, W. C., Powers, G. J. and Meier, D. M. (1977) Inhalation carcinogenesis of high-fired $^{238}PuO_2$ in rats. Radiat. Res. **71**: 528–546.
10. Sanders, C. L. and Mahaffey, J. A. (1978) Inhalation carcinogenesis of high-fired $^{244}CmO_2$ in rats. Radiat. Res. **76**: 384–401.
11. Sanders, C. L. and Mahaffey, J. A. (1983) Inhalation carcinogenesis of high-fired $^{241}AmO_2$ in rats. Radiat. Res. **94**: 66–80.
12. Sanders, C. L., Lauhala, K. E. and McDonald, K. E. (1993) Lifespan studies in rats exposed to $^{239}PuO_2$ aerosol. III. Survival and lung tumors. Int. J. Radiat. Biol. **64**: 417–430.
13. Sanders, C. L. and Lundgren, D. L. (1995) Pulmonary carcinogenesis in the F344 and Wistar rat after inhalation of plutonium dioxide. Radiat. Res. **144**: 206–214.
14. Lundgren, D. L., Haley, P. J., Hahn, F. F., Diel, J. H., Griffith, W. C. and Scott, B. R. (1995) Pulmonary carcinogenicity of repeated inhalation exposure of rats to aerosols of $^{239}PuO_2$. Radiat. Res. **142**: 39–53.
15. Dagle, G. E., Park, J. F., Gilbert, E. S. and Weller, R. E. (1989) Risk estimates for lung tumors from inhaled $^{239}PuO_2$, $^{238}PuO_2$, and $^{239}Pu(NO_3)_4$ in beagle dogs. Radiat. Protect. Dosimetry **26**: 173–176.
16. Guilmette, R. A., Diel, J. H., Muggenburg, B. A., Mewhinney, J. A., Boecker, B. B. and McClellan, R. O. (1984) Biokinetics of inhaled $^{239}PuO_2$ in the beagle dog: effects of aerosol particle size. Int. J. Radiat. Biol. **45**: 563–581.
17. Oghiso, Y., Yamada, Y., Iida, H. and Inaba, J. (1998) Differential dose responses of pulmonary tumor types in the rat after inhalation of plutonium dioxide aerosols. J. Radiat. Res. **39**: 61–72.
18. Oghiso, Y. and Yamada, Y. (2000) Pathogenetic process of lung tumors induced by inhalation exposures of rats to plutonium dioxide aerosols. Radiat. Res. **154**: 253–260.
19. Mohr, U., Rittinghausen, S., Takenaka, S., Ernst, H., Dungworth, D. L. and Pylev, L. N. (1990) Tumours of the lower respiratory tract and pleura in the rat. In: Pathology of Tumours in Laboratory Animals, Vol. I. Tumours of the Rat, 2nd ed., Eds. V.S. Turusov and U. Mohr, pp. 275–299., IARC Scientific Publications No. 99, Lyon, France.
20. Hahn, F. F. and Boorman, G. A. (1997) Neoplasia and preneoplasia of the lung. In: Pathology of Neoplasia and Preneoplasia in Rodents, Eds. P. Bannasch and W. Gössner, pp. 29–42., EULEP Color Atlas Vol. 2, Chattauer, Stuttgart & New York.
21. Coggle, J. E. (1988) Lung tumor induction in mice after X-rays and neutrons. Int. J. Radiat. Biol. **53**: 585–598.
22. Fritsch, P., Dudoignon, N., Guillet, K., Oghiso, Y., Morlier, J. P. and Monchaux, G. (2003) Does mean lung dose calculated after inhalation of α emitters actually reflect the risk of malignant lung tumor induction? Radiat. Protect. Dosimetry (in press).
23. Hahn, F. F., Lundgren, D. L., Griffith, W. C. and Boecker, B. B. (1993) Effects of thoracic and whole-body exposure of F344 rats to X-rays. In: Inhalation Toxicology Research Institute Annual Report 1992–1993, pp. 64–65, Report ITRI-140, National Technical Information Service, Springfield, VA.
24. Lafuma, J., Chmelevsky, D., Chameaud, J., Morin, M., Masse, R. and Kellerer, A. M. (1989) Lung carcinomas in Sprague-Dawley rats after exposure to low doses of radon daughters, fission neutrons or gamma rays. Radiat. Res. **118**: 230–245.
25. Batchelor, A. L., Buckley, P., Gore, D. J., Jenner, T. J. and Major, I. R. (1980) The carcinogenic effect of localized fission fragment irradiation of rat lung. Int. J. Radiat. Biol. **37**: 249–266.
26. Morin, M., Masse, R. and Lafuma, J. (1994) Experimental study of different histologic types of pulmonary cancers induced by irradiation. Comptes. Rend. Acad. Sci. Paris **317**: 90–93.
27. Hahn, F. F. and Lundgren, D. L. (1992) Pulmonary neoplasms in rats that inhaled cerium-144 dioxide. Toxicol. Pathol. **20**: 169–178.
28. Lundgren, D. L., Hahn, F. F., Griffith, W. C., Hubbs, A. F., Nikula, K. J., Newton, G. J., Cuddihy, R. G. and Boecker, B. B. (1996) Pulmonary carcinogenicity of relatively low doses of beta-particle radiation from inhaled $^{144}CeO_2$ in rats. Radiat. Res. **146**: 525–535.
29. Mitchel, R. E., Jackson, J. S. and Heinmiller, B. (1999) Inhaled uranium ore dust and lung cancer risk in rats. Health Phys. **76**: 145–155.
30. Oghiso, Y. and Yamada, Y. (2002) Immunohistochemical study on cellular origins of rat lung tumors induced by inhalation exposures to plutonium dioxide aerosols as compared to those by X-ray irradiation. J. Radiat. Res. **43**: 301–311.
31. ICRP (1994) Human respiratory tract model for radiological protection. ICRP Publication 66, Annals of the ICRP 24(1-3), Pergamon Press, Oxford.
32. NCRP (1997) NCRP Report No. 125 on Deposition, Retention and Dosimetry of Inhaled Radioactive Substances. Recommendations of the National Council on Radiation Protection and Measurements.
33. Lundgren, D. L., Hahn, F. F., Carlton, W. W., Griffith, W. C., Guilmette, R. A. and Gillett, N. A. (1997) Dose responses from inhaled monodisperse aerosols of $^{244}Cm_2O_3$ in the lung, liver and skeleton of F344 rats and comparison with $^{239}PuO_2$. Radiat. Res. **147**: 598–612.
34. Dudoignon, N., Guillet, K., Rateau, G. and Fritsch, P. (2001) Survival, lung clearance, dosimetry and gross pathology of rats exposed to either NpO_2 or PuO_2 aerosols. Int. J. Radiat. Biol. **77**: 979–990.
35. Sanders, C. L., McDonald, K. E. and Mahaffey, J. A. (1988) Lung tumor response to inhaled Pu and its implications for radiation protection. Health Phys. **55**: 455–462.
36. Sanders, C. L., McDonald, K. E. and Lauhala, K. E. (1988) SEM autoradiography: aggregation of inhaled $^{239}PuO_2$. Int. J. Radiat. Biol. **54**: 115–121.
37. Sanders, C. L., McDonald, K. E. and Lauhala, K. E. (1988) Promotion of pulmonary carcinogenesis by plutonium particle aggregation following inhalation of $^{239}PuO_2$. Radiat. Res. **116**: 393–405.
38. Lundgren, D. L., Mauderly, J. L., Rebar, A. H., Gillett, N. A. and Hahn, F. F. (1991) Modifying effects of preexisting pulmonary fibrosis on biological responses of rats to inhaled $^{239}PuO_2$. Health Phys. **60**: 353–363.

39. Morlier, J. P., Morin, M., Monchaux, G., Fritsch, P., Pineau, J. F., Chameaud, J., Lafuma, J. and Masse, R. (1994) Lung cancer incidence after exposure of rats to low doses of radon: influence of dose rate. Radiat. Protect. Dosimetry **56**: 93–97.
40. Gilbert, E. S., Cross, F. T. and Dagle, G. E. (1996) Analysis of lung tumor risks in rats exposed to radon. Radiat. Res. **145**: 350–360.
41. Monchaux, G., Morlier, J. P., Altmeyer, S., Debroche, M. and Morin, M. (1999) Influence of exposure rate on lung cancer induction in rats exposed to radon progeny. Radiat. Res. **152**: S137–S140.

Received on April 28, 2003
1st Revision on June 24, 2003
Accepted on July 2, 2003

J. Radiat. Res., 45, 69–76 (2004)

Regular Paper

Comparative Study on *Tp53* Gene Mutations in Lung Tumors from Rats Exposed to ^{239}Pu, ^{237}Np and ^{222}Rn

Yutaka YAMADA[1]*, Yoichi OGHISO[1], Jean-Paul MORLIER[2], Kristell GUILLET[3], Paul FRITSCH[3], Nicolas DUDOIGNON[4] and Georges MONCHAUX[4]

***Tp53*/Mutation/Alpha emitters/Rat/Lung tumors.**

The tumor suppressor gene *Tp53* was analyzed by polymerase chain reaction-amplification of genomic DNA extracted from paraffin-embedded tissue sections of rat lung tumors to compare mutations that occurred after inhalation exposures to plutonium dioxide, neptunium dioxide, or radon and radon progenies. Exons 5 to 8 of the gene were amplified in 16 plutonium-, 23 neptunium- and 15 radon-induced lung tumors, and their polymerase chain reaction products were examined for mutations by single strand conformational polymorphism analysis and direct sequencing method. Two point mutations were detected in the plutonium-induced tumors, i.e., a guanine to adenine transition at codon 219 of exon 6 and a cytosine to thymine transition at codon 266 of exon 8. Although only one point mutation was found at codon 175 of exon 5 (cytosine to thymine transition) from neptunium-induced tumors, no mutations were detectable from radon-induced tumors. These results indicate that the abnormalities of the *Tp53* gene might not be so critical for the pulmonary carcinogenesis after the inhalation of different alpha emitters, even though the presence and frequencies of the *Tp53* gene mutations were different.

INTRODUCTION

Inhalation exposures to alpha emitters have been shown to most effectively induce lung tumors through an alpha particle irradiation of target pulmonary epithelial cells.[1,2] These alpha emitters include transuranium elements such as plutonium (^{238}Pu or ^{239}Pu; Pu), americium (^{241}Am), and neptunium (^{237}Np; Np) from nuclear facilities and naturally present radionuclides, radon (^{222}Rn; Rn), and its progenies. Life-span animal studies conducted in our laboratories have revealed dose-response relationships of lung tumors induced by inhalation exposures to alpha emitters.[3–8] It has been also reported that the pulmonary carcinogenesis is affected by the granulometric parameters, solubility, and the specific activity of inhaled aerosols of alpha emitters.[9] However, molecular mechanisms related to the carcinogenic responses following alpha irradiations remain unclear.

Concerning the molecular carcinogenesis, alterations of the *Tp53* tumor suppressor gene have been investigated because its mutations are the most frequently occurring molecular events in many types of human cancers.[10–11] Although the *Tp53* gene mutations have been described in lung tumors from uranium miners to be inducible by the inhalation of Rn and its progenies,[12–14] there have also been some reports on the *Tp53* gene mutations observed in rat lung tumors induced by variable carcinogens, such as beryllium,[15] diesel exhaust,[16] X-ray irradiation,[17] and Pu dioxide.[18] Our previous study, however, indicated that the intranuclear *Tp53* protein accumulation was detectable only in a slight percentage of pulmonary carcinomas from ^{239}Pu-exposed rats,[7] whereas point mutations of the *Tp53* gene were detectable in 13% (11 of 82 Pu-induced rat lung tumors) by both polymerase chain reaction-single strand conformation polymorphism (PCR-SSCP) analysis and direct sequencing analysis.[19] This value appears to be relatively higher in frequency in comparison to the other report.[18] These results suggest the plausibility that the *Tp53* gene mutations could at least partly play a role in the development of rat lung tumors after the inhalation of Pu dioxide. To our knowledge, however, it has never been described whether any of the *Tp53* gene mutations are present in rat lung tumors induced by alpha emitters other than Pu.

Our laboratories (NIRS, LCE/DRR/CEA, and LRT/DRR/

*Corresponding author: Phone: +81-43-206-3098,
Fax: +81-43-284-1389,
E-mail: yt_yamad@nirs.go.jp

[1]Internal Radiation Effects Research Group, National Institute of Radiological Sciences, 9-1, 4-chome, Anagawa, Inage-ku, Chiba 263-8555, Japan; [2]CEA-Direction des Sciences du Vivant, Département de Radiobiologie et de Radiopathologie, Laboratoire de Cancérologie Expérimentale, BP 6, F92265 Fontenay-aux-Roses Cedex, France; [3]CEA-Direction des Sciences du Vivant, Département de Radiobiologie et de Radiopathologie, Laboratoire de Radiotoxicologie, BP 12, F91680 Bruyères-le-Châtel, France; [4]Institut de Radioprotection et de Sûreté Nucléaire, BP 17, F92262 Fontenay-aux-Roses Cedex, France.

CEA) have been engaged in a collaborative research program to compare carcinogenic responses and risks among Pu-, Np-, and Rn-induced rat lung tumors. The purpose of this study is to compare the frequencies and types of *Tp53* gene mutations in rat lung tumors after inhalation exposures to these different alpha emitters.

MATERIALS AND METHODS

Tumor induction and samples

Histological sections of rat lung tumors were prepared at NIRS (Pu-induced tumors), LRT/DRR/CEA (Np-induced tumors), and LCE/DRR/CEA (Rn-induced tumors). Experimental design, inhalation regimens, pathology, and dose estimation have been reported in the previous papers in detail.[3–9] Briefly, female Wistar rats were exposed once to ^{239}Pu dioxide aerosol at 8 weeks of age in a nose-only inhalation chamber device. After the inhalation, the animals were kept under a barrier-filtered air condition during their life times. The activity median aerodynamic diameter (AMAD) of the Pu aerosol ranged from 0.3–0.5 μm in a geometric standard deviation 1.9–2.0, and initial lung deposition (ILD) ranged 0.1–3.1 kBq. The dose response curve for lung tumor incidences was obtained with a peak value of approximately 97% at 5–6 Gy and a threshold-like dose range of less than 0.2 Gy for malignant tumors. Male Sprague-Dawley rats were exposed to aerosols of ^{237}Np dioxide (AMAD of 2.6 μm in a geometric standard deviation 2.2) at 7–8 weeks of age by single-nose-only inhalation to obtain ILD ranging 0.1–7 kBq. The rats were kept until they were dead or moribund. The incidence of malignant lung tumors increased in a linear-quadratic dose-dependent manner and reached 93% at 26 ± 7 Gy of lung dose in the highest ILD group. In the Rn-inhalation experiment, Male Sprague-Dawley rats (TR and RD) and male hybrid rats of Wistar and F344 (RF) were used. The rats were exposed to ^{222}Rn gas and its progeny (1,200 WL) at 12 weeks of age in a radon chamber for 6 h per day for 5 days a week until the cumulative dose had reached a range of 500–1,000 WLM. Treatment with beta naphto flavone (BNF) was started two months later from the last inhalation of radon to promote the

Table 1. *Tp53* mutation in rat lung tumors after inhalation of plutonium dioxide ($^{239}PuO_2$).

Case No.	Survival period (day)	Dose (Gy)	Type and site of tumors*	PCR-SSCP and direct sequencing	Amino acid
R-1-2-5	993	2.07	AD/AC	Wild type	
			AC #1	Wild type	
			AC #2	Wild type	
			SCC	Wild type	
R-1-4-2	824	2.36	AC #1	Wild type	
			AC #2	Wild type	
S-1-3-2	665	3.1	ASC	Wild type	
			AD/AC	Wild type	
S-1-3-3	692	3.06	AC #1	Wild type	
			AC #2	Wild type	
S-2-4-5	1040	0.8	AD/AC	Wild type	
			AC/ASC	Wild type	
T-1-3-5	761	1.62	AD	Wild type	
V-3-3-3	807	1.97	AD/AC	Wild type	
			SCC	Wild type	
			AC/SCC	Wild type	
V-3-4-2	518	1.56	AC #1	Wild type	
			AC #2	Codon 266, GA**C** to GA**T**	Aspartic acid (D)–Aspartic scid (D)
W-1-1-4	828	2.62	ASC	Wild type	
W-1-2-2	559	2.78	AC	Wild type	
W-1-3-3	770	2.87	AD/AC	Wild type	
			FAC	Wild type	
W-1-3-4	778	2.81	AC	Wild type	
W-2-2-4	873	0.38	AD/AC	Wild type	
			SCC	Wild type	
Y-1-2-2	839	2.86	SCC	Wild type	
Y-2-1-2	780	2.08	AD/AC	Wild type	
			MP/AD	Wild type	
Y-2-3-1	486	2.28	FAC	Codon 219, **G**AG to **A**AG	Glutamic acid (E)–Lysine (K)

*AD: adenoma, AC: adenocarcinoma, ASC: adenosquamous carcinoma, SCC: squamous cell carcinoma, FAC: fibroadeno carcinoma, MP: metaplasia.

Table 2. *Tp53* mutation in rat lung tumors after inhalation of neptunium dioxide ($^{237}NpO_2$).

Case No.	Survival period(day)	Dose (Gy)	Type and site of tumors*1	PCR-SSCP and direct sequencing*2	Amino acid
003	453	15.3	FAC	Wild type	
012	499	32	FAC	Wild type	
			SCC	—	
013	500	0.8	AC/LN metastasis	Wild type	
			AC/Pleural metastasis #1	Codon175, CCC-TCC	Proline (P)-Serine (S)
			AC/Pleural metastasis #2	Wild type	
			AC/Pleural metastasis #3	Wild type	
018	528	13.6	FAC	Wild type	
020	539	29.3	ASC	Wild type	
022	554	32.7	AC	Wild type	
026	582	28.3	FAC	Wild type	
027	581	5.9	AC	Wild type	
029	597	17.7	SCC	Wild type	
030	589	5.9	FAC	Wild type	
034	609	9.5	SCC	—	
			AC/Pleural	Wild type	
035	613	28.7	AC/ASC	Wild type	
			SCC	—	
041	646	6.5	AC/ASC	—	
			ASC/SCC	Wild type	
			Papillary AC	Wild type	
058	743	19.3	SCC	Wild type	
			Solid AC	Wild type	
060	747	42.9	SCC/AC	Wild type	
			AC	-	
062	749	12.6	AC	Wild type	
073	771	1.3	AC/Pleural	Wild type	
077	800	10.6	AC	Wild type	
078	799	8.4	AC	Wild type	
			SCC	—	
086	819	15	AC	Wild type	
103	891	9.7	AC/Pleural	Wild type	
			AC/LN metastasis	Wild type	
110	661	2.4	SCC	Wild type	
			AC/Pleural	Wild type	
114	681	1.6	AC-Alveolar	Wild type	
			AC-Bronchial	Wild type	

*1AD: adenoma, AC: adenocarcinoma, ASC: adenosquamous carcinoma, SCC: squamous cell carcinoma, FAC: fibroadeno carcinoma, LN: lymph node. *2–: not amplified by PCR.

tumor development. BNF in a dose of 25 mg per kg of body weight was injected intramuscularly to the rats six times every 2 weeks. The incidence of lung tumor in rat exposed to radon/radon progeny increased with cumulative exposure, and the BNF treatment accelerated the tumor development. The survival, exposure, or absorbed lung dose and pathological diagnosis of each case are given in Tables 1–3.

DNA extraction

DNA extraction from lung tissue sections mounted on glass slides were done as previously described[20,21] with slight modification. Briefly, the lung tissues were fixed in 10% phosphate-buffered formalin, processed in graded ethanol and xylene, and embedded in paraffin. Several serial sections were prepared from each specimen and placed on glass slides. A 5- to 6-μm-thick section was stained with hematoxylin-eosin (HE) to identify the location and type of lung tumors, and the area of tumor was marked with a marking pen after identification. A 15-μm-thick unstained paraffin section on glass slide was dewaxed by immersions two times in xylene, 100% ethanol, and 70% ethanol for 1–2 min, then washed two times with distilled water and TE buffer (10 mM Tris-HCl, pH 7.5 and 1 mM EDTA). The glass slide was placed in a glass plate and immersed in 10 ml of TE buffer, then put

Table 3. *Tp53* mutation analysis in rat lung tumors after inhalation of Radon (^{222}Rn).

Case No.	Survival period (day)	Dose (WLM)	Treatment[*1]	Type and site of tumors[*2]	PCR-SSCP[*3]
RD07	148	1,000	+BNF	SCC	Wild type
RD14	169	1,000	+BNF	SCC #1	Wild type
				SCC #2	Wild type
				SCC #3	Wild type
				SCC #4	Wild type
RD24	331	1,000	+BNF	AC/ASC	Wild type
RD27	386	1,000	+BNF	AC/ASC	Wild type
RD28	386	1,000	+BNF	SCC	Wild type
RD29	413	1,000	+BNF	Papillary AC	Wild type
RD31	413	1,000	+BNF	Solid AC	Wild type
RD34	413	1,000	+BNF	Papillary AC	Wild type
RD35	448	1,000	+BNF	SCC	Wild type
RF33	316	500	+BNF	SCC	Wild type
RF37	425	500	+BNF	SCC #1	Wild type
				SCC #2	Wild type
TR06	553	800	—	ASC/SCC	Wild type
TR11	678	800	—	AC	Wild type
TR09	654	800	+BNF	AC	Wild type
TR10	670	800	+BNF	AC #1	Wild type
				AC #2	Wild type
				AC #3	Wild type
				AC/Cardiac metastasis	—

[*1]BNF: β-naphthoflavone, intramuscularly injection after inhalation of radon. [*2]AC: adenocarcinoma, ASC: adenosquamous carcinoma, SCC: squamous cell carcinoma. [*3]–: not amplified by PCR.

into a microwave oven at 400 W for 10 s to allow easy detachment of the section from the glass slide. The dewaxed 15-μm-thick section was matched up to the HE-stained serial section, and the tumor area was dissected from the 15-μm-thick section with fine needles under a stereoscopic microscope (Fig. 1, a and b). To avoid cross-contamination of the samples, disposable sterile needles, individual washing buffer, and glass plates were used. Multiple tumor areas were occasionally dissected from the same section.

The dissected tumor samples were incubated overnight at 37°C in lysate buffer consisting of 10 mM Tris-HCl, pH 7.5; 5 mM EDTA; 0.5% sodium dodecyl sulfate; and 20 μg/ml Proteinase K. DNAs were isolated from the lysate solution by using phenol-chloroform extraction and precipitated by ethanol with DNA carrier (Ethachinmate, Wako, Japan). The DNA samples were dissolved in 20 μl of TE buffer. DNA (40 μg/ml) from normal rat lung tissues was used for wild-type control, and a rat fibroblast cell line (Rat 2) was used as the positive control for mutation. The mutation is a thymine (T) to guanine (G) transversion at the second base of codon 171 in exon 5 of *Tp53* gene as confirmed first by us. TE buffer was used as the negative control in the PCR amplification.

PCR-SSCP analysis

The screening for mutations of lung tumor samples were done in the conserved regions of the *Tp53* gene, exon 5 to 8, by PCR-SSCP analysis, because the majority of *Tp53* gene mutations in human tumors are found in exons 5 to 8.[22] The primers specific to exons 5 (upper and lower regions), 6, 7, and 8 in the rat *Tp53* gene were synthesized according to the previous paper.[23] The primer pairs were designed from the intron-exon junction sites for preventing an amplification of rat pseudo *Tp53* gene, and two overlapping primer pairs for exon 5 were used for increasing the efficiency of the detection of a single base change in the PCR-SSCP analysis. To improve the amplification of a small amount of template DNA, the "Hot Start" method was utilized for all samples. PCR products of the *Tp53* gene were generated from 1 μl of the template DNA in a 10 μl reaction mixture containing 5 picomoles of each primer pair, 10 mM Tris-HCl (pH 8.3), 50 mM KCl, 2.5 mM $MgCl_2$, 0.2 mM of each dNTP, and 0.4 unit of "AmpliTaq Gold" DNA polymerase (Applied Biosystems). Pre-heating for activation of the DNA polymerase was performed at 95°C for 9 min. PCR was carried out for 35–60 cycles on an automated thermal cycler (GeneAmp PCR System 9600; Applied Biosystems) with denature at 95°C for 1 min, annealing at 55 to 62°C for 1 min, and extension at 72°C for 1 min. The PCR products were analyzed by 2% agarose gel electrophoresis to examine optimal amplifications.

The second PCR for SSCP analysis was performed under the same conditions as those used for the first PCR in the presence of the 5′-end-labeled forward and reverse primers with [gamma-^{32}P] ATP using T4 polynucleotide kinase. The labeled products were mixed with loading buffer of 10 mM NaOH, 95% formamide, 0.1% bromophenol blue, and 0.1% xylene cyanol. The samples were denatured at 94°C for 2 min

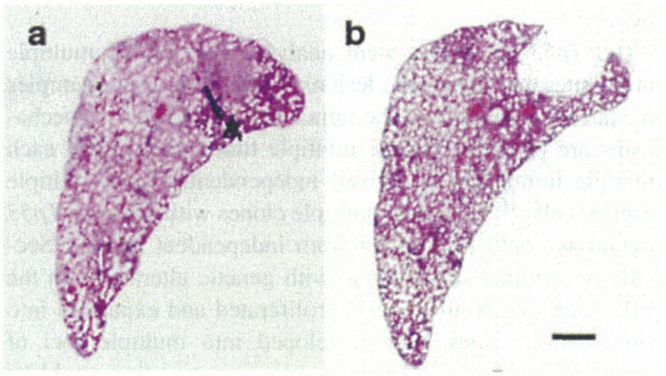

Fig. 1. A representative sample of dissection from rat lung tumor. a: a HE-stained lung tissue section containing a tumor site. b: a serial section of the lung tissue after dissection of the tumor site. The tumor site was removed from the unstained serial section, and the section was then stained with HE after the dissection. A bar indicates one mm.

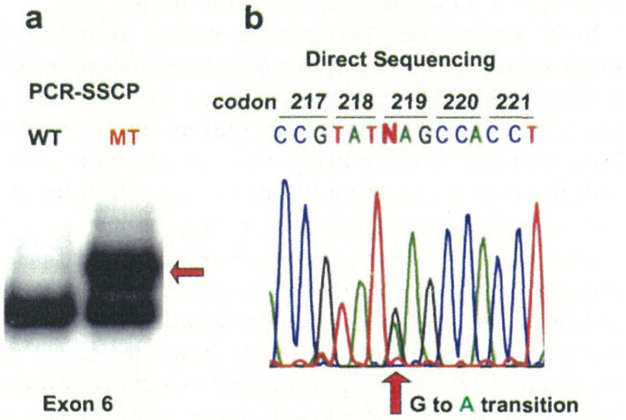

Fig. 2. SSCP analysis and direct sequencing of *Tp53* of DNA from rat lung tumor. a: sample of lung tumor (MT; case Y-2-3-1) had altered the banding pattern compared to wild-type control (WT; normal lung). Labeled forward primer and unlabeled reverse primer for exon 5 upper of *Tp53* were used in this SSCP analysis. b: sequence diagram showed a G to A transition at codon 219 in the sample above.

and put on ice. Three μl of each sample were run at 8 watts for 5 h on the "Mutation Detection Enhancement" gels (FMC BioProducts). The gels were subjected to autoradiography with X-ray film (Fuji Photo Film, Co., Ltd.) for the detection of mutations (Fig. 2a).

Direct DNA sequencing

The DNA samples showing abnormal mobility in SSCP analysis were amplified again by the PCR in 100 μl reaction mixture. The PCR products were electrophoresed in low melting agarose gel. The band showing authentic PCR product size was cut out from the gel, and the DNA fragment was eluted and purified with glass powder. The purified samples were processed for direct sequencing analysis with a DNA sequencing system (ABI Prizm 377; Applied Biosystems) according to the manufacturer's instructions (Fig. 2b). The primer pairs for each exon used in the PCR-SSCP analysis were employed for the sequencing of both 5′- and 3′-strands to identify the mutations.

RESULTS

PCR-SSCP analysis was performed in 29 tumor sites of 16 Pu-induced tumors (Table 1), 37 tumor sites of 23 Np-induced tumors (Table 2), and 22 tumor sites of 15 Rn-induced tumors (Table 3). The number of lung tumor sites that were generated per rat varied depending on the absorbed dose. It ranged from 0.4 to 2.7 in carcinomas and from 0.6 to 1.8 in adenomas of Pu-inhaled animals.[24] The PCR fragments showing different mobility in PCR-SSCP analysis were examined to identify the mutations by direct sequencing analysis. Two point mutations were detected from Pu-induced tumors (cases Y-2-3-1 and V-3-4-2), a G to A transition in the first base at codon 219 within exon 6, and a C to T transition in the third base at codon 266 within exon 8 (Table 1). One point mutation was identified in Np-induced tumors (case 013), a C to T transition in the first base at codon 175 within exon 5 (Table 2). All the mutations were G to A or C to T transition in a non-CpG dinucleotide. On the other hand, no mutation was observed in the PCR-SSCP analysis of the DNA from any Rn-induced lung tumors in the present study (Table 3). The frequencies of the confirmed mutations were calculated to be 13% (2 of 16 cases) in Pu-induced tumors and 5% (1 of 23 cases) in Np-induced tumors.

Mutation analysis of separate foci in the same lung tumor samples indicated a different state of mutation. In case V-3-4-2 of Pu containing two separate tumor sites of adenocarcinoma (AC), one site (AC #2) showed a point mutation, but the other (AC #1) showed a wild type (Table 1). In case 013 of Np, one metastatic lesion of adenocarcinoma in a lymph node (AC/LN) and 3 different sites of adenocarcinomas in pleural surfaces (AC/pleural #1 to #3) were separately analyzed. The results showed that only one (#1) of the AC/pleural sites possessed the *Tp53* gene mutation (Table 2).

DISCUSSION

Frequencies of Tp53 mutation in alpha-emitter-induced lung tumors

In the present study, the observed mutation frequency (13%) of *Tp53* by direct sequence analysis on Pu-induced tumors is almost equivalent to the observed frequency of 13% (11 out of 82 cases) found in our previous data from the different Pu-induced lung tumor samples.[19] This frequency is relatively higher than the other report, 5% (2 out of 38 cases) in Pu-induced lung tumors in the rat.[18] When the actual number of tumors examined were treated as the individual unit, the mutation frequency was 7% (2 out of 29 tumor sites); that

was more in line with the data obtained by the other investigators.

The frequency of *Tp53* mutation was 5% in the Np-induced tumors, and it was 0% in Rn-induced tumors. Although it is difficult to explain the reasons underlying such different frequencies of *Tp53* mutations of rat lung tumors among three alpha emitters, the dose rate or half-life of Rn may explain differences in the mutation frequency compared to the other alpha emitters. Alpha particle irradiation by Rn and progenies might have been completed within relatively shorter periods even after repeated exposures; Pu and Np dioxides are retained in the lung during a much longer period, then leading to a continuous alpha particle irradiation. In fact, the frequency of *Tp53* gene mutations of rat lung tumors induced by fractionated or single X-ray irradiation during a shorter period was very low.[17] Further investigations are needed to establish whether *Tp53* mutations are a dose-rate-dependent phenomenon in radiation-induced tumors.

The *Tp53* gene is considered as one of the most reliable genes to be altered in human cancers and is the primary molecular target under the process of carcinogenesis.[10,11] It has been described that more than half of all human cancers has *Tp53* gene mutations. On the other hand, *Tp53* mutation frequencies in rodent tumors are generally lower than in human ones,[25] except for some chemically induced tumors. These include tamoxifen-[26] and 2-acetylaminofluorene-[27] induced hepatocellular carcinomas, vinyl chloride-induced liver angiosarcomas,[28] *N*-methyl-*N*-nitrosourea-induced forestomach squamous cell carcinomas,[29] *N*-butyl-*N*- (4-hydroxybutyl) nitrosamine-induced urinary bladder carcinomas,[30] formaldehyde-induced nasal squamous cell carcinomas,[31] and 1,6-dinitropyrene-induced lung tumors.[32] Furthermore, it has been reported that methylene chloride-,[33] aflatoxin B_1-,[34] and urethane-induced lung tumors[35] of mice showed low frequencies of *Tp53* mutations in the early stage of pulmonary tumorigenesis, although the incidences of mutation increased in the late period of tumorigenesis. These reports indicate that the *Tp53* mutation frequencies of the chemical carcinogen-induced tumors in rodents appear to depend on the type of carcinogens and the progression stage of tumors.[27,29,30] Miller[36] also indicates that *Tp53* mutations may not be necessary for rodent lung tumorigenesis, but may occur as a late event. However, it has been shown that the *Tp53* mutations are a rare event in radiation-induced lung tumors[17,18,37] and skin cancer.[38] Such low frequencies of *Tp53* mutation in radiation-induced tumors of rodents might be due to carcinogenic mechanisms that are more complex and involve genetic and epigenetic factors, including species differences. It was recently reported that hypermethylation of the promoter region of $p16^{INK4a}$ could also be related to carcinogenesis of rat lung tumors.[39,40] More attention needs to be focused on potential alterations that may occur in other genetic pathways instead of screening for *Tp53* mutation.

Tp53 mutations in multiple tumor sites and metastaic lesions

The *Tp53* mutations were analyzed in each of multiple tumor sites and metastatic lesions in the same tumor samples to examine the origin of the tumor cells. At least two mechanisms are plausible for the multiple tumor sites. First, each multiple tumor site is derived independently from multiple original cells.[41] Therefore multiple clones with different *Tp53* mutations could be derived from independent origins. Second, the original single clone with genetic alterations in the early stage of carcinogenesis proliferated and expanded into surrounding tissues, then developed into multiple foci of tumors.[42] In the second case, a common mutation could be detected in the multiple foci. Franklin *et al.* have reported that the expansion and dispersion of a mutant progenitor epithelial cell clone throughout the air way resulted in the widespread presence of a single somatic *Tp53* point mutation in the bronchi of a smoker.[43] On the other hand, Waridel *et al.* detected an expansion of multiple clones of a *Tp53* mutant in the esophagus of a human using a yeast functional assay.[44]

In the present study, the mutation analysis of separate foci in the same lung tumor samples indicate a different state that is described in the result section. These results suggest that the cellular origins of each tumor lesion and the occurrence of *Tp53* mutations could be independent; or otherwise the tumor cells from the same origin metastasized into other intrapulmonary sites to form separate lesions, and the mutations then occurred in each of the metastatic lesions. Matched pairs of chemically induced primary and metastatic mouse squamous cell carcinomas also had no concordance between the *Tp53* mutation found in the primary tumor site and the distant metastatic site.[44] These findings suggested that the occurrence of *Tp53* mutations in the primary tumor and the metastatic lesions could be independent events in the Pu- and Np-induced rat lung tumors.

Types of Tp53 mutations in alpha-emitter-induced lung tumors

All the mutations found in the present study were G to A or C to T transition in a non-CpG dinucleotide (Tables 1 and 2), though half of the *Tp53* mutations in Pu-induced lung tumors of rat were observed at CpG dinucleotide in our previous report.[19] The other investigations also showed similar results because rodent lung tumors tend to exhibit G to A or C to T transition in the late period of tumorigenesis.[18,34,40] As well as exogenous mutagens, endogenous products such as metabolites and free radicals are known to cause mutations. Cytosine and methyl cytosine residues are deaminated to uracil and thymine by the endogenous products respectively, which, if not repaired, will result in G:C to A:T transition.[46] Nitric oxide (NO) radicals have the ability to deaminate the cytosine and the methyl cytosine, and the NO-related deaminations of DNA cause also the G:C to A:T transition.[47,48] This type of mutation in the *Tp53* has been most commonly observed in

human cancers,[46,49] including colorectal cancers,[11] brain tumors[11] and gastric carcinomas.[50] These results that only G:C to A:T transition was found in the present and the previous study[18,19] indicate that the mechanism of mutagenesis in alpha-emitter-induced lung tumors could involve the deamination of cytosine and methylated cytosine at non-CpG and CpG site, depending on the endogenous mechanisms of mutation.

In conclusion, the present data showed first the comparable results on *Tp53* mutations in rat lung tumors induced by three different alpha emitters. The frequencies of the confirmed mutations were calculated to be 13% in Pu-induced tumors and 5% in Np-induced tumors, but 0% in Rn-induced tumors. However, there would not be enough sizes for examinations to determine whether *Tp53* mutations play a significant role in the onset and development of lung tumors. The discordant *Tp53* mutations in multiple tumor sites indicate that the mutations may occur independently in each tumor site. Only G:C to A:T transition was found, suggesting that the *Tp53* mutation could be dependent on endogenous mechanisms.

REFERENCES

1. ICRP (1980) Biological effects of inhaled radionuclides. Publication **31**, Annals of the ICRP 4 (1–2), Pergamon Press, Oxford.
2. ICRP (1994) Human respiratory tract model for radiological protection. Publication **66**, Annals of the ICRP 24 (1–3), Pergamon Press, Oxford.
3. Dudoignon, N., Guezingar-Liebard, F., Guillet, K., L'Hullier, I., Rateau, G., Monchaux, G. and Fritsch, P. (1999) Lung carcinogenesis in rats after inhalation exposure to $^{237}NpO_2$. Radiat. Res. **152**: S31–S33.
4. Morlier, J. P., Morin, M., Monchaux, G., Pineau, J. F., Chameaud, J., Lafuma, J. and Masse, R. (1994) Lung cancer incidence after exposure of rats to low doses of radon: Influence of dose rate. Radiat. Prot. Dosim. **56**: 93–97.
5. Monchaux, G., Morlier, J. P., Morin, M., Chameaud, J., Lafuma, J. and Masse, R. (1994) Carcinogenic and cocarcinogenic effects of radon and radon daughters in rats. Environ. Health Perspect **102**: 64–73.
6. Oghiso, Y., Yamada, Y., Ishigure, N., Fukuda, S., Iida, H., Yamada, Y., Sato, H., Koizumi, A. and Inaba, J. (1994) High incidence of malignant lung carcinomas in rats after inhalation of $^{239}PuO_2$ aerosol. J. Radiat. Res. **35**: 222–235.
7. Oghiso, Y., Yamada, Y., Iida, H. and Inaba, J. (1998) Differential dose responses of pulmonary tumor types in the rat after inhalation of plutonium dioxide aerosols. J. Radiat. Res. **39**: 61–72.
8. Oghiso, Y. and Yamada, Y. (2000) Pathogenetic process of lung tumors induced by inhalation exposures of rats to plutonium dioxide aerosols. Radiat. Res. **154**: 253–260.
9. Dudoignon, N., Guillet, K., Rateau, G. and Fritsch, P. (2001) Survival, lung clearance, dosimetry and gross pathology of rats exposed to either NpO_2 or PuO_2 aerosols. Int. J. Radiat. Biol. **77**: 979–990.
10. Levine, A. J., Momand, J. and Finlay, C. A. (1991) The *p53* tumor suppressor gene. Nature **351**: 453–456.
11. Hollstein, M., Sidransky, D., Vogelstein, B. and Harris, C. C. (1991) *p53* mutations in human cancers. Science **253**: 49–53.
12. Taylor, J. A., Watson, M. A., Devereux, T. R., Michels, R. Y., Saccomanno, G. and Anderson, P. (1994) *p53* mutation hotspot in radon-associated lung cancer. Lancet **343**: 86–87.
13. Vähäkangas, K. H., Samet, J. M., Metcalf, R. A., Welsh, J. A., Bennett, W. P., Lane, D. P. and Harris, C. C. (1992) Mutation of *p53* and ras genes in radon-associated lung cancer from uranium miners. Lancet **339**: 576–579.
14. Hollstein, M., Bartsch, H., Wesch, H., Kure, E. H., Mustonen, R., Muhlbauer, K. R., Spiethoff, A., Wegener, K., Wiethege, T. and Muller, K. M. (1997) *p53* gene mutation analysis in tumors of patients exposed to α-particles. Carcinogenesis **18**: 511–516.
15. Nickell-Brady, C., Hahn, F. F., Finch, G. L. and Belinsky, S. A. (1994) Analysis of *K-ras, p53* and *c-raf-1* mutations in beryllium-induced rat lung tumors. Carcinogenesis **15**: 257–262.
16. Swafford, S. D., Nikula, K. J., Mitchell, C. E. and Belinsky, S. A. (1995)Low frequency of alterations in *p53*, *K-ras*, and *mdm2* in rat lung neoplasms induced by diesel exhaust or carbon black. Carcinogenesis **16**: 1215–1221.
17. Belinsky, S. A., Middleton, S. K., Picksley, S. M., Hahn, F. F. and Nikula, K. J. (1996) Analysis of the *K-ras* and *p53* pathways in X-ray-induced lung tumors in the rat. Radiat. Res. **145**: 449–456.
18. Kelly, G., Stegelmeier, B. L. and Hahn, F. F. (1995) *p53* alterations in plutonium-induced F344 rat lung tumors. Radiat. Res. **142**: 263–269.
19. Yamada, Y. and Oghiso, Y. (1999) Mutations in *Tp53* gene sequences from lung tumors in rats that inhaled plutonium dioxide. Radiat. Res. **152**: S107–S109.
20. Chung, K. Y., Mukhopadhyay, T., Kim, J., Casson, A., Ro, J. Y., Goepfert, H., Hong, W. K. and Roth, J. A. (1993) Discordant *p53* gene mutations in primary head and neck cancers and corresponding second primary cancers of the upper aerodigestive tract. Cancer Res. **53**: 1676–1683.
21. Sarkar, F. H., Kupsky, W. J., Li, Y.-W. and Sreepathi, P. (1994) Analysis of *p53* gene mutations in human gliomas by polymerase chain reaction-based single-strand conformation polymorphism and DNA sequencing. Diag. Mol. Pathol. **3**: 2–8.
22. Harris, C. C. (1993) p53: At the crossroads of molecular carcinogenesis and risk assessment. Science **262**: 1980–1981.
23. Wang, D., You, L., Sneddon, J., Cheng, S.-J., Jamasbi, R. and Stoner, G. D. (1995) Frameshift mutation in codon 176 of the *p53* gene in rat esophageal epithelial cells transformed by benzo[a]pyrene dihydrodiol. Mol. Carcinogenesis **14**: 84–93.
24. Oghiso, Y. and Yamada, Y. (2003) Comparisons of pulmonary carcinogenesis in rats following inhalation exposure to plutonium dioxide or X-ray irradiation. J. Radiat. Res. **44**: 261–270.
25. Buzard, G. S. (1996) Studies of oncogene activation and tumor suppressor gene inactivation in normal and neoplastic rodent tissue. Mutat. Res. **365**: 43–58.
26. Vancutsem, P. M., Lazarus, P. and Williams, G. M. (1994) Frequent and specific mutations of the rat *p53* gene in hepatocarci-

nomas induced by tamoxifen. Cancer Res. **54**: 3864–3867.
27. Ho, Y. S.Cheng, H. T. Wang, Y. J. Lin, J. K. (1995) *p53* gene mutational spectra in hepatocellular carcinomas induced by 2-acetylaminofluorene and *N*-nitroso-2-acetylaminofluorene in rats. Mol. Carcinogenesis **13**: 182–190.
28. Barbin, A., Froment, O., Boivin, S., Marion, M. J., Belpoggi, F., Maltoni, C. and Montesano, R. (1997) *p53* gene mutation pattern in rat liver tumors induced by vinyl chloride. Cancer Res. **57**: 1695–1698.
29. Matsumoto, K., Iwase, T., Hirono, I., Nishida, Y., Iwahori, Y., Hori, T., Asamoto, M., Takasuka, N., Kim, D. J., Ushijima, T., Nagao, M. and Tsuda, H. (1997) Demonstration of ras and *p53* gene mutations in carcinomas in the forestomach and intestine and soft tissue sarcomas induced by N-methyl-N-nitrosourea in the rat. Jpn J. Cancer Res. **88**: 129–136.
30. Masui, T., Dong, Y., Yamamoto, S., Takada, N., Nakanishi, H., Inada, K., Fukushima, S. and Tatematsu, M. (1996) *p53* mutations in transitional cell carcinomas of the urinary bladder in rats treated with *N*-butyl-*N*-(4-hydroxybutyl)-nitrosamine. Cancer Lett. **105**: 105–112.
31. Recio, L., Sisk, S., Pluta, L., Bermudez, E., Gross, E. A., Chen, Z., Morgan, K. and Walker, C. (1992) *p53* mutations in formaldehyde-induced nasal squamous cell carcinomas in rats. Cancer Res. **21**: 6113–6116.
32. Smith, B. A., Manjanatha, M. G., Pogribny, I. P., Mittelstaedt, R. A., Chen, T., Fullerton, N. F., Beland, F. A., Heflich, R. H. (1997) Analysis of mutations in the *K-ras* and *p53* genes of lung tumors and in the *hprt* gene of 6-thioguanine-resistant T-lymphocytes from rats treated with 1,6-dinitropyrene. Mutat. Res. **379**: 61–68.
33. Hegi, M. E., Söderkvist, P., Foley, J. F., Schoonhoven, R., Swenberg, J. A., Kari, F., Maronpot, R., Anderson, M. W. and Wiseman, R. W. (1993) Characterization of *p53* mutations in methylene chloride-induced lung tumors from B6C3F1 mice. Carcinogenesis **14**: 803–810.
34. Tam, A. S., Foley, J. F., Devereux, T. R., Maronpot, R. R. and Massey, T. E. (1999) High frequency and heterogeneous distribution of *p53* mutations in alatoxin B_1-induced mouse lung tumors. Cancer Res. **59**: 3634–3640.
35. Horio, Y., Chen, A., Rice, P., Roth, J. A., Malkinson, A. M. and Schrump, D. S. (1996) Ki-ras and p53 mutations are early and late events, respectively, in urethane-induced pulmonary carcinogenesis in A/J mice. Mol. Carcinogenesis **17**: 217–223.
36. Miller, M. S. (1999) Tumor suppressor genes in rodent lung carcinogenesis- Mutaion of *p53* does not appear to be an early lesion in lung tumor pathogenesis. Toxicol. Applied Pharmacol. **156**: 70–77.
37. Belinsky, S. A., Swafford, D. S., Finch, G. L., Mitchell, C. E., Kelly, G., Hahn, F. F., Anderson, M. W. and Nikula, K. J. (1997) Alterations in the *K-ras* and *p53* genes in rat lung tumors. Environ. Health Perspec. **105**: 901–906.
38. Jin, Y., Burns, J., Garte, S. J., Hosselet, S., (1996) Infrequent alterations of the *p53* gene in rat skin cancers induced by ionizing radiation. Carcinogenesis **17**: 873–876.
39. Swafford, D. S., Middleton, S. K., Palmisano, W. A., Nikula, K. J., Tesfaigzi, J., Baylin, S. B., Herman, J. G. and Belinsky, S. A. (1997) Frequent aberrant methylation of $p16^{INK4a}$ in primary rat lung tumors. Mol. Cellular Biol. **17**: 1366–1374.
40. Belinsky, S. A., Snow, S. S., Nikula, K. J., Finch, G. L., Tellez, C. S. and Palmisano, W. W. (2002) Aberrant CpG island methylation of the $p16^{INK4a}$ and estrogen receptor genes in rat lung tumors induced by particulate carcinogens. Carcinogenesis **23**: 335–339.
41. Sozzi, G., Miozzo, M., Pastorino, U., Pilotti, S., Donghi, R., Giarola, M., De, Gregorio, L., Manenti, G., Radice, P., Minoletti, F., Porta, G. D. and Pierotti, M. A. (1995) Genetic evidence for an independent origin of multiple preneoplastic and neoplastic lung lesions. Cancer Res. **55**: 135–140.
42. Sidransky, D., Frost, P., Von, Eschenbach, A., Oyasu, R., Preisinger, A. C. and Vogelstein, B. (1992) Clonal origin of bladder cancer. New Engl. J. Med. **326**: 737–740.
43. Franklin, W. A., Gazdar, A. F., Haney, J., Wistuba, I. I., La, Rosa, F. G., Kennedy, T., Ritchey, D. M. and Miller, Y. E. (1997) Widely dispersed *p53* mutation in respiratory epithelium. A novel mechanisms for field carcinogenesis. J. Clin. Invest. **100**: 2133–2137.
44. Waridel, F., Estreicher, A., Bron, L., Flaman, J.- M., Fontolliet, C., Monnier, O., Frebourg, T. and Iggo, R. (1997) Field cancerisation and polyclonal *p53* mutation in the upper aero digestive tract. Oncogene **14**: 163–169.
45. Zhang, S. Y., Bauer, B., Mitsunaga, S., Goodrow, T. L. and Klein-Szanto, A. J. (1995) Lack of concordant *p53* mutations in some paired primary and metastatic mouse squamous cell carcinomas induced by chemical carcinogenesis. Mol. Carcinogenesis **12**: 77–81.
46. Greenblatt, M. S., Bennett, W. P., Hollstein, M. and Harris, C. C. (1994) Mutations in the *p53* tumor suppressor gene: clues to cancer etiology and molecular pathogenesis. Cancer Res. **54**: 4855–4878.
47. Wink, D. A., Kasprzak, K. S., Maragos, C. M., Elespuru, R. K., Misra, M., Dunams, T. M., Cebula, T. A., Koch, W. H., Andrews, A. W. and Allen, J. S. (1991) DNA deaminating ability and genotoxicity of nitric oxide and its progenitors. Science **254**: 1001–1003.
48. Nguyen, T., Brunson, D., Crespi, C. L., Penman, B. W., Wishnok, J. S. and Tannenbaum, S. R. (1992) DNA damage and mutation in human cells exposed to nitric oxide in vitro. Proc. Natl. Acad. Sci. USA **89**: 3030–3034.
49. Hainaut, P., Hernandez, T., Robinson, A., Rodriguez-Tome, P., Flores, T., Hollstein, M., Harris, C. C. and Montesano, R. (1998) IARC database of *p53* gene mutations in human tumors and cell lines: updated compilation, revised formats and new visualisation tools. Nucleic Acids Res. **26**: 205–213.
50. Tsuji, S., Tsuji, M., Sun, W.-H., Gunawan, E. S., Murata, H., Kawano, S. and Hori, M. (1997) *Helicobater pylori* and gastric carcinogenesis. J. Clin. Gastroenterol. **25**: S186–S197.

Received on March 19, 2003
1st Revision on August 16, 2003
2nd Revision on September 1, 2003
3rd Revision on November 4, 2003
Accepted on November 4, 2003

プルトニウム内部被ばく研究報告書
補遺　研究成果資料集

平成１８年９月刊行

放射線医学総合研究所
放射線防護研究センター　発達期被ばく影響研究グループ
企画部　企画課

〒263-8555　千葉県千葉市稲毛区穴川 4-9-1